



Lithostratigraphy, geology and geochemistry of the volcanic rocks of the Maligat Formation and associated intrusions on Disko and Nuussuaq, Paleocene of West Greenland

Pedersen, Asger Ken; Larsen, Lotte Melchior; Pedersen, Gunver Krarup

Published in:
Geological Survey of Denmark and Greenland Bulletin (GEUS)

Publication date:
2018

Document version
Publisher's PDF, also known as Version of record

Document license:
[CC BY](#)

Citation for published version (APA):
Pedersen, A. K., Larsen, L. M., & Pedersen, G. K. (2018). Lithostratigraphy, geology and geochemistry of the volcanic rocks of the Maligat Formation and associated intrusions on Disko and Nuussuaq, Paleocene of West Greenland. *Geological Survey of Denmark and Greenland Bulletin (GEUS)*, 40, 1-239.

Lithostratigraphy, geology and geochemistry of the volcanic rocks of the Maligât Formation and associated intrusions on Disko and Nuussuaq, Paleocene of West Greenland

Asger Ken Pedersen, Lotte Melchior Larsen
& Gunver Krarup Pedersen



**Lithostratigraphy, geology and geochemistry of
the volcanic rocks of the Maligât Formation and
associated intrusions on Disko and Nuussuaq,
Paleocene of West Greenland**

Asger Ken Pedersen, Lotte Melchior Larsen and Gunver Krarup Pedersen

Geological Survey of Denmark and Greenland Bulletin 40

Keywords

Maligât Formation, basalt, lithostratigraphy, intrusions, crustal contamination, native iron, graphite, Nuussuaq Basin, Paleocene

Cover illustration

Uppalluk/Giesecke Monument, a landmark peak reaching 1574 m a.s.l. on the south coast of Nuussuaq. Subaerial lava flows of the upper Rinks Dal Member of the Maligât Formation constitute the major part of the peak, which is topped by a remnant of a Nordfjord Member basalt flow. The exposed section is 550 m thick. Photo: Erik Vest Sørensen.

Frontispiece: facing page

The north-east coast of Disko in midnight sun. A wall of subaerial lava flows of the Rinks Dal Member of the Maligât Formation rises above a slope dominated by numerous landslides. The slides are caused by an unstable configuration of basalts overlying poorly consolidated Cretaceous to Paleocene sediments. The ice-capped peak to the left is the 1366 m high Qinnugsaq mountain. In the foreground, the cutter Porsild of the Arctic Station in Qeqertarsuaq is anchored in the bay at Tartunaq, Nuussuaq, 1986.

Chief editor of this series: Adam A. Garde

Editorial board of this series: John A. Korstgård, Department of Geoscience, Aarhus University; Minik Rosing, Geological Museum, University of Copenhagen; Finn Surlyk, Department of Geosciences and Natural Resource Management, University of Copenhagen

Scientific editor: Adam A. Garde

Editorial secretary: Jane Holst

Referees: C.H. Emeleus and R. Wilson

Illustrations: Jette Halskov, Willy L. Weng, Benny M. Schark, Jacob Lind Bendtsen and Allan Lindy.

Photographs: All photographs were taken by the authors except where otherwise stated.

Layout and graphic production: Henrik Klinge Pedersen and Jacob Lind Bendtsen

Printers: Rosendahls-Schultz Grafisk A/S, Albertslund, Denmark

Manuscript received: 9 June 2017

Final version approved: 15 May 2018

Printed: September 2018

ISSN (print) 1604-8156

ISSN (online) 1904-4666

ISBN (print) 978-87-7871-498-5

ISBN (online) 978-87-7871-499-2

Citation of the name of this series

It is recommended that the name of this series is cited in full, viz. *Geological Survey of Denmark and Greenland Bulletin*.

If abbreviation of this volume is necessary, the following form is suggested: *Geol. Surv. Den. Green. Bull.* 40, 239 pp.

Available from

Geological Survey of Denmark and Greenland (GEUS)

Øster Voldgade 10, DK-1350 Copenhagen K, Denmark

To buy bulletin in printed form please contact bogsalg@geus.dk

and at www.geus.dk/bulletin40 (open access)

© De Nationale Geologiske Undersøgelser for Danmark og Grønland (GEUS), 2018

For the full text of the GEUS copyright clause, please refer to www.geus.dk/bulletin



Dedicated to the memory of Finn Ulff-Møller

Contents

Abstract	9
Introduction	10
Geological setting	14
The sedimentary substrate	16
Deposition of the volcanic succession and equivalent sediments	16
Methods	20
Stratigraphic subdivision and numerical coding system	20
Nomenclature	20
<i>Geological sections and profiles</i>	20
West Greenland Basalt Group	22
Summary of the petrology of the Vaigat and Maligât formations	22
Maligât Formation	23
<i>Revision of the Maligât Formation</i>	23
Lithostratigraphy of the Maligât Formation	23
General features of the Maligât Formation	24
Subdivision	24
Lithological variations and the filling of the Assoq Lake	25
Boundaries	39
<i>Lower boundary</i>	39
<i>Upper boundary</i>	42
Rinks Dal Member	43
Lithostratigraphy of the Rinks Dal Member	43
Subdivision of the Rinks Dal Member	44
Lower Rinks Dal Member	45
<i>Summary of the main features of the lower Rinks Dal Member</i>	45
Unit 505 (lowest flows)	46
Unit 506	46
Unit 507 (low-Ti flows)	47
Unit 509	55
<i>South coast of Disko: Infilling of the southern part of the Assoq Lake</i>	56
<i>The northern basin in the Kuugannguaq–Qullissat area</i>	61
Unit 511 (Skarvefjeld unit)	65
<i>South coast of Disko around Skarvefjeld</i>	70
<i>East Disko around Kvandalen</i>	71
<i>North coast of Disko around Qullissat</i>	75
Unit 512 (lower transition flows)	76
<i>Invasive lava flows on eastern Disko</i>	77
<i>Invasive lava flows on southern Nuussuaq</i>	77
Middle Rinks Dal Member	80
<i>Summary of the main features of the middle Rinks Dal Member</i>	80
Unit 513 (Akuarut unit)	80
<i>South coast of Disko between Marraat Qaqqaat and Tuapaat Qaqqaat</i>	83
<i>South coast of Nuussuaq</i>	85
Upper Rinks Dal Member	88
<i>Summary of the main features of the upper Rinks Dal Member</i>	88
Unit 514 (upper transition flows)	88
Units 515, 516 and 517 (the main upper Rinks Dal Member)	89

Unit 518 (uppermost flows)	91
Lithologies of the upper Rinks Dal Member	91
<i>Eruption sites on western Disko</i>	92
<i>Lithologies on Disko</i>	92
<i>Lithologies on Nuussuaq</i>	99
Lava volumes in the upper Rinks Dal Member	101
Chemical compositions of the Rinks Dal Member	104
<i>Major elements</i>	104
<i>Trace elements</i>	104
Eruption sites for the Rinks Dal Member	113
Uncontaminated basalt dykes and sills	113
Feeder systems for the Rinks Dal Member	114
Nordfjord and Niaqussat members	115
<i>Revision of the boundary between the Nordfjord and Niaqussat members</i>	115
Nordfjord Member	116
<i>Summary of the main features of the Nordfjord Member</i>	116
Lithostratigraphy of the Nordfjord Member	116
Internal structure of the Nordfjord Member	117
Igneous rock types	119
Basalt	119
Basaltic andesite	122
Andesite	123
Dacite	124
Rhyolite	128
Geological themes and locality descriptions	131
Sediment horizons at the base of the Nordfjord Member	131
The West Disko Graphite Rhyolite (WDGR) volcano	134
<i>Tuff successions</i>	136
Conglomerates and volcanoclastic sandstones	138
<i>Sediments with clasts from the WDGR volcano</i>	141
<i>Sediments without clasts from the WDGR volcano</i>	144
Simple dacite lava flows between Hammer Dal and Jamma	144
Composite lava flows	146
Crater site lithologies	153
Chemical compositions of the Nordfjord Member	156
<i>Major elements</i>	156
<i>Trace elements</i>	161
<i>Composite lava flows</i>	162
Niaqussat Member	169
<i>Summary of the main features of the Niaqussat Member</i>	169
Lithostratigraphy of the Niaqussat Member	169
Lower Niaqussat Member (unit 530)	170
<i>Western Disko</i>	171
<i>Eastern Disko</i>	174
<i>Eastern Nuussuaq</i>	175
Middle Niaqussat Member (unit 531)	176
Upper Niaqussat Member (unit 532)	177
<i>Disko</i>	178
<i>Eastern Nuussuaq</i>	179
Chemical compositions of the Niaqussat Member	182
<i>Major elements</i>	183

<i>Trace elements</i>	183
Sapernuvik Member	192
<i>Summary of the main features of the Sapernuvik Member</i>	192
Lithostratigraphy of the Sapernuvik Member	192
Geology and geochemistry of the Sapernuvik Member	193
Dyke systems of the Nordfjord and Niaqussat members	195
<i>Summary of the main features of the contaminated dyke systems</i>	195
Weakly contaminated dykes	195
Main dyke systems of the strongly contaminated magmas	195
<i>Intrusions in dyke system A</i>	197
<i>Intrusions in dyke system B</i>	207
<i>Intrusions in dyke system C</i>	208
<i>Other dyke intrusions</i>	209
<i>Concluding remarks on the strongly contaminated dyke systems</i>	210
Chemical compositions of the Nordfjord and Niaqussat Member dykes and feeder systems	210
Volume relations of the Maligât Formation	215
<i>Thickness of the removed succession</i>	216
Crustal contamination of the volcanic rocks	217
<i>Summary of the main features of the crustal contamination processes</i>	217
Possible contaminants	217
<i>Basement</i>	217
<i>Sediments</i>	217
<i>Distinction between contaminants</i>	223
Degrees of contamination	224
Contamination processes and geochemical changes during contamination	225
<i>Mixing and AFC processes</i>	225
<i>Reduction processes</i>	226
<i>Exchange of elements</i>	228
Concluding remarks	230
Acknowledgements	230
References	231
List of geological map sheets and sections	236
Appendix: Place names	238

Abstract

Pedersen, A.K., Larsen, L.M. & Pedersen, G.K. 2018: Lithostratigraphy, geology and geochemistry of the volcanic rocks of the Maligât Formation and associated intrusions on Disko and Nuussuaq, Paleocene of West Greenland.

Geological Survey of Denmark and Greenland Bulletin 40, 239 pp.

The Paleocene volcanic rocks in the Nuussuaq Basin on Disko and Nuussuaq comprise the picritic Vaigat Formation (*c.* 62–61 Ma) and the overlying basaltic Maligât Formation (*c.* 60 Ma). The Maligât Formation is up to 2000 m thick on western Disko where the top of the formation is least eroded. The formation is divided into four members, the Rinks Dal, Nordfjord, Niaqussat and Sapernuik members, which are formally defined here. On central and eastern Disko and Nuussuaq the Maligât Formation lavas are interbedded with fluvial and lacustrine sandstones and mudstones of the Atanikerluk Formation.

The Rinks Dal Member is the lowest member and originally constituted around 61% by volume of the formation. It is divided into 12 informal units based on chemically recognisable oscillations in the fractionation state of the basalts. The oldest units are present on central and south Disko close to the Disko Gneiss Ridge. The younger lavas spread farther to the east, north and west, filled the Assoq Lake basin east of the ridge and gradually overlapped the shield of the earlier Vaigat Formation that rose to the north. Only the lavas of the upper Rinks Dal Member reached far into Nuussuaq. The lavas are generally not crustally contaminated and comprise evolved basalts with 4.4–9.2 wt% MgO and a few picrites. The most evolved basalts with 3.2–4.8 wt% TiO₂ occur in the middle part of the member where they form the Akuarut unit.

The Nordfjord Member originally constituted around 6% by volume of the formation. It is not subdivided because the lithological variability is local. The member is widespread but has its depocentre on north-western Disko where thicknesses reach 350 m and eruption sites, intermediate lavas and acid tuffs are present. Over most of the area the member consists of just a few lava flows with combined thicknesses of 30–100 m. The member has a very diverse lithology with rock types ranging from silicic basalt with 5.3–10.0 wt% MgO through magnesian basaltic andesite and andesite with 2.4–10.6 wt% MgO to dacite with 1.2–2.2 wt% MgO. Rhyolite with 0.2–1.2 wt% MgO and up to 77 wt% SiO₂ occur in tuffs and conglomerate clasts. All rocks are crustally contaminated and some are native-iron-bearing.

The Niaqussat Member originally constituted around 33% by volume of the formation. It is subdivided into three informal units. The member is widespread, but much of it has been removed by erosion. Lithologies in the lower unit range from silicic picrite with up to 15 wt% MgO to basalt with 6–12 wt% MgO and a few basaltic andesite flows. The middle and upper parts of the Niaqussat Member comprise more evolved basalts with respectively 6.1–7.2 wt% MgO and 4.9–6.4 wt% MgO. All rocks are crustally contaminated and a few lava flows are native-iron-bearing.

The Sapernuik Member comprises three uncontaminated basalt flows with 7.5–10.7 wt% MgO. It is only preserved in a small area on western Disko.

Dyke systems with up to 80 km long dykes and subvolcanic intrusions associated with the Nordfjord and Niaqussat members occur on western and north-eastern Disko. The rocks are crustally contaminated and range from silicic basalt with 4–13 wt% MgO to magnesian andesite with 3–10 wt% MgO. They commonly form composite intrusions, some of which contain accumulations of native iron and sulfides.

The contaminants are carbon- and sulfur-bearing sediments of the Nuussuaq Group. Major contamination mechanisms were mixing with partial melts from the sediment sidewall and xenoliths and selective exchange of some elements, including carbon and sulfur, between magma and sediment. Degrees of contamination vary from 2–5% in the basalts to 10–50% in the more silicic rocks. No rocks more evolved than basalt were produced by ordinary fractional crystallisation.

A.K.P., *Natural History Museum of Denmark, University of Copenhagen, Øster Voldgade 5-7, DK-1350 Copenhagen K, Denmark, and Geological Survey of Denmark and Greenland, Øster Voldgade 10, DK-1350 Copenhagen K, Denmark.* E-mail: akp@snm.ku.dk

L.M.L., *Geological Survey of Denmark and Greenland, Øster Voldgade 10, DK-1350 Copenhagen K, Denmark.* E-mail: lml@geus.dk

G.K.P., *Geological Survey of Denmark and Greenland, Øster Voldgade 10, DK-1350 Copenhagen K, Denmark.* E-mail: gkp@geus.dk

Introduction

The Nuussuaq Basin is one of a series of linked basins that extend along the entire western continental margin of Greenland with a basin fill comprising Mesozoic to Tertiary sediments and Tertiary volcanic rocks (Chalmers & Pulvertaft 2001). The basins are partly situated in the offshore areas, but between 69° and 73°N the rocks of the Nuussuaq Basin are exposed on Disko, Nuussuaq, Ubekendt Ejland and Svartenhuk Halvø (Fig. 1). The Nuussuaq Basin contains a Cretaceous to Paleocene

sedimentary succession overlain by a Paleocene to Eocene volcanic succession. The rocks have been studied since the mid-1850s with an academic focus on the well-preserved fossils and the occurrence of native iron in the volcanic rocks. The economic interest has been focused on the coal beds and, in later years, on the presence of hydrocarbons. The lithostratigraphy of the sediments (the Nuussuaq Group) was defined and described by Dam *et*

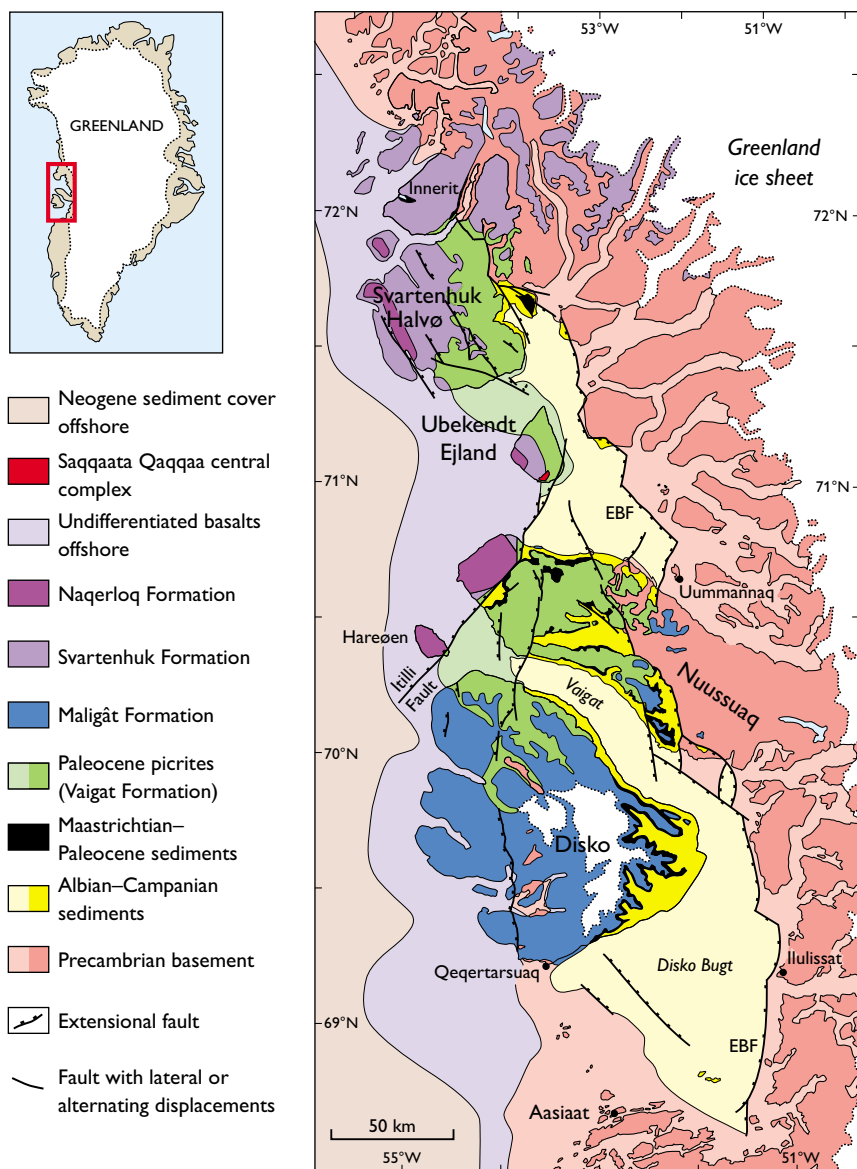


Fig. 1. Simplified map of the pre-Quaternary geology of the Nuussuaq Basin. Light colours denote sea-covered areas. **EBF**: Eastern boundary fault system.

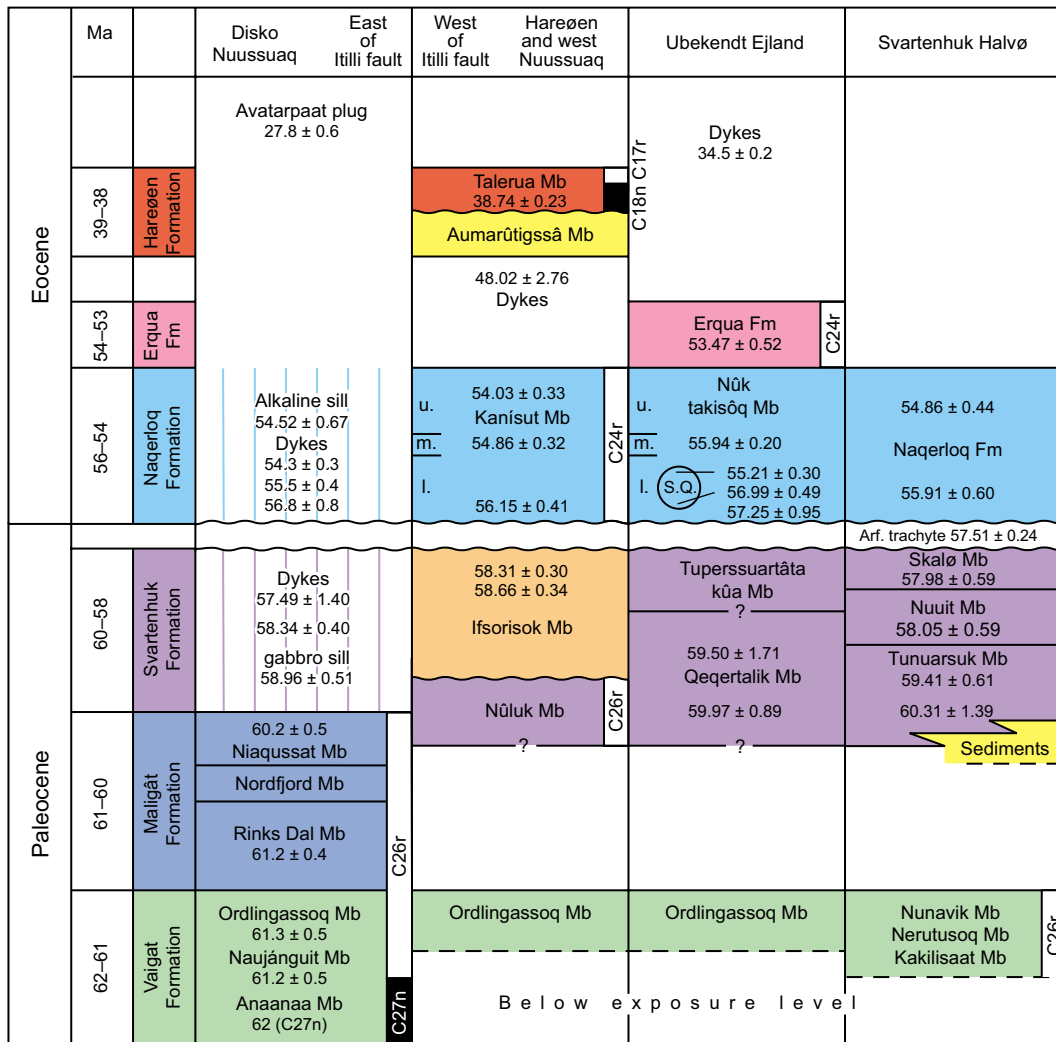


Fig. 2. Stratigraphic scheme for the volcanic rocks in the Nuussuaq Basin, based on Hald & Pedersen (1975) for Disko and Nuussuaq, Hald (1976) for Hareøen and western Nuussuaq, J.G. Larsen (1977) for Ubekendt Ejland, and J.G. Larsen & Grocott (1991) and J.G. Larsen & Pulvertaft (2000) for Svartenhuk Halvø. Radiometric ages (Ma) with one digit after the decimal point are from Storey *et al.* (1998) and Larsen *et al.* (2009); ages with two digits after the decimal point are from Larsen *et al.* (2016). The age for the Anaanaa Member is not radiometric but based on its normally magnetised character. Note that the vertical 'age scale' is not equidistant. **S.Q.**: Saqqaata Qaqqaa central complex. **l.**, **m.** and **u.** denote lower, middle and upper. **Arf.**: Arfetuarsuk trachyte. Sediments with a quartzo-feldspathic component are yellow; purely volcanoclastic sediments are brown. Wavy lines indicate unconformities. Palaeomagnetic directions with magnetochrons are indicated at the right side of some lithological units, from Riisager & Abrahamsen (1999), Riisager *et al.* (1999, 2003), Schmidt *et al.* (2005) and unpublished data by P. Riisager, 2006). Modified from Larsen *et al.* (2016).

al. (2009). The present work on the volcanic rocks may be considered a sequel to this work.

The volcanic rocks in the Nuussuaq Basin crop out over *c.* 20 000 km² within a basinal area of *c.* 120 km × 400 km (*c.* 50 000 km²); however, volcanic rocks extend over a total area of *c.* 200 km × 550 km (*c.* 110 000 km²), much of which is below sea level (Chalmers *et al.* 1999; Oakey & Chalmers 2012). The rocks in the Nuussuaq Basin were erupted at highly variable rates into a

tectonically very active environment, and there was a complex interplay between the volcanic, sedimentary and tectonic evolution of the basin, which resulted in a highly complex architecture of the volcanic succession. Moreover, the range of magma compositions was large. West Greenland contains an unusually high proportion of primitive, Mg-rich picritic rocks that represent almost unmodified mantle melts (Drever 1953, 1956; Clarke 1970; Clarke & Upton 1971; Clarke & Pedersen 1976;

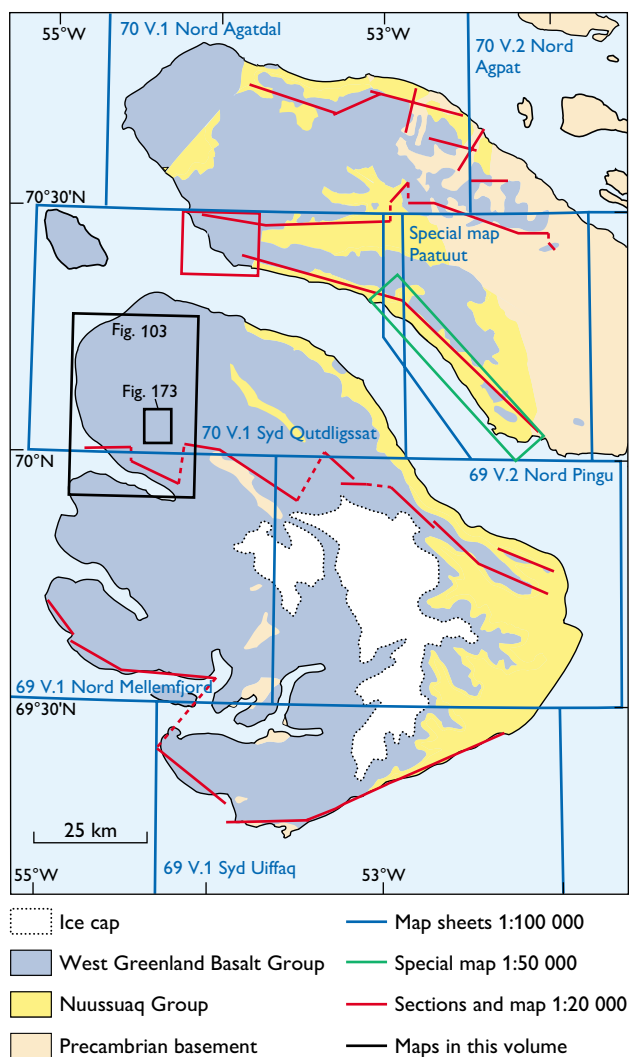


Fig. 3. Index map of published geological maps and photogrammetric sections covering Disko and Nuussuaq. Also shown are the local geological maps that appear as figures in this bulletin. A list of all published maps and sections is found at the end of the reference list.

Holm *et al.* 1993; Larsen & Pedersen 2000, 2009). However, repeated episodes of assimilation of crustal material, including organic-rich sediments, led to formation of units of silica-enriched rocks, including native-iron- and graphite-bearing basalts, andesites and dacites as well as graphite-bearing rhyolites (e.g. Törnebohm 1878; Steenstrup 1883; Pedersen 1977a, 1981, 1985; Pedersen & Larsen 2006; Larsen & Pedersen 2009).

The volcanic succession is divided into two major parts. The lower part is dominated by picrites and has been formalised as the Vaigat Formation, which is present from Disko and northwards to Svartenhuk Halvø (Hald & Pedersen 1975; Clarke & Pedersen 1976). The upper part is dominated by basalts and has previously been referred to different formations in different areas; based on ^{40}Ar - ^{39}Ar age determinations Larsen *et al.* (2016) concluded that the basalts on Disko and Nuussuaq east of the Itilli fault belong to the Maligât Formation which is not present in other areas (Figs 1, 2).

This bulletin on the Maligât Formation and its companion on the Vaigat Formation (Pedersen *et al.* 2017) describe the lithostratigraphy, geology and geochemistry of the volcanic succession on Disko and Nuussuaq east of the Itilli fault. They represent a synthesis of work that has been going on since 1968 and from which many results have been published. The two bulletins may be viewed as a comprehensive map description covering the Paleocene volcanic rocks in all the geological maps of the area, which is covered by seven geological maps on a scale of 1:100 000, two geological maps on scales of 1:50 000 and 1:20 000 covering different parts of Nuussuaq, and five vertical geological sections on a scale of 1:20 000 across Disko and Nuussuaq (Fig. 3). An important task for the two bulletins has been the definition and documentation of the several volcanic units that appear on the published maps and sections but have not been described before. The documentation includes geochemical data because chemostratigraphy is important in both formations and crucial for the Maligât Formation. Emphasis is placed on descriptions with pictures of the variable lithologies in selected key areas and on geochemical descriptions and plots of the stratigraphic units, facilitated by a numerical coding system, data tables and a comprehensive electronic appendix with analytical data. In short, the bulletins are intended to serve as guides for future field, geochemical and petrological studies.

The companion bulletin on the Vaigat Formation (Pedersen *et al.* 2017) contains detailed introductory chapters on previous investigations, geological setting and methods that also cover the Maligât Formation; however short chapters on the geological setting and methods are also included here because they are necessary for the independent use of the present bulletin. Petrogenetic considerations have been published by Larsen & Pedersen (2000, 2009) and Larsen *et al.* (2003), and the two bulle-

tins therefore only give short summaries of the petrology of the rocks. On the other hand, the present bulletin contains a final chapter on crustal contamination of the volcanic rocks, with descriptions of possible contaminants and discussion of contamination processes, that covers both the Vaigat and Maligât Formations.

Our late friend and colleague Finn Ulf-Møller studied the native-iron-bearing intrusions on western Disko

extensively, but at his death in 2009, much of his knowledge was left unpublished. In this bulletin, the chapter on dyke systems of the Nordfjord and Niaqussat members includes much information extracted from his PhD thesis, field notes, sketches, photographs and samples.

Geological setting

The Tertiary volcanic rocks in West Greenland form part of the North Atlantic Igneous Province. The volcanism was associated with the breakup of the North Atlantic Craton, as described by Noe-Nygaard (1974), Upton (1988), Saunders *et al.* (1997) and Pedersen *et al.* (2017). The *c.* 20 000 km² of exposed volcanic rocks in West Greenland make it the second largest exposed volcanic succession on the continental margins of the North Atlantic, surpassed only by the plateau basalts in central East Greenland.

The exposed rocks in the Nuussuaq Basin consist of Cretaceous to Palaeogene sediments and Palaeogene volcanic rocks. The three most important structural elements of the Nuussuaq Basin on Disko and Nuussuaq are the eastern boundary fault system (EBF), the Kuu-gannguaq–Qunnilik (K–Q) fault system and the Itilli fault system (Figs 1, 4). These fault systems divide the basin into a central–eastern part where the volcanic rocks are close to flat-lying and their substrate is well exposed, a western part where the substrate is rarely exposed and the volcanic succession is faulted and commonly tilted, and a westernmost part west of the Itilli fault system where, due to kilometre-scale downthrow to the north-west, a very different and mainly younger succession is preserved.

The eastern boundary fault system delimits the basin towards the elevated Precambrian basement in the east. The system consists of a number of fault segments with orientations from N–S to NW–SE. Within the basin, important faults run mainly N–S. The Disko Gneiss Ridge is a pre-basaltic fault block that is down-tilted towards the east, whereas to the west it is delimited by a N–S-running fault system that is an extension of the K–Q fault system. The surface of the gneiss ridge is shaped by prevolcanic erosion (Bonow 2005); the later lavas have lapped onto the hilly landscape of the ridge and eventually covered it. The ridge stands up to *c.* 700 m a.s.l. on central Disko, lowers to *c.* 300 m a.s.l. on southern Disko and extends southward, mainly below sea level, across Disko Bugt to the low-lying gneiss areas in the Aasiaat area. The ridge is not exposed at the north coast of Disko; this has been attributed to a NW–SE-trending fault on northern Disko (Chalmers *et al.* 1999).

The K–Q fault system runs S–N across both Disko and Nuussuaq, and pre-, syn- and postvolcanic movements have taken place along the faults. A clustering of volcanic eruption sites along the fault system demon-

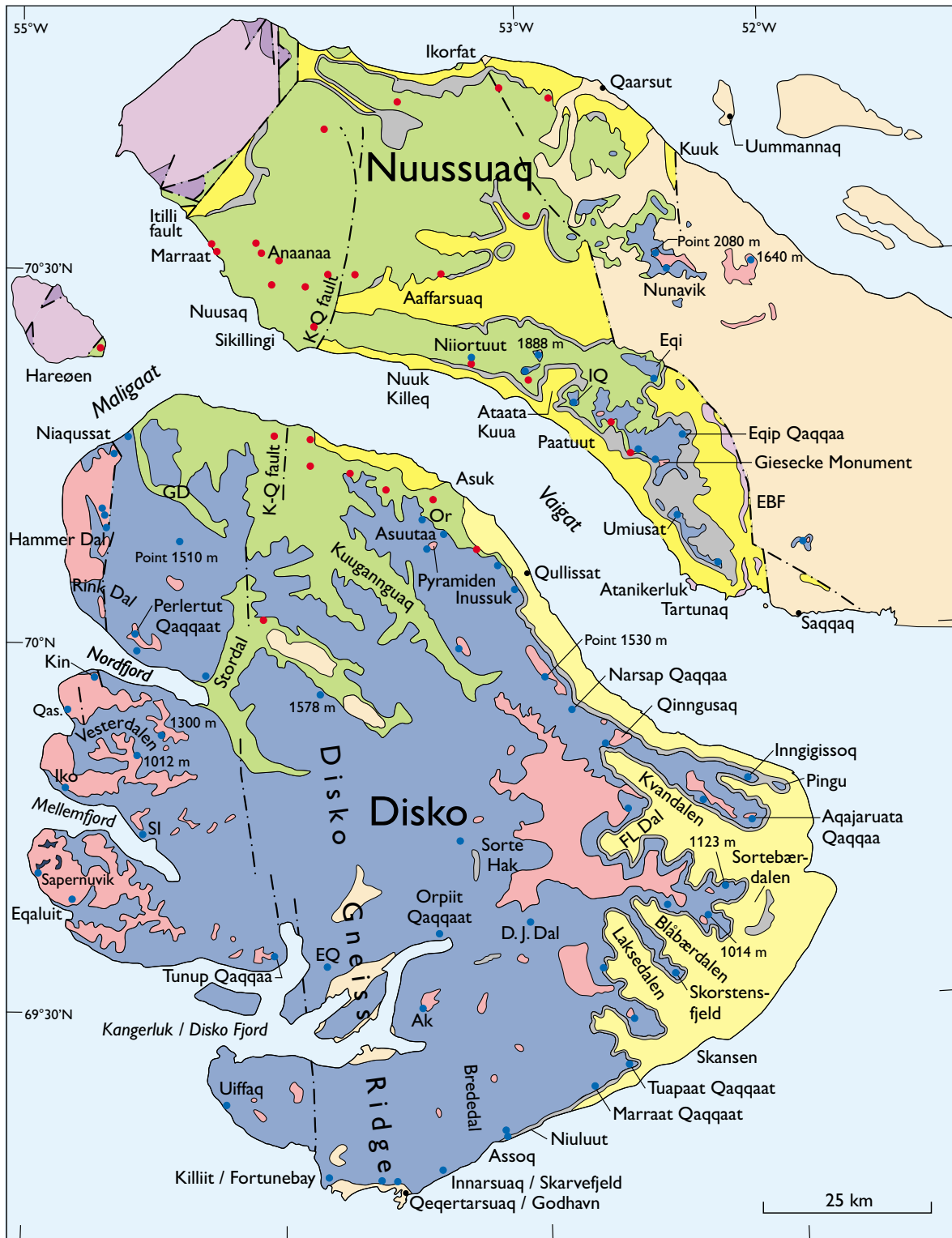
strates its deep-seated nature as a preferred pathway for magmas. West of the K–Q fault system no prevolcanic sediments are exposed on Disko, but sediment-contaminated volcanic rock units and sandstone and mudstone xenoliths in these attest to the presence of sediments at depth (e.g. Pedersen 1977a). Thick sedimentary successions are known from Nuussuaq west of the K–Q fault system (Dam *et al.* 2009).




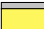



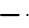


Western Disko, west of the K–Q fault system, is cut by several N–S-oriented post-Paleocene faults with steeply E-dipping fault planes. They divide the volcanic succession into a number of antithetic fault blocks in which the lavas dip 2–22° W, thus exposing the youngest parts of the succession in the westernmost blocks. The antithetic fault system does not continue offshore but rather has given rise to a monocline of limited width (Skaarup 2002; Skaarup & Pulvertaft 2007; Gregersen & Bidstrup 2008). According to refraction seismic data, Paleocene oceanic crust is situated 120 km west of Disko (Funck *et al.* 2012; Oakey & Chalmers 2012).

The Itilli fault system is a major structural boundary (Fig. 1; Chalmers & Pulvertaft 2001). Downthrow is to the NW, with net displacements of more than 1 km on Hareøen and Nuussuaq. As a result, the volcanic successions on the two sides of the Itilli fault system are fundamentally different (Fig. 2). Some relatively young (latest Paleocene to Eocene) volcanic formations occur west of the fault system but not east of it; these have not been included in this work.

Facing page:

Fig. 4. Simplified geological map of Disko and Nuussuaq with locations of the major profiles used for the mapping of the Maligât Formation (blue dots) and also shown in the stratigraphic panels of Figs 7–14. A few profiles are not shown. Profiles in the Vaigat Formation (red dots) are shown for completeness. Some localities are measured points with altitudes as given on the 1: 250 000 scale topographic maps. Abbreviated names: **Ak**: Akuliarusersuaq. **DJ Dal**: Daugaard-Jensen Dal. **EQ**: Eqalunnguaqqat Qaqqaat. **FL Dal**: Frederik Lange Dal. **GD**: Giesecke Dal. **Iko**: Ikorfarsuit. **IQ**: Ivissussat Qaqqaat. **Kin**: Kingittuusaq. **Or**: Orlingasoq. **Qas.**: Qasigissat. **SI**: Saqqarliit Ilorliit. **EBF**: Eastern boundary fault system. **K–Q fault**: Kuu-gannguaq–Qunnilik fault. Additional localities are shown in Fig. 6 and for north-west Disko in Fig. 103. Note that on this map glaciers are not shown; the extent of the Nordfjord Member on central eastern Disko, which is largely covered by the Sermersuaq ice cap, is interpolated between many small exposures at the margin of the ice cap.



- | | | | |
|---|-----------------------------|---|---|
|  | Eocene lavas and intrusions |  | Vaigat Formation |
|  | Nûluk Member |  | Cretaceous-Tertiary sediments |
|  | Sapernuivik Member |  | Precambrian basement |
|  | Nordfjord and Niaqussat mbs |  | Fault |
|  | Rinks Dal Member |  | Profile in the Vaigat (red) and Maligât (blue) formations |

The sedimentary substrate

The Nuussuaq Basin was a depositional area for clastic sediments for at least 40 Ma from the Albian to the Paleocene (Dam *et al.* 2009). Geophysical investigations have shown sediment thicknesses of at least 6 km and possibly up to 10 km in the western part of the basin (Christiansen *et al.* 1995; Chalmers *et al.* 1999); in the eastern part the sediments are only 1–2 km thick. Most of the exposed sediments were deposited in a large delta complex which fanned out from south-east of Disko towards the west and north-west; thus fluvial to deltaic environments predominate on Disko and southern Nuussuaq, while marine deep-water environments are found on north-western Nuussuaq and on Svartenhuk Halvø (G.K. Pedersen & Pulvertaft 1992). The Albian to Campanian non-marine and marginally marine sediments are referred to the Kome, Slibestensfjeldet, Upernivik Næs and Atane formations (Dam *et al.* 2009) and comprise yellowish quartzo-feldspathic sandstones interbedded with mudstones and coal layers (Midtgaard 1996; G.K. Pedersen *et al.* 2006). Dark marine mudstones of the Itilli and Kangilia formations are exposed on north-western Nuussuaq. On western Nuussuaq, the Itilli Formation is more than 2 km thick in the GRO#3 well. The Itilli Formation comprises Upper Cretaceous turbiditic sandstones and mudstones deposited on a submarine slope west of the Kuugannguaq–Qunnilik fault (Dam & Sønderholm 1994; Dam *et al.* 2009).

An early Campanian angular unconformity is observed on Central Nuussuaq (Dam *et al.* 2000) and interpreted as representing a regional event (Gregersen *et al.* 2013). During the Maastrichtian and early Paleocene, the basin was affected by faulting and changes in relative sea level. At least three phases of uplift during the Late Cretaceous and early Paleocene are interpreted from deeply incised submarine canyons with conglomerates, turbidites and mudstones, as well as an incised fluvial valley with pebbly sandstones as the dominant lithology (Dam & Sønderholm 1994, 1998; Dam 2002; Dam *et al.* 2009).

Deposition of the volcanic succession and equivalent sediments

At the onset of the volcanism, a marine embayment stretched from the open sea in the north-west (western Nuussuaq and beyond this) towards south and south-east where it was bounded by the Disko Gneiss Ridge in the west, an active delta depositing sediments in the south and south-east, and the gneiss highland in the east and north-east (Dam *et al.* 2009, fig. 12). Detailed studies of

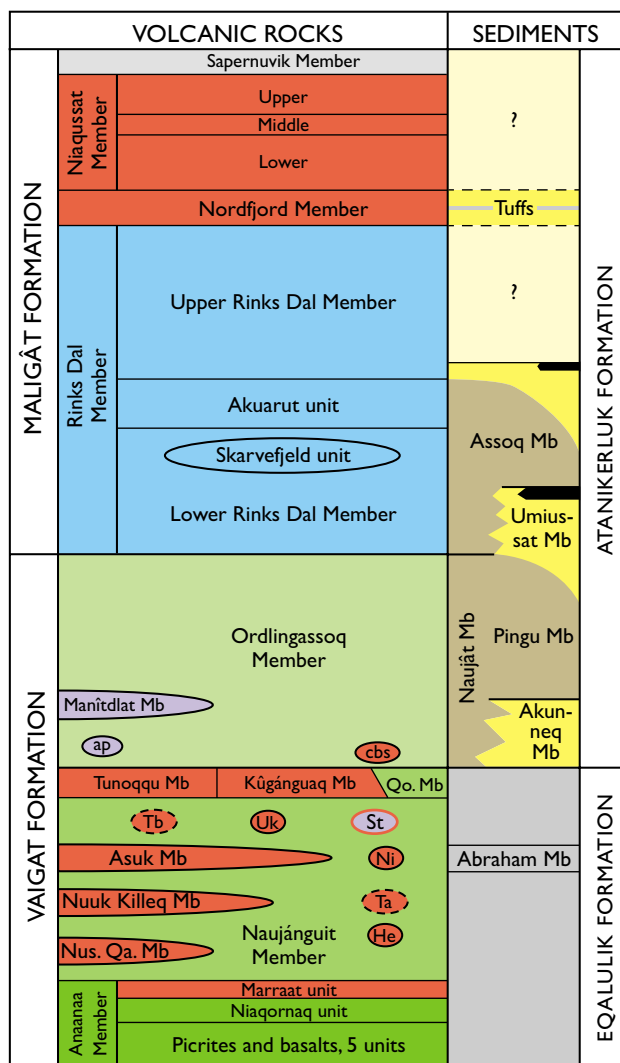


Fig. 5. Stratigraphic subdivision of the Paleocene volcanic rocks and sediments on Disko and Nuussuaq. The ‘thicknesses’ of the volcanic units in the diagram are intended to approximately reflect their volumes, although this is not always possible. The units with elliptical outlines do not extend laterally throughout the contemporaneous succession, and the small ones are distinctly local. Crustally contaminated units are shown in red, alkaline units in purple (with a red outline if crustally contaminated), and geochemically enriched units have dashed outlines. Abbreviations (in stratigraphic order): **Nus. Qa. Mb**: Nusap Qaqqarsua Member. **He**: Henderson unit. **Ta**: Tunorsuaq-a unit. **Ni**: Niiortuut unit. **Tb**: Tunorsuaq-b unit. **Uk**: Ukallit unit. **St**: Stordal alkaline unit. **Qo. Mb**: Qordlortorsuaq Member. **cbs**: contaminated basalts in Stordal. **ap**: alkali picrites associated with the Manitdlat Member. The lower and upper Rinks Dal Member are further subdivided into a number of chemostratigraphic units not shown here (but see Fig. 21). Sediment members from Dam *et al.* (2009): Marine mudstones are grey, non-marine mudstones are brownish-grey, sandstones are yellow and coal layers are black. The tuffs correlated with the Nordfjord Member were found in 2016.

volcanic facies transitions have documented very high subsidence rates in excess of 20 m/ka during the deposition of the early part of the Vaigat Formation (Pedersen *et al.* 2002b), making regional palaeogeographical reconstructions difficult. Deposition of the volcanic rocks began in the north-west and took place concomitantly with continued deposition of sediments in other parts of the basin, leading to a complex interplay between volcanic and sedimentary members. A lithostratigraphic scheme for both volcanic rocks and sediments is shown in Fig. 5. Lateral basin fill from west to east, shifting eruption sites with time and frequent facies changes between subaerial and subaqueous facies within most volcanic units resulted in an unusually complex stratigraphy of the volcanic succession, as described in Pedersen *et al.* (2017).

In the volcanic succession, the Vaigat Formation is dominated by primitive, olivine-rich picritic rocks, which in subaerial facies form thin, grey, crumbly lava flows. The overlying Maligât Formation is dominated by evolved, plagioclase-phyric to aphyric basalts which in subaerial facies form thicker, darker grey to brownish, massive lava flows. Both formations contain a number of lithologically and chemically distinct units; several of these form marker horizons and have been assigned member status (Fig. 5).

The Vaigat Formation forms a S–N elongate, 260 km long, shield-like feature in the Nuussuaq Basin. It is thickest, up to *c.* 5 km, on Ubekendt Ejland north of Nuussuaq (J.G. Larsen 1977). On central and western Nuussuaq it is up to 1.6 km thick, and on northern Disko up to 1.5 km; it wedges out eastwards on eastern Nuussuaq and eastwards and southwards on eastern and north-central Disko (Fig. 1). Its lower boundary towards the sediments is strongly diachronous and youngs towards the east because of progradation of the volcanic pile from west to east. It was deposited in three major episodes of activity, which gave rise to its three main members (Anaanaa, Naujánguit and Ordlingassoq). The marine embayment with mudstones of the Eقالulik Formation (Dam *et al.* 2009) was gradually filled from the west, and at the end of the second episode the advancing volcanic front reached the eastern gneiss highland on north-east Nuussuaq and blocked the connection to the sea; as a result the embayment was transformed into a freshwater lake, the Naajaat Lake (Piasecki *et al.* 1992; Pedersen *et al.* 1996), in which sediments of the non-marine Atanikerluk Formation were deposited (Koch 1959; Dam *et al.* 2009). This lake persisted through the third episode of the Vaigat Formation with deposition of mudstones of the Naujât and Pingu members, but it was greatly diminished

towards the end of the episode by the combined infill of volcanic rocks and sandstones of the Umiussat Member (G.K. Pedersen *et al.* 1998; Dam *et al.* 2009).

The Maligât Formation is centred on Disko, and its oldest exposed part is found on south-central Disko. It is thickest on western and central Disko where its base is generally below exposure level; on eastern Disko it rests on sediments, and in the north it onlaps the Vaigat Formation with increasingly younger lavas at the contact going north from Disko to Nuussuaq. Eastwards the Maligât Formation thins and interfingers with lake sediments of the Assoq Lake basin and the sand-dominated delta deposits from a large, north-west- to west-flowing river (Dam *et al.* 2009). As a result, the eastern fringes of the formation changed with time from subaqueous lava flows and hyaloclastites through invasive flows intruded like sills into the wet sediments, to subaerial lava flows, which finally covered much of the basinal area and stepped onto the gneiss highland on eastern Nuussuaq.

Both the Vaigat and Maligât formations are Paleocene (Danian–Selandian) in age. The oldest part of the Vaigat Formation is normally magnetised and was emplaced during geomagnetic chron C27n (Riisager & Abrahamson 1999), 62.5–62.2 Ma (Vandenberghé *et al.* 2012). The middle and upper parts of the Vaigat Formation, and all of the Maligât Formation, are reversely magnetised (Deutsch & Kristjansson 1974; Athavale & Sharma 1975; Riisager *et al.* 1999), fitting into the long-lived geomagnetic chron C26r. The top of the Maligât Formation has an ^{40}Ar – ^{39}Ar age of 60.2 ± 0.5 Ma (Storey *et al.* 1998).

In the northern part of the Nuussuaq Basin, the basalts are referred to the Svartenhuk, Naqerloq and Erqua formations (Fig. 2; J.G. Larsen 1977; J.G. Larsen & Grocott 1991; Larsen *et al.* 2016). These are younger than the Maligât Formation except for the lowest part of the Svartenhuk Formation, which may be coeval with it. The 60–58 Ma Svartenhuk Formation is present on Svartenhuk Halvø and north of it, on Ubekendt Ejland, and possibly also on Hareøen and on Nuussuaq west of the Itilli fault (Larsen *et al.* 2016; Figs 1, 2). It is overlain by the 56–54 Ma Eocene Naqerloq Formation in the same areas, followed by the 54–53 Ma Erqua Formation on Ubekendt Ejland. Dykes similar to the basalts of the Svartenhuk and Naqerloq formations are widespread on Disko and Nuussuaq (Larsen *et al.* 2016).

A map of Disko and Nuussuaq with detailed place names used in this bulletin is shown in Fig. 6.

Methods

Detailed descriptions of the methods for field work, photogrammetry and geochemistry are included in Pedersen *et al.* (2017) and are not repeated here. However, the following information is necessary for the independent use of this bulletin.

Geochemistry: For the Maligât Formation, 1440 samples were analysed for major elements and 400 for trace elements by X-ray fluorescence spectrometry (XRF); 150 samples were analysed for trace elements by Inductively coupled Plasma Mass Spectrometry (ICP-MS). For sills and dykes, 560 samples were analysed for major elements by XRF, 170 for trace elements by XRF, and 140 for trace elements by ICP-MS. To represent the range of possible contaminants for the magmas, 79 samples of mudstones and sandstones (partly as xenoliths in the igneous rocks) and Precambrian basement rocks were analysed for major elements by XRF, 33 for trace elements by XRF and 16 for trace elements by ICP-MS.

Stratigraphic subdivision and numerical coding system

The volcanic succession is subdivided into many lithological units both large and small. In order to handle both the units and the large number of samples of the various units, a four-digit sample coding system was established, shown in Table 1. The first digit signifies the formation (e.g. 5 for the Maligât Formation), and the second and third digits signify the unit (e.g. unit 20 in the Maligât Formation is the Nordfjord Member); thus all units in the succession have unique three-digit codes. The fourth digit signifies the lithological character of a sample (e.g. 4 for a xenolith). Thus, a sample coded 5204 is a xenolith from the Nordfjord Member of the Maligât Formation. In the descriptions and figures in this bulletin, individual units are frequently denoted by their identifying three-digit codes, e.g. unit 520 is the Nordfjord Member. Other units are also included in the numerical coding system; intrusion codes have first digit 6 (Table 1). The codes covering the Vaigat Formation have first digit 4 (Pedersen *et al.* 2017, table 1).

The numerical coding system was not used in the published geological maps and sections because it was completed after the publication of most of these. The unit codes have been added on many of the excerpts of maps and sections shown in this bulletin.

Nomenclature

The rules of the International Stratigraphic Guide (Murphy & Salvador 1999) state that the spelling of a name of an established stratigraphic unit must not be changed even if the spelling of the place name has changed. Therefore, the old spellings of the Maligât Formation and the Rinks Dal Member are maintained although the place names are now spelled Maligaat and Rink Dal.

The igneous rocks are named in accordance with the conventional chemical classification of Le Maitre (2002), based on the total-alkali – silica (TAS) diagram. Picrites have $\text{MgO} \geq 12$ wt%. We use ‘magnesian basalts’ for basalts with 10–12 wt% MgO which are usually visibly olivine-phyric. We use ‘silicic basalts’ for basalts which are crustally contaminated but have $\text{SiO}_2 < 52$ wt% (the boundary to basaltic andesites), because uncontaminated basalts in the Nuussuaq Basin rarely contain more than 50 wt% SiO_2 . It should be noted that the silicic rocks in West Greenland are quite distinct from orogenic rocks with the same TAS names. The basaltic andesites and andesites in West Greenland have much higher contents of MgO, Ni, and Cr than their orogenic namesakes, and ‘magnesian basaltic andesite’ and ‘magnesian andesite’ are appropriate but cumbersome names.

The lithological terms ‘hyaloclastite’ and ‘pillow breccia’ are frequently used synonymously. Following White & Houghton (2006), we use hyaloclastite as a general term to denote primary clastic subaqueous volcanic deposits. However, we sometimes use pillow breccia for coarse, clast-rich deposits even though these may include finer-grained, clast-poor parts. The term ‘volcaniclastic’ is used as a nongenetic term to denote any clastic deposit with a large component of volcanic material and includes both primary volcanic and nonvolcanic deposits such as mass-flows and other redeposited sediments.

Geological sections and profiles

In this bulletin, we frequently refer to the five published, photogrammetrically interpreted, long geological sections across the Nuussuaq Basin (Pedersen *et al.* 2006b). To facilitate reading, they will usually be referred to in short form as follows:

“North Nuussuaq section” is Pedersen *et al.* (2006a).

“Central Nuussuaq section” is Pedersen *et al.* (2002a).

“South Nuussuaq section” is Pedersen *et al.* (1993).

Table 1. Numerical codes for units and samples of the Maligât Formation and equivalent intrusions

Digit 1: Major division	Digits 2–3: Member or unit	Digit 4: Sample lithology
6 Intrusives	29 Dykes in Giesecke Dal and inner Hammer Dal	<i>Intrusives:</i> 9 Other 4 Xenolith 3 Plug or feeder dyke 2 Sill 1 Dyke
	28 Contaminated dykes, unspecified	
	27 Nordfjord complex	
	26 Hammer Dal complex	
	18 Weakly contaminated dykes, eastern Disko and Nuussuaq	
	17 Killiit dyke	
5 Maligât Fm	16 Hanekammen complex	<i>Maligât Fm:</i> 9 Other, incl. zeolites 8 Invasive lava or sill 7 Pebbles 6 Tuff 5 Sediment 4 Xenolith 3 Hyaloclastite matrix 2 Pillow 1 Lava flow
	99 Other	
	40 Sapernuvik Member	
	32 Upper Niaqussat Member	
	31 Middle Niaqussat Member	
	30 Lower Niaqussat Member	
	20 Nordfjord Member	
	18 Upper Rinks Dal Member, top flows	
	17 Upper Rinks Dal Member, upper main part	
	16 Upper Rinks Dal Member, low-Ti flows	
	15 Upper Rinks Dal Member, lower main part	
	14 Upper Rinks Dal Member, upper transition flows	
	13 Middle Rinks Dal Member, Akuarut unit	
	12 Lower Rinks Dal Member, lower transition flows	
	11 Lower Rinks Dal Member, Skarvefjeld unit	
	09 Lower Rinks Dal Member between low-Ti flows and Skarvefjeld unit	
	07 Lower Rinks Dal Member, low-Ti flows	
	06 Lower Rinks Dal Member between lowest flows and low-Ti flows	
	05 Lower Rinks Dal Member, lowest flows	
	01 Rinks Dal Member, unspecified	

For definition of the divisions based on TiO₂ contents, see Table 2 and Fig. 21.

“Central Disko section” is Pedersen *et al.* (2005).

”South Disko section” is Pedersen *et al.* (2003).

All these sections possess a horizontal distance scale along the base (an ‘x axis’) with origin at the westernmost (left) end of the 82–131 km long sections. The scales are preserved in the excerpts shown here, and an expression such as “at 9–10 km” refers to the distance scale.

‘Profiles’ are visited, measured and sampled local sections, usually on mountain sides, and are presented in diagrams as vertical columns. The profiles constitute the basis for the definitions and correlations of the volcanic succession. The lithostratigraphic type and reference sections are illustrated by their corresponding profiles.

West Greenland Basalt Group

The Tertiary volcanic rocks in West Greenland are all included in the West Greenland Basalt Group defined by Hald & Pedersen (1975). The present work does not involve any revision of the original definition of the Group as such. The volcanic succession on Disko and Nuussuaq (with Hareøen) east of the Itilli fault (Figs 1, 2, 4) comprises the Vaigat Formation and the revised Maligât Formation and is all of Paleocene age.

Summary of the petrology of the Vaigat and Maligât formations

The petrology of the Vaigat and Maligât formations was presented by Larsen & Pedersen (2009), and their conclusions are summarised below.

The primary magmas for both formations were highly magnesian, picritic, with at least 16.6 wt% MgO. Melting in the asthenosphere took place in garnet facies because the melting column was curtailed by the 100 km thick lithosphere. The Vaigat Formation magmas fractionated olivine in the feeder channels before eruption but generally did not stop in magma chambers. Only minor magma batches stopped in high-level magma chambers where many of them became crustally contaminated. At the time of transition to the Maligât Formation large, long-lived magma chambers developed, presumably in the lower crust. The Maligât Formation basalts have compositions buffered by magma chamber processes; large-scale cyclicity can be seen, with more and less fractionated steady-state compositions (see Fig. 21). Repeated pulses of new picritic magmas can be identified in both formations.

The Sr, Nd and Pb isotope data show that the asthenospheric mantle source was heterogeneous and the dominant component was depleted, MORB-like mantle with Nb/La <1. An additional, less-depleted mantle component akin to the Iceland mantle source is evident in the upper Vaigat Formation (Ordlingassoq Member) but disappeared again at the transition to the Maligât Formation. An incompatible-element-rich lithospheric mantle component is seen in the alkaline Manîtdlat Member of the Vaigat Formation. Single scattered tholeiitic lavas somewhat enriched in the same trace elements occur in both formations and are considered to be slightly contaminated with this component. The volume of these rocks is diminutive.

In the Vaigat Formation, crustal contamination was episodic within the short-lived, high-level magma chambers in the sedimentary succession. In the Maligât Formation, the earliest part, the Rinks Dal Member, is uncontaminated. In the subsequent Nordfjord and Niaquusat members, weak contamination was continuous in the deep, long-lived magma chambers, possibly because these had moved upwards in the crust, whereas additional episodes of strong contamination took place in local high-level, subvolcanic magma chambers. The predominant contaminants were the sediments in the Nuussuaq Basin. When carbon-rich mudstones were assimilated, severe reduction led to formation of graphite or native iron. All rocks more evolved than basalt arose by contamination processes, which will be discussed in more detail in the final chapter of this bulletin.

Maligât Formation

Revision of the Maligât Formation

The Maligât Formation was defined by Hald & Pedersen (1975) with distribution not specified but mentioned on Disko, Hareøen, Nuussuaq, Ubekendt Ejland, Svartenhuk Halvø and north of this. The type section was defined along the north and west coasts of Nuussuaq "because of the greater thickness of the formation there as compared with Disko". For the Svartenhuk Halvø area, the lava succession thought to be laterally correlative with the Maligât Formation was later termed the Svartenhuk Formation by J.G. Larsen & Grocott (1991) and J.G. Larsen & Pulvertaft (2000). Subdivisions of the Maligât Formation have been made for separate areas: for Disko by Pedersen (1975a), for western Nuussuaq and Hareøen by Hald (1977) and for Ubekendt Ejland by J.G. Larsen (1977). The Svartenhuk Formation was subdivided by J.G. Larsen & Grocott (1991).

Radiometric age dating of the volcanic succession in the Nuussuaq Basin by the ^{40}Ar – ^{39}Ar method has revealed the presence of three age groups in the Maligât Formation as originally defined (Fig. 2). Throughout Disko and Nuussuaq east of the Itilli fault, the Maligât Formation is of Paleocene age, 61.2–60.3 Ma (Storey *et al.* 1998, ages recalculated to an age of 28.201 Ma for the FCT-3 standard, following the Geologic Time Scale 2012). On Ubekendt Ejland and Svartenhuk Halvø, the basalts referred to the Svartenhuk Formation are of latest Paleocene age, 60.3–58.0 Ma, i.e. younger than the Maligât Formation on Disko and Nuussuaq (Larsen *et al.* 2016). On Nuussuaq west of the Itilli fault, Hareøen, western Ubekendt Ejland and western Svartenhuk Halvø, an Eocene basalt succession is present, dated to 56.2–54.0 Ma and recently referred to the Naqerloq Formation (Larsen *et al.* 2016). This includes the Kanisut Member of the original Maligât Formation, which is present on western Nuussuaq and on Hareøen (Hald 1976, 1977) where it overlies sediments with a large volcanoclastic component, suggestive of a break in the volcanic activity.

In view of the age differences, we here revise the Maligât Formation to exclude the Eocene part of the succession on Hareøen and Nuussuaq. As the old type section on western Nuussuaq was centred on the Eocene lavas, a new composite type section has been defined on central and north-west Disko.

Lithostratigraphy of the Maligât Formation

Revised formation

History. Originally defined by Hald & Pedersen (1975) to cover Disko, Hareøen, Nuussuaq, Ubekendt Ejland and Svartenhuk Halvø. The present revision restricts its known extent to Disko and Nuussuaq east of the Itilli fault.

Name. After Maligaat (old spelling Maligât), the strait between Disko and Hareøen (Fig. 4).

Distribution. The Maligât Formation extends over the whole of Disko and parts of southern and eastern Nuussuaq (Fig. 4). The depocentre was situated on south-central Disko from where the successive volcanic units spread gradually towards west, east and north. The Rinks Dal Member did not extend north of Nuussuaq, and this is most probably also the case for the younger members. The eastern and northern limits are relatively well defined, whereas the southern and western limits are unknown. The formation is assumed to be present on the shelf west and south-west of Disko.

Type section. The type section is composite. For the Rinks Dal Member: the south side of the mountain **Orpiit Qaqqaat** at 0–1080 m, central Disko (Fig. 8, profile 4; Fig. 24); the uppermost flows in the member are missing. For the Nordfjord Member and the lower and middle Niaqussat Member: **Point 440 m, northern gully**, north-west Disko (Fig. 14, profile 11; also Fig. 104). For the upper Niaqussat and Sapernuvik members: **Sapernuvik** on central west Disko (Fig. 14, profile 1; also Fig. 161).

Reference section. The uppermost flows of the Rinks Dal Member and the boundary to the Nordfjord Member are covered by a short profile on the eastern side of the mountain **Akuliarusersuaq** at 990–1045 m, 13 km south of the type section (Fig. 8, profile 3).

Thickness. The thickness varies from around 2000 m on western Disko where the top of the formation is least eroded and the base is below exposure level, through present (eroded) thicknesses of 500–1000 m over large parts of Disko and southern Nuussuaq, to 200–300 m in the

easternmost parts of Disko and Nuussuaq where the formation peters out towards the east and north.

Lithology. The main lithology of the Maligât Formation is plagioclase-phyric to aphyric tholeiitic basalts that typically form 10–40 m thick lava flows of considerable lateral extent. The major part of the Rinks Dal Member is made up of such flows, which form subaerial lava flows and also subaqueous and invasive flows and hyaloclastites. The rocks of the overlying Nordfjord and Niaquusat members are more variable and comprise slightly contaminated basalts and picrites and strongly contaminated basaltic andesites, andesites, dacites and rhyolites. These rocks form subaerial lava flows, high-level intrusions and craters, rhyolitic tuff layers and tuffaceous sediments and conglomerates. Some of the more contaminated rocks are highly reduced and carry native iron.

Subdivisions. The Maligât Formation is subdivided into four members based on lithologies and chemical compositions. These are the Rinks Dal Member of normal tholeiitic basalts, the Nordfjord and Niaquusat members of weakly to strongly crustally contaminated rocks, and the small Sapernuik Member of uncontaminated tholeiitic basalts. The thick Rinks Dal Member is further informally subdivided into 12 chemostratigraphic units.

Boundaries. The lower boundary is below exposure level on western Disko. Where exposed, the lower boundary is unconformable and the Maligât Formation rests on the Disko Gneiss Ridge on central and south Disko, on the lavas of the Vaigat Formation on northern Disko and south and central Nuussuaq, on contemporaneous fluvial and lacustrine sediments on eastern Disko and south-eastern Nuussuaq, and on the gneiss highland on eastern Nuussuaq.

The upper boundary is erosional. The youngest known flows are preserved at Sapernuik on western Disko and on the high ground above 2000 m altitude on eastern Nuussuaq.

Age. Paleocene, 61–60 Ma, magnetochron C26r, based on radiometric dating (Storey *et al.* 1998; Larsen *et al.* 2016).

Correlation. See Fig. 2. No correlation across the Itilli fault to Hareøen and westernmost Nuussuaq has been established. In particular, the relationship to the Nûluk Member on Hareøen and westernmost Nuussuaq (Hald 1976) is uncertain. On Ubekendt Ejland, the Maligât

Formation may be time-equivalent to the lower part of the 3000–3500 m thick Qeqertalik Member. On Svartenhuk Halvø, the Maligât Formation is possibly time-equivalent to the sediments of the lowest member of the Svartenhuk Formation (Larsen *et al.* 2016).

General features of the Maligât Formation

Subdivision

On north-western Disko, Pedersen (1975a) subdivided the Maligât Formation into the Rinks Dal, Nordfjord and Niaquusat members. This subdivision has been used in many subsequent works on the Maligât Formation, e.g. Pedersen (1977a, b); Pedersen & Larsen (1987); Larsen & Pedersen (1988, 1989, 1990, 1992); Pedersen *et al.* (1993, 2000, 2001, 2002a, 2003, 2005). In Larsen & Pedersen (2009) and in the present work we distinguish a fourth member, the small but distinct Sapernuik Member at the top of the formation. We also extend the three main members throughout Disko and Nuussuaq and subdivide them into a number of informal units. At the same time, we revise the boundary between the Nordfjord and Niaquusat members.

The lithological and compositional variation pattern of the Maligât Formation is different from that of the underlying Vaigat Formation, and consequently it is not subdivided in a similar way. In particular, the crustally contaminated and uncontaminated rocks do not form interspersed units, as seen in the Vaigat Formation, but the crustally contaminated rocks follow above the uncontaminated rocks. Because of the lithological uniformity of large parts of the succession, in particular the Rinks Dal Member, much of the subdivision is based entirely on geochemical differences. This has required analysis of many flow-by-flow sampled profiles and several samples outside profiles. As the geochemical variations are commonly gradational, the assignment of a flow to a specific unit is subjective in some boundary cases, and most units cannot be mapped in the field. For this reason, most of the units of the three main members of the Maligât Formation are maintained as informal units. On the other hand, several of the units are of large lateral extent because the major part of the formation is in subaerial lava facies. This is in contrast to the strong lateral variation and progradation of the hyaloclastites and subaerial lava flows of the successive units in the Vaigat Formation (Pedersen *et al.* 2017).

The complete subdivision of the Maligât Formation used in this bulletin is shown in Table 1. This table shows the 4-digit sample coding system used in order to handle the large number of samples of the various lithological units (see chapter on methods above). All geochemical analyses of the rocks of the Maligât Formation, their xenoliths, associated dykes and sediments representing possible contaminants are available in a supplementary data file at www.geus.dk/bulletin40.

Distribution of units. The location of the major profiles that form the basis for the mapping of the Maligât Formation is shown in Figs 4 and 6. Stratigraphic panels with the subdivided profiles are shown in Figs 7–14 which cover 1130 out of 1450 analysed samples. Several short profiles, particularly on western Disko, are not shown.

Successive stages in the deposition of the Maligât Formation are shown in Fig. 15. The oldest known parts are found on southern Disko on and near the Disko Gneiss Ridge. From here, the successive volcanic units spread northwards, overlapping the low picrite shield of the Vaigat Formation, and eastwards, filling in the Assoq Lake (see below). The middle part of the Rinks Dal Member (the Akuarut unit) reached southern Nuussuaq, and the upper part of the Rinks Dal Member extended to north-eastern Nuussuaq and transgressed the eastern boundary fault there. In the easternmost lava exposures on northern Nuussuaq, lavas of the Niaqussat Member rest directly on the gneiss or are invasive into sediments of the Atanikerluk Formation.

Lithological variations and the filling of the Assoq Lake

In order to provide a framework for understanding the lithological variations described in the following, particularly in the Rinks Dal Member, the history of the Assoq Lake is summarised here.

The existence of a large lake on central and eastern Disko and southern Nuussuaq is indicated by the wide extent of a succession of non-marine mudstones coarsening upwards into sandstones; these sediments form the Assoq and Umiussat members of the Atanikerluk Formation (Larsen *et al.* 2006; Dam *et al.* 2009, fig. 131). The history of filling of the lake by contemporaneous volcanic rocks and sediments is revealed by the distribution of lavas in subaerial, subaqueous, water-influenced and invasive facies and their relations to the sediments. The various volcanic facies and their diagnostic characters are as follows.

Subaerial lava flows have massive central parts and vesicular, slaggy or ropy top zones that commonly, but not always, are red-oxidised. In places, there are brick-red laterite horizons between flows.

Flows emplaced over wet surfaces or into shallow water have regularly columnar-jointed zones (colonnades) at the base and commonly zones with small, irregular, blocky columns (entablatures) in the centre. The vesicular top zones may be red-oxidised.

Flows emplaced into deeper water at high rates have colonnades and entablatures and thick to very thick, glass-rich, brecciated top zones; if the water depth was larger than the thickness of the flows the tops are yellowish brown and there is no red-oxidation.

Flows emplaced into deeper water at low rates are brecciated throughout and form hyaloclastite deposits, which are commonly foreset-bedded; if these are capped by subaerial flows from the same eruption the height of the foresets is a reliable measure of the water depth. Examples of these four types of flows are seen in the coastal cliff beneath Skarvefjeld (see Fig. 56).

Invasive lava flows are subaerial flows that have met unconsolidated sediment during their course and continued their flowage as sheets intruding laterally into the sediment, in places for distances of several kilometres. Such flows have the appearance of sills in the sediment but are stratigraphically in place in the volcanic succession (Figs 7–11) and can in some cases be followed laterally into normal subaerial facies. Invasive flows are usually water-influenced with colonnades and entablatures, in places double colonnades (see e.g. Fig. 42); their tops are chilled against the overlying sediment and have commonly developed small lobes intrusive into the sediment (see Fig. 76). The overlying sediment may be only a few metres thick, in which case the lava flow may have extruded up through the sediment to produce rootless craters, as at Marraat Qaqqaat (see Fig. 70). The flows may invade either mud or sand horizons; mud horizons seem to be more prone to invasion than sand horizons.

Invasive lava flows were first described from the Columbia River basalts by Schmincke (1967) and later by e.g. Byerly & Swanson (1978) and Ross (1989).

The Assoq Lake, or possibly system of lakes, presumably had its largest extent at the onset of extrusion of the Maligât Formation (Fig. 16); it was bounded to the west by the Disko Gneiss Ridge, and to the north it covered the edge of the lava shield of the Vaigat Formation, whereas its eastern boundary was most probably towards a low plain formed by siliciclastic sediments sourced from the east and south. Its southern boundary is unconstrained

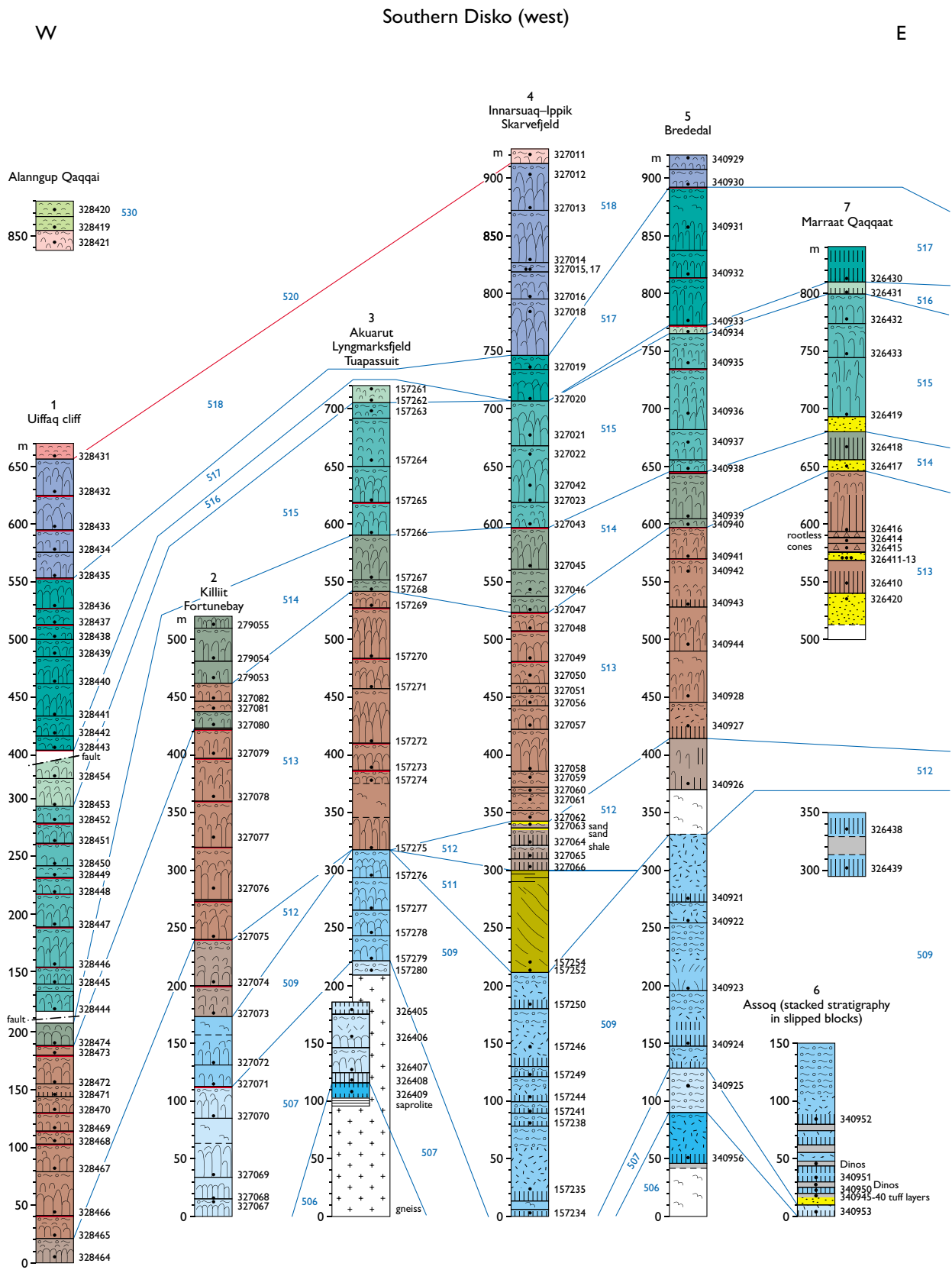
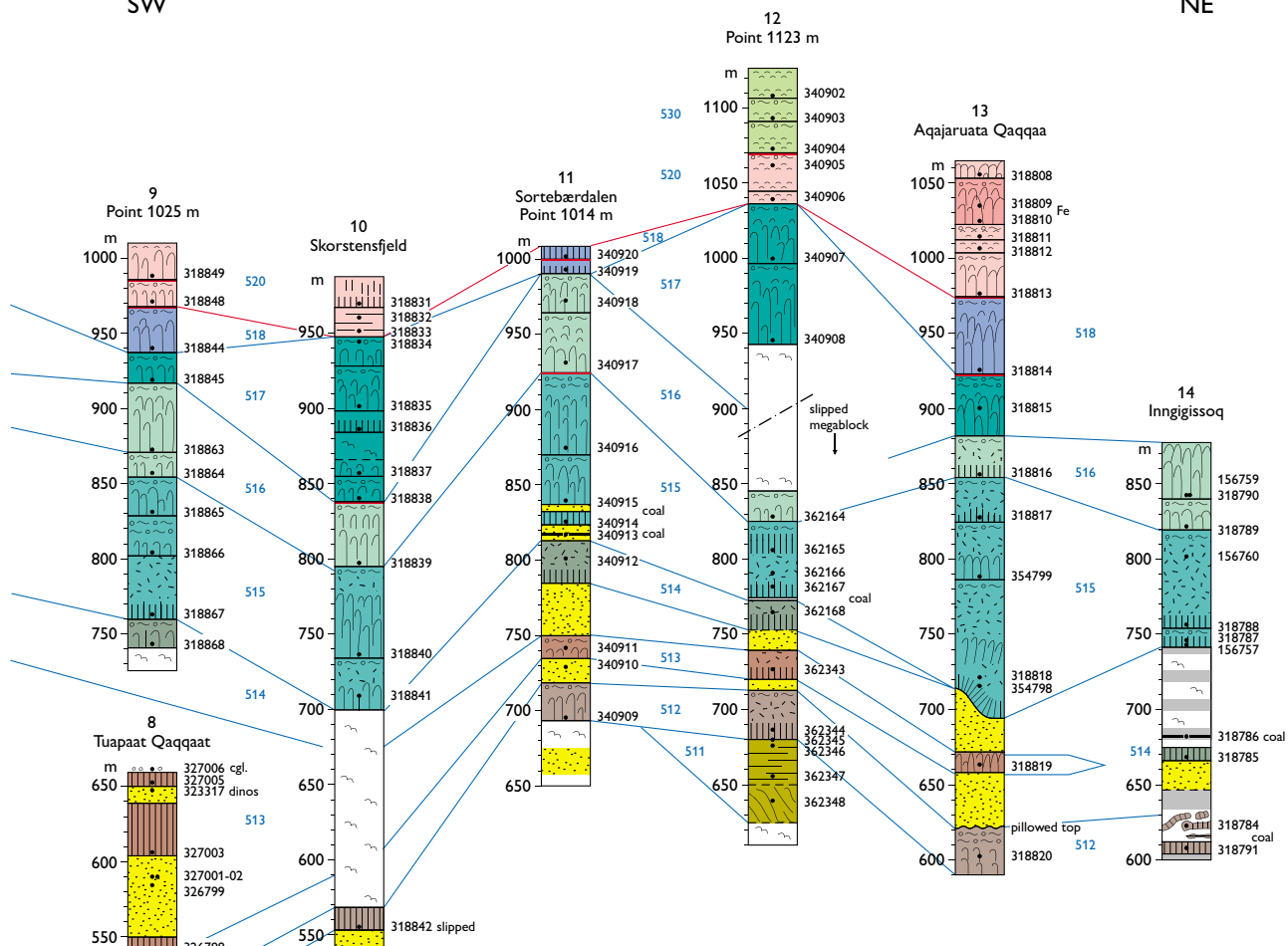


Fig. 7 (two pages). Profiles through the Maligat Formation on southern and eastern Disko. The legend applies to all profiles in the Maligat Formation in subsequent figures.

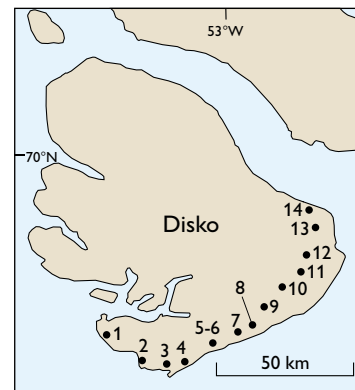
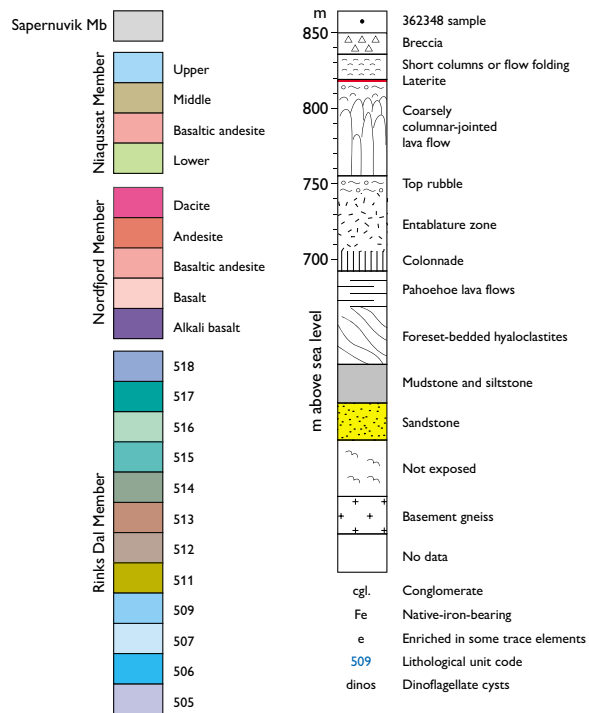
Southern Disko (east)

SW

NE



Legend for all Maligât Formation profiles



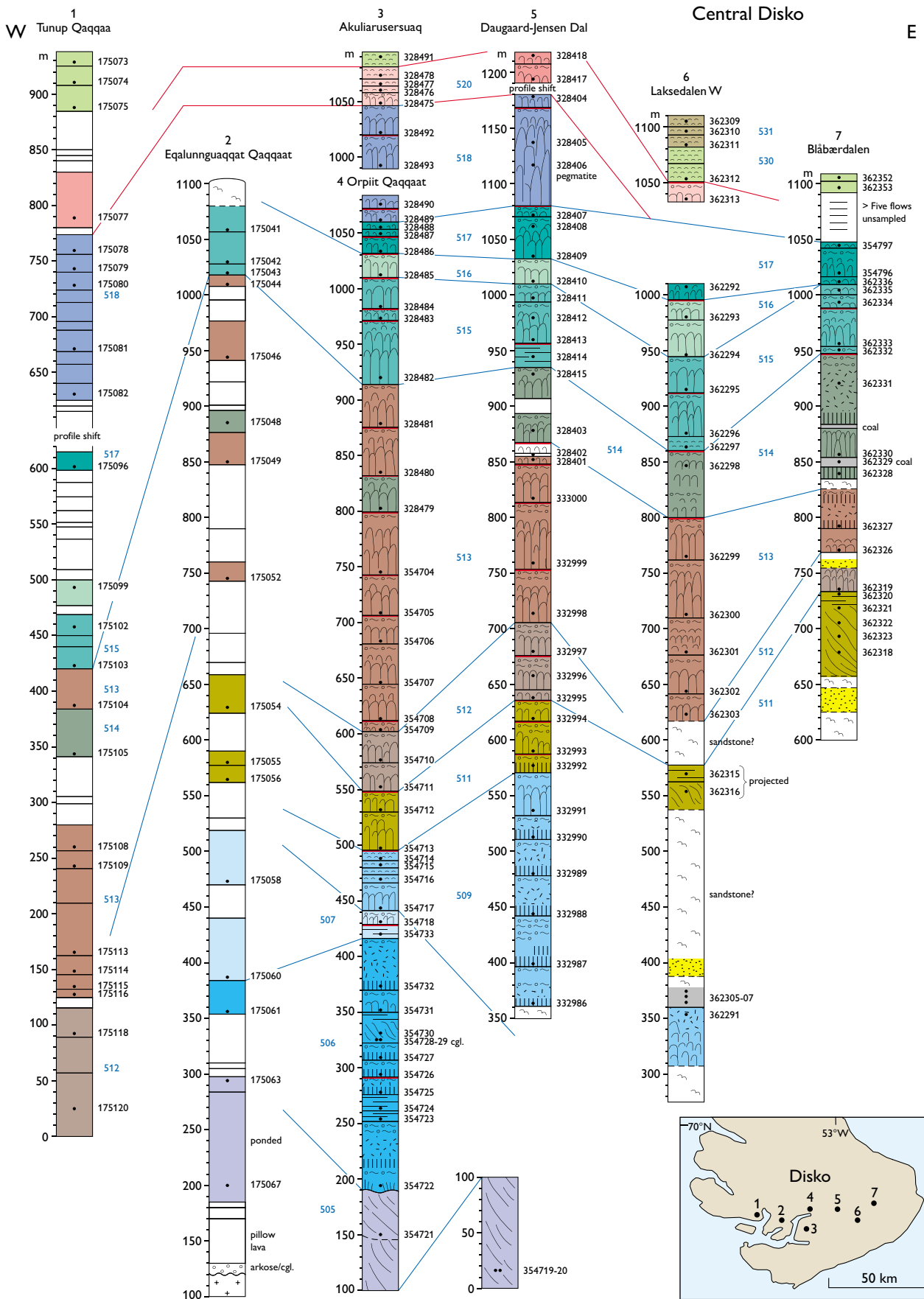


Fig. 8. Profiles through the Maligât Formation in a W-E panel across south-central Disko. The Orpiit Qaqqaat profile (no. 4) represents the type section for the Rinks Dal Member. For legend, see Fig. 7.

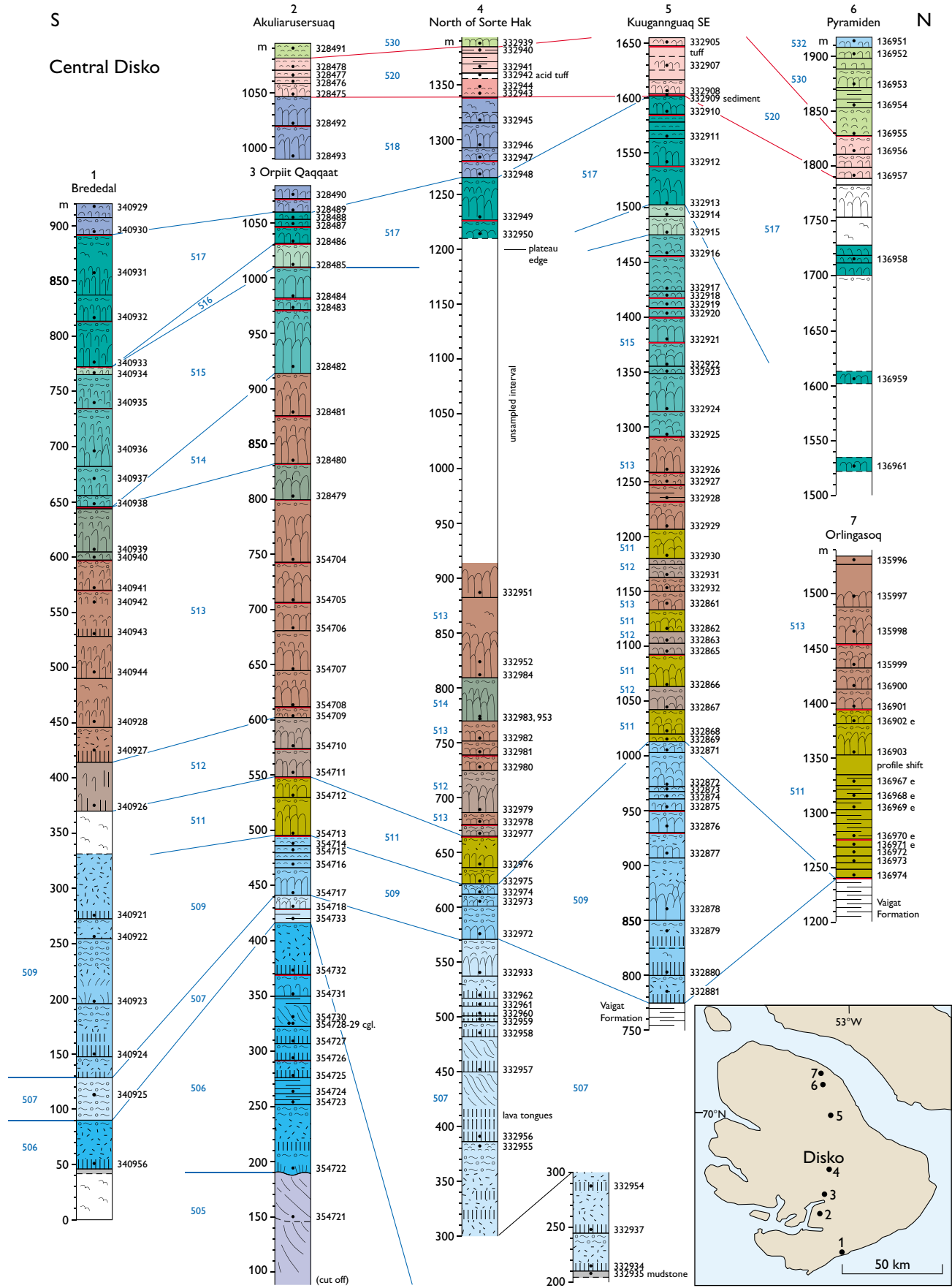


Fig. 9. Profiles through the Maligât Formation in a S–N panel across Disko. For legend, see Fig. 7.

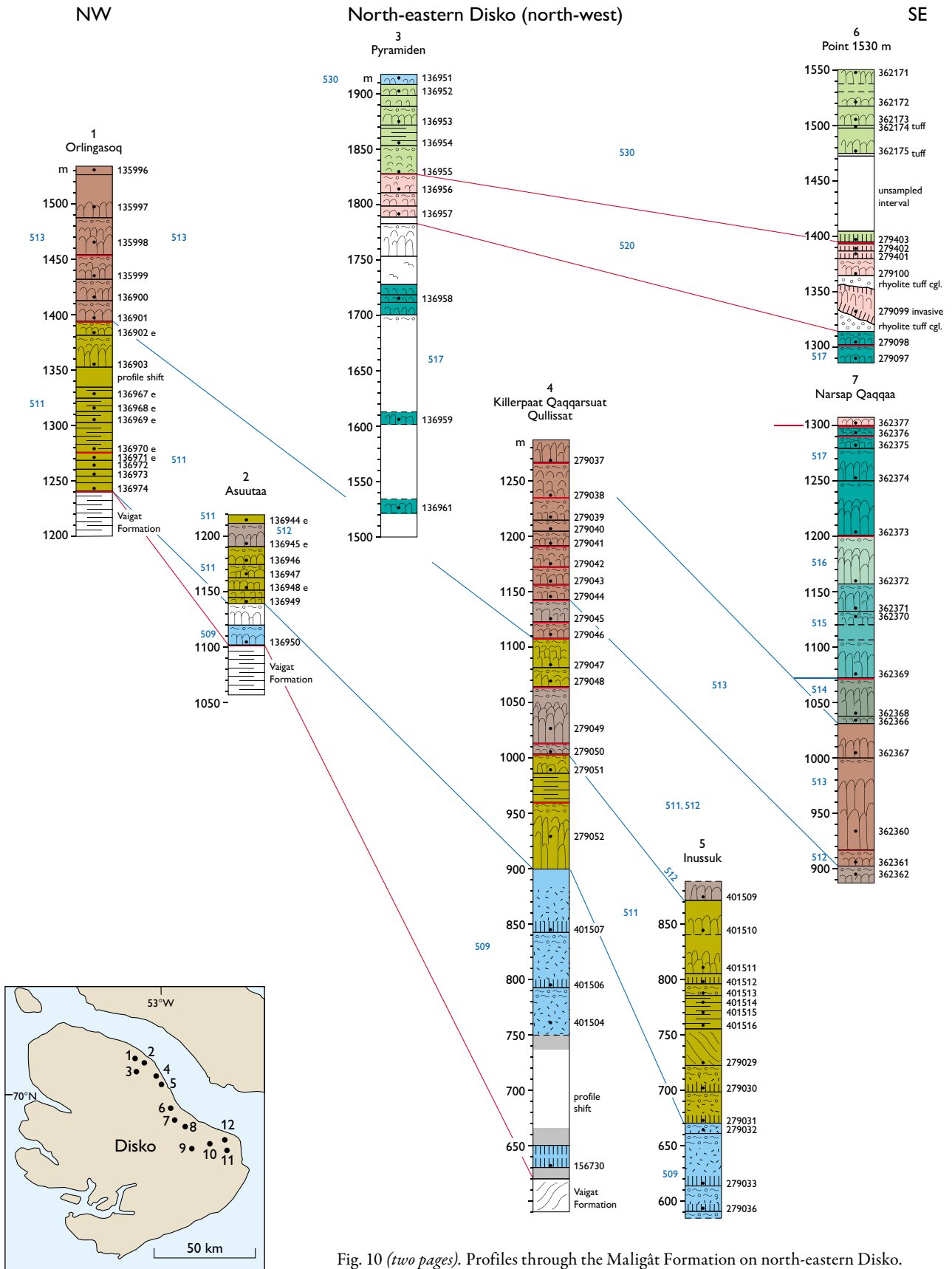
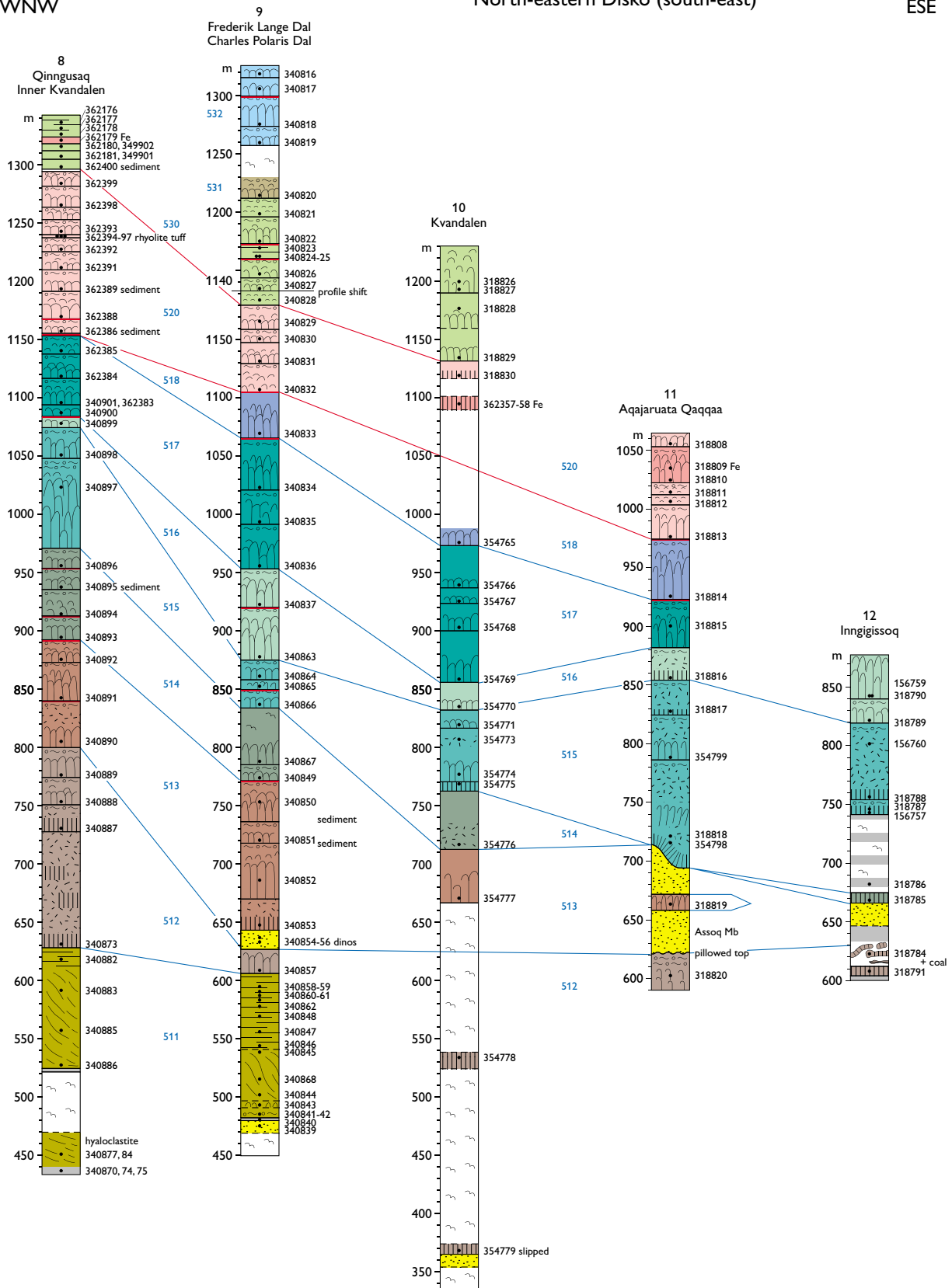


Fig. 10 (two pages). Profiles through the Maligât Formation on north-eastern Disko. For legend, see Fig. 7.

WNW

North-eastern Disko (south-east)

ESE



NW

S. Nuussuaq (north-west)

SE

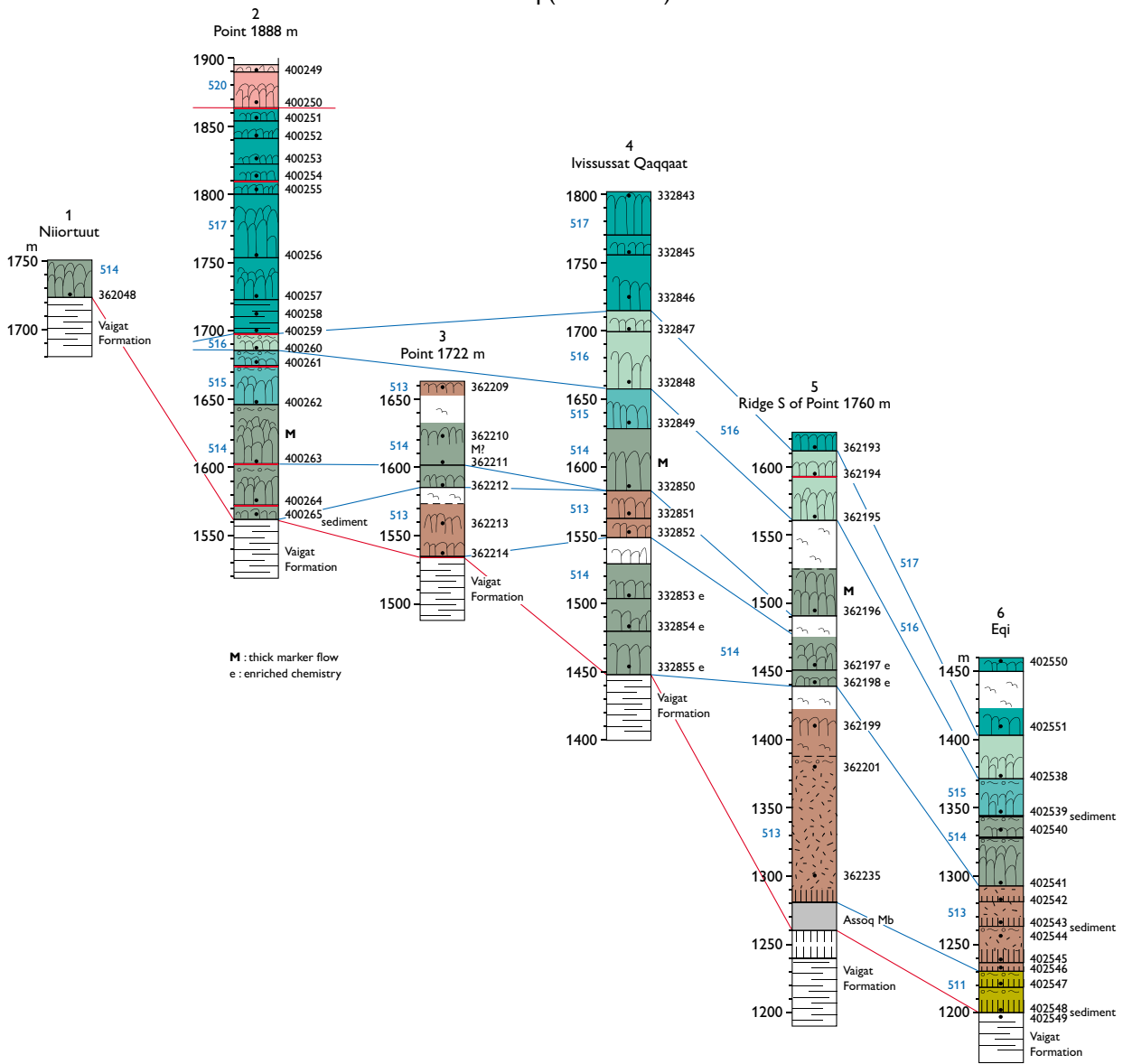


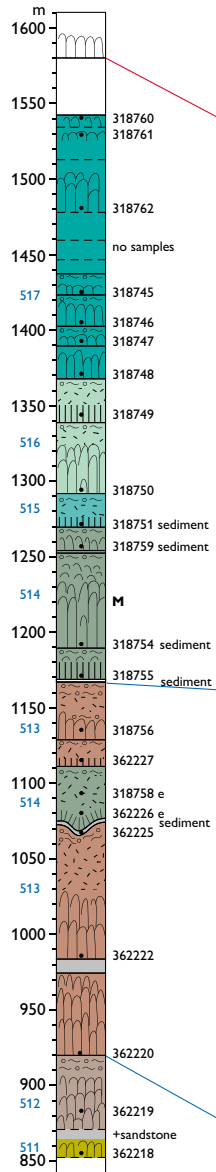
Fig. 11 (two pages). Profiles through the Maligat Formation along the south coast of Nuussuaq. For legend, see Fig. 7.

NW

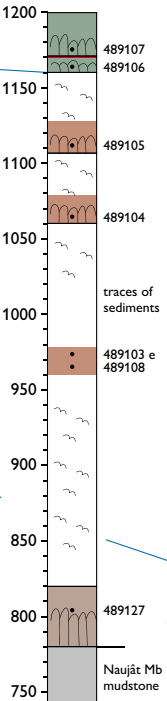
S. Nuussuaq (south-east)

SE

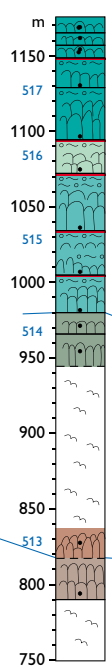
7
Giesecke Monument
Uppalluk



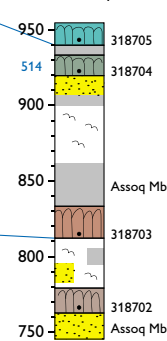
8
Eqip Qaqqaa



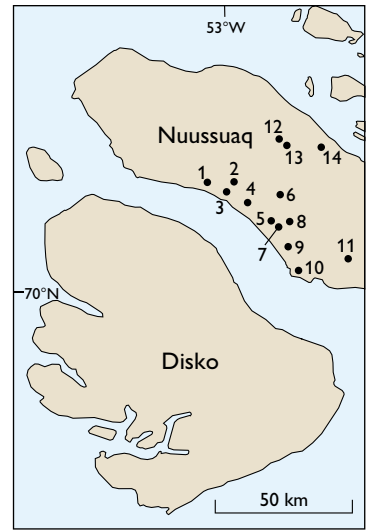
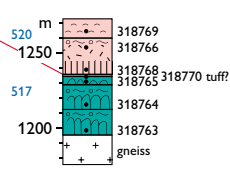
9
Umiasat



10
Tartunaq



11
Saqqaa



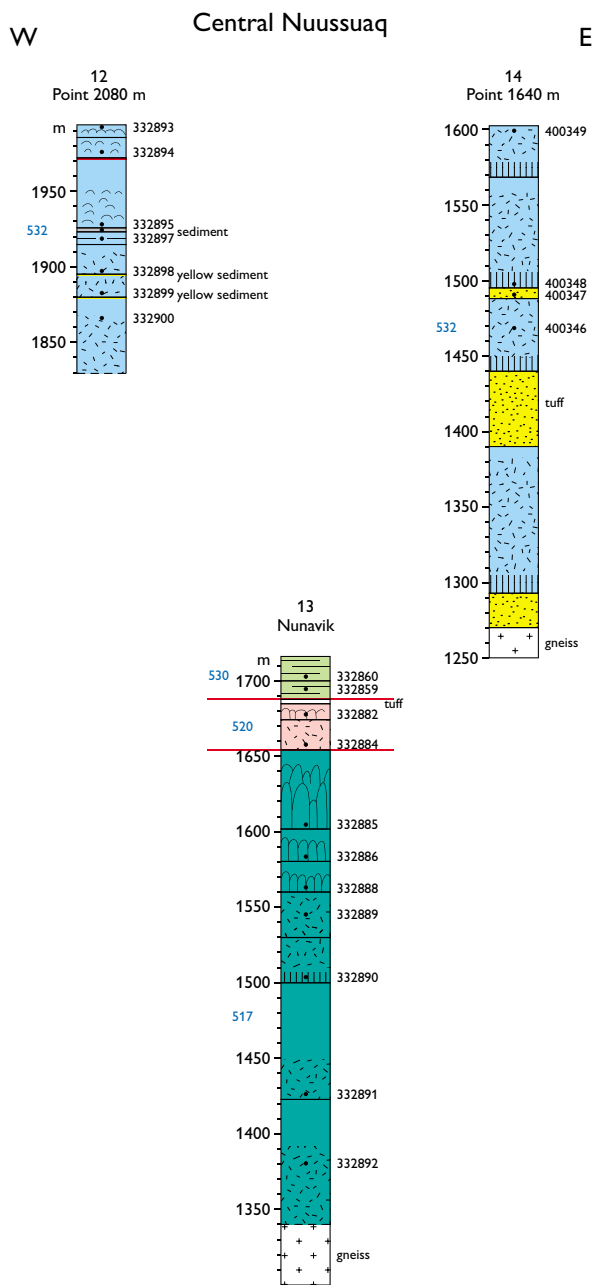


Fig. 12. Profiles through the Maligât Formation on central eastern Nuussuaq. Profile locations in Fig. 11. For legend, see Fig. 7.

(Dam *et al.* 2009). Scarce marine dinoflagellate cysts in samples from eastern and south-eastern Disko indicate that the lake was subject to marine inundations, most probably from the south (Dam *et al.* 2009). The western shoreline towards the Disko Gneiss Ridge and later volcanic rocks was probably steep; *c.* 200 m of foreset-bedded hyaloclastites at Orpiit Qaqqat just east of the gneiss ridge (Fig. 8, profile 4) suggest early water depths of this magnitude. The water depths shallowed towards east and north, and the north-western shoreline towards the Vaigat Formation and the eastern and northern siliciclastic shorelines all had low gradients. The height of the hyaloclastite foresets of the Skarvefjeld unit (511) indicates the depth of the water at one point in time during the filling of the lake: up to 100 m at Skarvefjeld, 60 m in Blåbærdalen, 60 m in Frederik Lange Dal, at least 90 m at Qinnngusaq (inner Kvandalen), more than 30 m at Inussuk on north-east Disko, and 0 m at Qullissat only 4–5 km farther north where the corresponding flows are subaerial. Extensive peat swamps developed along the eastern shoreline (eastern Disko).

As shown in Figs 15 and 16 the filling of the Assoq Lake began on southern Disko on and near the Disko Gneiss Ridge. Subaqueous lava flows and hyaloclastites of the lower Rinks Dal Member (units 505–511) prograded eastwards and northwards into the lake (Figs 7–10). The voluminous unit 509 pushed the western shoreline 10–20 km eastwards, and the hyaloclastites of unit 511 pushed it farther 10–40 km eastwards (Fig. 16). The filling tended to decrease the accommodation space and the water level may have risen, but as the basin floor also subsided the balance was delicate. In all, the lake gradually became shallower. At the eastern shore, the sediment accumulation kept pace with the aggrading lava plateau, or outpaced it. Around the transition to the middle Rinks Dal Member (unit 513, the Akuarut unit), there was apparently a decrease in the magma production rate because sediments, particularly sands, spread widely across the lava plain as far west as to Skarvefjeld (Figs 7, 8, 10). Unit 512 and the thick unit 513 are in subaerial lava facies over large parts of Disko, but on eastern Disko where the number of flows is strongly reduced, the flows commonly invaded the rising sediment pile as invasive flows. Units 512 and 513 were also the first flows of the Maligât Formation to reach southern Nuussuaq where they flowed northwards and occur, successively northwards, in invasive, near-shore and subaerial facies (Fig. 11). After the deposition of unit 513, the Assoq Lake was reduced to small temporary pools, coal swamps and fluvial plains. The flows of the upper Rinks Dal Member (units 514–518) are everywhere subaerial, but on easternmost

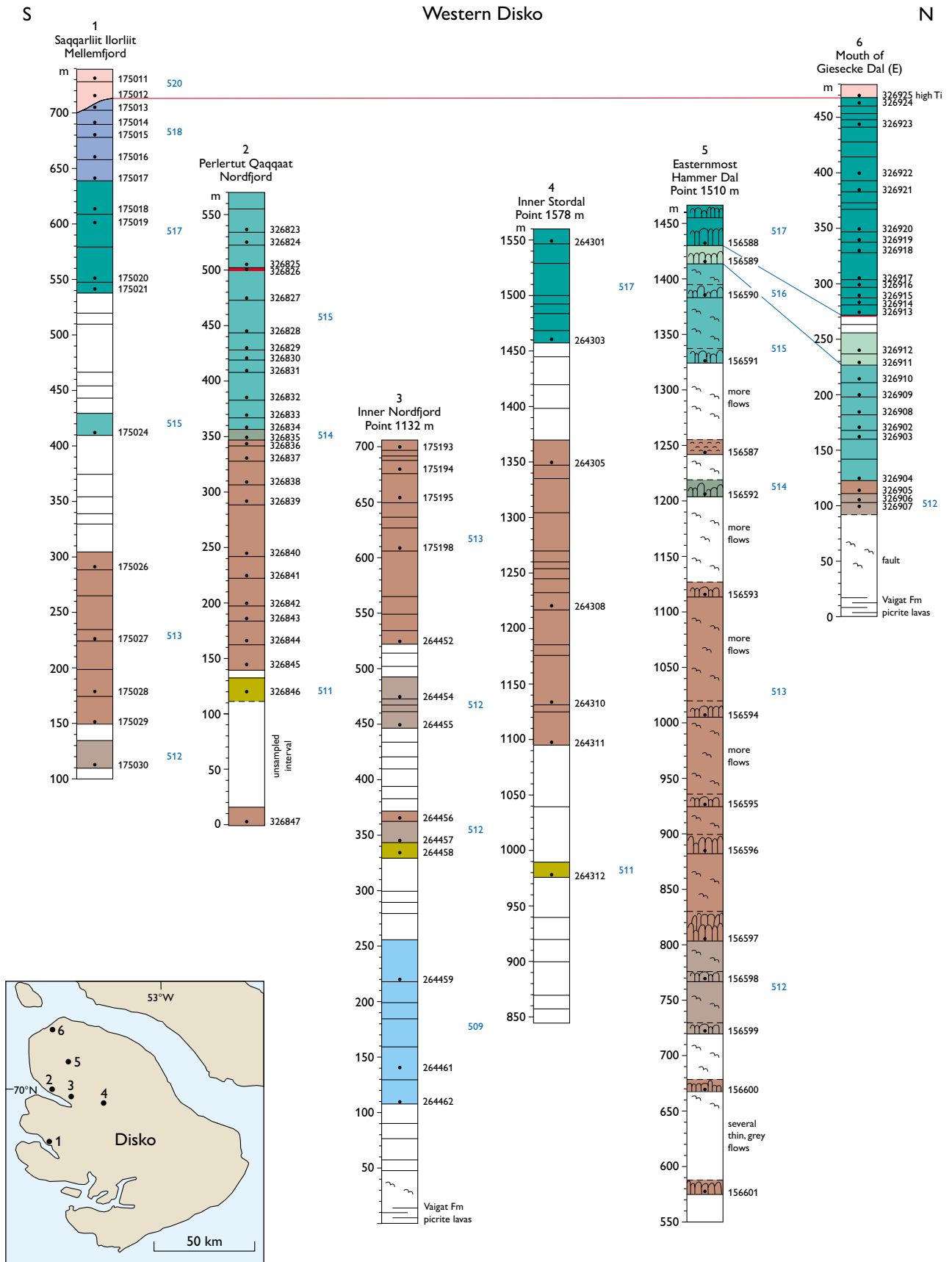


Fig. 13. Profiles through the Maligat Formation (mainly the Rinks Dal Member) in a S–N panel on western Disko. For legend, see Fig. 7.

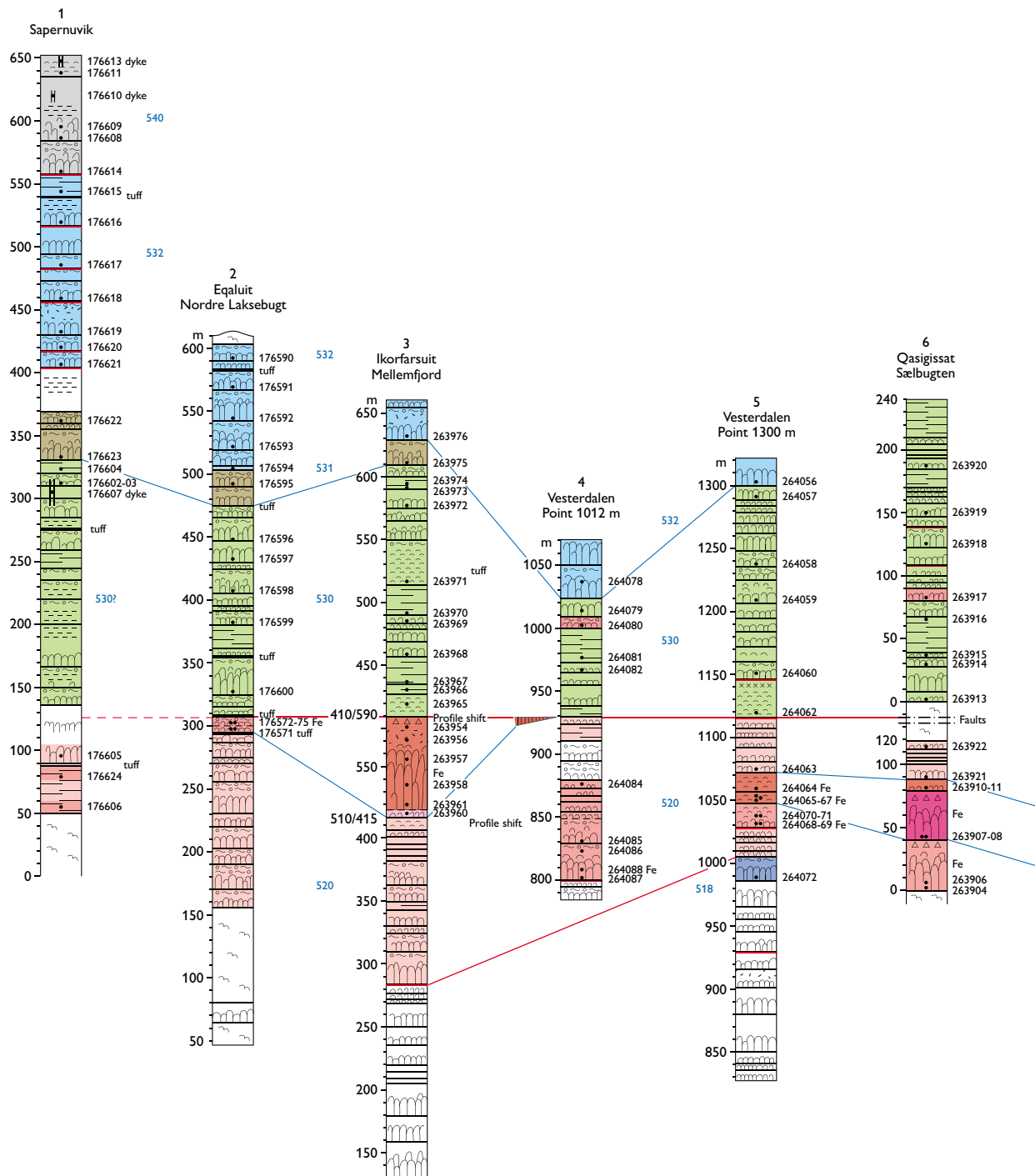
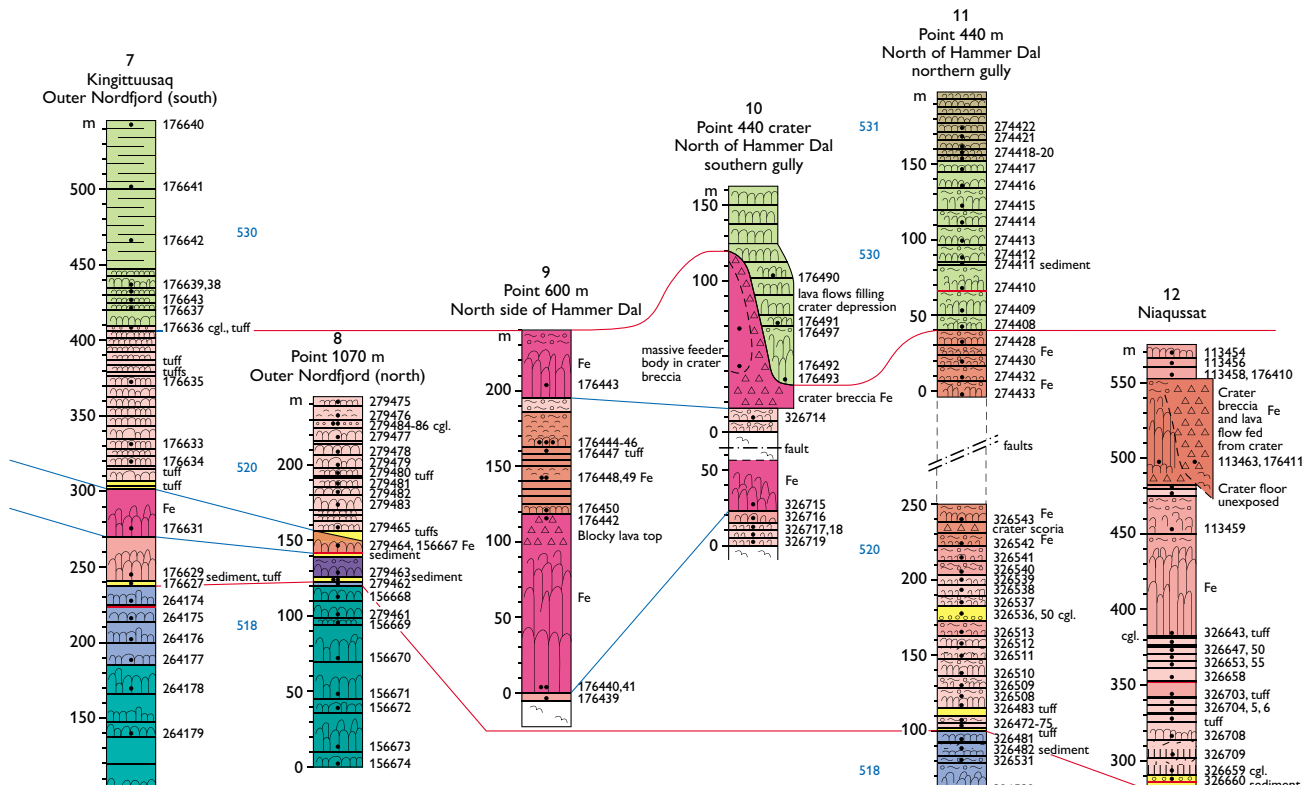
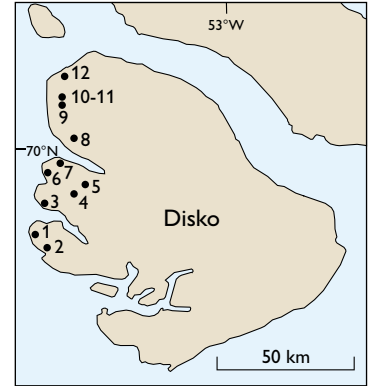
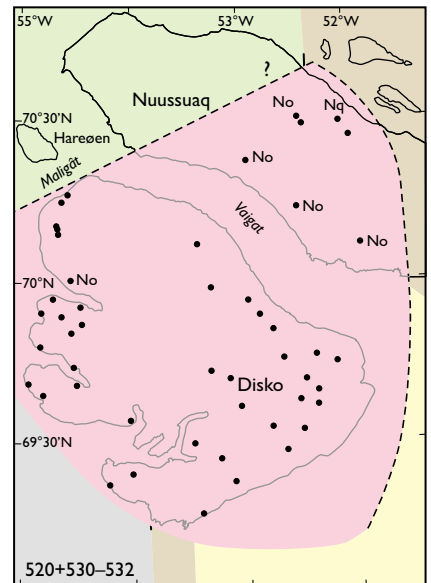
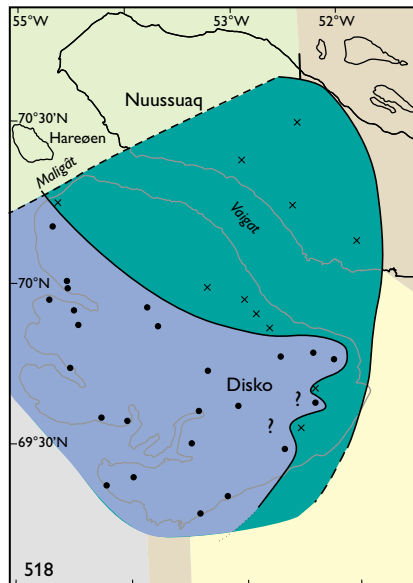
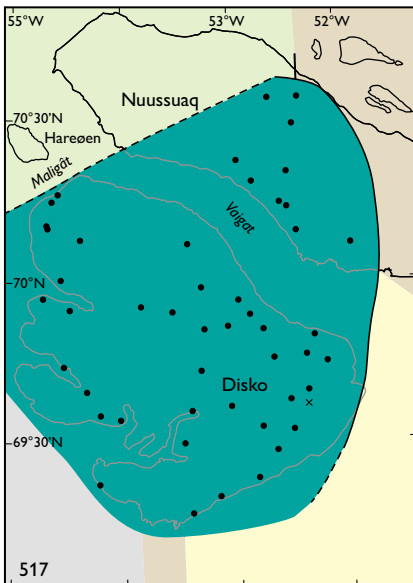
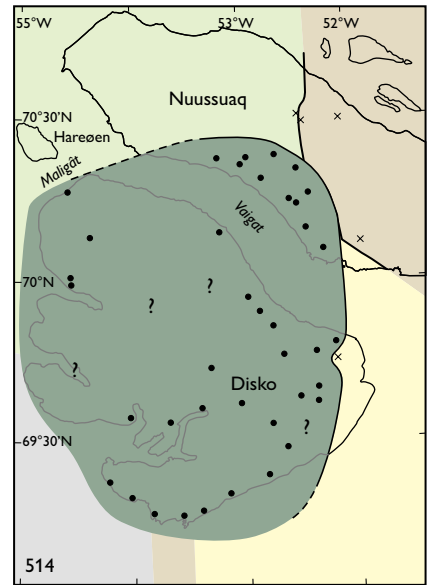
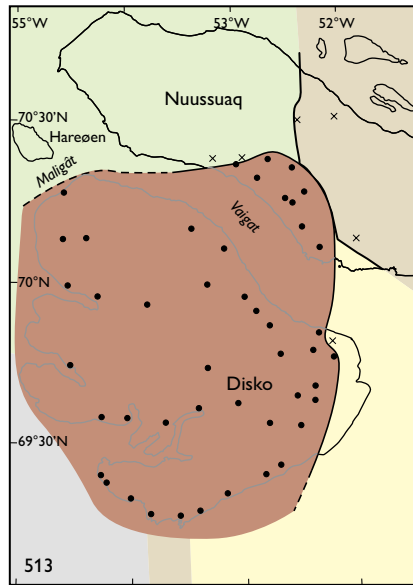
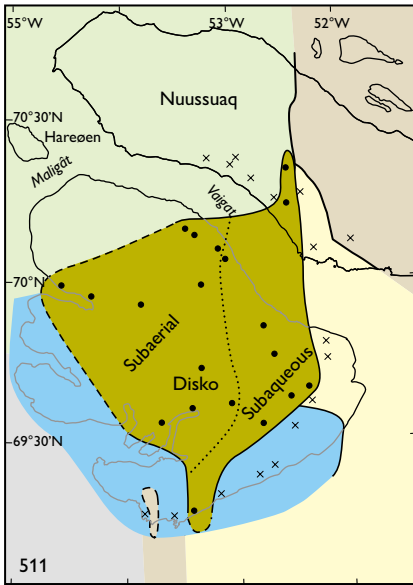
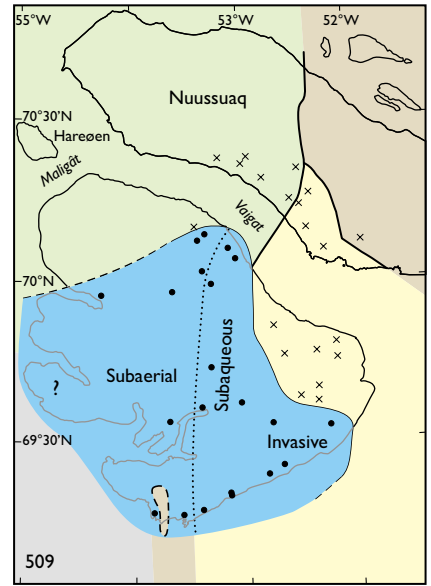
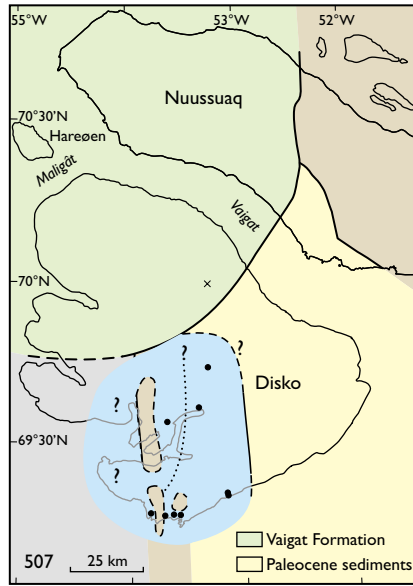
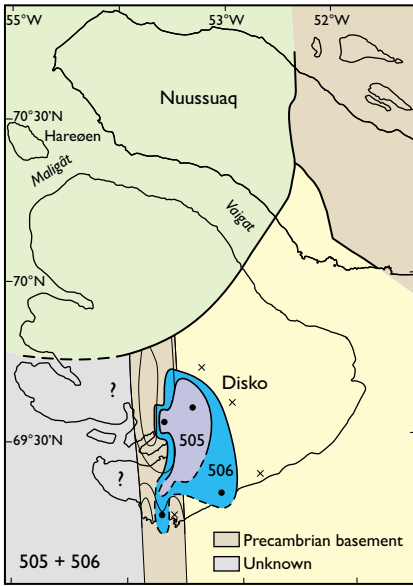


Fig. 14 (*two pages*). Profiles through the Maligât Formation (mainly the Nordfjord and Niaquassat Members) on westernmost Disko. For legend, see Fig. 7. All profiles are corrected for dips and faults to show the real thicknesses. For profiles 1–5 the heights are approximate m a.s.l.; the heavily faulted profiles 6–12 are reconstructed to local baselines and correlated relative to the base of the Niaquassat Member.





Facing page:

Fig. 15. Cartoons showing the substrate and extent of the successive units of the Maligât Formation. The lithological unit codes are indicated in the lower left corner of each cartoon. Units 512 and 515–516 are not shown; their extents are similar to those of units 513 and 514, respectively. Substrate in pale colours, legend in cartoons for units 505–507; the largest hills on the Disko Gneiss Ridge are shown with contour lines. The presence of a unit in a profile (Figs 4, 6) is marked with a black dot; the observed absence of a unit is marked with an x. The dotted lines for units 507, 509 and 511 show the position of the western shoreline of the Assoq Lake at the beginning of the infill of each unit into the lake. Units 505 and 506 are mainly in subaqueous facies except on the gneiss ridge, and units 513 and younger are mainly in subaerial facies, changing to invasive in the easternmost areas.

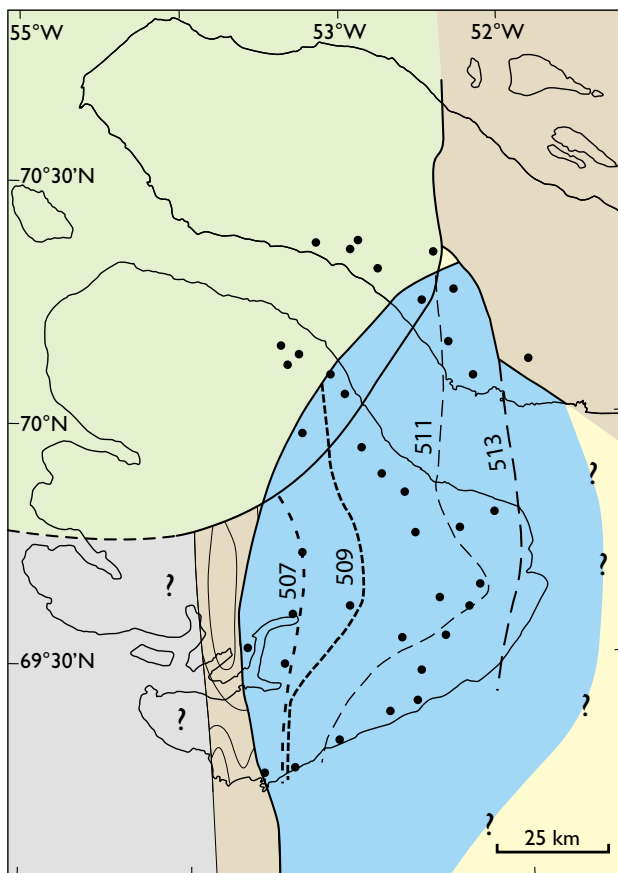


Fig. 16. The extent of the Assoq Lake (blue) during its early stage when it probably reached its largest extent, and during stages of deposition of the Maligât Formation. Substrate colours as in Fig. 15. The infill of the four units 507, 509, 511 and 513 of the Maligât Formation pushed the western shore of the lake successively eastwards: the four dashed lines show the position of the western shoreline at the end of the infill of each unit into the lake. Compare with the cartoons in Fig. 15 where the shorelines at the beginning of the infill of the units are shown. Black dots indicate the sample profiles in Figs 7–11 used to delimit the lake.

Disko and north-eastern Nuussuaq they are still water-influenced and in some places ponded. Remnants of the lake may have existed east of the present exposures.

Later lava flows of the Nordfjord and Niaqussat members are subaerial except for the uppermost flows of the Niaqussat Member in the easternmost profile on north-eastern Nuussuaq. These flows are intercalated with non-marine sediments and are water-influenced and partly invasive (Fig. 12, profile 14; see also Figs 164, 165). The sediments are referred to the Atanikerluk Formation and may have been deposited in the youngest remnant of the Assoq Lake or in an independently formed local lake in a depression on the gneiss highland.

Boundaries

Lower boundary

The lower boundary of the Maligât Formation is everywhere unconformable. The formation overlies Precambrian gneiss on southern and central Disko and eastern Nuussuaq, volcanic rocks of the Vaigat Formation on north-western and northern Disko and central Nuussuaq, and sediments of the Atanikerluk Formation on central and eastern Disko and south-eastern Nuussuaq (Fig. 15). In many places, the boundary is not exposed because it is either covered, below sea level or above erosion level. On south-western Disko the character of the substrate is unknown because it is everywhere below sea level.

Precambrian gneiss. The Disko Gneiss Ridge on southern and central Disko has an irregular surface with 'hilly relief' created in the Cretaceous by deep weathering and subsequent stripping of material, as described in detail by Bonow (2005). The local altitude differences between palaeo-hills and -valleys are to up to 400 m, and the long-exposed gneiss surface is in many places covered by thick residual deposits (saprolite). The successive volcanic units of the Maligât Formation gradually drowned this irregular surface, and at the time of deposition of the middle part of the Rinks Dal Member, all the gneiss hills were covered (Fig. 15). The relations between gneiss and volcanic rocks are well illustrated in the South Disko photographic section. A few examples are described below.

At the entrance to the narrow canyon that separates Navaranaat/Apostelfeld and Akuarut/Lyngmarksfeld, a weathered and eroded gneiss surface is directly covered by a basaltic lava flow of unit 507 in transitional subaqueous–subaerial facies (Fig. 17), see also Fig. 36 and Bonow (2005, fig. 15).



Fig. 17. The lower boundary of the Maligât Formation on south Disko between Akuarut/Lyngmarksfjeld and Navaranaat/Apostelfjeld. A basalt lava flow (unit 507) transitional to pillow lava rests directly on an eroded, but not weathered, gneiss surface.

The contact is well exposed near Tuapassuit 3–4 km farther west (South Disko section at 74.1–74.2 km, see also Fig. 36). The deeply weathered gneiss surface is covered by 3–4 m of saprolitic sediment and overlain by subaerial basaltic lava flows from the Maligât Formation unit 506 (Fig. 7, profile 3; Figs 18, 19).

In Kuannersuit Sulluat (the easternmost part of Kangerluk/Diskofjord) the contact is well exposed on the west coast below Eqalunnguaqqat Qaqqaat in one of the gullies below Point 1109 m (Fig. 8, profile 2). A strongly weathered gneiss is gradually transformed into metre-sized blocks packed in a matrix of kaolinised arkose (F. Ulf-Møller, unpublished field notes 1978). The upper part of the sediment contains layers of mica-rich sandstone and arkose with inter-layered reddish, clay-rich areas. The sediment is about 10 m thick and is covered by a basaltic pillow lava of unit 505.

On Nuussuaq the Maligât Formation overran the high gneiss terrain east of the Saqqaq–Ikorfat part of the eastern boundary fault. North of Saqqaq a few small remnants of lava flows (of unit 517) rest on the gneiss and represent an originally much more widespread lava cover (Pedersen *et al.* 2007a; Fig. 11, profile 11). There are no well-preserved contacts.

North of the Aaffarsuaq valley and east of the Saqqaq–Ikorfat boundary fault the Maligât Formation covered first the Vaigat Formation and farther east came into direct contact with the weathered gneiss, which had a considerable topography (Central Nuussuaq section at 64.5 to 71 km; Pedersen *et al.* 2007a; Fig. 12, profiles 13, 14). Only a few of these localities have been visited in the field.

Vaigat Formation. On northern Disko and southern and central Nuussuaq, lava flows of the Maligât Formation overlie lava flows of the Ordlingassoq Member of the Vaigat Formation, either directly or separated from them by a few decimetres to metres of residual soil with varying amounts of plant remains. At any one locality, the contact between the two formations is simple and subhorizontal (Fig. 20). However, because of the shield shape of the Vaigat Formation and also subtle syn-volcanic basin movements, the Vaigat Formation is in fact onlapped by a range of units of the Maligât Formation. This onlap can be observed in long and well-exposed mountainsides, as in the Kuugannguaq valley on Disko (see Fig. 45). In total, the units of the Maligât Formation resting on the Vaigat Formation change from the lower Rinks Dal Member (unit 509–511) on Disko to the lower to upper Rinks Dal Member (unit 511–514) on Nuussuaq (Figs 9–11, 15). The older units (505–507) are not known to be in contact with the Vaigat Formation and it is theoretically possible that they may be contemporaneous with the youngest part of the Vaigat Formation.

Atanikerluk Formation. Within the large sedimentary basin with the Assoq Lake on eastern Disko and southeastern Nuussuaq (Figs 15, 16), the lower boundary of the Maligât Formation is marked by basaltic lava flows and hyaloclastites which overlie or are emplaced into mudstones and sandstones of the Assoq and Umiussat members of the Atanikerluk Formation (see section on the Assoq Lake above). The boundary zone is characterised by a range of volcanic morphologies created as the volcanic rocks entered the lake, swamps and fluvial plains



Fig. 18. The lower part of the Maligât Formation on south Disko at Tuapassuit, resting on gneiss (see Fig. 27). The boundary to the gneiss is concealed by talus fans except at the small white circle, which indicates the location of the images in Fig. 19. All lava flows are subaerial, and the lowest flow here belongs to unit 506. The plateau top to the left is at 560 m a.s.l.



Fig. 19. Deeply weathered surface of the basement gneiss beneath lava flows of the Maligât Formation. **A:** Saprolite consisting of weathered and oxidised gneiss overlain by a lava flow of unit 506. The sediment is undercut by a small stream. **B:** Kaolinised and disintegrated gneiss (at hammer) overlain by dark grey mudstone. In the centre of the mudstone is a small debris flow with angular, poorly sorted clasts of kaolinised gneiss and mudstone that has a load-deformed base. The mudstone is covered by highly oxidised lateritic soil containing a dark stone (in shadow). The base of the overrunning lava flow of unit 506 is traced. Length of hammer 32 cm. Tuapassuit, south Disko (for location, see Fig. 18).



Fig. 20. Near-conformable boundary between the Vaigat and Maligât formations in subaerial facies. Thick brown lava flows of Maligât Formation units 513–514 overlie thin grey picrite flows of the Ordlingassoq Member of the Vaigat Formation. The preserved part of the Maligât Formation is 150 m thick in the central peak. North wall of Ataata Kuua, Nuussuaq.

with unconsolidated mud, sand and peat. The units of the Maligât Formation in contact with the sediments range from the lowest Rinks Dal Member (unit 506) on central Disko to the middle Rinks Dal Member (unit 513) on eastern Disko and south-eastern Nuussuaq. On north-eastern Nuussuaq east of the boundary fault, lava flows of the upper Niaqussat Member (unit 532) are intercalated with sediments assigned to the Atanikerluk Formation. The detailed contact relations are described in the sections on the individual members and units of the Maligât Formation.

Upper boundary

The upper boundary of the Maligât Formation on Disko and Nuussuaq is erosional. On Disko the highest parts of the formation are exposed on western Disko where they include three lava flows of the Sapernuvik Member (unit 540). On north-eastern Nuussuaq the uppermost part of the Maligât Formation comprises basaltic lava flows from the uppermost Niaqussat Member (unit 532).

Rinks Dal Member

Lithostratigraphy of the Rinks Dal Member

Revised member

History. The Rinks Dal Member was informally established by Pedersen (1975a) on north-western Disko. Here the definition is formalised and extended to cover the volcanic areas on both Disko and Nuussuaq east of the Itilli fault.

Name. After Rink Dal (formerly spelled Rinks Dal) on north-western Disko.

Distribution. The Rinks Dal Member extends over the whole of Disko and parts of southern and central Nuussuaq (Fig. 15). The eastern and northern limits are depositional and relatively well defined, whereas the southern and western limits are unknown.

Type section. The south side of the mountain **Orpiit Qaqqaat** at 0–1080 m, central Disko. This comprises the thickest and most complete section through the Rinks Dal Member although the uppermost flows are missing (Fig. 8, profile 4); Fig. 24 (photogrammetrically measured section), Fig. 28 (geological map) and Figs 25, 31, 63 (photographs). The uppermost flows and the boundary to the Nordfjord Member are covered by a short profile on the eastern side of the mountain **Akuliarusersuaq** at 990–1045 m, 13 km farther south (Fig. 8, profile 3).

Reference sections. The eastern wall of **Brededal** at 0–920 m, c. 3 km from the south coast of Disko (Fig. 7, profile 5; South Disko section at 95–96 km). The eastern wall of the **Kuugannguaq** valley just south of 70°N, at 760–1600 m, northern Disko (Fig. 9, profile 5; Central Disko section at 56–57 km). The southern shoulder of the mountain **Qinngusuaq** leading down to the innermost part of Kvandalen, at c. 500–1150 m, eastern Disko (Fig. 10, profile 8; Central Disko section at 79–83 km). **Giesecke Monument** (Uppalluk) and the neighbouring mountain (Point 1580 m) at c. 850–1550 m, south coast of Nuussuaq (Fig. 11, profile 7; South Nuussuaq section at 57–59 km; Figs 74, 75, 94). The mountain **Point 1888 m** west of Ataataa Kuua, at 1565–1860 m, 7.5 km from the south coast of Nuussuaq (Fig. 11, profile 2). **Nuna-**

vik, the southern slopes below the mountain Point 2000 m, at c. 1300–1650 m, eastern Nuussuaq (Fig. 12, profile 13; Central Nuussuaq section at 67–68 km, Fig. 95).

Thickness. The Rinks Dal Member is thickest on western and central Disko around the Disko Gneiss Ridge where the lower boundary is usually below exposure level. The exposed thickness here is generally around 1000 m and reaches up to 1460 m. The member is thinner where it engulfs the Disko Gneiss Ridge with elevations up to 750 m a.s.l.. East of the ridge, where both the lower and upper boundaries are exposed, the thickness is 1000 m on southern and central Disko, thinning towards the north where the Rinks Dal Member onlaps the Vaigat Formation, and also thinning towards the east where the member interfingers with contemporaneous fluvial and lacustrine sediments. The member is c. 300 m thick around Aqajaruata Qaqqaa on easternmost Disko, and 800 m thick in the inner part of the Kuugannguaq valley on northern Disko. On Nuussuaq, a maximum thickness of 600 m is attained around Giesecke Monument, whereas on central and eastern Nuussuaq the thickness is reduced to 200–300 m because of the onlap on the Vaigat Formation and on the eastern gneiss highland. Thicknesses on western and northern Nuussuaq cannot be estimated because of erosion.

Lithology. Plagioclase-phyric and aphyric tholeiitic basalts of uniform aspect. Mainly subaerial lava flows, but east of the Disko Gneiss Ridge also subaqueous and invasive lava flows and hyaloclastites. The lava flows vary in thickness from less than 5 m to 60 m; most flows are 15–30 m thick. In a few cases, ponded flows are up to 100 m thick. Interbasaltic sediments in the subaerial lava succession are mainly thin lateritic top soils on lava flows.

Subdivisions. The Rinks Dal Member (RDM) is subdivided into 12 chemostratigraphic units which are all informal because they are generally not lithologically distinguishable. However, one large and extensive unit in the middle of the RDM is partly mappable and is shown on the geological maps on a scale of 1:100 000 of Disko south of 70°N (unit β i) and south-east Nuussuaq (unit Mi). This unit is characterised by high contents of iron and titanium and was called the FeTi unit by Larsen & Pedersen (1990); it is here named the Akuarut unit. A

smaller unit is only mappable east of the Disko Gneiss Ridge where it is in hyaloclastite facies; this unit is here named the Skarvefjeld unit (formerly the 'pahoehoe unit' of Larsen & Pedersen 1990) and is shown on the geological maps on a scale of 1:100 000 of eastern and southern Disko (unit β fph2).

In the following, it has been convenient to assemble the 12 units of the RDM into three parts, the lower, middle and upper RDM, with the Akuarut unit constituting the middle RDM.

Boundaries. The lower boundary is below exposure level on western Disko. Where exposed, the lower boundary is unconformable. It is also diachronous, younging towards the east and north. The Rinks Dal Member onlaps the Disko Gneiss Ridge on central and south Disko, as well as the lavas of the Vaigat Formation on northern Disko and Nuussuaq. It invades and interfingers with contemporaneous fluvial and lacustrine sediments on southern and eastern Disko and south-eastern Nuussuaq. At the upper boundary the Rinks Dal Member is conformably overlain by lava flows of the Nordfjord Member; there is commonly, but not always, a sediment horizon at the boundary.

Age. Paleocene, 61–60 Ma, magnetochron C26r, based on radiometric dating (Storey *et al.* 1998; Larsen *et al.* 2016).

Correlation. None certain. The relationship to the Nùluk Member on Hareøen and westernmost Nuussuaq west of the Itilli fault is uncertain.

Subdivision of the Rinks Dal Member

The Rinks Dal Member is the thickest and most extensive member of the Maligât Formation. It constitutes the major part of the preserved succession and extends over all of Disko where it is well exposed along the south coast (South Disko section) and along many valley sides, e.g. in the Central Disko section. It caps the high mountaintops of southern and south-eastern Nuussuaq (South Nuussuaq section) and is present at high altitudes on north-eastern Nuussuaq (Central Nuussuaq section, North Nuussuaq section).

Because of the lithological uniformity of the Rinks Dal Member, its subdivision is based on geochemical variations in many flow-by-flow sampled profiles. In the following, all quoted element concentrations are from analyses recalculated to 100 wt% on a volatile-free basis.

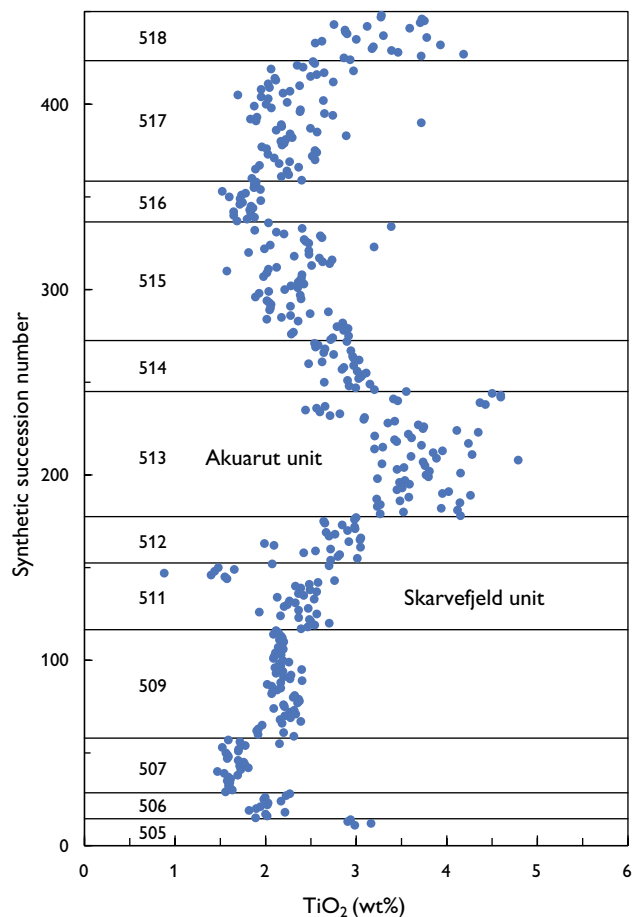


Fig. 21. The variation in TiO₂ content with height in the Rinks Dal Member. The vertical axis is a synthetic succession numbered 1–450, comprising 440 analysed samples arranged in stratigraphic order; the number of samples in each unit approximately reflects the correct volume proportions. Unit divisions are shown with three-digit unit codes (Table 1) on the left. Low TiO₂ contents in some samples in the Skarvefjeld unit (511) are due to high MgO contents not seen in this plot.

The Rinks Dal Member overwhelmingly consists of three-phase-cotectic basalts, i.e. relatively evolved melts in equilibrium with olivine, plagioclase and clinopyroxene. Of 1011 analysed samples, 998 have MgO = 4.4–9.2 wt% (average 6.4 wt%); only 13 samples have MgO > 10 wt% and most of these contain accumulated olivine. The 998 samples have TiO₂ = 1.47–4.78 wt% (average 2.73 wt%) and K₂O = 0.06–1.05 wt% (average 0.30 wt%). SiO₂ contents are 46.4–50.7 wt% except for two samples with 51.3–51.4 wt%; crustal contamination is thus very rare.

Table 2. Subdivision of the Rinks Dal Member by TiO₂ contents

Unit code	Designation	TiO ₂ range (wt%)
518	Uppermost flows	2.3–4.5
517		1.7–3.4
516	Upper low-Ti unit	1.5–2.0
515		1.8–3.4
514	Upper transition flows	2.4– <3.2
513	Akuarut unit	≥ 3.2
512	Lower transition flows	2.4– <3.2
511	Skarvefjeld unit*	2.06–2.78†
509		1.8–2.5
507	Lower low-Ti unit	1.5–1.8
506		1.8–2.6
505	Lowest flows	2.9–3.2

*This unit is distinguished by higher TiO₂ for a given MgO.

†Except in samples with MgO contents >12 wt%.

Unit codes 508 and 510 are unused.

The main subdivision of the Rinks Dal Member is three-fold (Fig. 5). The backbone of the subdivision is the Akuarut unit, a succession of Ti-rich flows in the middle part of the Rinks Dal Member that is easily recognisable in the analysed profiles and is present over all of Disko and southern Nuussuaq. The Akuarut unit conveniently divides the Rinks Dal Member into the three parts shown on the newer geological maps and the geological sections. In detail, the Rinks Dal Member is subdivided into 12 chemostratigraphic units based on oscillations in the TiO₂ content with height (Fig. 21 and Table 2). This subdivision forms the basis for lateral correlations over wide areas (Figs 7–14).

The subdivision by chemical means has some drawbacks. The boundaries between units are ‘artificial’, the more so when the geochemical changes with height are gradual. For instance, the Akuarut unit is surrounded by ‘transitional’ flows that have compositions intermediate between the Akuarut unit and the older and younger flows (Fig. 21). Moreover, flows from some units may interdigitate; a good example of this is again the Akuarut unit, which on northern Disko and southern Nuussuaq splits up in two intervals with ‘transitional’ flows between them.

Lower Rinks Dal Member

Summary of the main features of the lower Rinks Dal Member

- Uneven substrate: Disko Gneiss Ridge hills, Assoq Lake basin east of the ridge and Vaigat Formation picrite shield rising to the north. Substrate to the west unknown.

- Earliest units (505, 506, 507) are only present on south-central Disko. Later units (509, 511, 512) spread gradually over all of Disko; 511 and 512 also occur on south Nuussuaq.
- Unit 509 is the first unit known to step onto the Vaigat Formation picrite shield on central Disko.
- Gradual drowning of nearly all the remaining hills of the Disko Gneiss Ridge by lava flows.
- Gradual eastward filling of the Assoq Lake basin with hyaloclastites and subaqueous lava flows. Several filling episodes can be distinguished.
- Lava flows at the eastern margins of the lava plateau frequently invasive into fluvial and lake sediments of the Assoq Member.
- Individual units are distinguishable chemically but generally not lithologically. Parts of units 507 (Low-Ti unit) and 511 (Skarvefjeld unit) are mappable because they form hyaloclastites and thin-bedded pahoehoe flow groups.
- Unit 511 (Skarvefjeld unit) represents an episode with eruption of Mg-rich magmas interpreted as due to incomplete mixing with a new picritic magma batch intruded into the deep-seated magma chamber.
- Unit 512 has increased TiO₂ and forms a transition to unit 513 (Akuarut unit, middle Maligât Formation).

The lower Rinks Dal Member comprises units 505, 506, 507, 509, 511, and 512 (there are no units 508 and 510). The depositional history of this part of the succession is strongly influenced by the uneven substrate and the existence of the large Assoq Lake basin east of the Disko Gneiss Ridge (Fig. 16; Dam *et al.* 2009).

The lowermost units (505, 506, 507) are only present on south and central Disko (Fig. 15). Subaerial lava flows spread on the Disko Gneiss Ridge, and subaqueous lava flows, pillow lavas and hyaloclastites filled out the western part of the Assoq Lake east of the ridge (Fig. 16). The two lowest units are below the present sea level or exposure level west of the Disko Gneiss Ridge. They may have been erupted locally, as they most probably could not cross the high-standing ridge, whereas the following unit (507) is also found on the western side of the ridge at Killiit/Fortunebay (Fig. 7, profile 2). The following unit 509 was the first to spread over large areas of Disko (Fig. 15), overlapping the Vaigat Formation in the north and extending farther into the subsiding Assoq Lake basin. Units 511 and 512 continued this spreading and infilling pattern until most of Disko was a flat subaerial lava plain bordering a fluvial plain with coal swamps on eastern Disko and southern Nuussuaq.

Unit 505 (lowest flows)

Composition and petrography. The lowest flows have relatively high TiO_2 contents of 2.9–3.2 wt%. The typical basalt contains scattered microphe-nocrysts and small glomerocrysts (less than 2 mm in size) of plagioclase and augite.

Distribution. The lowermost flows have only been sampled in two profiles in a narrow area on the eastern flank of the Disko Gneiss Ridge (Fig. 15). At Eqalunnguaqqat Qaqqaat (Fig. 8, profile 2), unit 505 is at least 170 m thick, and *c.* 10 km to the east at the type locality Orpiit Qaqqaat (Fig. 8, profile 4) it is more than 190 m thick.

Lithologies. At Eqalunnguaqqat Qaqqaat the lowermost basalt is a 40 m thick flow overlying conglomerate and sediment developed on the gneiss surface; it is transitional between a subaqueous lava flow and a pillow lava with pillows several metres in size. It is covered by a few small lava flows and by a large, *c.* 100 m thick ponded lava (F. Ulf-Møller, unpublished field notes 1978) which is in turn covered by several subaerial lava flows with red-oxidised, scoria-rich flow tops.

Unit 505 can be followed eastwards to Orpiit Qaqqaat as poorly exposed hyaloclastite (Fig. 22) and pillow tongues dipping in an easterly direction. Several flow units of hyaloclastite, each thickening eastwards, are present; the lowermost of these is *c.* 150 m thick and indicates a water depth in the lake basin of this size (Fig. 8, profile 4). The base of unit 505 is below sea level near Orpiit Qaqqaat, but other exposures in the area indicate

that the hyaloclastites here overlie lacustrine mudstones of the Assoq Member of the Atanikerluk Formation.

Unit 506

Composition and petrography. Unit 506 has TiO_2 contents of 1.8–2.3 wt% with a few values of up to 2.6 wt%. Typical basalts are phenocryst-poor with scattered microphe-nocrysts and phenocrysts of plagioclase and less common augite up to 2 mm in size, and with pseudomorphs after olivine less than 1 mm in size (Fig. 23). These basalts are lithologically and chemically similar to those of unit 509 but are separated from them by the distinctive unit 507.

Distribution. The basalts of unit 506 occupy an elongate, *c.* 25 km wide, N–S-trending belt confined to the west by the Disko Gneiss Ridge and to the east by lack of exposures (Fig. 15). On the Disko Gneiss Ridge the distribution and thickness of the unit is affected by the considerable palaeo-topography (Bonow 2005). The unit here comprises just a few flows, but its thickness increases eastwards to up to 225 m on central Disko at Orpiit Qaqqaat (Figs 8, 24) where the lavas prograded towards the east and north into the Assoq Lake basin.

Lithologies. Unit 506 has been sampled and recorded at a few localities on the south coast of Disko. A single lava flow overlies saprolite at Tuapassuit (Fig. 7, profile 3), and about 100 m north of Qeqertarsuaq town pillow lavas and hyaloclastites overlie local sands (the main aquifer of the town). At Brededal, a *c.* 40 m thick subaqueous



Fig. 22. Oldest exposed deposits of the Maligât Formation: Hyaloclastites rich in pillow fragments, unit 505, lowest Rinks Dal Member. Length of Swiss army knife 8 cm. Orpiit Qaqqaat, south-central Disko.

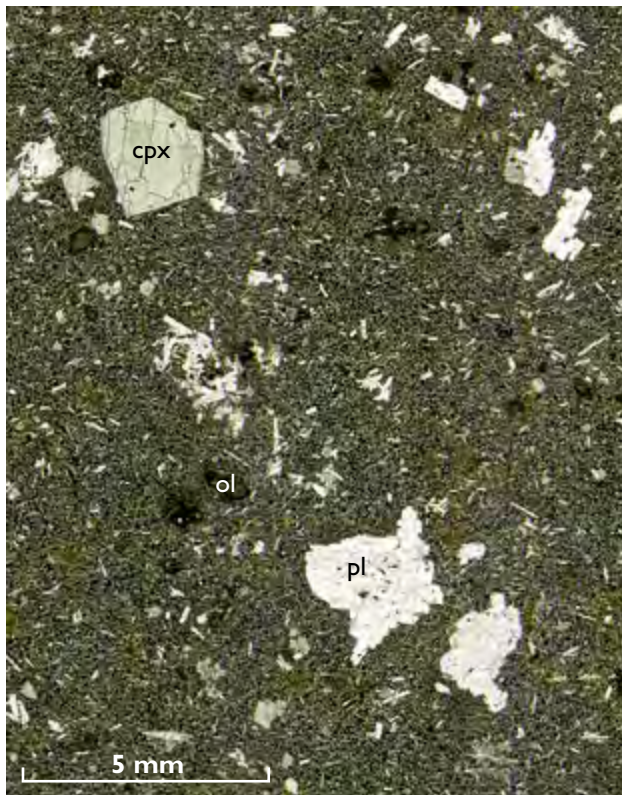


Fig. 23. Thin section (scanned) of a typical lava from Rinks Dal Member unit 506. Basalt with scattered phenocrysts of plagioclase (pl), olivine (ol, altered to dark green clay) and augite (cpx) in a fine-grained matrix. Sample GGU 354727, Orpiit Qaqqaat, south-central Disko.

lava flow overlies mudstone of the Assoq Member (Fig. 7, profile 5).

The main studied occurrence of unit 506 is situated along the inner part of the Kuannersuit Sulluat fjord on the lower slopes of the mountain Orpiit Qaqqaat (Fig. 8, profile 4; Fig. 24) where the unit is moderately well exposed over *c.* 5 km (Fig. 25). It is *c.* 225 m thick and comprises a number of lava flow fields showing general thickening from west to east as they filled the growing accommodation space in the subsiding lake basin. A well-exposed gully (Fig. 25) displays a considerable lithological variation showing that subsidence and basin filling were episodic. Here, unit 506 rests on foreset-bedded hyaloclastites of unit 505, and four episodes of deposition of unit 506, as well as two episodes of drowning, can be distinguished (Fig. 24).

Filling episode 1 led to the deposition of several subaqueous lava flows with very well-developed colonnades and hyaloclastite tops (in all *c.* 60 m thick), followed by a *c.* 10 m thick flow unit with mega-pillows and pillow

tubes. This is capped by a 12 m thick flow unit of thin subaerial pahoehoe lobes with lateritic soil on the top, indicating complete emergence.

A first drowning episode is indicated by the renewed occurrence of subaqueous volcanic facies.

Filling episodes 2 and 3 led to the deposition of two subaqueous lava flows covered by 3–4 m of basalt gravel and conglomerate (episode 2, partial filling), followed by *c.* 14 m of foreset-bedded hyaloclastite and 10 m of associated thin subaerial pahoehoe flows which constitute one flow field. This is followed by a *c.* 15 m thick, distinctly subaerial lava flow with an oxidised, scoria-rich flow top, capped by lateritic soil (episode 3, complete filling).

A second, lesser drowning episode is indicated by a renewed occurrence of water-influenced lava morphologies.

Filling episode 4 led to the deposition of a 40–45 m thick lava flow with a regular colonnade and entablature indicating flow into a wet environment. However, the metre-thick, oxidised flow top shows that the basin was filled well above the wet zone. Unit 506 is here capped by a flow field of thin subaerial pahoehoe lobes of unit 507.

Unit 507 (low-Ti flows)

Composition and petrography. Unit 507 is a distinctive lithological and chemical marker horizon. It consists of low-titanium basalts with TiO_2 contents of 1.4–1.8 wt% (Fig. 21), rich in phenocrysts of plagioclase and less common augite. The phenocrysts tend to form glomerophyric clusters up to *c.* 4 mm in size but occasionally up to 10 mm. Olivine (pseudomorphs) form scattered microphenocrysts less than 1 mm in size. (Fig. 26). In wet facies the basaltic groundmass is very fine-grained, whereas subaerial basalts have well crystallised, almost doleritic groundmass textures.

Distribution. The basalts of unit 507 occupy a *c.* 35 km wide, north–south elongate belt confined towards both west and east by being below exposure level (Fig. 15). On the Disko Gneiss Ridge, the distribution and thicknesses are still affected by the palaeo-topography. The unit is thickest in its easternmost parts (360 m in the profile north of Sorte Hak, Fig. 9, profile 4) because of infill of the Assoq Lake basin.

The lavas of unit 507 are known from two main areas on south and central Disko. They occur in a 17 km long section along the south coast of Disko from Killiit in the west to Blæsedalen in the east; they are shown as units m_1

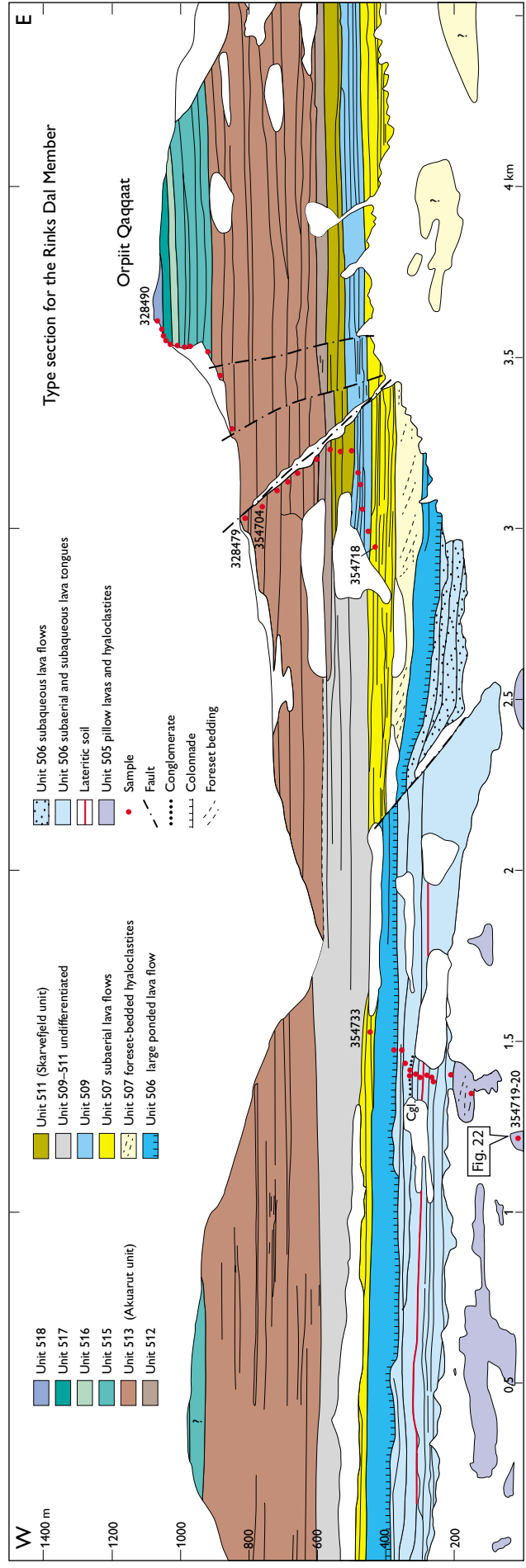


Fig. 24. The type section for the Rinks Dal Member with the thickest and most complete section through the member. See map in Fig. 28 and photographs in Figs 25, 31, 63. The indicated samples are used to construct the profile shown in Figs 8, 9. Photogrammetrically measured section, south side of the mountain Orpitt Qaqqaat, south-central Disko.



Fig. 25. The western part of the type section for the Rinks Dal Member; unit codes are indicated. **cgl.**: conglomerate. The photo corresponds to Fig. 24 at 0.9–2 km; unit 506 (subaqueous and ponded flows) is 230 m thick. South side of the Orpiit Qaqqat mountain, south-central Disko.

and m_2 in the South Disko section at 65–82 km (see Fig. 36) and as parts of the units $\beta f1$ and $\beta f1u$ on the geological map sheet Uiffaq (Fig. 27).

On central Disko, unit 507 occurs on both sides of the inner part of the fjord Kuannersuit Sulluat and on both sides of the valley Kuannersuit Kuussuat and its side valley Sorte Hak. It is mapped as unit $\beta fph1$ on the geological map sheet Pingu (Pedersen *et al.* 2001; Fig. 28). Unit 507 has a total thickness of 360 m north of Sorte Hak (Fig. 9, profile 3) of which the lower 295 m is in subaqueous facies which makes it one of the thickest subaqueous successions in the Maligât Formation.

South coast of Disko. The Disko Gneiss Ridge is exposed and reaches heights up to *c.* 350 m at the south coast of Disko between Killiit in the west and Rødeelv in the east (Figs 6, 27). The relationship between the gneiss topography, subaerial lava flows and subaqueous hyaloclastite

breccias is discussed below at four localities (South Disko section at 67–81 km, see Fig. 36).

At Killiit at least four subaerial lava flows of unit 507 onlap the western flank of the Disko Gneiss Ridge, but the contact is not exposed. The flow packet is 115 m thick and the flows vary in thickness between 15 and 50 m (Fig. 7, profile 2). The uppermost flow is overlain by *c.* 30 cm of reddish lateritic soil. About 4–5 km farther to the east, north-east of Tini, 30–35 m of unit 507 are exposed in a gully. The two localities are separated by a gneiss hill that rises up to 200 m above the level of the lavas of unit 507 (see also Fig. 36 at 69–72 km), indicating that the flows near Tini must have followed an unexposed palaeovalley. The succession near Tini starts with a strongly columnar-jointed subaqueous lava flow covered by a hyaloclastite composed of decimetre-sized pillows and matrix glass shards. The hyaloclastite contains decimetre-sized clasts of claystone and lateritic soil and

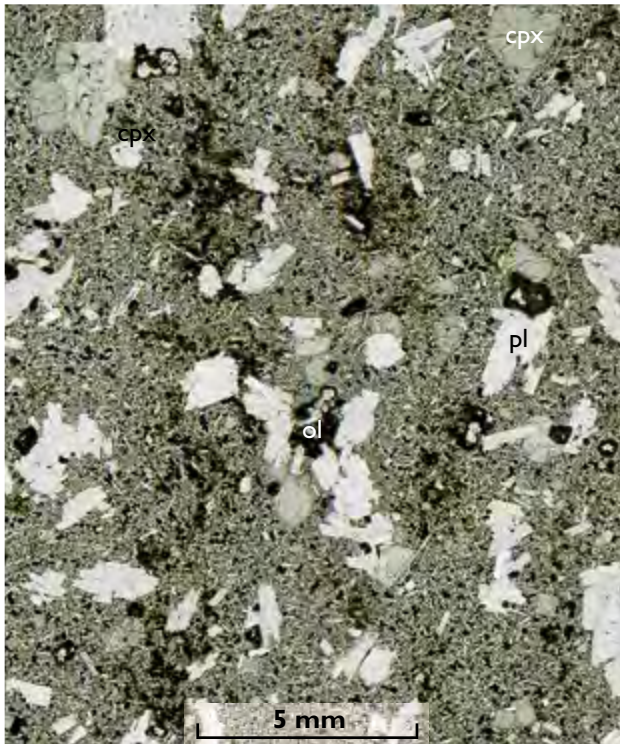


Fig. 26. Thin section (scanned) of a typical lava from Rinks Dal Member unit 507. Highly porphyritic basalt with many phenocrysts of plagioclase (**pl**), olivine (**ol**, altered to brown clay and white zeolite) and augite (**cpx**) in a medium-grained matrix. Sample GGU 332960, Sorte Hak, central Disko.

centimetre-sized clasts of gneiss, all of which have been stripped off a weathered gneiss surface. At the contact between the subaqueous flow and the hyaloclastite there are patches of red-oxidised scoria and up to 15 cm of lateritic soil. The top of the hyaloclastite is covered by several decimetres of reddish-brown soil of subaerial origin. This is in turn covered by a compound pahoehoe flow indicating subaerial conditions.

East of Tini, at Tuapassuit, unit 507 forms a 115 m thick succession of six subaerial lava flows above a 55 cm thick horizon of sandstone and siltstone with plant remains overlying unit 506 (Fig. 7, profile 3). Most of unit 507 must bank up against the Disko Gneiss Ridge northwest of Qeqertarsuaq town because it is not present on the top of the ridge (see Fig. 36 at 76–77.5 km). A single flow of unit 507 overlies the gneiss ridge in the canyon between Apostelfjeld and Lyngmarksfjeld (Fig. 29).

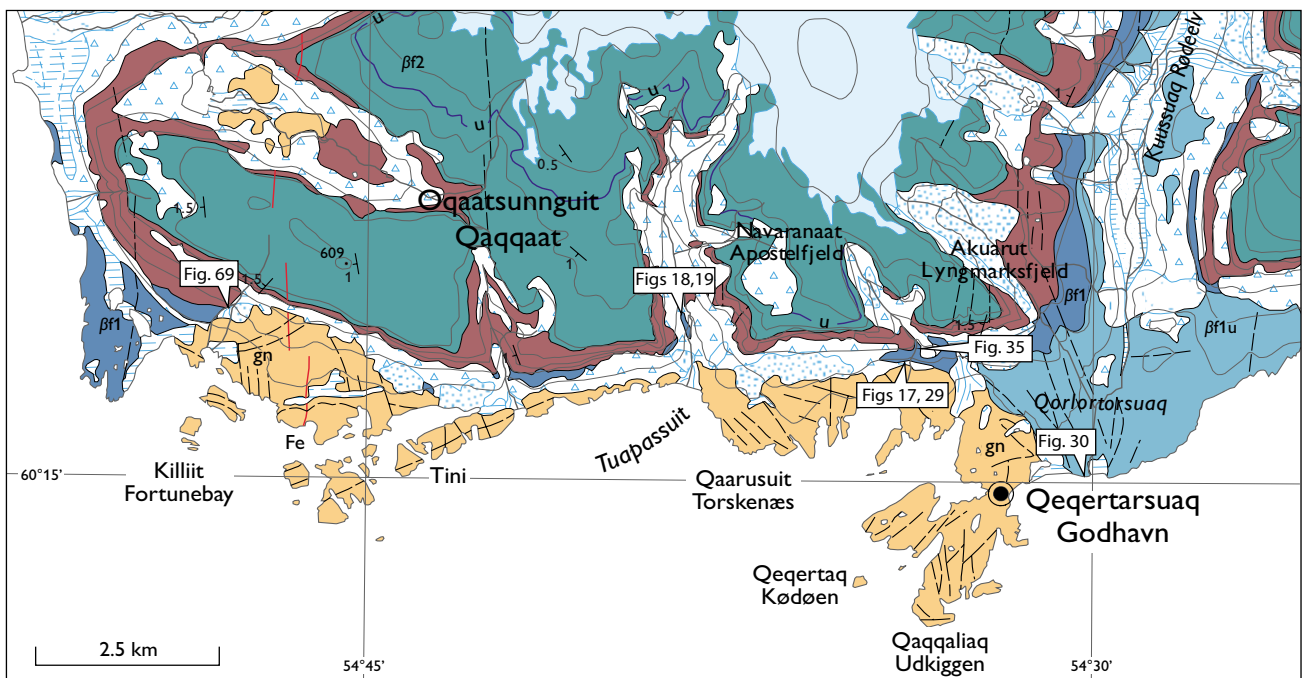
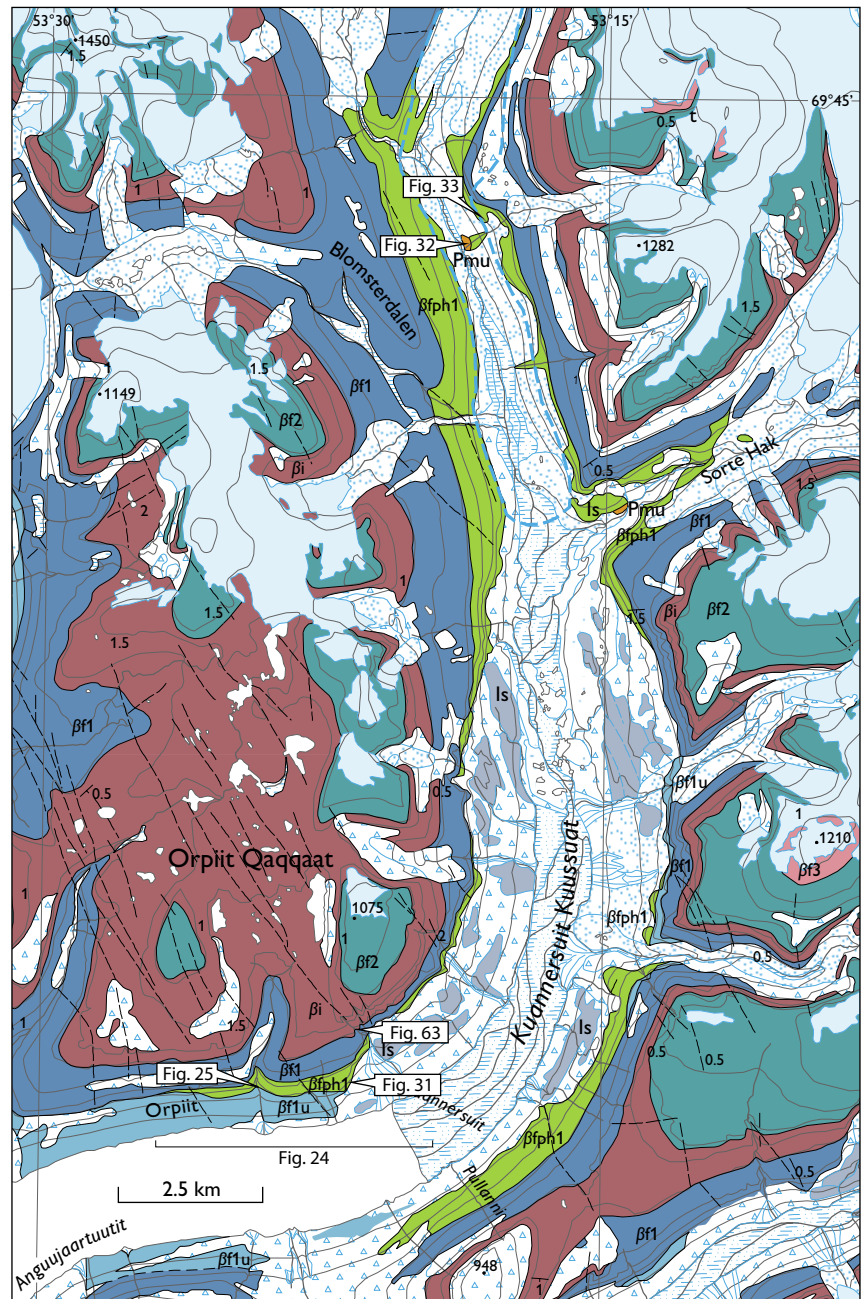


Fig. 27. Excerpt from the 1:100 000 scale geological map sheet 69 V.1 Syd Uiffaq, showing the lava succession of the Rinks Dal Member covering the hilly relief on the Disko Gneiss Ridge. The brown unit comprises the Fe-Ti-rich lava flows of the Akuarut unit (513). Annotation as on the original map, see Fig. 28. The native-iron-bearing Killiit dyke is shown as red lines marked Fe. The locations of some figures are indicated.

Fig. 28. Excerpt from the 1:100 000 scale geological map sheet 69 V.2 Nord Pingu, showing almost the full stratigraphy of the Rinks Dal Member. Annotation as on the original map. This corresponds to the more detailed lithological units in this work as follows: $\beta f1u$ is units 505–506, $\beta fph1$ is unit 507, $\beta f1$ is units 509–512, βi is unit 513 and $\beta f2$ is units 514–518. $\beta f3$ is the overlying lava flows of the Nordfjord Member, and Pmu is small exposures of the underlying mudstones of the Assoq Member. The line of view of the type section (Fig. 24) is shown, as well as the locations of some figures.



This flow has a brecciated lower part and a thin top zone with oxidised scoria and traces of sediment.

Between Tuapassuit and Qeqertarsuaq the Disko Gneiss Ridge is *c.* 200 m high. On its eastern flank, towards the outflow of Rødeelv, unit 507 reappears. Subaqueous lava flows of this unit are exposed for about 2 km along a rocky beach and a coastal cliff. Here a varied succession of large pillow lobes, subaqueous basalt breccias and fine-clastic hyaloclastites formed when a number

of subaerial pahoehoe lava lobes entered the Assoq Lake basin. The elongate pillow lobes (Fig. 30) show a general flow direction from the north-west. Parts of the lobes have cavities now filled by zeolites. The breccias are composed of pillows with thin glassy rims in a coarse matrix of brownish-weathering palagonitised glass.



Fig. 29. Lava flow of unit 507 overlying the Disko Gneiss Ridge in the canyon between Apostelfjeld and Lyngmarksfjeld (South Disko section at 77.6 km, Fig. 36). The flow is *c.* 30 m thick and in transitional facies between subaqueous and subaerial: it has a brecciated lower part, its interior is a coarse entablature, and there is a thin rubbly top zone with oxidised scoria.

Central Disko. The basalts of unit 507 extend from the south coast of Disko northwards to central Disko, but they have not been studied or sampled between the south coast and the inner part of Kuannersuit Sulluat (easternmost Kangerluk). Unit 507 is present in the profile at Eqalunnguaqqat Qaqqat (Fig. 8, profile 2) as two more than 30 m thick subaerial lava flows overlying unit 506. In the gully on the south slope of Orpiit Qaqqat, unit 507 consists of a small flow field of pahoehoe lobes about 12 m thick covered by a *c.* 12 m thick lava flow (Fig. 8, profile 4). Eastwards from there unit 507 rapidly increases in thickness to more than 100 m just 2 km farther to the east, where it changes facies to form foreset-bedded hyaloclastite infill into the Assoq Lake. The foresets show infilling from the west and north-west, but a very dense joint system striking NW to NNW locally obscures the breccia structure when seen at a distance (Fig. 31). The infill into the lake occurred over a more than 20 km long, north-south-extending front that prograded more than 5 km eastwards, reducing the western lake area by more than 100 km² (Figs 15, 16).



Fig. 30. Metre-long pillow lobe from a pahoehoe flow of unit 507 that flowed into the Assoq Lake. The lobe has a near-tubular central cavity filled by zeolites. Near the outflow of Rødeelv east of Qeqertarsuaq town, south Disko.



Fig. 31. Middle part of the type section of the Rinks Dal Member. The photo corresponds to Fig. 24 at 2.8–3.5 km. Unit 506 is in subaqueous lava facies (506 sLa). A subaerial succession of thin pahoehoe flows of unit 507 (507 La) entered the Assoq Lake from the west and formed a thick horizon of massive foreset-bedded hyaloclastites (507 hy) that prograded more than 5 km into the lake. The foresets are obscured by a very pronounced vertical joint system. The overlying flows are all subaerial. The combined unit 507 (flows and hyaloclastites) is 150 m thick. South side of the Orpiit Qaqaat mountain, south-central Disko.

Up to 10 m of black mudstone of the Assoq Member from the lake floor is exposed at the base of the volcanic rocks at a few localities (unit Pmu on the map sheet Pinggu, Fig. 28). In the profile 5 km north of Sorte Hak, the contact between mudstone and infilling hyaloclastites has produced a chaotic mixture like very coarse peperite where pillow tongues invaded unconsolidated mud (Fig. 32).

On both walls of the Kuannersuit Kuussuat valley and its side valley Sorte Hak (Fig. 28), unit 507 consists of foreset-bedded hyaloclastites and overlying subaerial pahoehoe lava flows. Excellent exposures in the eastern wall of Kuannersuit Kuussuat north of Sorte Hak formerly

showed the presence of several distinct hyaloclastite beds which cannot have been formed during a single eruptive event. These exposures were covered in 1995 by a surging glacier lobe. The highest foresets produced in a single filling event, which record the water depth in the Assoq Lake at that time, are around 100–150 m high and occur in the northern wall of Sorte Hak.

The subaerial pahoehoe lava flows comprise 10 to 15 individual lava lobes in vertical section and represent several flow fields. The uppermost lava flow of unit 507 north of Sorte Hak is thick (35–40 m) and massive and has a regular colonnade indicating that it solidified in a moist environment (Fig. 33).

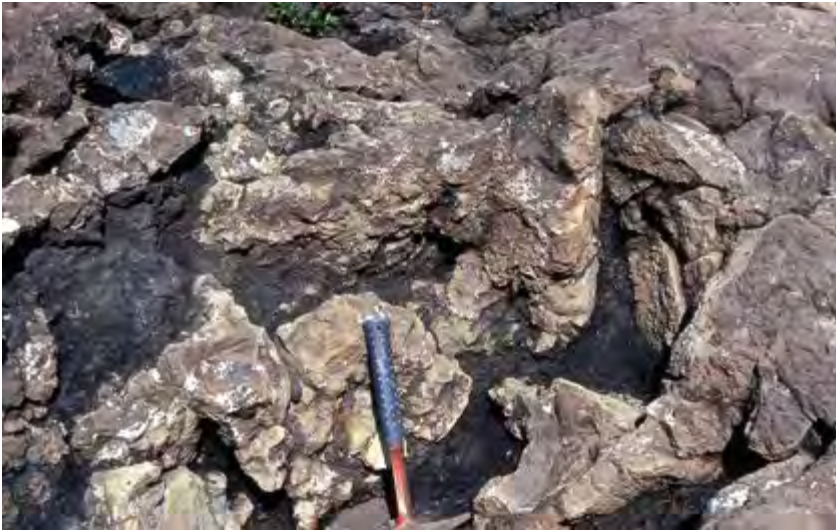


Fig. 32. Lava lobes and pillows of a subaqueous lava flow invading black mudstones of the Assoq Member. The hammer is 32 cm long. Valley bottom 5 km north of Sorte Hak (Fig. 28; Fig. 9, base of profile 4); the locality was covered by ice after a major glacier surge in 1995–1999.

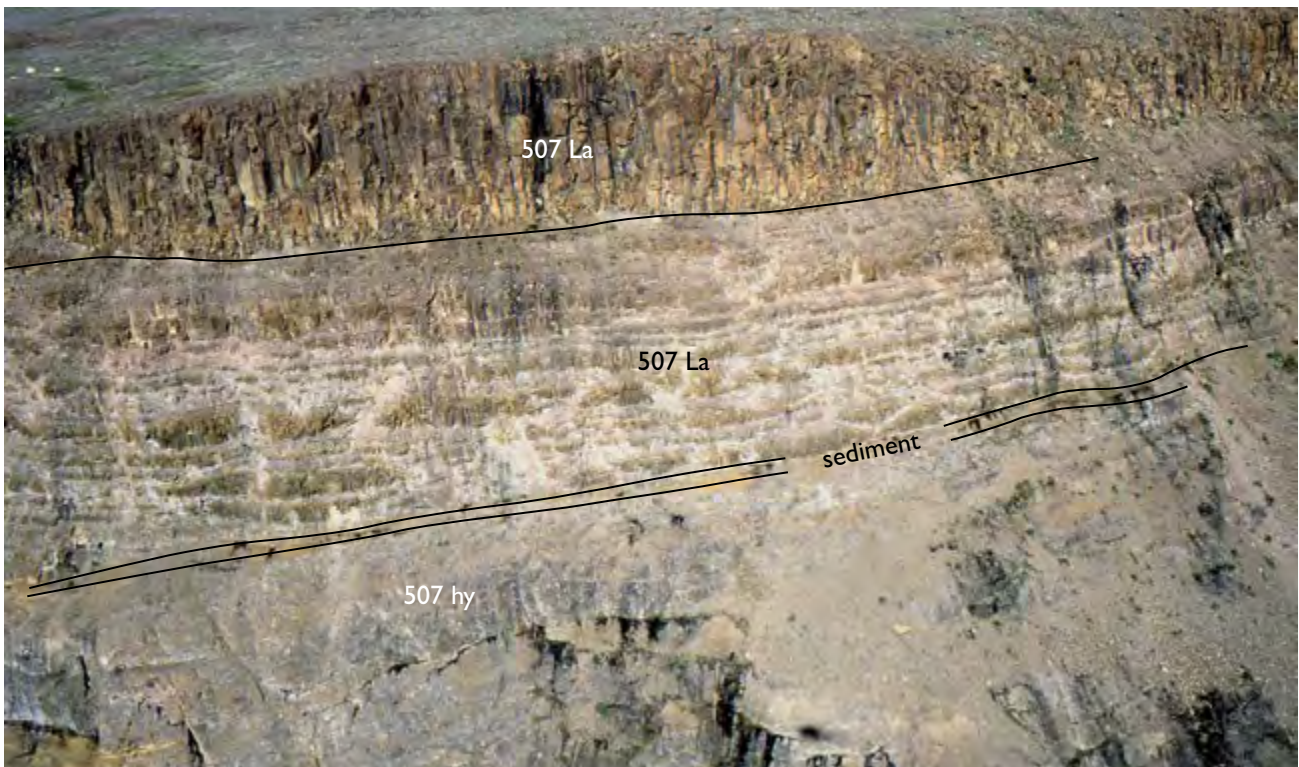


Fig. 33. Lithological variations in unit 507. The unit comprises hyaloclastites (507 hy, the foresets dip away from the viewer), a thin sediment horizon, subaerial pahoehoe flows (507 La) and a thick, massive flow with a well-developed colonnade (also 507 La). The thick flow is 35–40 m thick. Kuannersuit Kuussuat north of Sorte Hak, central Disko.

Unit 509

Composition and petrography. Unit 509 is composed of basalts with TiO_2 contents of 1.8–2.5 wt% (Fig. 21). They contain scattered plagioclase and augite glomerocrysts between 1 and 3 mm in size and pseudomorphs up to 1 mm large after olivine crystals (Fig. 34A) in a fine-grained to glassy groundmass. Some regional variations are present. The subaqueous lava flows along the south coast of Disko from Ippik (east of Skarvefjeld) to Tuapaat Qaqqaat have very uniform compositions with TiO_2 contents of 2.0–2.2 wt% and *mg*-numbers of 48–55; these flows were called the Ippik unit by Larsen *et al.* (2006). On central and northern Disko, several lava flows of unit 509 have higher *mg*-numbers (57–62), corresponding to MgO contents of 7.7–8.8 wt%; these flows may be aphyric to slightly olivine-microphyric (Fig. 34B). Other northern flows are very similar to those on southern Disko.

Distribution. Unit 509 is present over large parts of central and southern Disko (Fig. 15); to the north, it reaches Qullissat and Asuutaa but peters out before Orlingasoq

(Fig. 10). It also peters out on eastern Disko and is not present east of Tuapaat Qaqqaat (Fig. 7), Laksedal (Fig. 8) and Inussuk (Fig. 10). It is present on western Disko around inner Nordfjord (Fig. 13) and is assumed to be present beneath sea or exposure level in large areas west of the Disko Gneiss Ridge. Excluding onlap settings, thicknesses are between 50 m and 240 m. Unit 509 almost, but not completely, covered the Disko Gneiss Ridge. The unit is in subaerial facies on the gneiss ridge and west of it. East of the gneiss ridge the lavas plunged into the Assoq Lake and continued as coherent subaqueous lava flows. The unit prograded far into the Assoq Lake where the flows burrowed into lacustrine and fluvial sediments and continued as invasive lava flows that resemble sills (South Disko section).

Lithologies. In subaerial facies, unit 509 comprises 2–10 lava flows per profile, commonly around five flows. The combined thickness of the flows may exceed 150 m. Individual flows vary in thickness from less than 5 m to more than 50 m, typical flows being 10–30 m thick. The greyish weathering flows are of blocky pahoehoe type (Fig.

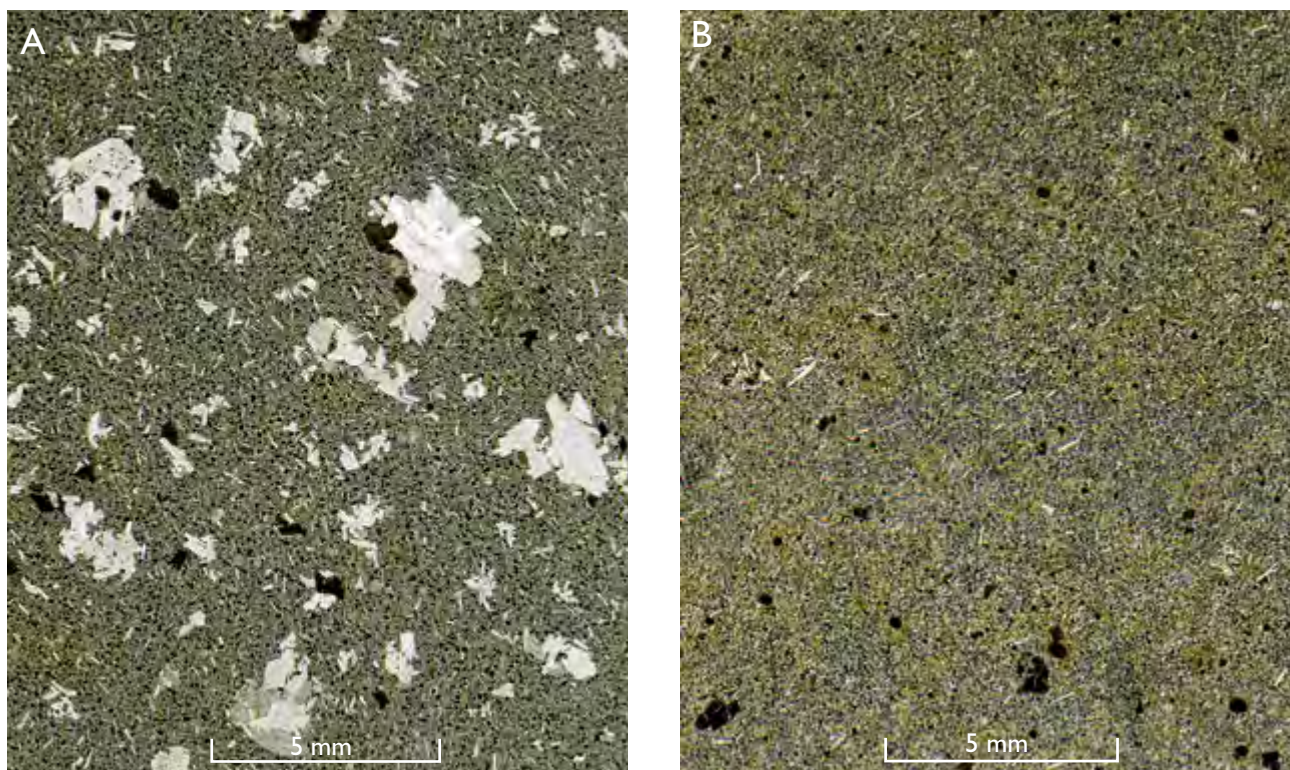


Fig. 34. Thin sections (scanned) of typical lavas from Rinks Dal Member unit 509. **A:** Basalt with numerous glomerocrysts of plagioclase (white), augite (grey) and olivine (dark brown, altered to clay) and smaller single plagioclase and olivine phenocrysts in a fine-grained matrix. Sample GGU 332986, Daugaard-Jensen Dal, south Disko. **B:** Nearly aphyric basalt with a few microphenocrysts of olivine (dark brown, altered to clay) and plagioclase. Sample GGU 332881, Kuugannguaq, northern Disko.



Fig. 35. Typical, c. 30 m thick subaerial lava flow of blocky pahoehoe type with a massive, crudely jointed central part and an oxidised rubbly top. Traces of red lateritic soil occur at the top and base. A patch of brick-red laterite is worked into the flow near its base. Rinks Dal Member unit 509, Lyngmarksfjeld, south Disko.

35; Kilburn 2000) and are visually indistinguishable from most other subaerial flows of the Rinks Dal Member. The flows onlap the flank of the Disko Gneiss Ridge at Killiit (Fig. 7) and west of Tini but overflowed the ridge farther to the east and north (Fig. 36).

The lava flows entered the Assoq Lake in an easterly direction along a palaeoshore that extended for more than 50 km from the south coast of Disko at Blæsedalen and northwards, where much is presently below exposure level. The infill of unit 509 into the lake must have reduced the lake area by more than 1750 km². A northern lake or wetland, which may have been continuous or contemporaneous with the Assoq Lake, existed on north-eastern

Disko between Kuugannguaq and Qullissat (Fig. 15, see also Fig. 48).

The large and relatively thick lava flows of unit 509 that entered the Assoq Lake maintained their coherence, also at subaqueous conditions (e.g. Fig. 56). This is in contrast to the small pahoehoe lobes in the flow fields of unit 507 (as well as the overlying unit 511) which were transformed into pillow lavas and foreset-bedded hyaloclastites. A factor contributing to this difference is probably higher magma flow rates in the large flows of unit 509.

South coast of Disko: Infilling of the southern part of the Assoq Lake

The lake floor. Mudstones of the Assoq Member underlie the volcanic units in the Assoq Lake over large areas on south and south-east Disko (Dam *et al.* 2009, fig. 124), but there are very few exposures due to extensive landslides and solifluction. The contact relations between the subaqueous lavas of unit 509 and the mudstones are therefore only seen at few localities. The westernmost mudstone crops out beneath Skarvefjeld in a small landslide, but the main exposures are farther to the east at Assoq (Larsen *et al.* 2006, fig. 5; Dam *et al.* 2009, figs 138, 139; Fig. 7, profile 6), Niuluut (Larsen *et al.* 2006, fig. 13), and Tuapaat Qaqqaat (Dam *et al.* 2009, fig. 140; Fig. 7, profile 8).

The depth of the Assoq Lake when unit 509 was emplaced was estimated to 200 ± 100 m by Larsen *et al.* (2006).

Subaqueous lava flows. The south coast of Disko contains remarkable exposures of strongly columnar-jointed basalts with brecciated tops interpreted to be subaqueous lava flows (Heinesen 1987; Larsen *et al.* 2006). The subaqueous lava flows extend for more than 25 km from Blæsedalen in the west to east of Siniffik (South Disko section at 82–107 km, unit m₃) and their total thickness is at least 200 m, but over large distances east of Assoq the exposures are poor and fragmented by landslides. The best and most coherent exposures are found between Blæsedalen and Brededal.

The individual subaqueous flows may well exceed 10 km in length; however, the chemical and petrographical homogeneity of unit 509 make correlation across valleys, landslides and talus virtually impossible. Several flows have been mapped continuously for 2–3 km along cliff exposures. The thickness of individual flows varies from 5 m to more than 100 m due to local ponding. In typical cliff sections unit 509 consists of 4–5 subaqueous flows.

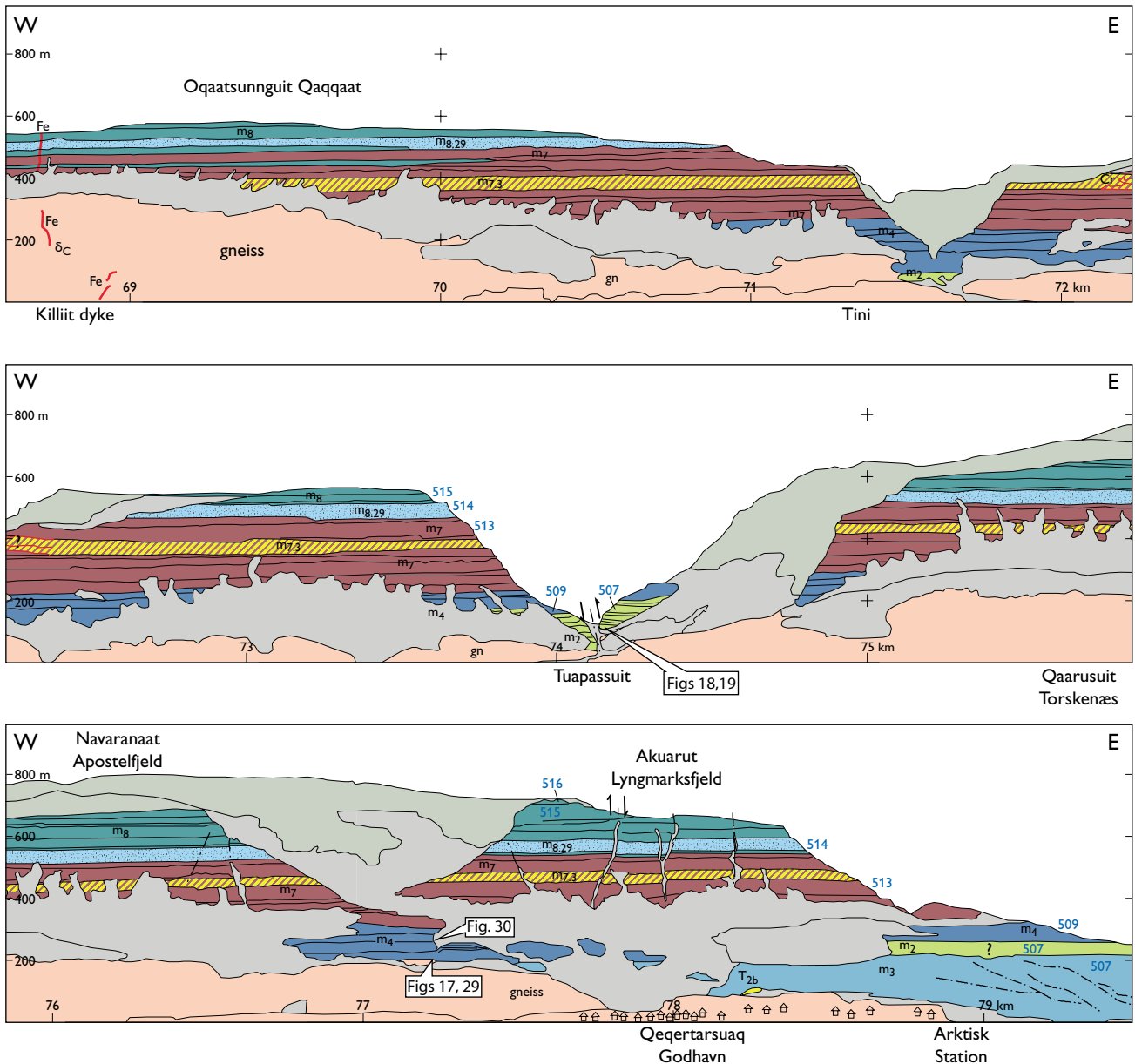


Fig. 36. Photogrammetrically measured section along the coastal cliffs on south Disko between Killit and Arktisk Station near Qeqertarsuaq. Blue three-digit numbers are lithological codes; other annotations as in the original. The brown lava succession is the Akuarut unit (513). Some marker flows are coloured and numbered individually. The locations of some figures are indicated. Excerpt from the South Disko section (Pedersen *et al.* 2003).

Despite their compositional homogeneity, the flows seem to be well separated in time because there are commonly small patches of sediment between them.

Just east of Blæsedalen hyaloclastite and breccia of unit 507 form an E-dipping palaeoslope which is overlain by a thick flow of unit 509 with a regular colonnade at the base and a thick entablature with several tiers; the top is not exposed. There are traces of sediment in small basins at the base of the flow. At sea level around Kuannit the

spectacular columnar-jointed masses of basalt form a local tourist attraction.

In the cliff beneath Skarvefjeld the lowermost flow extends from sea level to *c.* 60 m and has a wavy top surface on which there are accumulations of a few centimetres to decimetres of mudstone in the local depressions (see also Fig. 56).

A typical subaqueous lava flow such as seen at Ippik (Fig. 37) has at its base a few metres thick regular colon-

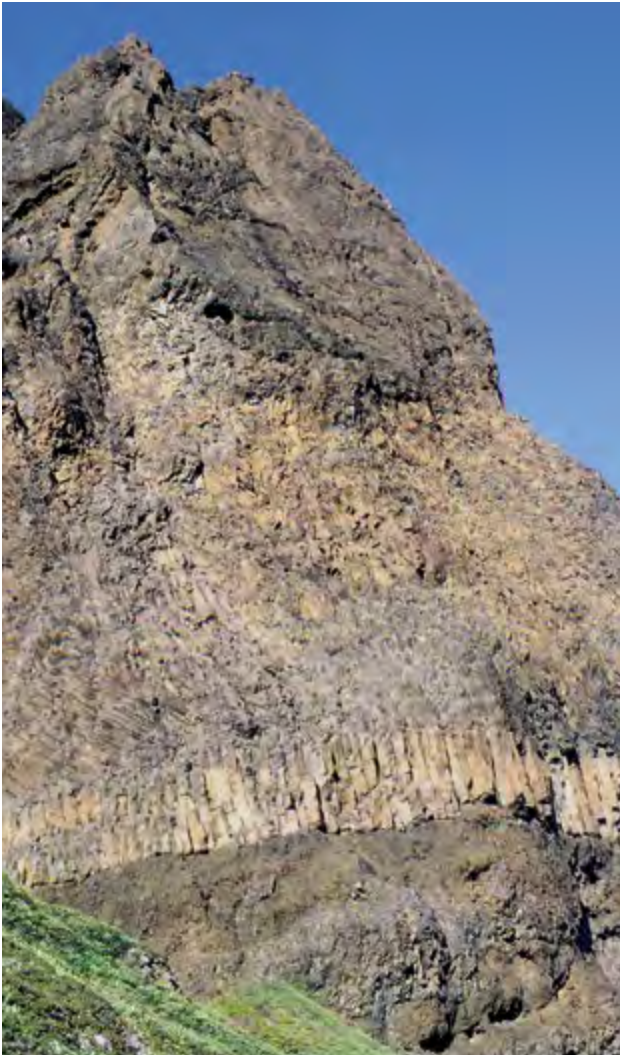


Fig. 37. Typical subaqueous lava flow of unit 509. The basal zone is a regular colonnade a few metres thick, whereas the major part of the flow is in entablature facies with smaller, curved columns that commonly form swirls. The top zone (not seen) is thoroughly brecciated. The part of the flow visible in the photo is *c.* 35 m thick. Ippik, south coast of Disko.

nade which changes abruptly into a 10 m to more than 20 m thick entablature from which lobes may extend upwards into a 5–10 m thick, thoroughly brecciated top zone. Within the top zone itself, and in small depressions on the surface, there may be pockets of volcanoclastic sand and gravel (Fig. 38) that may contain layers of mudstone with plant remains. There is no red-oxidation at the flow top or between flows. The top zone itself is disturbed by the overlying subaqueous flow. Disturbances of the substrate by bulldozing and loading are especially



Fig. 38. Fine-grained volcanoclastic sediment between two subaqueous lava flows (the lower flow is just beneath the outcrop). The lower part of the sediment is normally graded with a weak lamination; the upper part is homogeneous. Note the absence of red oxidation colours. The basal zone of the overlying flow is thoroughly brecciated. Ippik, south coast of Disko.

pronounced where a subaqueous lava flow has run onto unconsolidated mudstone (Fig. 39).

Subaqueous rootless cones. At Niuluut about 20 km from the lake shore, a rootless cone field developed when the first subaqueous lava that flowed onto the lake floor was locally brecciated throughout, providing outlet points for hydroclastic explosions of the pressurised and heated water in the underlying mud (Larsen *et al.* 2006). The cliff section cuts through the centres of two cones (Fig. 40; also shown on a scale of 1:2500 in the South Disko sec-



Fig. 39. A large subaqueous lava flow of unit 509 that has filled a depression within unconsolidated mudstones of the Assoq Member and deformed and probably partly replaced the mud. The colonnade columns are of different heights but always perpendicular to the lower boundary of the flow. Person for scale. The locality is also seen in Fig. 40. Niuluut, south coast of Disko.

tion), and others are probably present both seawards and landwards. The cones are small mounds about 25 m high and 100–200 m wide, composed of normally graded and well-bedded volcanoclastic material intimately mingled with mudstone in up to metre-sized clasts, frequently with plant fragments. In both cones, the bedding dips

away from a central ‘chimney’ that is considered to be the outlet point for the explosions and later filled with shaly sediment. Large pieces of apparent driftwood indicate the proximity of emerged and forested land. Detailed descriptions and interpretations are found in Larsen *et al.* (2006).



Fig. 40. Section through a subaqueous rootless cone. The flank of an adjacent cone is seen to the right. See text and Larsen *et al.* (2006) for descriptions. The cone was covered with mud (**m**) that also filled the central explosion site (chimney). A thick lava flow (white line traces its base) subsequently overran the cones; thin lava tongues invaded the mud overlying the cone flank to the left, and the massive lava subsided into the mud between the cones (Fig. 39). Height of cliff section *c.* 25 m. Niuluut, south coast of Disko.

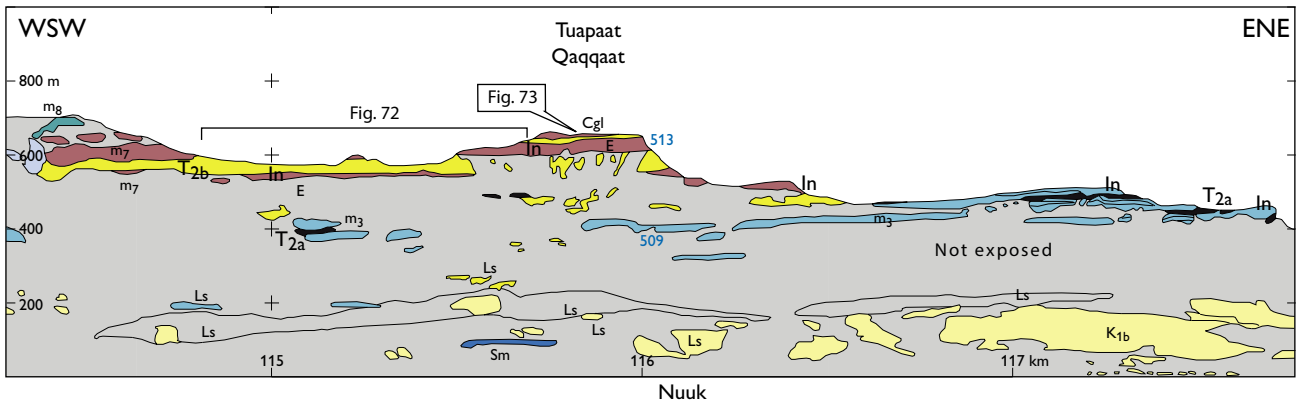


Fig. 41. Lava flows of Rinks Dal Member units 509 (blue) and 513 (brown) invasive (**In**) into Paleocene mudstones (**T_{2a}**) and sandstones (**T_{2b}**) of the Assoq Member of the Atanikerluk Formation. **Cgl**: conglomerate. **Sm**: sill. Pale yellow **K_{1b}**: Cretaceous sandstone. **E**: Entablature. **Ls**: land-slipped exposures. The locations of some figures are indicated. Tuapaat Qaqaat, south coast of Disko, excerpt from the South Disko section (Pedersen *et al.* 2003).

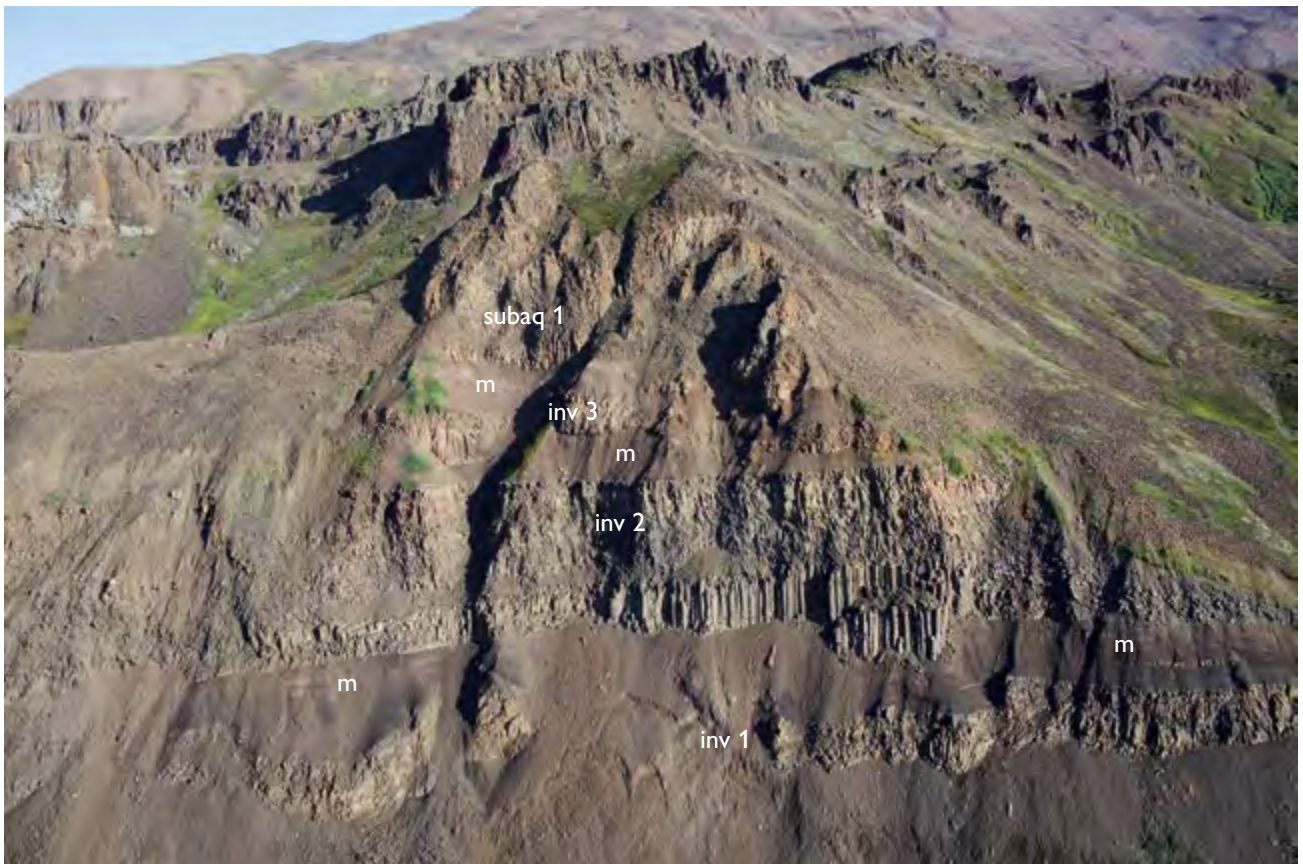


Fig. 42. Lava flows of Rinks Dal Member unit 509 invasive into dark brown mudstones (**m**) of the Assoq Member at its type locality. There are three successive, invasive, sill-like flows (**inv 1** to **inv 3**) and a thick subaqueous flow (**subaq 1**). Note the colonnades at both base and top of **inv 2**. The exposure is about 100 m high and is slightly slipped and rotated. Assoq just east of Brededal, south coast of Disko. Photo: Erik Vest Sørensen.

Invasive lava flows. A number of basaltic sill-like bodies crop out over a distance of more than 23 km between Assoq and Tuapaat Qaqqaat (South Disko section at 95–118 km (Fig. 41); in small gullies along the coast there are sometimes fragmentary exposures of mudstone beneath, between and above them. The sills are chemically and petrographically identical to the subaerial and subaqueous lava flows of unit 509. The complete absence of any feeder bodies led Larsen & Pedersen (1990) to conclude that the sills are invasive lava flows formed when subaqueous flows invaded unconsolidated Assoq Member sediments and continued their eastward flow as sills.

The sill-like invasive lava flows may show planar, concordant lower and upper contacts to the mudstone, or they may form more irregular bodies. At the upper contacts, there may occasionally be pillow bodies, and small apophyses may extend from the lavas to form auto-brecciated hyaloclastite. The 'sills' may show well-developed upper and lower colonnades and, in the central part, an entablature zone of small, irregular columns. The best exposures are in the type section of the Assoq Member in a landslide at Assoq just east of Brededal (Fig. 42; Dam *et al.* 2009, fig. 138 and 139; Larsen *et al.* 2006, fig. 6). Here three to four successive invasive lava flows are embedded in mudstone and underlying sandstone (Fig. 7, profile 6). They are covered by 3–4 subaqueous lava flows, which are broken up into several smaller landslides and are not seen in continuity (Fig. 42). Some samples of the mudstones between the flows contain dinoflagellate cysts (Piasecki *et al.* 1992; H. Nøhr-Hansen, personal communication 2017).

On the south coast of Disko invasive lava flows are relatively well preserved along a W–E oriented ridge extending from Tuapaat Qaqqaat to Tuapaat at the coast (South Disko section at 116 to 118 km (Fig. 41; Fig. 7, profile 8). Here both the lower and upper contacts between mudstone of the Assoq Member and four invasive lava flows of unit 509 are preserved. They are overlain by sand with at least two invasive flows of unit 513.

The upper boundary of unit 509 is poorly exposed between Assoq and Tuapaat Qaqqaat but seems to have been entirely beneath the surface of the Assoq Lake (Fig. 7). To the west, beneath Skarvefjeld, subaqueous lava flows of unit 509 with traces of mudstone on top are covered by up to 160 m of regularly foreset-bedded hyaloclastites of unit 511 (see also Fig. 56). Heinesen (1987) provided evidence of semi-continuous subsidence of the Assoq basin in the western part of Skarvefjeld in the time interval of the eruption of the overlying lava plateau; if subsidence also took place during the emplacement of

the subaqueous parts the 160 m height of the foresets is a maximum depth for the lake overlying unit 509.

Daugaard-Jensen Dal. Complete filling of the central Assoq Lake took place about 30 km farther to the north in Daugaard-Jensen Dal (Fig. 8, profile 5) where 210 m of subaqueous lavas and a single subaerial lava flow of unit 509 can be observed in the northern wall of the valley (Fig. 43). There are several typical subaqueous lava flows with well-preserved, thick top zones of pillow breccia with metre-sized pillows and pillow tubes. One of the top zones encloses up to metre-sized boulders of basaltic lava, which are talus fragments from the palaeoshore carried into the lake by the later lava flow (Fig. 44). The uppermost subaqueous flow is covered by a 35–40 m thick lava flow that has a well-developed colonnade and entablature zone and a thick scoriaceous top zone which is slightly high-temperature oxidised and obviously subaerial.

The northern basin in the Kuugannguaq–Qullissat area

Lava flows and breccias of unit 509 form the basal part of the Maligât Formation over large areas on north-eastern Disko between the inner Kuugannguaq valley and the Vaigat coast around Qullissat (see also Fig. 48). Here unit 509 onlaps the Vaigat Formation, and the volcanic rocks display a considerable range of morphologies depending on the nature of the environment in which they were emplaced. In large areas unit 509 is concealed below younger basalts or glaciers, scree or landslides. However, semi-continuous exposures of the succession occur in three, more than 10 km long, subparallel sections oriented approximately NW–SE. Two sections form the walls of the inner part of the Kuugannguaq valley and are only 2–3 km apart, whereas the third section comprises the coastal slopes along the Vaigat strait 15 km north-east of Kuugannguaq.

Kuugannguaq valley. On both walls of the inner part of the Kuugannguaq valley (map sheets Qutdligssat and Pingu), lava flows of unit 509 are seen onlapping the gently SE-sloping top surface of the Vaigat Formation. The geology of both walls has been compiled from long photogrammetric panels, and the succession has been sampled in a profile on the north-eastern wall where unit 509 is 240 m thick (Fig. 9, profile 5); the north-eastern wall is shown in the Central Disko section at 51.5–60.5 km where the sample profile is situated at 55–56 km. The

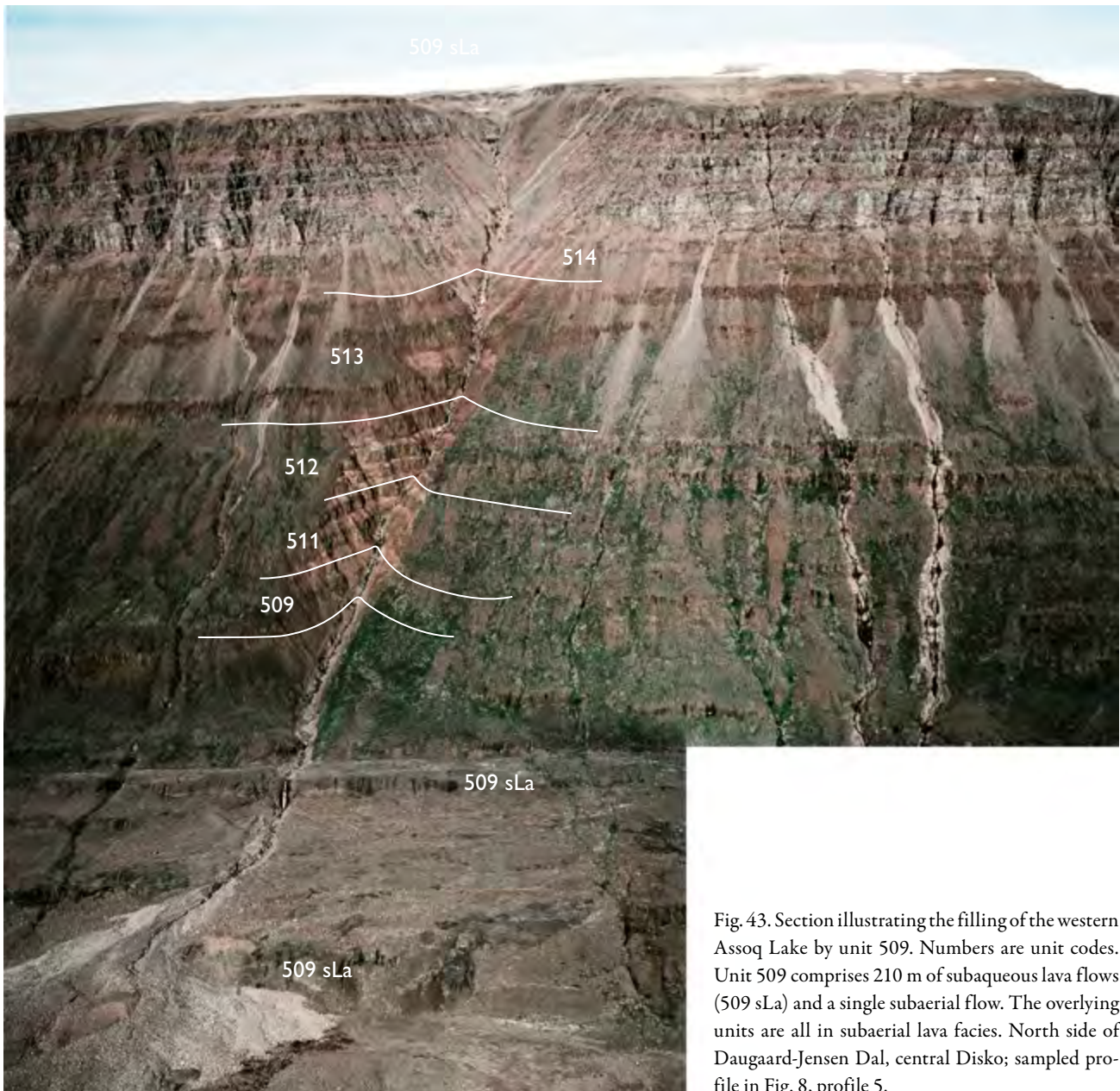


Fig. 43. Section illustrating the filling of the western Assoq Lake by unit 509. Numbers are unit codes. Unit 509 comprises 210 m of subaqueous lava flows (509 sLa) and a single subaerial flow. The overlying units are all in subaerial lava facies. North side of Daugaard-Jensen Dal, central Disko; sampled profile in Fig. 8, profile 5.

distances to the nearest investigated exposures of unit 509 to the south and south-east are around 25 km.

In Kuugannguaq the lavas of unit 509 encountered waterlogged or water-covered areas which were either an extension of the Assoq Lake or a separate wetland. The volcanic morphologies record two phases of interaction between the inflowing magmas and water in the subsiding basin. The first phase is seen in both valley walls but is best exposed in the south-western wall. Here the basal part of unit 509 comprises a group of several strongly brecciated lava flows up to 40 m thick, which can be followed for about 5 km towards north-west, petering out

to 0 m by onlap onto the Vaigat Formation. These flows are overlain by a few entirely subaerial lava flows, which step directly onto the Vaigat Formation for 5–6 km farther towards north-west (Fig. 45). There are three such flows in the south-west wall and two thinner ones in the north-east wall (Fig. 46), indicating that the flows arrived from a south-westerly direction. The flows were probably deflected by the SE-sloping surface of the Vaigat Formation and channelled along this.

Continued basin subsidence led to renewed accumulation of water in the area. A second water-influenced phase is indicated by a renewed occurrence of brecci-



Fig. 44. Top zone of a subaqueous lava flow of unit 509 enclosing a large boulder of subaerial basalt lava as well as the usual pillows and pillow fragments. The lava boulders are older talus fragments from the palaeoshore carried into the lake by the lava flow. North side of Daugaard-Jensen Dal, central Disko.

ated flows and flows with distinct development of colonnades and entablature zones, followed by a huge ponded lava flow with a large, regular colonnade (Figs 45, 46). This lava packet is well exposed on both valley walls and is thicker in the north-east wall than in the south-west wall, suggesting a somewhat deeper basin to the north-east, filled during continued volcanic inflow from the south-west. These lavas extended 5–10 km farther to the north-west than those of the first phase. The large ponded lava flow can be followed for at least 9–10 km on both valley sides and locally attains a thickness of 70–80 m. It covers more than 50 km² and has a volume

well above 2–3 km³. Towards the south-east it seems to consist of several separate subaqueous lava tongues. Towards the north-west it forms a single distinct flow with load structures towards the underlying volcanoclastic sediment (Fig. 46); its colonnade becomes thicker, continuous, and extremely regular, whereas its top gradually develops scoria and becomes high-temperature oxidised. Farther towards the north and north-west the flow thins against the sloping surface of the Vaigat Formation and the colonnade becomes coarse and less regular until the flow has the appearance of an entirely subaerial lava flow (Fig. 47). This flow provides the best example from the Maligât Formation of the morphological variations of a basaltic lava flow emplaced under changing wet and dry conditions.

Qullissat coastal section. The exposures along the Vaigat coast comprise a c. 11 km long, SE–NW-oriented section extending from just north of Qullissaaqqat (Gamle Qullissat) in the south-east to Killerpaat Qaqqarsuat north-west of Qullissat, shown in Fig. 48. In the north (Fig. 48 at 7.3–>11 km), subaerial picritic lava flows of the Vaigat Formation form a gently SE-sloping surface, similarly to the setting in the inner part of Kuugannguaq. At 6.2 to 7.3 km, the Vaigat Formation terminates in c. 200 m high fans of bedded hyaloclastite deposits. These are covered by lacustrine mudstone except where the sediments have been removed by a glacier. The mudstone is tentatively referred to the Assoq Member on the basis of its mineralogy, indicating that the Assoq Lake, or a contemporaneous lake, extended into this area. Maligât Formation lavas of unit 509 overlie sediments and the Vaigat Formation throughout the section, but to the south, the boundary and the lower part are poorly exposed because of talus and landslides (Fig. 48 at 2–6.5 km).

Unit 509 is up to 150 m thick in the Qullissat section and composed of one to four lava flows, most of which are strongly affected by emplacement over a wet or fully water-covered surface (Fig. 10, profiles 4, 5). In the mountain wall beneath Killarpaat Qaqqarsuat three voluminous lava flows are exposed which have very prominent dark grey entablature zones and olive grey brecciated tops (Fig. 49). The top zone of the lowermost flow is entirely a subaqueous pillow breccia, whereas the second flow top is dominated by pillow breccia with metre-sized pillows and also contains patches of high-temperature air-oxidised scoria, showing that this flow for a time completely displaced the water. The third flow also has a top of partly glassy breccia and partly oxidised scoria and was emplaced after return of the water to this part of the

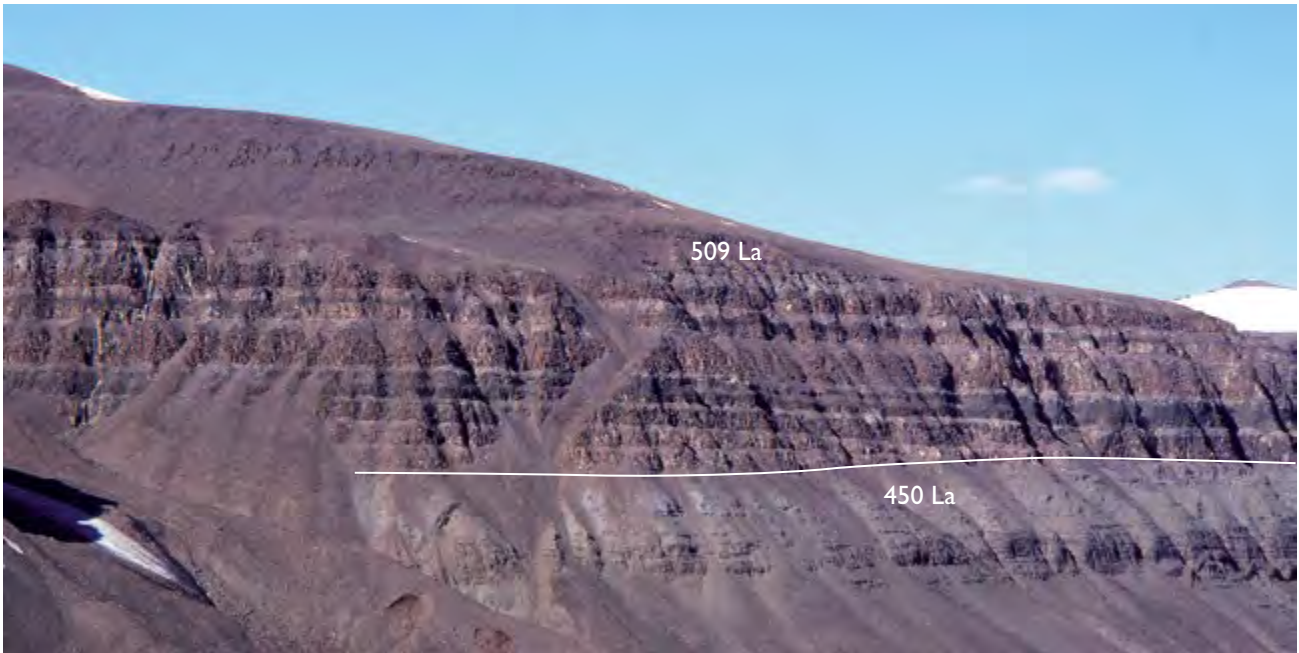


Fig. 45. Lava flows of Maligât Formation unit 509 onlapping the gently sloping surface of the Vaigat Formation (450 La). The three lowest flows of unit 509 are subaerial, the following dark flow is brecciated, and the overlying thick flow is ponded. Height of exposure *c.* 400 m. South-western wall of the inner Kuugannguaq valley *c.* 45 km from the mouth of the valley.



Fig. 46. Subaerial picrite flows of the Vaigat Formation unit 450 overlain by basalt flows of the Maligât Formation unit 509. There are two subaerial flows with a reddish soil horizon between them, a black volcaniclastic sediment and a thick subaqueous flow (509 sLa) with irregular base because of loading into the soft sediment. Height of field of view *c.* 100 m. North-eastern wall of the inner Kuugannguaq valley *c.* 45 km from the mouth of the valley.

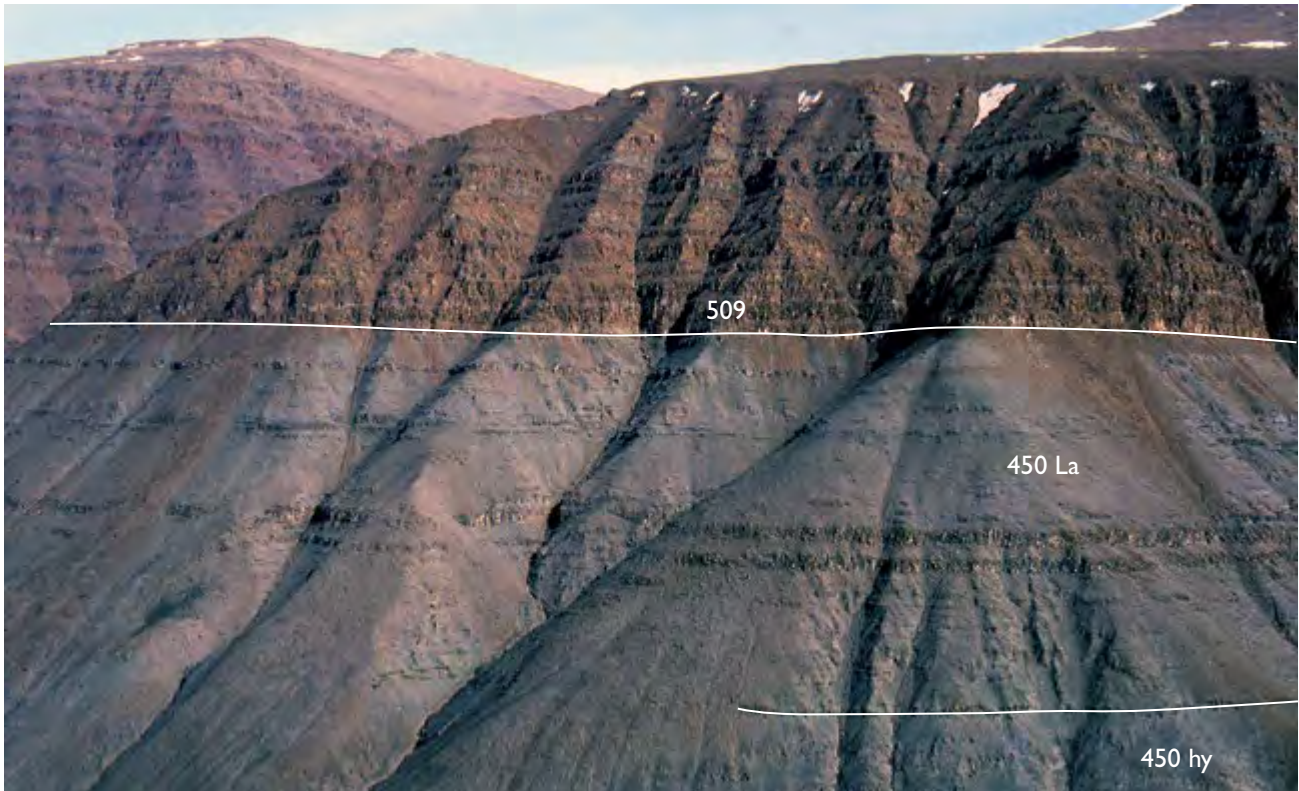


Fig. 47. Picrite hyaloclastites (450 hy) and subaerial lava flows (450 La) of the Vaigat Formation overlain by entirely subaerial flows of the Maligât Formation unit 509. The lowest flow, thinning towards the north (left), is the same as the thick ponded flow shown in Figs 45, 46. Height of field of view *c.* 500 m. North-eastern wall of the inner Kuugannguaq valley *c.* 40 km from the mouth of the valley.

subsiding basin. Farther to the north-west, just north of Fig. 48, only one of these flows has well developed colonnade and entablature; it has an entirely oxidised and scoriaceous top and marks the final infilling of the wetland in this part of Disko. Five kilometres farther to the north-west, at Asuutaa, unit 509 consists of one or two entirely subaerial lava flows with a total thickness of less than 40 m (Fig. 10, profile 2).

In the central part of the Qullissat section, where Vaigat Formation hyaloclastites are covered by mudstones and sandstones of the Atanikerluk Formation, a columnar-jointed sill is intruded into the sediments (Fig. 48); see also Pedersen *et al.* (2017, fig. 162). The sill has a composition typical for unit 509 and is interpreted as an invasive lava flow. Its continuation into the normal lava package is obscured by landslides.

In the south-eastern part of the Qullissat section, at Inussuk, unit 509 consists of three or four entirely subaqueous lava flows with glassy brecciated top zones. In one of the flows, the top zone is a 10 m thick stratified hyaloclastite. The lower part of unit 509 is here covered by landslides.

As in Kuugannguaq, the basalts of unit 509 reached the Qullissat area from the south-west and overlapped the gently SE-sloping top surface of the Vaigat Formation.

Unit 511 (Skarvefjeld unit)

Composition. The Skarvefjeld unit represents a shift in chemical composition. The defining feature is that, for a given *mg*-number (atomic $100\text{Mg}/(\text{Mg} + \text{Fe}^{2+})$), the lavas of the Skarvefjeld unit have significantly higher TiO_2 contents than the lavas of the earlier units, so much that in a plot of TiO_2 versus *mg*-number there is little or no overlap between the Skarvefjeld unit and the earlier units (see also Fig. 97). The lavas of the Skarvefjeld unit have TiO_2 contents of 1.9–2.8 wt%; most of them have MgO contents of 6–9 wt% but the unit also includes magnesian rocks with MgO contents of 10–25 wt%; of the 13 samples from the Rinks Dal Member with MgO >10 wt%, 11 are from the Skarvefjeld unit.

It is sometimes difficult to chemically distinguish the most evolved lavas of unit 511 from unit 512. This is understandable in view of the interpretation by Larsen &

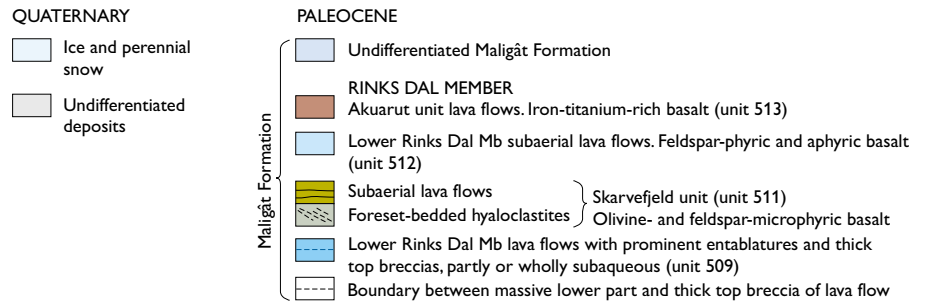
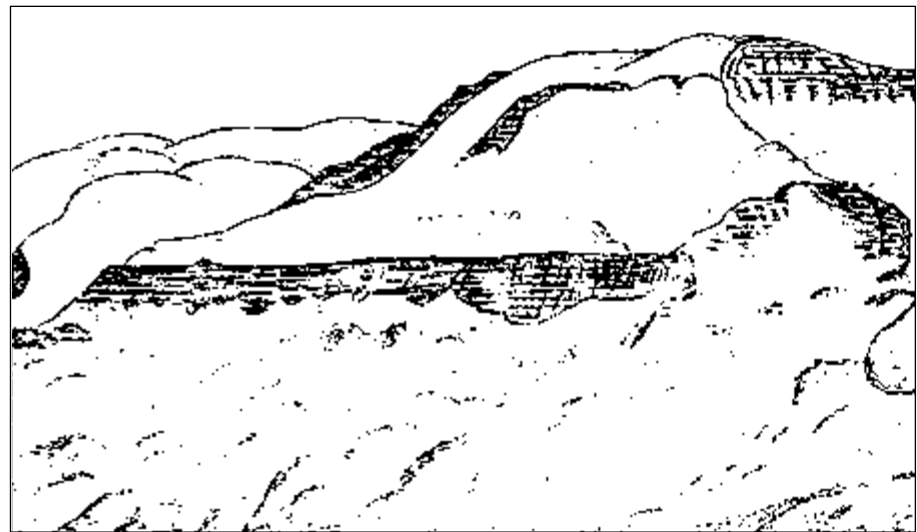
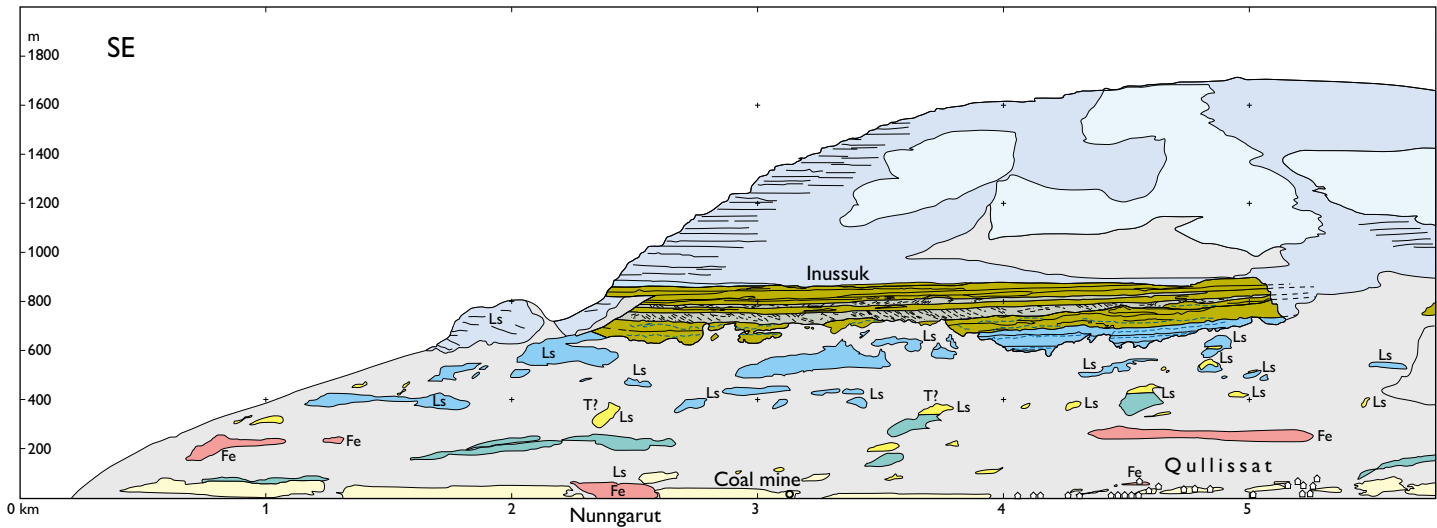
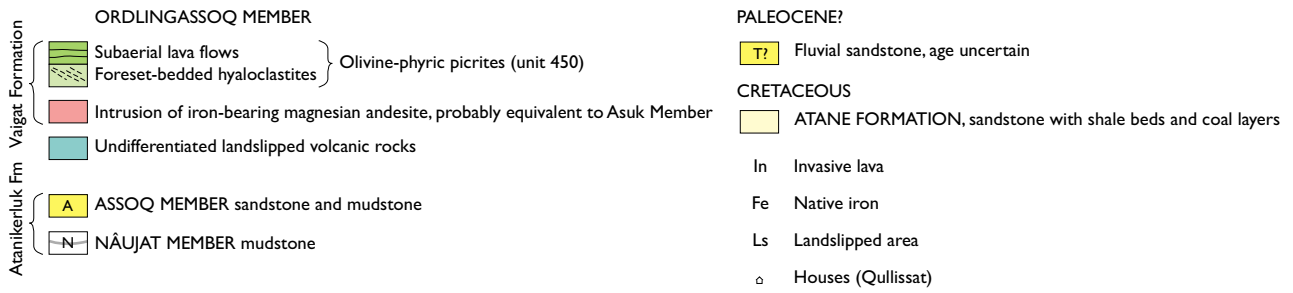
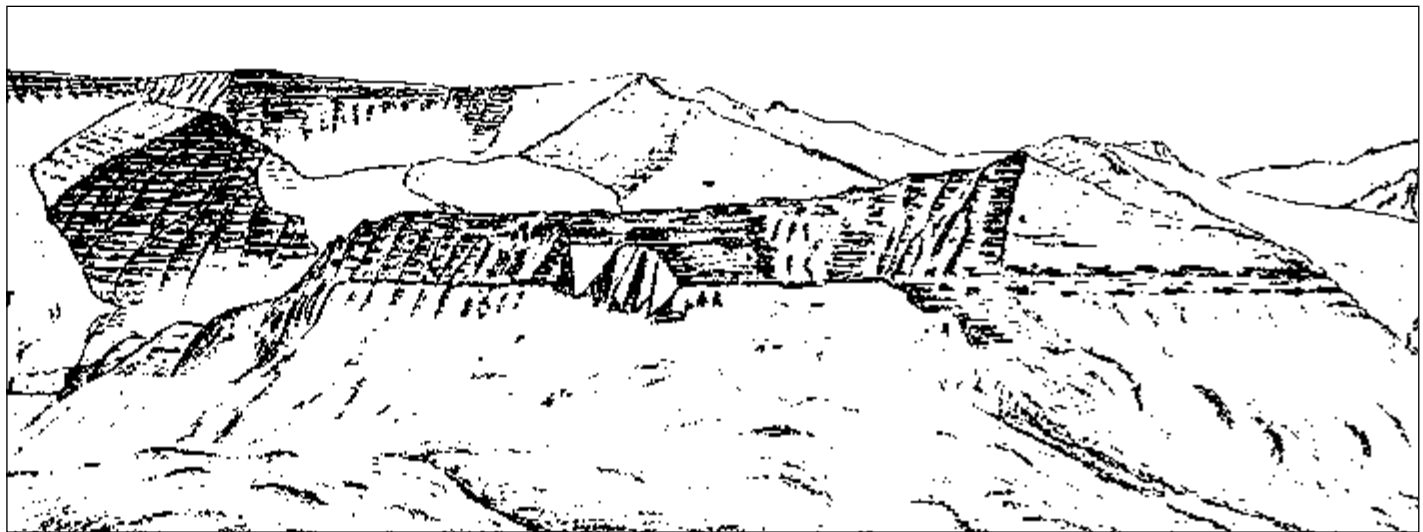
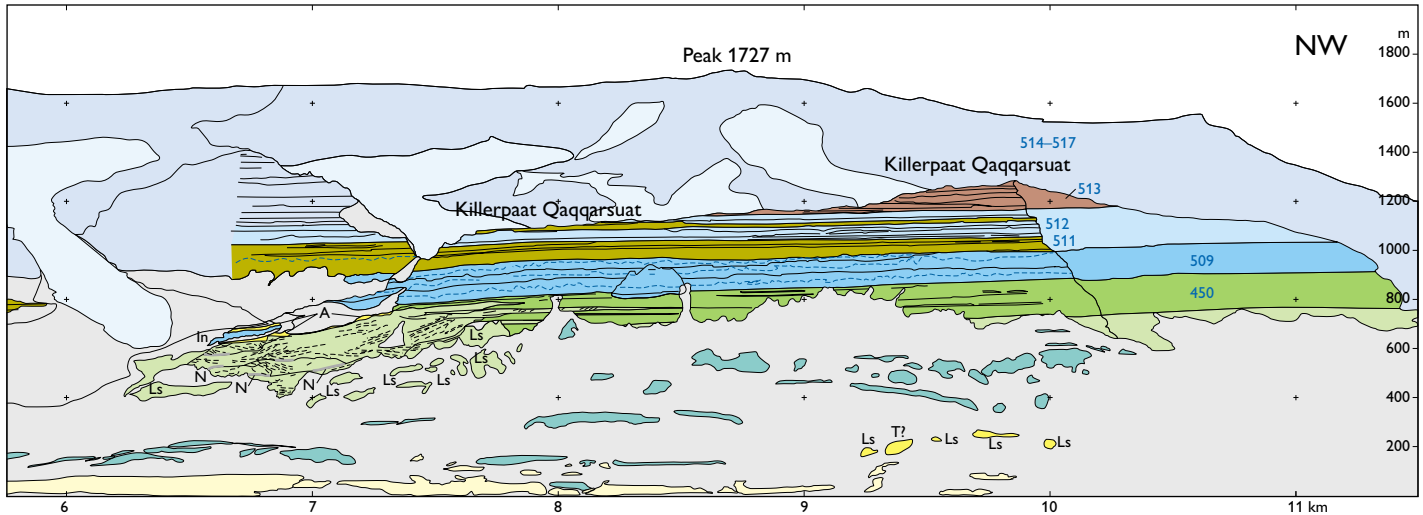


Fig. 48. Photogrammetrically measured section along the north coast of Disko around Qullissat. A pencil drawing by R.R.J. Hammer of the same coastal section (from Steenstrup 1900) is shown for comparison. Numbers are lithological unit codes.

Pedersen (2009) that the Skarvefeld unit is the result of incomplete mixing of the evolved magma residing in the deep-seated magma chamber with a new batch of primitive magnesian magma. Thus unit 512 represents the residing magma which in principle grades continuously into the mixed magma at the evolved end of the mixing curve. This also explains the local co-occurrence of lavas

of unit 511 and 512, as in the profiles in Kuugannguaq (Fig. 9), Asuutaa and Killerpaat Qaqqarsuat (Fig. 10).

Petrography. The most magnesian rocks of the Skarvefeld unit (with MgO >10 wt%) are strongly olivine-phyric and similar to picrites of the Vaigat Formation. These lavas are confined to a small area around Orlingasog on

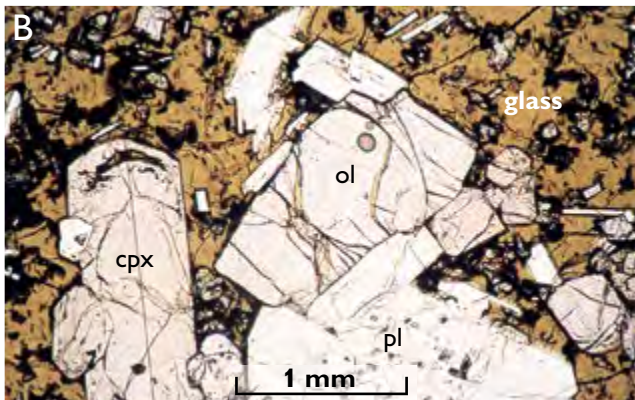
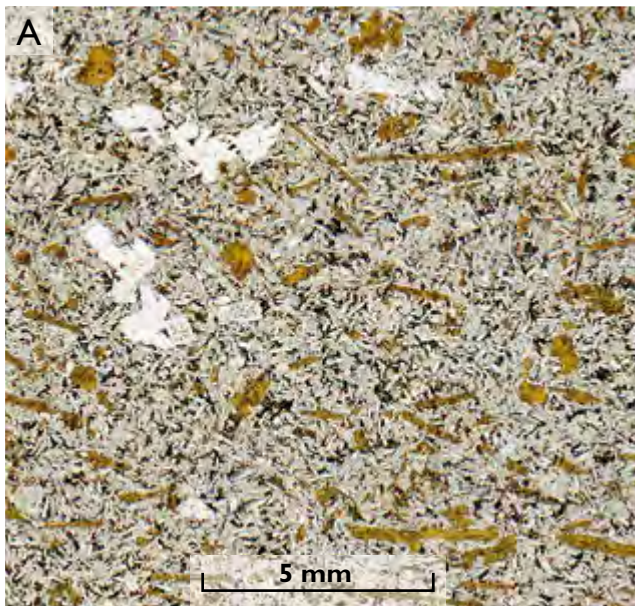


north-eastern Disko where they are intercalated with less magnesian lavas of the same unit (Fig. 10, profiles 1, 2). Basalts with 7–10 wt% MgO are characterised by a few equidimensional olivine phenocrysts and abundant skeletal, frequently platy, olivine microphenocrysts, and by microphenocrysts of plagioclase which increase in abundance as MgO decreases to 7 wt% (Fig. 50A). Tiny semi-

transparent chromite crystals occur enclosed in olivines in these rocks. Basalts with 6–7 wt% MgO have augite as an additional phenocryst phase to olivine and plagioclase, and some rocks contain glomerocrysts of augite, plagioclase and olivine (Fig. 50B).



Fig. 49. Facies of the Maligât Formation at the north-western shore zone of the Assoq Lake basin. Subaerial picrite flows of the Vaigat Formation unit 450 are overlain by two voluminous lava flows of Maligât Formation unit 509 with very prominent dark grey entablature zones and light grey brecciated tops, indicating emplacement into water. These are followed by subaerial flows of units 511–513. The height of the exposed section is c. 600 m. Killerpaat Qaqqarsuat, north Disko (north-western part of the coastal section in Fig. 48). Photo: Erik Vest Sørensen.



Distribution. The distribution of the Skarvefjeld unit is shown in Fig. 15. The Skarvefjeld unit is centred on Disko east of the gneiss ridge but is also present on western Disko and south-eastern Nuussuaq (Fig. 15; Larsen & Pedersen 1990, fig. 4). On eastern and southern Disko the unit is easily distinguished lithologically as a compact package of foreset-bedded hyaloclastites capped by their equivalent subaerial facies of thin pahoehoe lava flows. With this morphology the unit has been mapped on the 1:100 000 scale geological maps Uiffaq 69V.1S and Pingu 69V.2N (unit β fph2), as well as on the 1:20 000 geological sections (South Disko section, Central Disko section). The unit is well exposed on the south coast of Disko between Skarvefjeld and Ippik where it is up to 180 m thick, and on eastern Disko around Kvandalen and Blåbærdalen where thicknesses are 50–150 m. It is

Fig. 50. Thin sections of rocks from Rinks Dal Member unit 511, Skarvefjeld unit. **A:** Typical basalt lava with a few equidimensional olivine phenocrysts and abundant skeletal, commonly very elongate olivine phenocrysts (all altered to yellowish brown clay) together with a few plagioclase glomerocrysts (white) in a medium-grained groundmass. Scanned thin section. Sample GGU 362315 (MgO = 7.3 wt%), Laksedalen, eastern Disko. **B:** Pillow breccia of basalt with glomerocrystic plagioclase (pl), fresh olivine (ol) and augite (cpx) in a glassy groundmass with tiny crystals of the same phases. Microphotograph, plane polarised light. Sample GGU 176765 (MgO = 6.5 wt%), Skarvefjeld, south Disko.

also present on northern Disko around Qullissat where it is *c.* 200 m thick and shows a morphological variety comprising subaqueous lava flows, foreset-bedded hyaloclastites and associated thin subaerial pahoehoe lava flows, and thick subaerial lava flows (Figs 48, 49).

On central and northern Disko, lavas of the Skarvefjeld unit are in subaerial facies and lithologically indistinguishable from the surrounding lavas. Two to five flows referred to the Skarvefjeld unit are present in nearly all profiles from Orpiit Qaqqat to Daugaard-Jensen Dal, Sorte Hak, Kuugannguaq, Orlingasoq and Qullissat, commonly intercalated with flows referred to unit 512, as explained above. On southern Nuussuaq one to two water-influenced flows are found lowest in the profiles at Giesecke Monument and Eqi.

Lithologies. The volcanic rocks of the Skarvefjeld unit occur as subaerial and subaqueous lava flows, pillow lavas, hyaloclastites and volcanoclastic beds. The successions of thin pahoehoe flows and foreset-bedded hyaloclastites, to which all the picritic rocks belong, show considerable lithological similarity to the picritic rocks of the Vaigat Formation. Many lavas form flow fields consisting of many thin flow lobes with ropy flow surfaces, testifying to the fluid character of the magma (Fig. 51). Subaerial lava flows with MgO > 10 wt% tend to develop subhorizontal, vesiculated segregation veins (Fig. 52).

Soil layers of centimetre to decimetre thickness within the succession show that the Skarvefjeld unit was erupted in several phases separated by sufficient time intervals to allow soil formation.



Fig. 51. Well-preserved ropy surface of a thin pahoehoe lava flow in the Skarvefjeld unit. South-western slope of Qinnngusaq mountain, innermost head of Kvandalen valley, east Disko.



Fig. 52. A 7 m thick subaerial pahoehoe flow of olivine-rich basalt of the Skarvefjeld unit (511) with subhorizontal, vesiculated segregation veins. The overlying flow is a feldspar-phyric basalt also of unit 511. Ridge between Frederik Lange Dal and Charles Polaris Dal, east Disko (Fig. 10, profile 9 around 600 m). The background shows the same succession in the north wall of Charles Polaris Dal. For location, see Fig. 140.



Fig. 53. Pillow lava of the Skarvefjeld unit: basalt pillows in a brown-weathering matrix of volcanic glass, formed close to the entry point of the flow into the Assoq Lake. Length of hammer 32 cm. North side of Frederik Lange Dal, east Disko; for location, see Fig. 140.



Fig. 54. Relatively fine-grained hyaloclastite with a few larger clasts deposited as a sediment gravity flow distally from the entry point of the lava flow into the Assoq Lake. About 15 cm of the underlying Assoq Member siltstone are seen lowest in the photo. Length of hammer 55 cm. Innermost head of Kvandalen, east Disko; for location, see Fig. 140.

Where the pahoehoe flows entered the Assoq Lake, pillow lavas (Fig. 53) and hyaloclastites were formed, and volcanoclastic sediments occur as distal deposits along the basin floor (Fig. 54). These sediments frequently contain scattered fragments of silicified wood or coal. Mudstone of the Assoq Member is occasionally exposed beneath the volcanic rocks (Fig. 55).

The Skarvefjeld unit formed the western shore zone of the Assoq Lake for nearly 100 km from south to north across Disko (Fig. 15). It prograded into the lake in a general easterly direction until the magma was exhausted. Despite the fact that much of unit 511 is composed of pahoehoe flow fields which are unlikely to have flowed individually for more than at most a few tens of kilometres and hence must have been erupted on the present Disko, no trace of any feeder dykes or necks have been

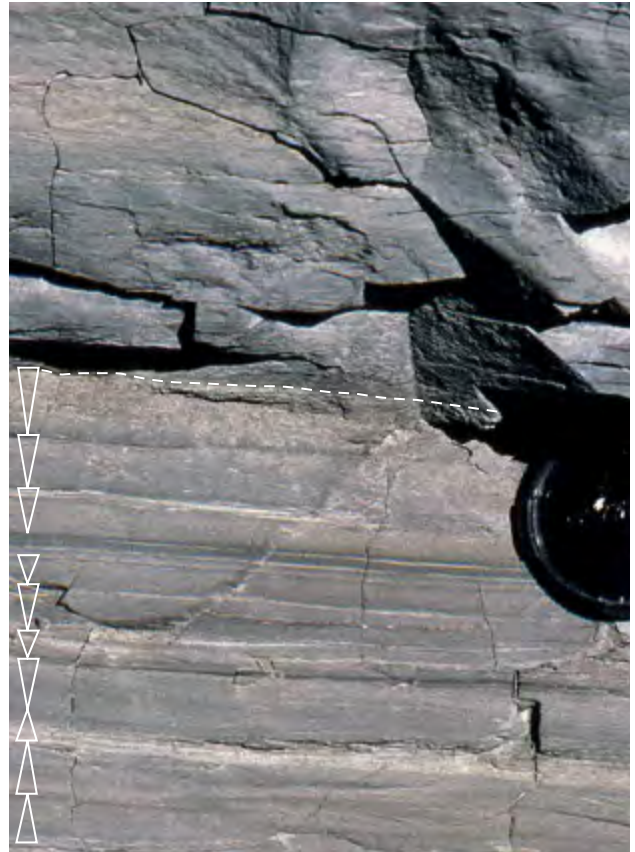


Fig. 55. Laminated, silt-streaked mudstone with normal and inverse grading (shown by white open triangles at left) deposited from distal density currents, overlain by nearly homogeneous mudstone (above dashed line). Assoq Member underlying the Skarvefjeld unit, detail of loose boulder; diameter of lens cap 5 cm. Innermost head of Kvandalen, east Disko; for location, see Fig. 140.

located. Three subareas of inflow into the Assoq Lake can be recognised and are described below.

South coast of Disko around Skarvefjeld

The south coast of Disko around Skarvefjeld has been described by Heinesen (1987), Larsen & Pedersen (1990) and documented by Pedersen *et al.* (2000) and in the South Disko section. The Skarvefjeld unit is exposed in the coastal cliffs over a distance of *c.* 7 km from Skarvefjeld in the west to the western side of Brededal in the east (South Disko section at 84.3–91.3 km). Here it forms a 80–100 m thick succession of foreset-bedded hyaloclastites and an overlying 30–40 m thick succession of pahoehoe flow lobes with transitional breccia facies at the interface between lavas and hyaloclastites (Fig. 7,

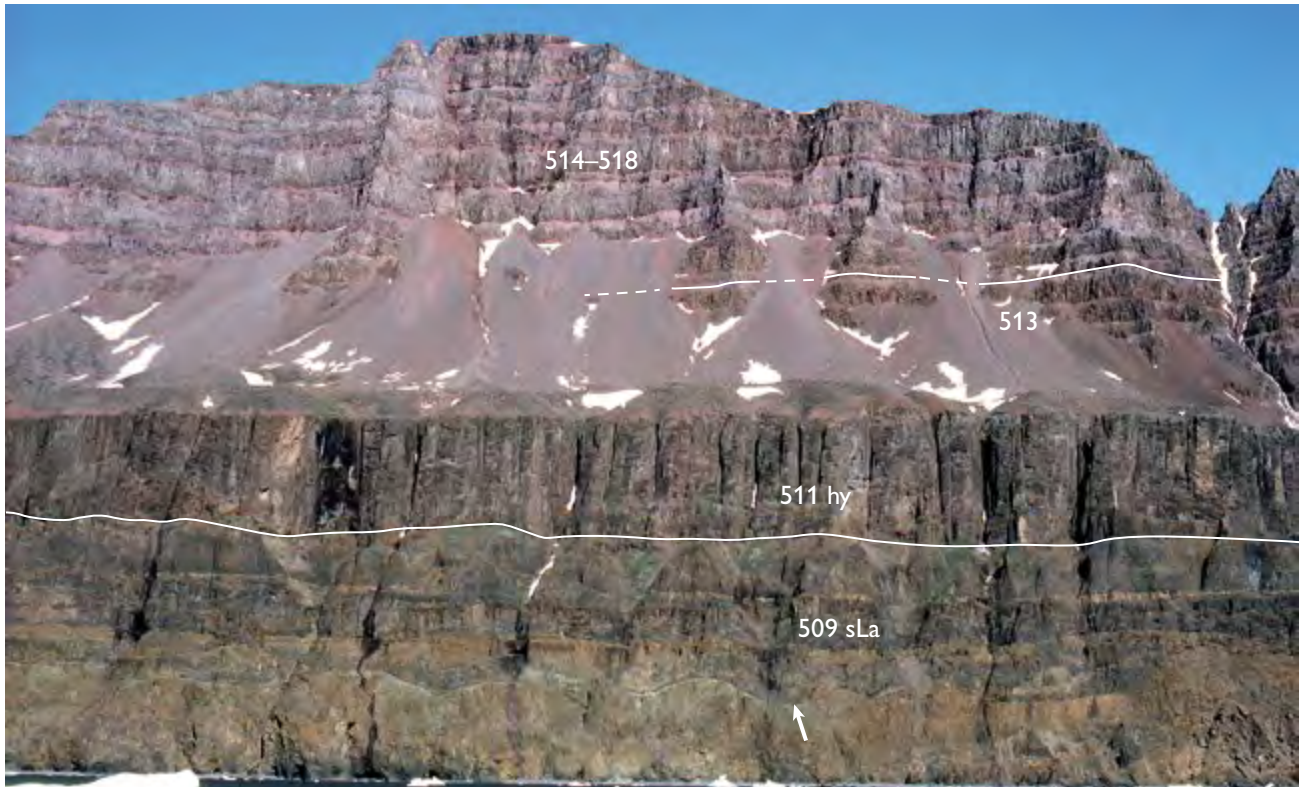


Fig. 56. Systematic upward changes of volcanic facies in the succession beneath Skarvefjeld, demonstrating the filling of the Assoq Lake basin. The lowest unit (509) is 160 m thick and comprises at least four subaqueous lava flows with thick, yellowish brown breccia tops (509 sLa); deposits of mudstone have accumulated in the lows on the undulating surface of the lowest flow (arrow). The overlying Skarvefjeld unit comprises an 80 m thick horizon of foreset-bedded hyaloclastite (511 hy; the foresets dip towards the viewer); the associated overlying subaerial pahoehoe flows are concealed beneath scree. Scree also conceals a few flows of unit 512 and a thin horizon of quartzo-feldspathic sandstone, probably a fluvial deposit. The following units 513 to 518 are all in subaerial facies with red-oxidised top rubble. Cliff face, 920 m high, beneath Skarvefjeld, south coast of Disko just east of Qeqertarsuaq town; see also Figs 57, 58, 89.

profile 4). The foresets dip consistently S to SE, showing that the subaerial lavas flowed into the Assoq Lake basin from the north and north-west. Individual foresets can be followed from the palaeoshore to the basin floor and demonstrate a lake depth of 80–100 m at the time (Figs 56–57, 89). The hyaloclastites are separated from the underlying subaqueous lava flows of unit 509 by an up to a few decimetres thick veneer of dark mudstone, which may be disturbed by the hyaloclastites. The western and eastern margins of unit 511 are unexposed due to scree or erosion.

At Ippik the top of the subaerial lava flows of the Skarvefjeld unit is eroded and covered by a *c.* 2 m thick bed of fine-grained yellow sandstone with millimetre-sized clasts of quartz and chert but entirely devoid of Tertiary volcanic components. The sandstone is a distal facies of sandstone from the Assoq Member (Dam *et al.* 2009) which is well exposed at Tuapaat Qaqqat some 25

km to the east (Fig. 41; also Fig. 72). The sandstone at Ippik is covered by lava flows of unit 512 (Figs 57–58). All the basalts of the Skarvefjeld unit along the south coast of Disko show a narrow compositional range (6.1–6.5 wt% MgO) and could have originated from the same flow field.

East Disko around Kvandalen

The lavas and hyaloclastites of the Skarvefjeld unit are shown as unit $\beta_{\text{fph}2}$ on the map sheet Pingu (Pedersen *et al.* 2001). On the Central Disko section at 79.5–93 km, they comprise units m_5 (foreset-bedded hyaloclastites) and m_6 (lava flows) in the inner part of Kvandalen. Three localities aligned NW–SE for about 30 km (inner Kvandalen, Charles Polaris Dal and Point 1123 m) illustrate the compositional and lithological variation of the Skarvefjeld unit on eastern Disko.

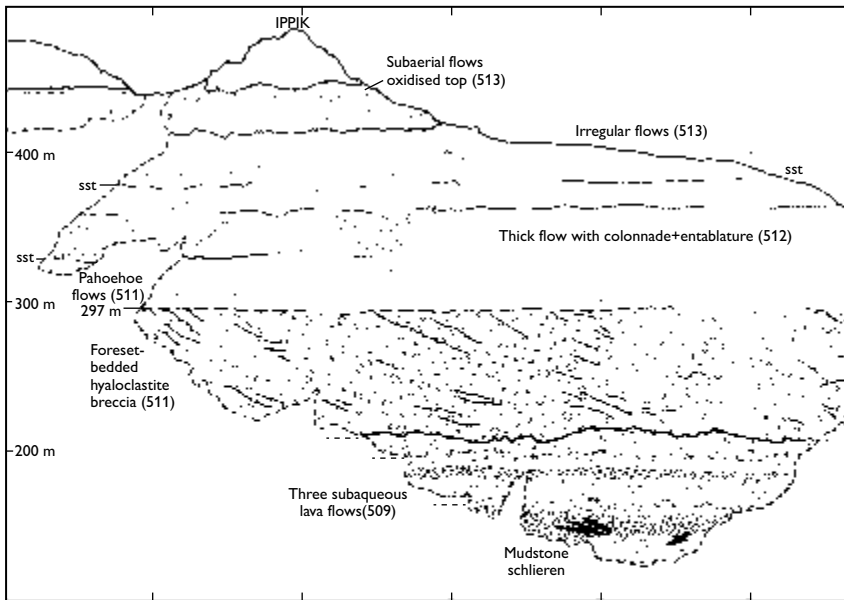


Fig. 57. Photogrammetric interpretation of the volcanic succession at Ippik 4 km east of Skarvefjeld, south coast of Disko. Subaqueous lava flows of unit 509 and hyaloclastites of unit 511 filled in the Assoq Lake. The foresets can be traced from top to bottom of the hyaloclastite, indicating a lake depth of around 85 m. Note two very thin levels of sandstone (sst). Lithological unit codes in parentheses. See also Fig. 58. From Heinesen (1987), with slightly modified text.



Fig. 58. The volcanic succession at Ippik. Hyaloclastites of the Skarvefjeld unit (511 hy) and subaerial lava flows of units 511, 512 and 513. The single flow of unit 512 has a well-developed colonnade indicating emplacement on a wet surface; thin layers of quartzo-feldspathic sandstone (sst), probably fluvial, are seen both below and above this flow. See also Fig. 57. Ippik, south coast of Disko (south Disko section at around 90 km).



Fig. 59. The Skarvefjeld unit (511) in the south wall of Charles Polaris Dal, eastern Disko. Thick foreset-bedded hyaloclastites (511 hy) showing infill from the west (right), and associated subaerial thin pahoehoe flows ending with one or two thicker flows (511 La). A *c.* 10 m horizon of quartzo-feldspathic sandstone (sst) separates the overlying flows of unit 512 and 513. The subaerial part of the Skarvefjeld unit (511 La) is *c.* 60 m thick. For location, see Fig. 140.

Inner Kvandalen. Fig. 10, profile 8. In the innermost part of Kvandalen the Skarvefjeld unit is about 200 m thick. It overlies more than 20 m of Assoq Member mudstones, which contain plant fossils and thin shell fragments of a small bivalve. The lowermost *c.* 180 m of the unit is in subaqueous facies and forms various hyaloclastites and volcanoclastic beds, which were derived from at least three different eruptive events separated in time by beds of non-volcanic clastic sediments.

The lower hyaloclastite unit comprises some of the most evolved basalts of unit 511 (with *c.* 5.5 wt% MgO) and is composed of glassy clasts and pillow fragments of plagioclase-augite microphyric basalt together with clasts of subaerial basalt, mudstone and scarce siderite concretions derived from clastic sediments. The unit comprises several beds with varying amounts of moderately baked mudstone and conglomeratic layers of up to decimetre-sized basalt clasts derived by coastal erosion of subaerial lava flows of unit 511. Some of the beds are dominated by volcanoclastic gravel and are separated by up to dec-

imetre-thick beds of deformed mudstone (Fig. 54). A middle unit is composed of slightly more magnesian hyaloclastite (with *c.* 6 wt% MgO) with scattered clasts of mudstone. The uppermost unit is up to 100 m thick and consists of foreset-bedded hyaloclastite and pillow lava of distinctly more magnesian basalt (with 8–9 wt% MgO) which were fed from overlying, compositionally similar subaerial pahoehoe lava flows.

Charles Polaris Dal. Fig. 10, profile 9. About 11–12 km south-east of profile 8, the Skarvefjeld unit is excellently exposed on both walls of Charles Polaris Dal, in particular the south wall at the corner to Frederik Lange Dal. The Skarvefjeld unit is here about 125 m thick and overlies quartzo-feldspathic sandstone and *c.* 80 cm of poorly exposed mudstone of the Assoq Member. The lowermost part of unit 511 is an about 7 m thick volcanoclastic bed composed of glassy basalt clasts and pillow fragments together with scattered millimetre-sized polished quartz grains, rare centimetre-sized clasts of polished chert, and



Fig. 60. The easternmost exposures of the Skarvefjeld unit in Kvandalen. The view is from west-south-west (Point 1123 m) and shows hyaloclastites (511 hy) and subaerial lava flows (511 La) of the Skarvefjeld unit, in total *c.* 55 m thick. Units 512–516 are each represented by a single flow. The flow of unit 513 has yellow quartzo-feldspathic sandstone (sst) at its base and top and is probably invasive (inv). See also Dam *et al.* (2009, fig. 131). The exposure is slightly slipped. The white outcrops in the background are Cretaceous sandstones in Kvandalen. South side of Kvandalen *c.* 1.5 km east of Point 1123 m, east Disko (Fig. 7, profile 12).

fragments of coal and silicified wood picked up from the underlying sediments. This bed is overlain by a 7 m thick columnar-jointed basalt of unit 511 with poorly exposed lower and upper contacts, interpreted as an invasive flow. This is overlain by a *c.* 45 m thick, foreset-bedded hyaloclastite showing inflow from the west, covered by a *c.* 50 m thick succession of thin pahoehoe lava flows feeding the hyaloclastites (Fig. 59).

The upper part of the Skarvefjeld unit in Charles Polaris Dal is composed of two olivine-rich lava flows with up to 12.2 wt% MgO and a top flow of feldspar-phyric basalt (Fig. 52). The olivine-rich flows have very dark grey, partly olivine-cumulative basal zones with prominent sub-horizontal segregation veins, and upper light grey zones, which are vesicular and less rich in olivine. The top zones of both flows are high-temperature oxidised and

the upper flow has a *c.* 5 cm cover of lateritic soil. The upper picritic flow shows a distinct local up-doming and a thickening of its olivine-rich lower part which might indicate proximity to an eruption site, but no trace of a volcanic feeder has been recognised.

The uppermost flow of unit 511 is a *c.* 7 m thick feldspar-phyric basalt with red-oxidised top with traces of lateritic soil. It is covered by a thick lava flow of unit 512.

South wall of Kvandalen east of Point 1123 m. Fig. 7, profile 12. The easternmost exposures of the Skarvefjeld unit are situated on the south wall of Kvandalen about 29 km south-east of profile 8. At least 55 m of the Skarvefjeld unit are exposed in a slightly slipped block *c.* 1.5–2 km east of Point 1123 m (Fig. 60; Larsen & Pedersen 1990, fig 7; Dam *et al.* 2009, fig. 131). The lower boundary is

not exposed. The Skarvefjeld unit here comprises 20–25 m of foreset-bedded hyaloclastites covered by *c.* 30 m of subaerial pahoehoe flows feeding the hyaloclastites. The compositional variation is much smaller than in the localities described above (8.0–8.2 wt% MgO in the hyaloclastites and the lavas just above them, and about 6.5 wt% MgO in the uppermost lava flows), which suggests that the Skarvefjeld unit here is distal relative to its source and represents just one or two flow fields. The upper boundary of the pahoehoe lavas is a planar erosion surface covered by about 10 cm of coaly mudstone. The final volcanic front, which marks the exhaustion of unit 511 is not exposed at any locality.

North coast of Disko around Qullissat

The northern part of the Assoq Lake deposits and volcanic infill are virtually unexposed over a distance of *c.* 30 km along the Vaigat coast between innermost Kvandalen and Qullissat. The lack of exposures is caused by large landslides, which have covered both the lowermost part of the Maligât Formation and the underlying Cretaceous to Tertiary sediments (Pedersen *et al.* 2001; Central Disko section). However, blocks of hyaloclastites of

the Skarvefjeld unit occur in the landslipped masses at several localities, and the unit may therefore be present along the whole distance. Exposures of the Skarvefjeld unit reappear in the coastal mountain walls at Inussuk and Qullissat (Fig. 10, profiles 4, 5; Fig. 48).

Over a distance of about 8 km the near-vertical walls of the Inussuk mountain in the south-east and the Killerpaat Qaqqarsuat mountain in the north-west show an up to 200 m thick succession of subaerial and subaqueous lava flows and foreset-bedded hyaloclastites of the Skarvefjeld unit. The basalts have a limited chemical variation (6–7 wt% MgO) but form both thick individual flows and successions of thin pahoehoe tongues. The repeated facies variations, with two hyaloclastite horizons (Fig. 48 at 2.5–5 km), demonstrate that the basalts were emplaced in a number of individual eruption events that were sufficiently spaced in time to record synvolcanic subsidence. In the Killerpaat Qaqqarsuat mountain, only the lowermost lava flow of the Skarvefjeld unit records wet conditions at the time of inflow. This flow overlies partly subaqueous flows of unit 509 (see section on unit 509) and has an intensely jointed colonnade and entablature but a vesiculated and oxidised top surface and a thin coat of lateritic soil. A few kilometres to the south-east

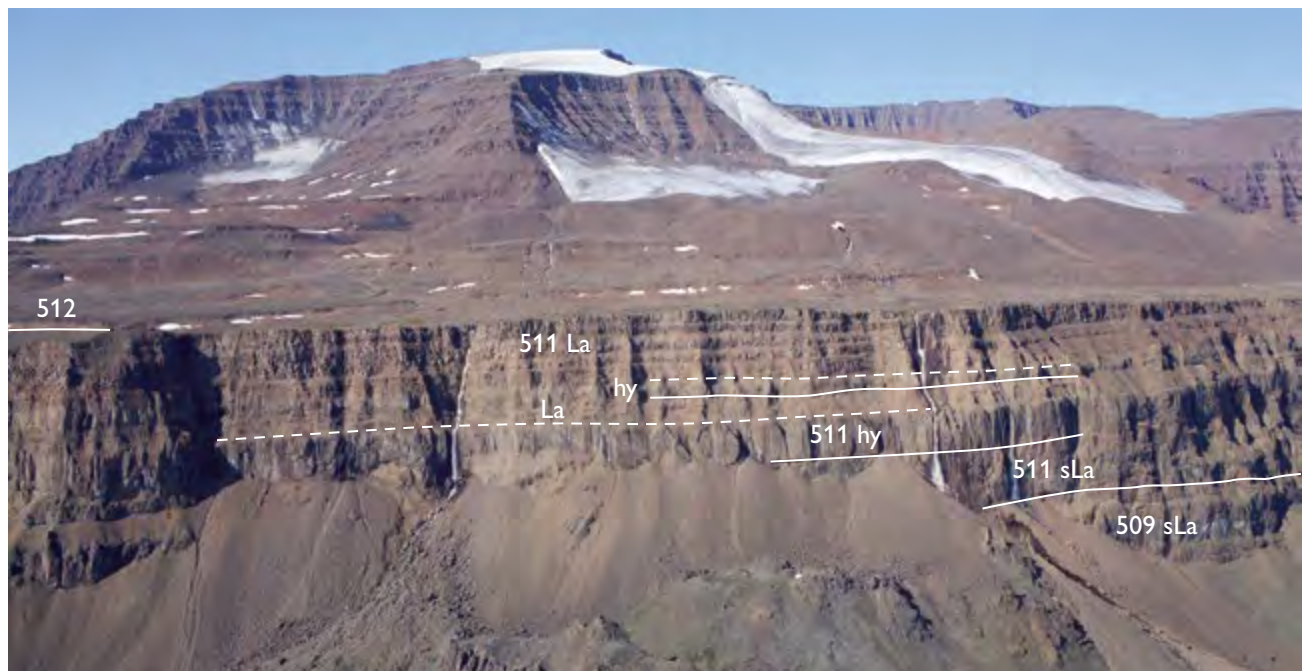


Fig. 61. The eastern part of the mountain wall Inussuk just south of Qullissat, north-eastern Disko (Fig. 48 at 3–4.2 km). The major part of the wall comprises the Skarvefjeld unit in subaqueous lava facies (511 sLa), foreset-bedded hyaloclastite facies (511 hy) and subaerial lava facies (511 La). The foresets of the lower hyaloclastite horizon are NW-inclined whereas the foresets of the upper hyaloclastite horizon are SE-inclined (Fig. 48). The total thickness of unit 511 is here *c.* 200 m. Photo: Erik Vest Sørensen.

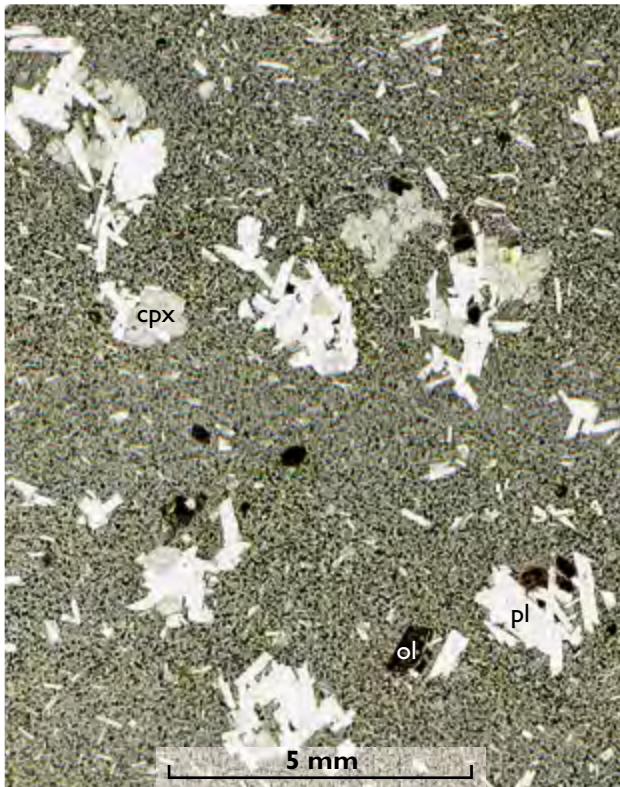


Fig. 62. Thin section (scanned) of a typical lava from Rinks Dal Member unit 512, lower transition flows. Basalt with many glomerocrysts and individual phenocrysts of plagioclase (pl) and less common augite (cpx) and olivine (ol, altered to dark brown clay), in a fine-grained matrix. Sample GGU 340873, Qinnusaq, north-east Disko.

the same flow is probably present as one or two entirely subaqueous, thick lava flows emplaced on top of subaqueous flows of unit 509 (Figs 10, 61). The palaeo-water depth cannot be estimated from these flows, but they are covered by a foreset-bedded hyaloclastite horizon fed from a flow field of pahoehoe lava lobes, and the 35–45 m high foresets truly reflect the water depth at that time. After the filling of the Assoq Lake, the area was inundated again and filled by a new series of pahoehoe flows of the Skarvefjeld unit, which form an upper, just 5–10 m thick, foreset-bedded hyaloclastite. This marks the final filling of the Assoq Lake in this part of Disko, and the final flows of unit 511 are entirely subaerial (Fig. 61).

Unit 512 (lower transition flows)

Composition and petrography. These flows form a transition from the Skarvefjeld unit to the overlying Fe-Ti-rich Akuarut unit. In a plot of TiO_2 vs *mg*-number (see Fig.

97) they form a partially more evolved extension of the trend of the Skarvefjeld unit, with equal or higher TiO_2 contents (2.4–3.2 wt%) and lower *mg*-numbers caused by higher FeO^* and relatively low MgO (5.8–6.8 wt%). A few exceptions with lower TiO_2 are found on eastern Disko. The lower transition flows are moderately phyric to almost aphyric basalts with some phenocrysts, commonly glomerocrysts, of plagioclase up to 6 mm in size, scarce augite up to 1 mm in size, and olivine up to 1 mm in size but always pseudomorphed by smectite (Fig. 62). Chromite has not been observed.

Distribution. The lower transition flows are found throughout Disko; on eastern Disko the unit oversteps unit 509 and the Skarvefjeld unit (511) and forms invasive flows which are the oldest in the area (Fig. 7, profiles 8, 10, 11, 13, 14). On most of Disko unit 512 is 20–100 m thick and consists of only one to three flows; an exception is seen at Qinnusaq on north-eastern Disko where a succession of four flows reaches 170 m thickness and two flows have a combined thickness of 100 m because of ponding (Fig. 10, profile 8).

Unit 512 is present in the southernmost part of Nuusuaq where it is represented by a single invasive flow, the lowest one in the profiles at Tartunaq, Umiusat and Eqip Qaqqaa, and flow 2 at Giesecke Monument (Fig. 11).

Transition flows are absent in a few profiles (Lyngmarksfjeld, Orlingasaq).

Lithology. The lower transition flows are widespread, massive, blocky pahoehoe lava flows, and except for their chemical composition, they are indistinguishable from most other Rinks Dal Member basalts (Fig. 63). At most localities, the one to four flows of unit 512 are situated between the Skarvefjeld unit (511) and the overlying prominent Akuarut unit (513). However, at Kuu-gannuaq SE and Killarpaat Qaqqarsuat (Fig. 9, profile 5; Fig. 10, profile 4) unit 512 lavas interdigitate with flows of both units 511 and 513.

On eastern Disko (Frederik Lange Dal, Blåbærdalen and Point 1123 m in Kvandalen) unit 512 is represented by a single 20–30 m thick subaerial lava flow, which overlies subaerial pahoehoe lava tongues of the Skarvefjeld unit (Fig. 60). The flow top is eroded and covered by a widespread, around 10 m thick horizon of non-volcanic, quartzo-feldspathic sand and siltstone of the Assoq Member (Fig. 60; Dam *et al.* 2009, fig. 131). At Frederik Lange Dal this horizon contains marine dinoflagellate cysts in some samples (Piasecki *et al.* 1992), indicating marine incursions into the Assoq Lake at this stage. The



Fig. 63. The eastern part of the type section for the Rinks Dal Member at Orpiit Qaqqaat. The photo corresponds approximately to Fig. 24 at 3–4 km but is viewed at a different angle. From unit 509 upwards, all flows are subaerial. The sample profile follows the left edge of the gully (Fig. 24). The Fe-Ti-rich Akuarut unit (513) is recognised by having stronger reddish-brown colours than the other units. See also Figs 25 and 31. South side of the Orpiit Qaqqaat mountain, south-central Disko.

sediment horizon on top of unit 512 extends for more than 50 km to the south coast of Disko and farther westwards where it thins gradually; a sand layer a few decimetres thick persists into the lava plateau at Skarvefjeld and Ippik (Fig. 7, profile 4; Fig. 57).

Invasive lava flows on eastern Disko

The subaerial lava flows of unit 512 are nowhere directly observed to pass onto or into the Assoq Member sediments, but basaltic sill-like bodies in the sediments are widespread on eastern Disko. They have chemical compositions similar to unit 512 lavas and occur at an equivalent stratigraphic level, and they are interpreted as invasive lava flows (Larsen & Pedersen 1990). They occur from Tuapaat Qaqqaat on the south coast to Pingu and Inngigissoq on the east coast (Fig. 7, profiles 8–14; Fig. 10, profiles 10–12; Fig. 64). At Inngigissoq the upper of two such lavas is thoroughly pillowed (Fig. 7, profile

14), indicating that the sediments were wet and unconsolidated at the time of intrusion.

Invasive lava flows on southern Nuussuaq

A very well-exposed invasive lava flow of unit 512 (Figs 65, 66) can be followed semi-continuously for about 18 km along the south coast of Nuussuaq from Giesecke Monument in the west to Tartunaq in the east (South Nuussuaq section at 59–77 km). Samples from three profiles (Fig. 11, profiles 7, 9, 10) have virtually identical chemical compositions, confirming that the flow represents a single eruption. The flow burrowed into unconsolidated mud of the Assoq Member (formerly named the Aussvik Member). Figure 66 shows that at *c.* 72.7 km the boundary between sandstone of the Umiussat Member and mudstone of the Assoq Member is located below unit 512. Farther to the east unit 512 is invasive into the Umiussat Mb (Fig. 11, profile 10). Unit 512 is at least locally composed of two columnar-jointed bodies



Fig. 64. Sediments and lava flows on eastern Disko. Two invasive lava flows belong to units 512 and 514, whereas unit 513 is absent. The flows of unit 515 are in normal subaerial facies (Fig. 10, profile 12). The sediments belong to the Atanikerluk Formation. The boundary between the upper part of the Pingu Member (P) and the Umiussat Member (U) is indicated. The lower boundary of the Assoq Member (A) is not well exposed in this section, but is probably located above 512 inv. The north-east facing slope of Inngigissoq, east Disko. The outcrop is shown on the Central Disko section around 103 km (viewed at a different angle) and in Dam *et al.* 2009, fig. 132. Photo: Erik Vest Sørensen.

with upper and lower contacts chilled against mudstone (Pedersen 1975b; see also Fig. 76). The flow is 20–50 m thick along the coastal section and extends for more than 5 km inland (Pedersen *et al.* 2007b); it has an estimated volume in excess of 2 km³. This is a much larger volume than that of the preceding thin lavas of unit 511, and the

flow evidently had volume enough to extend the lava area much farther into the Assoq Lake basin.

A separate sill-like body which covers at least 4 km² *c.* 5 km north-north-east of Giesecke Monument (Pedersen *et al.* 2007b), represents the northernmost extension of unit 512.



Fig. 65. Invasive lava flows of units 512 and 513 in mudstones (the 512 flow) and sandstones (the 513 flow) of the Assoq Member. Flows of units 514–515 are in normal subaerial facies. The sandstone seen in the lower part of the photo is the Umiussat Member. The fine-grained sandstones are interpreted as low-energy fluvial deposits. Slope beneath Point 975 m, south coast of Nuussuaq (Fig. 66 at *c.* 71.8–72.5 km).

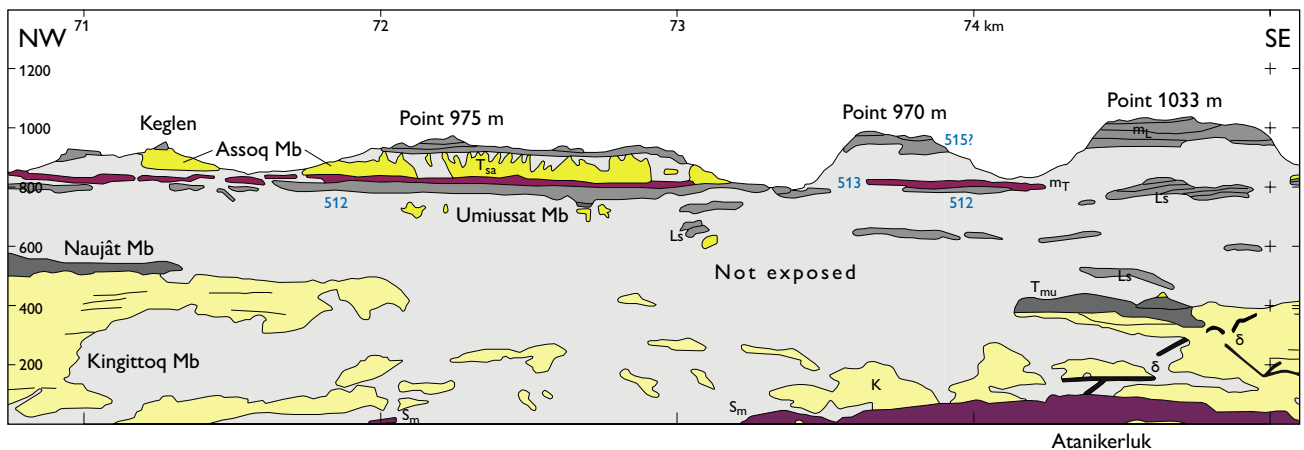


Fig. 66. Photogrammetrically measured section of the south coast of Nuussuaq around Point 975 m, showing invasive lava flows of units 512 and 513 and subaerial lava flows of unit 515(?). Blue three-digit numbers are lithological codes. The invaded sediments are sandstones (yellow, labelled T_{sa}) and mudstones (dark grey) of the Assoq Member of the Atanikerluk Formation. Lower sediments are mudstones of the Naujât Member (T_{mu}) of the Atanikerluk Formation and sandstones of the Kingittoq Member (K) of the Cenomanian Atane Formation. L_s : land-slipped blocks. δ : dykes. The dark purple area at Atanikerluk is an Eocene sill. Excerpt from the South Nuussuaq section (Pedersen *et al.* 1993). Note that the horizontal scale is at the top.

Middle Rinks Dal Member

Summary of the main features of the middle Rinks Dal Member

- Comprises a single unit, the Akuarut unit (513), with high TiO_2 (≥ 3.2 wt%).
- Stratigraphic ‘backbone’ of the Rinks Dal Member. Generally mappable by a combination of chemistry and strong brown colours. Not well distinguished on north-west Disko and not shown on the 1:100 000 map sheet Qullissat. Otherwise shown on all relevant geological maps and photogrammetric sections.
- Covered the last remaining hills of the Disko Gneiss Ridge on southern Disko.
- Spread on a flat plain on Disko and stepped farther north onto the Vaigat Formation picrite shield on south Nuussuaq.
- All lava flows are subaerial. On eastern Disko and southern Nuussuaq they are also invasive into Assoq Member sediments. Rare dinoflagellate cysts in the Assoq Member indicate episodic marine incursions on Disko.
- The most evolved basalts of the Rinks Dal Member. Tilted REE spectra suggest garnet fractionation in deep-seated magma chambers.

Unit 513 (Akuarut unit)

The Akuarut unit is an important stratigraphic marker and is shown as unit β_i on the three 1:100 000 scale geological map sheets covering Disko south of 70°N (Mellemfjord, Uiffaq and Pingu) and as unit M_i on the 1:100 000 geological map sheet Paatuut covering southern Nuussuaq. It is also shown on the 1:20 000 scale geological sections showing the south coast of Disko, central Disko and the south coast of Nuussuaq.

Composition. The flows of this unit are characterised by high contents of iron and TiO_2 , and the unit was called the ‘Fe-Ti unit’ by Larsen & Pedersen (1990) and ‘iron-titanium-rich basalts’ on the maps and sections. It is here defined as all flows around the middle level of the Rinks Dal Member with $\text{TiO}_2 \geq 3.2$ wt% (Table 2; Fig. 21). This value was chosen because it is practically applicable and results in the clearest divisions between units. Thus defined, the flows of the Akuarut unit have 3.2–4.8 wt% TiO_2 , 4.4–6.8 wt% MgO, and 12.3–16.8 wt% FeO^* . These flows are the most evolved basalts in the Rinks Dal Member, yet their *mg*-numbers show a large overlap with other units (Fig. 97).

Petrography. The basalts of the Akuarut unit range from almost aphyric to distinctly porphyritic or glomeroporphyritic with phenocrysts of plagioclase, augite and olivine (always altered; Fig. 67). Almost aphyric basalts occur through the entire compositional range in TiO_2 . Cognate dolerite inclusions occur occasionally. Some of the invasive lava flows have a doleritic groundmass texture.

Distribution. The distribution of the Akuarut unit is shown in Fig. 15. The Akuarut unit is present over nearly all of Disko but is missing in a small area around Pingu on eastern Disko (Fig. 7, profile 14; Pedersen *et al.* 2001; Central Disko section). In some places, e.g. at Lyngmarks-



Fig. 67. Thin section (scanned) of a typical lava from Rinks Dal Member unit 513, Akuarut unit. Basalt with a few small plagioclase phenocrysts and a glomerocryst of plagioclase (pl), augite (cpx) and pseudomorphosed olivine (ol) in a fine-grained matrix with a dark, glass-rich streak at top of photo. Sample GGU 279038, Killerpaat Qaqqarsuat, northern Disk

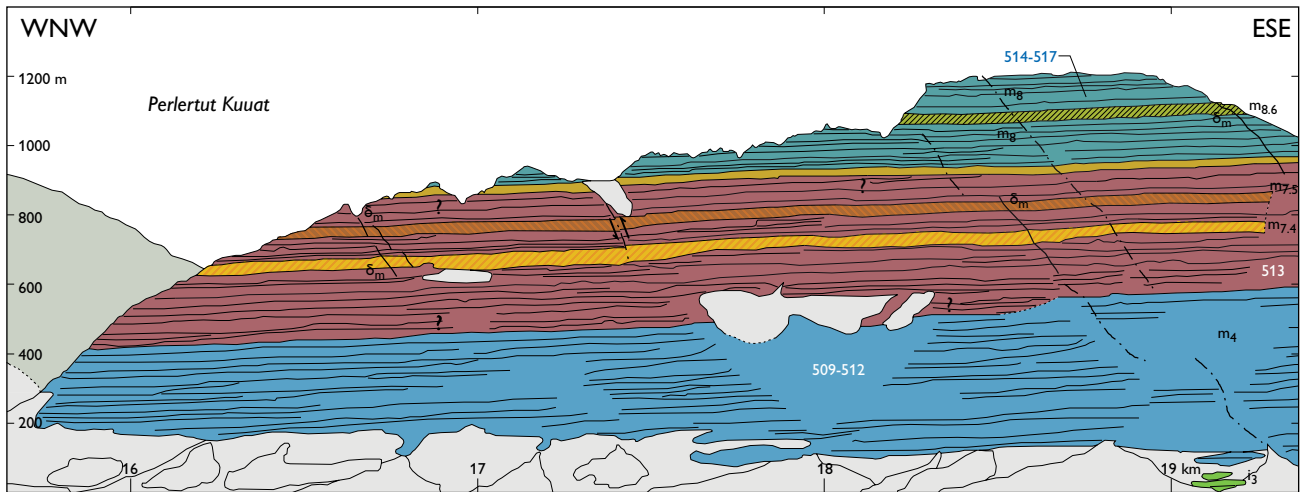


Fig. 68. The Rinks Dal Member at Perlertut, north coast of Nordfjord, west Disko, characterised by a large number of relatively thin lava flows. White and blue three-digit numbers are lithological codes; other annotations are from the original. Some individual marker flows are shown with deviating colours. Picritic lava flows of the Vaigat Formation are denoted i_3 . Excerpt from the Central Disko section (Pedersen *et al.* 2005).

field, the unit can be distinguished lithologically because the flows are very brown and have thick, purple top breccias, but commonly it is not clearly visually distinguishable. The unit is thickest on western and central Disko where there are from five to about 20 flows present (Fig. 68) with a combined thickness of 150–400 m. It is probable that the unit is up to 600 m thick on north-western Disko, but due to lack of flow-by-flow sampled profiles in that area this cannot be ascertained. It is represented by a single lava flow at the mouth of Giesecke Dal on north-western Disko (Fig. 13, profile 6), whereas its distribution among the mountain tops on northern Disko on both sides of the Kuugannguaq valley is unknown due to lack of sampling. On eastern Disko, the Akuarut unit thins eastwards; it goes into invasive facies, is reduced to five to one flows and peters out. A single flow reached Sortebærdalen, Kvandalen and Aqajaruata Qaqqaa, but the unit never reached Pingu.

On south and south-east Nuussuaq, the Akuarut unit is present south of the central Aaffarsuaq valley (Fig. 15) where it comprises one to four flows (Fig. 11). The flows onlap the surface of the Vaigat Formation, which rises towards the north and west. It is thickest at Giesecke Monument and Eqip Qaqqaa where it is represented by four thick flows of which the lowest two are invasive. One subaerial flow reached Point 1722 m just west of Ataata Kuua as the lowest flow of the Rinks Dal Member, resting directly on the flows of the Vaigat Formation, but none reached Point 1888 m only 8 km northeast of Point 1722 m. In the south-eastern profiles of Umiusat and Tartunaq

a single thin invasive flow is present, the same in the two profiles.

Over much of Disko the Akuarut unit forms a single, well-defined unit. This is the case on southern and eastern Disko as seen in the South Disko section, e.g. Fig. 36. However, in some profiles on central Disko there are a few flows with less than 3.2 wt% TiO_2 intercalated in the Akuarut unit (Fig. 9, profiles 3, 4, 5). On Nuussuaq, a group of flows with less than 3.2 wt% TiO_2 is intercalated within the upper part of the Akuarut unit, as seen on the South Nuussuaq section at 50–56 km and Fig. 11. The intercalated lavas are considered to belong to unit 514 (the upper transition unit) described below.

Lithology. The Akuarut unit is mainly composed of subaerial lava flows. On eastern Disko and Nuussuaq the flows are water-influenced and commonly invasive. The flows are mostly blocky pahoehoe flows, but aa flow morphology is also encountered. Typical flow morphologies are seen in the steep wall above Ippik (Fig. 58). In parts of southern, central and eastern Disko and Nuussuaq the flows have a distinctive, rusty brown weathering colour (Figs 20, 43), but in other areas, such as north-western Disko, the flows are greyish brown and do not show sufficient colour contrast to the surrounding flows to allow visual identification of the Akuarut unit.

Individual lava flows extend over large areas and individual flow volumes must commonly exceed 1 km^3 . In general, the mean flow thickness is about 20 m on western Disko and more than 30 m on central and eastern

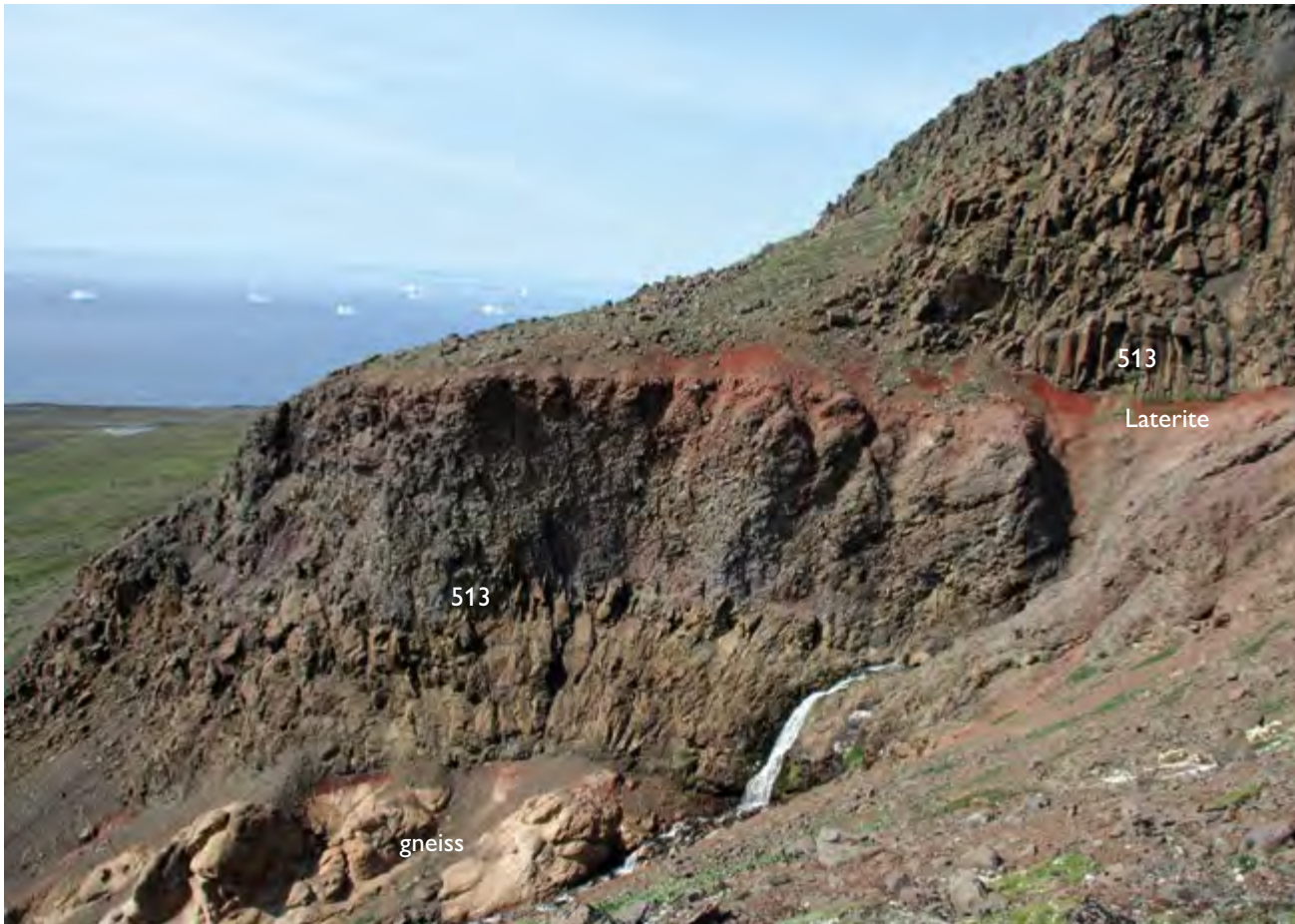


Fig. 69. Two lava flows of the Akuarut unit (513) onlapping the Disko Gneiss Ridge. The lower flow was weathered and eroded and an up to 1 m thick brick-red laterite horizon was developed before the upper flow arrived. South coast of Disko above Killiit (South Disko section at 68 km).

Disko. Some individual flows can be traced photogrammetrically on southern and central Disko, and the sectioned length of these is 3.7–12.5 km (South Disko section, Central Disko section). If a typical flow occupies a circular area with a diameter of 10 km, this amounts to *c.* 80 km², and with a thickness of 20 m, it has a volume of *c.* 1.6 km³. One or two flows can be distinguished by a particular chemical composition; of these, one flow on Nuussuaq extends over 17 × 10 km between six profiles with an estimated volume around 3.4 km³. Another flow on south-western Disko appears to be present over 55 × 35 km in five profiles; if it is truly a single flow its volume is in the order of 30 km³.

No primary eruption sites or dykes have been found and it is assumed that the Akuarut unit was erupted on western Disko or in the western offshore areas, but eruption sites on central and south-central Disko cannot be excluded.

The time intervals between eruptions of the flows of the Akuarut unit were frequently large enough to allow deep weathering, erosion of the lava tops and deposition of decimetre-thick layers of lateritic soil, well exemplified by lava flows in the Killiit area (Fig. 7, profile 2; Fig. 69).

The Akuarut unit seems to have spread over a flat plain very close to sea level on Disko and to have onlapped the low shield of Vaigat Formation picrites on Nuussuaq. To the east, it was bordered by the shallow Assoq Lake basin. The lava flows progressed from a westerly direction and invaded and interacted with the sediments of the basin over a more than 100 km long shore zone extending from the south coast of Disko to the Aaffarsuaq valley on Nuussuaq (Fig. 16). On Disko, dinoflagellate cysts have been recovered from interbasaltic sediments associated with the Akuarut unit at two localities, indicating a brackish environment, whereas similar sediments on Nuussuaq appear to be non-marine (Piasecki *et al.* 1992).



Fig. 70. Volcanic breccias interpreted as rootless cones. The lower lava flow (513 inv) is 30 m thick and has a columnar-jointed lower half with a sharp transition to entablature facies in its upper half. This flow has invaded a sandstone horizon (ss) only *c.* 5 m below the palaeosurface and re-erupted up through the sandstone, forming a volcanic breccia with sediment matrix (**vbr 1**). After a pause indicated by a red, weathering surface (red line), a 4–6 m thick lava flow arrived, and on top of this a brecciated zone of rootless phreatic cones (**vbr 2**) was created by explosions of heated vapour in the wet sand underlying the flow. See text for detailed descriptions. South coast of Disko at Marraat Qaqqaat (South Disko section at 109.2 km).

Exposures of the Akuarut unit in the eastern shore zone are scarce on much of eastern Disko and south-eastern Nuussuaq because of extensive landslides and solifluction, but the lithological variations are well-exposed in an 8 km long section along the south coast of Disko between Marraat Qaqqaat and Tuapaat Qaqqaat, and also in a 24 km long section along the Vaigat coast on Nuussuaq between Point 1760 m and Tartunaq. These are described in the following.

South coast of Disko between Marraat Qaqqaat and Tuapaat Qaqqaat

East of Brededal good partial exposures of the contacts between lava flows and the largely contemporaneous sediments of the Assoq Member are seen over a distance of *c.* 8 km between Marraat Qaqqaat and Tuapaat Qaqqaat (South Disko section at 108–116 km; Fig. 41). Here the Akuarut unit interacted with the quartzo-feldspathic

sands, which in this region form the upper part of the Assoq Member (Dam *et al.* 2009). Two exposures illustrate the interaction between subaerial lava flows and unconsolidated sand.

Rootless phreatic cones at Marraat Qaqqaat. At the slope of Marraat Qaqqaat (South Disko section at *c.* 109 km; Fig. 7, profile 7), the lowermost of three lava flows of unit 513 forms a *c.* 30 m thick invasive flow with a pronounced colonnade and a well-defined upper chill zone against a sandstone horizon which is no more than 5 m thick (Fig. 70). Above the sandstone, there is a 5–8 m thick mixed horizon consisting of a volcanic breccia with pillow-like clasts in a matrix of sand and glass fragments; the deposit may be called a peperite (Fig. 71). This bed has a 20–30 cm thick, oxidised weathering surface. It is overlain by a 4–6 m thick, irregular, subaerial lava flow, which in places grades upwards into a number of spatter cones with beds of centimetre- to decimetre-sized achne-



Fig. 71. Peperite deposit from rootless cones: a breccia consisting of volcanic clasts in a matrix of quartzo-feldspathic sand and glass fragments. Length of hammer 32 cm. Marraat Qaqqaat, South Disko.

liths (rounded pyroclastic fragments) at the top. This is covered by a massive, about 50 m thick subaerial lava flow with a several metres thick, blocky and scoriaceous top, which is the uppermost flow of the Akuarut unit. This flow is in turn covered by 5 m of yellow sandstone.

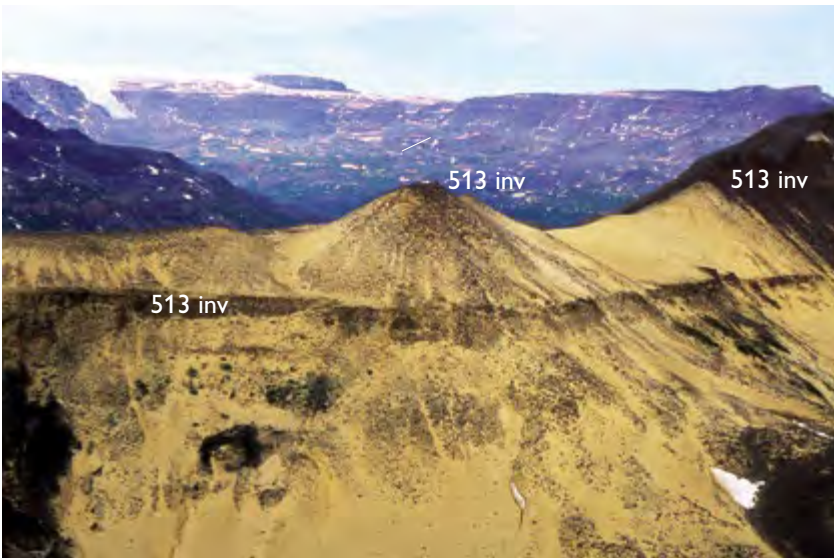


Fig. 72. Lava flows of the Akuarut unit (513) invasive into sandstone of the upper Assoq Member. The fine-grained, friable sandstone shows cross-lamination indicative of deposition from low-energy currents, but the exposure is generally very poor. The sandstone between the two flows is *c.* 50 m thick, and more than 100 m of sand is indicated by patchy outcrops in the scree below the lower flow. Ridge just west of Tuapaat Qaqqaat, south coast of Disko (South Disko section at 114.9–115.7 km, Fig. 41).

The breccia above the lower invasive lava flow is interpreted as basalt from the same flow, re-erupted through the very thin sandstone cover, while the spatter cones from the middle flow are interpreted as rootless phreatic cones created by explosions of heated vapour in the underlying wet sand. The oxidised weathering surface and the subaerial spatter cones show that the water was very shallow, probably a shore-near lake or a riverbed. Thus, the Assoq Lake had shrunk and shallowed considerably since the formation of the rootless cones at Niuluut, only 10 km east-south-east of Marraat Qaqqaat, beneath around 200 m of water in the lake at the time of deposition of unit 509 (Larsen *et al.* 2006).

Invasive lava flows and conglomerate at Tuapaat Qaqqaat. About 6 to 7 km east of the rootless spatter cones at Marraat Qaqqaat, there are remarkable exposures of Akuarut unit lava flows interacting with unconsolidated yellow sand of the upper part of the Assoq Member (Fig. 41). As at Marraat Qaqqaat, there are three invasive flows. The two lower ones are compositionally identical to the two lower flows at Marraat Qaqqaat, but here they are separated by *c.* 50 m of sand (Fig. 7, profile 8; Fig. 72). The upper flow is compositionally identical to the 50 m thick upper flow at Marraat Qaqqaat, but here its thickness has decreased to 14 m and it overlies a thin mudstone horizon on top of 11 m of sand. The top of the flow is eroded and covered by several metres of a conglomerate with rounded, polished basalt clasts and a mixed matrix of quartzo-feldspathic yellow sand and basalt gravel (Fig. 73).



Fig. 73. Conglomerate overlying the thin top flow on Tuapaat Qaqqaat, south Disko, consisting of polished, rounded basalt clasts in a matrix of basalt gravel and yellow, quartzo-feldspathic sand. Marine dinoflagellate cysts in a thin mudstone beneath the lava flow suggest that the rounded cobbles and pebbles could have resulted from marine coastal erosion and abrasion. The ruler is 15 cm long. The conglomerate is indicated in Fig. 41.

The presence of marine dinoflagellate cysts in the mudstone beneath the flow (Piasecki *et al.* 1992) suggests that the conglomerate on top of the flow could have resulted from marine coastal erosion and abrasion. Samples from the lower sand horizons at Tuapaat Qaqqaat do not contain dinoflagellate cysts. However, dinoflagellate cysts are also found in the mudstones at Assoq that are invaded by flows of unit 509 (see text on unit 509). The dinoflagellate *Taurodinium granulatum*, which is indicative of brackish-water conditions (Fensome *et al.* 2016), is present at some levels (H. Nøhr-Hansen, personal communication 2017). The kinds and distribution of dinoflagellate cysts thus suggest that the Assoq Lake was subject to periodic marine inundations.

The other known sediment locality with dinoflagellate cysts associated with subaerial lava flows of the Akuarut unit is situated in Frederik Lange Dal *c.* 40 km north of Tuapaat Qaqqaat. Taken together and combined with the very extensive regional distribution of subaerial lava flows of the Akuarut unit over most of Disko and parts of southern Nuussuaq (Fig. 15), this supports the interpretation that the Akuarut unit was erupted over a flat plain very close to sea level at that time.

South coast of Nuussuaq

Large ponded flow. The Akuarut unit forms the base of the Maligât Formation between Paatuut and Point 1760 m west of Giesecke Monument (South Nuussuaq section at 50–58 km) where it directly overlies picritic subaerial lavas and hyaloclastites of the Vaigat Formation. Beneath Point 1760 m (Fig. 11, profile 5; Fig. 74) the Akuarut unit contains an up to 150 m thick, ponded lava flow that consists of a number of irregular, strongly columnar-jointed basalt bodies with distinct but thin colonnades and very thick entablature zones. The flow has a top zone of highly vesiculated, blocky and scoriaceous basalt which clearly solidified subaerially. Towards the east, the large flow overlies mudstones of the Assoq Member. The large flow is interpreted as having ponded in a lake basin, leading to temporary complete displacement of the water from the area. It is covered by a poorly exposed, 10–20 m thick subaerial lava flow also of unit 513.

Invasive lava flows along the Vaigat coast. About 5 to 6 km south-east of Point 1760 m, beneath the ridge just south of Giesecke Monument, more than 200 m of invasive lava flows of the Maligât Formation are exposed, interbedded with contemporaneous or slightly older mudstones of the lower part of the Assoq Member (Fig. 11, profile 7, Figs 74, 75). Above two older invasive flows of units 511 and 512, there are two massive sill-like flows of the Akuarut unit, which both have a chemical composition that differs significantly from that of the large ponded flow beneath Point 1760 m. The lower flow is *c.* 60 m thick and was emplaced in a single pulse. It has a poorly exposed contact against Assoq Member mudstones at both the base and the top. The upper flow is 80–90 m thick and composed of at least two cooling units (note the columnar-jointing pattern in Fig. 75); it has a bulging, irregular top composed of decimetre-sized pillow bodies. The flow has baked and hydrothermally affected the overlying mudstones, which include a *c.* 0.5 m thick coal-rich layer with a deposit of well-preserved, compacted, close-lying fossil leaves. The pillowed structure indicates that the flow invaded unconsolidated wet sediment.

On top of the large invasive flow there is a lava flow of unit 514, which has a subaerial flow top; it is followed by two subaerial flows which form the upper part of the Akuarut unit.

Along the Vaigat coast south-east of Giesecke Monument the number of flows in the Akuarut unit decreases, and south-east of Umiusat there is only a single flow present. Most contacts to sediments are covered by scree, but over a distance of 7 km from just west of Keglen to the

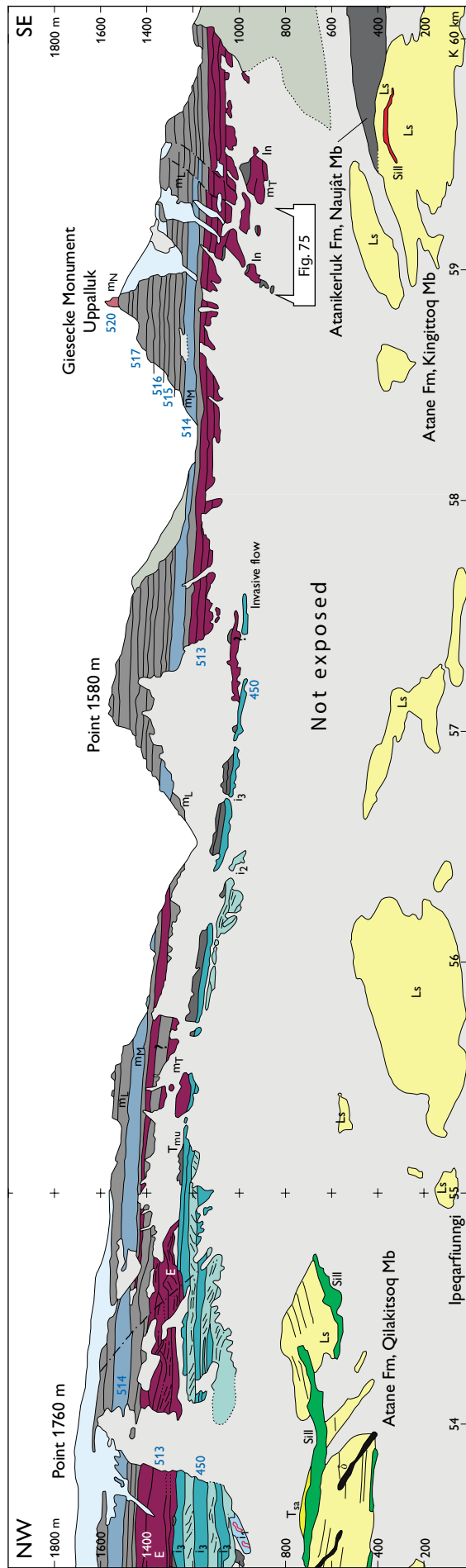


Fig. 74. Photogrammetrically measured section along the south coast of Nuussuaq at the easternmost occurrence of the Vaigat Formation (unit 450), showing hyaloclastites and lava flows above poorly exposed sediments (many landslips, Ls). The easternmost lava of the Vaigat Formation is an invasive picrite flow. Farther eastward, this was overstepped by flows of the Akuarut unit (513) of the Maligat Formation, which invaded the sediments (In) beneath Giesecke Monument. Blue three-digit numbers are lithological codes, other annotations as in the original. Excerpt from the South Nuussuaq section (Pedersen *et al.* 1993).



Fig. 75. Lava flows of the Akuarut unit (513) and an intercalated flow of unit 514, invasive (**inv**) into mudstones (**sed**) of the Assoq Member. Ridge just south of Giesecke Monument, south Nuussuaq (South Nuussuaq section at 58.9–59.3 km, see Fig. 74). Photo: Erik Vest Sørensen.

ridge above Tartunaq (South Nuussuaq section at 70 to 76.5 km) there are semicontinuous exposures of this flow showing that it is invasive. It is particularly well exposed beneath Point 975 m (Figs 65, 66). The flow, which is compositionally quite similar to the invasive lava flows south of Giesecke Monument, has intruded within the top part of a mudstone overlain by a sandstone horizon. The mudstone belongs to the lower part of the Assoq Member (formerly the Aussivik Member). The overlying 100 m of sandstone belongs to the upper part of the Assoq Member (formerly the Point 976 Member of Koch

1959). The upper contact of the flow is developed as a pillowed sill (Fig. 76) similar to that beneath Giesecke Monument. Koch (1959, p. 28–29) noted the curious combination of extrusive and intrusive features of the lavas around Point 975 m, but the concept of invasive lava flows was not developed at the time.

In the inland areas around the valley Puiatussuaq north-east of the Vaigat coast, this flow and an underlying, similar invasive flow of unit 512 can be followed as two prominent ledges in the sediment-dominated and scree-covered terrain.

Upper Rinks Dal Member

Summary of the main features of the upper Rinks Dal Member

- Comprises five units (514–518) defined by chemistry (intervals with variations in TiO_2 contents) but lithologically indistinguishable from each other; therefore shown as one group on maps and photogrammetric sections.
- Covered the flat surface of the Akuarut unit on Disko and part of southern Nuussuaq and extended farther east onto the fluvial plain of the Assoq Member by onlap and invasion. Stepped farther north onto the Vaigat Formation picrite shield. Extends in remnants to the north coast of Nuussuaq and onlaps gneisses on eastern Nuussuaq.
- Eruption sites are known from west Disko.
- Individual lava flows extend over large areas. Flow volumes are up to 10 km^3 but generally between 0.5 and 5 km^3 .
- The uppermost unit (518) is retracted in distribution relative to the earlier units of the upper Rinks Dal Member; it is also the most evolved unit and may reflect waning magma production in the final stage of the Rinks Dal Member volcanism.

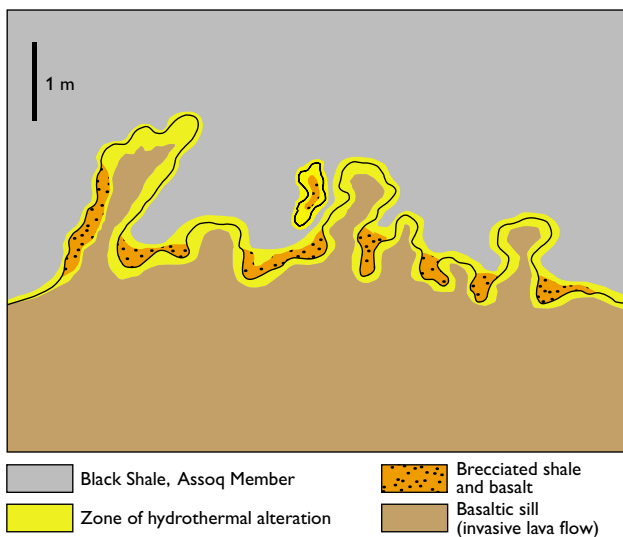


Fig. 76. The upper contact between an invasive lava flow of the Akuarut unit and mudstone of the Assoq Member. The flow forms a 'pillowed sill': irregular lava tongues intrude the mudstone in a zone that is more than a metre thick, and both mudstone and basalt are brecciated and hydrothermally altered at the contact. The relations show that the flow invaded the mudstone while this was still water-rich and only partly consolidated. South coast of Nuussuaq, the slope beneath Point 975 m (Fig. 65). Redrawn after Pedersen (1975b).

The upper Rinks Dal Member has been divided into five chemostratigraphic units (514–518). The division relies solely on chemical analyses (Fig. 21), and distinction is not possible outside the analysed profiles. The geological maps and sections therefore show the upper Rinks Dal Member as one undivided unit.

The upper Rinks Dal Member is present throughout Disko and central to eastern Nuussuaq from the south coast to the north coast. Thicknesses are greatest, 500–600 m, on western Disko and decrease to around 400 m on central and southern Disko and 300 m on northern and eastern Disko. On Nuussuaq, the upper Rinks Dal Member is 340 m thick between Paatuut and Giesecke Monument and decreases eastwards to 300 m. On central-eastern and north-eastern Nuussuaq only the upper Rinks Dal Member is present, and its thickness is reduced to *c.* 200 m due to onlap on the picrites of the Vaigat Formation and on the gneiss in the easternmost areas. Around Point 2000 m in the easternmost lava areas on Nuussuaq, thicknesses locally reach 360 m due to ponding of flows in depressions on the old gneiss surface.

The number of flows is largest on western Disko, where there are around 25 flows present in any vertical succession, giving an average flow thickness of around 20 m, but with considerable variation as seen in the geological profiles and sections. The number of flows decreases and the average flow thickness increases eastwards, and at Skarvefjeld on southern Disko, there are 13 flows with an average thickness around 30 m. At Qinnngusaq on eastern Disko, there are nine flows with an average thickness of 37 m. At Giesecke Monument on south-eastern Nuussuaq, there are 13 flows with an average thickness of 26 m, and at Nunavik on eastern Nuussuaq there are four flows with an average thickness of 60 m. The five units (514–518) are present over most of the region, which shows that the eastwards decrease in the number of flows affected all units equally.

Unit 514 (upper transition flows)

Composition. These flows form a transition from the Akuarut unit (513) into the main upper Rinks Dal Member. The development with time towards lower TiO_2 contents was gradual (Fig. 21), and the lower boundary of the upper Rinks Dal Member is therefore not always well defined. The flows of unit 514 have 2.4–3.2 wt% TiO_2 and 5.4–7.6 wt% MgO , and in a plot of TiO_2 vs *mg*-number they fall in the same field as the lower transition flows (unit 512) to which they are very similar.

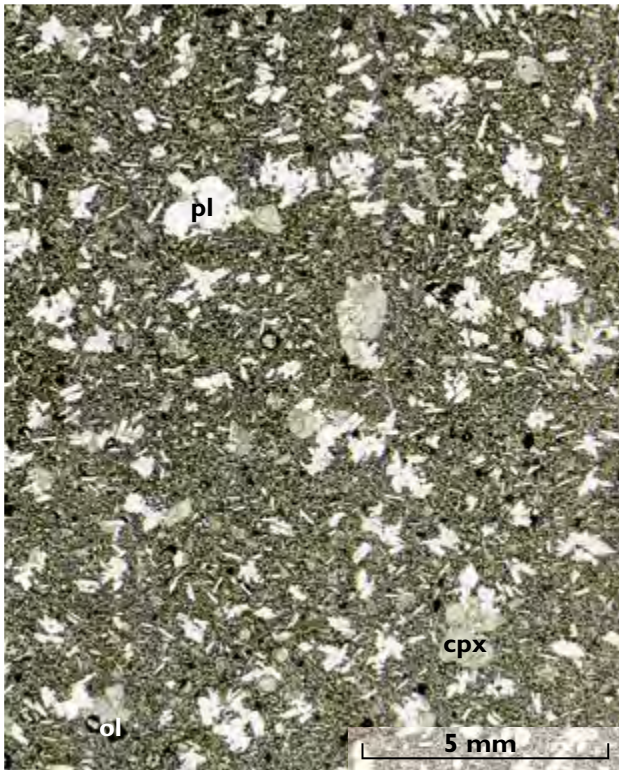


Fig. 77. Thin section (scanned) of a lava of Rinks Dal Member unit 514, upper transition flows. Basalts with abundant microphenocrystic plagioclase (pl) and augite (cpx) and scarce olivine (ol) pseudomorphs. Sample 332813, Paatuut, southern Nuussuaq.

Petrography. Unit 514 basalts are commonly almost aphyric with very scarce phenocrysts of plagioclase. The aphyric rocks range in TiO_2 between 2.4 and 3.02 wt%. Some unit 514 basalts contain abundant microphenocrystic plagioclase and augite and scarce pseudomorphs after olivine, exemplified by Fig. 77. Basalts with a very fine-grained groundmass and glomerocrystic plagioclase and pseudomorphed olivine and scarce augite also occur.

Distribution. The flows of unit 514 are found throughout Disko and south-eastern Nuussuaq (Fig. 15). They form a 20–80 m thick succession of one to five flows, some of which may interdigitate with the upper part of the Akuarut unit, as described above, and some interdigitate with unit 515, particularly on southern Nuussuaq. Unit 514 is absent in a few profiles.

Lithologies. Descriptions are included in the lithology section on the entire upper Rinks Dal Member.

Units 515, 516 and 517 (the main upper Rinks Dal Member)

Composition. These three units, which constitute the main part of the upper Rinks Dal Member, comprise basalts with TiO_2 contents within the rather wide range of 1.5–3.4 (3.7) wt%. The variation at any stratigraphic level is usually within one per cent TiO_2 , typically in the interval 2–3 wt% TiO_2 , but in all profiles there is an interval around the middle part with lower TiO_2 contents of 1.5–2.0 wt% (unit 516), which is used as a stratigraphic partitioning (Fig. 21). The flows below and above this interval (units 515 and 517) are chemically indistinguishable and all three units are considered to be closely related. They are treated here under one heading.

In a TiO_2 vs *mg*-number diagram (see Fig. 97), most samples of units 515, 516 and 517 plot together with the lower Rinks Dal Member and separate from the Akuarut unit and the two units of transition flows. Some flows of unit 515 show compositional overlap to unit 514, and the two units interdigitate on southern Nuussuaq.

Petrography of unit 515. Unit 515 is dominated by basalts with abundant plagioclase phenocrysts and plagioclase-augite glomerocrysts up to 2 mm in size in a fine-grained groundmass. Pseudomorphs after olivine less than 1 mm in size are scarce but present in all rocks (Fig. 78A). The range of TiO_2 in this main type is 1.7–3.2 wt%. Another common type has only scattered, 1 to 2 mm large plagioclase and augite glomerocrysts but carries abundant microphenocrystic plagioclase and augite less than 0.5 mm in size. Pseudomorphs after microphenocrystic olivine are also present. A few basalts are almost aphyric and contain only scarce microphenocrysts and phenocrysts of plagioclase, augite and olivine pseudomorphs (Fig. 78B). The range in TiO_2 for this type is 2.5–3.4 wt%.

Petrography of unit 516. The low- TiO_2 basalts of unit 516 (1.5–2.0 wt% TiO_2) are all strongly plagioclase and augite glomerophytic with 1–3 mm glomerocrysts. Pseudomorphs after olivine are also present. No phenocryst-poor or aphyric samples were found. Groundmasses range from very fine grained to almost doleritic. None of the samples are obvious plagioclase cumulates, and none are distinctive petrographical markers as compared to basalts of units 515 and 517.

Petrography of unit 517. The basalts of unit 517 show a considerable range in texture, varying from a few very phenocryst-poor basalts with fine-grained groundmass, through microphyric or micro-glomerophytic basalts



Fig. 78. Thin sections (scanned) of typical lavas from Rinks Dal Member unit 515. **A:** Basalt with abundant plagioclase phenocrysts and plagioclase-augite-olivine glomerocrysts in a fine-grained groundmass. Plagioclase is colourless, augite (near lower edge) grey and olivine pseudomorphosed by brown and yellow clay. Sample 354773, Kvandalen, eastern Disko. **B:** Nearly aphyric basalt with scarce microphenocrysts and phenocrysts of plagioclase, augite and olivine pseudomorphs. Sample 332917, Kvandalen, eastern Disko.



Fig. 79. Thin section (scanned) of a lava from Rinks Dal Member unit 517. Basalt with common plagioclase-augite glomerocrysts and individual phenocrysts of plagioclase (**pl**), augite (**cpx**) and distinctive olivine (**ol**, black pseudomorphs). Sample 326430, Marraat Qaqqaat, south-eastern Disko.

with very abundant microphenocrystic plagioclase and augite, to common, distinctly porphyritic basalts; these have plagioclase and augite glomerocrysts up to 5–10 mm in size, individual plagioclase phenocrysts up to 5 mm, augites up to 4 mm, and distinctive olivine phenocrysts (pseudomorphed) up to 2 mm (Fig. 79).

Distribution. Units 515 and 516 have the same distribution as unit 514 throughout Disko and south-eastern Nuussuaq and are not found east of the boundary fault on Nuussuaq. Unit 517 is the most widespread of the 12 units in the Rinks Dal Member; it crossed the eastern boundary fault and reached northern Nuussuaq where it overlapped the picrite shield of the Vaigat Formation and the high gneiss terrain in the east (Fig. 15). It is present in sampled profiles at both Saqqaq and Nunavik (Figs 11, 12).

Lithologies. Descriptions are included in the lithology section on the entire upper Rinks Dal Member.

Unit 518 (uppermost flows)

Composition. The uppermost flows of the Rinks Dal Member have increased TiO_2 contents relative to the underlying succession (units 514–517), and more than half of them have just as high TiO_2 as the Akuarut unit (Fig. 21). In general, they have more than 2.5 wt% TiO_2 and mostly more than 2.8 wt%. In particular, one to two flows with up to 4.4 wt% TiO_2 occur in many profiles. This unit plots in a TiO_2 vs *mg*-number diagram in the same area as the Akuarut unit and the transition flows; however, unit 518 and the Akuarut unit can be distinguished by their trace elements (see below and Larsen & Pedersen 2009).

Petrography. The basalts of unit 518 show a considerable range in textures. Slightly less than half of the rocks are phenocryst-poor or almost aphyric. Many basalts are rich in plagioclase and augite microphenocrysts and glomerocrysts. One such lava flow contains decimetre-sized lava pegmatites (Fig. 80A) which were dated by Storey *et al.* (1998). Finally, there are glomerophyric basalt samples with up to 6 mm large glomerocrysts of plagioclase, augite and pseudomorphs after olivine (Fig. 80B).

Distribution. Unit 518 is the only unit of the Rinks Dal Member that has a more limited distribution than its predecessor (Fig. 15). On western Disko, it typically consists of four to five flows with a combined thickness of 100–150 m; on central and parts of eastern Disko, there are one to two flows with a combined thickness between 20 m and 100 m. No flows reached north-eastern Disko and Nuussuaq. The unit is interpreted as representing a waning stage of the volcanism of the Rinks Dal Member, when dwindling volumes of increasingly evolved magmas were erupted, centred on western Disko or west of Disko.

Lithologies. Descriptions are included in the lithology section on the entire upper Rinks Dal Member.

Lithologies of the upper Rinks Dal Member

All lava flows in the upper Rinks Dal Member are subaerial. On easternmost Disko and south-easternmost Nuussuaq, they are also invasive into, or flowed onto, wet sediments, with ensuing development of colonnades and entablatures in the flows. However, at this stage the Assoq Lake was reduced to small temporary pools, coal swamps and fluvial plains. On north-easternmost Nuussuaq, the flows of unit 517 ponded in water-filled depressions on the gneiss surface, leading to development of thick flows with prominent entablatures.

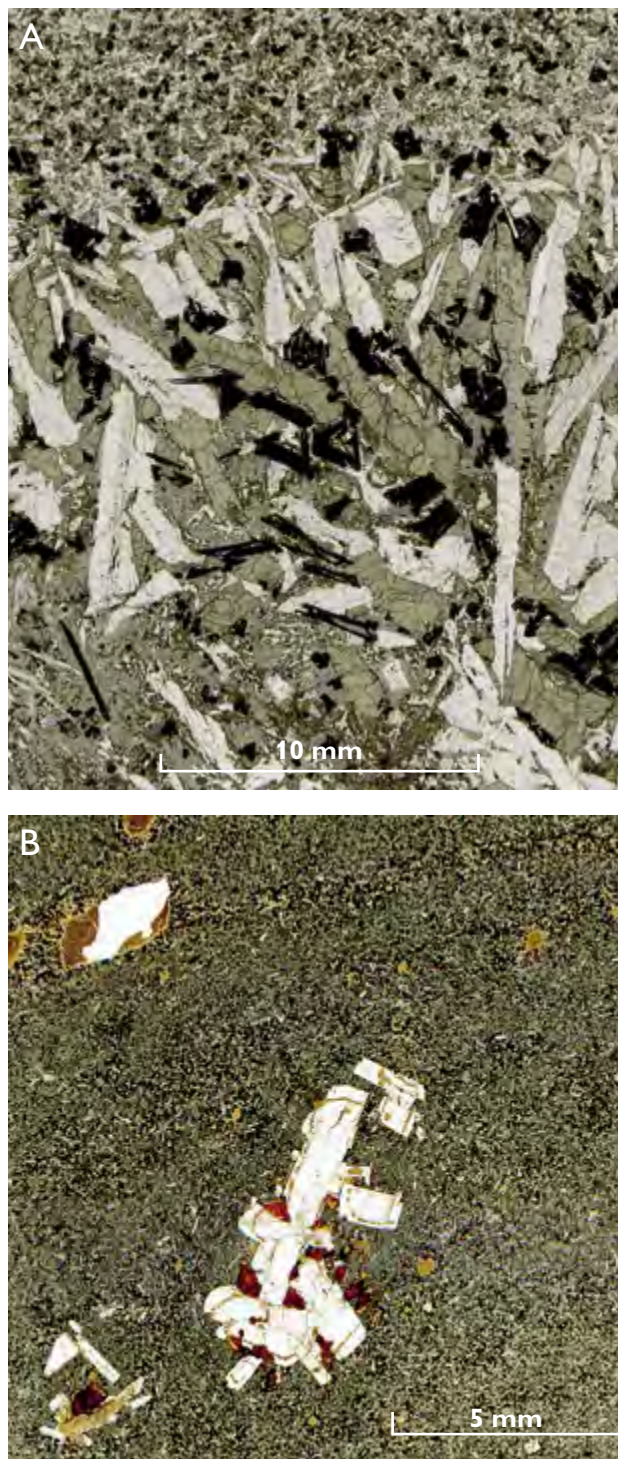


Fig. 80. Thin sections (scanned) of Rinks Dal Member unit 518. **A:** Pegmatitic vein with large crystals of plagioclase (white) and augite (grey) and smaller crystals of ilmenite and magnetite (black). The matrix of the same phases shows micrographic intergrowths. Dated sample 328406 (Storey *et al.* 1998), Dagaard-Jensen Dal, south-central Disko. **B:** Sparsely glomerophyric basalt with up to 6 mm large glomerocrysts of plagioclase and olivine (pseudomorphosed) in a very fine-grained groundmass. Sample 327016, Skarvefjeld, south Disko.

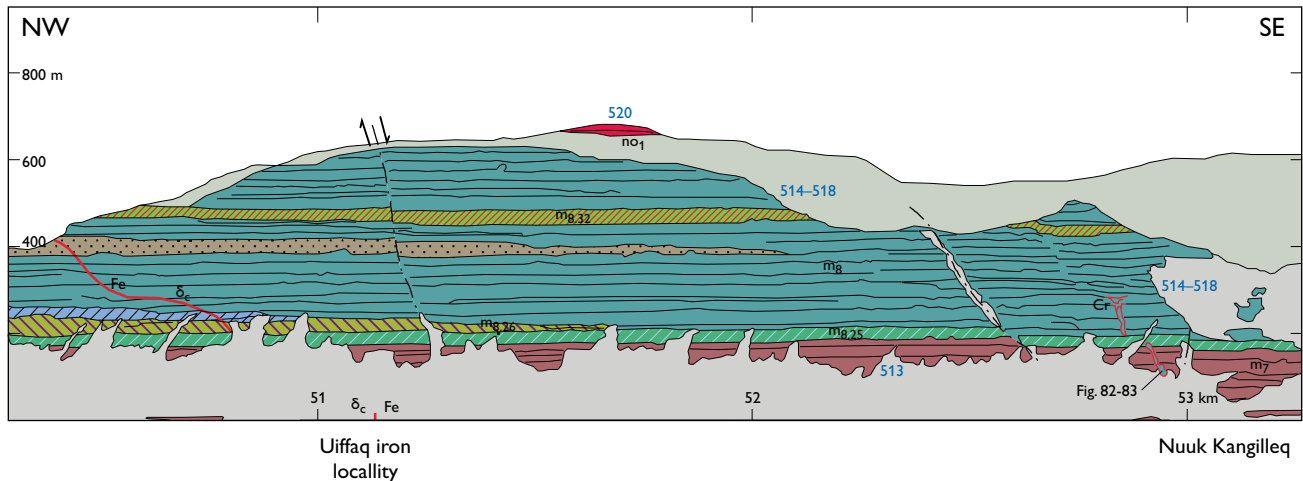


Fig. 81. Photogrammetrically measured section of a part of the south-west-coast of the Uiffaq peninsula, south Disko. A feeder dyke and small eruption crater (Cr) in the upper Rinks Dal Member are located at 52.9 km (shown in Figs 82, 83). A native-iron-bearing dyke (red) described later cuts obliquely through the exposure at 50–51 km and appears at the coast at 51.2 km in the famous locality where native iron was first described (Nordenskiöld 1871). Blue three-digit numbers are lithological codes; other annotations as in the original. Excerpt from the South Disko section (Pedersen *et al.* 2003).

On western Disko, the upper Rinks Dal Member displays a significant variation in lava flow thickness and morphology, whereas these are more uniform on central and eastern Disko and Nuussuaq. The few eruption sites that have been found are all located on western Disko. Together with the higher number of flows and larger total thicknesses in the west, these features support the interpretation that the primary source areas of these basalts were on western Disko and west of Disko.

Eruption sites on western Disko

Uiffaq, unit 515. A volcanic eruption site is exposed in the steep coastal cliff on the Uiffaq peninsula *c.* 14 km west of the Disko Gneiss Ridge at Nuuk Kangilleq (Fig. 81). Here a brecciated basaltic feeder dyke can be followed vertically for about 180 m until it ends in a funnel-shaped, reddish scoria zone within a basaltic lava flow (Fig. 82) situated in the middle of nine successive lava flows of unit 515. The lower part of the feeder dyke is strongly brecciated and crudely bedded (Fig. 83) and was described briefly by Pedersen (1977c, p. 63) who suggested that the dyke was brecciated when it came into contact with a local aquifer.

Nordfjord, unit 517. A prominent basaltic volcanic neck is exposed high in the steep mountain wall along the south side of Nordfjord/Kangersooq *c.* 2 km WNW of Point 1137 m (see Fig. 103, loc. 25). It was originally

mapped as part of the Nordfjord Member by Pedersen & Ulff-Møller (1987). A later visit revealed that the neck is an eruption site feeding basalts of unit 517 of the upper Rinks Dal Member. The semi-cylindrical neck has a diameter of *c.* 500 m and comprises two basalt bodies, of which the upper one is part of a lava flow originating from the neck (Fig. 84). The top of the neck is poorly exposed except in the near-vertical northern wall, but a more than 50 m thick coarsely columnar-jointed lava flow of unit 517 can be seen south-west of the neck at a distance of *c.* 500 m (Fig. 85). Two sample profiles, at distances of *c.* 500 m and 900 m from the neck, through the top of the upper Rinks Dal Member and the Nordfjord Member (Fig. 86) demonstrate that at the time of eruption of the Nordfjord Member (unit 520), the neck and its top lava constituted a prominent hill which allowed airborne tuffs to settle on it, while a total of 85 m of andesitic and dacitic lava flows were banked up against its flank. The neck constitutes the largest known basaltic eruption site of the Maligât Formation.

Lithologies on Disko

West of the Disko Gneiss Ridge. The general lithologies are well illustrated by the section along the north coast of Kangerluk between Naqerloq and Illukasik (South Disko section at 18–42 km). The upper Rinks Dal Member is here *c.* 520 m thick and consists of about 25 lava flows (Fig. 8, profile 1, and Fig. 87). West of Tunup Qaqqaa,



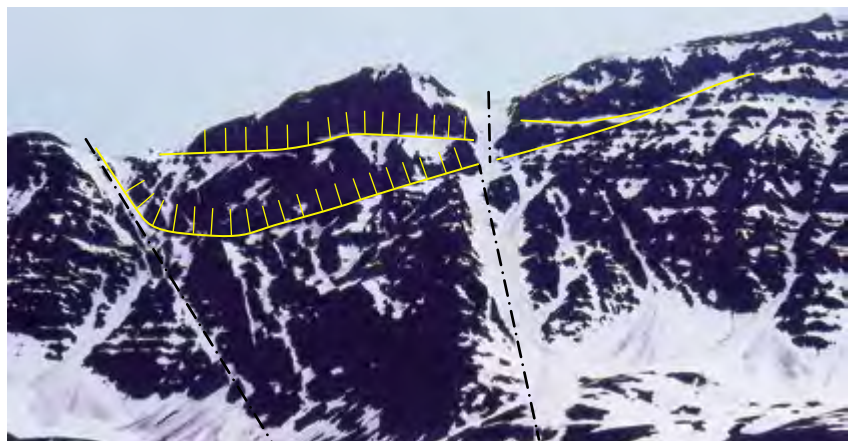
Fig. 82. Eruption site for a lava flow of unit 515, Nuuk Kangilleq, Uiffaq (Fig. 81). The brecciated feeder dyke can be followed vertically for about 180 m until it ends in a funnel-shaped reddish scoria zone within a lava flow. Photo: Finn Ulff-Møller.



Fig. 83. The lower part of the brecciated feeder dyke shown in Fig. 82. Height of field of view 8–10 m.

the thickness variation of the flows is particularly large, as illustrated by the South Disko section at 23–30 km, where individual lava flows range in thickness from less than 10 m to 60 m (the thick marker flow $m_{8,11}$) and there are intercalated flow fields of thin pahoehoe flows (e.g. unit $m_{8,13}$) that can be followed over more than 14 km and which were at least partially erupted from a crater site near Ukaleqartarfik (Fig. 88).

Fig. 84. Eruption site for Rinks Dal Member unit 517 on the south side of Nordfjord, west Disko (for locality, see Fig. 103, loc. 25). The dark exposure faces north; yellow lines schematically trace neck outline, base of thick lava flow and columnar jointing. The semi-cylindrical neck has a diameter of *c.* 500 m. It is composed of a lower body of compact basalt showing coarse columnar jointing roughly perpendicular to the wall, and an upper basalt body with a compact lower part with vertical columns up to several metres thick and an upper vesiculated part. The upper body is part of a lava flow originating from the neck (Fig. 85).



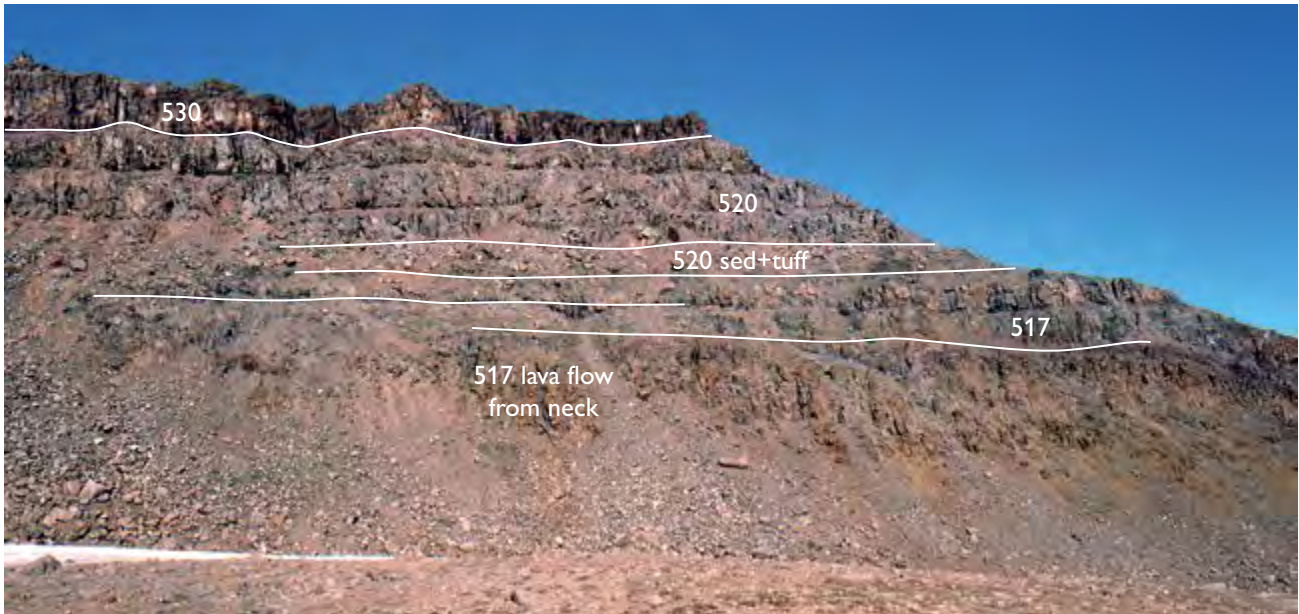


Fig. 85. The lava succession *c.* 500 m south-west of the volcanic neck in Fig. 84. The more than 50 m thick flow of unit 517 was erupted from the neck; it is the third flow beneath the top of the Rinks Dal Member. The flows of unit 517 are covered by sediments, including tuffs, and basalt lava flows of the Nordfjord Member (unit 520), followed by flows of the Niaquassat Member (unit 530).

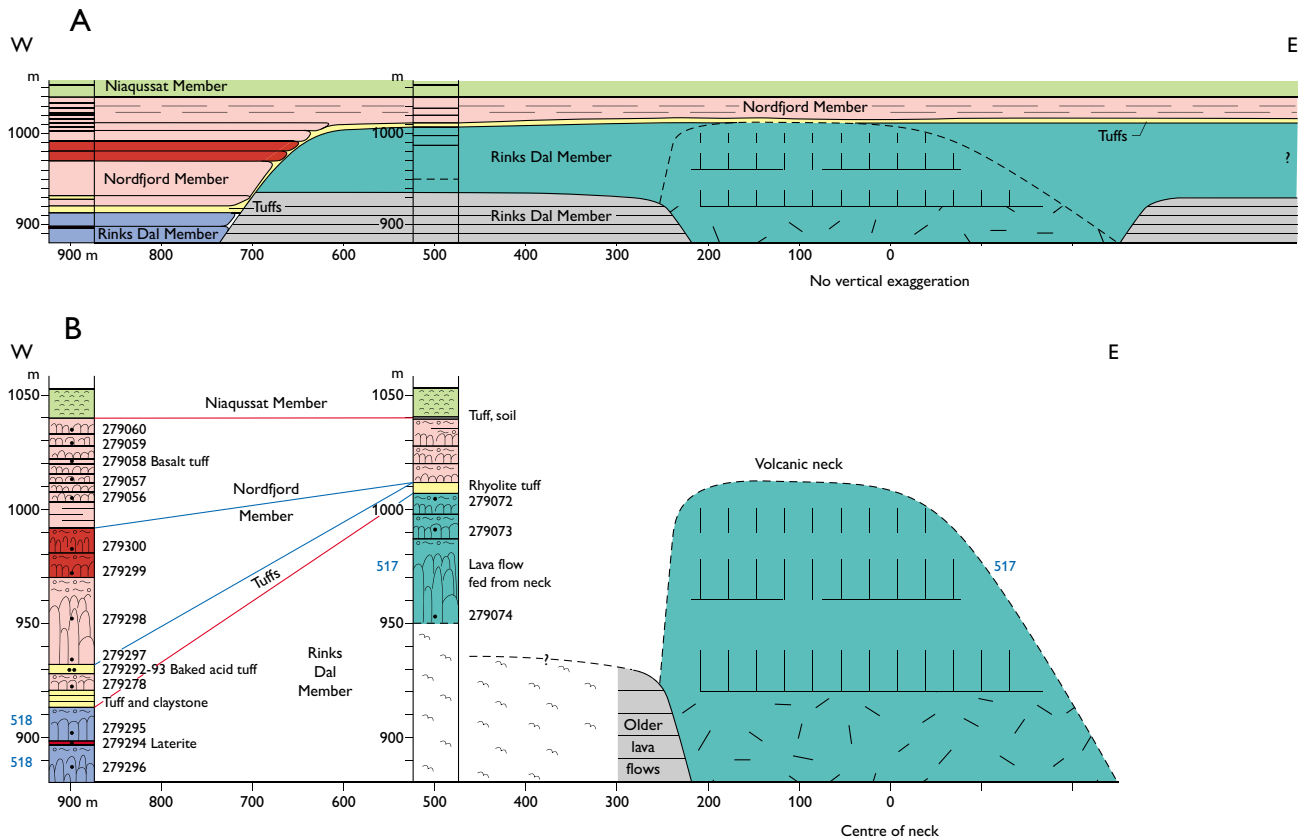


Fig. 86. Eruption site for Rinks Dal Member unit 517 on the south side of Nordfjord (Figs 84, 103). **A**: schematic reconstruction. **B**: profiles through the neck and the surrounding lava succession. For colours and symbols, see Fig. 7. See text for interpretation.

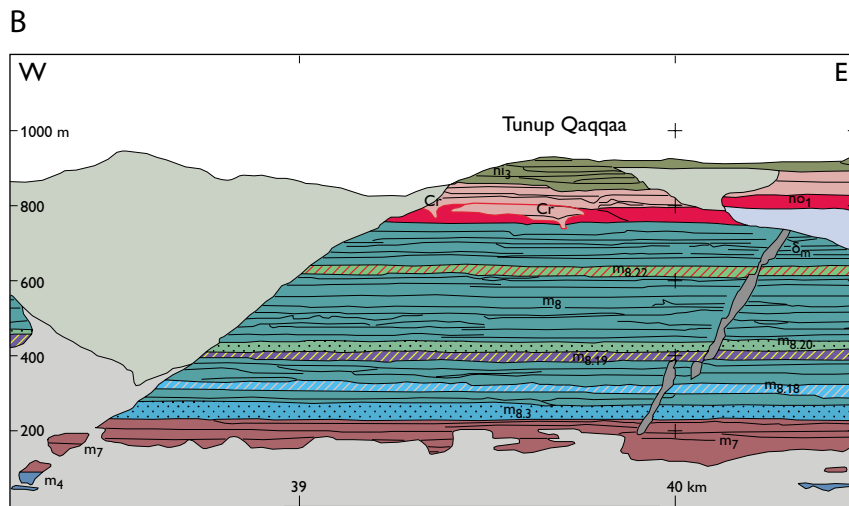


Fig. 87. The full upper Rinks Dal Member, 520 m thick, on south-central Disko. The boundaries between the successive units in the upper Rinks Dal Member are not precisely located because the Tunup Qaqqaa sample profile was not flow-by-flow sampled (Fig 8, profile 1). **A:** Photograph. **B:** Photogrammetric interpretation, excerpt from the South Disko section (Pedersen *et al.* 2003). Some characteristic marker flows are separately coloured and annotated. The Rinks Dal Member is overlain by the Nordfjord Member (unit 520, red and pink) and the Niaqussat Member (unit 530, olive green). Note the red scoria of the eruption crater (cr) for the lowest Nordfjord Member flow. South side of the Tunup Qaqqaa mountain, south-central Disko.

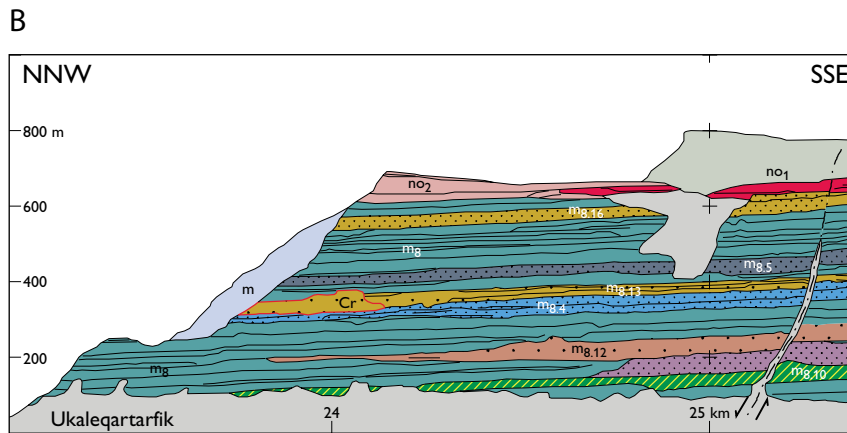


Fig. 88. The upper Rinks Dal Member on south-west Disko. **A:** Photograph. **B:** Photogrammetric interpretation, excerpt from the South Disko section (Pedersen *et al.* 2003). Some characteristic marker flows are separately coloured and annotated. Note the intercalated thick and thin flows and the eruption crater (Cr) for the flow field of thin flows of marker unit mg.13, marked with a black star in A. The boundaries between the successive units in the upper Rinks Dal Member cannot be located because no sample profiles are close enough. Flows of the Nordfjord Member (unit 520) overlie the Rinks Dal Member. Ukaleqartarfik 15 km west of Tunup Qaqqa, south-west Disko.

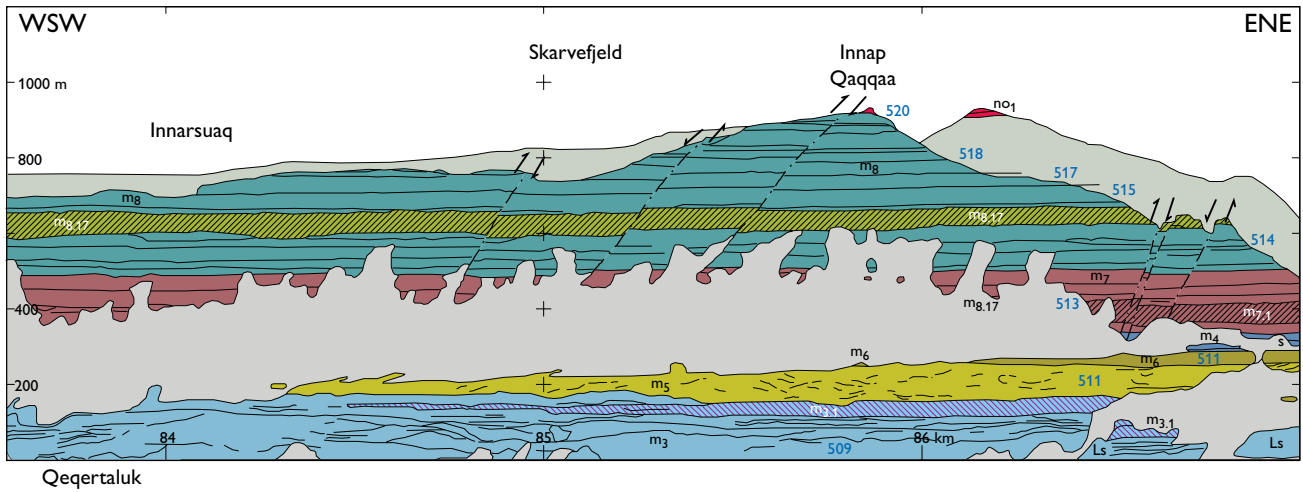


Fig. 89. Skarvefjeld on the south coast of Disko, exposing a large part of the Rinks Dal Member and the upper boundary to the Nordfjord Member. Some characteristic marker flows are separately coloured and annotated. Blue three-digit numbers are lithological codes; other annotations as in the original. The photo in Fig. 56 covers the section from 85.3 to 86.7 km on the base line. Excerpt from the South Disko section (Pedersen *et al.* 2003).

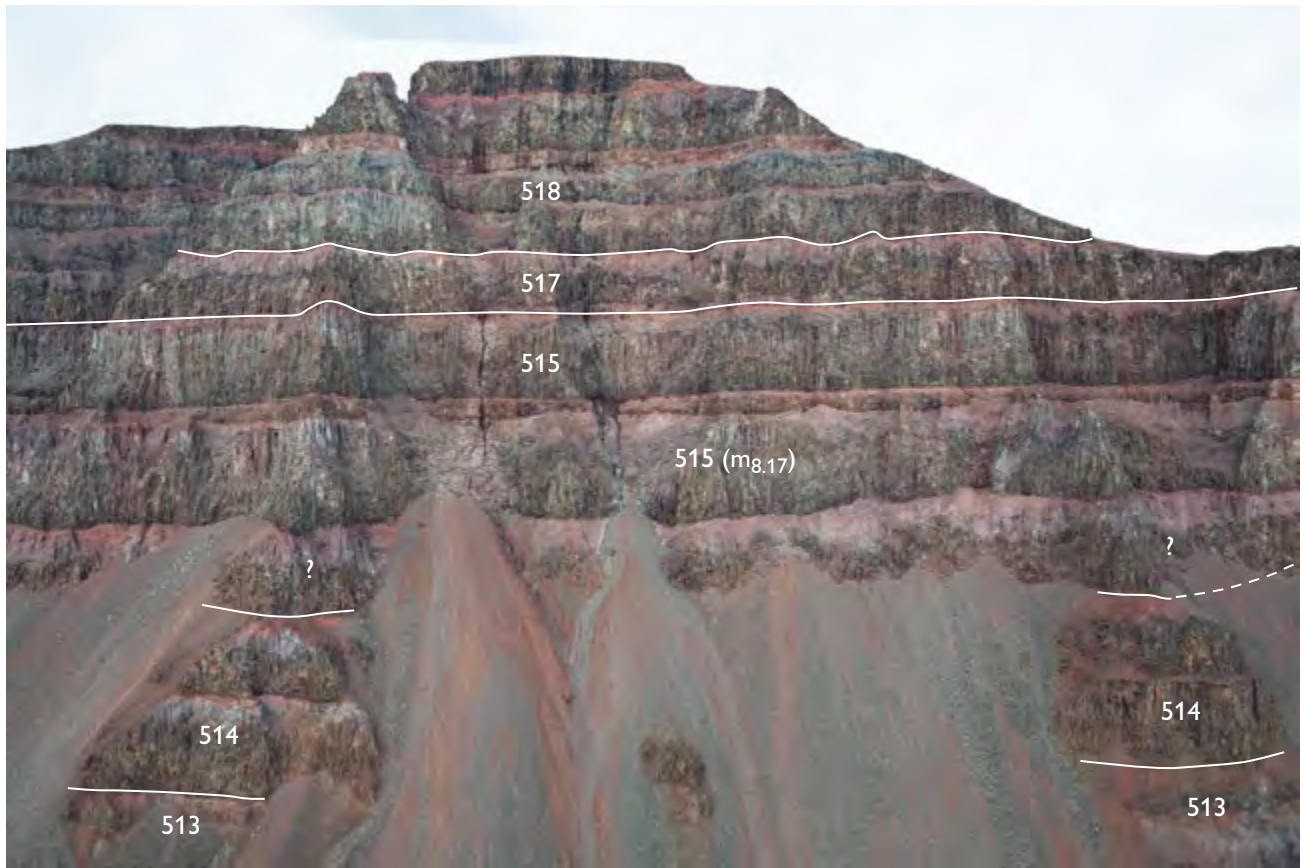


Fig. 90. Lava flows of the upper Rinks Dal Member at Innap Qaqqaa, the highest part of the Skarvefjeld mountain. Compare with the photogrammetric interpretation in Fig. 89 where the flow labelled m8.17 is identified. Photo: Erik Vest Sørensen.



Fig. 91. The middle and upper Rinks Dal Member on eastern Disko. A single flow of the Akuarut unit (513 inv) is invasive into sediments of the Assoq Member. The following two flows of the upper Rinks Dal Member (unit 514) are subaerial and ponded in wet depressions where they developed pronounced columnar jointing; the upper flow is capped by a prominent laterite horizon (**lat**). The overlying two flows (unit 515) are purely subaerial. North-exposed corrie wall in Blåbærdalen 2 km north-west of Skorstensfjeld, eastern Disko. Photo: Erik Vest Sørensen.

Central and southern Disko. On the Disko Gneiss Ridge and just east of it, the upper Rinks Dal Member forms a fairly monotonous succession of subaerial lava flows with blocky pahoehoe flow morphology and with only very limited lithological variation. The lava succession is well illustrated by the coastal wall at Skarvefjeld between Blåsedalen and Brededal on the south coast of Disko, shown in Fig. 89 and Fig. 7, profile 4. The upper Rinks Dal Member is here 390 m thick and consists of 13 subaerial lava flows, which vary in thickness between 10 m and *c.* 50 m. (Fig. 90). Some of the flows have slightly eroded top surfaces with a few centimetres of lateritic soil while others are devoid of soil. The lava flows show a crude columnar jointing with no indication of the presence of water.

Eastern Disko. On eastern Disko, the upper Rinks Dal Member thins gradually eastwards from 300 m to less than 200 m, and the number of lava flows decreases to less than ten. Individual lava flows more than 40 m thick occur, e.g. Fig. 7, profile 10 (Skorstensfjeld) or profile 12 (Point 1123 in Kvandalen). The lower part of the succession shows eastwards increasing interaction with un-

consolidated sand and coal swamps of the upper part of the Assoq Member. The flows ponded in topographic lows and are strongly columnar-jointed as illustrated by the two lowermost flows of the upper Rinks Dal Member exposed in a corrie in Blåbærdalen 2 km north-west of Skorstensfjeld (Fig. 91). The upper of these two flows is capped by a prominent horizon of red soil.

An example of a very thick, ponded flow, which reaches 90 m in thickness is seen at Aqajaruata Qaqqaa (Fig. 7, profile 13). Well developed, curved colonnades and prominent entablature zones attest to ponding in a water-filled depression.

The uppermost part of the Rinks Dal Member is particularly well illustrated by the basalt plateau exposed at Point 1014 m in Sortebærdalen (Fig. 7, profile 11). In the lower part of the succession, three lava flows of units 512–514 have invaded friable sandstone with a thick coal bed referred to the Assoq Member. The overlying six lava flows of units 515–518 have no traces of sandstone between them (Fig. 92), suggesting that at this stage the Assoq Lake basin was obliterated throughout the Disko area.

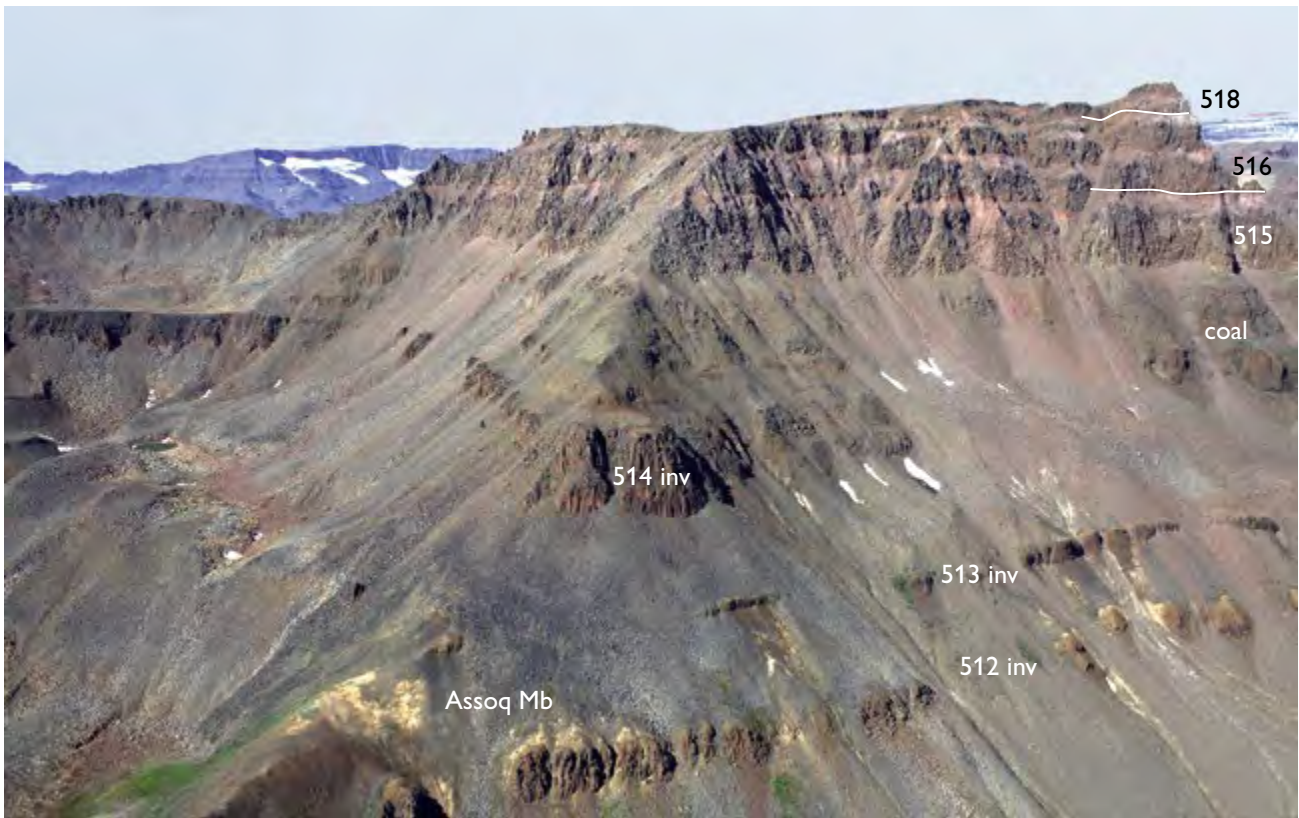


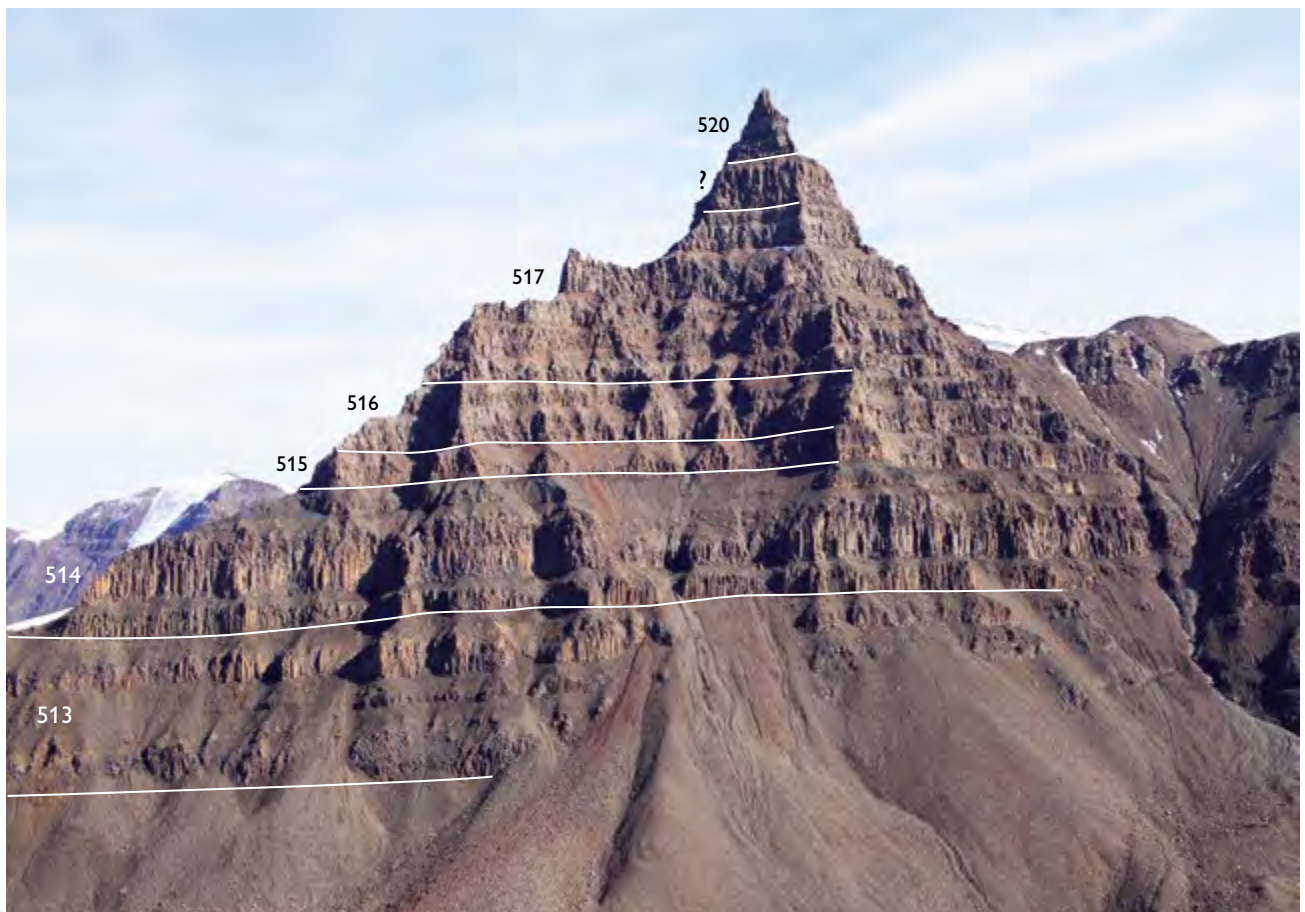
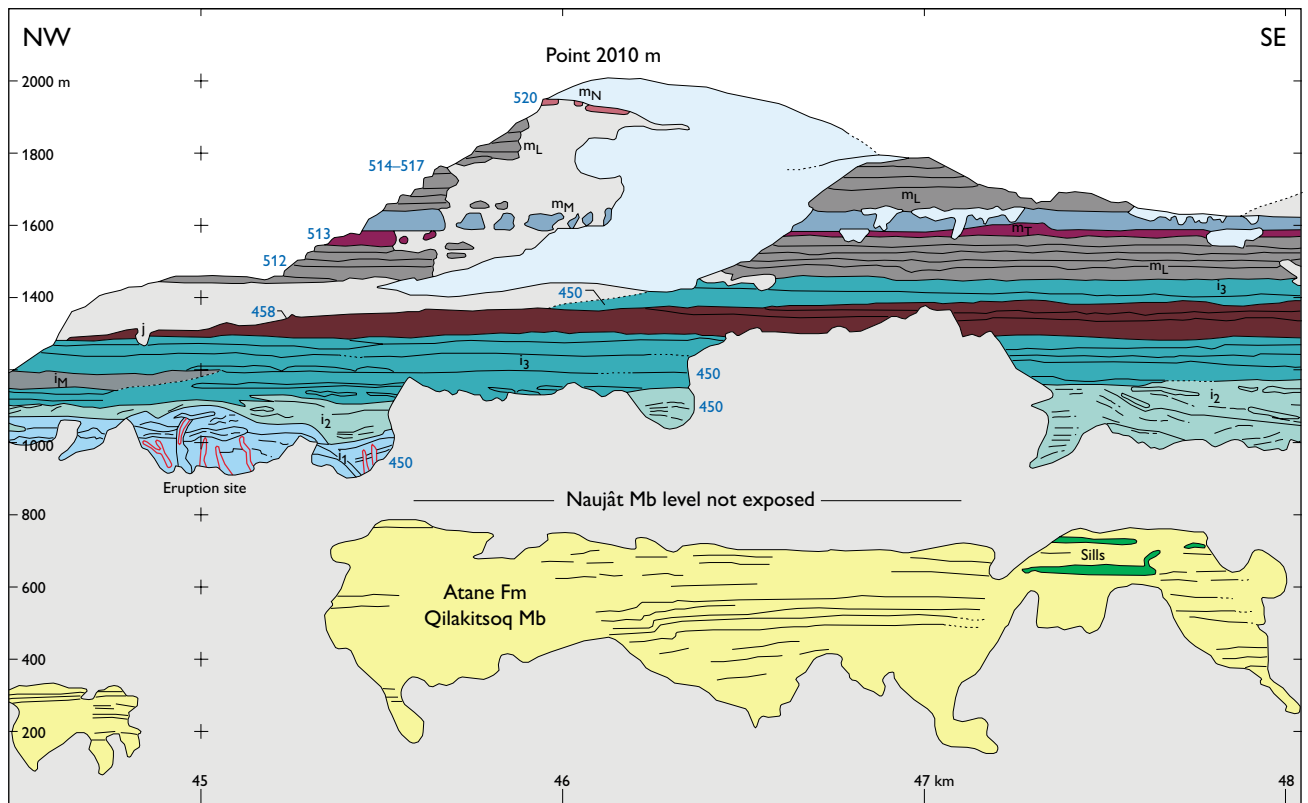
Fig. 92. The Rinks Dal Member on eastern Disko. Single flows of units 512 and 513 are invasive into Assoq Member sandstones. The overlying upper Rinks Dal Member comprises a unit 514 flow invasive into coal-bearing Assoq Member sands, followed by six subaerial flows of units 515–518 without traces of sandstone between them. The upper part of sample profile 11 in Fig. 7 is situated just left of the ridge in the centre of the image, and the lower part is situated to the right of the ridge. The level of a poorly exposed coal layer more than 1.5 m thick is indicated (coal). Height of field of view 300 m. Basalt plateau at Point 1014 m in Sorte bærdaalen, eastern Disko, seen from the south-west. Photo: Erik Vest Sørensen.

Lithologies on Nuussuaq

South coast of Nuussuaq. The original thickness of the upper Rinks Dal Member can only be assessed at a few localities where the overlying Nordfjord Member is preserved. Along the south coast, the upper Rinks Dal Member is *c.* 300 m thick at Point 1888 m north of Ataata Kuua (Fig. 11, profile 2) where it consists of *c.* 15 flows. Farther to the east the upper Rinks Dal Member is *c.* 340 m thick at Point 2010 m (Fig. 93) and at Giesecke Monument where it consists of 12–13 flows (Figs 74, 94). The flow thickness varies from less than 10 m to a maximum of *c.* 70 m for the large flow m_M in the South Nuussuaq section (Fig. 93). This flow may have a local origin (see map Fig. 96), but most of the other flows are considered to have flowed in from the south-west, partly channelled along the south-easterly sloping surface of the Vaigat Formation picrite lava shield.

The easternmost exposure of the upper Rinks Dal Member is a just 40 m thick succession of three subaerial lava flows of unit 517, which have crossed the eastern boundary fault to be emplaced on gneiss north of Saqqaq (Pedersen & Larsen 1987; Pedersen *et al.* 2007a; Fig. 11, profile 11) where they are covered by lava flows of the Nordfjord Member and separated from these by traces of soil.

Nunavik ridge. North of the Aaffarsuaq valley, lava flows of the upper Rinks Dal Member unit 517 rest either on picrite lavas from the Vaigat Formation or on gneisses. They cap a number of local high mountaintops and are overlain by lavas of the Nordfjord and Niaquusat members. They are best illustrated by their occurrence along the mountain ridge Nunavik (Nuugajukassak Alleq and Qulleq; Larsen & Pedersen 1992, figs 3 and 4, Central



Facing page (top):

Fig. 93. Photogrammetrically measured section along the south coast of Nuussuaq, showing subaerial lava flows of the Rinks Dal Member (units 512–517) and the Nordfjord Member (unit 520) overlying the Vaigat Formation (Ordlingassoq Member, units 450 and 458). Blue three-digit numbers are lithological codes; other annotations as in the original. The synvolcanic mudstones of the Naujât Member are not exposed; their approximate level is indicated. Point 2010 m near Paatuut, excerpt from the South Nuussuaq section (Pedersen *et al.* 1993).

Nuussuaq section at 59 to 71 km, units m_u and m_M ; Fig. 163, unit M_{f2}). They are shown in Fig. 12, profile 13 and Fig. 95, where they form a succession of about seven lava flows with a total thickness of up to 315 m. Some of the flows are ponded and as much as 75 m thick, and one flow locally reaches a thickness of 90 m. Several flows have prominent colonnades and entablatures suggesting solidification in a wet environment.

Lava volumes in the upper Rinks Dal Member

Despite the fairly monotonous character of the upper Rinks Dal Member, photogrammetric studies have identified a number of individual lava flows or flow fields. These are indicated with colours and/or annotation on the photogrammetric sections where they can be followed over distances ranging from a few kilometres to more than 15 km, commonly over 4–8 km (Table 3). These measurements are not easy to convert into areas, but if the lengths are simply squared, and if a typical thickness of *c.* 30 m is assumed, many flows will have volumes between 0.5 and 3 km³, and very few will exceed 5 km³.

The largest of the measured flows belongs to unit 514 and can be followed for a distance of 25 km along the south coast of Nuussuaq from west of Ataata Kuua to Giesecke Monument. It is shown as marker unit m_M in the South Nuussuaq section (Fig. 93). The thickness of this flow was measured by Pedersen & Ducholm (1992, fig. 13), who found that it varies from less than 45 m to more than 70 m within a 'measurable' area of 18 × 3–4 km (Fig. 96). The flow has a minimum area of *c.* 240 km² and its minimum volume can be estimated at 10 km³. The thickness measurements can be contoured and show a maximum near Paatuut, suggesting either ponding or that the feeder zone might have been located in this part of Nuussuaq; no actual feeders have been observed. The real volume of the flow may substantially exceed 10 km³.

By comparison, the most voluminous lava flow known in the Maligât Formation is a native-iron-bearing composite lava flow of the Nordfjord Member in the Mellemfjord area on south-western Disko which has a volume of at least 14 km³ (Pedersen 1977b, fig. 19 and page 41).

Facing page (bottom):

Fig. 94. Giesecke Monument, a landmark peak reaching 1574 m a.s.l. on the south coast of Nuussuaq. Subaerial flows of the upper Rinks Dal Member (units 514–517) constitute the major part of the peak, which is topped by a remnant of a Nordfjord Member basalt flow (unit 520). The exposed section is 550 m thick. See also Fig. 74. Photo: Erik Vest Sørensen.

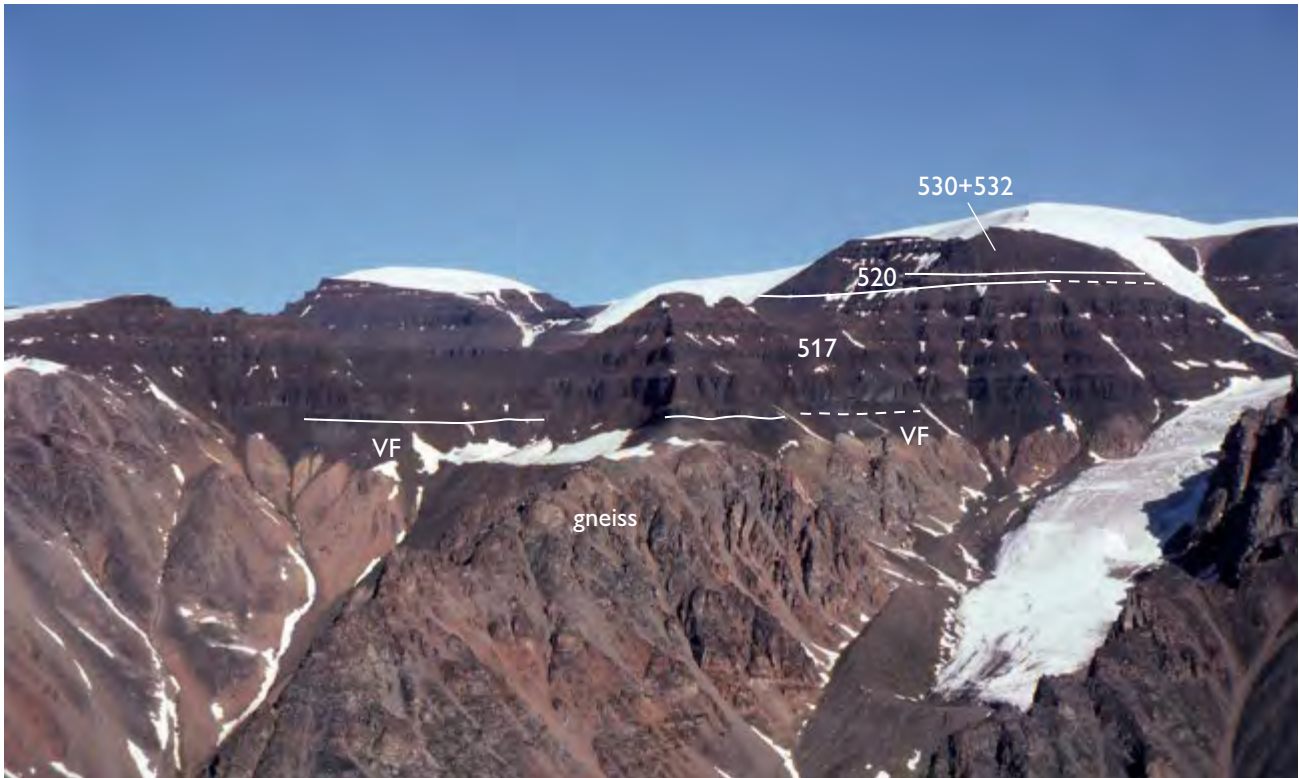


Fig. 95. The Nunavik mountain ridge on northern Nuussuaq, just east of the eastern boundary fault. Here the gneiss rises to 1300–1500 m altitude and is overstepped by the Vaigat Formation (VF) in lows, overlain by seven flows of unit 517 of the upper Rinks Dal Member, two basalt flows of the Nordfjord Member (520) and a series of picrite and basalt flows of the lower and upper Niaqussat Member (530, 532). Unit 517 is here 315 m thick. The ridge is located in Figs 4, 6.

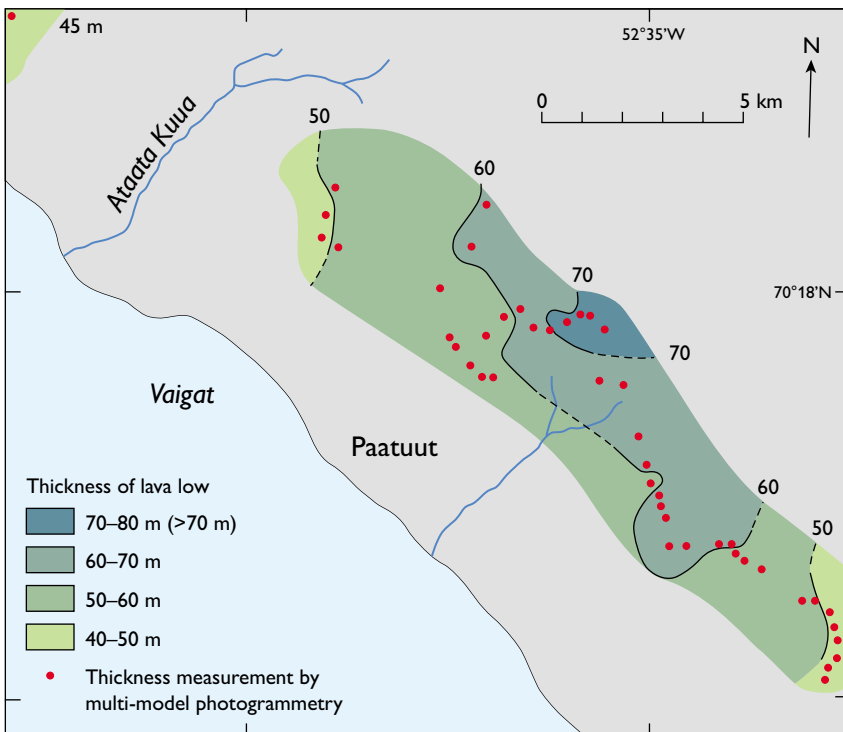


Fig. 96. Thickness map of the most voluminous lava flow measured in the upper Rinks Dal Member. The thickness measurement points, tracing the coastal wall, are spaced over a sufficiently wide coastal strip that a contoured thickness map can be made. The flow has a minimum area of *c.* 240 km² and a minimum volume of 10 km³. Paatuut, south coast of Nuussuaq. After Pedersen & Dueholm (1992, fig. 13).

Table 3. Measured minimum lengths of individual lava flows in the Rinks Dal Member

Annotation	Localities	Length, km	Western end	Eastern end
Akuarut unit (513)				
<i>South Disko section (west to east)</i>				
m 7.2	Naqerloq to Tunup Qaqqaa	7.4	Scree	Scree
m 7.3	Kangaarsuk to Akuarut	12.5	Air	Air
m 7.1	Skarvefjeld to Ippik	3.3	Scree	Air
<i>Central Disko section (west to east)</i>				
m 7.1	Perlertut Qaqqaat	2.4	Scree	Scree
m 7.2	Perlertut Qaqqaat	1.6	Scree	Scree
m 7.3	Perlertut Qaqqaat	2.0	Scree	Scree
m 7.4	Perlertut Kuuat to Stordal	3.0	Air	Scree
m 7.5	Perlertut Kuuat to Stordal	2.9	Air	Scree
m 7.6	Perlertut Kuuat to Stordal	2.8	Air	Air
m 7.7	Stordal	8.5	Featheredge	Featheredge
m 7.8	Stordal	6	Featheredge	Featheredge
m 7.9	Stordal	3.9	Featheredge	Scree
m 7.10	Kuugannuaq	2.8	Scree	Scree
m 7.11	Narsap Qaqqaa	5.0	Scree	Scree
<i>South Nuussuaq section</i>				
m	Umiasat to Tartunaq	c. 12	Air	Air
Median length 3.3 km; mean length 5.1 km.				
Upper Rinks Dal Member (units 514–518)				
<i>South Disko section (west to east)</i>				
m 8.8	Point 639 m to Nuuk Qiterleq	6.1	Scree	Air
m 8.7	Point 639 m to Point 691 m	7.0	Scree	Air
m 8.15	Point 639 m to Point 691 m	6.6	Scree	Air
m 8.6	Nuuk Killeq to Point 691 m	4.5	Fault	Air
m 8.14	Point 691 m	2.6	Air	Air
m 8.5	Nuuk Killeq to Umiiarneq	13.1	Scree	Air
m 8.13	Nuuk Killeq to Umiiarneq	13.8	Scree	Air
m 8.4	Nuuk Kangilleq to Naqerloq	8.9	Scree	Air
m 8.2	Point 691 m	2.6	Scree	Air
m 8.12	Ukaleqartarfik to Umiiarneq	5.6	Featheredge	Featheredge
m 8.11	Ukaleqartarfik to Kuussuaq	8.0	Featheredge	Near featheredge
m 8.10	Ukaleqartarfik to Naqerloq	3.2	Scree	Air
m 8.1	Naqerloq to Kuussuaq	5.1	Air	Air
m 8.9	Naqerloq to Kuussuaq	7.7	Scree	Featheredge
m 8.21	Kuussuaq	1.6	Featheredge	Air
m 8.24	Tunup Qaqqaa	3.5	Air	Air
m 8.22	Tunup Qaqqaa	3.5	Air	Air
m 8.20	Tunup Qaqqaa	4.9	Featheredge	Air
m 8.19	Tunup Qaqqaa	6.0	Featheredge	Air
m 8.18	Tunup Qaqqaa	7.0	Featheredge	Air
m 8.3	Tunup Qaqqaa	6.0	Featheredge	Scree
m 8.32	Kangerluk to Itilleq (Uiffaq)	13.8	Air	Air
m 8.23	Kangerluk to Uiffaq	5.0	Air	Featheredge
m 8.27	Uiffaq	5.0	Air	Featheredge
m 8.26	Uiffaq	5.8	Air	Featheredge
m 8.25	Uiffaq	10.0	Featheredge	Scree
m 8.28	Uiffaq to Itilleq	6.0	Featheredge	Air
m 8.29	Killiit to Lyngmarksfjeld	11.8	Air	Air
m 8.17	Skarvefjeld to Ippik	6.8	Air	Air
m 8.30	Brededal to Nuugaarsunnguaq	4.7	Air	Featheredge
m 8.31	Brededal to Niuluut	2.1	Air	Scree
<i>Central Disko section (west to east)</i>				
m 8.2	Perlertut Qaqqaat	4.3	Fault	Air
m 8.3	Perlertut Qaqqaat	2.8	Scree	Scree
m 8.6	Perlertut Qaqqaat to Stordal	5.2	Featheredge	Air
m 8.8	Stordal	6.3	Air	Featheredge
m 8.9	Stordal	3.1	Featheredge	Air
m 8.12	Kuugannuaq	4.3	Air	Featheredge
m 8.16	Point 1530 m	5.7	Air	Air
m 8.14	Point 1530 m to Qinngusaq	17.5	Featheredge	Air
m 8.17	Point 1530 m	6.0	Panel boundary	Air
m 8.15	Narsap Qaqqaa to Qinngusaq	10.0	Featheredge	Featheredge
m 8.18	Qinngusaq	3.0	Panel boundary	Scree
m 8.19	Kvandalen	4.8	Featheredge	Scree
m 8.20	Kvandalen	12.5	Air	Scree
<i>South Nuussuaq section</i>				
m M	Point 1722 m to Upalluk	25.6	Air	Featheredge
<i>Central Nuussuaq section</i>				
m M	Point 2080 m to Point 2000 m	12.9	Air	Air

Median length 5.9 km; mean length 7.0 km.

Note: Similarly annotated flows in different sections are not identical flows.

The annotation numbers were made during compilation and are not systematic with height or longitude.

Ends noted as scree or air are 'open', i.e. the flow may be longer. Featheredges are true ends.

Chemical compositions of the Rinks Dal Member

As stated earlier, the Rinks Dal Member almost exclusively consists of three-phase cotectic basalts evolved in deep-seated magma chambers (Larsen & Pedersen 2009). The crystallisation sequence is olivine (+ rare chromite) → olivine + plagioclase → olivine + plagioclase + clinopyroxene. Fe-Ti oxides are late. Most lava samples contain small amounts of interstitial clay, probably altered glass. However, the samples are generally fresh, with an average volatile content of 1.27 ± 0.70 wt%; of 1011 chemically analysed samples only 14 have more than 4 wt% volatiles. Mobile elements such as K, Rb, and Ba do, however, show some scatter. Representative analyses are shown in Table 4.

In contrast to the Vaigat Formation, MgO is a poor variation parameter for the Rinks Dal Member because of its narrow variation interval (mainly 4.4–9.2 wt% MgO; only 13 samples have higher MgO up to 25.4 wt%). The *mg*-number ($mg = \text{atomic } 100\text{Mg}/(\text{Mg} + \text{Fe}^{2+})$) provides a much better data spread (mainly *mg* 35–64, but up to 83) and has therefore been chosen as the main variation parameter for the Rinks Dal Member. This means that the geochemical plots for the Vaigat and Maligât Formations shown in Pedersen *et al.* (2017), and in the present work, are not directly comparable. For plots of the Maligât Formation with MgO as the common variation parameter, see Larsen & Pedersen (2009).

The 12 chemostratigraphic units of the Rinks Dal Member are difficult to show individually in chemical plots. Therefore, in many plots the analyses have been grouped into the Lower Rinks Dal Member (units 505–509, 512), the Skarvefjeld unit (511), the Akuarut unit (513), and the Upper Rinks Dal Member (units 514–518).

Major elements

Variation diagrams for the major elements are shown in Fig. 97. Crystallisation proceeds from right to left in the diagrams. Only the most Mg-rich samples have crystallised olivine alone. Plagioclase began crystallising around *mg*-number 58 (MgO around 7.5 wt%) where Al_2O_3 began to decrease. It was followed shortly by clinopyroxene, and CaO began to decrease also. Na_2O increased slightly but was also removed with the plagioclase. FeO^* increased markedly, and so did TiO_2 , K_2O and P_2O_5 . The most fractionated basalts, with *mg*-number <40 (MgO <*c.* 4.8 wt%), may perhaps have started to fractionate titanomagnetite, whereas K_2O and P_2O_5 remained in-

compatible throughout. The K_2O diagram shows a fair amount of scattering due to secondary alteration.

The SiO_2 trend forms a broad arc with maximum values that generally do not exceed 50.3 wt% SiO_2 . Of the analysed samples, 361 (36%) are *Q* normative, but only 120 (12%) have >1% *Q*. Some flows with around and above 50 wt% SiO_2 may be slightly crustally contaminated. Two flows with 51.3–51.4 wt% SiO_2 are clearly contaminated.

The Skarvefjeld unit does not follow the general fractionation trend shown by the other units. Its major element trends have higher TiO_2 , FeO^* and P_2O_5 and lower CaO and Al_2O_3 than the other units at similar *mg*-numbers; however, the trends merge into the main trend at low *mg*-numbers. As pointed out by Larsen & Pedersen (2009), the Skarvefjeld unit is best explained as a result of an episode of mixing followed directly by eruption: A batch of picrite magma, perhaps unusually large, entered the deep-seated magma chamber and mixed with the residing fractionated melt there; the mixed magma was then erupted without further equilibration and fractionation. The Skarvefjeld trends in Fig. 97 are thus not fractionation trends but mixing curves. Curves calculated by mixing of average unit 512 basalt with 6.2 wt% MgO (the residing melt in the chamber at the time) with a calculated unit 511 picrite with *c.* 21 wt% MgO model the Skarvefjeld trends very well (Fig. 97). There is also petrographic support for this explanation because some of the samples with 12–13 wt% MgO contain plagioclase glomerocrysts although plagioclase is not on the liquidus in such MgO-rich magmas. Three samples with 18–24 wt% MgO (*mg*-number >75) contain accumulated olivine; plagioclase phenocrysts were not observed in these.

Trace elements

Variation diagrams for trace elements are shown in Figs 98, 99. The incompatible elements (Fig. 98) show a general increase with decreasing *mg*-number, but significant scatter is apparent for some elements. This is primarily due to the fact that the Skarvefjeld unit and the upper and lower transition units comprise some lavas that are significantly enriched in Rb, Ba, Sr, Nb, Ce, and Zr/Y relative to the 'normal' lavas. These enriched lavas are only present in a small area on north-eastern Disko and on southern Nuussuaq (Figs 10–11). It is also notable that most flows of the Akuarut unit have particularly high contents of Sr and high Zr/Y.

Of the transition elements (Fig. 99), V, Cu, and Zn increase throughout the sequence of melt evolution.

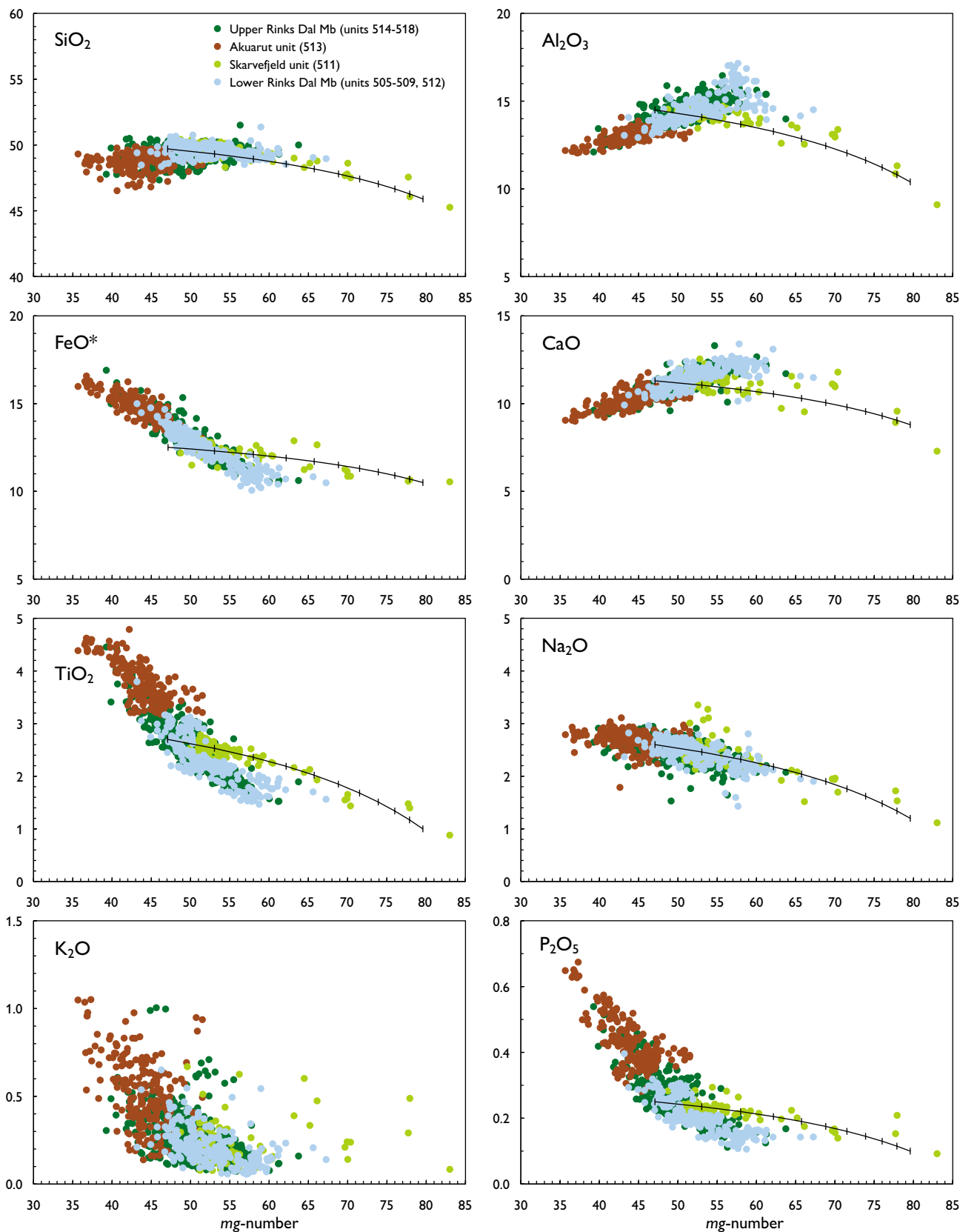


Fig. 97. Major element variation diagrams for rocks of the Rinks Dal Member. Data in wt% oxides recalculated volatile-free. FeO* is total iron as FeO. The curves in all diagrams are mixing curves calculated by mixing of an average unit 512 basalt with a modelled unit 511 picrite composition (tick marks shown for every 10% increment). The mixing trend reproduces the Skarvefjeld trend well; see text for discussion.

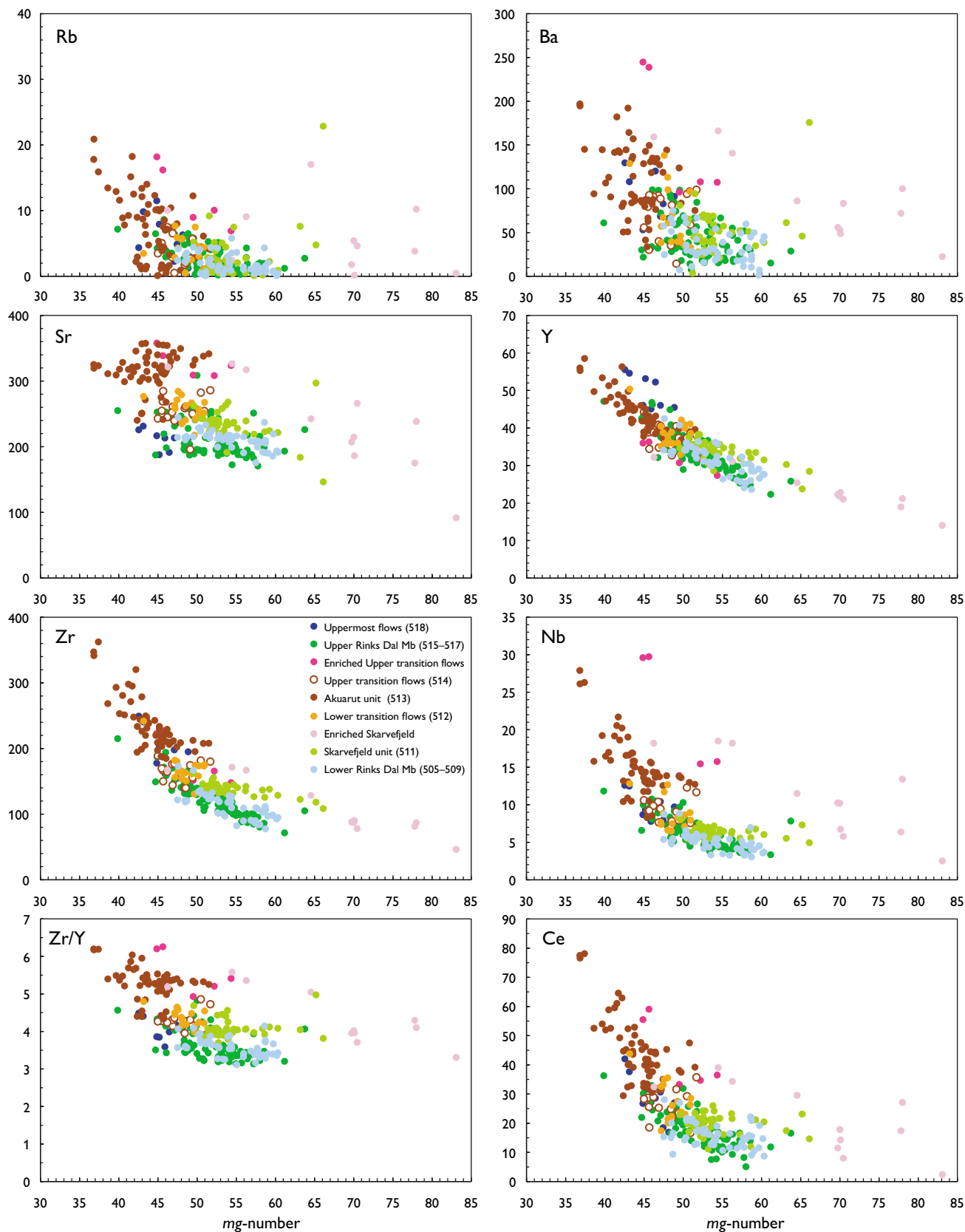


Fig. 98. Incompatible trace-element variation diagrams for rocks of the Rinks Dal Member. Data in ppm.

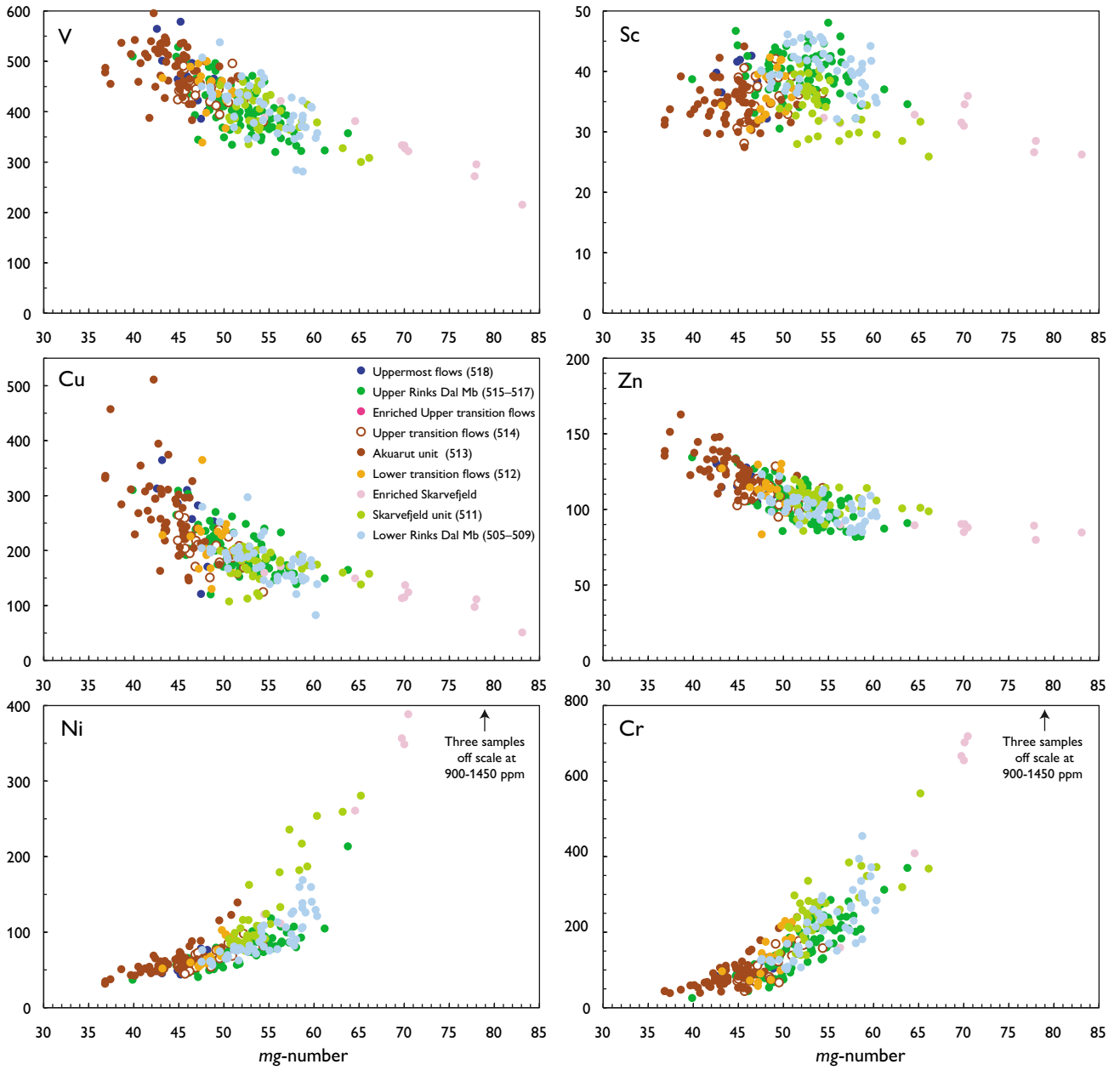


Fig. 99. Transition-element variation diagrams for rocks of the Rinks Dal Member. Data in ppm.

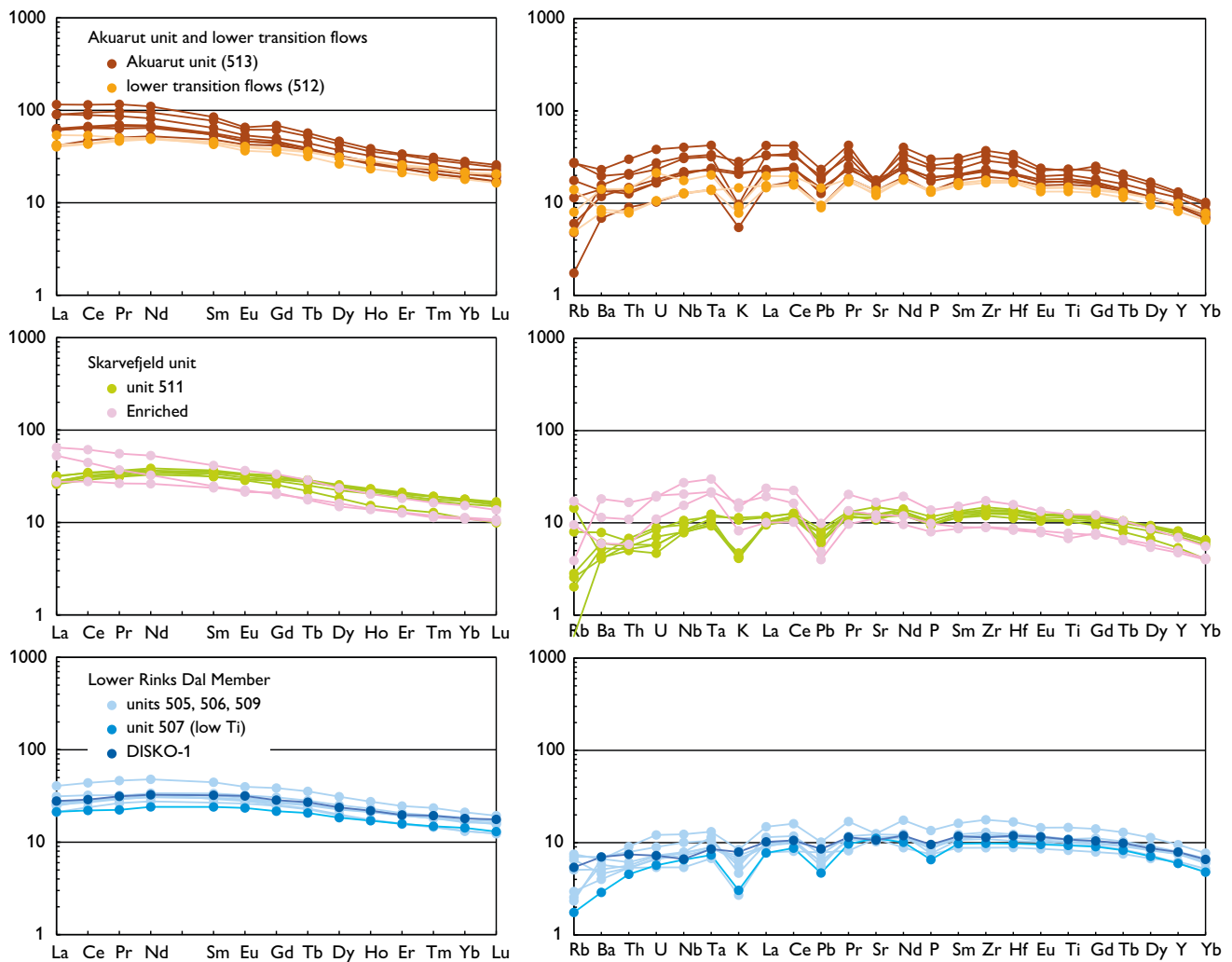


Fig. 10 (*first of two parts*). REE and multi-element diagrams for representative rocks of the Rinks Dal Member. Left diagram: chondrite normalised; right diagram: primitive mantle normalised; normalisation factors from McDonough & Sun (1995). DISKO-1 from unit 509 is GEUS' in-house geochemical standard.

Sc peaks around *mg*-number 50–55 and is then lowered by fractionation of clinopyroxene. Ni and Cr are compatible in olivine, chromite and clinopyroxene and decrease throughout the sequence of melt evolution. The Skarvefjeld unit has relatively low Sc and high Ni and Cr which is an effect of magma mixing, as described above.

REE and multi-element diagrams are shown in Fig. 100. With few exceptions, the REE patterns are parallel and show hump-backed shapes with $(La/Sm)_N < 1$ and $(Tb/Lu)_N > 1$. Parallel displacement of patterns correlate well with *mg*-numbers and is due to ordinary olivine-plagioclase-augite fractionation. The low-Mg, evolved rocks of the Akuarut unit show small Eu troughs, presumably due to extended plagioclase fractionation.

The REE patterns of the Akuarut unit are steeper than those of the other units and are tilted relative to these, with higher LREE and lower or equal HREE. This can be modelled by involving stabilisation and fractionation of small amounts of garnet (*c.* 1%) in the deep-seated magma chamber at this stage (Larsen & Pedersen 2009), which will also explain the high Zr/Y.

The multi-element patterns have curved shapes like the REE patterns, with relative depletion of the most incompatible elements Rb–Ba–Th–U, and distinct troughs for K, Pb and P. There are some variations in the levels of Rb and K of individual samples which may be due to secondary alteration. The increased levels of the most incompatible elements in the enriched samples

B

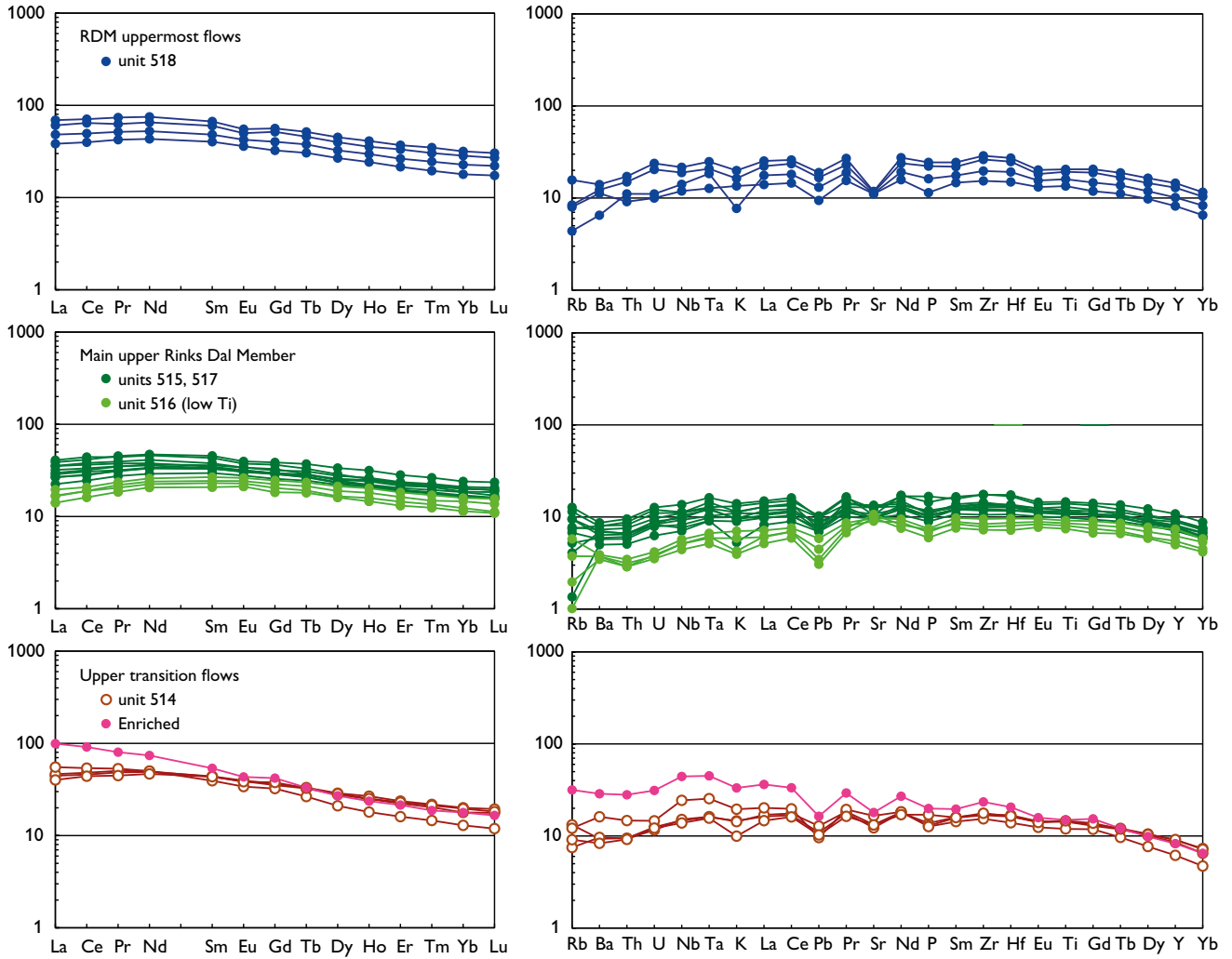


Fig. 100 (second of two parts). REE and multi-element diagrams for representative rocks of the Rinks Dal Member. Left diagram: chondrite normalised; right diagram: primitive mantle normalised; normalisation factors from McDonough & Sun (1995).

shown in Fig. 98 are clearly seen in Fig. 100 as well. In the most enriched samples, such as 136969 of the Skarvefjeld unit and 318758 of the upper transition flows (Table 4), the increase comprises all elements from Rb to Ti but not the HREE. These enriched flows bear an imprint of accidental contamination with an enriched mantle com-

ponent, as discussed in Larsen & Pedersen (2009). Sample 327065 of the lower transition flows (Table 4) has a different enrichment pattern with a small increase in the most incompatible elements from Rb to Pb but not other elements; the Sr–Nd isotope analyses suggest that this increase is caused by slight crustal contamination.

Table 4a. Chemical analyses of rocks of the Rinks Dal Member

Unit	Lower Rinks Dal Member					Skarvefjeld unit				Lower transition flows		Akuarut unit
	5052	5061	5071	5091	5092	5111	5111	5112	5111	5121	5121	5131
Lith. code	5052	5061	5071	5091	5092	5111	5111	5112	5111	5121	5121	5131
GGU No.	354719	332881	326406	340961	157246	136969	332930	362348	136973	362344	327065	279041
Deg. W	5324.25	5319.33	5338.17	5342.09	5314.41	5324.06	5318.62	5215.44	5324.11	5215.40	5319.79	5307.77
Deg. N	6935.355	6958.587	6916.251	6915.768	6918.378	7009.380	6958.831	6939.040	7009.392	6939.014	6917.262	7005.896
Altitude, m	18	786	162	103	148	1256	1184	639	1207	687	312	1193
SiO ₂	48.43	48.72	48.24	49.57	49.10	44.82	47.88	48.21	48.17	48.93	48.88	49.13
TiO ₂	2.94	1.88	1.66	2.00	2.15	1.36	2.10	2.16	2.41	2.94	2.69	3.44
Al ₂ O ₃	13.69	14.59	15.26	14.48	13.91	11.01	13.27	13.92	13.85	13.64	13.12	13.12
Fe ₂ O ₃	5.25	4.70	4.58	1.73	3.70	2.08	5.54	2.25	4.92	3.05	4.80	4.53
FeO	8.62	6.76	6.91	10.20	8.90	8.50	6.24	9.49	7.39	9.94	8.67	9.25
MnO	0.24	0.18	0.20	0.18	0.20	0.17	0.18	0.18	0.19	0.19	0.21	0.21
MgO	5.99	8.06	6.92	6.86	6.47	18.09	10.39	8.07	6.65	6.33	5.83	5.76
CaO	10.68	12.14	11.96	11.54	11.47	9.31	10.85	11.41	10.39	10.55	10.33	10.17
Na ₂ O	2.52	2.14	2.23	2.46	2.38	1.49	2.05	2.27	2.97	2.60	2.68	2.59
K ₂ O	0.243	0.088	0.078	0.210	0.180	0.475	0.329	0.136	0.125	0.226	0.266	0.624
P ₂ O ₅	0.279	0.135	0.154	0.179	0.190	0.203	0.198	0.196	0.213	0.287	0.273	0.399
Volatiles	1.16	0.74	1.77	1.02	0.95	2.63	0.94	1.98	2.68	0.95	2.29	0.94
Sum	100.03	100.13	99.96	100.44	99.60	100.14	99.96	100.26	99.96	99.62	100.04	100.16
FeO*	13.34	10.99	11.03	11.76	12.23	10.37	11.22	11.51	11.82	12.68	12.99	13.33
mg number	47.59	59.73	55.92	54.13	51.69	77.91	65.18	58.64	53.23	50.23	47.58	46.65
Zn	118	83.4	91.6	99.1	106	76.9	88.5	99.6	108	124	123	125
Cu	282	176	171	194	216	126	146	200	178	294	407	270
Ni	71.7	132	76.7	84.7	76.6	774	266	220	96.4	110	60.9	68.7
Sc	48.7	46.7	36.6	41.5	39.5	27.4	38.2	33.6	35.7	39.0	33.1	34.1
V	558	422	330	404	403	243	364	350	409	453	354	465
Cr	134	381	158	201	173	1049	683	348	277	206	167	92.11
Ga	22.6	19.4	19.8	20.8	20.7	13.4	19.2	20.4	20.9	24.0	22.7	25.0
Rb	4.50	1.05	1.77	1.53	3.04	10.3	4.79	1.69	1.21	2.95	4.81	10.6
Sr	249	222	221	215	224	243	296	228	212	253	274	342
Y	40.9	25.6	26.8	32.3	32.4	20.4	23.1	30.7	32.9	42.5	35.1	39.4
Zr	186	103	92.4	123	128	93.5	125	132	140	186	175	232
Nb	8.11	4.30	3.55	4.79	5.06	13.5	6.98	5.25	5.43	8.48	11.6	13.5
Cs	0.067	0.017	0.109	0.008	0.062	0.035	0.145	0.034	0.028	0.046	0.110	0.124
Ba	43.5	19.1	26.4	37.9	33.8	75.6	51.9	39.8	34.9	52.2	93.5	90.0
La	9.63	5.01	5.05	6.02	6.19	12.52	7.59	6.15	6.52	9.55	12.78	14.54
Ce	26.9	14.6	13.5	16.5	17.8	27.3	21.0	17.8	19.7	26.4	32.8	39.4
Pr	4.30	2.46	2.08	2.71	2.74	3.44	3.33	2.89	3.04	4.31	4.66	5.88
Nd	21.9	12.6	11.0	14.0	14.7	14.9	16.7	15.0	16.5	22.2	22.9	29.5
Sm	6.58	3.96	3.56	4.47	4.69	3.66	4.62	4.68	5.15	6.55	6.33	8.08
Eu	2.24	1.47	1.32	1.61	1.71	1.20	1.61	1.64	1.83	2.23	2.06	2.62
Gd	7.67	4.92	4.31	5.28	5.46	4.19	5.09	5.61	5.96	7.46	7.02	8.66
Tb	1.28	0.819	0.747	0.903	0.932	0.635	0.789	0.910	1.04	1.27	1.14	1.33
Dy	7.64	4.79	4.53	5.54	5.63	3.66	4.50	5.48	6.10	7.62	6.47	7.61
Ho	1.50	0.948	0.932	1.16	1.16	0.755	0.833	1.12	1.22	1.55	1.27	1.42
Er	3.94	2.50	2.53	3.09	3.13	2.03	2.20	2.97	3.24	3.97	3.39	3.74
Tm	0.580	0.359	0.367	0.449	0.446	0.280	0.317	0.422	0.470	0.582	0.473	0.508
Yb	3.39	2.11	2.30	2.64	2.72	1.76	1.79	2.55	2.81	3.44	2.89	3.02
Lu	0.476	0.305	0.320	0.394	0.384	0.252	0.244	0.368	0.399	0.502	0.404	0.415
Hf	4.75	2.76	2.51	3.21	3.35	2.36	3.18	3.48	3.73	4.92	4.72	5.76
Ta	0.487	0.272	0.250	0.313	0.329	0.801	0.430	0.343	0.371	0.523	0.749	0.886
Pb	1.52	0.704	1.17	0.950	0.920	0.731	0.973	1.17	0.918	1.34	2.19	2.19
Th	0.720	0.361	0.424	0.421	0.449	0.868	0.501	0.439	0.412	0.624	1.14	1.01
U	0.246	0.115	0.110	0.134	0.145	0.401	0.171	0.143	0.117	0.214	0.433	0.337
<i>Isotope ratios calculated at 60 Ma</i>												
⁸⁷ Sr/ ⁸⁶ Sr ₆₀	0.703389	0.703283				0.703318	0.703444	0.703253	0.703354			0.703819
εSr	-16.49	-17.99				-17.49	-15.71	-18.41	-16.99			-10.39
¹⁴³ Nd/ ¹⁴⁴ Nd ₆₀	0.512945	0.512942				0.512959	0.512794	0.512965	0.512990			0.512785
εNd	7.50	7.43				7.78	4.56	7.89	8.37			4.38
²⁰⁶ Pb/ ²⁰⁴ Pb ₆₀	17.650	17.719				17.754	18.068	17.982	17.860			17.761
²⁰⁷ Pb/ ²⁰⁴ Pb ₆₀	15.346	15.307				15.352	15.533	15.419	15.395			15.301
²⁰⁸ Pb/ ²⁰⁴ Pb ₆₀	37.425	37.408				37.552	37.831	37.665	37.661			37.494

For explanation of lithological codes, see Table 1. For petrographical notes on the samples, see Table 4c.

Geographical coordinates in WGS 84. First two digits are degrees, then follow minutes in decimal form.

Major elements in wt% (XRF analyses). Trace elements in ppm (Zn–Ga: XRF analyses; Rb–U: ICP-MS analyses).

FeO* = total iron as FeO. mg number = 100 × atomic Mg/(Mg+Fe²⁺), with the iron oxidation ratio adjusted to Fe₂O₃/FeO = 0.15.

Table 4b. Chemical analyses of rocks of the Rinks Dal Member

Unit	Akuarut unit				Upper transition flows		Upper Rinks Dal Member				Uppermost flows	
	5131	5131	5131	5131	5141	5141	5151	5161	5171	5171	5181	5181
Lith. code	5131	5131	5131	5131	5141	5141	5151	5161	5171	5171	5181	5181
GGU No.	327049	332861	332852	362227	362168	318758	327023	157261	400255	340908	332945	327014
Deg. W	5324.88	5318.69	5247.61	5228.36	5215.17	5227.90	5326.28	5333.01	5256.76	5216.78	5313.35	5321.72
Deg. N	6916.722	6958.798	7018.247	7012.534	6938.994	7013.426	6916.755	6916.575	7022.688	6938.608	6944.899	6917.239
Altitude, m	409	1140	1551	1129	766	1095	620	719	1803	945	1318	829
SiO ₂	47.92	47.02	47.86	47.95	48.75	46.43	48.68	48.71	49.33	49.54	48.95	48.17
TiO ₂	4.08	4.71	4.51	4.26	2.94	3.00	2.81	1.62	1.98	2.15	2.71	3.87
Al ₂ O ₃	12.25	12.82	11.85	11.86	12.97	13.75	13.33	14.59	14.51	14.57	13.44	12.22
Fe ₂ O ₃	5.48	6.57	4.94	3.95	3.79	4.97	5.99	5.22	6.00	4.53	4.97	4.82
FeO	9.99	8.97	11.33	12.02	10.84	9.10	8.15	6.27	6.11	7.75	9.39	10.90
MnO	0.22	0.23	0.26	0.23	0.22	0.22	0.21	0.17	0.18	0.19	0.24	0.23
MgO	5.24	5.37	4.66	4.49	5.88	5.46	5.90	7.49	6.72	6.19	6.12	5.58
CaO	9.50	9.81	9.16	9.02	10.52	10.69	10.23	12.19	11.60	11.17	10.13	9.57
Na ₂ O	2.83	2.72	2.71	2.71	2.70	2.79	2.77	2.26	2.43	2.44	2.41	2.67
K ₂ O	0.817	0.281	0.688	0.936	0.288	0.962	0.404	0.170	0.153	0.272	0.391	0.472
P ₂ O ₅	0.495	0.525	0.620	0.630	0.351	0.410	0.345	0.150	0.184	0.210	0.236	0.458
Volatiles	1.29	1.03	0.96	1.35	0.74	1.83	0.86	0.92	0.65	0.77	1.14	1.22
Sum	100.11	100.04	99.54	99.40	99.98	99.61	99.68	99.76	99.84	99.78	100.12	100.18
FeO*	14.92	14.88	15.78	15.57	14.25	13.57	13.54	10.97	11.51	11.83	13.86	15.24
mg number	41.53	42.19	37.40	36.83	45.49	44.86	46.85	58.01	54.15	51.43	47.17	42.55
Zn	154	147	164	160	129	115	127	88.0	92.8	101	120	155
Cu	354	500	443	396	281	253	304	151	208	218	202	400
Ni	55.4	69.5	36.9	36.5	51.7	58.7	53.3	86.0	85.2	63.1	63.6	49.8
Sc	36.1	40.8	39.7	30.9	39.1	32.4	34.9	36.3	37.1	39.2	33.7	36.2
V	506	630	522	416	457	405	419	328	359	404	396	497
Cr	62.0	104	39.3	32.4	65.6	65.5	58.6	232	279	171	91.7	75.9
Ga	25.9	27.2	26.2	26.2	23.6	21.8	22.9	19.7	20.5	21.0	23.3	24.3
Rb	16.5	2.88	16.3	22.6	5.47	19.0	7.65	2.25	0.81	5.71	4.79	5.04
Sr	308	347	327	334	263	358	245	212	192	214	220	230
Y	49.5	54.1	56.9	55.1	39.3	35.5	39.9	23.6	30.4	33.8	35.2	55.7
Zr	303	348	390	384	186	246	185	82.2	111	128	161	275
Nb	20.9	20.1	26.6	26.5	9.11	29.2	8.98	3.36	4.63	6.39	7.84	12.43
Cs	0.116	0.064	0.285	0.387	0.084	0.128	0.099	0.010	0.009	0.153	0.053	0.049
Ba	130	104	153	155	55.0	190	57.1	24.6	33.0	46.5	74.0	81.0
La	21.5	21.3	27.4	26.5	9.51	23.5	9.68	3.93	5.32	6.79	9.08	14.4
Ce	54.4	57.9	70.5	68.2	27.0	56.0	27.1	11.6	15.0	18.8	24.4	39.5
Pr	8.03	9.03	10.78	9.88	4.15	7.45	4.09	1.90	2.55	2.95	3.93	5.82
Nd	37.4	43.4	50.4	47.5	21.3	33.8	21.0	10.3	13.3	15.5	19.8	29.9
Sm	9.55	11.4	12.5	11.8	6.44	7.95	6.38	3.41	4.38	4.91	5.96	8.88
Eu	3.02	3.48	3.69	3.48	2.16	2.44	2.11	1.28	1.56	1.71	2.03	2.81
Gd	9.94	12.3	13.7	13.0	7.50	8.35	7.25	4.06	5.10	5.74	6.46	10.3
Tb	1.60	1.89	2.05	1.90	1.18	1.20	1.19	0.691	0.885	0.969	1.10	1.65
Dy	9.11	10.6	11.4	10.6	7.00	6.65	7.06	4.08	5.45	5.77	6.59	9.80
Ho	1.76	1.95	2.10	2.01	1.37	1.29	1.39	0.866	1.14	1.21	1.32	1.94
Er	4.51	5.27	5.39	5.23	3.68	3.43	3.71	2.31	2.99	3.26	3.44	5.33
Tm	0.634	0.716	0.765	0.709	0.525	0.463	0.535	0.335	0.441	0.479	0.482	0.751
Yb	3.72	4.28	4.50	4.28	3.16	2.86	3.29	1.99	2.58	2.96	2.88	4.58
Lu	0.555	0.595	0.632	0.593	0.447	0.407	0.470	0.277	0.395	0.416	0.427	0.663
Hf	7.54	8.33	9.52	9.36	4.65	5.82	4.75	2.28	3.02	3.36	4.23	7.03
Ta	1.24	1.18	1.57	1.54	0.578	1.67	0.599	0.218	0.336	0.457	0.471	0.769
Pb	2.94	2.71	3.49	3.66	1.54	2.46	1.48	0.519	1.04	1.34	1.41	2.50
Th	1.66	1.61	2.38	2.29	0.730	2.23	0.757	0.230	0.403	0.522	0.726	1.19
U	0.555	0.471	0.777	0.745	0.247	0.634	0.258	0.078	0.127	0.181	0.203	0.415
<i>Isotope ratios calculated at 60 Ma</i>												
⁸⁷ Sr/ ⁸⁶ Sr ₆₀		0.703242	0.703392	0.703182			0.703252	0.703271		0.703390		0.703329
εSr		-18.57	-16.45	-19.42			-18.44	-18.16		-16.47		-17.33
¹⁴³ Nd/ ¹⁴⁴ Nd ₆₀		0.512962	0.512965	0.512964			0.512993	0.512987		0.512951		0.512978
εNd		7.83	7.88	7.87			8.43	8.32		7.61		8.13
²⁰⁶ Pb/ ²⁰⁴ Pb ₆₀		17.923	17.957	17.960			17.863	17.987		17.847		17.708
²⁰⁷ Pb/ ²⁰⁴ Pb ₆₀		15.404	15.399	15.398			15.383	15.403		15.333		15.338
²⁰⁸ Pb/ ²⁰⁴ Pb ₆₀		37.613	37.711	37.711			37.706	37.709		37.591		37.560

Table 4c. Notes on analysed samples of the Rinks Dal Member

354719	Very fine-grained basalt with tiny microphenocrysts of plagioclase, clinopyroxene and olivine. Foreset-bedded pillow breccia, c. 190 m thick, deposited in the Assoq Lake. Unit 1 in the Orpiit Qaqqaat profile, south-central Disko just east of the gneiss ridge.
332881	Very fine-grained, nearly aphyric basalt with sparse microphenocrysts of olivine and plagioclase. From entablature zone in lava flow with well-developed entablature, 25 m thick, resting directly on weathered picrite of the Vaigat Formation. Flow 1 in the Kuugannguaq SE profile, inner Kuugannguaq valley, north-central Disko.
326406	Fine-grained basalt with numerous plagioclase-olivine glomerocrysts and scattered clinopyroxene phenocrysts. From entablature zone in lava flow with well-developed colonnade and entablature, 30 m thick. Flow 4 in the Tuapassuit profile, south Disko, on depression in the gneiss ridge just west of Qeqertarsuaq town.
340961	Fine-grained basalt with plagioclase-olivine-clinopyroxene glomerocrysts. Lava flow, 60 m thick. Flow 4 in the Fortunebay East profile, south Disko, on depression in the gneiss ridge.
157246	Very fine-grained basalt with plagioclase-olivine-clinopyroxene glomerocrysts. From entablature zone in subaqueous lava flow with well-developed colonnade and entablature and thick yellow top breccia, 40 m thick, deposited in the Assoq lake. Flow 8 in the Ippik profile, south Disko well east of the gneiss ridge.
136969	Picrite with numerous olivine phenocrysts with inclusions of chromite crystals. Pahoehe lava flow, 7 m thick, one of a group of four picrite flows enriched in some incompatible trace elements. Flow 7 in the Orlingasoq profile, north Disko.
332930	Fine-grained basalt with scattered phenocrysts of olivine and clinopyroxene. Lava flow, 30 m thick. Flow 24 in the Kuugannguaq SE profile, inner Kuugannguaq valley, north-central Disko.
362348	Fine-grained intersertal basalt with many microphenocrysts of skeletal olivine and a few plagioclases. Foreset-bedded pillow breccia, >25 m thick, deposited in the Assoq lake. Unit 1 in the Point 1123 profile, south side of Kvandalen, east Disko.
136973	Fine-grained almost aphyric basalt. Lava flow, 5 m thick. Flow 2 in the Orlingasoq profile, north Disko.
362344	Fine-grained basalt with sparse plagioclase phenocrysts and olivine microphenocrysts. From entablature zone in 30 m thick lava flow with well-developed colonnade and entablature and red-oxidised top breccia, resting on 10 cm black shale and overlain by 8 m yellow sand (filling stage of the Assoq lake). Flow 4 in the Point 1123 profile, south side of Kvandalen, east Disko.
327065	Well-crystallised basalt with phenocrysts and glomerocrysts of plagioclase. Slightly contaminated. Lava flow, 12 m thick, with 40 cm thick yellowish brown sediment on top. Flow 2 in the Skarvefjeld profile, south Disko.
279041	Very fine-grained basalt with small phenocrysts of plagioclase and olivine and clusters of clinopyroxene. Lava flow, 8 m thick. Flow 18 in the Qullissat profile, north Disko.
327049	Basalt with scattered plagioclase phenocrysts and glomerocrysts of plagioclase and augite. Lava flow, 45 m thick. Flow 15 in the Skarvefjeld profile, southern Disko.
332861	Very fine-grained basalt with tiny microphenocrysts of plagioclase, olivine and clinopyroxene. Highest TiO ₂ content in the Rinks Dal Member. Lava flow, 13 m thick. Flow 20 in the Kuugannguaq SE profile, inner Kuugannguaq valley, north-central Disko.
332852	Very fine-grained basalt with tiny microphenocrysts of plagioclase, olivine and clinopyroxene. Lava flow, 14 m thick. Flow 5 in the Ivissussat Qaqqaat profile, east of Ataata Kuua, south Nuussuaq.
362227	Very fine-grained basalt with sparse small plagioclase phenocrysts and tiny clinopyroxene microphenocrysts. Lava flow, 7 m thick. Flow 6 in the Giesecke Monument profile, south Nuussuaq.
362168	Fine-grained, nearly aphyric basalt with rare small phenocrysts of plagioclase and clinopyroxene. From entablature zone in 25 m thick lava flow with well developed entablature zone, overlain by c. 2 m of black, coal-bearing sediment. Flow 6 in the Point 1123 profile, south side of Kvandalen, eastern Disko.
318758	Very fine-grained basalt with scattered phenocrysts of clinopyroxene, plagioclase and olivine, and many microphenocrysts of the same minerals. Lava flow, 20 m thick. Flow 5 in the Giesecke Monument profile, south Nuussuaq. Enriched in some incompatible trace elements.
327023	Very fine-grained, nearly aphyric basalt with a few tiny microphenocrysts of plagioclase, olivine and clinopyroxene. Lava flow, 45 m thick. Flow 21 in the Skarvefjeld profile, south Disko.
157261	Very fine-grained basalt with glomerocrysts of plagioclase and olivine. Lava flow, >13 m thick. Flow 19 (top flow) in the Lyngmarksfjeld profile, south Disko.
400255	Fine-grained basalt with small plagioclase phenocrysts and plagioclase-olivine-clinopyroxene glomerocrysts. Lava flow, 12 m thick. Flow 9 in the Point 1888 profile, west of Ataata Kuua, south Nuussuaq.
340908	Fine-grained basalt with numerous plagioclase-clinopyroxene-olivine glomerocrysts. Lava flow, 55 m thick. Flow 9 in the Point 1123 profile, south side of Kvandalen, east Disko.
332945	Fine-grained, nearly aphyric basalt with rare plagioclase phenocrysts. Lava flow, 25 m thick, with laterite-impregnated top zone, uppermost flow in the Rinks Dal Member. Flow 33 in the Sorte Hak profile, central Disko.
327014	Very fine-grained, nearly aphyric basalt with scattered small phenocrysts of plagioclase and microphenocrysts of clinopyroxene and olivine. Lava flow, 45 m thick, next-highest flow in the Rinks Dal Member. Flow 28 in the Skarvefjeld profile, south Disko.

Phenocryst phases as observed in thin section are mentioned in order of decreasing abundance.

Samples of subaerial lava flows are usually taken in massive columns a few metres above the flow base.

Eruption sites for the Rinks Dal Member

Very few eruption sites for the Rinks Dal Member are known. It would be natural to assume that the member was fed from the widespread uncontaminated basalt dykes in the region, but this is not the case, as shown below.

Uncontaminated basalt dykes and sills

Many dykes of uncontaminated basalt on Disko and Nuussuaq cut the Rinks Dal Member. In addition, seismic sections and aeromagnetic maps suggest that the sediments beneath Disko Bugt are intruded by sills; one such sill crops out on a group of small islands in the south-eastern corner of Disko Bugt (Fig. 1), and another has been sampled by dredging in eastern Disko Bugt (Larsen & Dalhoff 2007; Larsen *et al.* 2016). South of Disko Bugt, three large young dykes are known; these are the >60 km long N–S-trending ‘globule dyke’, the 110 km long NNE–SSW-trending Manermiut dyke and the >13 km long WNW–SSE-trending Sydostbugt dyke (Ellitsgaard-Rasmussen 1951; Henderson 1969; Ártung 2004; Larsen 2006). On the aeromagnetic maps (Rasmussen 2002) the globule dyke and the Manermiut dyke form conspicuous linear features with reversed magnetic signature that can be followed northwards into Disko Bugt and almost to the south coast of Disko. No Tertiary intrusions have been found on the mainland east of the eastern boundary fault.

Some dykes are clearly younger than the lava succession because they cut through the whole succession. Naturally, such dykes have mainly been identified in the complete lava succession on western Disko. Such identification cannot be made over large areas, and the age of the dykes must be constrained by other methods.

Uncontaminated basalt dykes have major element compositions in the same general range as the lavas of the Rinks Dal Member, i.e. 4–8 wt% MgO and 1.4–5 wt% TiO₂. However, in detail the dykes and sills on Disko and Nuussuaq are compositionally different from the lavas of the Rinks Dal Member.

All dykes with more than 3.2 wt% TiO₂ (similar to the Akuarut unit lavas) have much higher contents of K₂O (0.7–1.3 wt%) and P₂O₅ (0.4–0.7 wt%) and other incompatible elements than the Akuarut Member lavas and are therefore clearly not feeders for the lava flows. These dykes also have higher Ce/Y and Nb/Y than any Rinks Dal Member lavas (Fig. 101). Most of the cross-cutting dykes on western Disko are of this type. They are interpreted to be associated with Eocene lavas of the Naqerloq Formation (Larsen *et al.* 2016).

Uncontaminated dykes and sills with less than 3.2 wt% TiO₂ have trace element contents and ratios that are slightly but significantly different from those of the lavas of the Rinks Dal Member. Almost all analysed dykes of this kind have lower Zr/Nb for similar Ce/Y ratios, and most of them have higher Nb/Y for similar Zr/Y ratios (Fig. 101) and mainly plot in the Iceland field of Fitton

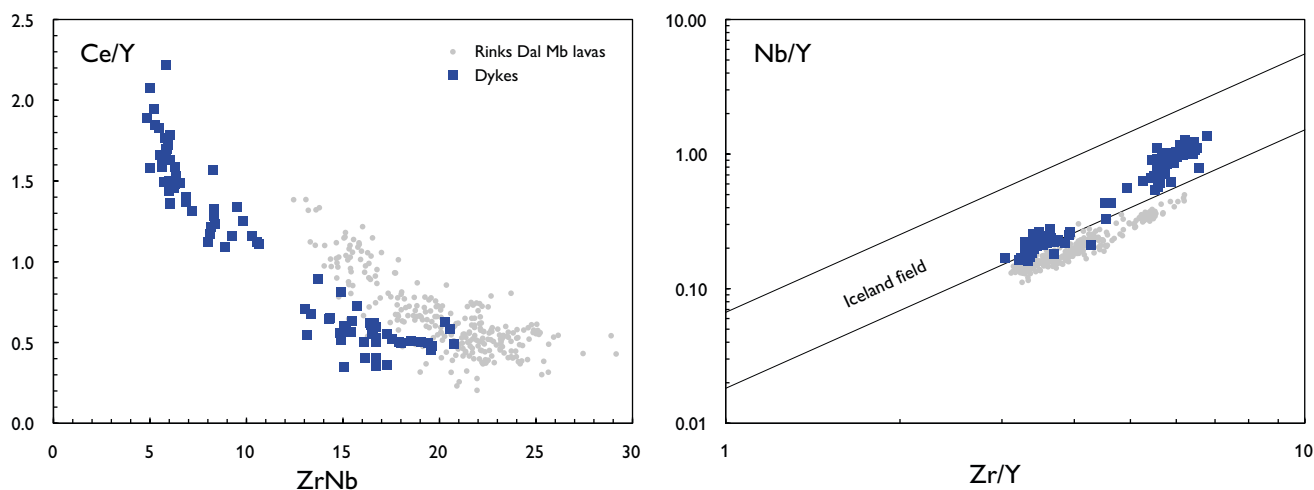


Fig. 101. Immobile trace-element ratios of uncontaminated dykes on Disko and Nuussuaq compared with those of the lavas of the Rinks Dal Member, showing that the dykes were not feeders for the lava flows. Three apparent exceptions are discussed in the text. The dykes are interpreted as associated with lavas of the Svartenhuk Formation (the low-Ce/Y group) and the Naqerloq Formation (the high-Ce/Y group; Larsen *et al.* 2016).

et al. (1998). These dykes are interpreted to be associated with lavas of the latest Paleocene Svartenhuk Formation (Larsen *et al.* 2016).

Only two intrusions are compositionally similar to the Rinks Dal Member lavas: the Manermiut dyke south of Disko Bugt (two analyses) and an apparent dyke at Niuluut on the south coast of Disko. The Niuluut dyke as observed in 1984 cut a highly fractured subaqueous lava flow with a similar chemistry and was later interpreted as a fracture filling in the flow; the dyke had disappeared completely from the coastal cliff when the locality was revisited in 2011. Thus, no analysed dykes on Disko and Nuussuaq are feeders for the lavas of the Rinks Dal Member.

Radiometric age determinations confirm the compositional differences because the dated uncontaminated dykes and sills are younger than the Maligât Formation (Fig. 2). The low-Ti intrusions are latest Paleocene in age, 59–57.5 Ma (Larsen *et al.* 2016) whereas the high-Ti intrusions, including the ‘globule dyke’ in the Aasiaat district, are earliest Eocene in age, 56–54 Ma (Storey *et al.* 1998; Larsen 2006; Larsen *et al.* 2009).

The undated low-Ti Manermiut dyke (1.7 wt% TiO₂) in the Aasiaat district is considered to be contemporaneous with the Rinks Dal Member lavas, i.e. 61–60 Ma. This long, thick dyke, which skirts the outermost west coast south of Aasiaat, may be connected northwards to feeder systems for the Rinks Dal Member on western Disko and farther west.

Feeder systems for the Rinks Dal Member

Only in two localities on western Disko, a dyke and a neck have been observed feeding lava flows of the Rinks Dal Member (units 515 and 517, see p. 92–94). As shown above, the dyke systems in the region are unrelated to the Rinks Dal Member, and thus the locations of the

feeders for the member largely have to be inferred. Several lines of evidence suggest that the main feeder systems are situated west of the Disko Gneiss Ridge: the successive units of the Rinks Dal Member spread eastwards from areas on the gneiss ridge (Fig. 15); the lava morphologies are more variable in the west than in the east, the number of flows is higher and the total thicknesses are larger west of the ridge, and the two eruption sites that have been found are both situated west of the ridge. The lack of potential feeder dykes east of the gneiss ridge points in the same direction. West of the gneiss ridge, the feeders will be covered by younger flows, but east of the ridge, erosion has cut sufficiently deep to expose them, if they were present. Already Henderson (1973) speculated that the primary source areas of these basalts were on western Disko and west of Disko.

The Skarvefjeld unit (unit 511) may have been erupted from more easterly sites. The very thin pahoehoe flows of this unit that filled the Assoq Lake on eastern Disko could not have flowed for very long distances and may be fed from sites east of the Gneiss Ridge. Support for this may be found in the distribution of geochemically enriched flows of unit 511: these occur in a limited area on eastern north Disko around Orlingasoq, where the strongly enriched flows of the Manitdlat Member of the Vaigat Formation also occur (Larsen *et al.* 2003; Pedersen *et al.* 2017). The enriched unit 511 magmas could have acquired their composition during passage through old feeder systems for the Manitdlat Member in the crust, leaving the main, deep crustal magma chambers unaffected.

Another small succession of thin pahoehoe flows (unit 507; flows β fph1 on the map of Pedersen *et al.* 2001) only known from a 20 × 6 km area in the Kuannersuit Kuussuat valley on central Disko was probably also erupted locally.

Nordfjord and Niaquassat members

Revision of the boundary between the Nordfjord and Niaquassat members

The upper part of the Maligât Formation is lithologically very variable and comprises crustally contaminated rocks ranging from basalts and picrites to andesites, dacites and rhyolites. The rocks form lava flows, high-level intrusions, crater breccias and rhyolitic tuff layers, with crater areas centred on western Disko. Pedersen (1975a, 1977a, b) divided this succession into two members, the Nordfjord and Niaquassat members, based on lithological differences between the basic rocks coupled with compositional differences. The Nordfjord Member was restricted to comprise relatively evolved basalts together with silicic rocks derived from evolved basaltic parent magmas, whereas the Niaquassat Member also comprised picrites and magnesian basalts, as well as more silicic rocks with magnesia-rich parents. Included in the Niaquassat Member were silicic rocks in a number of craters and feeder dykes on north-western Disko, with Niaquassat as the type area for the Member. The Niaquassat Member was interpreted to represent a major new influx of primitive picritic melt into the main crustal magma reservoir.

Subsequent investigations have shown that the original distinction between the two members is difficult to uphold, particularly for the more silicic rocks. Pedersen (1981) showed that some of the andesites and dacites of the Niaquassat Member have evolved basaltic parents. Moreover, at various stratigraphic levels, the Nordfjord Member comprises subordinate magnesian basalts with up to 10.5 wt% MgO; this indicates that the influx of primitive magma that culminated with the basic magmas

of the Niaquassat Member with up to 15 wt% MgO had already begun in Nordfjord Member time. In consequence, we here revise the boundary between the Nordfjord and Niaquassat members as follows.

The base of the Niaquassat Member is now placed at the base of a succession of flow-folded pahoehoe lavas of olivine-microphyric magnesian basalts and picrites. This succession is lithologically distinctive and has a large regional extent over all of Disko and parts of eastern Nuussuaq. All the crater facies rocks on north-western Disko, including the Niaquassat crater, as well as a large composite native-iron-bearing lava flow in the Mellemfjord area, are thereby moved to the Nordfjord Member. This leaves no andesites and dacites, and only few basaltic andesites, in the Niaquassat Member.

The revision has no consequence for the boundary between the two members on central and eastern Disko and Nuussuaq, which stays in place. It also has no consequence for the geological map sheets on a scale of 1:100 000 because these combine the Nordfjord and Niaquassat members on western Disko. The two members are shown separately on the geological map of the Mellemfjord area on a scale of 1:50 000 (Pedersen 1977b) and in the photogrammetric sections on a scale of 1:20 000 (South Disko section, Central Disko section), and the only consequence for these is that the large native-iron-bearing Mellemfjord lava flow, which appears as the lowest flow of the Niaquassat Member on the 1:50 000 scale map and in the South Disko section at 8–16.3 km, is now considered to be the uppermost flow of the Nordfjord Member (Fig. 102).

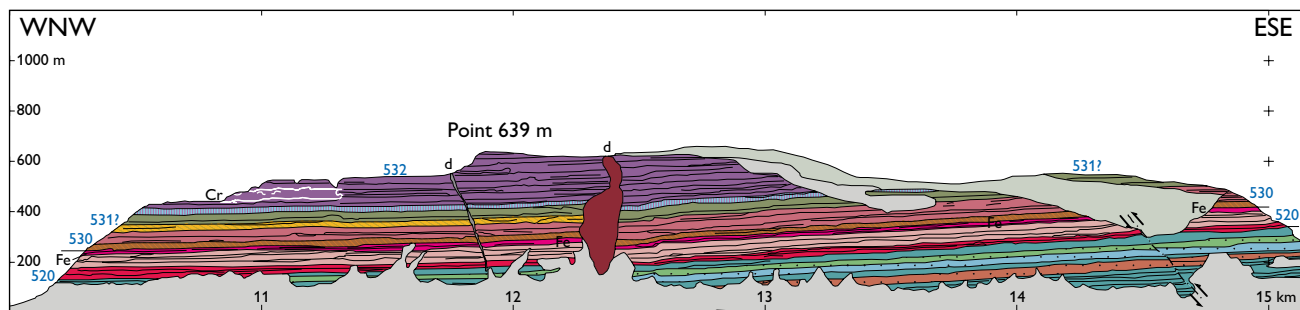


Fig. 102. Photogrammetrically measured section of the coastal cliff at Eqaluit on south-west Disko, documenting the boundaries between the Rinks Dal, Nordfjord and Niaquassat members. After the present revision of the boundary between the Nordfjord (520) and Niaquassat (530–532) members, the native-iron-bearing lava flow (Fe) is shifted from the lowest Niaquassat Member to the uppermost Nordfjord Member (this flow is the composite Mellemfjord lava flow described later). Green flows beneath the Nordfjord Member belong to the upper Rinks Dal Member. Some characteristic marker flows are separately coloured. An eruption crater (Cr) in unit 532 is traced with a white outline. Two dykes (d) cut the succession, one very obliquely. Slightly modified excerpt from the South Disko section (Pedersen *et al.* 2003).

Nordfjord Member

Summary of the main features of the Nordfjord Member

- Original extent over all of Disko and southern and eastern Nuussuaq, with depocentre on western Disko.
- Cannot be subdivided based on stratigraphy. Descriptions based on rock types and localities.
- Very wide igneous compositional range, from basalt to rhyolite, with no stratigraphic significance. Numerous tuff layers.
- All igneous rocks are more or less crustally contaminated except for one alkali basalt flow. Sediment xenoliths are common in the more silicic lavas and tuffs.
- The dominant lithology is basalt lava flows. Andesites, dacites and rhyolites are confined to north-west and central-west Disko where eruption sites are known and inferred.
- Native iron occurs in some basaltic andesites, andesites and dacites, and rarely in basalts.
- Composite lavas with more basic lower parts and more silicic upper parts, and many with native iron, occur on west Disko and northern east Disko. They indicate the presence of several individual high-level magma chambers within sediments west of the Disko Gneiss Ridge and, on northern east Disko also east of the ridge.
- An unexposed central volcano, the West Disko Graphite Rhyolite Volcano, is situated somewhere on north-west Disko or just offshore from there. The volcano produced massive rhyolites (now only found in conglomerates) and graphite-bearing tuffs which are the most strongly sediment-contaminated and evolved rocks of the Maligât Formation.
- A metre-thick sediment deposit at the base of the member suggests an interruption of the volcanic activity after the formation of the Rinks Dal Member.
- Volcanogenic conglomerates and sandstones with plant fossils occur at several levels on north-west Disko and indicate an active erosive environment with river transport. Picrite blocks in the conglomerates indicate exposure and erosion of the Vaigat Formation to the north.

Lithostratigraphy of the Nordfjord Member

Revised member

History. The Nordfjord Member was informally established by Pedersen (1975a) in the area between Hammer Dal and Nordfjord on north-western Disko. It was further investigated on north-western Disko by Pedersen (1977a) and on western and south-western Disko by Pedersen (1977b, 1981) who gave the first detailed descriptions. The Nordfjord Member was subsequently mapped on southern, south-eastern and eastern Disko (Pedersen & Larsen 1987; Larsen & Pedersen 1989) and on Nuussuaq (Pedersen & Larsen 1987; Larsen & Pedersen 1992). The definition is here formalised and extended to cover the whole of Disko and Nuussuaq.

Name. After Nordfjord, north-western Disko (Fig. 4).

Distribution. The Nordfjord Member originally extended over the whole of Disko and southern and eastern Nuussuaq (Fig. 15); its main occurrence now is in the down-faulted, west-dipping blocks of western Disko where it is preserved over wide areas (Fig. 103). It is eroded away on central and north-central Disko (Fig. 4), whereas on eastern and southern Disko it is present as erosional remnants on peaks and ridges, particularly on nunataks in and around the central glacier Sermersuaq (e.g. Pedersen *et al.* 2001, 2003, 2005). It caps the highest peaks on southern Nuussuaq (Point 2010 m and Giesecke Monument) and is present at high altitudes on eastern Nuussuaq (Larsen & Pedersen 1992).

Type section. **Point 440 m, northern gully**, on north-western Disko (Fig. 14, profile 11). The locality is an E–W-oriented gully 3.5–4 km north of the river in Hammer Dal (Fig. 103); the succession is faulted and tilted and dips 22°W (photogrammetrically measured section in Fig. 104A). The Nordfjord Member is exposed over a lateral distance of *c.* 2000 m at around 350 m altitude.

Reference sections. **Point 440 m, southern gully**, an E–W-running gully *c.* 1.2 km south of the gully with the type section (Fig. 14, profile 10; Figs 103, 104B). **Niaqussat** at 280–380 m altitude, north-western Disko (Fig. 14, profile 12). **Point 600 m**, north side of Hammer Dal (Fig.

14, profile 9; Figs 103, 104C). **Sedimentkløften** at the south side of the mouth of Hammer Dal, north-western Disko (Fig. 117). **Point 1070 m** at *c.* 950–1200 m altitude, north of outer Nordfjord, western Disko (Fig. 14, profile 8; Central Disko section at 7.5–9 km). **Sapernu-vik** at *c.* 50–140 m altitude, west coast of Disko north of Kangerluk (Fig. 14, profile 1; South Disko section at 4 km). The eastern side of the mountain **Akuliaru-sersuaq** at 1045–1080 m altitude, central Disko (Fig. 9, profile 2). The eastern wall of the **Kuugannguaq** valley just south of 70°N, at 1600–1670 m altitude, northern Disko (Fig. 9, profile 5; Central Disko section at 55–57 km). The southern shoulder of the mountain **Qinngusaq** above the innermost part of Kvandalen, at *c.* 1150–1290 m altitude, eastern Disko (Fig. 10, profile 8; Central Disko section at 81–83 km). The mountain **Point 1888 m** west of Ataata Kuua, at 1860–1893 m altitude, 7.5 km from the south coast of Nuussuaq (Fig. 11, profile 2). The southern slopes (**Nunavik**), at *c.* 1650–1680 m altitude, of the mountain Point 2000 m, eastern Nuussuaq (Fig. 12, profile 13; Central Nuussuaq section at 67–68 km). **Saqqaq**, Point 1266 m at 1235–1270 m altitude, 10 km north of the village Saqqaq, south-eastern Nuussuaq (Fig. 11, profile 11).

Thickness. The Nordfjord Member has its depocentre on western Disko where it is up to 290 m thick and where 10 or more lava flows are present in some profiles. Another, smaller, depocentre seems to exist on eastern Disko around Kvandalen where the member is up to 180 m thick and comprises nine lava flows in the Qinngusaq section. In most other places on Disko where the upper boundary to the Niaqussat Member is preserved, the Nordfjord Member is less than 100 m thick and comprises only 2–5 lava flows. In many profiles only 1–2 flows are left after erosion. On eastern Nuussuaq, the Nordfjord Member is only about 30 m thick and comprises 2–3 lava flows.

Lithology. Lava flows comprise plagioclase-phyric tholeiitic basalts, plagioclase-phyric to aphyric basaltic andesites and andesites some of which carry native iron, and weakly plagioclase-orthopyroxene-phyric dacites, some with native iron. Some lava flows are composite. One flow is an alkali basalt. Quartz-feldspar-biotite-phyric rhyolite, some with almandine garnet, forms tuff layers. All lava flows are subaerial. Volcaniclastic sediments occur at several horizons and comprise conglomerates with clasts of dacite and rhyolite, and sandstones of redeposited tuffaceous material, some with plant remains. Sedi-

ment xenoliths showing variable degrees of reaction with the magma are common in the silicic lavas and tuffs.

Subdivisions. The Nordfjord Member has not been subdivided.

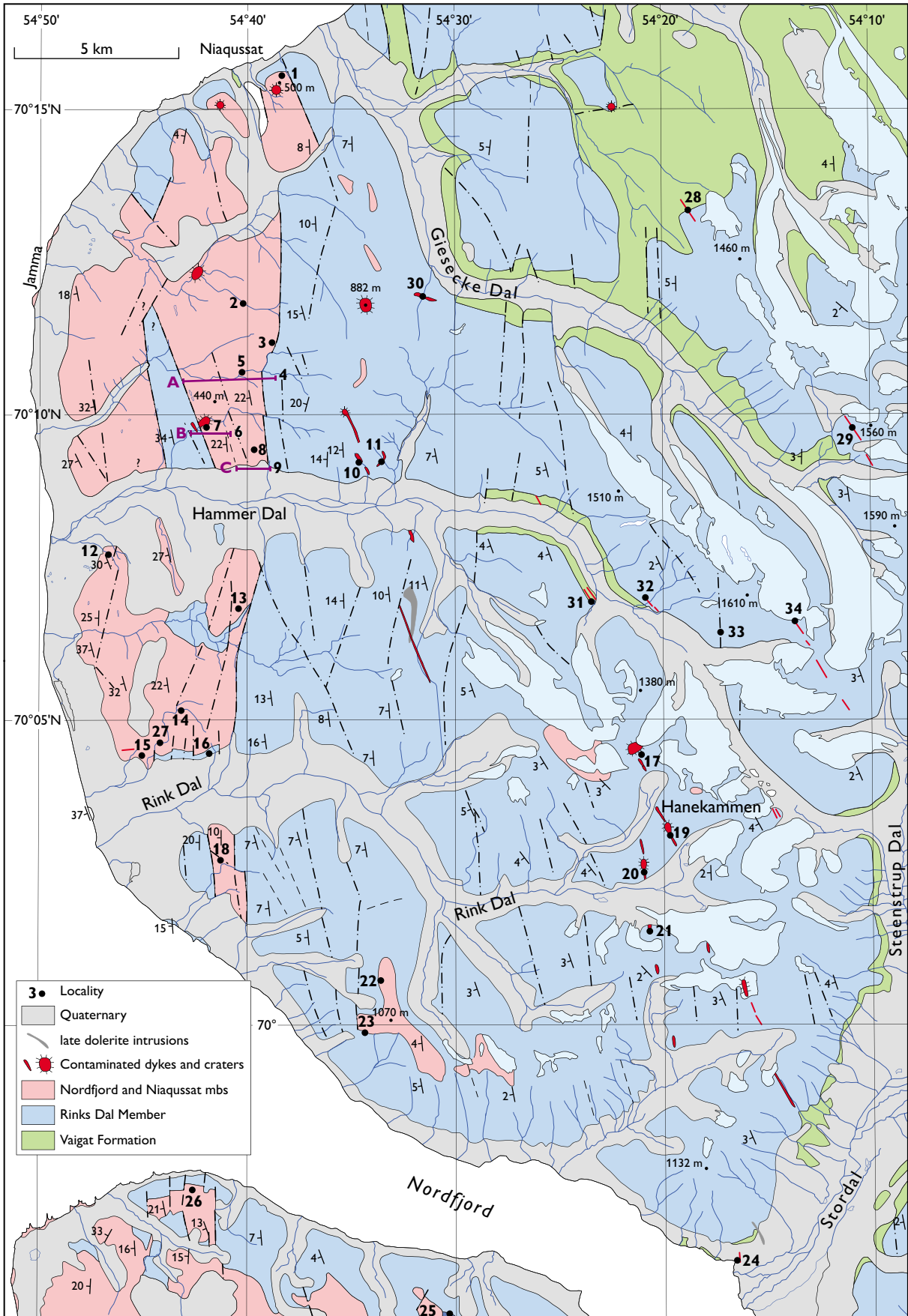
Boundaries. The Nordfjord Member conformably overlies the lava flows of the Rinks Dal Member; as described below there is commonly, but not always, a sediment horizon at the base. At the upper boundary, the Nordfjord Member is conformably overlain by a distinctive succession of flow-folded pahoehoe lavas of olivine-microphyric magnesian basalts and picrites of the Niaqussat Member.

Age. Paleocene, 61–60 Ma, magnetochron C26r, based on radiometric dating (Storey *et al.* 1998; Larsen *et al.* 2016).

Correlation. None certain.

Internal structure of the Nordfjord Member

Despite its modest thickness, the Nordfjord Member is the most variable and complex member in the Maligât Formation. In contrast to the Rinks Dal and Niaqussat members with their laterally continuous units, the Nordfjord Member contains a patchwork of local eruption sites surrounded by various lithologies of limited areal extent. A subdivision into chemostratigraphic units is consequently not possible, and the entire member is referred to as unit 520. The description of the geology of the Nordfjord Member in the following is therefore structured differently from the descriptions of the other members. The Nordfjord Member descriptions comprise, firstly, a section with descriptions of the different igneous rock types and, secondly, a section arranged according to geological themes illustrated by many locality descriptions. Many of these localities are situated on north-western Disko and their locations are shown in Fig. 103.



Facing page:

Fig. 103. Geological map of north-west Disko showing mentioned localities and figured photographs. Localities 1–26 are numbered in a general direction from north to south; localities 27–34 are scattered. **1:** Logs c and d in Fig. 113, photos in Figs 114–116. **2:** Airfall tuff locality 3 km north-north-east of Point 440 m north of Hammer Dal; log in Fig. 117, photos in Fig. 122. **3:** Photo in Fig. 129. **4:** Purple line: ‘Point 440 m, northern gully’, Type section for the Nordfjord and lower and middle Niaqussat members, Fig. 104A. **5:** Figures from the type section: base of the Nordfjord Member log b in Fig. 113, airfall tuff log in Fig. 117, photos in Figs 121, 123B, 127. **6:** Purple line: ‘Point 440 m, southern gully’, Reference section for the Nordfjord and Niaqussat members, Fig. 104B. **7:** Point 440 crater, photos in Figs 143, 144. **8:** Point 600 m, photo in Fig. 132. **9:** Purple line: ‘Point 600 m, north side of Hammer Dal’, Reference section for the Nordfjord Member, Fig. 104C. **10:** Hammer Dal complex, drawing and photo in Figs 175, 176. **11:** Hammer Dal transgressive sill, drawing and photos in Figs 177–179. **12:** Sedimentkløften with tuffaceous sediments, log in Fig. 117, photos in Figs 118–120. **13:** Conglomerate, photo in Fig. 128. **14:** Volcaniclastic sandstone, photo in Fig. 131. **15:** Prominent conglomerate, photo in Fig. 130. **16:** Picritic lava succession of the Niaqussat Member, photo in Fig. 151. **17:** Hanekammen complex, neck, photo in Fig. 180, map in Fig. 181. **18:** Niaqussat Member basalt lava flow packed with xenoliths, photo in Fig. 154. **19:** Hanekammen complex, crater, map in Fig. 181, photo in Fig. 182, drawing in Fig. 183. **20:** Nordfjord complex, map in Fig. 181. **21:** Nordfjord complex, tubular intrusion, photo in Fig. 184. **22:** The Point 1070 section (Fig. 14, profile 8) with sediments at the base of the Nordfjord Member, log a in Fig. 113. **23:** Nordfjord Member lava flows, photo in Fig. 134. **24:** Nordfjord complex, important sediment xenolith locality. **25:** Rinks Dal Member, volcanic neck in unit 517, photo in Fig. 84. **26:** The Kingituaq section (Fig. 14, profile 7). **27:** Tuff locality, 2.5 km SSW of Point 521 m (Avatarpaat Qaqqaat). **28–29:** Inner Giesecke Dal dyke zone. **30:** Outer Giesecke Dal dyke. **31–34:** Innermost Hammer Dal dyke swarm.

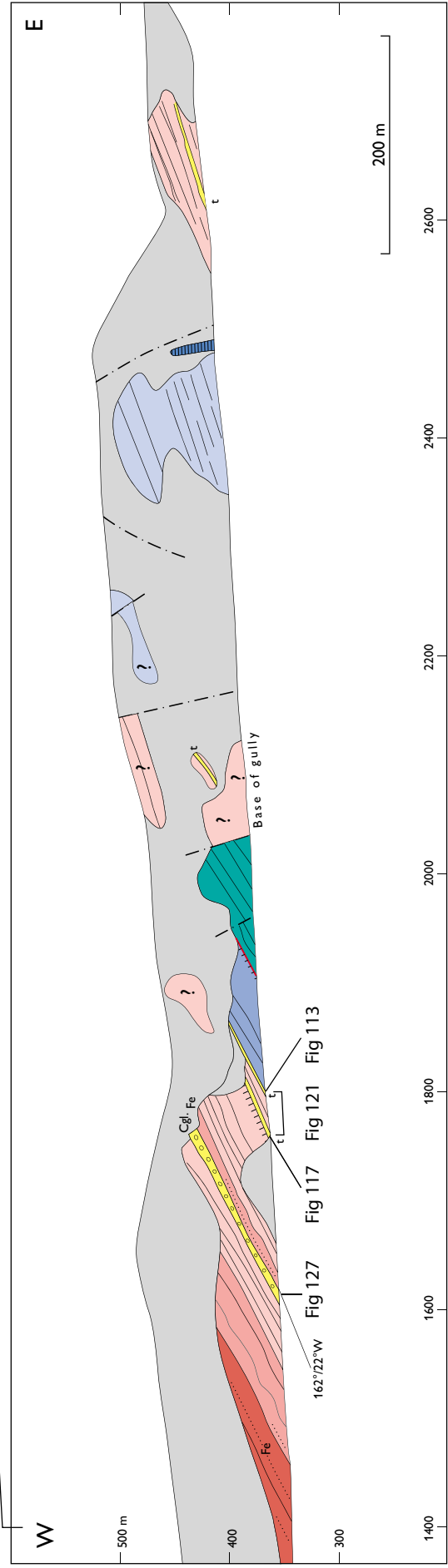
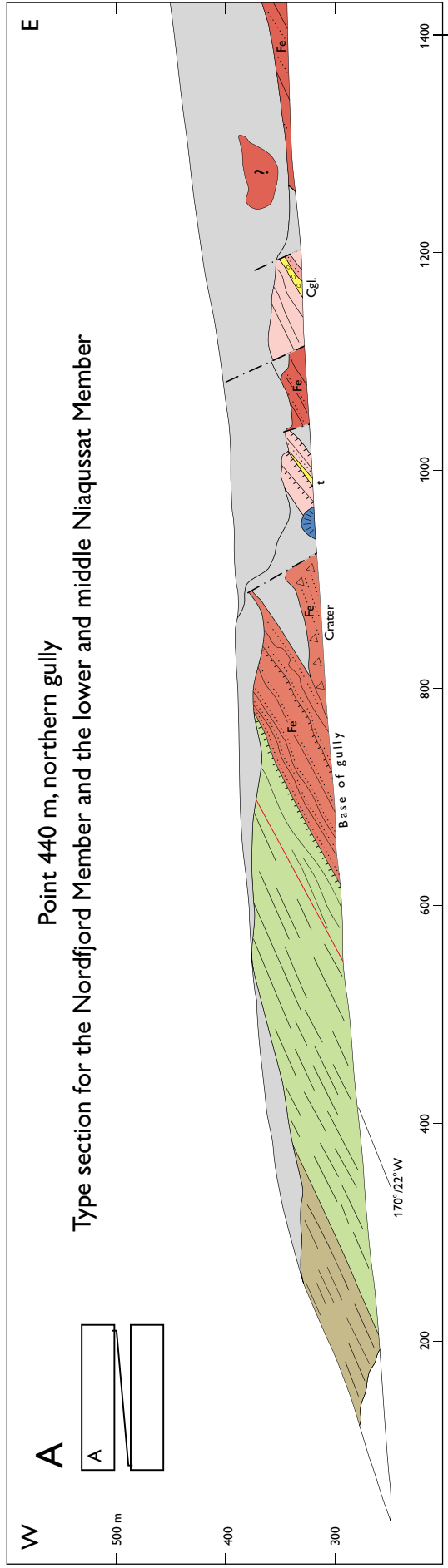
Igneous rock types

The major part of the Nordfjord Member consists of subaerial basalt lava flows. Lava flows and crater deposits of basaltic andesite, andesite and dacite, some of which carry native iron, are subordinate and mainly occur on western Disko except for a few flows of basaltic andesite on eastern Disko. Some lava flows are composite, typically with more basic lower parts and more silicic, commonly native-iron-bearing main parts. The most characteristic component of the Nordfjord Member, although volumetrically insignificant, is rhyolite, which solely occurs as tuffs and conglomerate blocks on western Disko and at one locality on north-eastern Disko.

Basalt

Composition and petrography. The basalt lava flows of the Nordfjord Member are commonly very similar to the basalts of the underlying Rinks Dal Member. Compositionally, the Nordfjord Member lavas are ordinary tholeiitic basalts; compared to the Rinks Dal Member basalts they show small but systematic differences (see below) suggesting that almost all the Nordfjord Member basalts are slightly crustally contaminated, as discussed by Larsen & Pedersen (2009). They show wide ranges in MgO (5.3–10.0 wt%) and TiO₂ (1.3–3.9 wt%). Basalts with 50–52 wt% SiO₂ are also called *silicic basalts*.

Petrographically the basalts vary from aphyric to strongly plagioclase-phyric. The most magnesian basalts (Fig. 105A) are olivine-microphyric and may in addition carry scarce microphenocrysts of plagioclase. There are many almost aphyric basalts which comprise a considerable compositional range. Several basalts carry microphenocrysts of plagioclase, augite and scarce olivine and are petrographically indistinguishable from typical Rinks Dal Member basalts. The lithologically most distinctive Nordfjord Member basalts, which are widespread and common, are highly plagioclase-phyric with many individual phenocrysts larger than 5 mm and glomerocrysts up to 15–20 mm in size (Fig. 105B). These basalts also contain phenocrysts of augite and olivine and represent a range in TiO₂ of 2.2–3.0 wt%. The silicic basalts may also carry microphenocrysts of low-Ca clinopyroxene or orthopyroxene. The slight to strong crustal contamination of the Nordfjord Member basalts is also demonstrated by the widespread occurrence of xenocrysts and xenoliths of crustal (mostly sedimentary) origin. Some xenoliths comprise plagioclase-spinel-graphite aggregates derived from mudstone.



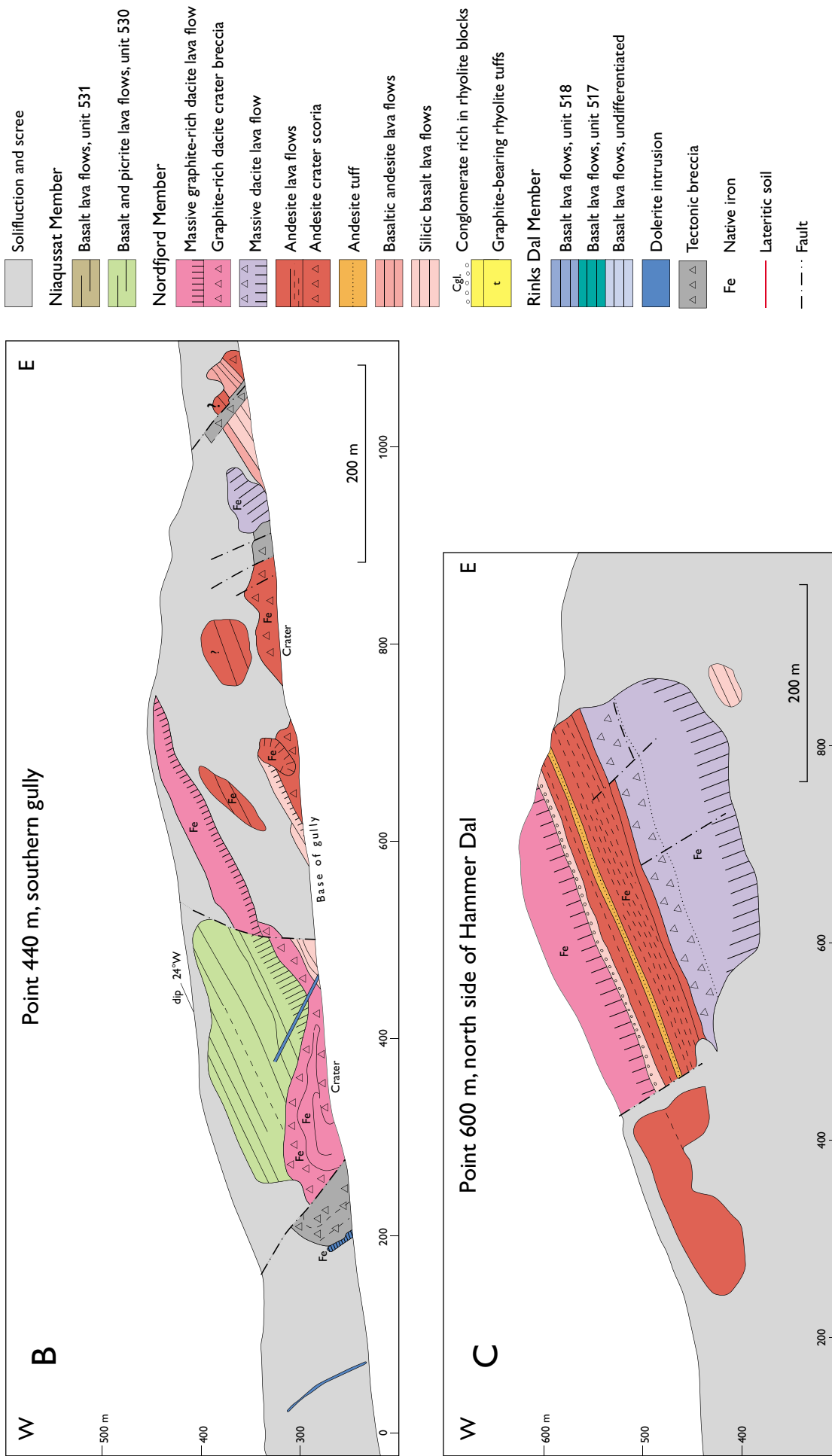
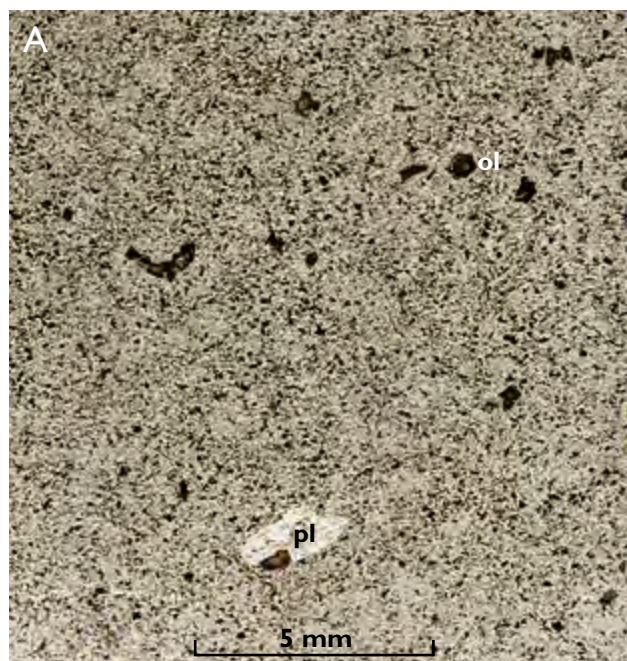


Fig. 104 (pages 120, 121). Photogrammetric drawings of tilted and faulted sections north of Hammer Dal, western Disko. **A:** Point 440 m, northern gully (shown in two overlapping panels), the type section for the Nordford Member and the lower and middle Niaquassat Member. **B:** Point 440 m, southern gully. **C:** Point 600 m. B and C are reference sections. Compare the reconstructed profiles in Fig. 14, profiles 9–11, and the photograph of Point 600 m in Fig. 132. The traces of the three projection planes are shown in Fig. 103.

Over a distance of around 5 km along the north coast of Nordfjord, the first lava flow above the basal sediment horizon is an alkali basalt, the only alkaline rock in the entire Maligât Formation. Pebbles of this flow occur in a



conglomerate in the Hammer Dal area *c.* 7 km north of the exposures of the flow. The alkali basalt is a very fine-grained, aphyric rock and differs from other basalts by containing traces of dark mica in micropegmatitic vugs in slowly cooled parts of the lava.

In a few profiles on western Disko, notably in the Giesecke Dal and Niaqussat profiles (Figs 13, 14), the first lava flow above the basal sediment horizon is a high-Ti basalt flow with 3.3–3.9 wt% TiO₂, similar to some of the flows in the uppermost unit (518) of the Rinks Dal Member. However, the sediment horizon provides an unequivocal boundary between the two members.

Distribution. Basalt lava flows constitute the volumetrically dominant rock type in the Nordfjord Member and are present throughout the member on Disko and Nuusuaq (Fig. 15; see also e.g. Figs 155, 156 and 159).

Basaltic andesite

Composition and petrography. By definition, the basaltic andesites have 52–57 wt% SiO₂; the transition from basalt is gradual. They show wide ranges in MgO (3.4–10.6 wt%) and TiO₂ (1.2–3.2 wt%).

The majority of the basaltic andesites carry phenocrysts of plagioclase and orthopyroxene and frequently xenocrysts of plagioclase and plagioclase-spinel aggregates. Several of these rocks carry native iron and sulfides, and many have a very fine-grained groundmass with a globular texture (Fig. 106A). Patches of decomposed magma-equilibrated mudstone are common in these rocks.

Some of the most magnesian rocks of the Nordfjord Member are basaltic andesites in Vesterdalen/Qasigissat Kuussuat. These rocks have more than 800 ppm Cr and are clearly derived from a much more primitive magma than represented by the basalts of the upper Rinks Dal Member. The glassy sample 263934 (Fig. 106B) is one of the most magnesian basaltic andesites and the only one

Fig. 105. Thin sections (scanned) of basalts of the Nordfjord Member. **A:** Basalt with olivine microphenocrysts (**ol**, pseudomorphed) and a plagioclase phenocryst (**pl**) in a fine-grained groundmass. Sample GGU 327011, Skarvefjeld, south Disko; SiO₂ = 50.2 wt%, TiO₂ = 1.69 wt%, MgO = 8.9 wt%. **B:** Characteristic Nordfjord Member basalt type with many large phenocrysts and glomerocrysts of plagioclase (**pl**), augite (**cpx**) and smaller olivine crystals (**ol**, pseudomorphed) in a fine-grained groundmass. Rounded vesicles are filled with zeolite (**ze**). Sample GGU 332964, nunatak near Point 1440 m, central Disko; SiO₂ = 49.2 wt%, TiO₂ = 2.90 wt%, MgO = 6.0 wt%. Concentrations are recalculated volatile-free.

with fresh, well-preserved phenocrysts and microphe-
nocrysts of olivine. In addition, the rock contains scarce
microphenocrysts of orthopyroxene, spongy plagioclase
xenocrysts and tiny microphenocrysts of clinopyroxene.
The glass contains 55.4 wt% SiO₂ and 6.5 wt% MgO.
One of the least magnesian basaltic andesites is exempli-
fied by sample 332944 with 53.3 wt% SiO₂ and 5.8 wt%
MgO. This rock is very fine-grained, flow-laminated, and
virtually aphyric except for very scarce plagioclase micro-
phenocrysts (not illustrated).

Distribution. Basaltic andesites mainly occur on western
and north-western Disko. Here they form simple lava
flows intercalated with basalt or andesite flows, as in the
Hammer Dal area (Fig. 14), or several successive flows, as
in Vesterdalen. Basaltic andesite also forms part of com-
posite lava flows, as described later.

A few basaltic andesite flows occur on southern and
eastern Disko and Nuussuaq. At Uiffaq, Tunup Qaqqaa,
Daugaard-Jensen Dal, Sorte Hak and Point 1888 m, the
first lava flow in the Nordfjord Member is a basaltic an-
desite (Figs 7–9, 11). In the Kvandalen area on eastern-
most Disko, an up to 30 m thick flow of basaltic andesite
with native iron occurs in the middle of the Nordfjord
Member (Fig. 10).

Andesite

Composition and petrography. By definition, the andesites
have 57–63 wt% SiO₂; the transition from basaltic an-
desite is gradual. They show a wide range in MgO (2.4–
7.9 wt%) and less in TiO₂ (1.1–2.3 wt%).

The andesites range from very fine-grained, nearly
aphyric rocks to very phenocryst-, xenocryst- and ante-
cryst-rich, native-iron-bearing rocks exemplified by the
andesite erupted from a crater at Niaquassat (Fig. 107A).
The phenocrysts include orthopyroxene, pigeonite, pla-
gioclase and armalcolite. There are traces of ilmenite, ru-

tile, native iron, troilite and graphite, and xenocrysts of
plagioclase, spinel, corundum, cordierite, mullite, quartz
and graphite. There is an abundance of magma-modified
xenoliths of mudstone and sandstone, and cognate clus-
ters of relatively coarse noritic rocks.

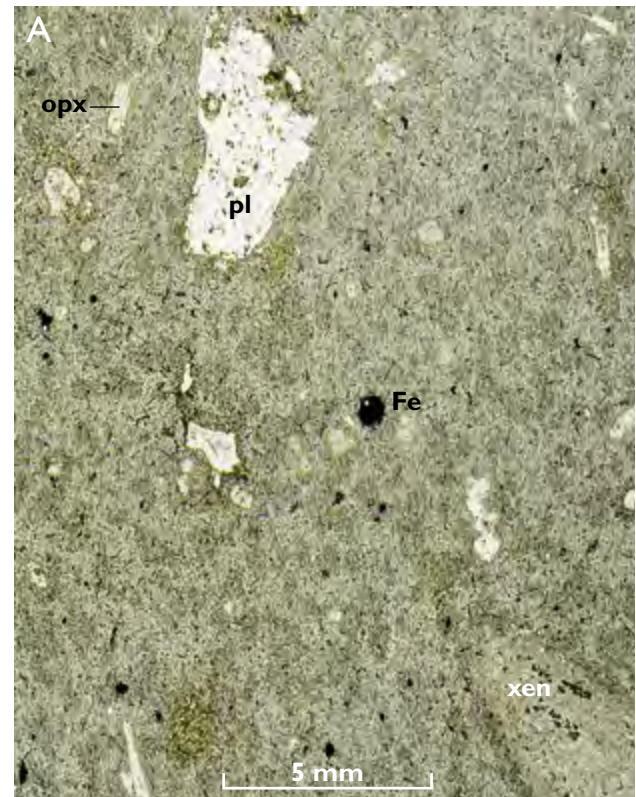
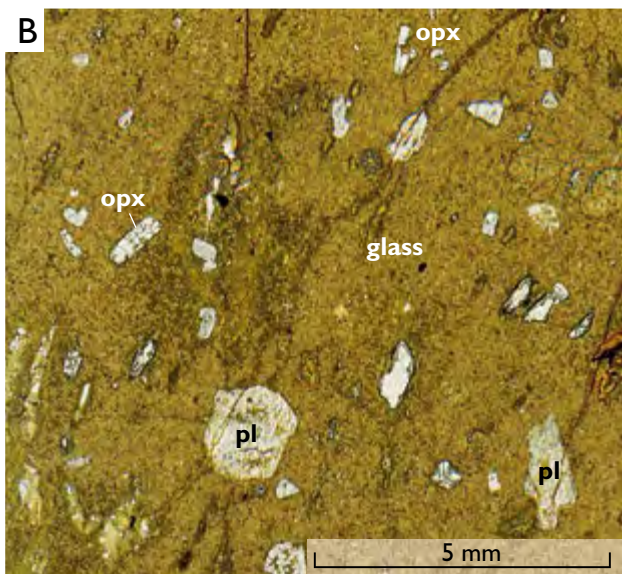
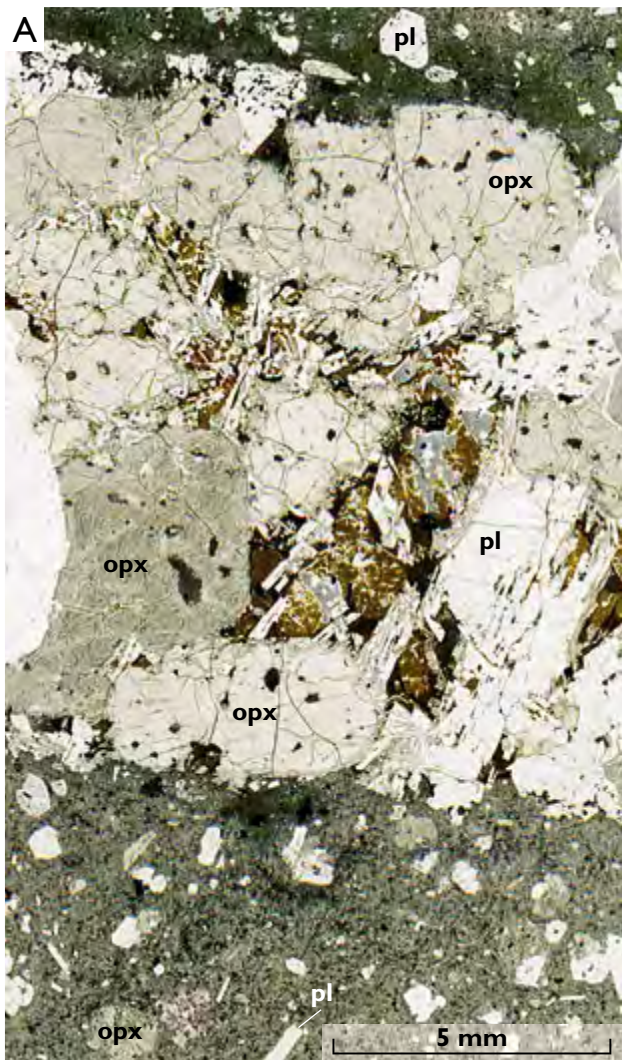


Fig. 106. Thin sections (scanned) of basaltic andesites of the Nord-
fjord Member. **A:** Native-iron-bearing magnesian basaltic andesite
with phenocrysts of plagioclase (**pl**) and microphe-
nocrysts of orthopyroxene (**opx**) in a very fine-grained groundmass with globular texture
and blebs of native iron (**Fe**). A xenolith (**xen**) is seen in the lower right
corner. Sample GGU 264076, Vesterdalen, west Disko; SiO₂ = 56.1
wt%, TiO₂ = 1.53 wt%, MgO = 6.8 wt%. **B:** Magnesian basaltic an-
desite, nearly aphyric glassy rock with brown alteration rims of the glass
along cracks and vesicle walls. Sample GGU 263934, pahoehoe tongue,
Point 1114 m, Vesterdalen, west Disko; SiO₂ = 55.2 wt%, TiO₂ = 1.58
wt%, MgO = 9.2 wt%. Concentrations are recalculated volatile-free.



A low- Al_2O_3 , high- P_2O_5 variety of andesite associated with similar dacite (see below) contains microphenocrysts of tridymite in a glassy groundmass (Fig. 107B).

Distribution. Andesites in the Nordfjord Member are restricted in occurrence to western and north-western Disko from Mellemfjord to Niaquassat (Fig. 108). The Niaquassat crater erupted a thick andesite flow (Fig. 14, profile 12).

Dacite

Composition and petrography. The dacites have SiO_2 in the range 63–67.7 wt% and contain 1.3–3.0 wt% MgO and 1.3–2.3 wt% TiO_2 . There are four main types of dacite, which are distinguishable both chemically and petrographically.

Native-iron-bearing dacite with ilmenite. This is the most voluminous dacite type. It is confined to north-western Disko around and north of Hammer Dal, where it occurs as a few lava flows and as pebbles in conglomerate. Three samples of this type were described in detail by Pedersen (1981). The type is exemplified here by sample 176486 (Fig. 109A); this is a very fine-grained rock with phenocrysts of plagioclase and orthopyroxene and scarce microphenocrystic ilmenite, which has been modified by progressive reduction and sulfidation to aggregates of ilmenite, armalcolite, rutile, native iron and troilite (Fig. 110). There are small, dispersed grains of native iron and troilite and flakes of graphite in the groundmass. Xenoliths and xenocrysts derived from mudstone and sandstone and antecrysts and cognate noritic inclusions are widespread.

Fig. 107. Thin sections (scanned) of andesites of the Nordfjord Member. **A:** Andesite (lower and upper part of the image) with phenocrysts of plagioclase (**pl**) and orthopyroxene (**opx**) in a fine-grained groundmass with tiny black specks of native iron. Most of the image is occupied by a cognate inclusion of orthopyroxene and plagioclase with a dark brown, altered residuum. Detailed description and mode of this sample in Pedersen (1981). Sample GGU 176411, Niaquassat, north-west Disko; $\text{SiO}_2 = 60.6$ wt%, $\text{TiO}_2 = 2.02$ wt%, $\text{MgO} = 2.51$ wt%. **B:** Low- Al_2O_3 , high- P_2O_5 andesite with microphenocrysts of orthopyroxene and xenocrysts of sieve-textured plagioclase in a glassy groundmass. Pie-sector-shaped microliths of tridymite in the groundmass are too small to be discernible in this image. Sample 263910, Qasigissat, west Disko; analysed bulk rock 263911 has $\text{SiO}_2 = 60.7$ wt%, $\text{TiO}_2 = 2.00$ wt%, $\text{MgO} = 4.45$ wt%.

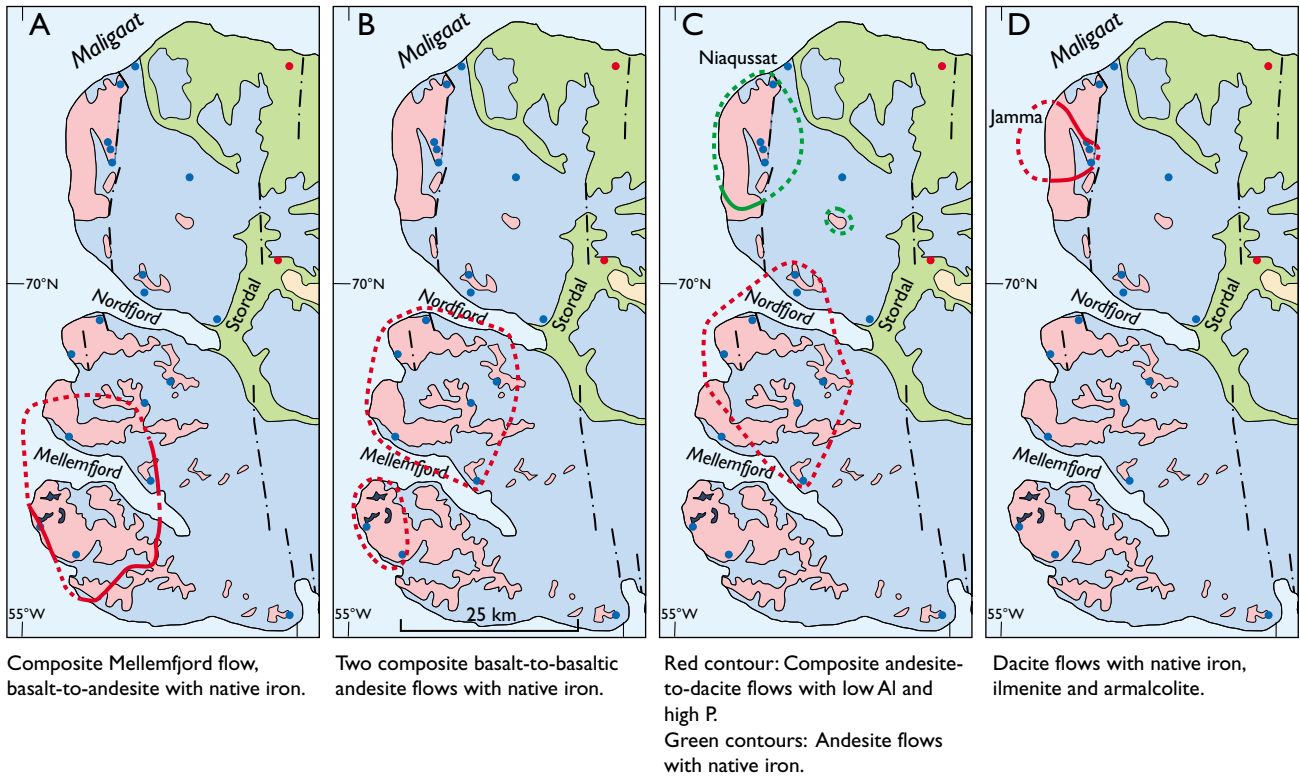


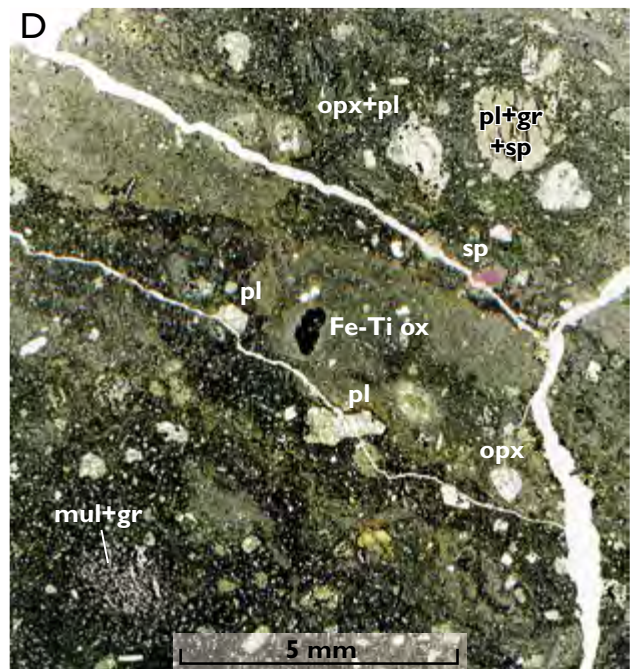
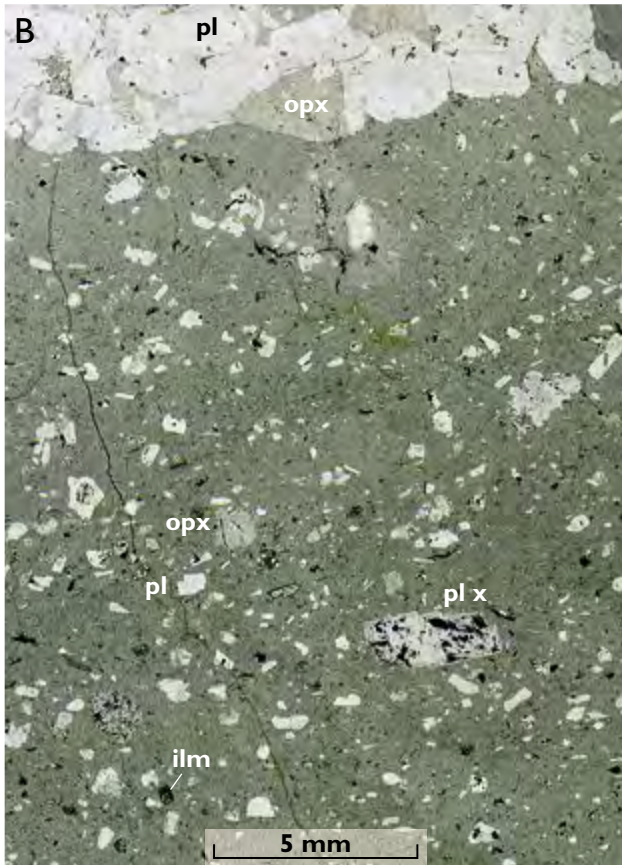
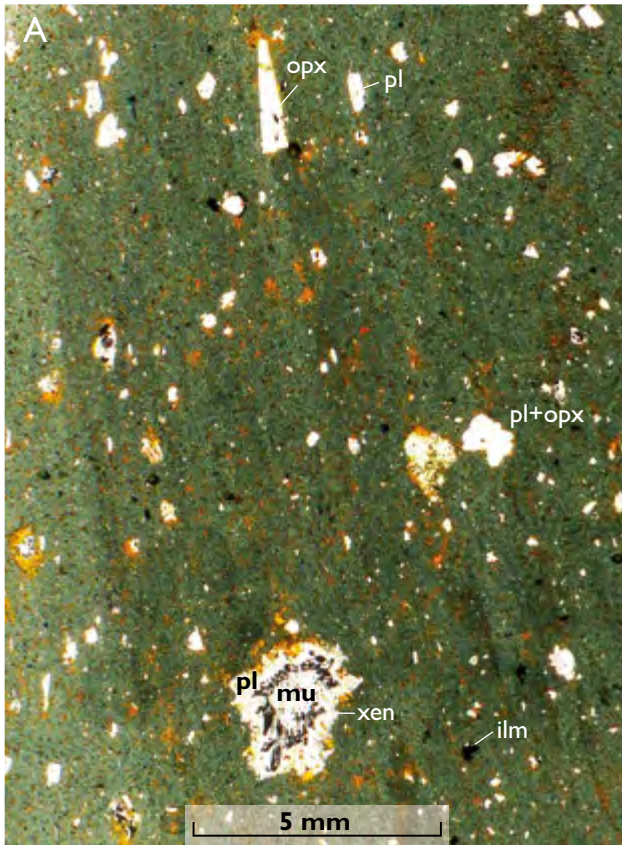
Fig. 108. Distribution of some composite flows, andesite flows and dacite flows in the Nordfjord Member, outlined in red (A–D) and green (C); dashed lines are inferred boundaries. Blue dots are the location of profiles shown in Fig. 14, but several samples from outside these profiles were also used to construct the figure. There are no systematic age differences between the flows.

A closely related native-iron-bearing dacite with 66–67 wt% SiO_2 is only known from a coastal exposure at Jamma. It is the most silicic igneous rock with native iron known from the Nuussuaq Basin and has been described in detail by Pedersen (1981). It carries phenocrysts of orthopyroxene, pigeonite, plagioclase and ilmenite and a range of xenocrysts derived from sediments and sediment xenoliths, and cognate noritic inclusions (Fig. 109B).

Low- Al_2O_3 , high- P_2O_5 dacite. Dacite of this type is characterised by relatively high P_2O_5 and TiO_2 and low Al_2O_3 and K_2O . It is confined to western Disko between Mellemfjord and the north coast of Nordfjord (Fig. 108C), where it forms part of a composite lava flow with a range of compositions from high-Si andesite to dacite that share similar chemical characteristics. The dacitic rocks are generally very fine-grained and phenocryst-poor but may contain up to a few per cent phenocrysts of orthopyroxene and plagioclase and scarce microphe- nocrysts of clinopyroxene and pseudomorphed olivine. The orthopyroxene phenocrysts commonly have reaction rims of clinopyroxene. Resorbed xenocrysts of quartz and

quartz aggregates and scattered, sieve-textured plagioclase grains are common, whereas fine-grained plagioclase-spinel-graphite microxenoliths are scarce. Most rocks contain scarce native iron and troilite. The groundmass, especially when well crystallised, reveals the presence of tridymite in addition to plagioclase, clinopyroxene, ilmenite and residuum, and in glassy rocks, the tridymite is seen to be an early crystallising phase. This magma type is inferred to have been formed by the reaction of evolved basalt (delivering the P_2O_5 and TiO_2) with a sandstone-dominated contaminant (delivering the quartz xenocrysts).

High-Ni dacite. Dacite of this type is characterised by relatively low TiO_2 and CaO and significantly higher Ni than in the other dacites (*c.* 200 ppm, see Table 6 (pages 164–168), sample 176443). It forms a thick crater deposit with an associated lava flow in the Hammer Dal area where it is the highest unit in the Nordfjord Member (Fig. 14, profiles 9, 10). The dacite has phenocrysts, glomerocrysts and microphe- nocrysts of orthopyroxene and plagioclase together with minor ilmenite, armalco-



Facing page:

Fig. 109. Thin sections (scanned) of dacites of the Nordfjord Member. **A:** Dacite with phenocrysts of plagioclase (**pl**), orthopyroxene (**opx**) and scarce microphenocrystic ilmenite (**ilm**). The groundmass contains small dispersed grains of native iron and troilite (both weathered to brown rusty spots) and flakes of graphite (tiny black specks). A re-equilibrated xenolith (**xen**) consists of mullite (**mu**) rimmed by plagioclase (**pl**). Detailed description and mode of this sample in Pedersen (1981). Sample 176486, clast in conglomerate north of Hammer Dal, north-west Disko; $\text{SiO}_2 = 65.4 \text{ wt\%}$, $\text{TiO}_2 = 1.52 \text{ wt\%}$, $\text{MgO} = 1.42 \text{ wt\%}$. **B:** Dacite with phenocrysts of plagioclase (**pl**) and orthopyroxene (**opx**) as well as xenocrysts (**x**) derived from sediments and sediment xenoliths. Native iron forms tiny black specks in the groundmass. A cognate noritic inclusion is seen at the top. Detailed description and mode in Pedersen (1981). Sample 176471, Jamma, north-west Disko; $\text{SiO}_2 = 67.7 \text{ wt\%}$, $\text{TiO}_2 = 1.28 \text{ wt\%}$, $\text{MgO} = 1.31 \text{ wt\%}$. **C:** High-Ni-dacite with phenocrysts, glomerocrysts and microphenocrysts of orthopyroxene (**opx**) and plagioclase (**pl**). Native iron forms small black specks in the groundmass. Several xenocrystic clusters of plagioclase, spinel and graphite (**pl+sp+gr**) are seen. A picrite xenolith (**xen**) is present near the base. Sample 176443, Hammer Dal, north-west Disko; $\text{SiO}_2 = 66.0 \text{ wt\%}$, $\text{TiO}_2 = 1.29 \text{ wt\%}$, $\text{MgO} = 2.11 \text{ wt\%}$. The sample contains 1.14 wt% carbon. **D:** High-Al graphite dacite with phenocrysts of orthopyroxene (**opx**) and plagioclase (**pl**) in a dark groundmass with dispersed graphite flakes. Small xenocrystic aggregates consist of aluminous phases and graphite (**gr**). The aluminous phases include mullite (**mul**), cordierite and red aluminous spinel (**sp**). The rock is inhomogeneous due to the mixing and mingling of more and less contaminated magma. Sample 326550, clast in conglomerate north of Hammer Dal, north-west Disko; $\text{SiO}_2 = 63.5 \text{ wt\%}$, $\text{TiO}_2 = 1.76 \text{ wt\%}$, $\text{MgO} = 3.02 \text{ wt\%}$. The sample contains 2.7 wt% carbon.

lite and rutile (Fig. 109C). It also contains native iron, troilite and disseminated graphite. The very fine-grained groundmass contains disseminated flakes of graphite and has a composition transitional between dacite and rhyolite, with 68–71 wt% SiO_2 . There is an abundance of medium- to fine-grained igneous clasts of picrite and noritic dolerite together with a large range of magma-modified xenocrysts and xenoliths derived from mudstone and sandstone. Xenocrysts of resorbed quartz and cordierite rimmed by plagioclase are common, together with plagioclase-spinel-cordierite-mullite-graphite rocks and many other similar rocks. Scarce plagioclase-quartz-pyroxene rocks with glassy residuum and tiny flakes of phlogopitic mica and graphite also occur. Residual glass within the xenoliths is rhyolitic.

High-Al graphite dacite. Dacite of this type is characterised by relatively high Al_2O_3 and MgO and low P_2O_5 and FeO^* . Graphite is abundant. It is only found as cobbles in a Nordfjord Member conglomerate just north of Hammer Dal. It has not been located *in situ* and is speculated to have originated from the West Disko rhyolite volcano. It is a very fine-grained volcanic rock with phenocrysts of orthopyroxene and plagioclase in a dark groundmass with about 2.7 wt% TOC (total organic carbon) in dispersed graphite flakes. There are abundant small xenocrystic aggregates of aluminous phases and graphite in various stages of equilibration with the magma. The aluminous phases include mullite, cordierite, aluminous spinel and corundum and are derived from carbonaceous mudstone. Rare xenocrystic aggregates with calcic clinopyroxene and without graphite are probably derived from sandstone. The rock is inhomogeneous with a veined

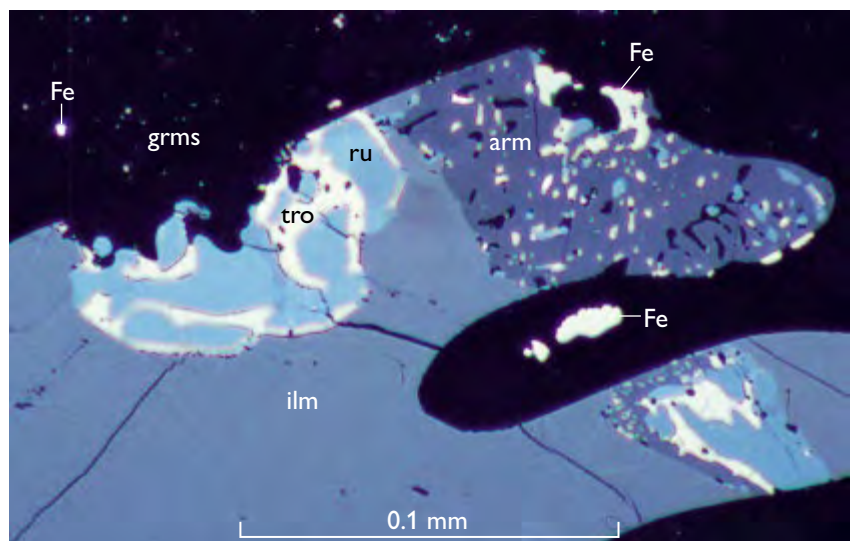


Fig. 110. Reflected-light image of oxides and native iron in dacite, same sample as in Fig. 109A. An ilmenite microphenocryst (**ilm**) is affected by progressive reduction and sulfidation and has partly recrystallised to rutile (**ru**), armalcolite (**arm**), troilite (**tro**) and native iron (**Fe**). It is surrounded by the dacitic groundmass (**grms**), also with native iron. See detailed description in Pedersen (1981). Sample 176486, clast in conglomerate north of Hammer Dal, north-west Disko.

structure due to the mixing and mingling of more and less contaminated magma, as exemplified by sample 326550 (Fig. 109D; Table 6, pages 164–168).

Distribution. The dacites are restricted in occurrence to western and north-western Disko from just north of Mellemfjord to north of Hammer Dal and Jamma at the coast (Figs 108C, D).

Rhyolite

Composition and petrography. The rhyolitic rocks contain 70.5–76.9 wt% SiO₂; they include two samples that plot just inside the dacite field in a TAS diagram (Le Maitre 2002) but are closely related to the rhyolites. The rhyolites are low in MgO (1.2–0.2 wt%) and TiO₂ (0.67–0.04 wt%). They comprise two compositional and petrographic groups both of which are peraluminous. These are *garnet rhyolite*, which is strongly porphyritic and sometimes transitional to dacite, and *sanidine rhyolite*, which is much less porphyritic and more evolved and has higher SiO₂ contents.

Because no ferromagnesian silicate or oxide mineral analyses have been published from the rhyolites, a selection of pyroxene, garnet, biotite, ilmenite and hercynite analyses is presented here in Table 5.

Garnet rhyolite. These rocks, exemplified by sample 156518 (Fig. 111A), consist of 65–70% glassy groundmass, *c.* 25% crystals and *c.* 5% xenoliths. The crystals comprise phenocrysts of quartz, plagioclase, orthopyroxene, biotite and almandine garnet, cognate clusters of plagioclase, orthopyroxene, pigeonite and garnet (Fig. 111B), minor ilmenite, apatite, zircon and graphite, and various xenocrysts of sillimanite (Fig. 111C), corundum, hercynitic spinel and feldspar. There is a variety of sediment xenoliths dominated by equilibrated mudstone (Fig. 111A) and also some highly equilibrated clasts, perhaps of sandstone, with intergrown quartz, garnet and plagioclase (Fig. 111D). Graphite is as a significant component of many xenoliths and xenocrysts.

At a locality described below, garnet rhyolite clasts were picked up by a subaerial basalt lava flow that engulfed a conglomerate bed. These rhyolite clasts are rounded, weathered and oxidised; pyrometamorphism by the basalt magma has transformed the biotite, orthopyroxene, garnet and ilmenite into ferric-oxide-rich oxide-silicate assemblages (Fig. 111E), while the original textures are preserved. In particular, the very characteristic quartz-garnet intergrowth patterns are now preserved

as pseudomorphs consisting of quartz, iron oxide and silicate.

Sanidine rhyolite. This rock type mainly forms dark, glassy pitchstone (Fig. 112A) but also microcrystalline laminated rocks. The glassy sanidine rhyolite contains *c.* 95% glassy groundmass, about 5% phenocrysts of quartz, plagioclase, sanidine and biotite (Fig. 112B), and very minor ilmenite, zircon, apatite, monazite and almandine-rich garnet. The rocks also contain very scarce xenocrysts of aluminous phases and highly equilibrated sediment xenoliths, which are now aggregates of feldspar, hercynite, biotite, orthopyroxene, ilmenite, sillimanite and graphite. The graphite occurs in xenoliths, enclosed in ilmenite and biotite, and as small flakes in the groundmass glass (Fig. 112C).

The microcrystalline sanidine rhyolites are strongly flow-laminated rocks with 80–85% groundmass and <20% phenocrysts of quartz, plagioclase, sanidine and biotite. The minor phases have not been investigated. The rocks are carbon-poor (organic C <0.02%) and graphite may have been oxidised away completely.

Facing page:

Fig. 111. Thin sections (scanned) of garnet rhyolites of the Nordfjord Member. **A:** Garnet rhyolite with phenocrysts of feldspar (**fsp**), quartz (**qz**), biotite (**bi**), orthopyroxene (**opx**) and garnet (not in image). The upper right half is a graphite-rich, magma-modified mudstone xenolith (**xen with graphite**). Sample 156518, clast in conglomerate in Sedimentkløften, Hammer Dal, north-west Disko; SiO₂ = 72.6 wt%, TiO₂ = 0.49 wt%, MgO = 0.56 wt%. **B:** Cognate cluster of garnet (**gt**), quartz (**qz**) and plagioclase (**pl**) in a glassy groundmass (**grm**). Garnet rhyolite sample 113508, clast in conglomerate in Sedimentkløften, Hammer Dal, north-west Disko. **C:** Sillimanite xenocryst (**sil**) and quartz phenocrysts (**qz**) in garnet rhyolite sample 113508, clast in conglomerate in Sedimentkløften, Hammer Dal, north-west Disko. **D:** The upper right half of this image is a cluster of highly equilibrated clasts, perhaps of sandstone, with intergrown quartz, garnet and plagioclase (**gt+qz+pl**) and interstitial smectite. The lower left half is the host rock, a garnet rhyolite with plagioclase (**pl**), quartz (**qz**), orthopyroxene (**opx**) and garnet (**gt**). Sample 326468, clast in Sedimentkløften, Hammer Dal, north-west Disko. **E:** A former garnet rhyolite pebble that has been picked up in a basalt lava flow and metamorphosed at high temperature and low pressure. Garnet-quartz-plagioclase aggregates have recrystallised to iron oxide-quartz-plagioclase aggregates (**Feox+qz+pl**), whereas the rhyolite textures with groundmass (**grm**), plagioclase (**pl**) and quartz (**qz**) are preserved. Sample 274424, Hammer Dal, north-west Disko; SiO₂ = 72.6 wt%, TiO₂ = 0.47 wt%, MgO = 0.84 wt%.

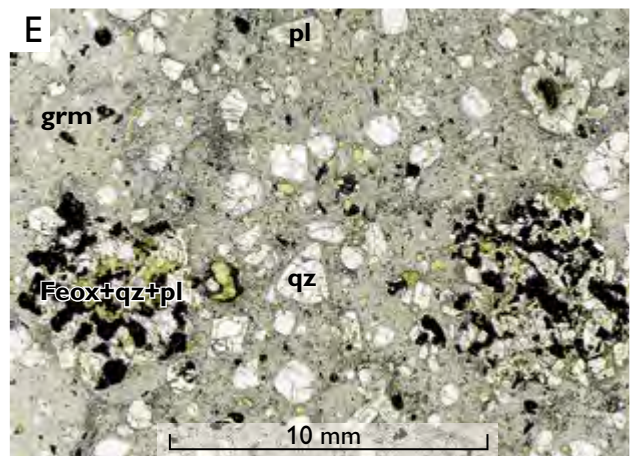
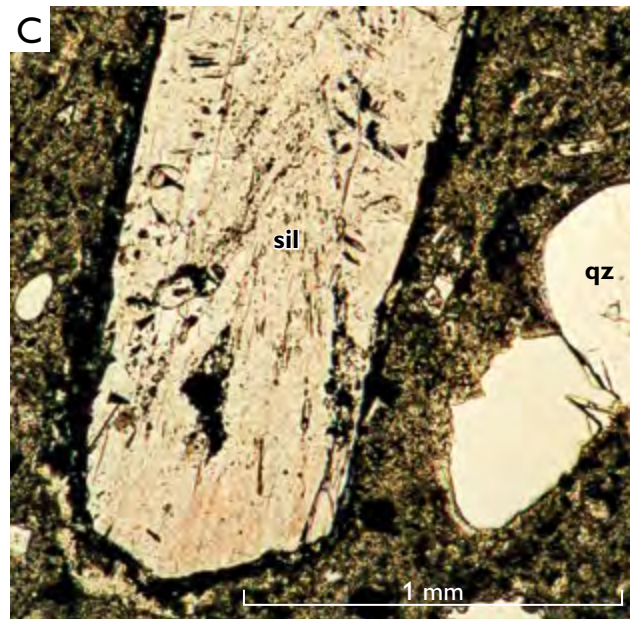
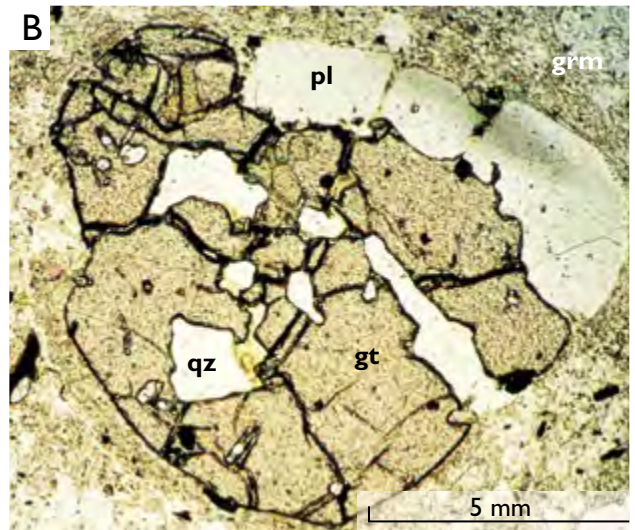
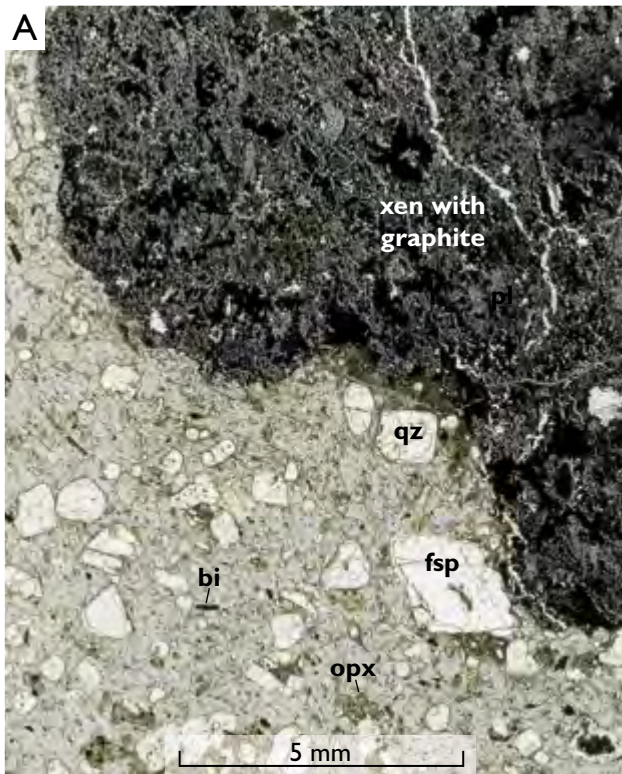


Table 5. Microprobe analyses of minerals in rhyolites of the Nordfjord Member

No.	1	2	3	4	5	6	7	8	9	10	11	12
GGU No.	156518.1	156518.1	113508	156518.1	113508	113515	156518.1	113515	156518.1	113515	156518.2	156518.2
Mineral	Pigeonite	Orthopyx	Orthopyx	Garnet	Garnet	Garnet	Biotite	Biotite	Ilmenite	Ilmenite	Hercynite	Hercynite
<i>Oxides, wt%</i>												
SiO ₂	49.43	46.61	47.71	37.51	36.86	37.21	33.28	33.47				
TiO ₂	0.39	0.22	0.13	0.14	0.24	0.12	5.72	4.90	50.01	51.76	0.44	1.85
Al ₂ O ₃	1.09	1.42	0.98	22.28	21.48	22.15	14.78	16.44	0.23	0.29	59.33	37.53
Cr ₂ O ₃											0.16	12.80
FeO*	30.12	43.89	44.35	32.16	35.19	36.90	29.14	28.97	46.86	46.17	34.15	42.11
MnO	0.55	0.46	0.73	0.62	1.23	2.16			0.35	0.53	0.25	0.23
MgO	13.06	6.24	6.60	6.00	2.99	2.20	4.63	4.27	0.80	0.63	5.67	2.14
CaO	5.11	0.77	0.52	1.51	2.62	1.65	0.11					0.17
Na ₂ O	0.24	0.54	0.58				0.74	1.03				
K ₂ O							8.81	8.90				
Sum	99.99	100.15	101.60	100.22	100.61	102.39	97.21	97.98	98.25	99.38	100.00	96.83
<i>Recalculated to cations</i>												
No of cations	4	4	4	8	8	8	16	16	2	2	3	3
Si	1.937	1.928	1.944	2.946	2.946	2.943	5.375	5.330	0.000	0.000	0.000	0.000
Al	0.050	0.069	0.047	2.063	2.024	2.065	2.814	3.086	0.007	0.009	1.950	1.404
Ti	0.011	0.007	0.004	0.008	0.014	0.007	0.695	0.587	0.957	0.982	0.009	0.044
Cr											0.004	0.321
Fe ²⁺	0.987	1.518	1.511	2.112	2.352	2.441	3.936	3.858	0.998	0.974	0.796	1.118
Mn	0.018	0.016	0.025	0.041	0.083	0.145	0.000	0.000	0.008	0.011	0.006	0.006
Mg	0.763	0.385	0.401	0.702	0.356	0.259	1.114	1.013	0.030	0.024	0.236	0.101
Ca	0.215	0.034	0.023	0.127	0.224	0.140	0.019					0.006
Na	0.018	0.043	0.046				0.232	0.318				
K							1.815	1.808				
mg number	43.59	20.21	20.96	24.95	13.15	9.60	22.07	20.80	2.95	2.37	22.83	8.30

1. Pigeonite in glomerocryst in garnet rhyolite 156518.1
 2. Orthopyroxene margin on cognate pyroxene-feldspar cluster in garnet rhyolite 156518.1
 3. Orthopyroxene in pyroxene-garnet aggregate in garnet rhyolite 113508
 4. Garnet fragment in glass in garnet rhyolite 156518.1
 5. Garnet in garnet-ilmenite aggregate in garnet rhyolite 113508
 6. Small garnet clast in glass in sanidine rhyolite 113515
 7. Biotite in glass in garnet rhyolite 156518.1
 8. Biotite in glass in sanidine rhyolite 113515
 9. Ilmenite intergrown with biotite in garnet rhyolite 156518.1
 10. Ilmenite in glass in sanidine rhyolite 113515
 11. Hercynite in magma-modified mudstone xenolith 156518.2 in garnet rhyolite
 12. Chromian hercynite in magma-modified mudstone xenolith 156518.2 in garnet rhyolite
- Analyses of bulk rocks 156518.1 and 156518.2 are shown in Tables 6c and 13, respectively.

FeO* is total iron as FeO. mg number is $100 \times \text{Mg}/(\text{Mg}+\text{Fe})$. 156518.2 is a xenolith in sample 156518.1

When recast to equivalent oxygen, the pyroxenes, garnets and oxides show no significant Fe₂O₃, with one exception: the chromian hercynite no. 12 with 0.2 Fe³ cations. The oxidation state of biotite cannot be calculated because of possible vacancies in the crystal lattice.

Xenoliths in rhyolite. Mudstone xenoliths in the native-iron-bearing rocks elsewhere on Nuussuaq and Disko comprise a suite of more or less equilibrated rocks, from melted but unequilibrated buchites composed of glass, cordierite, mullite, sulfide and graphite to highly magma-equilibrated rocks with plagioclase, spinel, corundum and graphite (e.g. Törnebohm 1878; Pedersen 1979a; Pedersen & Larsen 2006). The equilibrated rocks have exchanged elements with the basic magma, and a marked depletion in some elements and a strong enrichment in others, e.g. Ca, has taken place. Of the xenoliths in rhyolite, a single *c.* 3 cm large, equilibrated mudstone xenolith has been analysed (see Table 13, sample 156518.2). This shows that the reaction between the mudstone and the rhyolite magma was different from the reaction with the

basic magma: the mudstone has taken up K and Ba from the rhyolite to stabilise biotite and K-feldspar, whereas the uptake of Ca is small. The xenolith now contains 6.15 wt% K₂O, which is much more than measured in any sediment in the Nuussuaq Basin, and has retained much of its carbon as graphite (11.72 wt% C).

Distribution. Rhyolite as glassy and microcrystalline massive rock has only been found as transported cobbles and pebbles in conglomerates on west Disko from Vesterdalen north-east of Hammer Dal, and in a river deposit on north-east Disko (described below). However, Rhyolite is extensively distributed as primary airfall tuffs and altered and redeposited tuffaceous sediments.

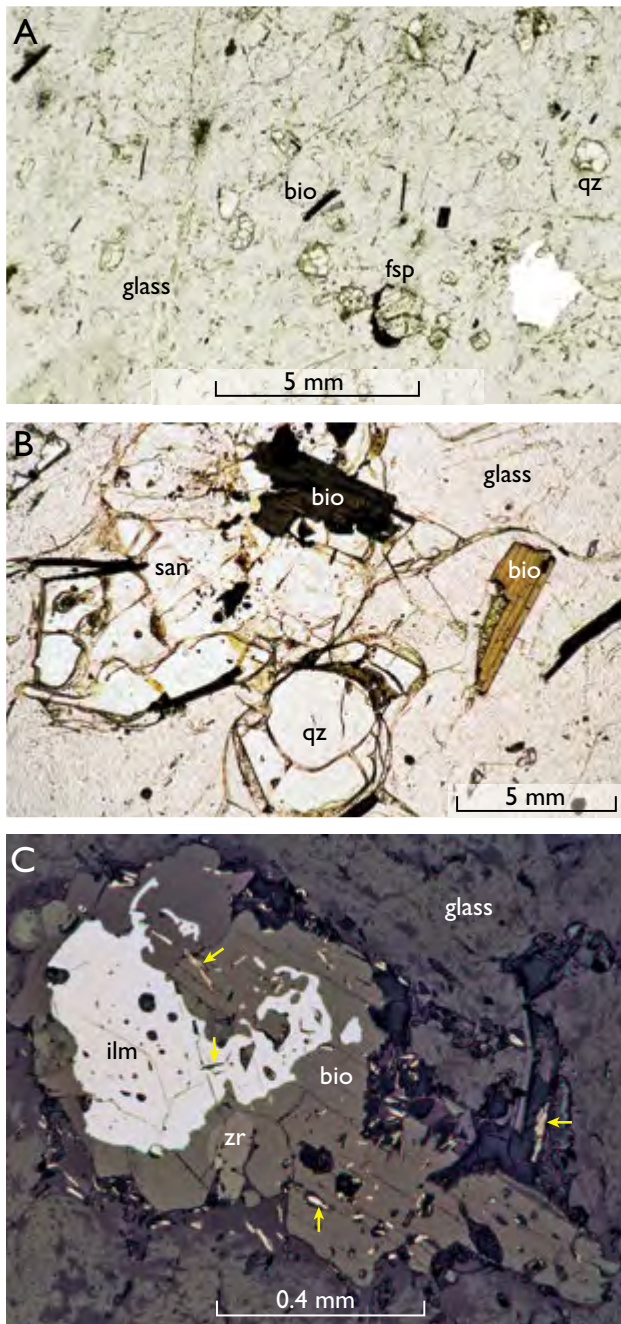


Fig. 112. Thin sections of sanidine rhyolites of the Nordfjord Member. **A:** Glassy pitchstone with about 5% phenocrysts of quartz (**qz**), feldspar (**fsp**) and biotite (**bio**). Sample 156516, clast in conglomerate in Sedimentkløften, Hammer Dal, north-west Disko; $\text{SiO}_2 = 76.6 \text{ wt\%}$, $\text{TiO}_2 = 0.10 \text{ wt\%}$, $\text{MgO} = 0.17 \text{ wt\%}$. Plane polarised light. **B:** Cluster of phenocrysts of quartz (**qz**), sanidine (**san**) and biotite (**bio**) in glass in sanidine rhyolite sample 156559, clast in conglomerate north of Rink Dal, north-west Disko. Plane polarised light. **C:** Reflected-light image of sanidine rhyolite showing flakes of graphite (at yellow arrows) enclosed in ilmenite (**ilm**), in biotite (**bio**) that forms a reaction rim on ilmenite, and in the groundmass glass. Note also minor zircon (**zr**) in biotite. Sample 113515, clast in conglomerate in Sedimentkløften, Hammer Dal, north-west Disko.

Geological themes and locality descriptions

Sediment horizons at the base of the Nordfjord Member

The base of the Nordfjord Member is marked by a prominent sediment horizon deposited on the eroded top surface of basaltic lavas of the upper Rinks Dal Member. Depending on local topography the sediment may exceed 2 m in thickness but may also be just a few decimetres thick (Fig. 113).

On north-western Disko, the lower part of the sediment horizon is a yellowish-brown claystone which sometimes contains beds of extensively weathered volcanic material interpreted as derived from rhyolitic pumice tuffs, sometimes with graphite. This indicates that formation of strongly sediment-contaminated and evolved rhyolitic magmas took place from the very beginning of the formation of the Nordfjord Member, in this case even before the beginning of the basaltic to andesitic activity (several similar events took place later). Three particularly significant localities are described below.

Niaqussat (Fig. 103, loc. 1; Fig. 14, profile 12; Fig. 113, profiles c, d). The locality is shown from a distance in Fig. 114. The eroded basalt lava surface of the upper Rinks Dal Member (unit 517) is overlain by a few metres of claystone and tuffaceous sandstone with strongly altered rhyolitic pumice. This sediment is covered, partly by a subaerial basalt lava flow, and partly by *c.* 10 m of stratified conglomerate deposited by a river, which eroded laterally into the lava flow (Fig. 113). The lava flow and the conglomerates are in turn covered by two basaltic lava flows with prominent colonnades and entablatures indicative of emplacement over a wet surface (Fig. 115). The conglomerate comprises three beds. The lowest bed has a matrix of claystone and mostly carries clasts of basalt from the Rinks Dal Member but also a minor component of highly weathered clasts of picrite, indicating that parts of the Vaigat Formation must have been exposed to erosion at that time. The upper two conglomerate beds likewise carry basalt clasts but also clasts of rhyolitic pumice and pitchstone (Fig. 115), and parts of the matrix are rich in quartz crystals and decomposed rhyolite pumice (Fig. 116). Altogether, the basal conglomerates of the Nordfjord Member at *Niaqussat* indicate tectonic activity between the deposition of the Rinks Dal and Nordfjord members.

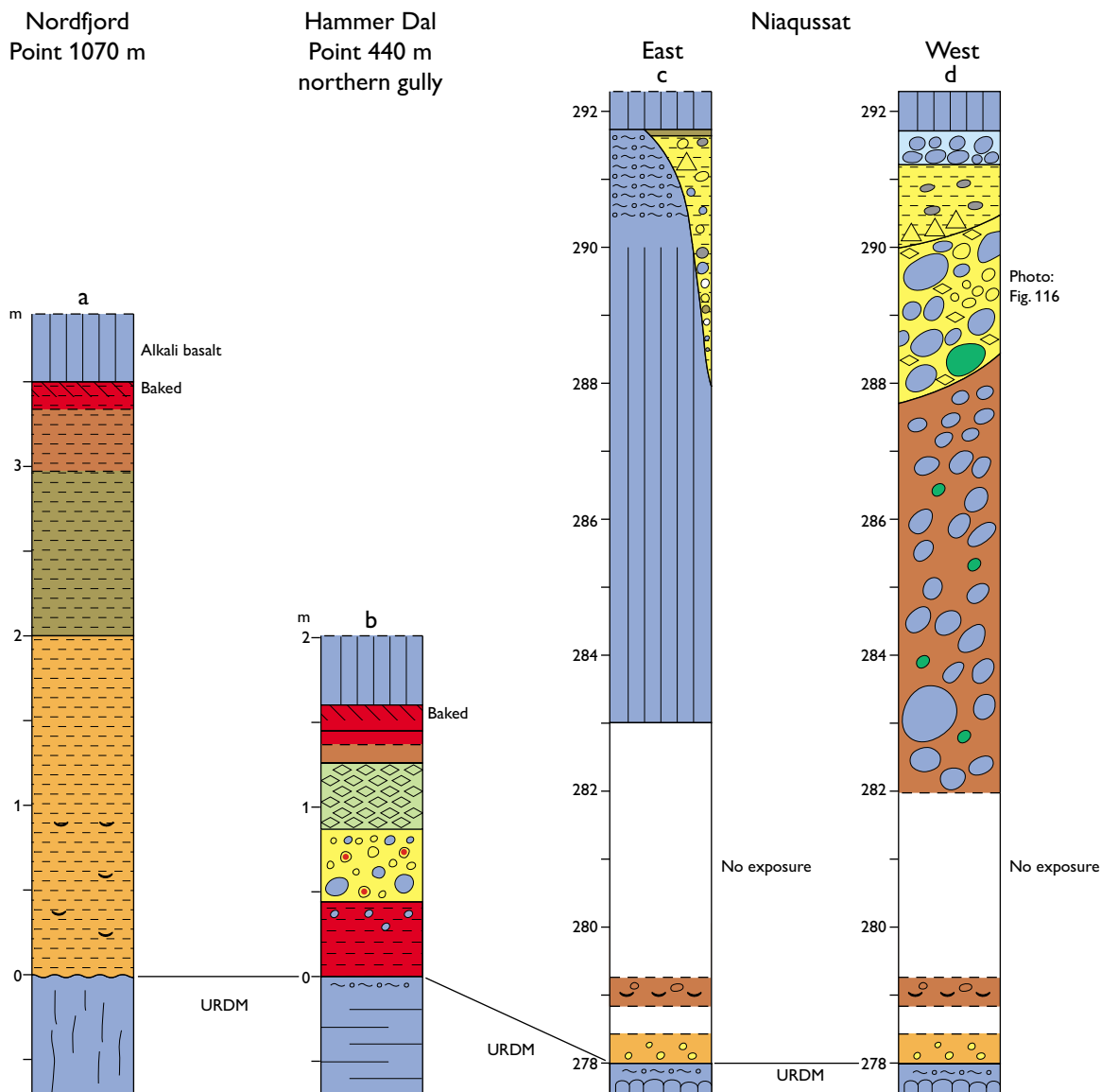


Fig. 113. Detailed logs through the sediment horizon at the base of the Nordfjord Member. Note different vertical scales. For legend, see Fig. 117, for localities, see Fig. 103, locs 1, 5, 22.

The type section of the Nordfjord Member north of Hammer Dal (Fig. 103, loc. 5; Fig. 104; Fig. 14, profile 11; Fig. 113, profile b). This section includes two sediment horizons with a lava flow between them near the lower boundary (Fig. 104 around 1800 m). The lower sediment horizon is a 10–20 cm thick, yellowish-brown claystone; the chemical composition of the overlying lava flow suggests, without being definitely diagnostic, that it belongs to the upper Rinks Dal Member (unit 518). The base of the Nordfjord Member is therefore placed at the base of the upper sediment horizon. This is a 1.6 m thick volcanoclastic sediment composed of several units of which the lower *c.* 45 cm is a lateritic soil with scattered volcanic

clasts (Fig. 113). The soil is covered by a *c.* 40 cm thick, matrix-rich conglomerate bed with up to 4 cm large clasts of basalt and, remarkably, clasts of garnet rhyolite and scarce millimetre-sized clasts of almandine garnet. The matrix is partly derived from a rhyolitic source. The conglomerate is covered by *c.* 60 cm of claystone, greenish-grey and reddening upwards, with altered rhyolite clasts containing recognisable phenocrysts of quartz and biotite. The 10–15 cm thick top zone consists of tuff and lateritic soil that has been strongly baked by the overlying lava flow. Again, it is evident that highly evolved rhyolitic rocks were available as a source for the initial sediments at the base of the Nordfjord Member.



Fig. 114. Overview photo of the Nordfjord Member at Niaquassat, north-west Disko. The Nordfjord Member begins with a basal sediment (520 sed) that is overlain by lava flows (520 La) of basalt, basaltic andesite and a single native-iron-bearing andesite erupted from a nearby crater. Some samples from profile 12 in Fig. 14 are indicated. The circle indicates the location of log d in Fig. 113 and Figs 115, 116. **URDM**: upper Rinks Dal Member.

The Point 1070 m section north of Nordfjord (Fig. 103, loc. 22; Fig. 14, profile 8; Fig. 113, profile a). This section shows the well-exposed base of the Nordfjord Member. The strongly weathered surface of a lava flow of the up-

per Rinks Dal Member (unit 518) is overlain by a 2.5 to *c.* 4 m thick succession of claystone. The lower *c.* 2 m of the claystone is yellowish-brown and contains a number of strongly altered tuff beds and beds with altered vol-



Fig. 115. The basal *c.* 12 m thick sediment horizon of the Nordfjord Member at Niaquassat (Fig. 113, log d). The locality is encircled in Fig. 114. The sediments comprise claystone, tuffaceous sandstone and bedded conglomerates described in the text. The prominent colonnade of the overlying lava flow indicates a wet environment during its emplacement.



Fig. 116. Clast-supported conglomerate in the basal sediment horizon of the Nordfjord Member at Niaqussat. The rounded clasts are mainly basalt but clasts of rhyolitic pumice also occur. The matrix is rich in quartz and decomposed rhyolite pumice. For location of the photo, see Fig. 113, log d. Length of ruler 15 cm.

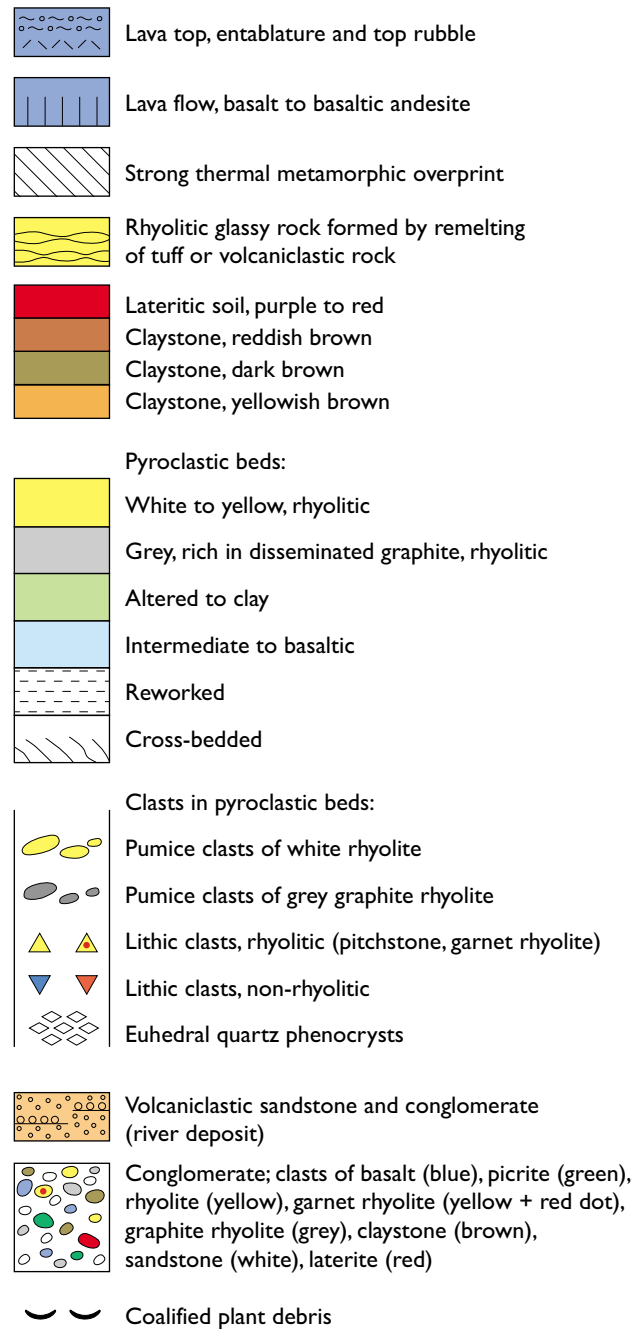
canic clasts and remnants of plant fossils. The upper half of the claystone gradually becomes more reddish, and the uppermost 20 cm is a red lateritic soil, which is strongly baked by the overlying alkali basaltic lava flow.

The West Disko Graphite Rhyolite (WDGR) volcano

The West Disko Graphite Rhyolite volcano (WDGR) denotes one or several volcanoes located somewhere in the westernmost part of north-western Disko or on the shallow shelf offshore Disko. The volcano erupted rhyolitic tuffs but also massive glassy lavas and perhaps bombs. One of the unusual features of the erupted rocks is the ubiquitous presence of graphite, which, together with scattered magma-modified sediment xenoliths, shows that the rhyolitic magmas evolved in high-level reservoirs within carbonaceous mudstones and sandstones.

The main occurrences of WDGR rocks are situated on north-western Disko. They were first noted by GGU geologists in a small gully in the south wall of Hammer Dal (V. Münther, personal communication 1968); the gully was subsequently named Sedimentkløften ('Sediment gully'). They were described by Pedersen (1969, 1975a, 1977a), Pedersen & Pedersen (1987) and Hansen & Pedersen (1985).

Legend (facing page, Figs 113, 124)



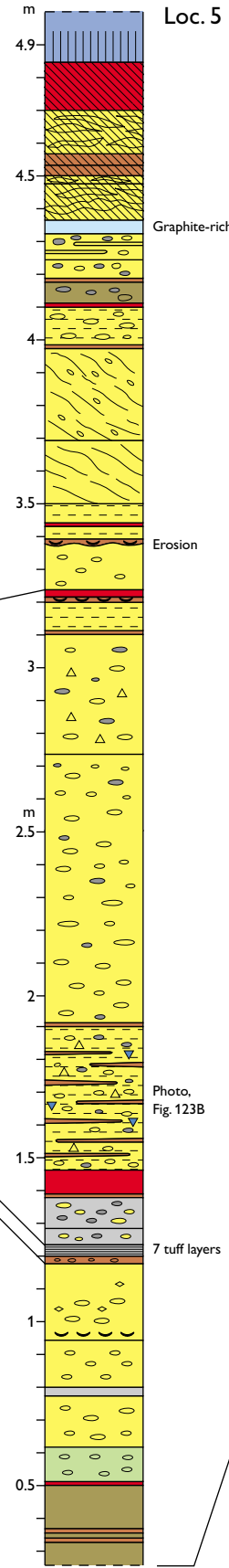
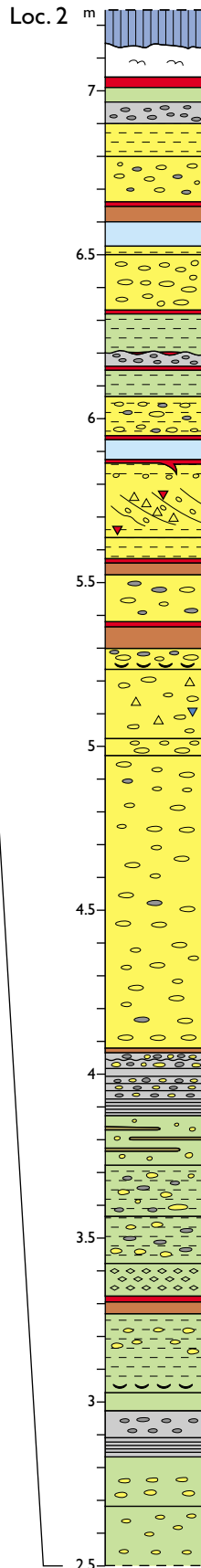
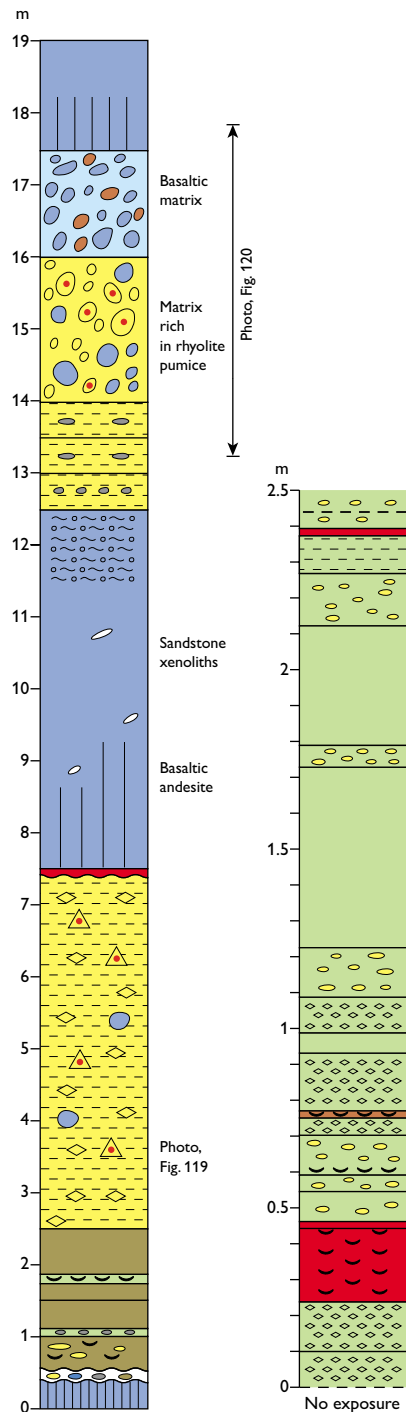
Facing page:

Fig. 117. Detailed logs of three successions with rhyolite tuffs on north-west Disko. Locality numbers are those in Fig. 103. Unreworked, primary airfall tuffs are only found north of Hammer Dal. Note the different vertical scales in the Sedimentkløften and north of Hammer Dal logs. Several photographs are located on the logs. The legend also covers Figs 113 and 124.

North of Hammer Dal

Sedimentkløften

Loc. 12



The area on north-western Disko with the main occurrences of WDGR rocks is generally poorly exposed and extensively faulted, and large areas along the coasts and in the valleys are covered by Quaternary deposits. Because of the unique nature of the rocks, and in order to locate the volcano or lava flows from the volcano, all the gullies and valley sides in the western part of the area between Giesecke Dal and Nordfjord have been systematically searched. While many individual exposures of WDGR tuffs and coarser volcanoclastic beds were located, no feeders, craters or rhyolitic lava flows from the WDGR volcano have ever been found.

Timing and duration of the WDGR volcanism. Tuffs and conglomerates with WDGR rocks occur in the volcanoclastic deposits at the base of the Nordfjord Member, immediately overlying the Rinks Dal Member, and the volcano must therefore have developed in the time interval represented by the basal sediment horizon. On the other hand, there are no traces of primary WDGR rocks within the uppermost part of the Nordfjord Member, and the volcano thus appears to have become extinct before the formation of this member ended.

Tuff successions

Tuffs derived from the WDGR volcano occur on western and north-eastern Disko, but undisturbed tuffs many metres

thick are only preserved in a limited area on north-western Disko from Rink Dal to north of Hammer Dal (Fig. 103).

Redeposited tuffs and conglomerates in Sedimentkløften. An about 18 m thick succession of volcanoclastic sandstone, conglomerate and lava flows is exposed within Sedimentkløften in the south wall of Hammer Dal. The strata dip 30°W and are disturbed by faulting. The succession belongs to the lower part of the Nordfjord Member but is not stratigraphically well constrained. It contains the most diverse assemblage and the largest rhyolite blocks found and is probably the exposure that is most proximal to the volcano. It is reconstructed here as a vertical log in Fig. 117.

At the base of the succession, a weathered basalt flow with a surface of basalt blocks in a claystone matrix is covered by 2 m of claystone and rhyolite tuff. The most conspicuous unit is the following, *c.* 5 m thick, light grey-white tuffaceous sandstone which is visible from a distance of several kilometres and has given the gully its name (Fig. 118). This sandstone contains rounded pebbles and cobbles of garnet rhyolite and must have been derived by reworking of material produced by explosive activity associated with one of the main rock types of the WDGR volcano, the garnet rhyolite (Fig. 119). It is covered by a sediment-contaminated basalt lava flow with sandstone xenoliths. On top of the flow is a *c.* 5 m thick bedded succession composed of reworked rhyolite tuff, a



Fig. 118. The tuffaceous sediment succession in Sedimentkløften; a log is shown in Fig. 117. Note encircled person for scale.



Fig. 119. Rhyolitic tuffaceous sandstone in Sedimentkløften. The two red arrows point to garnet rhyolite clasts. For location of the photo, see the log in Fig. 117.

conglomerate with a large diversity of clasts up to boulder size ranging from several types of rhyolite to basalt and alkali basalt, and an upper oxidised conglomerate with clasts of basalt, laterite and basaltic scoria (Fig. 120).

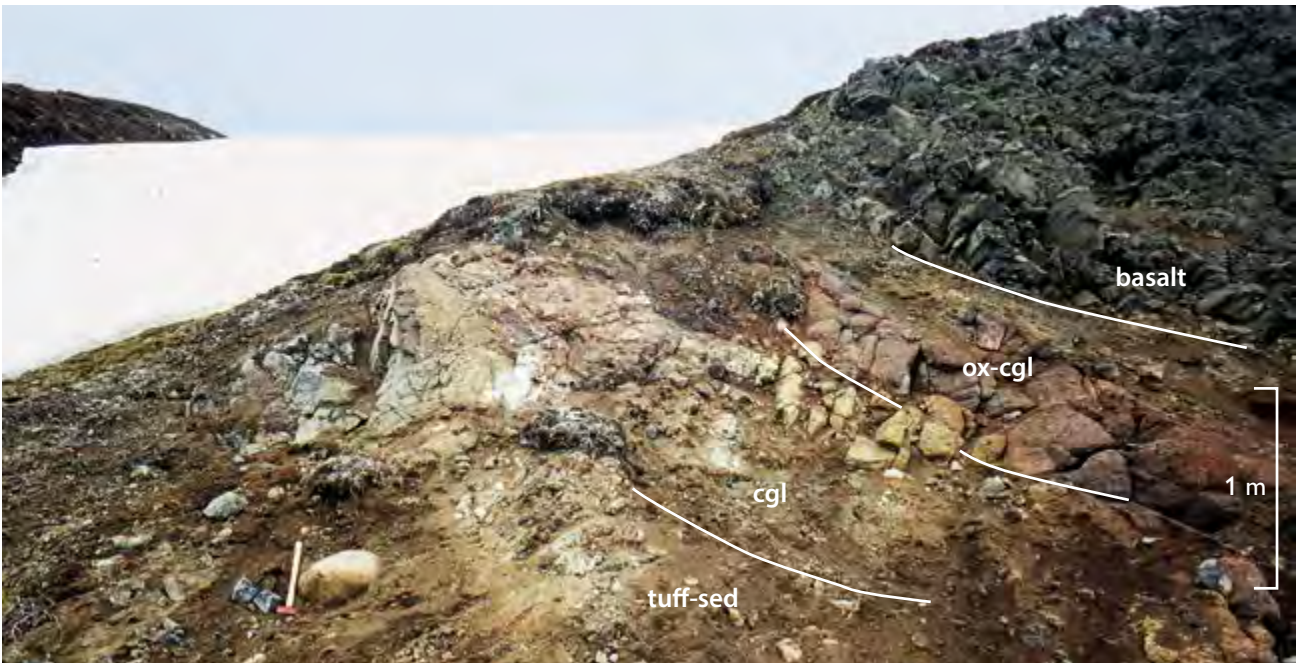


Fig. 120. The upper part of the tuffaceous sediment succession in Sedimentkløften: a bedded succession of reworked rhyolite tuff (**tuff-sed**), a light-coloured conglomerate (**cgl**) and an upper oxidised conglomerate (**ox-cgl**), overlain by a basalt lava flow. The succession dips towards the viewer. The boulder at the hammer has rolled down from the light conglomerate; it is the largest rhyolite boulder found on Disko. Length of hammer 47 cm. For location of the photo, see the log in Fig. 117.

Airfall tuffs north of Hammer Dal. The three best preserved tuff localities occur in the Hammer Dal area, two north of Hammer Dal and a third south of Hammer Dal (Fig. 103, locs 2, 5, and 27). The tuffs have minimum thicknesses of 7.1 m, 4.85 m and 5.3 m, respectively. Detailed logs of the successions at the two northern localities are shown in Fig. 117. Figure 121 is an overview photo of tuff locality 5.

The most distinctive constituent of the tuffs, which is recognised in all profiles through airfall tuffs, is a *c.* 20 cm thick horizon of bedded, graphite-rich rhyolitic tuffs (Fig. 122). Graphite gives the pumice a dark grey to black colour. The horizon comprises five to six thin, fine-clastic beds, which vary in colour between light grey and black, followed by seven coarser pumice beds, some of which are mixtures of white rhyolite pumice and dark grey graphitic rhyolite pumice. The horizon is overlain by a white-grey rhyolitic pumice bed (Fig. 122A), which is more than 1 m thick at the two northern localities but only 30 cm at the southern locality.

Hand-picked separates of a white and a dark grey pumice clast from a mixed pumice layer were analysed for TOC and sulfur (see Table 7, sample 326497). The white clast contains 0.51 wt% TOC whereas the dark grey clast is graphite-rich and contains 3.1 wt% TOC;



Fig. 121. Tuff horizon north of Hammer Dal, loc. 5 in Fig. 103. A detailed log is shown in Fig. 117.

the difference demonstrates a significant heterogeneity in the erupting high-level magma chamber.

In the thick tuff succession at locality 2, the lower 3.8 m are dominated by a number of claystone beds varying in colour between greyish-green and dark grey, which contain altered clasts of rhyolitic pumice. Notably, a number of these beds contain clear bipyramidal quartz crystals (phenocrysts) that are perfectly preserved, whereas their host pumice has decomposed to clay. Together, the thick tuffs at the two northern localities have preserved evidence of 24 explosive eruptive events, with many more small, individual beds; 20 events were rhyolitic and three non-rhyolitic. Graphite is important in four of these eruptive events.

Plant fossils occur at four to five levels, and clay and lateritic soil at six to eleven levels. Loose trunks of silicified wood occur at locality 2 and must have been eroded out of the tuff succession. These occurrences indicate significant time gaps between the individual eruptions of the tuffs. Moreover, there are signs of local erosion and reworking by water of several tuffs (Fig. 123), notably in the southern locality 27, which comprises two prominent conglomerate beds.

The intensive weathering to clay of the lower part of the succession and the better-preserved state of the upper 3 m of the tuffs indicate a considerable duration of the

explosive eruptive phase and a much higher eruption rate for the uppermost 3 m of the tuffs.

Altogether, the distribution of the airfall tuffs indicates a location of the WDGR volcano around or just north of Hammer Dal or within the neighbouring offshore area.

Conglomerates and volcaniclastic sandstones

In addition to the conglomerates and sandstones described above, the Nordfjord Member contains a number of other conglomerate and volcaniclastic sandstone beds which all indicate active tectonic movements, recurrent phases of local erosion, and the presence of rivers.

The main occurrences of such sediments are on western and north-western Disko from Nordfjord to Giesecke Dal and in a limited area on north-eastern Disko. They seem to be absent on south-western Disko, and no evidence of conglomerate beds is found in the large areas where only erosional remnants of the Nordfjord Member are preserved.

In the poorly exposed and severely block-faulted western and north-western Disko, individual sediment beds are only preserved over short lateral distances from a few metres to at most a few hundred metres, and no reconstructions of palaeo-riverbeds are possible. In contrast, a



Fig. 122. A characteristic horizon of bedded, graphite-rich rhyolite tuff found in all profiles through airfall tuffs, here at locality 2 north of Hammer Dal. For description, see text. **A:** Overview of the succession with the \approx 15 cm thick, graphite-rich tuff horizon in the centre. **B:** Close-up of the graphite-rich tuff horizon. The thin tuff layers (1–2 cm) in the lower part show normal grading, which suggests that they may have been deposited in water. The absence of wave- or current-generated cross-lamination suggests rapid deposition in a low-energy environment. The thick, coarse-grained tuff layer in the middle indicates either a more violent eruption or a crater much closer to the locality. For location of the photos, see the log in Fig. 117 (where the measured tuff layer is 20 cm thick).



Fig. 123. Rhyolite tuffs north of Hammer Dal showing signs of reworking by water. **A:** Well-sorted rhyolite tuff with cross-bedding indicating fluvial transport and deposition. **B:** Moderately sorted, very coarse-grained tuffaceous sandstone with weak stratification, interbedded with two thin dark claystone layers in the upper part of the photo, suggesting settling from suspension in water. For locations of the two photos, see the logs in Fig. 117.

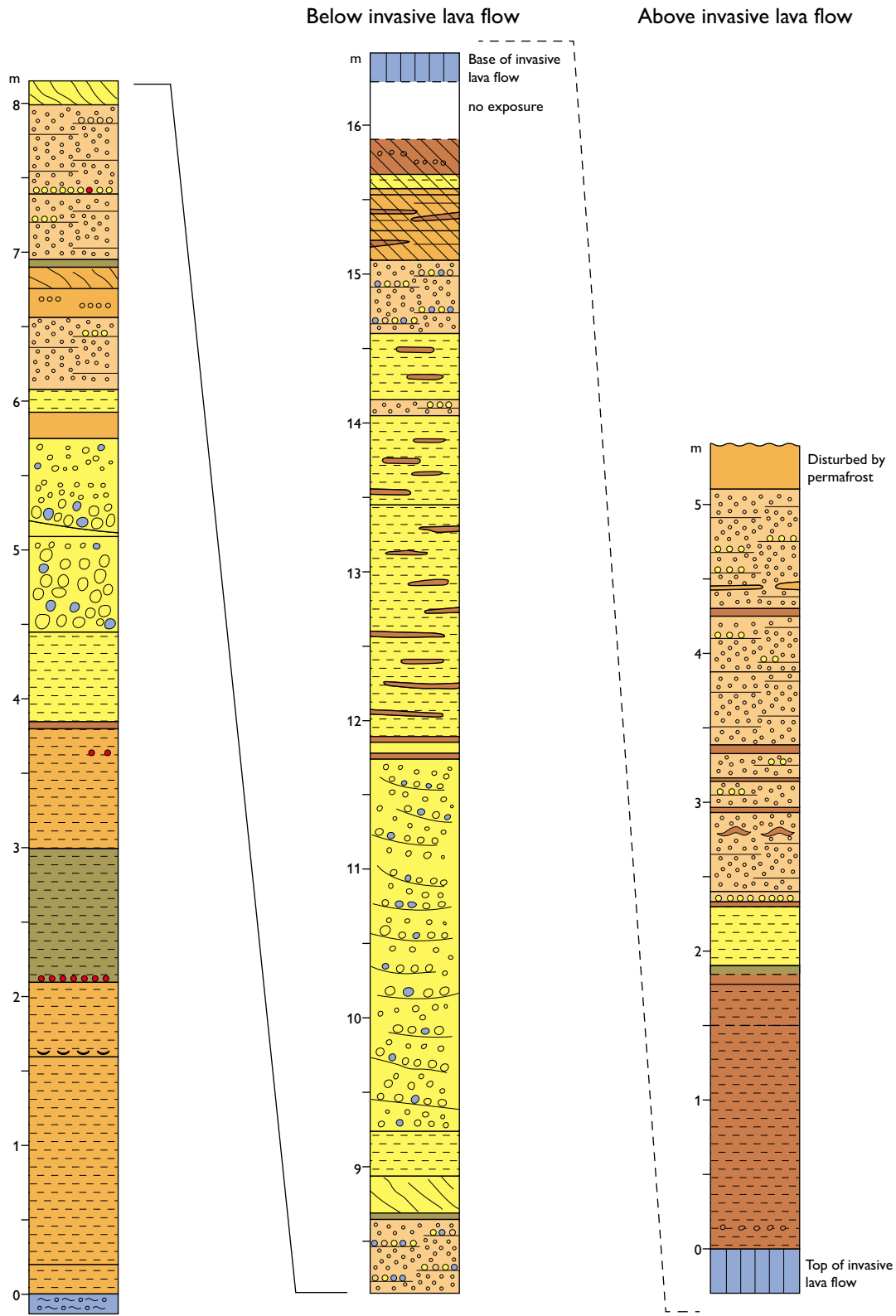


Fig. 124. Log of *c.* 21 m of rhyolitic tuffaceous sediments in a river deposit, north-eastern Disko. The succession is split in two by an invasive lava flow. Legend in Fig. 117. Three sedimentary facies are distinguished: mudstone, presumably altered tuff; pebbly sandstones with weak stratification, locally interbedded with thin mudstones; and conglomerates, massive or weakly cross-bedded. The mudstones are interpreted as floodplain deposits and the sandstones and conglomerates are fluvial. See text for descriptions and discussion.



Fig. 125. Few metres of rhyolitic, tuffaceous sediment deposited on the irregular, eroded top of the underlying lava flow. The sediment is relatively fine grained with parallel bedding and is baked (dark grey colour) by the overlying, invasive lava flow. The lower boundary of the tuff layer is mostly covered by down-washed tuffaceous material. Nordfjord Member below Point 1530 m, north-eastern Disko. The part of the invasive flow seen here is *c.* 20 m thick. See also Fig. 10, profile 6.

horizon of conglomerate and sandstone on north-eastern Disko is continuous over at least 3 km.

The conglomerate and sandstone beds contain very different clast populations. Here two types will be described, namely beds with a substantial component of rhyolitic rocks from the WDGR volcano and beds without rhyolitic rocks.

Sediments with clasts from the WDGR volcano

River deposit on north-eastern Disko. The most extensive conglomerate-bearing horizon within the Nordfjord Member is an up to 20 m thick deposit of tuffaceous sandstone and conglomerate rich in rhyolitic clasts and pumice, which is exposed in the steep coastal cliff below Point 1530 m near Unartuarsuk on north-eastern Disko (Central Disko section at 69 km; Fig. 10, profile 6 at 1315–1365 m; sediment log in Fig. 124). The deposit

forms a white sediment layer that can be followed for 3 km along the cliff face. No similar sediments are present in the surrounding areas, and the massive rhyolite clasts cannot have been deposited by airfall from a volcanic explosion in the WDGR volcano more than 75 km to the north-west. This, and the rounded and abraded state of the clasts, indicate that the sediment was deposited by a river, which must have transported rhyolitic rocks from the WDGR volcano on north-western Disko for at least 75 km towards south-south-east across northern Disko (Larsen & Pedersen 1989).

The deposit is only accessible at the eastern end of the exposure where it is partly disturbed by a *c.* 30 m thick invasive lava flow of the Nordfjord Member (Fig. 125; also Larsen & Pedersen 1989, figs 2 and 4). The flow has intruded the upper part of the succession and has melted the sediments at its lower and upper contacts into glassy zones in which reddish layers of oxidised claystone can



Fig. 126. Sediments in rhyolitic tuffaceous deposit on north-eastern Disko. Pebbly sandstone and fine-grained sandstone form trough-shaped sets. The parts with contrasting grain sizes are well separated, indicating abrupt changes from high to lower energy conditions; deposition could have taken place in a fluvial channel. The base of an invasive lava flow is seen in the upper part of the photo; the sediment at the contact has been melted into a glassy rock; the glassy interval is indicated by a white vertical line at upper right; the amount of glass decreases downwards from the contact. In the glassy interval, a reddish layer of oxidised claystone (a former soil horizon?) can be distinguished from blue-grey layers of melted volcanoclastic sediment rich in rhyolitic pumice. Length of field spade 67 cm.

still be distinguished from blue-grey layers of melted volcanoclastic sediment rich in rhyolitic pumice (Fig. 126). Close to a palaeo-riverbank cut into the lowermost lava flow of the Nordfjord Member, there are *c.* 15 m of sediment below the invasive lava flow and more than 5 m above the flow (Fig. 124). The lowermost *c.* 3.5 m of the sediment consist of yellowish-brown to dark-brown claystone beds with a few millimetre-thick layers of coalified plant remains. This is interpreted as a floodplain deposit. Upwards, the succession is composed of alternating beds of volcanoclastic sandstone and conglomerate, in places separated by thin layers of yellowish brown claystone. Numerous erosive structures are present (Fig. 126). The volcanoclastic beds have a whitish-grey matrix dominated by reworked rhyolitic pumice (Fig. 126). The conglomerate comprises basalt clasts up to 15 cm large and rhyolite and andesite clasts up to 5 cm large. Among the rhyolites,

which all carry graphite, are the three characteristic components of the WDGR volcano: glassy quartz-biotite-feldspar rhyolite (pitchstone), which is predominant; flow-laminated microcrystalline rhyolite (felsite, from lavas) with the same phenocrysts, which is common; and scarce, strongly porphyritic garnet rhyolite. Andesites, and possibly dacites, with xenoliths of magma-modified mudstone are also present. The main part of the sediment is transported from north-western Disko, and the many beds separated by claystone show that the succession was deposited over some time and not in a single catastrophic event.

Conglomerate deposits on north-western Disko. It is not possible to correlate any conglomerate bed on western Disko with the fluvial deposit on north-eastern Disko, although some similarities are seen in a conglomerate

Fig. 127. Conglomerate bed north of Hammer Dal, north-west Disko. Matrix-supported, poorly sorted conglomerate bed with rounded to sub-angular clasts. The clasts comprise basalt (**bas**), pitchstone (**pt**) and white rhyolitic pumice (**pu**). The light grey matrix has a large component of reworked rhyolitic pumice. The conglomerate may be a debris-flow deposit. For locality, see Fig. 103, loc. 5.



horizon about 70 m above the base of the Nordfjord Member in the type section (Fig. 103, loc. 5; Fig. 14, profile 11, lower part at 173 m), and in a parallel gully. This horizon is 10.2 m thick and composed of volcanoclastic sandstone and conglomerate rich in rhyolite clasts, with a matrix that is light grey due to a large component of reworked rhyolitic pumice. The clast size varies from pebbles to rare boulders. The clasts vary considerably in composition from bed to bed and from locality to locality, but strongly sediment-contaminated volcanic rocks are always abundant and particularly rhyolitic rocks from the WDGR volcano. A typical fresh conglomerate sur-

face is shown in Fig. 127. The rhyolitic rocks comprise pitchstones, felsites and garnet rhyolites just as in the north-east Disko conglomerates. Dacites with native iron are common, as are basaltic to andesitic rocks. A characteristic but rather scarce rock type, which is only known from these conglomerates is graphite-rich high-Al dacite. At some localities feldspar-phyric basalt clasts seem to be missing, at others they are subordinate. Pitchstone glass clasts are very common to dominant in the sand to gravel fraction.

South of Hammer Dal there is a conglomerate bed with a clast population dominated by basalt, but also

Fig. 128. Conglomerate bed south of Hammer Dal, north-west Disko. Matrix-supported, poorly sorted conglomerate bed, tentatively interpreted as a debris flow deposit. The clasts comprise basalt, garnet rhyolite, felsite, pitchstone and rare clasts of picrite derived from the Vaigat Formation. Length of hammer 32 cm. For locality, see Fig. 103, loc. 13.





Fig. 129. Conglomerate with rhyolitic clasts (**rhy**) engulfed by a Nordfjord Member basalt lava flow. North of Hammer Dal, north-west Disko. For locality, see Fig. 103, loc. 3.

with common clasts of garnet rhyolite, felsite and pitchstone (Fig. 128). A rare component is weathered and well-rounded clasts of picrite, which must have been derived from the Vaigat Formation.

Conglomerate engulfed by a lava flow. About 2.8 km north-east of Point 440 m north of Hammer Dal (Fig. 103, loc. 3), a more than 6 m thick feldspar-phyric basalt lava flow of the Nordfjord Member has engulfed a conglomerate with rhyolitic blocks from the WDGR volcano. The lower 2 m of the flow are very rich in rounded xenoliths of several types of basalt and rhyolite and show chill zones against the blocks (Fig. 129). Some of the blocks were weathered before they were picked up by the flow. During reheating in the flow, pumice clasts were partly remelted and the almandine garnets of the garnet rhyolites were transformed into oxide-silicate assemblages, which have preserved the original characteristic garnet-quartz intergrowth texture of this rock type (Fig. 111E).

Sediments without clasts from the WDGR volcano

A number of uncorrelatable exposures of metre-thick conglomerates and volcanoclastic sandstones without rhyolitic clasts occur in an area on north-west Disko from just south of the western part of Hammer Dal, through the western part of Rink Dal to the north coast of Nordfjord. The sediments are sandwiched between plagioclase-phyric basalts within the upper part of the Nordfjord Member. The most extensive of these sediment deposits is found in the northern and southern walls of the western part of Rink Dal (Fig. 130; Fig. 103, loc. 15). The succession is up to *c.* 10 m thick and composed of beds of volcanoclastic sandstone alternating with variably coarse conglomerate beds. The clasts vary in size from less than 1 cm to more than 2 m and predominantly consist of plagioclase-phyric and aphyric basalt; in addition, there are strongly sediment-contaminated basaltic andesites and andesites, some of which contain native iron and graphite-rich modified mudstone xenoliths. Native-iron-bearing lava flows are not preserved within this part of Rink Dal, but they are present to the north, south and east.

Within a few kilometres from the main conglomerate locality in the north wall of Rink Dal, there are several localities with cross-bedded volcanoclastic sandstones, one of which contains a rich assemblage of fossil leaf imprints and coal fragments (Fig. 103, loc. 14). The sandstones are covered by a decimetre-thick layer of lateritic soil, and at one locality there are two volcanoclastic sandstone beds separated by lateritic soil and an additional lateritic soil layer on top (Fig. 131). This demonstrates that the small stream that deposited the sand dried up several times before the sand was covered by lateritic soil and finally by the next basalt lava flow.

Simple dacite lava flows between Hammer Dal and Jamma

One or two dacite lava flows with native iron occur in the strongly faulted and poorly exposed area that extends from Hammer Dal and about 10 km northwards to Jamma (Fig. 108D). The mineralogy and textures are interpreted as recording a trend of progressive reduction in T-f_{O₂} space, as described in detail by Pedersen (1981). Most localities have only preserved part of a single dacite lava, but the north wall of Hammer Dal at Point 600 m shows a continuous exposure of the uppermost 240 m of the Nordfjord Member (Fig. 14, profile 9; Figs 104C, 132; also Pedersen 1977a, fig. 7). Here a *c.* 120 m thick dacite lava flow with native iron is exposed, the thickest recorded lava flow in the Paleocene of the Nuussuaq Ba-



Fig. 130. Succession of conglomerate and sandstone beds within the upper part of the Nordfjord Member. The conglomerates are moderately sorted and are overlain by red volcaniclastic sandstone. The sediments do not contain any rhyolitic component, and due to their predominantly basaltic composition, they are not visibly baked by the overlying lava flow. Length of hammer 47 cm. Rink Dal, north-west Disko. For locality, see Fig. 103, loc. 15.

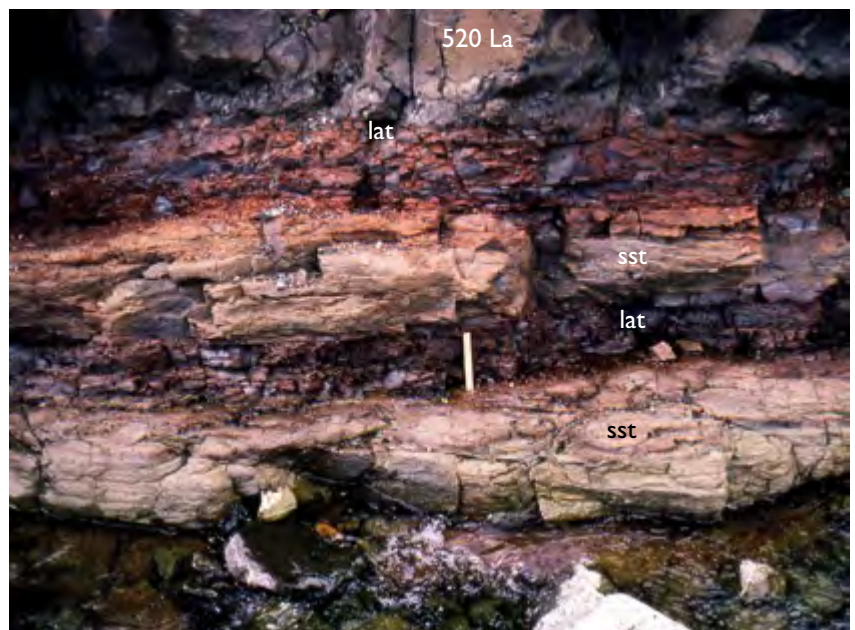


Fig. 131. Sediments within the Nordfjord Member. Two volcaniclastic sandstone beds (**sst**) each overlain by a lateritic soil (**lat**), indicating alternating wet and dry conditions. The sediments were eventually covered by a lava flow (520 La). Length of ruler 15 cm. North of Rink Dal, north-west Disko. For locality, see Fig. 103, loc. 14.

sin. Its lower part is very compact and has a rusty brown weathering colour; it is jointed into more than 1 m thick columns and blocks. The upper *c.* 20 m is a blocky lava top. Part of the same flow is exposed in an E–W-running gully *c.* 1.5 km to the north (Fig. 104B; Fig. 14, profile 10) and there are other small exposures in gullies 3 km to the south in the south wall of Hammer Dal, but no realistic map of the extent of the lava flow can be made. No feeders or intrusive rocks of similar composition are known.

A very similar rock (Pedersen 1981, table 1 sample 176466) is preserved as wave-eroded skerries around the small point Jamma at the coast (Fig. 103). The skerries consist of a dark grey, very fine-grained dacite with native iron (Table 6; Pedersen 1981, table 1 and 2, sample 176471). It is not seen in contact with other volcanic rocks.

In addition to the exposed native-iron-bearing dacite lavas in the upper part of the Nordfjord Member, native-iron-bearing dacite also occurs as clasts in conglomerate beds with rhyolite (see above) embedded within basaltic lavas older than the dacite lavas (Fig. 14, profile 11, lower part at 170 m). There are both native-iron-bearing dacite clasts that are very similar to the lavas (Pedersen 1981 table 1 and 2, sample 176486) and clasts of graphite-rich,

high-Al dacite of a type not known as lavas and likely to be associated with the WDGR volcano (see above).

Composite lava flows

Basaltic andesites, andesites and dacites commonly form part of composite lava flows or groups of flows from the same eruption centre. As shown in the last chapter, they are likely to have erupted from composite feeder dykes. The distribution and extent of some of the more characteristic composite flows is shown in Fig. 108.

Egaluit/Nordre Laksebugt. A *c.* 27 m thick, composite lava flow at the base of the Nordfjord Member occurs 2.5 km east-north-east of the river outlet at Egaluit (Fig. 133). The flow is only known from this locality. It has a 2.5–3.5 m thick lower part of columnar-jointed, nearly aphyric basaltic andesite with 53 wt% SiO₂, 2.2 wt% TiO₂ and 5.8 wt% MgO (Table 6, sample 176579). This passes upwards through a thin hybrid zone with incomplete mixing into a more than 20 m thick, more silicic basaltic andesite with 55 wt% SiO₂, 3.1 wt% TiO₂ and 3.6 wt% MgO (Table 6, sample 176582). This part is dotted with rusty spots of weathered native iron and troilite; it contains numerous xenoliths of graphitic, magma-mod-

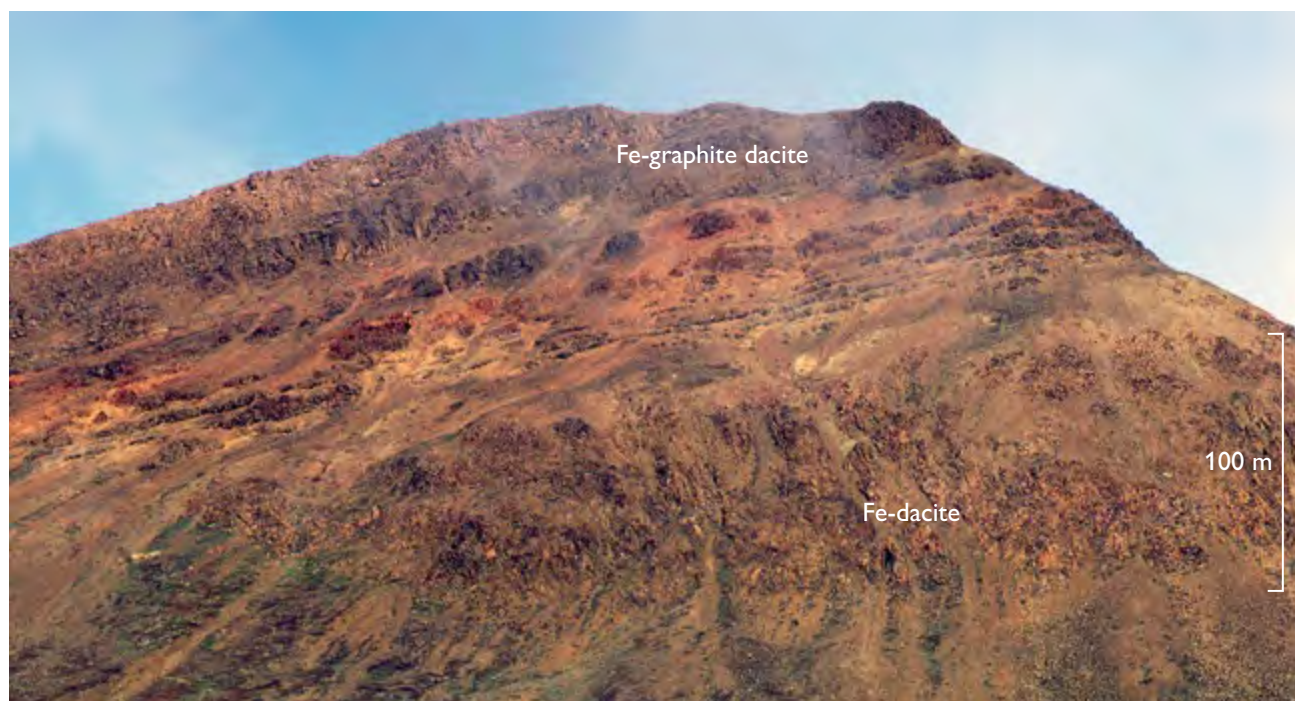


Fig. 132. A Nordfjord Member lava succession with two native-iron-bearing dacite flows, a lower 120 m thick and an upper 45 m thick, with a series of thinner andesite flows in between. Point 600 m, north side of Hammer Dal, west Disko, looking north. See also Fig. 14, profile 9 and the photogrammetric interpretation in Fig. 104C. For locality, see Fig. 103, loc. 8.

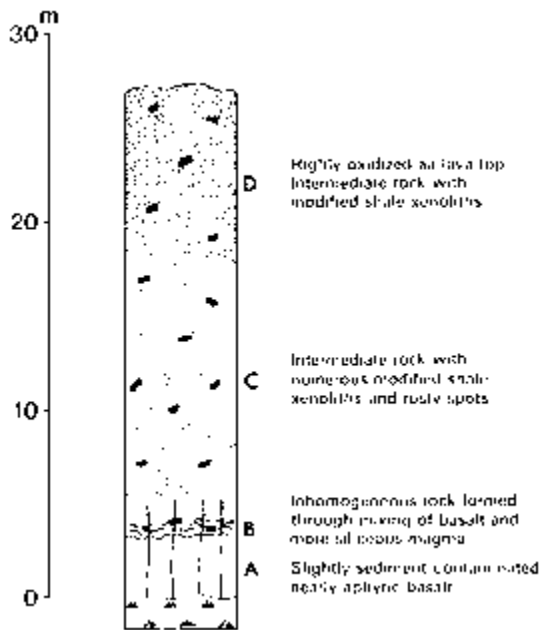


Fig. 133. Drawing of a composite lava flow at the base of the Nordfjord Member near Eqaqut, south-western Disko. From Pedersen (1977, fig. 18).

ified mudstone. The upper 5 m of the flow is vesiculated and strongly oxidised. The flow provides an example of contamination of a fairly evolved basaltic magma.

Qasigissat–Vesterdalen–Nordfjord. In the area between Mellemfjord and Nordfjord several lava flows of basaltic andesite to andesite form the lowermost part of the Nordfjord Member. Their total thickness is up to about 50 m (Fig. 14, profiles 4–7) and several of the flows are composite. All the rocks contain xenoliths of magma-modified mudstone and sandstone, and several carry native iron. The composite flows are exposed over an area of between 150 and 200 km² but must also have been present in the offshore areas in the west. Their feeder dykes are likely to be composite similar to some of the dykes of dyke system A described below (see also Fig. 174), but none have been found.

An example of the diversity of the erupting pulses is illustrated by a composite andesite lava flow with native iron in the Point 1300 m profile in Vesterdalen (Fig. 14, profile 5). The c. 12 m thick flow is composed of a lower part transitional between basaltic andesite and andesite and an upper part transitional between andesite and dacite. The lower part contains 57.0 wt% SiO₂, 1.7 wt% TiO₂, 8.1 wt% MgO and 0.57 wt% K₂O. The upper part has a very inhomogeneous groundmass; it contains 62.4

wt% SiO₂, 2.0 wt% TiO₂, 4.0 wt% MgO and 0.84 wt% K₂O (Table 6, sample 264067). Here two different, both strongly contaminated magmas were emplaced during the same eruption. This flow belongs to the low-Al₂O₃, high-P₂O₅ group of flows described below.

Low-Al₂O₃, high-P₂O₅ magmas in a group of composite lava flows. A group of one to three lava flows of andesitic to dacitic composition and sharing a unique geochemical character constitutes an important local marker horizon that was presumably produced from a single eruptive centre. The lavas are exposed along the outer part of Nordfjord and extend southward to the inner part of Mellemfjord, where the horizon is present at Saqqarliit Ilorliit (Pedersen 1977b, table 7 no. 5). It belongs to the lowest part of the Nordfjord Member and is known from a number of profiles (Fig. 14, profiles 5–8); its distribution is shown in Fig. 108C. One large dacitic lava flow varies in thickness from more than 50 m around Perlerut Qaqaat on the north wall of Nordfjord (Central Disko section at 7.6 to 12.6 km) to less than 10 m. This flow forms a prominent, rusty brown horizon due to the weathering of native iron and sulfides (Fig. 134). It is known from the south coast of Nordfjord to Mellemfjord. On the north side of Nordfjord, the dacite overlies an alkali basalt lava flow and is partly covered by rhyolitic tuff from the WDGR volcano (Fig. 14, profile 8; Central Disko section at 7.5–12.5 km). The horizon thins out just north of Nordfjord and is missing in Rink Dal. No eruption sites have been found and there are no known intrusive rocks of similar chemistry. The thickness variations suggest that the lavas originated in the outer part of the present Nordfjord.

The composite Mellemfjord lava flow. A large, native-iron-bearing composite lava flow in the Mellemfjord area on south-western Disko forms an important local marker horizon in the uppermost part of the Nordfjord Member (Figs 135, 136). The flow has been mapped photogrammetrically (Pedersen 1977b, plate 1 and an isopach map, fig. 19). It extends along the northern and southern shores of the central and western parts of Mellemfjord and must continue offshore well to the west of the coastline (Fig. 108A). The flow must have covered an area of more than 400 km² and its volume must have exceeded 14 km³, which makes it the most voluminous crustally contaminated lava flow on Disko and among the largest lava flows within the Nuussuaq Basin.

The flow was first discovered by K.J.V. Steenstrup in 1880 and was later described by Steenstrup (1883), Lor-

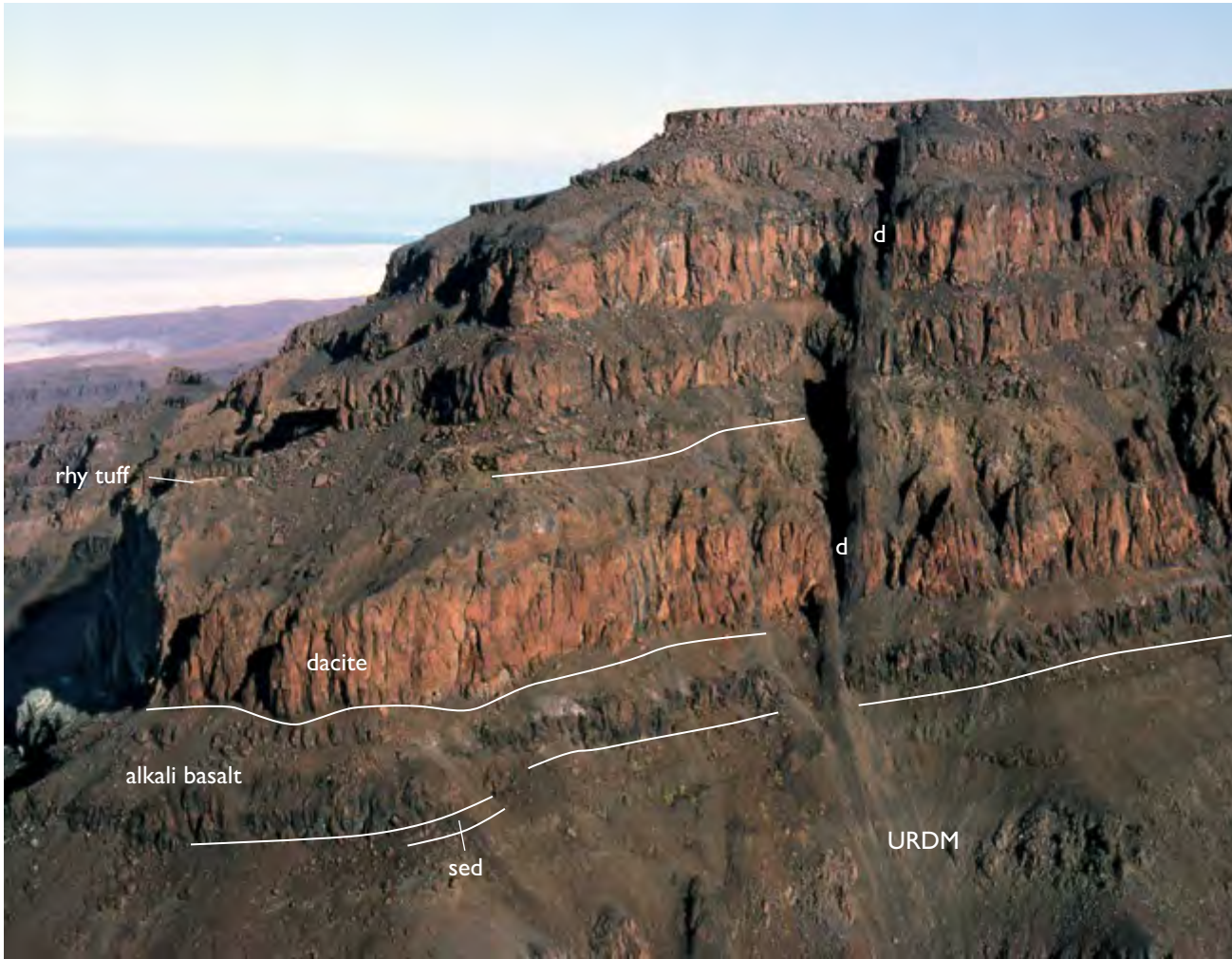


Fig. 134. Nordfjord Member lava flows and rhyolitic tuff layer (**rhy tuff**) in the north wall of Nordfjord, west Disko (central Disko section at around 7.8 km). The large dacite flow is 60 m thick and forms a prominent rusty brown horizon due to the weathering of native iron and sulfides. Thin sediments (**sed**) at the base of the Nordfjord Member are just visible below the alkali basalt flow. **URDM**: upper Rinks Dal Member. The succession is cut by a dyke (**d**).

enzen (1882), Nicolau (1900), Pauly (1969), Pedersen (1977b, p. 41–46) and Klöck *et al.* (1986). Pedersen (1977b) originally assigned the flow to the Niaqussat Member because of its estimated high-magnesium parental composition, but it is here reassigned to the uppermost Nordfjord Member (see Fig. 14, profile 3).

The Mellemfjord lava flow is lithologically very similar to the native-iron-bearing composite lava flows of the Asuk Member in the Vaigat Formation (Pedersen *et al.* 2017), but it has a much larger volume. A simplified section through the flow is shown in Fig. 137. The flow has a thin lower zone of basalt, a thin hybrid zone of basaltic andesite, and a thick upper zone of highly magnesian andesite. The lower few metres of the flow are a

very fine-grained basalt without native iron (Fig. 138A; Table 6, sample 176565). The basalt carries very scarce plagioclase phenocrysts up to 1 mm in size and abundant pseudomorphed olivine microphenocrysts together with scarce augite microphenocrysts. The groundmass is composed of plagioclase, pigeonite and augite, ilmenite and residuum. Native iron appears within the hybrid zone of basaltic andesite (Table 6, sample 176556), and 2–3 m above the base the rock becomes a magnesian andesite with native iron (Fig. 138B; Table 6, sample 176564) and with sufficiently high Cr (418 ppm) to demonstrate a highly magnesian parent.

The magnesian andesite has been described by Nicolau (1900) and Klöck *et al.* (1986). It is a very fine-



Fig. 135. The cliffs along the south coast of Mellemfjord. The large native-iron-bearing composite Mellemfjord lava flow (**Fe**) forms a major marker horizon over a large area. It is the highest flow in the Nordfjord Member and is overlain by lava flows of the Niaqussat Member (unit 530). The Nordfjord Member (unit 520) has a basaltic andesite (**ba**) flow at the base. **URDM**: upper Rinks Dal Member. The highest part of the cliffs reaches 900 m a.s.l. East of Ivisaarqut/Enok Havn, west Disko.



Fig. 136. The composite Mellemfjord lava flow at the north coast of Mellemfjord just east of Ikorfarsuit. The flow is here 75 m thick; the basaltic and andesitic parts are indicated.

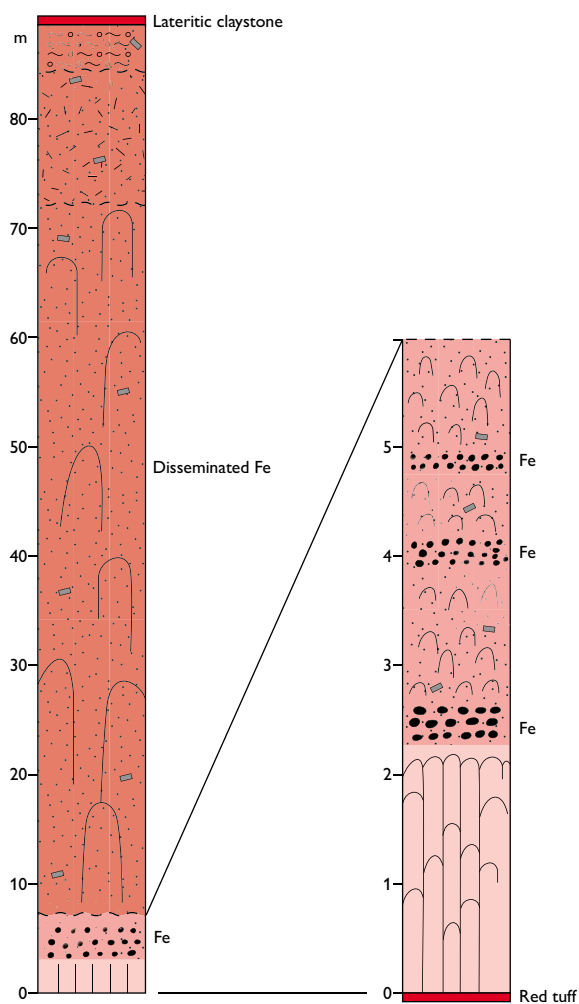


Fig. 137. Simplified section through the composite Mellemfjord lava flow; the basal part is shown expanded in the right column. The flow has a lower zone of basalt without native iron (pale red), a hybrid zone of basaltic andesite (stronger red) with disseminated native iron and three horizons of native iron accumulations (black), and a thick upper zone of highly magnesian andesite (reddish brown) with disseminated native iron (small black specks). Sediment xenoliths are grey. For further description, see text. The section represents the flow along the north coast of Mellemfjord between Ikorfarsuit (Fig. 14, profile 3) and Saqqarliit Silarliit (Fig. 6), where the flow attains its maximum thickness of about 88 m.

grained rock with an unusual assemblage of pyroxenes. There are common phenocrysts of low-Ca-clinopyroxene and abundant microphenocrysts of orthopyroxene and plagioclase. The cores of some pyroxene phenocrysts show intense lamellar twinning resembling twinning in clino-hypersthene commonly found in chondrites. Such twinned cores have not been found in any other andesites with native iron from Disko. The magnesian

andesite carries up to millimetre-sized bodies of native iron rimmed by troilite. There are scattered xenocrysts of olivine, red spinel and plagioclase with graphite, and xenoliths of magma-modified mudstone. The groundmass is composed of plagioclase, orthopyroxene and calcic clinopyroxene, ilmenite, native iron and troilite, and residual glass with a composition of potassic rhyolite. Rare grains of armalcolite have been found associated with the native iron (Klöck *et al.* 1986). In the lower part of the flow, the andesite groundmass is very fine-grained and fairly homogeneous (Fig. 138B), but upwards the fine-grained groundmass develops a distinct globular texture (Fig. 138C) resembling a product of liquid immiscibility, similar to the texture in native-iron-bearing basaltic andesite of the Asuk Member.

The composite Mellemfjord lava flow is covered by a thin layer of lateritic claystone, which has also impregnated the uppermost metre of the scoria of the flow. The overlying lava flows are olivine-microphyric and aphyric basaltic lavas assigned to the Niaqussat Member.

Minor flows from the Mellemfjord eruption site. Along the north coast of Mellemfjord, the composite Mellemfjord lava flow is underlain by several flows packed with cognate gabbroic olivine-clinopyroxene-plagioclase nodules and magma-modified sediment inclusions up to 20 cm in size; one of the flows contains up to 4 cm long olivine grains (Fig. 139). These lava flows have highly irregular upper parts where heaps of scoria alternate with thin pahoehoe lava tongues. Despite the absence of a feeder body and a visible crater, these features strongly indicate close proximity to an eruption site. The first eruptions must have comprised the xenolith-rich flows, later followed by the large native-iron-bearing lava flow.

Composite lava flow in the Kvandalen valley, eastern Disko. On eastern Disko, there are only two eruptive units more silicic than basalt, one in each of the Nordfjord and Niaqussat members. Both flows are believed to be associated with the NW-SE-trending dykes of system C described below (see Fig. 174), which seems to have been active over a long time period.

The lava flow of the Nordfjord Member is a large composite basaltic andesite flow with native iron in the Kvandalen area. It was briefly described by Pedersen & Larsen (1987, fig. 2) and Larsen & Pedersen (1989) and shown as marker unit τ (tau) on the geological map sheet Pingu (Fig. 140). The lava flow extends along the north wall of Kvandalen westwards from Aqajaruata Qaqqaa (Fig. 141; Fig. 10, profiles 10, 11; Central Disko section at

82.5–105.4 km); its northern and eastern delimitations are unconstrained because of erosion. Towards the northwest the lava flow terminates in the eastern part of the Qinggusaq mountain. On the south side of Kvandalen it is only present on the ridge towards Charles Polaris Dal.

The lava flow is up to 25–30 m thick and composite, with the lower few metres consisting of basaltic andesite very close to basalt (52.1 wt% SiO₂) while the rest of the flow is a basaltic andesite with 53–54 wt% SiO₂. Rusty spots of weathered native iron and troilite are widespread in

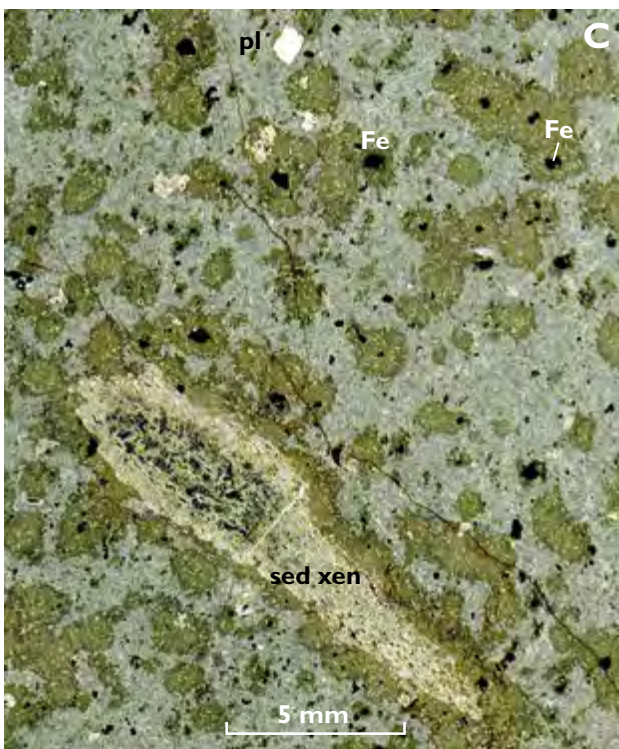
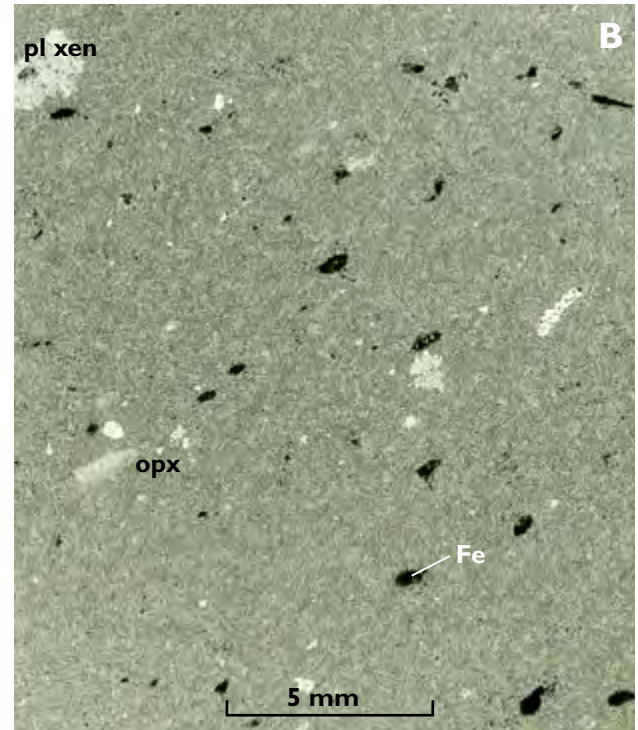
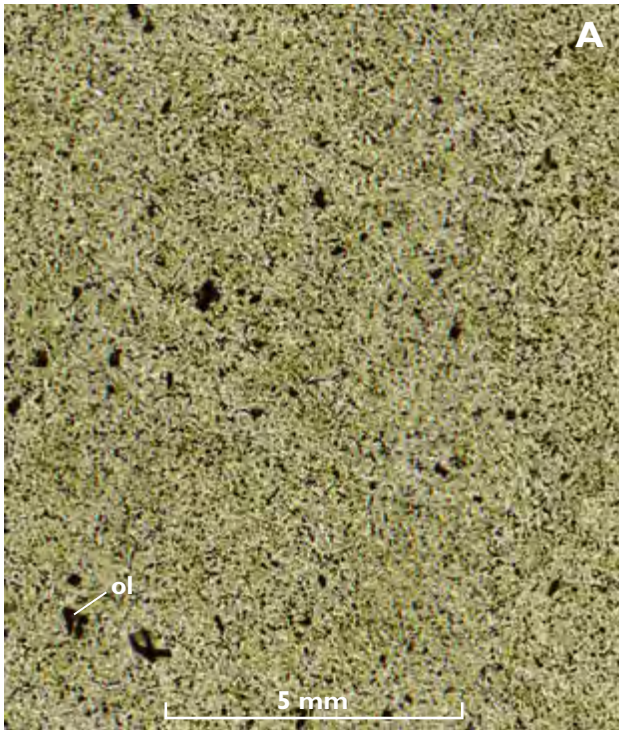
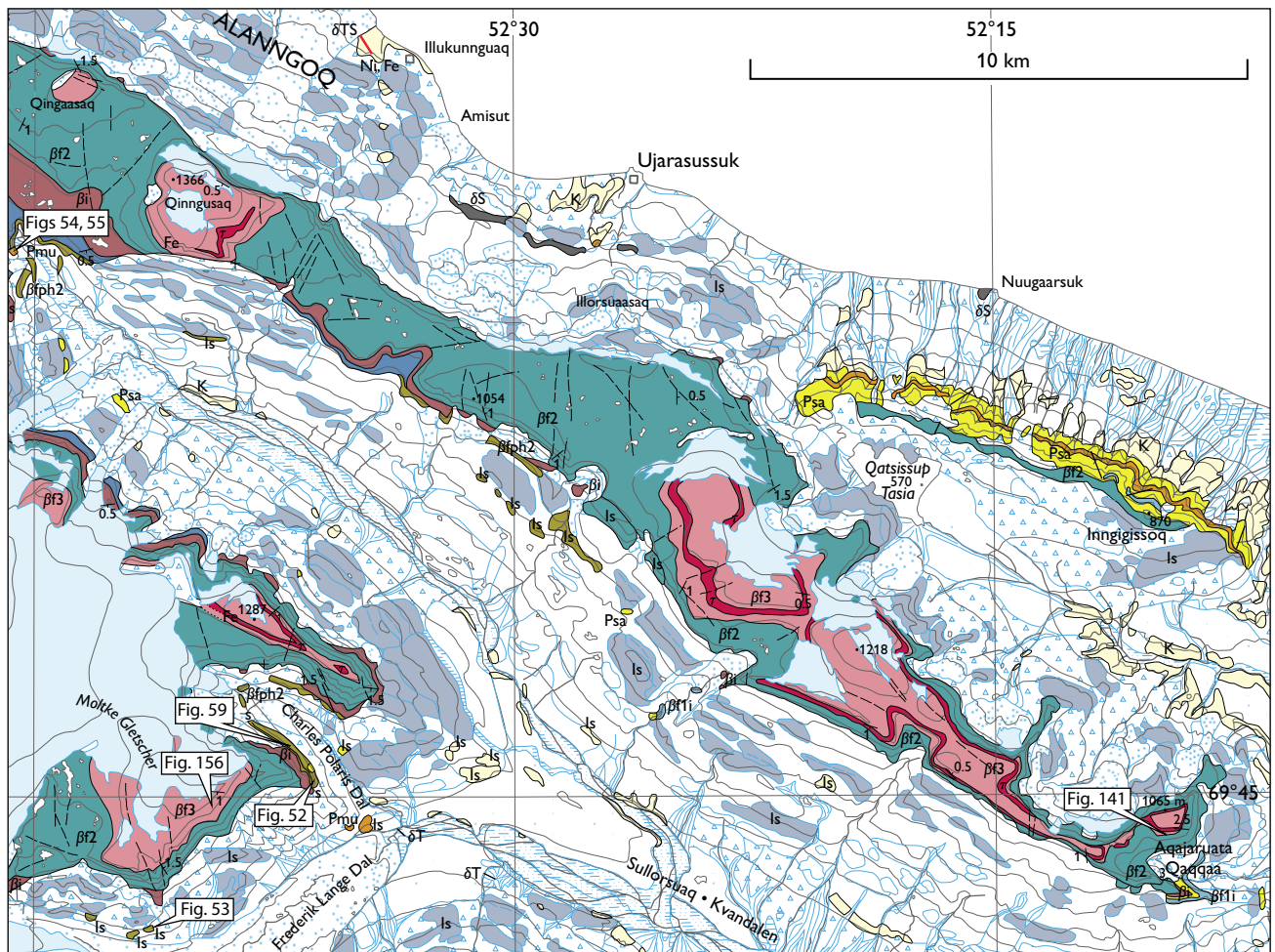


Fig. 138. Thin sections (scanned) of the composite Mellemfjord lava flow. **A:** Basal part of the flow: very fine-grained silicic basalt with scattered olivine (**ol**) that is mostly altered. No native iron is present. Sample 176565, Saqqarliit Ilorliit, north coast of Mellemfjord, western Disko. **B:** Upper zone: very fine-grained magnesian andesite with native iron (**Fe**), orthopyroxene (**opx**) and a plagioclase xenocryst (**pl xen**). Sample 176564, Saqqarliit Ilorliit, north coast of Mellemfjord, western Disko. **C:** Upper zone: magnesian andesite with native iron (**Fe**), a plagioclase microphenocryst (**pl**) and a large reacted sediment xenolith (**sed xen**). The fine-grained groundmass has a globular texture resembling a product of liquid immiscibility. Sample 447260, Jernpynten, western Disko.



Fig. 139. Nordfjord Member lava flow with cognate gabbroic plagioclase-olivine-clinopyroxene nodules and a magma-modified sediment xenolith (**sed**) that is *c.* 8 cm long. Two large olivine grains are indicated (**ol**). North coast of Mellemfjord just east of Ikorfarsuit (same locality as Fig. 136).
Photo: Finn Ulff-Møller.



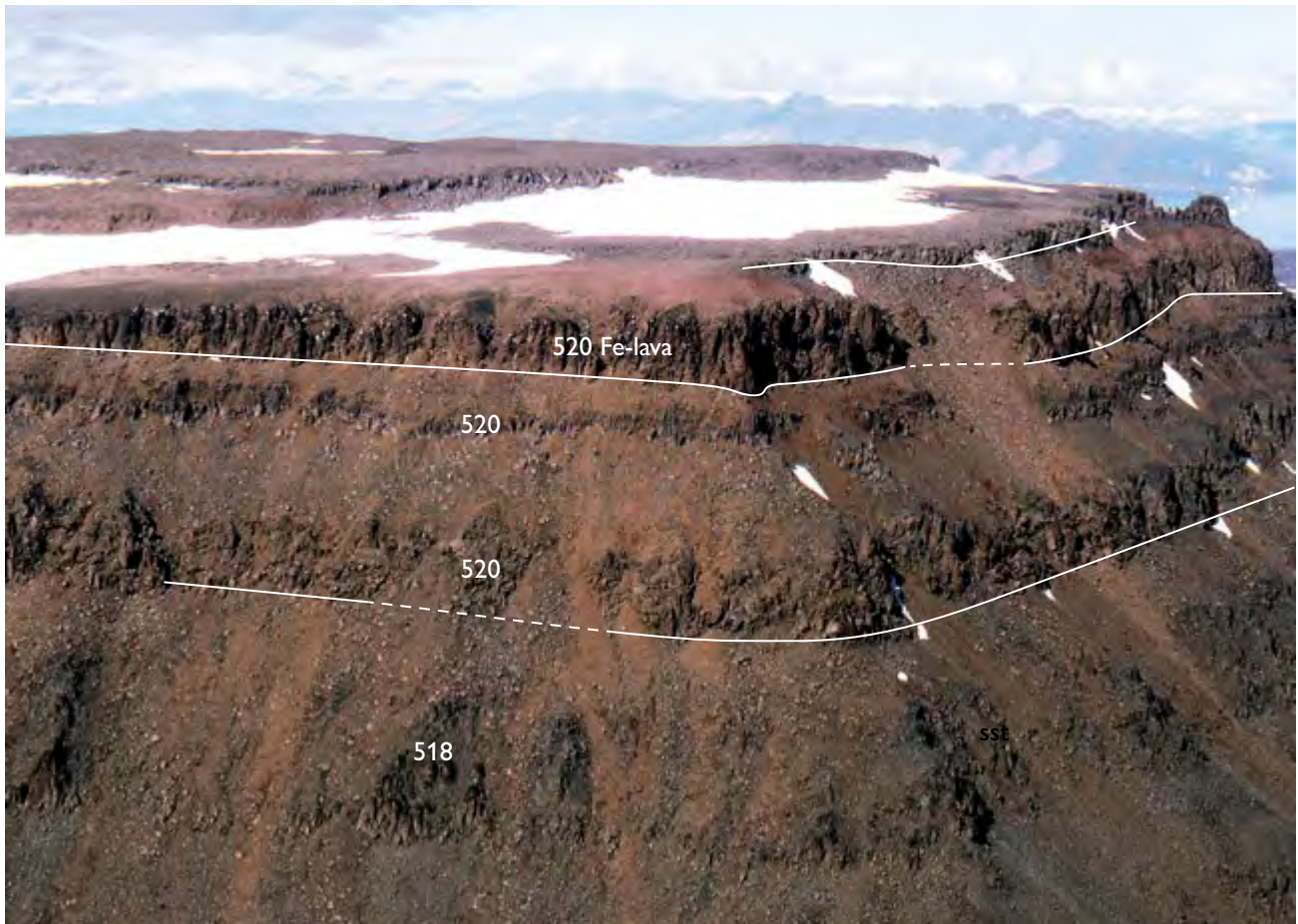


Fig. 141. The lava succession at the top of Aqajaruata Qaqqaa, eastern Disko (Fig. 7, profile 13). The Nordfjord Member (520) rests on flows of Rinks Dal Member unit 518. **Fe-lava**: the composite, c. 25 m thick, native-iron-bearing basaltic andesite flow shown in dark red in Fig. 140. For location, see Fig. 140.

the upper part of the flow, which has a light rusty brown weathering colour. The flow contains scattered xenoliths of magma-modified mudstone. The flow extends for more than 23 km in a general NW–SE to W–E direction and probably originally covered at least 100 km². The erupted volume was probably in excess of 1 km³. The apparent elongation of the flow suggests emplacement from

a NW–SE-trending feeder dyke, which has not been located.

Crater site lithologies

Basaltic fissure eruption site on north-eastern Disko. Features indicative of an eruption site are seen in the second lava flow of the Nordfjord Member in the excellently exposed vertical coastal cliff below Point 1530 m (Fig. 4). The flow is usually 15–20 m thick, but over a distance of c. 700 m its thickness increases to up to 35 m and it has a very thick scoriaceous top zone in which there are irregular lava tongues (Fig. 142). The feature is interpreted as a longitudinal section through an eruption fissure. The fissure runs SE–NW, parallel to the cliff face and parallel to the inferred eruption sites for the contaminated magmas (dyke system C in Fig. 174).

Facing page:

Fig. 140. Excerpt from the 1:100 000 scale geological map sheet 69 V.2 Nord Pingu, showing the extent of the native-iron-bearing lava flow (dark red) of the Nordfjord Member on eastern Disko. Other Nordfjord and Niaqussat Member lavas are pink. The Rinks Dal Member (RDM) flows are green (upper RDM), brown (middle RDM), and blue and olive-green (lower RDM). Sediments are yellow and orange. Light bluish grey areas are landslipped. The locations of some figures are indicated. Annotations as on map.

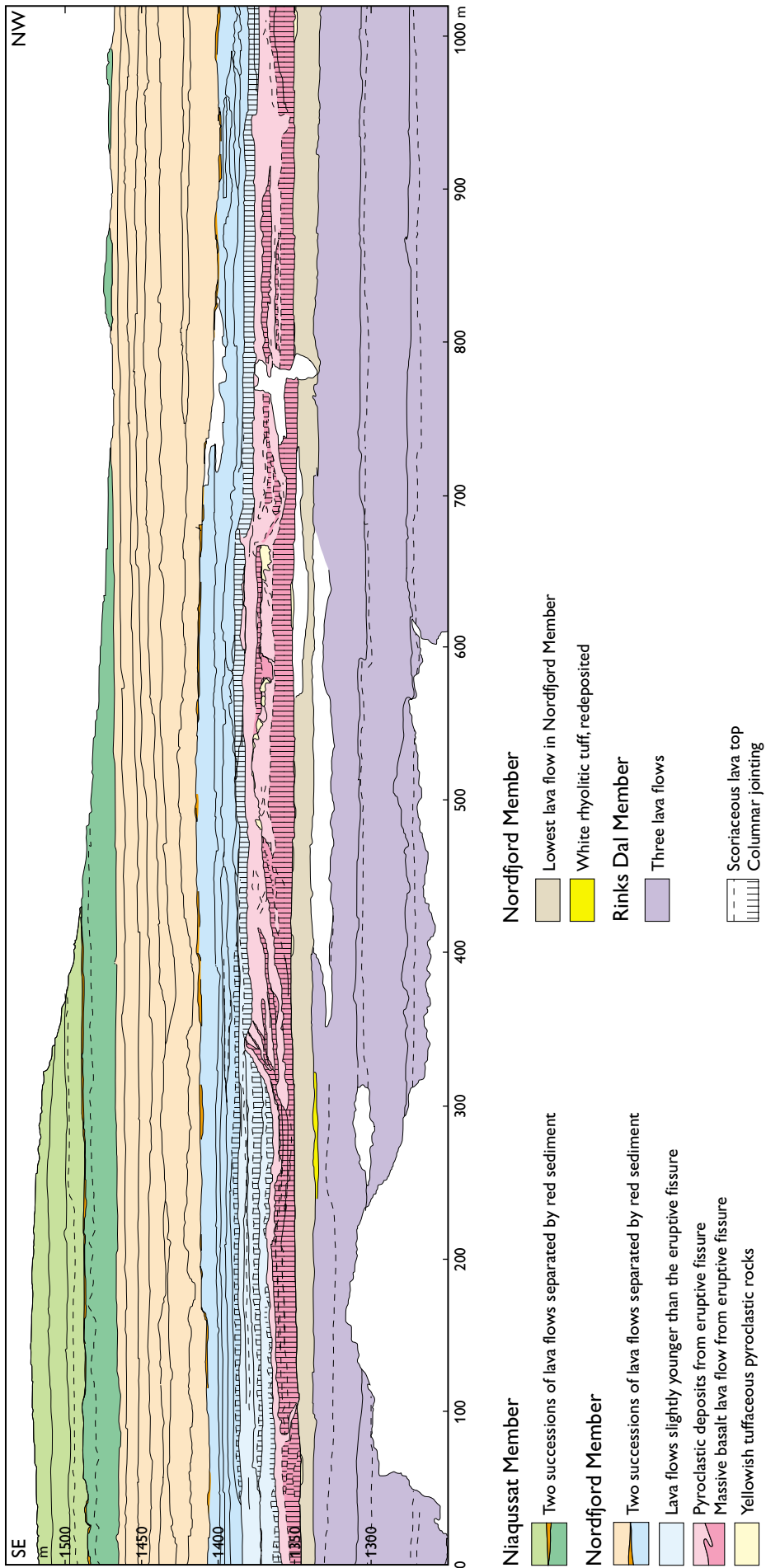


Fig. 142. Longitudinal section through a basaltic fissure eruption site in the Nordford Member. The fissure runs SE-NW, parallel to the cliff face. Photogrammetrically measured section along the coastal cliff below Point 1530 m, north-eastern Disko. For location, see Figs 4, 6.

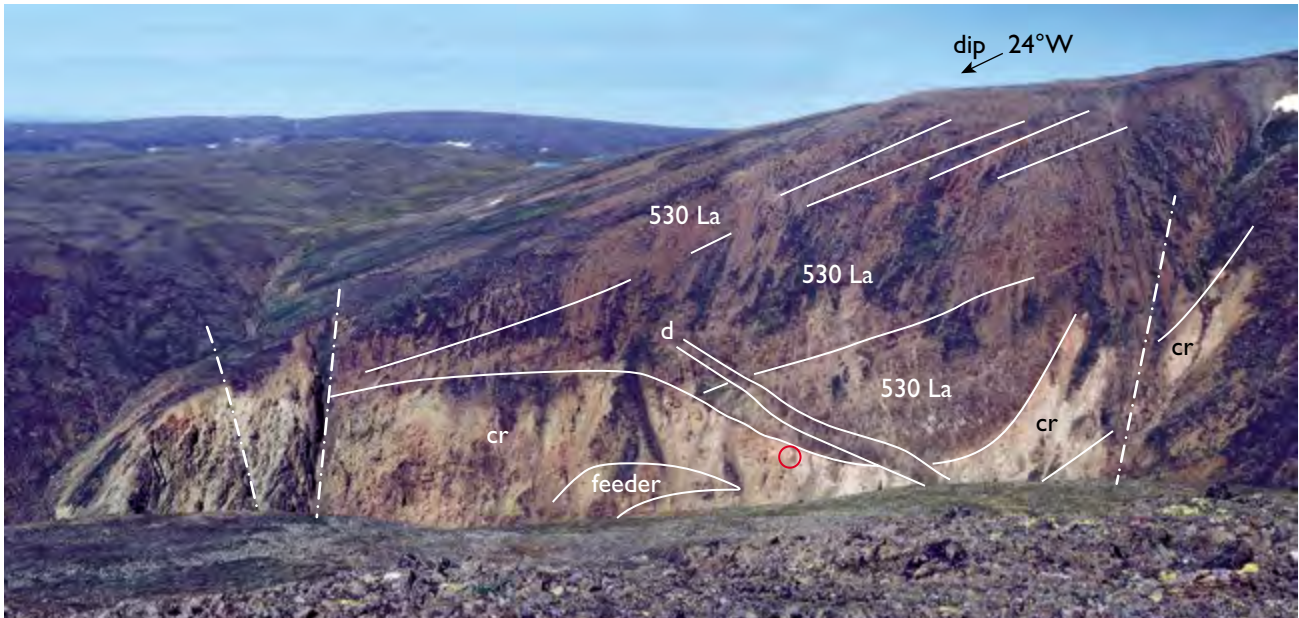


Fig. 143. Exposed section through the Point 440 crater north of Hammer Dal, north-western Disko. The light rock (**cr**) is a native-iron-graphite dacite crater breccia with a feeder body; the dark rocks comprise later infill of lava flows of the Niaquussat Member (530 La). The succession dips 24°W and is cut by a later dyke (**d**). The red circle indicates the position of Fig. 144. See text for detailed descriptions. For locality, see Fig. 103, loc. 7.

Craters and lava flows around Point 440 m near Hammer Dal. The top lava in the Point 600 m profile north of Hammer Dal is a more than 45 m thick, native-iron-bearing dacite with disseminated graphite (Figs 104C, 132) which was formerly assigned to the Niaquussat Member (Pedersen 1977a, fig. 7), but which is here reassigned to the Nordfjord Member (Fig. 14, profile 9). The lava was erupted from a crater site *c.* 1.7 km west-north-west of Point 600 m exposed in a gully close to Point 440 m and described as the Point 440 crater by Pedersen (1977a, p. 11–13, fig. 9). The locality shows preserved parts of a more than 250 m wide crater with a height of at least 110 m which is easily distinguished by rocks with a yellowish-grey colour speckled with red (Fig. 143; see also the photogrammetric interpretation in Fig. 104B). The crater is composed of a mushroom-shaped central feeder body of massive, native-iron-bearing dacite surrounded by vesiculated and fragmented, oxidised dacite forming a crater breccia rich in dark grey, graphite-bearing magma-modified mudstone xenoliths (Fig. 144). The crater deposit is covered by a thin layer of lateritic claystone. The crater was subsequently overflowed and gradually covered by more than six basaltic lava flows of the Niaquussat Member. These flows are olivine-microphyric pahoehoe lavas; the lowermost flow is 45 m thick and formed a local lava lake when it filled part of the crater. The succession was later tilted to dip 24°W.



Fig. 144. The volcanic breccia in the Point 440 crater (see Fig. 143). The breccia is composed of vesiculated and fragmented, oxidised dacite that is rich in dark grey, graphite-bearing, magma-modified mudstone xenoliths. Length of hammer 47 cm.

The site illustrates how an area rich in local craters was re-shaped into a lava plateau after the onset of the regional basaltic volcanism of the Niaqussat Member.

Craters and lava flows between Hanekammen, Hammer Dal and Giesecke Dal. The upper part of the Nordfjord Member (from the top of the dacites described above) in an area extending from Hanekammen and Hammer Dal to Giesecke Dal, north-western Disko, is dominated by basaltic to andesitic lavas and craters described by Pedersen (1977a, figs 1 and 2). The western part of the area has been extensively faulted, subsequently eroded into a Tertiary planation surface that now has a westerly dip (Bonow *et al.* 2006), cut by large incised valleys, and eroded again by the Holocene sea. It is now mostly covered either by Quarternary deposits or by extensive low-lying marine deposits. Despite the generally poor exposure, excellent sections are exposed in the north wall of Hammer Dal around Point 600 m (Fig. 14, profile 9; Fig. 104C), in two E–W-trending gullies north of Hammer Dal (Fig. 14, profiles 10, 11; Fig. 104A, B), and in the mountain walls around Point 500 m south of Niaqussat (Fig. 14, profile 12). The area contains scattered craters and volcanic necks, and many more must exist undetected beneath the Quaternary cover. Some of the craters and necks are connected to feeder dykes such as the Hammer Dal complex (Ulf-Møller 1977) and the Hanekammen complex (Ulf-Møller 1990). Some of the lavas and craters were probably fed by dyke system A described below. The basalts and andesites of the upper part of the Nordfjord Member are extensively sediment-contaminated and were clearly fed from high-level magma reservoirs; many lavas and crater breccias are packed with magma-modified mudstones and sandstones as well as cognate igneous inclusions (autoliths). However, the volcanism at the individual sites was short-lived, and except for the elusive West Disko Graphite Rhyolite volcano there is no evidence of large central volcanoes that sustained long-lived activity.

Tunup Qaqqaa, south-western Disko. The mountaintops in the area around Tunup Qaqqaa north of the inner part of Kangerluk are capped by lavas of the Nordfjord and Niaqussat members (Pedersen & Ulf-Møller 1987; South Disko section at 35.5–42 km). A feeder crater site is exposed in the mountain wall facing Kangerluk (Fig. 87). The crater was part of the feeder system for a *c.* 40 m thick basaltic andesite lava erupted at the base of the Nordfjord Member (Fig. 8, profile 1, sample 175077). The lava flow probably covered more than 20 km² with a

volume of around 0.5–1 km³; it is likely to be composite, but present knowledge is incomplete.

Chemical compositions of the Nordfjord Member

The Nordfjord Member comprises an almost continuous compositional suite from basalt over basaltic andesite, andesite and dacite to rhyolite. It should, however, be noted that these rocks are distinctly different from orogenic rocks with the same names. In particular, the Nordfjord Member rocks have much higher contents of MgO, Ni, and Cr than their orogenic namesakes.

Table 6 shows representative chemical analyses of the Nordfjord Member rocks, and all analyses are plotted in the variation diagrams in Figs 145–147. In contrast to the variation diagrams for the Rinks Dal Member, MgO was chosen as the main variation parameter because the Nordfjord Member rocks show strongly divergent trends in FeO* that invalidate the *mg*-number as a common variation parameter.

Major elements

The Nordfjord Member rocks are subalkaline, with total alkalis for basalts and basaltic andesites less than 3.5 wt% except for the above mentioned single alkali basalt flow which has 4 wt% total alkalis. Many basalts are quartz normative. Of the analysed samples four andesites, three dacites, and all the rhyolites are corundum normative. The alkali basalt samples are either slightly nepheline or slightly hypersthene normative, demonstrating its mildly alkaline character.

The Nordfjord Member basalts overlap compositionally with the Rinks Dal Member basalts but with a displacement towards slightly higher SiO₂ and lower CaO, TiO₂ and Na₂O contents (Fig. 145). The Nordfjord Member basalts have on average 49.8 wt% SiO₂, 31% of the analyses have SiO₂ > 50 wt%, and 76% are quartz normative. In comparison, the Rinks Dal Member basalts have on average 49.2 wt% SiO₂, 6% of the analyses have SiO₂ > 50 wt%, and 35% are quartz normative. FeO* contents are similar to those in the Rinks Dal Member.

The single alkali basalt flow (four analysed samples) is particularly discernible by its high Na₂O. It has correspondingly low CaO and low SiO₂, and high TiO₂, K₂O and P₂O₅.

Basaltic andesites and andesites span a larger range in MgO than the basalts and form trends parallel to the basalts at higher SiO₂ and K₂O and lower FeO*, CaO,

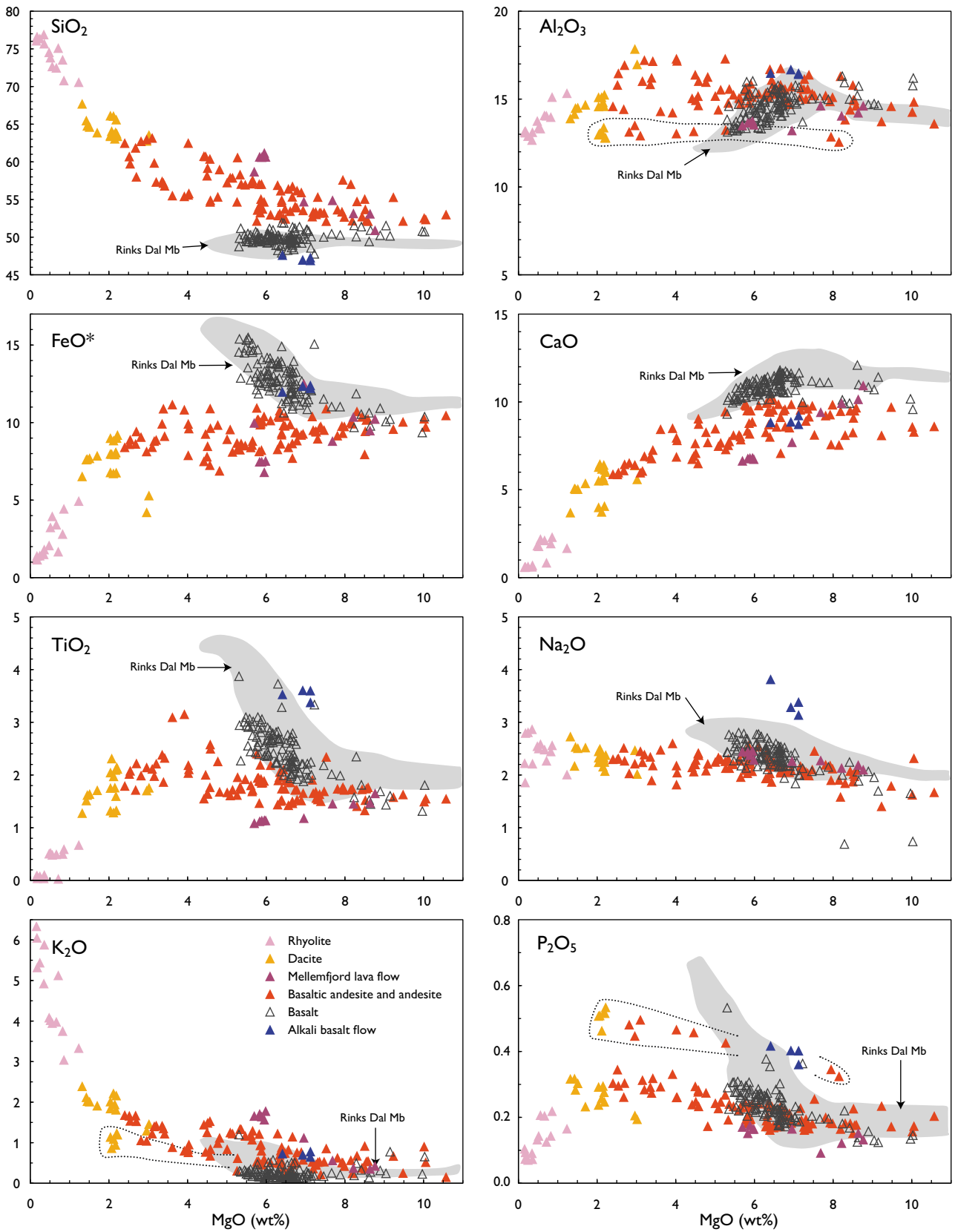


Fig. 145. Major-element variation diagrams for rocks of the Nordfjord Member. Data in wt% oxides recalculated volatile-free. FeO* is total iron as FeO. Dotted outlines in the Al₂O₃, P₂O₅ and K₂O diagrams show the fields of the low-Al₂O₃, high-P₂O₅ andesites and dacites.

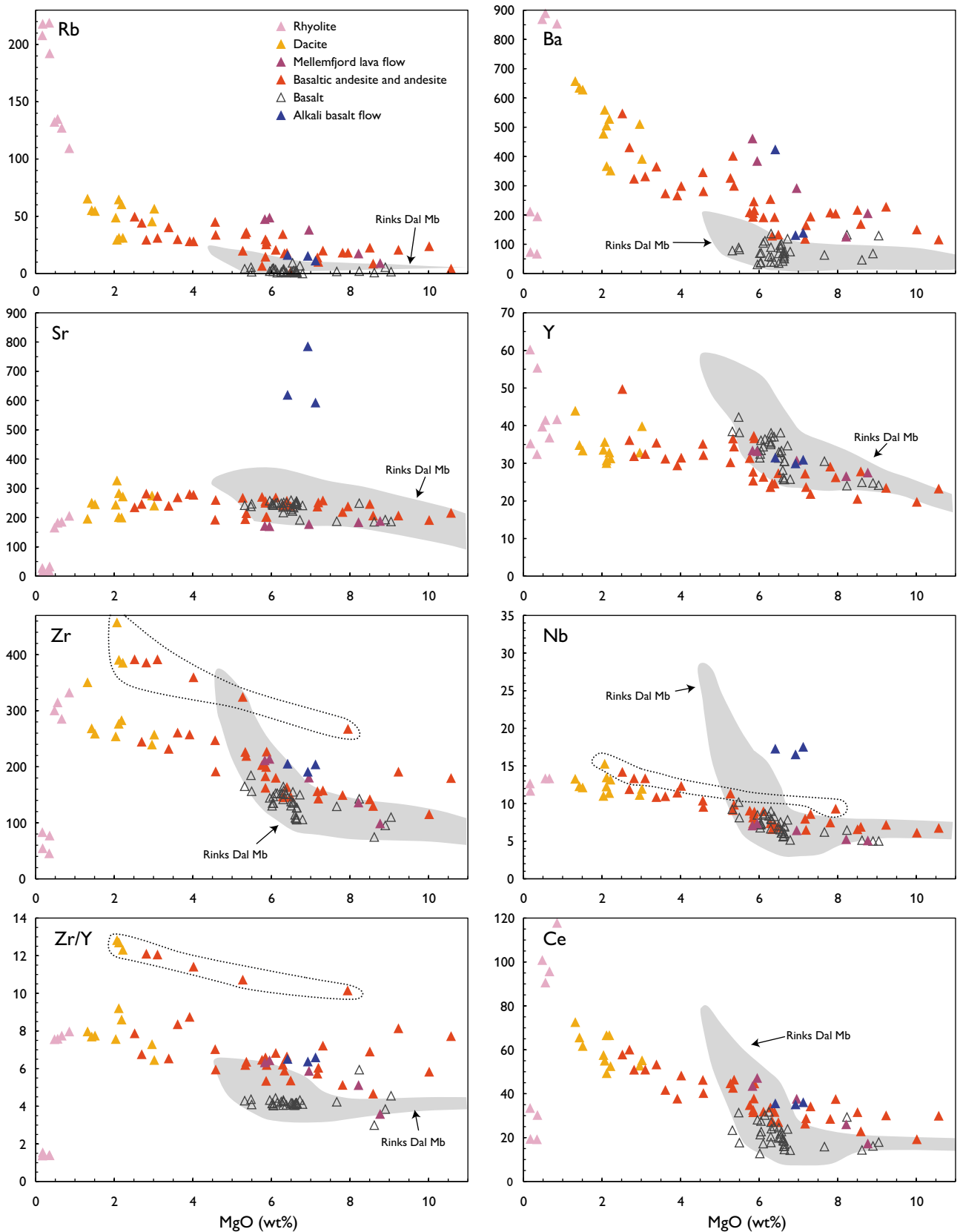


Fig. 146. Incompatible trace element variation diagrams for rocks of the Nordfjord Member. Data in ppm. Dotted outlines in some diagrams show the fields of the low-Al₂O₃, high-P₂O₅ andesites and dacites.

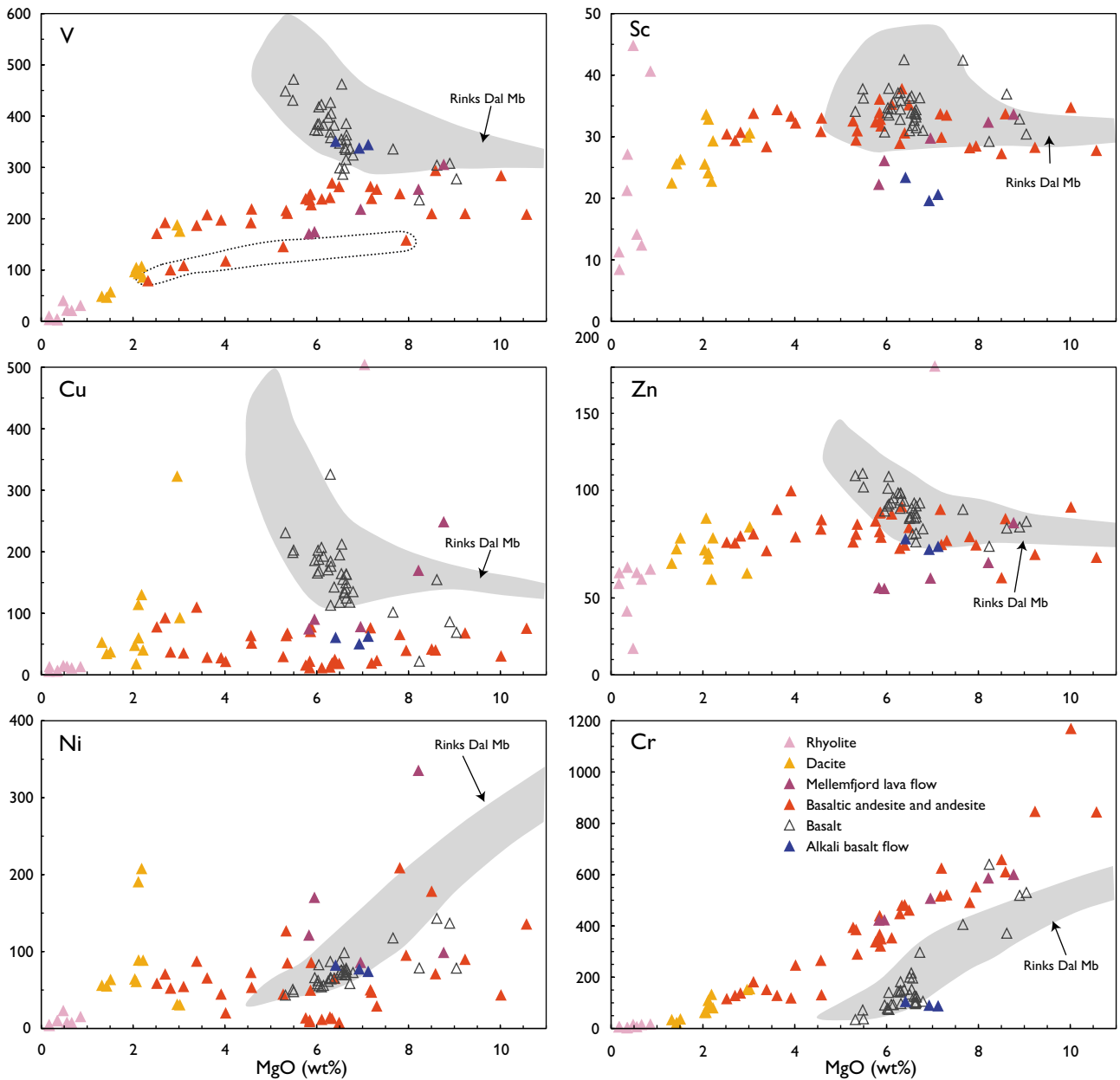


Fig. 147. Transition-element variation diagrams for rocks of the Nordfjord Member. Data in ppm. Dotted outline in the V diagram shows the field of the low- Al_2O_3 , high- P_2O_5 andesites and dacites.

TiO_2 and Na_2O . In contrast to the basalts, FeO^* is constant or decreases with decreasing MgO .

The dacites continue the trend from the andesites towards higher SiO_2 and K_2O and lower FeO^* and CaO and show no increase in TiO_2 and Na_2O .

A subgroup of andesites and dacites form separate trends, which are contoured in some of the diagrams in Fig. 145. These rocks have particularly high P_2O_5 and also high SiO_2 , low Al_2O_3 , and low K_2O . They represent

a group of related lava flows in a limited area of about 25 km^2 around Nordfjord and southwards to Mellemfjord. These flows are regarded as predominantly sandstone-contaminated, as discussed later.

The rhyolites contain 70–77 wt% SiO_2 and 0.2–1.2 wt% MgO and are the most evolved rocks on Disko. They comprise two compositional subgroups (best seen in the K_2O , TiO_2 and CaO diagrams, Fig. 145), a low-silica group (garnet rhyolites) with lower SiO_2 and K_2O

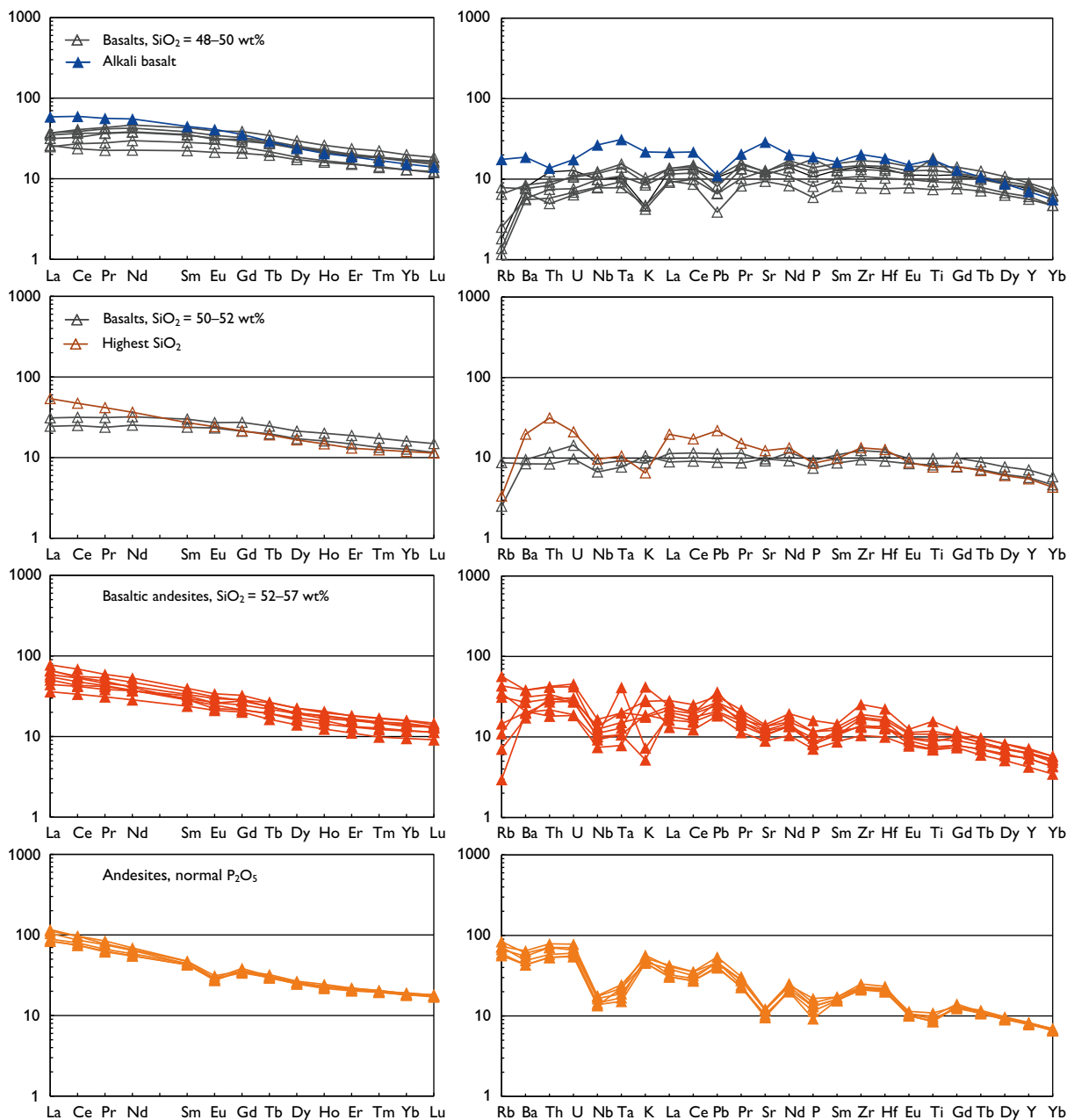


Fig. 148 (*first of two parts*). REE and multi-element diagrams for representative rocks of the Nordfjord Member. Dacites with 'normal P_2O_5 ' comprise high-Ni, high-Al and iron-ilmenite dacites. Left diagram, chondrite normalised; right diagram, primitive mantle normalised; normalisation factors from McDonough & Sun (1995).

and higher Al_2O_3 , CaO , FeO^* , TiO_2 and P_2O_5 than the other, high-silica group (sanidine rhyolites). The rocks contain 0.9–1.2 wt% FeO and the glasses have very low $MgO/(MgO+FeO)$ ratios of 0.04–0.08, indicative of a reduced state.

The most unusual feature of the strongly contaminated volcanic rocks of the Nordfjord Member is the presence of native iron (iron-carbon alloys), sulfur and

carbon in many of these rocks; analytical data for these elements are given in Table 7. The highest content of native iron analysed is 2.4 wt% Fe^0 in an andesite, and the highest TOC is 3.1 wt% in a rhyolite (apart from a sediment xenolith with 11.72 wt% TOC). The rhyolites do not contain native iron but are rich in graphite. Sulfur in rhyolite is generally low and has disappeared by degassing of the flow during eruption.

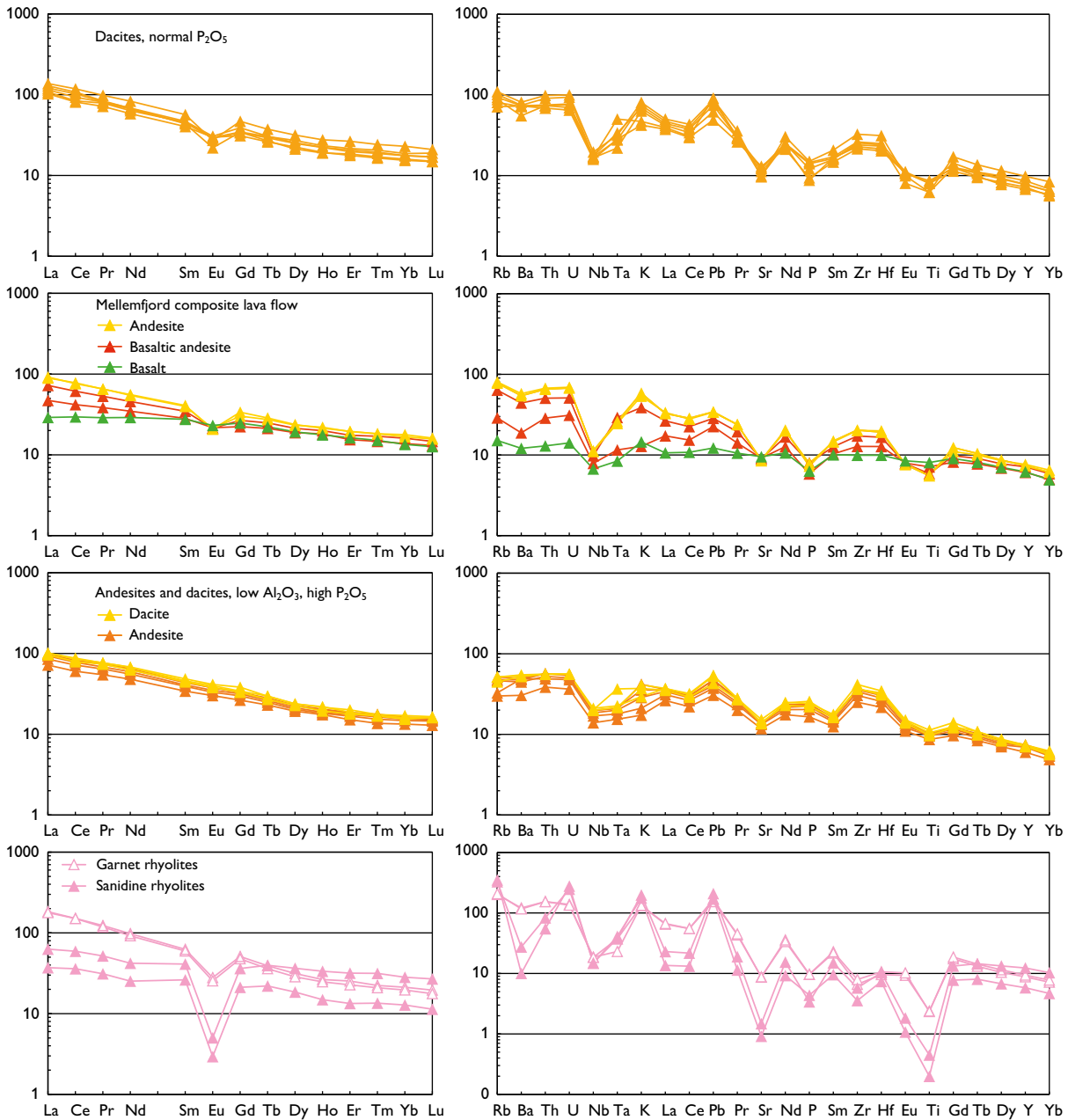


Fig. 148 (*second of two parts*). REE and multi-element diagrams for representative rocks of the Nordfjord Member. Dacites with ‘normal P_2O_5 ’ comprise high-Ni, high-Al and iron-ilmenite dacites. Left diagram, chondrite normalised; right diagram, primitive mantle normalised; normalisation factors from McDonough & Sun (1995).

Trace elements

Variation diagrams for trace elements are shown in Figs 146, 147. The basalts have trace-element contents within the same range as the Rinks Dal Member basalts although high values of Sr, Y, Zr, Nb, and Cu are not attained. The more silicic rocks have higher Rb, Ba, Ce and Cr, and lower V and Cu. Apparent trends for Sr, Y, Zr, Nb, Sc and Zn pass through the level of the basalts but do not in-

crease, or even decrease, with decreasing MgO. Ni shows rather erratic variations, which are tied to the presence or absence of native iron or sulfides in some flows.

The high- P_2O_5 andesites and dacites have high Zr, Nb and Zr/Y and distinctly low V without having low TiO_2 .

The high-silica sanidine rhyolites have higher Rb, lower Sr and V, and particularly much lower Ba, Zr and Ce than the low-silica garnet rhyolites.

The alkali basalt has high contents of incompatible trace elements, particularly Sr and Nb, and low Sc and Cu.

REE and multi-element diagrams are shown in Fig. 148. The REE patterns of the basalts are fairly similar to those of the basalts of the Rinks Dal Member except for slightly increased La–Nd limbs in five out of nine samples; these do not possess the humpback-shaped characteristic of the Rinks Dal Member. The basaltic andesites have significantly increased La–Nd and almost straight REE patterns; a few have negative Eu anomalies. The andesites and dacites have REE patterns parallel displaced towards higher values than the basaltic andesites, and, apart from the high- P_2O_5 group, have distinct negative Eu anomalies. The high- P_2O_5 group has REE patterns without Eu anomalies and lower HREE than the other rocks. The low-silica garnet rhyolites have very high REE patterns nearly parallel to those of the low- P_2O_5 dacites, whereas the high-silica sanidine rhyolites have very different patterns with decreased LREE and very deep Eu anomalies.

The multi-element patterns show that many of the basalts have slightly increased Ba–Th–U relative to the Rinks Dal Member. Basalts with <50 wt% SiO_2 have diminished K and Pb troughs, whereas basalts with >50 wt% SiO_2 have variable K and no Pb troughs. A high- TiO_2 basalt (328463, Table 6) has distinct peaks at Ti and P while other incompatible elements are not increased; there are four analyses (probably representing three flows, all on western Disko) of this basalt type (Fig. 145) which seems to have acquired its high Ti and P by other means than normal fractionation. The basaltic andesites have further increased Rb–Ba–Th–U limbs, Nb–Ta troughs, K and Pb peaks and small Zr–Hf peaks. The normal- P_2O_5 andesites and dacites have deepened Nb–Ta troughs because the elements on both sides are increased more than Nb and Ta; they also have distinct K and Pb peaks and relative troughs at Sr, P, Eu and Ti. The high- P_2O_5 andesites and dacites have lower contents of many incompatible elements but higher P and Zr–Hf–Eu than the corresponding low- P_2O_5 rocks. The garnet rhyolites have the highest contents of incompatible elements; a deep Ti trough indicates Ti-oxide fractionation. The sanidine rhyolites appear to have fractionated feldspar (very low Ba, Sr, Eu), apatite, Ti-oxide, zircon, and monazite. Monazite, which is identified petrographically, has removed Th (but not U) and light to middle REE.

Composite lava flows

The Nordfjord Member contains a number of composite lava flows as described above and in Pedersen (1977b). The chemical analyses (Fig. 149) show that the variation within the composite flows mainly occurs in the basaltic andesite compositional interval (52–57 wt% SiO_2). The basal parts of the flows are generally more MgO-rich and SiO_2 -poor than their main parts, with a few exceptions where the opposite is the case. Other elements behave variably and may decrease from base to main part in some flows and increase in others (e.g. TiO_2 and CaO), testifying that the variation is not caused by ordinary crystal fractionation processes. The incompatible elements normally increase from the base to the main part of a flow (Na_2O , P_2O_5 and many trace elements). Most of the compatible trace elements, including V, decrease from base to main part, but Ni increases.

The composite Mellemfjord lava flow has a compositional range of 50.9–61.1 wt% SiO_2 , 8.8–5.7 wt% MgO, 10.9–6.6 wt% CaO, 0.36–1.78 wt% K_2O , and 12.5–6.8 wt% FeO^* . The least contaminated basalt sample has 10.2 wt% FeO^* ; a single sample with higher FeO^* than this value (12.5 wt% FeO^*) has accumulated native iron.

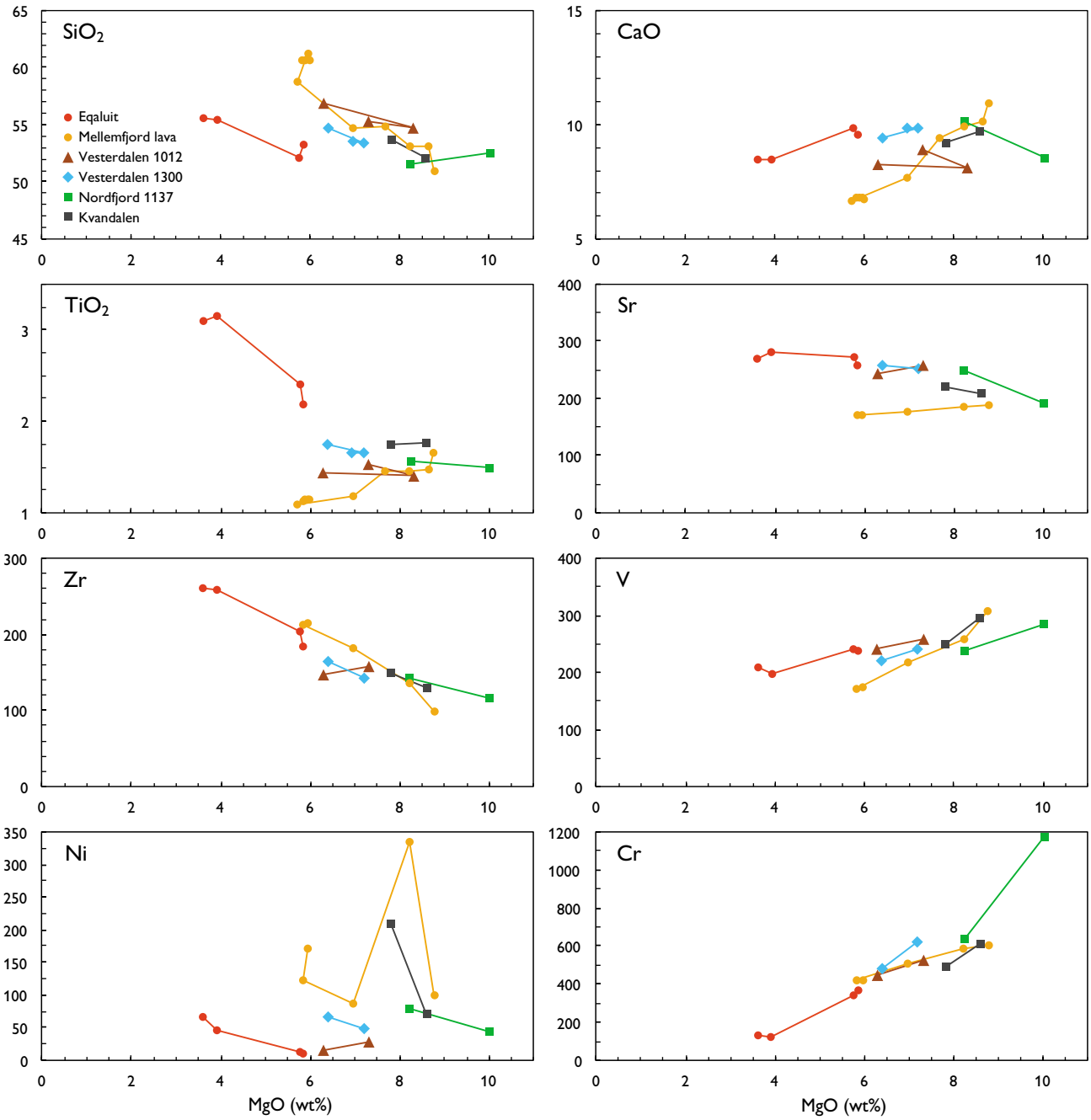


Fig. 149. Variation diagrams for composite lava flows of the Nordfjord Member.

Table 6a. Chemical analyses of rocks of the Nordfjord Member

Lithology	Basalt										Basaltic andesite		
	Alkali basalt	5201	5201	5201	5201	5201	5201	5201	5201	5201	5201	5201	5201
Lith. code	5201	5201	5201	5201	5201	5201	5201	5201	5201	5201	5201	5201	5201
GGU No.	156678	327011	332882	279298	326647	362398	279465	328463	318768	279297	263934	318809	
Deg. W	5440.66	5322.36	5221.55	5431.57	5438.32	5240.68	5433.37	5359.31	5151.96	5431.57	5439.11	5210.29	
Deg. N	7002.622	6917.510	7028.983	6955.205	7015.636	6950.968	7000.524	6923.916	7006.107	6955.189	6954.400	6944.761	
Altitude, m	406	921	1679	951	377	1267	1092	818	1238	931	761	1036	
SiO ₂	45.82	49.06	48.18	50.77	49.57	48.87	48.91	47.04	49.12	48.80	54.22	53.04	
TiO ₂	3.49	1.65	1.49	1.55	1.98	2.23	2.60	3.64	2.90	1.39	1.55	1.72	
Al ₂ O ₃	15.91	14.35	14.82	16.06	14.79	15.20	13.40	13.42	12.94	13.25	13.46	15.03	
Fe ₂ O ₃	4.27	6.38	3.85	1.49	3.25	2.98	4.23	6.49	4.60	6.67	2.25	1.04	
FeO	8.00	4.93	6.90	8.20	7.91	8.43	9.70	7.77	11.03	3.52	7.37	8.12	
MnO	0.17	0.18	0.17	0.16	0.17	0.17	0.22	0.20	0.23	0.14	0.15	0.17	
MgO	6.90	8.69	8.40	8.11	7.53	6.36	6.20	6.14	5.24	9.30	9.05	7.72	
CaO	8.46	10.59	11.79	9.96	10.91	11.23	10.43	10.43	9.95	7.97	7.94	9.12	
Na ₂ O	3.28	2.02	2.01	1.97	2.05	2.30	2.46	2.43	2.39	1.51	1.38	2.17	
K ₂ O	0.630	0.307	0.136	0.189	0.250	0.133	0.260	0.244	0.300	0.842	0.660	0.622	
P ₂ O ₅	0.390	0.154	0.122	0.178	0.192	0.220	0.254	0.368	0.286	0.146	0.230	0.198	
Volatiles	1.92	1.70	1.48	1.85	2.02	1.06	1.51	1.53	1.05	5.32	1.17	0.88	
Sum	99.24	100.01	99.35	100.49	100.62	99.18	100.17	99.69	100.04	98.86	99.43	99.83	
FeO*	11.84	10.67	10.36	9.54	10.83	11.11	13.51	13.61	15.17	9.52	9.39	9.06	
mg number	54.10	62.22	62.11	63.23	58.43	53.66	48.15	47.71	41.13	66.39	66.08	63.29	
Zn	92.0	93.1	77.3	82.3	94.1	96.2	116	106	128	80.1	76.8	86.2	
Cu	56.2	107	154	21.8	111	131	173	318	255	26.5	66.9	71.3	
Ni	76.6	136	142	77.4	116	73.7	63.4	84.8	47.0	39.0	88.2	165	
Sc	21.0	32.0	38.4	28.8	38.9	36.4	35.3	32.0	36.2	29.4	27.7	32.1	
V	311	282	317	233	319	334	398	360	432	265	206	261	
Cr	94.1	562	407	630	411	233	95.4	139	26.5	1198	830	552	
Ga	18.4	19.3	18.3	20.5	19.8	21.9	23.2	23.9	24.2	18.1	19.2	21.4	
Rb	10.5	5.26	0.83	2.02	1.51	1.09	3.89	1.51	4.71	21.0	20.4	19.3	
Sr	574	195	186	246	183	224	248	230	243	177	203	226	
Y	30.2	24.6	24.1	23.7	30.6	32.5	36.4	34.1	38.4	18.2	23.0	29.0	
Zr	213	99.9	81.1	141	130	150	155	138	178	110	188	161	
Nb	17.5	4.41	5.12	6.37	5.56	6.48	7.72	6.48	8.12	4.88	7.03	7.09	
Cs	0.137	0.087	0.004	0.065	0.007	0.022	0.050	0.116	0.072	0.543	0.788	0.477	
Ba	124	56.0	44.9	130	63.0	52.2	55.7	37.8	50.1	137	224	181	
La	13.9	5.79	6.13	12.8	7.36	8.27	8.85	7.48	8.73	8.53	13.2	13.5	
Ce	36.5	15.3	14.4	28.9	19.4	22.4	23.6	19.9	24.9	20.5	29.5	32.1	
Pr	5.21	2.20	2.08	3.86	2.91	3.43	3.86	3.38	4.02	2.89	4.05	4.28	
Nd	25.2	11.5	10.3	16.7	14.6	17.5	19.4	17.2	21.2	13.0	17.3	19.4	
Sm	6.61	3.52	3.29	4.01	4.44	5.24	5.66	5.14	6.36	3.53	4.29	4.97	
Eu	2.31	1.31	1.20	1.36	1.53	1.74	1.95	1.79	2.21	1.19	1.42	1.51	
Gd	7.06	4.22	4.12	4.28	5.44	6.15	6.43	5.83	7.67	4.00	4.39	5.78	
Tb	1.05	0.713	0.705	0.690	0.885	1.01	1.06	0.984	1.243	0.590	0.727	0.882	
Dy	5.89	4.22	4.24	4.07	5.24	6.01	6.27	5.82	7.27	3.44	4.10	5.17	
Ho	1.13	0.877	0.874	0.807	1.094	1.20	1.23	1.17	1.42	0.676	0.880	1.06	
Er	3.01	2.36	2.41	2.09	3.00	3.10	3.22	3.04	3.77	1.77	2.16	2.79	
Tm	0.416	0.330	0.351	0.308	0.428	0.453	0.459	0.449	0.548	0.244	0.313	0.382	
Yb	2.45	2.05	2.07	1.91	2.58	2.73	2.79	2.66	3.19	1.53	2.00	2.48	
Lu	0.343	0.285	0.302	0.280	0.367	0.393	0.410	0.371	0.454	0.224	0.284	0.347	
Hf	5.14	2.59	2.15	3.60	3.35	3.80	4.06	3.62	4.61	2.82	4.57	4.01	
Ta	1.15	0.285	0.289	0.391	0.344	0.386	0.518	0.405	0.569	0.290	0.470	0.679	
Pb	1.66	1.32	0.583	3.28	1.69	1.58	1.22	1.00	1.63	2.74	3.37	3.17	
Th	1.09	0.669	0.394	2.50	0.930	0.977	0.731	0.592	0.665	1.44	2.45	2.51	
U	0.355	0.198	0.129	0.429	0.292	0.260	0.214	0.155	0.223	0.375	0.645	0.641	
<i>Isotope ratios calculated at 60 Ma</i>													
⁸⁷ Sr/ ⁸⁶ Sr ₆₀	0.703419		0.703303							0.707465		0.708146	
εSr	-16.06		-17.70							41.37		51.04	
¹⁴³ Nd/ ¹⁴⁴ Nd ₆₀	0.512964		0.512883							0.512286		0.512222	
εNd	7.87		6.28							-5.36		-6.62	
²⁰⁶ Pb/ ²⁰⁴ Pb ₆₀	17.910		18.430							16.936		16.978	
²⁰⁷ Pb/ ²⁰⁴ Pb ₆₀	15.388		15.482							15.045		15.079	
²⁰⁸ Pb/ ²⁰⁴ Pb ₆₀	37.677		38.172							37.225		37.219	

For explanation of lithological codes, see Table 1. For petrographical notes on the samples, see Table 6d–e.

Geographical coordinates in WGS 84. First two digits are degrees, then follow minutes in decimal form.

Major elements in wt% (XRF analyses). Trace elements in ppm (Zn–Ga: XRF analyses; Rb–U: ICP-MS analyses).

FeO* = total iron as FeO. mg number = 100 × atomic Mg/(Mg+Fe²⁺), with the iron oxidation ratio adjusted to Fe₂O₃/FeO = 0.15.

Table 6b. Chemical analyses of rocks of the Nordfjord Member

Lithology	Basaltic andesite			Mellemfjord composite lava flow			Eqaluit composite flow		Andesite			
	5201	5201	5201	5201	5201	5201	5201	5201	5201	5201	5201	5201
Lith. code	5201	5201	5201	5201	5201	5201	5201	5201	5201	5201	5201	5201
GGU No.	264087	176626	274430	176565	176556	176564	176579	176582	176448	176473	113463	176411
Deg. W	5432.80	5452.49	5441.97	5447.61	5432.14	5447.61	5444.68	5444.68	5439.89	5441.43	5438.72	5438.76
Deg. N	6949.408	6944.605	7010.578	6947.511	6944.859	6947.511	6938.688	6938.688	7009.282	7012.046	7015.447	7015.246
Altitude, m	802	128	309	456	821	459	245	241	500	360	410	368
SiO ₂	56.11	52.55	56.19	49.90	54.60	59.93	52.93	54.87	57.40	58.71	56.93	59.80
TiO ₂	1.42	2.17	1.71	1.62	1.18	1.11	2.18	3.06	1.75	1.72	1.86	1.99
Al ₂ O ₃	15.14	15.17	15.34	14.33	13.19	13.49	15.11	14.14	14.55	14.75	16.14	15.57
Fe ₂ O ₃	2.69	1.84	1.06	2.02	4.13	0.62	2.02	1.33	0.95	2.54	0.00	0.00
FeO	5.74	8.40	7.57	8.21	8.76	6.83	8.15	9.84	7.27	4.77	10.85	8.48
MnO	0.12	0.19	0.15	0.20	0.16	0.15	0.17	0.17	0.15	0.12	0.13	0.14
MgO	6.20	6.06	5.28	8.59	6.94	5.76	5.81	3.57	5.25	4.44	3.37	2.48
CaO	8.16	9.72	7.64	10.72	7.69	6.70	9.50	8.35	7.42	6.32	6.75	5.79
Na ₂ O	1.91	2.52	2.10	2.06	2.26	2.41	2.54	2.45	2.27	2.34	1.89	2.27
K ₂ O	1.210	0.510	1.313	0.420	1.120	1.690	0.930	0.880	1.320	1.490	1.347	1.640
P ₂ O ₅	0.170	0.240	0.237	0.130	0.165	0.150	0.230	0.290	0.190	0.270	0.273	0.340
Volatiles	0.82	0.79	1.93	1.55	0.66	1.20	1.07	1.14	1.32	1.65	0.95	1.16
Sum	99.69	100.16	100.52	99.75	100.86	100.04	100.64	100.09	99.94	99.12	100.49	99.66
FeO*	8.16	10.06	8.52	10.03	12.48	7.39	9.97	11.04	8.12	7.06	10.85	8.48
mg number	60.58	54.93	55.61	63.41	52.94	61.19	54.11	39.55	56.65	56.00	38.58	37.17
TOC wt%												0.09
S wt%					0.22			0.03	0.18	0.00		0.41
Zn	81.2	89.3	86.0	80.3	62.9	55.7	92.6	106.3	90.2	89.6	80.4	81.2
Cu	12.7	11.3	71.9	225	78.4	79.9	11.7	28.4	68.1	63.4	110	101
Ni	14.8	10.3	67.5	84.1	85.8	113	9.1	65.0	63.6	69.2	87.2	90.4
Sc	28.5	30.4	31.0	33.3	29.7	22.3	33.7	34.0	29.1	28.8	28.3	26.0
V	238	211	215	272	218	160	236	206	218	209	186	155
Cr	442	359	301	586	507	411	365	128	334	297	152	106
Ga	20.5	21.8	22.1	18.7	19.4	19.1	22.5	23.9	21.3	21.6	23.7	23.3
Rb	34.0	18.8	33.7	9.07	38.2	46.8	29.7	29.7	35.6	43.2	40.2	50.3
Sr	240	268	208	189	178	172	255	266	197	190	239	234
Y	23.3	26.6	33.6	26.6	30.7	31.6	27.6	30.9	35.0	35.2	35.3	34.7
Zr	145	185	222	104	180	214	182	258	230	238	231	262
Nb	7.29	8.19	9.08	4.42	6.44	7.39	8.09	10.8	8.84	9.51	10.8	11.5
Cs	0.499	0.408	0.895	0.123	0.847	0.742	0.875	1.03	0.932	1.03	0.993	1.28
Ba	251	178	284	79.78	291	358	193	271	285	322	364	398
La	15.7	13.9	19.8	6.88	17.2	21.2	14.3	18.8	19.9	21.1	24.8	26.5
Ce	33.3	32.6	45.7	18.1	37.6	47.8	32.5	41.2	45.7	48.9	53.1	59.1
Pr	4.51	4.24	5.85	2.68	4.93	6.05	4.57	5.89	5.72	6.17	7.01	7.19
Nd	18.6	19.2	25.2	13.3	20.9	25.5	20.3	25.0	25.1	26.7	29.3	30.1
Sm	4.25	4.93	6.30	4.08	5.13	6.05	5.08	5.95	6.32	6.57	6.49	6.95
Eu	1.25	1.67	1.57	1.30	1.20	1.17	1.66	1.91	1.55	1.54	1.62	1.64
Gd	4.27	5.65	7.01	4.92	5.32	6.71	5.17	6.10	7.20	7.10	6.72	7.66
Tb	0.693	0.847	1.056	0.804	0.898	1.033	0.885	0.989	1.096	1.113	1.073	1.111
Dy	3.95	4.85	6.10	4.74	5.24	5.84	5.09	5.77	6.34	6.39	6.06	6.33
Ho	0.782	0.968	1.24	0.965	1.09	1.17	1.05	1.14	1.26	1.24	1.18	1.25
Er	2.10	2.62	3.31	2.61	2.80	3.13	2.66	2.93	3.50	3.47	3.24	3.42
Tm	0.302	0.357	0.483	0.373	0.419	0.451	0.380	0.406	0.488	0.504	0.479	0.497
Yb	1.89	2.29	2.93	2.17	2.58	2.69	2.24	2.57	3.08	3.01	2.90	2.88
Lu	0.280	0.315	0.417	0.311	0.361	0.386	0.335	0.378	0.441	0.439	0.437	0.430
Hf	3.76	4.59	5.63	2.81	4.70	5.42	4.78	6.33	5.98	6.17	5.75	6.61
Ta	0.478	0.561	0.561	0.311	1.080	0.963	0.544	0.935	0.818	0.623	0.699	0.817
Pb	5.43	3.68	5.94	1.83	4.27	5.14	3.98	4.78	6.16	7.01	6.82	6.93
Th	3.30	2.36	4.27	1.03	4.02	5.19	2.47	3.41	4.22	4.62	5.64	5.64
U	0.855	0.621	1.10	0.286	1.04	1.37	0.673	0.901	1.13	1.22	1.33	1.43
<i>Isotope ratios calculated at 60 Ma</i>												
⁸⁷ Sr/ ⁸⁶ Sr ₆₀		0.708947		0.704900		0.709988			0.709660			0.714259
εSr		62.40		4.96		77.17			72.53			137.79
¹⁴³ Nd/ ¹⁴⁴ Nd ₆₀		0.512195		0.512595		0.511918						0.511766
εNd		-7.14		0.66		-12.54						-15.50
²⁰⁶ Pb/ ²⁰⁴ Pb ₆₀		16.892		17.072		16.763						16.907
²⁰⁷ Pb/ ²⁰⁴ Pb ₆₀		15.044		15.105		15.010						15.041
²⁰⁸ Pb/ ²⁰⁴ Pb ₆₀		37.177		37.306		37.112						37.172

Table 6c. Chemical analyses of rocks of the Nordfjord Member

Lithology	Andesite		Dacite			Dacite	Dacite	Dacite	Sanidine		Garnet	
	high-P ₂ O ₅					high-P ₂ O ₅	high-Ni	high-Al graphite	rhyolite		rhyolite	
Lith. code	5201	5201	5201	5201	5201	5201	5201	5207	5207	5207	5207	5207
GGU No.	264064	264067	176441	176466	176471	176555	176443	326550	326465	156518.1	156516	156559
Deg. W	5428.35	5428.36	5439.52	5450.27	5449.50	5432.29	5440.02	5439.65	5446.30	5446.31	5446.31	5444.46
Deg. N	6952.312	6952.302	7009.224	7011.902	7012.836	6944.730	7009.311	7010.035	7007.630	7007.633	7007.633	7004.514
Altitude, m	998	990	434	3	1	734	525	417	164	160	160	266
SiO ₂	59.67	61.62	62.87	63.86	66.20	62.86	64.07	59.15	70.05	70.24	72.49	73.35
TiO ₂	1.93	2.01	1.74	1.62	1.25	2.27	1.25	1.64	0.48	0.47	0.09	0.04
Al ₂ O ₃	13.05	12.86	14.46	14.34	13.59	12.82	14.65	15.80	13.60	12.88	12.39	12.63
Fe ₂ O ₃	1.62	1.07	1.20	0.00	2.22	1.05	0.00	0.00	0.84	1.16	0.72	0.57
FeO	6.72	6.82	6.84	7.61	4.39	6.88	6.52	4.93	2.55	2.78	0.68	0.60
MnO	0.15	0.14	0.12	0.13	0.11	0.16	0.10	0.10	0.06	0.05	0.03	0.03
MgO	5.19	3.96	2.02	1.49	1.29	2.03	2.05	2.81	0.64	0.54	0.16	0.17
CaO	7.19	6.78	5.47	4.98	3.62	6.34	3.63	5.21	2.05	2.12	0.58	0.58
Na ₂ O	2.10	2.15	2.43	2.48	2.67	2.45	2.28	1.88	2.40	2.50	1.76	2.68
K ₂ O	0.610	0.830	1.830	1.990	2.340	0.850	2.150	1.358	3.848	3.820	5.730	5.100
P ₂ O ₅	0.420	0.460	0.290	0.300	0.310	0.500	0.250	0.181	0.198	0.200	0.070	0.090
Volatiles	1.06	1.12	0.98	0.95	1.40	1.69	2.40	6.19	3.33	2.61	4.15	3.59
Sum	99.71	99.82	100.25	99.75	99.39	99.90	99.35	99.24	100.05	99.37	98.85	99.43
FeO*	8.18	7.78	7.92	7.61	6.39	7.82	6.52	4.93	3.31	3.82	1.33	1.11
mg number	56.21	50.72	34.03	28.37	29.00	34.42	38.87	53.53	28.14	22.22	19.60	23.60
TOC wt%				0.07	0.27		1.17	2.72		0.17	0.22	0.01
S wt%			0.19	0.22	0.28		0.64	0.02				
Zn	85.1	88.5	80.67	89.0	79.7	92.9	68.2	89.6	62.1	57.1	60.7	57.6
Cu	29.5	21.7	47.71	41.1	58.6	31.2	131	86.7	7.50	9.13	4.10	7.67
Ni	44.0	20.1	63.91	71.5	59.9	44.1	201	28.8	5.57	4.86	2.09	1.33
Sc	32.1	31.8	25.37	22.9	20.5	32.6	20.2	28.5	13.2	17.8	8.73	6.23
V	144	116	96.20	70.5	60.5	89.5	108	164	20.9	21.6	5.72	0.80
Cr	389	244	62.64	36.8	37.1	64.5	124	145	9.19	6.96	0.80	1.29
Ga	20.7	21.1	22.88	22.3	22.3	21.7	20.6	26.3	22.8	22.1	22.7	22.3
Rb	19.7	27.8	48.50	56.1	65.9	26.9	61.1	52.7	121	125	197	211
Sr	264	274	242.37	249	193	304	198	225	174	172	29	18
Y	29.8	31.1	33.30	33.5	42.2	31.7	29.2	37.1	37.8	40.3	53.0	25.0
Zr	320	355	252.17	275	342	436	267	240	69.3	83.4	60.5	37.4
Nb	11.2	12.2	10.92	11.5	12.9	13.9	11.3	11.1	12.3	12.1	9.82	9.73
Cs	0.537	0.688	0.793	1.06	1.11	0.635	1.41	1.49	2.86	2.94	5.69	7.12
Ba	322	295	473.81	485	536	346	491	365	798	769	181	66.2
La	20.2	22.1	27.23	28.7	32.6	24.0	30.5	25.6	42.2	43.3	14.9	8.79
Ce	44.1	47.6	57.13	62.9	72.5	53.7	66.0	51.4	92.3	92.7	36.3	22.1
Pr	5.96	6.33	7.50	7.60	9.13	7.09	7.78	7.31	10.97	11.44	4.81	2.89
Nd	25.4	27.1	30.23	31.2	38.0	31.1	31.0	29.0	42.0	44.7	19.2	11.6
Sm	5.80	6.04	6.60	6.94	8.39	7.18	6.46	6.76	8.82	9.26	6.08	3.88
Eu	1.87	1.97	1.636	1.72	1.54	2.33	1.24	1.66	1.43	1.57	0.283	0.165
Gd	5.95	6.31	6.718	7.76	9.33	7.62	6.85	6.88	9.50	10.2	7.21	4.22
Tb	0.898	0.945	1.056	1.10	1.35	1.07	0.968	1.10	1.30	1.41	1.43	0.795
Dy	4.99	5.22	6.129	6.26	7.78	5.87	5.24	6.67	7.03	7.73	8.98	4.56
Ho	0.992	1.02	1.213	1.22	1.51	1.18	1.04	1.28	1.35	1.44	1.83	0.814
Er	2.68	2.79	3.157	3.31	4.24	3.21	2.95	3.45	3.63	4.05	5.08	2.14
Tm	0.379	0.406	0.463	0.480	0.598	0.433	0.420	0.508	0.517	0.552	0.779	0.333
Yb	2.38	2.47	2.828	2.84	3.70	2.74	2.57	3.01	3.16	3.42	4.55	2.06
Lu	0.358	0.369	0.420	0.415	0.516	0.406	0.369	0.465	0.435	0.481	0.662	0.279
Hf	7.25	7.99	6.561	7.06	8.87	9.80	6.78	6.07	2.71	3.01	2.93	2.09
Ta	0.663	0.740	0.814	1.25	1.17	0.836	1.02	1.86	0.852	1.38	1.39	1.52
Pb	5.6	6.1	9.289	11.2	13.1	8.12	12.5	13.7	25.3	23.1	31.4	26.0
Th	3.9	4.2	5.833	5.97	7.84	4.42	7.20	5.87	12.2	12.2	6.61	4.36
U	0.969	1.02	1.534	1.57	2.03	1.13	1.91	1.42	2.81	2.73	5.02	5.65
<i>Isotope ratios calculated at 60 Ma</i>												
⁸⁷ Sr/ ⁸⁶ Sr ₆₀				0.714161	0.714587	0.713227			0.720139	0.720129	0.714831	
εSr				136.41	142.45	123.15			221.25	221.12	145.92	
¹⁴³ Nd/ ¹⁴⁴ Nd ₆₀				0.511715		0.511812			0.511490		0.511671	
εNd				-16.49		-14.61			-20.89		-17.37	
²⁰⁶ Pb/ ²⁰⁴ Pb ₆₀				16.706		16.813			16.484		16.778	
²⁰⁷ Pb/ ²⁰⁴ Pb ₆₀				15.002		15.017			15.005		15.023	
²⁰⁸ Pb/ ²⁰⁴ Pb ₆₀				37.051		37.091			37.238		37.171	

Table 6d. Notes on analysed samples of the Nordfjord Member

156678	Alkali basalt with scarce microphenocrystic olivine and plagioclase in a very fine-grained, flow-laminated groundmass with tiny interstitial biotite. Lowest flow in the Nordfjord Member, Illuluarsuit Qaqqaa, mouth of Nordfjord, west Disko.
327011	Well crystallised basalt with scattered microphenocrysts of olivine (pseudomorphosed) and clinopyroxene and scarce sieve-textured plagioclase xenocrysts. Lowest flow in the Nordfjord Member, top flow in the Skarvefjeld profile, south Disko.
332882	Basalt with plagioclase glomerocrysts and microphenocrysts of olivine (mostly pseudomorphosed and rarely enclosing chromite) and scarce clinopyroxene. Up to 3 mm zeolite-filled vesicles. Lava flow, Nunavik profile, central Nuussuaq.
279298	Silicic basalt with scattered microphenocrysts of olivine (pseudomorphosed) in a very fine-grained groundmass. Lava flow, Point 1137 m south of Nordfjord, west Disko.
326647	Very fine-grained aphyric basalt with up to 3 mm smectite-filled vesicles. Lava flow, Niaqussat profile, north-west Disko.
362398	Strongly porphyritic basalt with glomerocrysts and phenocrysts of plagioclase, phenocrysts of olivine (pseudomorphosed) and glomerocrysts of calcic clinopyroxene. Lava flow, Qinnugasaq profile, Kvandalen, east Disko.
279465	Basalt with olivine phenocrysts (pseudomorphosed) and scarce plagioclase-clinopyroxene glomerocrysts in a fine-grained groundmass. Lava flow, Point 1070 m profile, outer Nordfjord, west Disko.
328463	Porphyritic basalt with phenocrysts and up to 8 mm glomerocrysts of plagioclase, olivine (pseudomorphosed) and clinopyroxene in a very fine-grained groundmass. Lava flow, Uiffaq, south-west Disko.
318768	Porphyritic basalt with phenocrysts and up to 10 mm glomerocrysts of plagioclase, minor olivine (pseudomorphosed) and scarce clinopyroxene in a very fine-grained groundmass. Lava flow, Saqqaq profile, south Nuussuaq.
279297	Basaltic andesite, aphyric. Lowest flow in the Nordfjord Member, Point 1137 m south of Nordfjord, west Disko.
263934	Basaltic andesite with phenocrysts of olivine (partly pseudomorphosed), scattered microphenocrysts of orthopyroxene and clinopyroxene, and scattered plagioclase xenocrysts in a glassy groundmass. Lava flow, Point 1114 m, Vesterdalen, west Disko.
318809	Iron-bearing basaltic andesite with orthopyroxene-plagioclase glomerocrysts, phenocrysts of orthopyroxene, and microphenocrysts of orthopyroxene, clinopyroxene and plagioclase. Up to 10 mm magma-modified sediment xenoliths with plagioclase and graphite, and groundmass with traces of native iron. Centre of composite lava flow, Aqajaruata Qaqqaa profile, east Disko.
264087	Basaltic andesite transitional to andesite with scattered phenocrysts of orthopyroxene and scarce microphenocrysts of plagioclase in an extremely fine-grained groundmass. Lava flow, Point 1012 m profile, Vesterdalen, west Disko.
176626	Basaltic andesite, aphyric. Lava flow, Enok Havn, outer Mellemfjord, west Disko.
274430	Basaltic andesite transitional to andesite with phenocrysts and microphenocrysts of orthopyroxene and plagioclase, glomerocrysts of orthopyroxene and plagioclase, and small xenocrystic aggregates of plagioclase, mullite, red spinel and graphite; traces of native iron. Lava flow, 'Point 440 m northern gully' profile, north of Hammer Dal, north-west Disko.
176565	Basalt with common olivine microphenocrysts (pseudomorphosed) and scarce plagioclase phenocrysts in a fine-grained groundmass. Basal part of the Mellemfjord composite lava flow, Saqqarliit Ilorliit, Mellemfjord, west Disko.
176556	Native-iron-bearing basaltic andesite with phenocrysts of orthopyroxene and plagioclase and microphenocrysts of clinopyroxene, scattered xenocrystic aggregates of plagioclase, red spinel and graphite, and rare xenocryst rosettes of mullite. The groundmass is very fine-grained and contains up to 2 mm native iron-troilite bodies. Lower part of the Mellemfjord composite lava flow, Saqqarliit Ilorliit, Mellemfjord, west Disko.
176564	Native-iron-bearing andesite with phenocrysts of resorbed plagioclase and lamellar-twinned low-Ca clinopyroxene mantled by orthopyroxene which also occurs as microphenocrysts. There are scattered xenocrystic aggregates of plagioclase with red spinel and graphite and up to 1 mm large native iron and sulphide grains in a very fine-grained groundmass. Central part of the Mellemfjord composite lava flow, Saqqarliit Ilorliit, Mellemfjord, west Disko.
176579	Basaltic andesite with scattered small plagioclase phenocrysts in a groundmass with inhomogeneous grain size distribution and with up to 0.3 mm large ilmenite grains. Lower part of composite lava flow, Equaluit (Nordre Laksebugt), south-west Disko.
176582	Native-iron-bearing basaltic andesite with phenocrysts of plagioclase and orthopyroxene (which may be mantled by lamellar-twinned pigeonite) in a well-crystallised groundmass with rusty spots after weathered native iron. There are scarce plagioclase xenocrysts with red spinel. Upper part of composite lava flow, Equaluit (Nordre Laksebugt), south-west Disko.
176448	Andesite with native iron in a partly glassy groundmass. Microphenocrysts of plagioclase, orthopyroxene, pigeonite and olivine, and scattered xenocrystic aggregates of plagioclase and mullite. Lava flow, Point 600 m profile, north side of Hammer Dal, north-west Disko.
176473	Native-iron-bearing andesite with phenocrysts of plagioclase and orthopyroxene and microphenocrysts of orthopyroxene, pigeonite and plagioclase; scattered plagioclase xenocrysts derived from sediments. Lava flow c. 5.5 km east of Jamma, north-west Disko.
113463	Native-iron-bearing andesite (transitional to basaltic andesite) with abundant phenocrysts of plagioclase and orthopyroxene and microphenocrysts of plagioclase, orthopyroxene and pigeonite. Abundant xenocrysts and xenocryst-aggregates of plagioclase, red spinel, mullite, graphite and quartz in a very fine-grained groundmass with native iron, troilite and graphite. Lava flow 60 m thick, fed from crater, Niaqussat profile, north-west Disko.
176411	Native-iron-bearing andesite with phenocrysts of plagioclase and orthopyroxene and a large range of microphenocrysts and xenocrysts (Pedersen 1981 table 2 no. 1 shows a detailed modal analysis). There are decimetre-sized cognate inclusions of norite. Lava flow within the Niaqussat crater, Niaqussat profile, north-west Disko.
264064	Native-iron-bearing andesite with common phenocrysts of plagioclase and orthopyroxene and microphenocrysts of plagioclase, orthopyroxene and clinopyroxene and possibly olivine pseudomorphs. The groundmass contains up to 0.5 mm grains of native iron. Lava flow, Point 1300 m profile, Vesterdalen, west Disko.
264067	Native-iron-bearing andesite with an inhomogeneous groundmass with variable grain size. Scarce up to 1 mm phenocrysts of plagioclase, orthopyroxene and clinopyroxene and common prismatic microphenocrysts of orthopyroxene and clinopyroxene. Scarce xenocrysts include quartz, plagioclase and mullite. Lava flow, Point 1300 m profile, Vesterdalen, west Disko.
176441.	Native-iron-bearing dacite (transitional to andesite) with common phenocrysts of plagioclase and orthopyroxene and microphenocrysts of plagioclase, orthopyroxene and clinopyroxene. Abundant aggregates of plagioclase and quartz and aggregates of plagioclase, spinel and graphite. Xenocrysts include plagioclase, quartz, spinel, cordierite, corundum and mullite. Base of 120 m thick lava flow, Point 600 m profile, north side of Hammer Dal, north-west Disko.

Phenocryst phases as observed in thin section are mentioned in order of decreasing abundance.
 Samples of subaerial lava flows are usually taken in massive columns a few metres above the flow base.

Table 6e. Notes on analysed samples of the Nordfjord Member

176466	Native-iron-bearing dacite with common phenocrysts of plagioclase and orthopyroxene and scarce ilmenite with armalcolite and rutile formed by progressive reduction and sulphidation. The very fine-grained groundmass contains native iron and troilite. A detailed mode, which also shows the range of xenocrysts, is given by Pedersen (1981 table 2 no. 3). Lava flow, Jamma, coast of north-west Disko.
176471	The most silicic native-iron-bearing volcanic rock in the Nuussuaq Basin. Dacite with common phenocrysts of plagioclase, orthopyroxene and pigeonite; microphenocrysts of ilmenite have been transformed to aggregates of ilmenite, rutile, native iron and troilite. The very fine-grained groundmass contains native iron, troilite and graphite. The abundance of various xenocrysts and cognate microxenoliths with plagioclase, orthopyroxene and pigeonite is described in Pedersen (1981). Lava flow, Jamma, coast of north-west Disko.
176555	Native-iron-bearing dacite with scattered small phenocrysts of plagioclase and orthopyroxene and abundant microphenocrysts of tridymite and plagioclase in a fine-grained groundmass with scarce native iron. There are scattered xenocrystic aggregates of quartz and plagioclase and rare spinel. Lava flow, Saqqarliit Ilorliit, Mellemfjord, west Disko.
176443	Native-iron-bearing dacite with abundant phenocrysts of plagioclase and orthopyroxene and microphenocrysts of ilmenite and armalcolite. Abundant xenocrysts and aggregates of plagioclase, quartz, cordierite, spinel and graphite; common xenoliths of picrite with chromite, and common cognate fine-grained norites. The very fine-grained groundmass contains native iron, troilite and graphite. Lava flow fed from the Point 440 crater; Point 600 m profile, north side of Hammer Dal, north-west Disko.
326550	High-Al graphite dacite with disseminated graphite and phenocrysts of orthopyroxene and plagioclase in a fine-grained groundmass. Abundant xenocrysts of mullite, cordierite, aluminous spinel and corundum. Rounded cobble from conglomerate in Nordfjord Member from the 'Point 440 m northern gully' profile north of Hammer Dal, north-west Disko.
326465	Garnet rhyolite with graphite flakes in the groundmass. More than 20% phenocrysts of plagioclase, quartz, orthopyroxene and garnet and minor ilmenite, apatite and zircon. Abundant xenocrysts include plagioclase, quartz, sillimanite, corundum and hercynite. Large (60 cm × 40 cm) rounded lava boulder in conglomerate. Sedimentkløften, south side of Hammer Dal, north-west Disko.
156518.1	Garnet rhyolite with graphite flakes in the groundmass. About 25% phenocrysts of plagioclase, quartz, orthopyroxene, garnet and biotite and minor ilmenite, apatite and zircon. There is a range of sediment xenoliths, xenocrysts and cognate clusters of plagioclase, orthopyroxene, pigeonite and almandine-rich garnet. Rounded lava cobble in conglomerate. Sedimentkløften, south side of Hammer Dal, north-west Disko.
156516	Sanidine rhyolite, pitchstone with tiny flakes of graphite in the groundmass glass. About 5% phenocrysts of plagioclase, quartz, sanidine, biotite and very minor ilmenite, zircon, apatite, monazite and almandine-rich garnet. There are very scarce aluminous xenocrysts and highly equilibrated sediment xenoliths composed of aggregates of feldspar, hercynite, orthopyroxene, ilmenite, sillimanite and graphite. Rounded lava cobble in conglomerate. Sedimentkløften, south side of Hammer Dal, north-west Disko.
156559	Sanidine rhyolite, vesiculated glassy rock with <10% phenocrysts of plagioclase, quartz, sanidine and biotite and very minor ilmenite, graphite and garnet. Lithic clast in pumice tuff. North side of outer Rink Dal, north-west Disko.

Table 7. Chemical analyses of carbon, sulfur and metallic iron in rocks of the Nordfjord Member

Rock type	GGU No.	TOC	S	Fe ⁰	SiO ₂
Andesite flow at Niaqussat	176411*	0.09	0.41	2.4	60.71
Dacite clast N of Hammer Dal	176486	0.9	0.22	0.9	65.49
Dacite clast N of Hammer Dal	326550	2.72	0.02	n.a.	63.52
Dacite clast N of Hammer Dal	326551	2.60	0.02	n.a.	62.75
<i>Hammer Dal</i>					
Point 600 m, dacite lava flow	176442	n.a.	0.2	1.6	63.07
Point 600 m, dacite lava flow	176443*	1.17	0.64	+	66.03
Point 440 crater, dacite	176497	0.8	0.67	+	66.09
<i>Jamma</i>					
Dacite lava	176466*	0.07	0.22	0.7	64.64
Dacite lava	176471*	0.27	0.28	0.14	67.71
<i>Mellemfjord composite lava flow</i>					
Lower part, basaltic andesite	176556*	n.a.	0.22	+	54.72
Central part, andesite	176564*	n.a.	n.a.	0.26	60.67
Central part, andesite	176548	n.a.	0.26	+	61.19
<i>Sedimentkløften, Hammer Dal</i>					
Sanidine rhyolite clast in conglomerate	113515	0.20	n.a.	0	75.68
Garnet rhyolite clast in conglomerate	113508	0.53	n.a.	0	70.76
Garnet rhyolite clast in conglomerate	156518.1*	0.17	n.a.	0	72.68
Sediment xenolith in rhyolite clast	156518.2**	11.72	n.a.	0	52.47
<i>Airfall tuffs north of Hammer Dal</i>					
White rhyolitic pumice clast in tuff	326497†	0.51	0.01	0	n.a.
Dark grey rhyolitic pumice clast in tuff	326497†	3.1	0.02	0	n.a.

TOC: total organic carbon. n.a.: not analysed. +: trace amounts.

*Sample included in Table 6 (major and trace elements, some isotopes). **Sample included in Table 13 (major and trace elements, some isotopes).

†: Hand-picked pumice clasts from tuff with a mixed population of white and dark grey pumice clasts.

Total sulfur determined by combustion using a LECO CS-200 induction furnace apparatus. Total organic carbon determined similarly after elimination of carbonate-bonded carbon through several stages of prolonged treatment with hot hydrochloric acid (HCl, 2N). Analyst: J. Bojesen-Koefoed. Metallic iron determined by the HgCl₂·NH₄Cl method. Analyst M. Mouritzen.

SiO₂ is recalculated on volatile-free basis except for the carbon-rich sediment xenolith.

Niaquussat Member

Summary of the main features of the Niaquussat Member

- Original extent over all of Disko and southern and eastern Nuussuaq, with depocentre on western Disko.
- Except for a thin soil at some localities, the member directly overlies the Nordfjord Member; the lava flows covered the cratered landscape on north-west Disko and formed a new level surface.
- The onset of the member indicates renewed upflow of magnesian magmas from depth.
- The lower Niaquussat Member is dominated by picrites and magnesian basalts. There are a few magnesian basaltic andesites, some of which are native-iron-bearing. The middle and upper Niaquussat Member comprise successively more evolved silicic basalts.
- All igneous rocks are more or less crustally contaminated; sediment xenoliths are scarce but in one case occur in abundance.
- Dykes with compositions similar to weakly contaminated Niaquussat Member basalt are found over large areas of Disko and Nuussuaq, suggesting eruption over wide areas.
- On north-east Nuussuaq, basalt flows of the upper Niaquussat Member extended the volcanic plateau *c.* 10 km eastward over the elevated gneiss country and invaded sediments with tuff layers believed to correlate with the Nordfjord Member.
- The two highest preserved lava flows of the upper Niaquussat Member on north-east Nuussuaq have a high-TiO₂, slightly enriched chemical composition very similar to that of the two highest flows on west Disko, suggesting that the member on Nuussuaq is close to completely represented.

Lithostratigraphy of the Niaquussat Member

Revised member

History. The Niaquussat Member was informally established by Pedersen (1975a) on north-western Disko. The definition is formalised here and extended to cover the whole of Disko and Nuussuaq.

Name. After Niaquussat, a coastal slope on north-western Disko (Fig. 4).

Distribution. The Niaquussat Member originally extended over the whole of Disko and eastern Nuussuaq; its main present occurrence is in the downthrown, west-dipping fault blocks on western Disko. It has been removed by erosion over wide areas on central and southern Disko but is preserved on peaks and ridges on eastern and north-eastern Disko (e.g. Pedersen *et al.* 2001; South Disko section; Central Disko section). It has been eroded away on southern and central Nuussuaq but is present at high altitudes on north-eastern Nuussuaq (Larsen & Pedersen 1992; Central Nuussuaq section).

Type section. The type section is composite. For the lower and middle Niaquussat Member: **Point 440 m, northern gully**, on north-western Disko (Fig. 14, profile 11; Figs 103, 104A). The locality is an E–W-oriented gully *c.* 4 km north of the river in Hammer Dal. The Niaquussat Member overlies the Nordfjord Member and is exposed over a lateral distance of *c.* 500 m at around 300 m altitude; the succession is faulted and tilted and dips 22°W (photogrammetrically measured section in Fig. 104A). The upper Niaquussat Member is eroded away at this locality; for this part, the type section is the **Sapernuik** profile above *c.* 140 m, north of outer Kangerluk, western Disko (Fig. 14, profile 1; see also Figs 161, 171).

Reference sections. **Ikorfarsuit**, outer Mellemfjord, western Disko, above *c.* 400 m (Fig. 14, profile 3). The high peak **Pyramiden**, at above 1830 m, northern Disko (Fig. 10, profile 3). The southern shoulder of the mountain **Qinngusaq** above the innermost part of Kvandalen, above *c.* 1290 m, eastern Disko (Fig. 10, profile 8; Central Disko section at 81–83 km). The north-western wall of **Frederik Lange Dal**, at above *c.* 1150 m, eastern Disko (Fig. 10, profile 9). The southern slopes (**Nunavik**), at above *c.* 1680 m, of the mountain Point 2000 m, eastern Nuussuaq (Fig. 12, profile 13; Central Nuussuaq section at 67–68 km).

Thickness. On western Disko, the Niaquussat Member attains thicknesses of up to 500 m at Sapernuik where it is most complete; more commonly it is 200–300 m thick, dependent on the level of erosion. Thicknesses are up to 160 m on north-western Disko, up to 180 m on eastern Disko and up to 200 m on eastern Nuussuaq. The maximum number of flows preserved in one section is *c.* 30 at

Sapernuvisk, *c.* 10 at Frederik Lange Dal on eastern Disko, and at least seven on eastern Nuussuaq. The youngest flows preserved occur on eastern Nuussuaq and at Sapernuvisk on western Disko.

Lithology. The Niaqussat Member consists of subaerial lava flows. These comprise olivine-phyric picrites and olivine-plagioclase-phyric and aphyric magnesian basalts and normal basalts. Many of the more magnesian lavas show a characteristic flow folding and flow lamination (Fig. 150). A few flows are basaltic andesites, some of which carry native iron.

Subdivisions. The Niaqussat Member has been subdivided into three informal units (units 530, 531 and 532), for convenience also called the lower, middle and upper Niaqussat Member. The subdivision is based on a step-wise decrease in MgO contents up-section; the units are clearly separated in geochemistry diagrams (see also Figs 167, 168), but the middle unit is generally indistinguishable in the field.

Boundaries. The Niaqussat Member conformably overlies the Nordfjord Member. Its lower boundary is placed at the base of a succession of lithologically distinctive, flow-folded pahoehoe lavas of olivine-phyric magnesian basalt and picrite. In places, there is a small sediment horizon at the base, but in most cases the Niaqussat Member lava flows rest directly on lavas and crater deposits of the Nordfjord Member. Particularly on north-western Disko, the top of the Nordfjord Member formed a very irregular and intensely cratered volcanic landscape which was drowned by the highly fluid lava flows of the Niaqussat Member so that an even lava field was re-established. This is for example seen at the Point 440 crater site (Fig. 143). Elsewhere, the flows continued to build up the existing lava field.

The upper boundary is erosional except in a small area at Sapernuvisk on westernmost Disko, where the Niaqussat Member is conformably overlain by the lava flows of the Sapernuvisk Member.

Age. Paleocene, 61–60 Ma, magnetochron C26r, based on radiometric dating (Storey *et al.* 1998; Larsen *et al.* 2016).

Correlation. None certain.

Lower Niaqussat Member (unit 530)

Composition and petrography. The onset of the Niaqussat Member volcanism is marked by a return to olivine-phyric, relatively primitive, picritic magma compositions. Unit 530 comprises picrites with up to 15 wt% MgO and olivine-microphyric magnesian basalts with more than 7 wt% MgO (except for three samples with 6–7 wt% MgO). There are also a few more silicic flows of basaltic andesite, some of which carry native iron.

Distribution and thickness. Unit 530 constitutes the major volume of the Niaqussat Member. The thickest and largest occurrences are on western Disko between Mellemfjord and Hammer Dal (Fig. 14), where thicknesses are close to 200 m and up to 240 m. Erosional remnants are widespread on peaks and ridges in other parts of Disko and on north-eastern Nuussuaq with thicknesses up to 100 m. On Nuussuaq unit 530 has only been sampled in one profile at Nunavik where a *c.* 30 m thick succession remains (Fig. 12); from photogrammetric studies (Central Nuussuaq section), the unit appears to comprise only a few flows in this area.

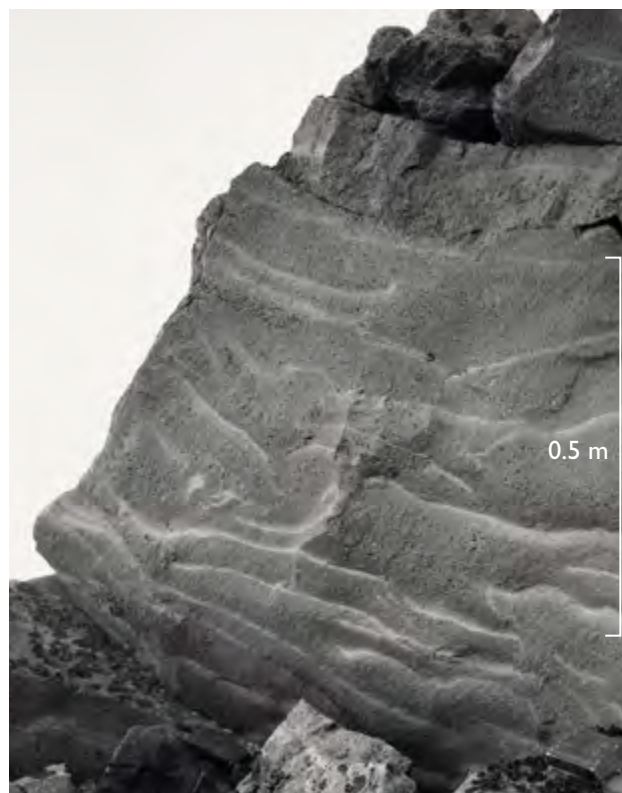


Fig. 150. Picrite lava flow of the lower Niaqussat Member showing the characteristic flow lamination and folding of this part of the member. Note compass in lower right corner.

Dykes with chemical compositions similar to the lower Niaquassat Member are known from both sides of the Vaigat strait on eastern Disko and south-eastern Nuussuaq, as well as on the south coast of Disko (Larsen & Pedersen 1992; see also Fig. 174 and Table 8). This suggests that the eruption sites were widespread.

Lithologies. The magnesian basalt to picrite flows occur as successions of pahoehoe lava flows from a few metres to more than 30 m thick. Many of the flows display a characteristic flow folding (Fig. 150) due to an inhomogeneous distribution of vesicles, which has given rise to grain-size variation throughout the flows.

Despite a universal chemical signature of crustal contamination (see below), the typical picrites and olivine-microphyric basalts of unit 530 are with few exceptions devoid of sediment xenoliths or xenocrysts. The few strongly contaminated lava flows, some of which carry native iron, contain numerous sediment xenoliths.

Western Disko

On western Disko, unit 530 forms a thick succession of many <10 m thick pahoehoe lava flows (Figs 151, 152), which seem to have built up small shield volcanoes.

Feeder dyke and lava flows on the northern wall of Rink Dal. An up to 4 m thick dyke of olivine-microphyric basalt is situated in the north-western corner of Rink Dal about 1.5 km east of the coast. The dyke strikes E–W over a distance of a few hundred metres. It is associated with a local up-doming of similar basalt and of a layer up to 5 m thick of partly welded tuff of olivine-microphyric basalt. The deposit is interpreted as having erupted from lava fountains along an eruptive fissure fed from the dyke, emitting pahoehoe lava flows and tuffs.

The northern wall of Rink Dal is strongly faulted and not well exposed (Pedersen 1975a, Plates 1, 2), but an excellent section through unit 530 is exposed about 3–4 km east of the feeder dyke (Fig. 103, loc. 16; Fig. 151). Here several strongly plagioclase-phyric basalts of the

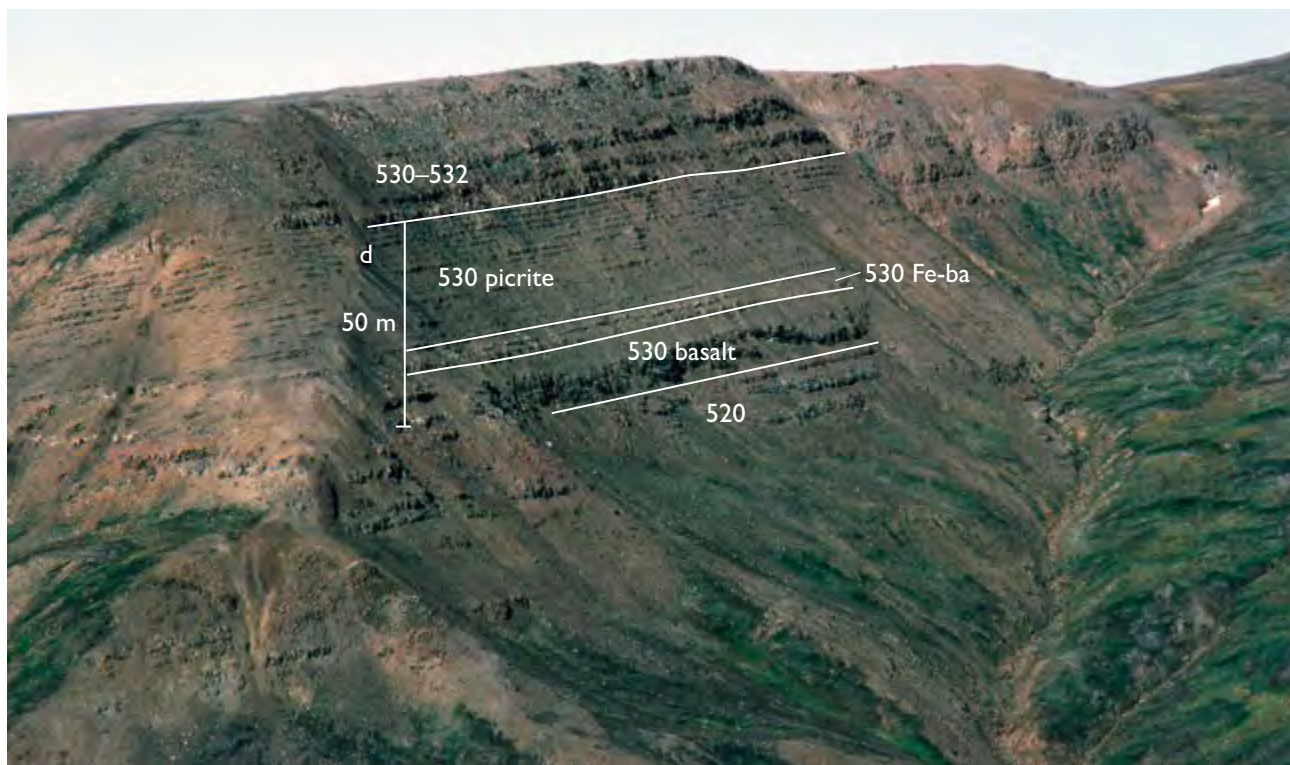


Fig. 151. Well-exposed lava succession of the Niaquassat Member. The lower Niaquassat Member (unit 530) comprises, lowest, a basaltic tuff layer (1.5 m thick, not seen in the picture), an olivine-microphyric basalt flow 15 m thick, two native-iron-bearing basaltic andesite flows (**Fe-ba**) and a characteristic succession of many thin picrite pahoehoe flows, *c.* 30 m thick. The thin picrites are overlain by thicker basalt flows of units 530–532. Unit 530 is underlain by tuffs and basalt flows of the Nordfjord Member (520). The succession is cut by a younger dyke (**d**). North side of the western Rink Dal, western Disko. For locality, see Fig. 103, loc. 16.



Fig. 152. A characteristic, thick succession of many thin picrite pahoehoe flows of unit 530 at Qasigissat, west Disko (Fig. 14, profile 6). Height of section in view 170 m.

Nordfjord Member are covered by a tuff partly altered to laterite, which defines the top of the member. The laterite is covered by an up to 1.5 m thick olivine-microphyric basaltic tuff assigned to the Niaquussat Member. The tuff has bluish black and reddish, fiamme-like tongues and is

similar in structure to the basaltic tuff overlying the feeder dyke described above. The tuff is covered by a *c.* 15 m thick, flow-folded and flow-laminated olivine-microphyric basalt with 10.4 wt% MgO; this is overlain by a >6 m thick basaltic andesite flow with 9.7 wt% MgO, with



Fig. 153. Accumulation of xenoliths at the base of a lava flow of unit 530. The close-packed xenoliths are rounded, up to 20 cm in size and consist of strongly magma-equilibrated mudstone that is now transformed into plagioclase-spinel-orthopyroxene rocks. The red arrows point to two xenoliths such as shown in Fig. 154B. Length of hammer 47 cm. Illuluarsuit Qaqqaa, westernmost Rink Dal. For locality, see Fig. 103, loc. 18. The occurrence is exposed in a small gully on the southern side of a fault block with lavas dipping 10°W.

native iron and sulfides in the basal part and abundant mudstone xenoliths up to 15 cm in size concentrated in the upper part. This flow is covered by a basaltic andesite flow several metres thick, with rusty spots and sediment xenoliths. Then follows a spectacular succession of *c.* 15 contaminated, picritic pahoehoe lava flows each a few metres thick (Fig. 151), on top of which there are several >5 m thick flows of olivine- and slightly plagioclase-phyric basalts. The monotonous succession of thin picrite flows suggests proximity to a feeder system in the western part of Rink Dal, which produced small lava shields.

Similar distinct successions of very thin, olivine-rich pahoehoe flows of unit 530 also occur along the west coast of Disko for 25 km farther south from Rink Dal to Qasigissat (Fig. 14, profiles 6, 7; Fig. 152), whereas fewer and thicker olivine-microphyric basalt flows are encountered farther south and east of the coast (Fig. 14, profiles 3–5).

Xenolith accumulation in olivine-microphyric basalt lava in Rink Dal. An exception to the general lack of sediment xenoliths is found in western Rink Dal (Fig. 103, loc. 18), where a thick accumulation of xenoliths occurs at the base of a lava flow (Fig. 153). At this locality, a strongly plagioclase-phyric basalt flow covered by a laterised, 30 cm thick tuff marks the top of the Nordfjord Member. This is overlain by an olivine-microphyric basalt tuff *c.* 0.8 m thick, with fiamme structure very similar to the basal Niaqussat Member tuff 4 km to the north-west described above. The tuff is covered by an olivine-microphyric basalt flow 9–17 m thick (Fig. 154A) with very prominent flow lamination and flow folding structures (Fig. 150). The lowermost part of this flow is an up to 2.5 m thick deposit of rounded, up to 20 cm large xenoliths of strongly magma-equilibrated mudstones transformed into plagioclase-spinel-orthopy-

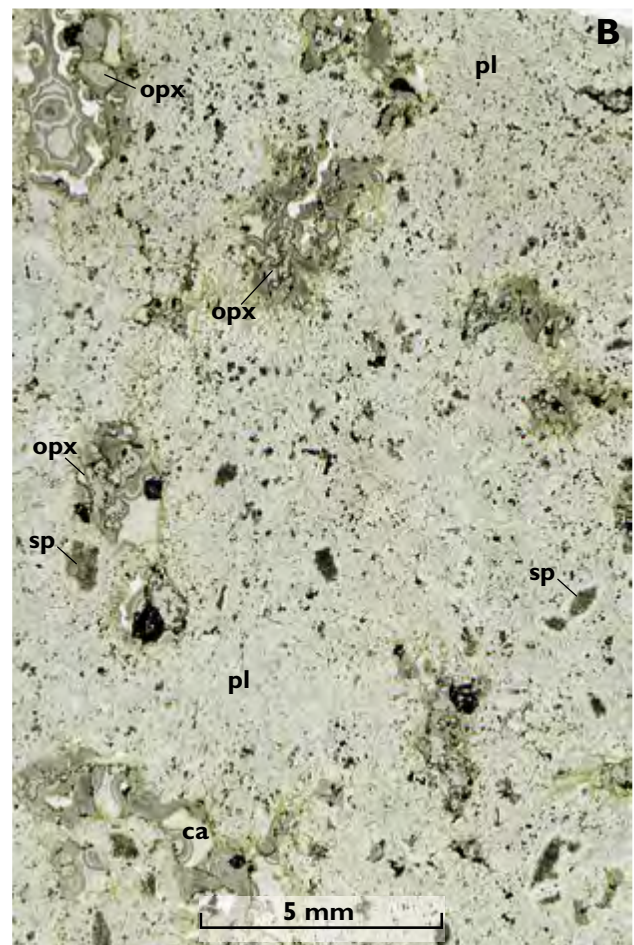
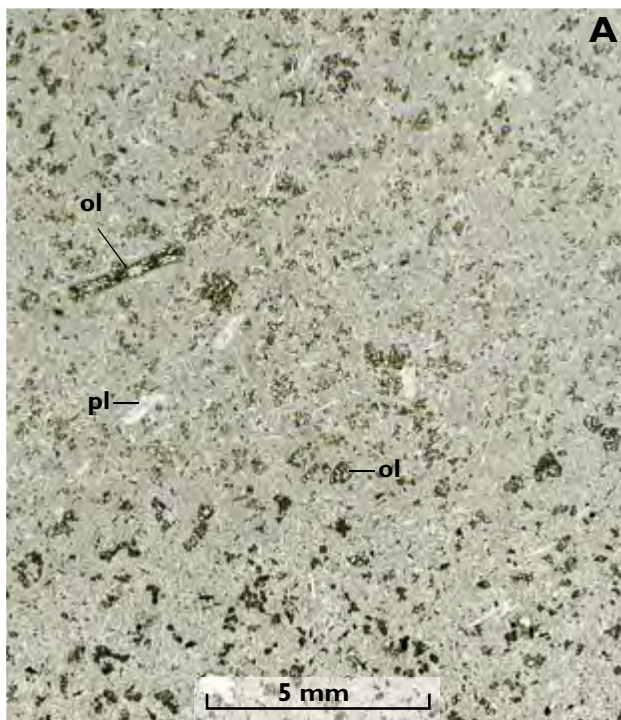


Fig. 154. Thin sections (scanned) of an olivine microphyric basalt flow packed with mudstone xenoliths. **A:** Flow-laminated basalt with microphenocrysts of olivine (**ol**) and plagioclase (**pl**) in a groundmass with zones of variable grain size. **B:** Pyrometamorphosed mudstone xenolith now consisting of an aggregate of plagioclase (**pl**, predominant), spinel (**sp**) and orthopyroxene (**opx**). Vesicles are filled with calcite (**ca**). See text for details. Sample 156677, Rink Dal, western Disko.

roxene rocks rich in plagioclase (Fig. 154B). The xenoliths are packed in a matrix of vesiculated basalt, and the deposit can be followed for 300 m along the base of the flow. On the northern part of the same fault block the lava flow is exposed again *c.* 1 km to the north of the xenolith-rich site, but here without visible xenoliths. The occurrence links the lavas of unit 530 to high-level magma reservoirs within sediments, and the huge accumulation of sediment xenoliths must indicate close proximity to another eruption site in the lowermost part of the Niaquassat Member.

Eastern Disko

Olivine-microphyric basaltic to picritic pahoehoe lava flows of unit 530 cap many plateaus and mountaintops on eastern Disko (Pedersen & Larsen 1987). This is well exemplified by Point 1123 m on the southern side of Kvandalen (Fig. 7, profile 12; Fig. 155; also Larsen & Pedersen 1988, fig. 4). Here, two basaltic lava flows of the Nordfjord Member are covered by a lateritic soil layer a few decimetres thick and overlain by three olivine-microphyric magnesian basalt lavas of unit 530. Some of the lava flows of the Niaquassat Member were erupted locally,

as attested by the occurrence of basaltic dykes of similar composition in the area (Larsen & Pedersen 1992, table 1, no. 8, sample 318824 with 12.64 wt% MgO from Akunneq).

Unit 530 is 90 m thick at Frederik Lange Dal (Fig. 10, profile 9) and *c.* 150 m thick at Point 1530 m north-west of Kvandalen (Fig. 10, profile 6). The lower part of unit 530 is dominated by olivine-microphyric to almost aphyric magnesian basalts, which are macroscopically almost devoid of sediment xenoliths or xenocrysts and carry neither native iron nor sulfides. However, at a level 40–55 m above the base of the member in Frederik Lange Dal and 25–30 m above the base at Qinnngusaq mountain, lava flows, which are clearly contaminated, occur in both profiles. This part of the profile at Point 1530 m (Fig. 10, profile 6) remains unsampled.

Compound lava flow with sediment xenoliths and sulfides in Frederik Lange Dal. About 40 m above the base of the Niaquassat Member in Frederik Lange Dal (Fig. 10, profile 9), a compound lava flow consisting of at least four flow lobes overlies a thin horizon of lateritic soil which in turn overlies three lava flows of olivine-microphyric



Fig. 155. The top of Point 1123 m on the south side of Kvandalen, eastern Disko (Fig. 7, profile 12). The lowest, thick lava flow belongs to unit 517 of the Rinks Dal Member. This is followed by two thinner flows of the Nordfjord Member (unit 520); these are covered by a few decimetres thick, brick-red lateritic soil layer and overlain by three olivine microphyric basalt flows of the lower Niaquassat Member (unit 530). The shown succession is 130 m thick.

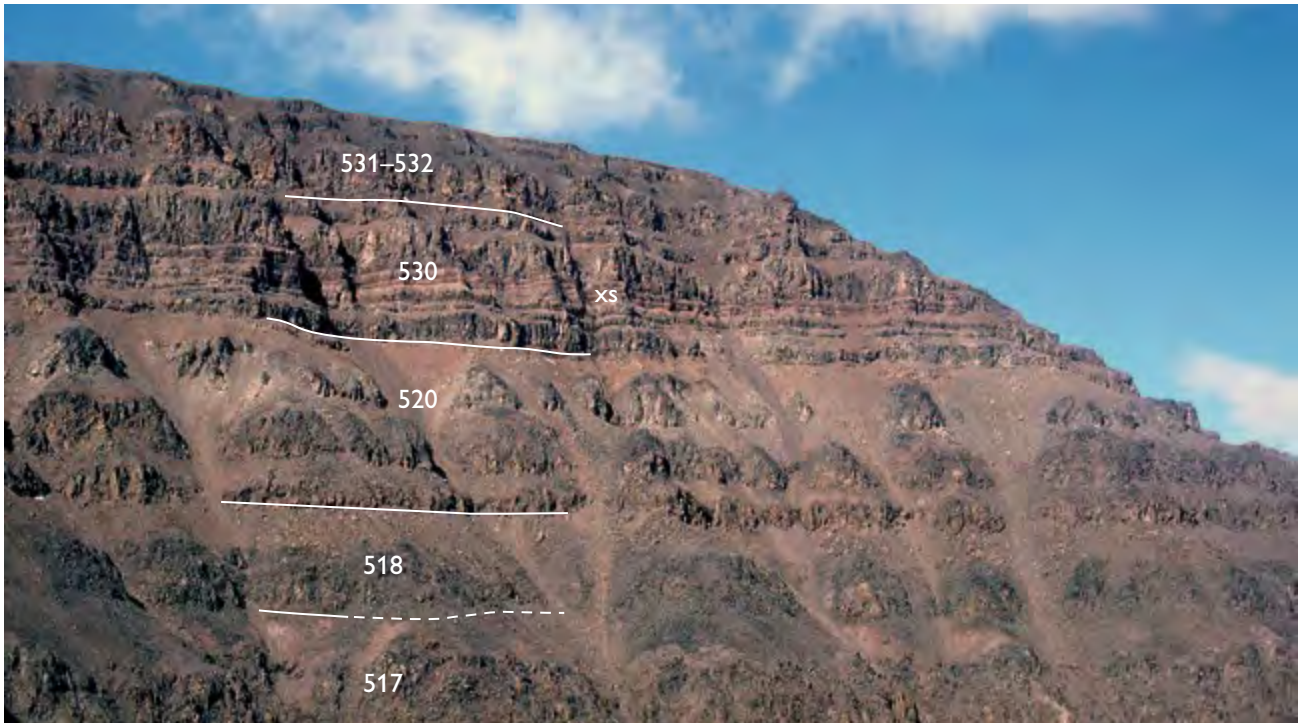


Fig. 156. Part of the sampled profile in Frederik Lange Dal, eastern Disko (Fig. 10, profile 9). Unit numbers are indicated. The compound flow of unit 530 with sediment xenoliths and sulfides is labelled *xs*. The shown succession is 350 m thick; there is a strong perspective shortening uphill, compare with Fig. 10, profile 9. For location, see Fig. 140.

basalt. The compound flow is 12–15 m thick and has a rusty brown weathering colour (Fig. 156). The lowermost flow lobe is composed of olivine-microphyric basalt (51 wt% SiO₂, 11 wt% MgO); its lower part contains disseminated iron sulfides (pyrrhotite or troilite) and scattered, few-millimetres-sized xenoliths of magma-modified mudstone with fine-grained plagioclase and reddish spinel which form radiating aggregates derived from reaction with mullite (as in Fig. 109A and in Pedersen *et al.* 2017, fig. 111). The flow must have been erupted locally on eastern Disko.

Basaltic andesite lava flow with native iron and sulfide at Qinnngusaq. A *c.* 4 m thick, light grey aa lava flow is exposed about 25 m above the base of the Niaqussat Member at Qinnngusaq (Fig. 10, profile 8). It is a highly magnesian basaltic andesite (55.8 wt% SiO₂, 9.2 wt% MgO) with scattered up to 8 mm aggregates of native iron and sulfide (Fig. 157). The rock contains resorbed olivine phenocrysts and abundant orthopyroxene phenocrysts and microphenocrysts. There are also scattered xenocrysts of quartz and abundant aggregates of sieve-textured plagioclase derived from sediment–magma

reaction. The flow also contains centimetre-sized, magma-modified mudstone xenoliths. The flow is the only native-iron-bearing lava flow in the Niaqussat Member on eastern Disko and Nuussuaq.

The chemical composition of the flow is comparable to that of the basaltic andesite dyke with native iron and sulfide at Illukunnguaq (Pauly 1958) at the Vaigat coast 5 km north-east of Qinnngusaq, and the dyke is therefore considered to be a likely feeder for the lava flow (Larsen & Pedersen 1992, dyke analysis table 1, no. 7, sample 362140).

Eastern Nuussuaq

Lava flows of the Niaqussat Member occur in the elevated country east of the eastern boundary fault on north-eastern Nuussuaq. Here, between Points 2080 m and 2000 m, there is a less than 50 m thick succession of 2–5 light grey picritic pahoehoe flows of unit 530 (Fig. 12, profile 13 (Nunavik); Figs 158, 159). The flows are separated from the underlying two basalt flows of the Nordfjord Member by 1–2 m of yellow brown tuffaceous volcanoclastic sandstone with up to 1 cm large fragments of plant

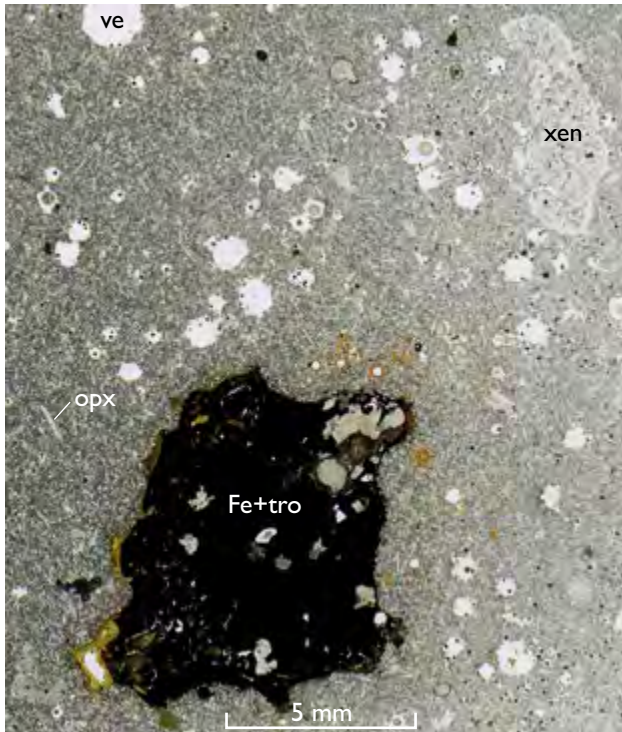


Fig. 157. Thin section (scanned) of a magnesian basaltic andesite of unit 530. The vesicular (ve) groundmass contains orthopyroxene microphenocrysts (opx) and a large aggregate of native iron and troilite (Fe+tro). The xenolith (xen) is a plagioclase-rich, strongly magma-modified mudstone. Sample 362179, Qinnuguaq, eastern Disko.

fossils. Traces of similar sandstone are also seen in the scree coming down from the top of the picritic succession. About 3–4 km east of the Nunavik profile both the picrites and the underlying lava flows of the Nordfjord and Rinks Dal members are banked up against a topographic high of Precambrian gneiss that blocked further eastward progression (Central Nuussuaq section at 71.6 km; see also Fig. 163).

Middle Niaqussat Member (unit 531)

Composition and petrography. Unit 531 comprises a few lava flows of silicic basalt with 50–52 wt% SiO₂, 6–7 wt% MgO and 1.7–2.2 wt% TiO₂. The rocks show only little petrographical variation; most have plagioclase phenocrysts and glomerocrysts varying in size between 0.5 and 2 mm, and in addition phenocrysts and glomerocrysts of augite <0.5–1 mm in size. Olivine is scarce or absent. Some rocks are almost aphyric. Xenocrysts of sedimentary origin have not been observed; however, occasional aggregates of plagioclase xenocrysts up to 7 mm in size with sieve-textured cores provide evidence for reaction between magma and crustal rocks.

Unit 531 is chemically well defined but is not recognisable as a field marker horizon.

Distribution and thickness. Flows of unit 531 overlie the more magnesian flows of unit 530 in four profiles on western Disko and three profiles on eastern Disko. The unit is absent in an area in Vesterdalen on western Disko

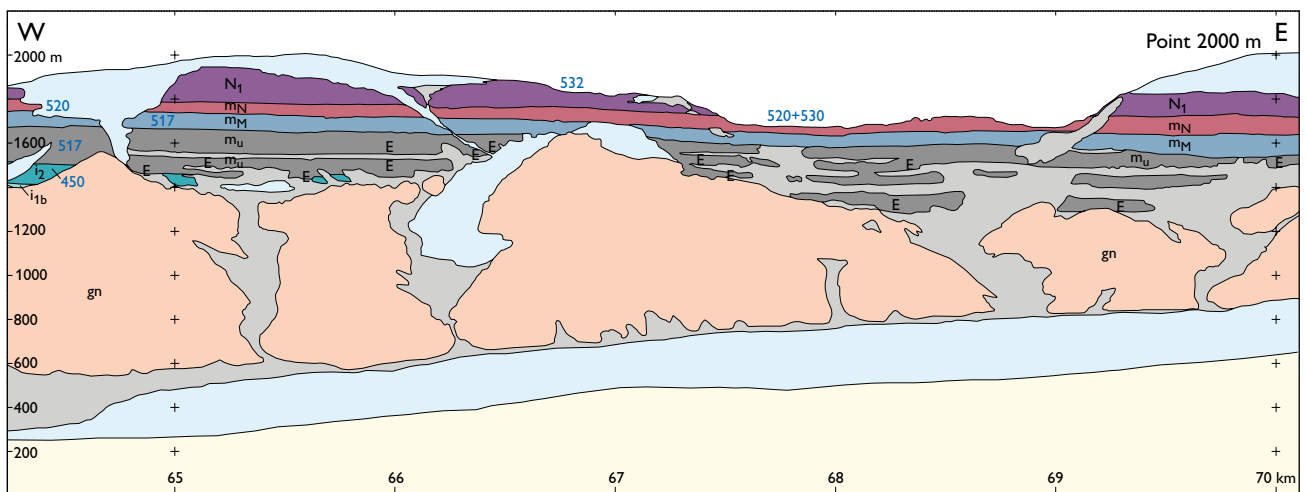


Fig. 158. Photogrammetrically measured section of the mountainside between Nunavik (just left of the picture) and Point 2000 m, eastern Nuussuaq. Blue three-digit numbers are lithological codes; other annotations as in the original. E: Entablature lava. The red horizon labelled m_N comprises both unit 520 and unit 530. Unit 531 is not present. Compare with Fig. 159. Excerpt from the Central Nuussuaq section (Pedersen *et al.* 2002a).



Fig. 159. Lava flows east of Nunavik, eastern Nuussuaq (Fig. 158 at *c.* 67 km). The Rinks Dal Member is present as unit 517; the Nordfjord Member (unit 520) comprises two basalt flows, the lower Niaqussat Member (unit 530) comprises 2–5 light grey picritic pahoehoe flows and the upper Niaqussat Member (unit 532) comprises about seven dark brown basalt flows. The combined thickness of units 520 + 530 is about 60 m. For location, see Fig. 163.

and at Pyramiden on northern Disko. In many other profiles, the level is eroded away. Its presence has not been confirmed on Nuussuaq. The unit is 15–35 m thick and only comprises one to three flows except at Point 440 m in the Hammer Dal area, where there are five flows with a combined thickness of 35 m, truncated upwards by erosion. At one locality (Fig. 14, profile 2), 10 cm of lateritic tuff or soil separate unit 531 and 530, but otherwise there are no indications of significant interruption in volcanic activity between the two units.

Upper Niaqussat Member (unit 532)

Composition. Unit 532 comprises lava flows of silicic basalt with 50–52 wt% SiO₂, 4.9–6.4 wt% MgO and 2.4–2.9 wt% TiO₂, which are capped by two or more flows of enriched basalt with *c.* 3.9 wt% TiO₂ on Nuussuaq (Fig. 12, profile 12) and by two flows of very enriched basalt

with 4.3 and 5.2 wt% TiO₂ at Sapernuvisk on south-western Disko (Fig. 14, profile 1).

Petrography. The basalts of unit 532 vary petrographically from rocks with distinctive millimetre-sized glomerophytic clusters of plagioclase, augite and pseudomorphed olivine (Fig. 160A) to almost aphyric rocks. Some of the more silicic basalts show flow lamination; besides scarce plagioclase phenocrysts and glomerocrysts, these basalts contain prismatic and commonly twinned microphenocrysts of clinopyroxene, some of which may be subcalcic or pigeonitic. In rare cases, these flows contain stellate clusters of prismatic clinopyroxene.

The enriched basalt flow no. 2 from the top of the Niaqussat Member at Sapernuvisk on Disko with 4.3 wt% TiO₂ has scarce glomerocrysts of plagioclase up to 4 mm in size and scattered microphenocrysts of plagioclase, augite and pseudomorphed olivine. The top flow with 5.2



Fig. 160. Thin sections (scanned) of basalts of the upper Niaqussat Member. **A:** Typical basalt with millimetre-sized, glomerophytic clusters of plagioclase (**pl**), pseudomorphed olivine (**ol**) and sparse augite (**cpx**) in a fine-grained groundmass. Sample 332900, Point 2080 m, Nunavik, eastern Nuussuaq. Dated sample (Storey *et al.* 1998). **B:** The Ti-rich uppermost flow of the Niaqussat Member: a fine-grained basalt with thin platy plagioclase (**pl**) phenocrysts, olivine microphenocrysts (**ol**) and scattered augite. Sample 176615, Sapernuik, west Disko.

wt% TiO_2 is a fine-grained basalt with thin, platy plagioclase phenocrysts up to 2 mm in size, scattered augites up to 0.5 mm in size and fairly abundant olivine microphenocrysts up to 0.3 mm in size (Fig. 160B). Many olivine microphenocrysts have an oxidised rim and an unaltered core. Despite the very high TiO_2 content, microphenocrysts of iron-titanium oxide are not seen.

Distribution and thickness. Unit 532 has been sampled in five profiles on western Disko, one on northern Disko (Pyramiden), one on eastern Disko (Frederik Lange Dal), and two profiles and a reconnaissance site on eastern Nuussuaq. It is most complete at Sapernuik where ten flows (160 m) are present. At Frederik Lange Dal, five flows (*c.* 60 m) are present. In other profiles on Disko, only one flow of this unit has been left by erosion. The unit is in fact better preserved on north-eastern Nuussuaq, where there are up to seven flows with a combined thickness of around 200 m and up to 300 m in the east-

ernmost parts of Nuussuaq where flows have ponded in lows on the gneiss surface.

Disko

Upper Niaqussat Member at Sapernuik on western Disko. The most complete exposures, and the only ones where the top of the Niaqussat Member is preserved, are found in the area between Sapernuik and Kingittup Qaqqaa on western Disko. The upper Niaqussat Member is here *c.* 230 m thick (Fig. 14, profile 1) and consists of about 12 robust flows with brownish weathering colour but becoming more greyish towards the top of the succession (Fig. 161). Thin horizons of lateritic soil occur between most flows, indicating a low eruption frequency for this part of the volcanic succession (Fig. 162; Fig. 14, profile 1). The area has been briefly described by Pedersen (1977b); it was mapped by Pedersen (1977b, Plate 1)



Fig. 161. The lava succession in the type section for the upper Niaqussat Member and the Sapernuvik Member. The sample profile runs along the ridge in the right foreground. The Niaqussat Member is well developed and comprises all of the lower (530), middle (531) and upper (532) parts of the member. It is overlain by the three preserved flows of the Sapernuvik Member (540). The top plateau is at around 600 m altitude. Photogrammetric interpretation in Fig. 171. Paakkarut, Sapernuvik, west Disko.

and Pedersen & Ulf-Møller (1987) and is shown on the South Disko section at 0–5 km (see Fig. 171).

The top of the Niaqussat Member, which ends with two unusually Ti-rich flows, is best exposed on the steep corrie wall *c.* 3 km south-west of Kingittup Qaqqaa (Fig. 162). The 20–30 m thick, second highest flow with 4.3 wt% TiO₂ here overlies a ‘normal’ flow with 2.54 wt% TiO₂, separated by a decimetre-thick lateritic soil layer. The flow can be observed as a local marker horizon in several corrie walls between Sapernuvik and Kingittup Qaqqaa (Fig. 161); it must once have covered an area of more than 16 km² and represents an original volume of at least 0.5 km³. The flow is capped by a thin lateritic soil layer, which is covered by two lava lobes (considered to be one flow) with a maximum thickness of *c.* 13 m and containing 5.2 wt% TiO₂. The volume of this flow cannot be assessed accurately but must be well below 0.1 km³; it must have been erupted close to the vicinity of Sapernuvik. A less than 20 cm thick horizon of lateritic soil on top of the flow separates it from the olivine-phyric

basalts of the Sapernuvik Member. There is no indication of prolonged volcanic quiescence between the formation of the Niaqussat and Sapernuvik members, despite a very marked contrast in their geochemical signatures.

Eastern Nuussuaq

Lava flows of unit 532 form a succession more than 200 m thick in the high area north and north-east of Nunavik (Larsen & Pedersen 1992, figs 3, 4). The lavas rest on basalt flows of the lower Niaqussat Member and, in the eastern parts, on Precambrian gneiss. The flows of unit 532 are the youngest preserved volcanic rocks on Nuussuaq east of the Itilli fault; their upper boundary is erosional.

About seven lava flows are preserved above the picrites of unit 530 (Fig. 12, profiles 12, 13). These basalts (the upper lava sequence of Larsen & Pedersen 1992) are very similar to the flows of unit 532 elsewhere. One of the flows (sample 332900) was dated by Storey *et al.* (1998)



Fig. 162. The lava succession in a steep corrie wall between Sapernuvik and Kingittup Qaqqaa, west Disko. The upper Niaqussat Member (unit 532) here comprises nine lava flows with lateritic soil (**lat**) horizons between them. The 20–30 m thick, second highest flow (with sample 176616) is a local marker horizon. The highest Niaqussat Member flow is compositionally unusual, with the highest TiO₂ content of all lavas in the Maligât Formation (sample 176615: 5.1 wt% TiO₂). It is overlain by the Sapernuvik Member flows (540). The two numbered samples were taken in the respective flows although not at this locality; the actual sample profile is shown in Fig. 161.

to 60.2 ± 0.5 Ma (recalculated), i.e. Selandian. The lava flows have a characteristic dark brown to almost black weathering colour (Fig. 159). They range in thickness from less than 5 m to more than 50 m; several have very prominent colonnades and entablature zones, indicating emplacement in a wet environment.

A 2 m thick horizon of laterised, red volcanoclastic sediment is exposed in the upper part of the succession,

indicating a distinct time gap in the volcanism; several more soil horizons may exist hidden in scree.

East of a palaeo-topographic high of Precambrian gneiss near Point 2000 m (Central Nuussuaq section at 71.6 km), the lava flows of unit 532 flowed directly onto the gneiss (Fig. 163). In this area the flows ponded in small basins where they invaded a thin succession of Paleocene quartzo-feldspathic clastic sediments (Cen-

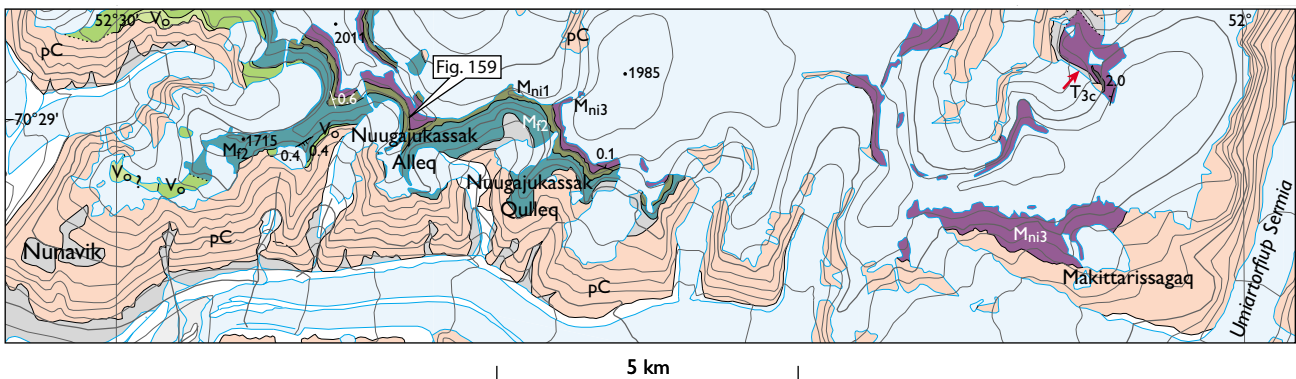
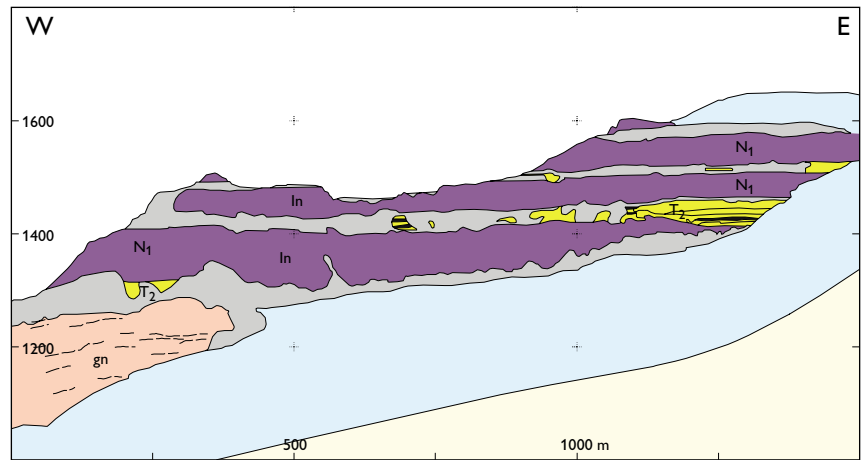


Fig. 163. Map demonstrating the eastward onlap of successively younger volcanic units onto the high gneiss terrain east of Nunavik on eastern Nuussuaq. The gneiss (**pC**) is pale red; Grass green (**V_o**) is the Vaigat Formation, dark green (**M_{ni1}**) is the upper Maligât Formation unit 517, olive green (**M_{ni1}**) is the combined Nordfjord and lower Niaqussat Members, and dark purple (**M_{ni3}**) is the upper Niaqussat Member (unit 532). The red arrow points to the location of Paleocene sediments (**T_{3c}**) and Figs 164–166. Excerpt from the 1:100 000 scale special map sheet Paatuut (Pedersen *et al.* 2007a). Annotations from the original.

Fig. 164. Photogrammetrically measured section of some of the easternmost exposures of lava flows on eastern Nuussuaq, 3 km north of Makittarissagaq (Fig. 163). The flows (N_1) belong to the upper Niaquussat Member and have invaded tuff-bearing sediments (T_2) assigned to the Atanikerluk Formation. Excerpt from the Central Nuussuaq section, panel L–M (Pedersen *et al.* 2002a). Annotations from the original.



tral Nuussuaq section at 59–79 km; Fig. 164; Pedersen *et al.* 2007a; Fig. 12, profiles 12, 14). These small basins may have reflected the local topography and may have been short-lived. The sediments may be referred to the Atanikerluk Formation, but it is uncertain whether they represent the youngest and most easterly remnants of the Assoq Member (Dam *et al.* 2009; Pedersen *et al.* 2007a,

unit T_{3c}). The lava flows can be followed for about 10 km towards the east but not continuously, and most contacts are obscured by scree or ice. At Makittarissagaq the succession is at least 200 m thick and consists of at least five flows, with traces of sediment between the two lowest flows (Central Nuussuaq section at 78.3 km). The easternmost localities with Niaquussat Member lava flows are



Fig. 165. Lava flows of the upper Niaquussat Member (unit 532) invading tuff-bearing sediments (*sed*) assigned to the Atanikerluk Formation. See photogrammetric interpretation in Fig. 164 and location in Fig. 163. The sediments are shown in more detail in Fig. 166.

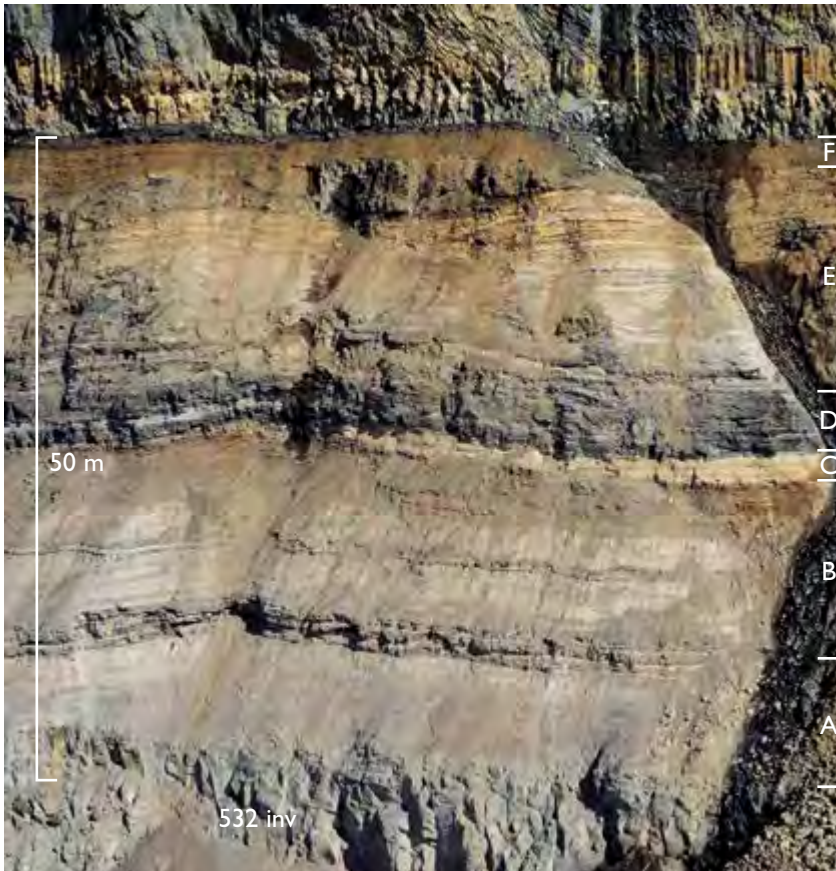


Fig. 166. Sediments between invasive lava flows of the upper Niaquassat Member on eastern Nuussuaq. The six intervals A to F are described in the text. The succession is tentatively interpreted as lacustrine deposits truncated by a minor fluvial channel. For location, see Fig. 165.

three small nunataks (at 70°25–26'N, 51°58–59'W) in the ice cap 6–8 km south of Umiartorfiup Qaqqaa. Mostly, only a few flows of dark basalt are seen together with traces of a sediment cover on the eroded gneiss (Central Nuussuaq section, panel J–K).

Lava flows and intercalated sediments. A c. 300 m thick section through the youngest volcanic and sedimentary lithologies is excellently exposed on a nunatak 3 km north of Makittarissagaq (Figs 163–166). The sediment locality is of difficult access and has only been investigated on the ground during a short helistop in 2016. Four flows are preserved, of which the uppermost is a small erosional remnant. The two upper flows appear to be subaerial, whereas the two lower ones have the appearance of sills intruded into more than 50 m of quartzo-feldspathic clastic sediments. The lowermost sill is up to 100 m thick. The sills are almost certainly invasive lava flows. Parts of the sediments are deformed and partially melted by the sills, but in the easternmost part of the exposure, there are more than 50 m of undeformed sediments (Fig. 164).

Figure 165 presents an overview of the sedimentary succession. The lower invasive lava flow cuts the succes-

sion at a low angle, whereas the flow above the sediments appears to be parallel to the bedding. The sedimentary succession is c. 50 m thick and comprises six intervals, A to F (Fig. 166). The lower sandstone (A) is cross-laminated, fine-grained and contains comminuted plant debris. The sandstone is interbedded with sand-streaked silty mudstone (B) with a few thin tuff beds. (C) is a channelised, cross-bedded, medium-grained sandstone. The overlying, coal-rich bed (D) is clayey, contains large pieces of coalified wood, and becomes sandier upwards. The sandstone (E) is similar to (A), and grades up into mudstone with tuff layers and coalified wood. The uppermost mudstone (F) is baked black towards the overlying lava. The succession is tentatively interpreted as lacustrine deposits, truncated by a minor fluvial channel (C).

Chemical compositions of the Niaquassat Member

The large majority of Niaquassat Member rocks are tholeiitic basalts and picrites; only a few flows of basaltic andesite occur. The basaltic andesites, like those of the Nordfjord Member, have much higher contents of MgO,

Ni, and Cr than their orogenic namesakes and are very different rocks.

Representative chemical analyses of the Niaquussat Member rocks are shown in Table 8, and all analyses are plotted in the variation diagrams, Figs 167–169. As for the Nordfjord Member, MgO was chosen as the main variation parameter because the variations in FeO* invalidate the *mg*-number as a common variation parameter.

Major elements

The successively more evolved character (lower MgO) of the three units of the Niaquussat Member is clearly seen in Fig. 167, where the separate identity of the middle unit is evident. The Niaquussat Member rocks are distinctly sub-alkaline, with total alkalis less than 3.4 wt%. Of the basalts (MgO < 12 wt%), 90 of 129 analysed samples (70%) are quartz normative. All basalts with MgO < 8 wt% (59 samples) are quartz normative.

The more silica-saturated character of the basalts and picrites compared with the Rinks Dal Member is seen in the silica diagram of Fig. 167, where the compositional field of the Niaquussat Member is situated at a higher level than that of the Rinks Dal Member. The Niaquussat Member basalts with less than 10 wt% MgO have on average 50.4 wt% SiO₂ compared with 49.2 wt% SiO₂ in similar basalts of the Rinks Dal Member. Likewise, the Niaquussat Member picrites (with 12–15.2 wt% MgO) have on average 49.3 wt% SiO₂ compared with 47.7 wt% SiO₂ in similar uncontaminated picrites of the Rinks Dal Member and the underlying Vaigat Formation. Thus *all* the rocks of the Niaquussat Member have increased SiO₂ relative to uncontaminated rocks of the earlier parts of the volcanic succession.

Further in comparison with the Rinks Dal Member, the Niaquussat Member basalts and picrites have generally higher Al₂O₃ and lower TiO₂, FeO*, Na₂O, and P₂O₅.

The Niaquussat Member basalts generally have TiO₂ contents lower than 2 wt%. Only in the upper Niaquussat Member are TiO₂ contents increased to 2–3 wt% (Fig. 167); four flows have unusually high TiO₂ (3.9–5.2 wt%). Two of these flows are the two uppermost Niaquussat Member flows in the Sapernuvik profile, lying immediately beneath the flows of the Sapernuvik Member; the uppermost flow has the highest TiO₂ content in the entire Maligât Formation. The two other flows are the uppermost two of the seven flows of the upper Niaquussat Member in the Point 2080 m profile on north-eastern Nuussuaq, situated 130 km from Sapernuvik. The four flows have many chemical characters in common, and it is

therefore likely that the upper Niaquussat Member is practically complete at Point 2080 m, despite the extensive erosion in the intervening area between the two profiles.

The few basaltic andesites only cover a fairly narrow range in MgO (7.2–10 wt%). This is in strong contrast to the Nordfjord Member where the basaltic andesites range down to 3.4 wt% MgO and grade continuously into andesites and dacites. The difference suggests fewer high-level magma chambers and much shorter residence times in these for the Niaquussat Member magmas.

Trace elements

Variation diagrams for trace elements are shown in Figs 168, 169. Many elements show more scatter than in the Rinks Dal Member, e.g. Rb, Ba, and Ce. In general, the lower Niaquussat Member rocks have lowered Sr, Nb, V, Cu and Ni, and increased Rb, Ba and Cr relative to the Rinks Dal Member. The middle and upper Niaquussat Member basalts are in many respects quite similar to the Rinks Dal Member basalts but have lower Sr and higher Sc.

The basaltic andesites have higher Rb, Ba, Zr, Zr/Y, Ce and Cr and lower V and Zn than the basalts and picrites.

REE and multi-element diagrams are shown in Fig. 170. The picrites and basalts, including the evolved basalts of the upper Niaquussat Member, have La_N/Sm_N ratios close to but above 1. This clearly distinguishes the basalts of the upper Niaquussat Member from the otherwise quite similar basalts of the Rinks Dal Member (Fig. 100). The basaltic andesites have higher La_N/Sm_N ratios than other rocks of the member. In the multi-element diagrams the picrites and basalts all have Nb-Ta troughs and do not show the K and Pb troughs that characterise the Rinks Dal Member basalts, or even have K and Pb peaks. The basaltic andesites show these features more pronouncedly and also have visible Eu-Ti troughs. The Ti-rich basalt flows just below the Sapernuvik Member are different from all other rocks in the Niaquussat Member: they have no Nb-Ta troughs, they have K and Pb troughs, and they appear not to be crustally contaminated.

In conclusion, except for the latest high-Ti flows all the rocks of the Niaquussat Member are to some degree crustally contaminated. Processes and degrees of contamination are discussed in the last chapter.

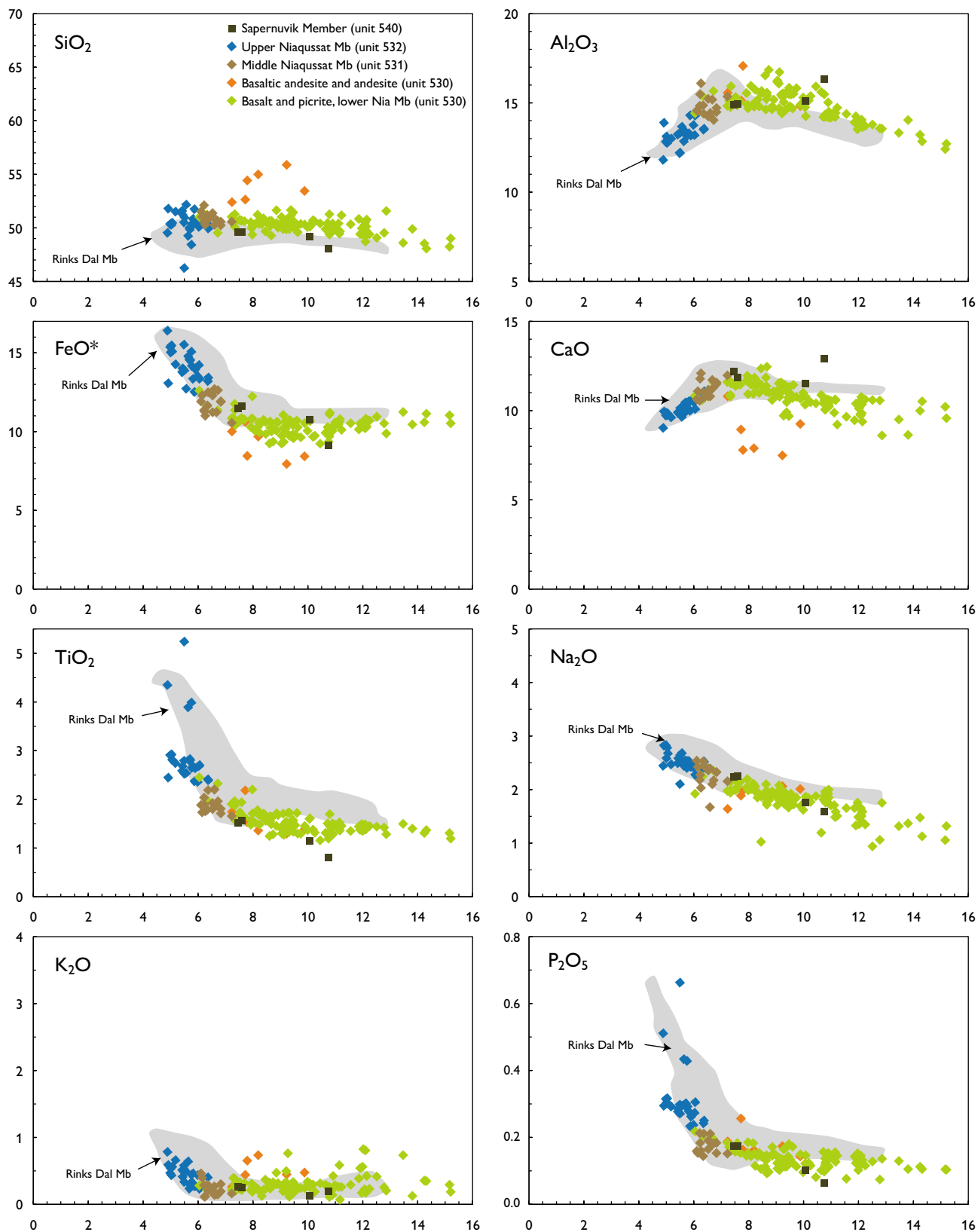


Fig. 167. Major-element variation diagrams for rocks of the Niaqussat Member. Four data points for the Sapernuik Member are included. Data in wt% oxides recalculated volatile-free. FeO* is total iron as FeO.

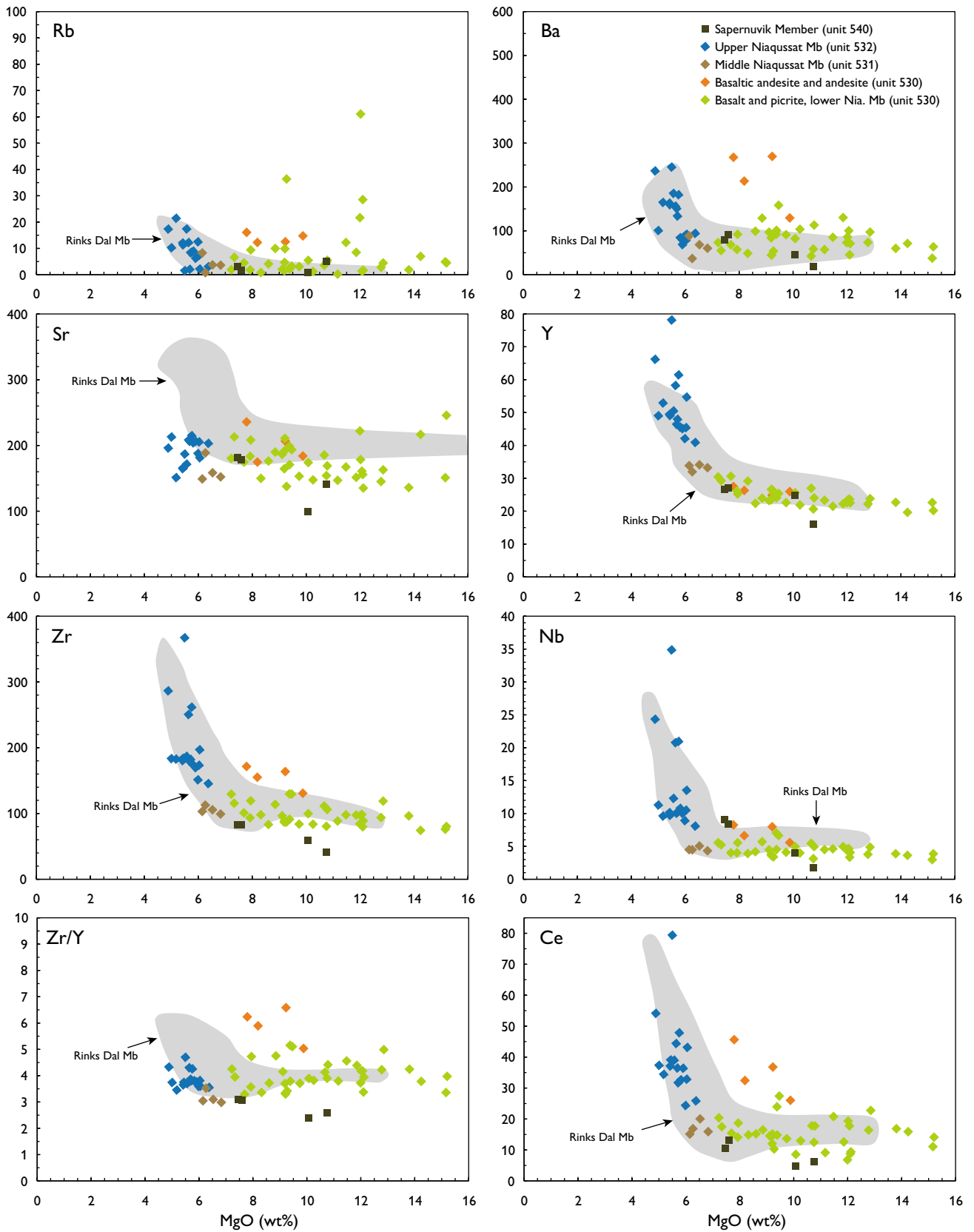


Fig. 168. Incompatible trace-element variation diagrams for rocks of the Niaquassat Member. Four data points for the Sapernuvik Member are included. Data in ppm.

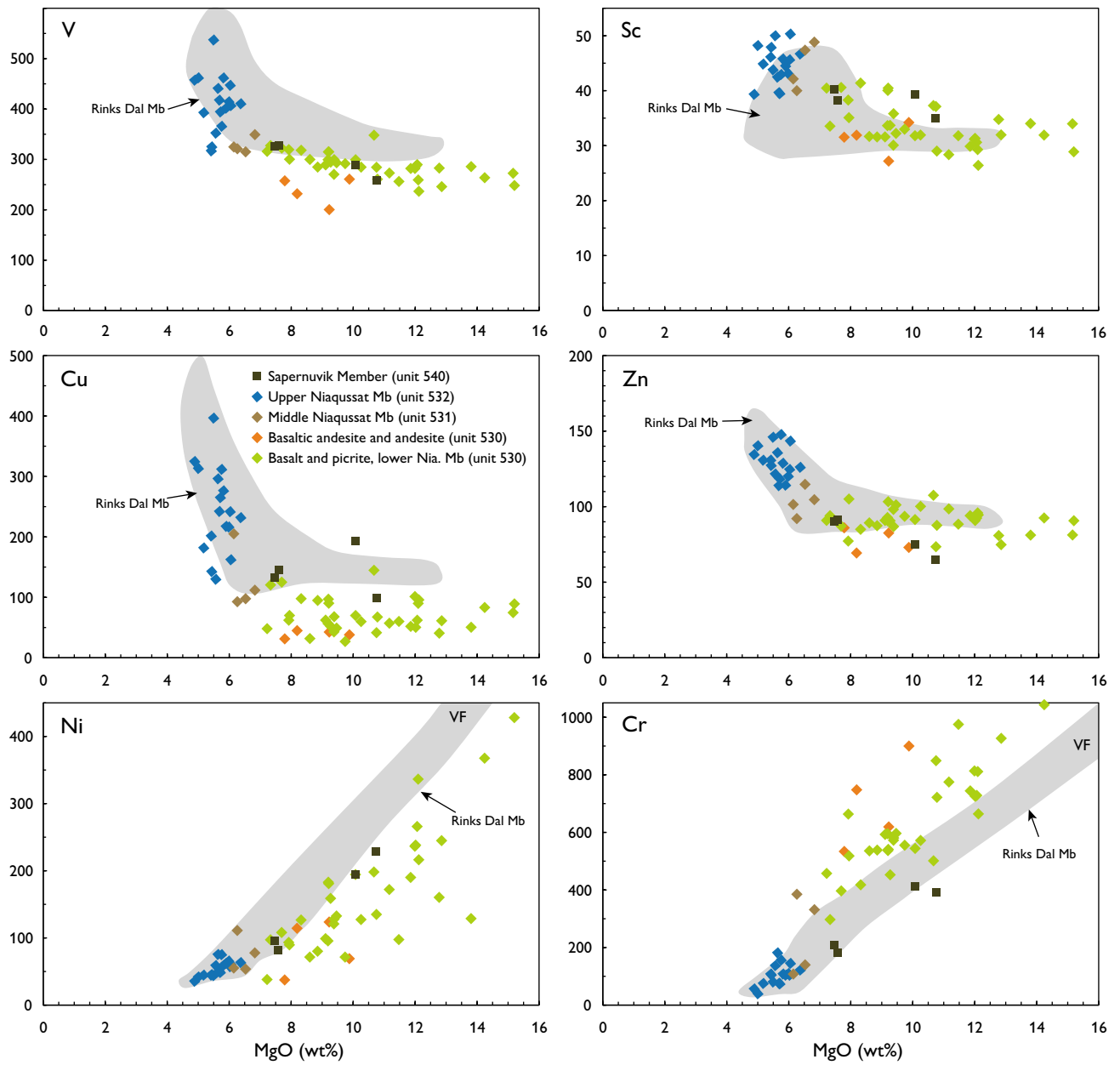


Fig. 169. Transition-element variation diagrams for rocks of the Niaquassat Member. Four data points for the Sapernuik Member are included. Data in ppm.

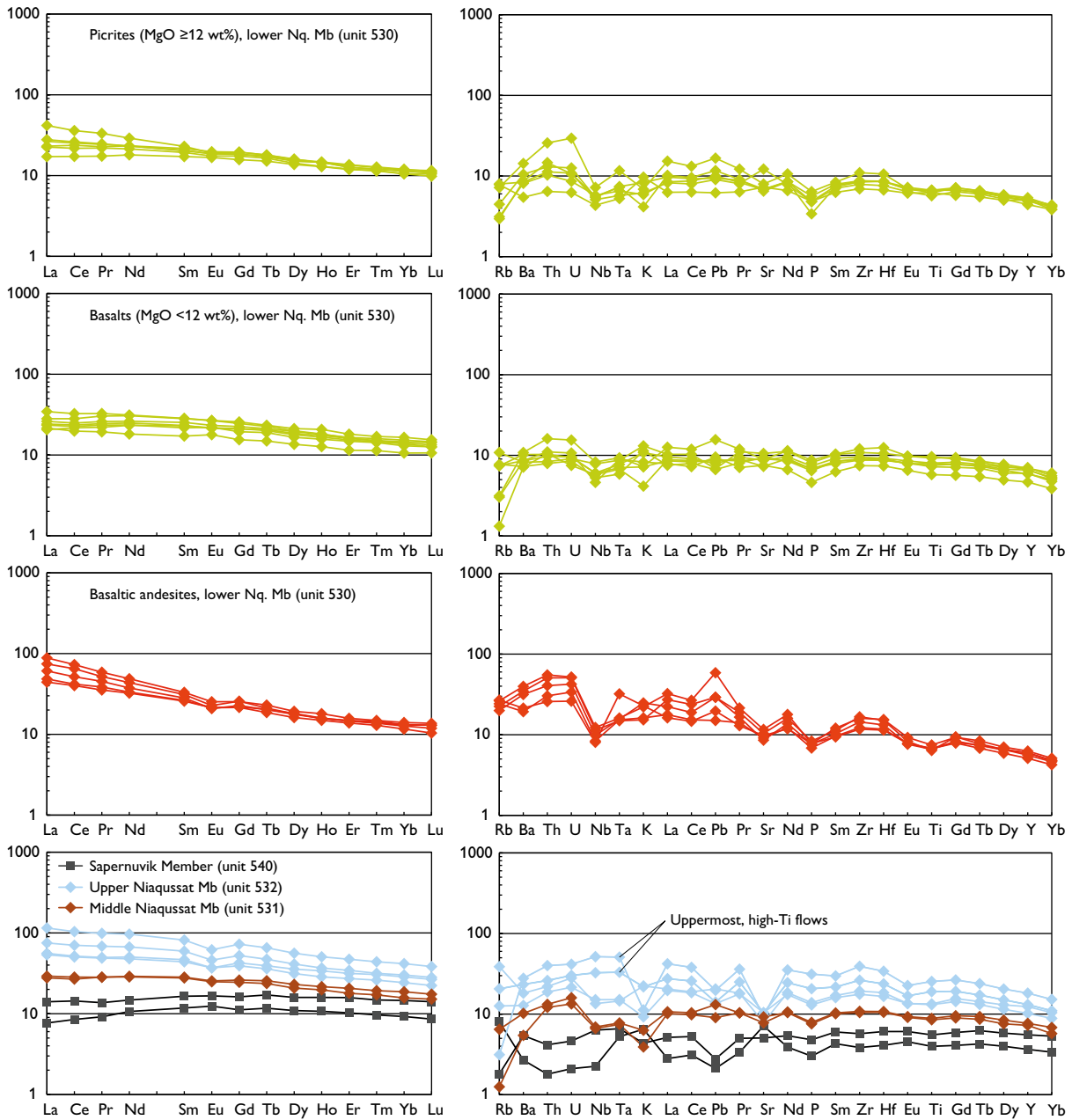


Fig. 170. REE and multi-element diagrams for representative rocks of the Niaquassat Member. Data for the Sapernuik Member are included. Left diagram, chondrite normalised; right diagram, primitive mantle normalised; normalisation factors from McDonough & Sun (1995).

Table 8a. Chemical analyses of rocks of the Niaquussat Member

Lithology	Lower Niaquussat Member										Basaltic andesite		
	Picrite					Basalt					5301	5301	
Lith. code	5301	5301	5301	5301	5301	5301	5301	5301	5301	5301	5301	5301	
GGU No.	332859	263973	156625	176642	340824	176603	264057	274415	318827	328420	362179	156571	
Deg. W	5219.82	5450.71	5445.76	5441.90	5240.88	5455.12	5427.73	5442.51	5220.01	5358.23	5240.45	5445.94	
Deg. N	7029.213	6948.649	7004.492	6957.254	6944.488	6940.704	6952.778	7010.641	6946.544	6923.912	6950.978	7004.470	
Altitude, m	1694	581	236	572	1162	312	1274	278	1193	872	1319	216	
SiO ₂	46.85	46.14	47.42	46.68	47.65	49.09	48.71	49.56	50.07	49.39	55.30	53.37	
TiO ₂	1.14	1.25	1.33	1.34	1.34	1.51	1.60	1.45	1.61	1.94	1.28	1.50	
Al ₂ O ₃	12.15	11.87	13.34	12.79	13.46	14.21	14.68	15.25	14.89	14.87	15.18	16.74	
Fe ₂ O ₃	1.68	2.61	2.95	1.45	3.03	2.63	3.09	4.59	3.91	5.77	0.40	0.89	
FeO	8.55	8.21	7.28	8.61	7.62	8.05	7.45	5.96	7.13	6.40	7.50	7.49	
MnO	0.16	0.17	0.16	0.20	0.17	0.18	0.18	0.17	0.18	0.19	0.14	0.14	
MgO	14.53	14.50	13.12	12.04	11.61	9.03	8.05	7.77	7.61	7.23	9.13	7.64	
CaO	9.15	9.77	8.21	9.96	9.44	11.29	11.25	11.45	11.33	10.73	7.41	7.64	
Na ₂ O	1.26	1.01	1.30	1.00	1.51	1.97	1.79	2.00	2.12	2.11	2.04	1.94	
K ₂ O	0.178	0.280	0.120	0.240	0.170	0.328	0.120	0.208	0.312	0.379	0.442	0.640	
P ₂ O ₅	0.099	0.100	0.100	0.070	0.116	0.133	0.140	0.142	0.152	0.167	0.172	0.160	
Volatiles	4.36	4.30	3.94	5.48	3.82	1.53	2.66	1.80	0.79	1.11	1.20	1.31	
Sum	100.11	100.21	99.27	99.86	99.93	99.95	99.72	100.35	100.10	100.28	100.19	99.46	
FeO*	10.06	10.56	9.93	9.91	10.35	10.42	10.23	10.09	10.65	11.59	7.86	8.29	
mg number	74.50	73.53	72.76	71.07	69.42	63.68	61.41	60.90	59.11	55.78	70.14	65.08	
Zn	72.2	77.7	77.1	76.2	81.6	78.2	82.2	75.8	86.2	92.7	69.8	84.3	
Cu	81.8	71.4	48.0	38.3	97.7	95.0	94.6	60.9	124	119	38.4	30.7	
Ni	413	465	122	151	208	171	123	91.5	107	95.9	113	36.7	
Sc	37.7	32.5	32.3	32.8	33.5	38.8	40.0	37.6	40.1	33.1	28.6	30.9	
V	278	261	272	267	274	301	308	313	319	323	215	253	
Cr	1401	1037	1055	1114	856	527	404	651	392	293	715	523	
Ga	12.3	12.6	17.2	13.2	17.1	20.0	18.5	18.5	19.7	20.9	19.9	22.8	
Rb	4.78	4.68	1.77	2.68	1.88	4.64	0.79	1.82	4.44	6.50	13.5	15.8	
Sr	242	144	129	137	135	188	145	180	173	210	206	231	
Y	19.0	21.6	21.6	20.9	22.2	25.3	28.2	25.7	30.3	28.8	24.0	27.0	
Zr	82.8	72.7	91.6	88.4	91.4	93.3	94.8	91.7	99.9	114	175	168	
Nb	3.35	2.85	3.69	3.57	3.78	3.47	3.78	3.94	3.98	5.15	7.48	8.09	
Cs	0.067	0.047	0.044	0.048	0.150	0.133	0.030	0.032	0.042	0.091	0.368	0.415	
Ba	55.3	36.0	57.0	69.3	53.5	48.0	47.1	56.3	67.5	54.2	229	262	
La	5.34	4.07	6.60	6.28	5.48	4.88	5.72	5.54	6.19	6.67	17.6	21.0	
Ce	13.3	10.6	16.0	15.5	14.5	13.3	14.4	13.9	15.2	17.2	39.8	44.7	
Pr	2.04	1.61	2.30	2.26	2.11	2.05	2.27	2.17	2.41	2.82	4.81	5.45	
Nd	9.78	8.24	10.6	10.6	10.7	10.6	11.4	10.8	12.0	14.0	20.0	22.3	
Sm	2.86	2.54	3.04	3.00	3.20	3.40	3.43	3.21	3.75	4.17	4.60	4.90	
Eu	0.984	0.943	1.04	1.05	1.11	1.22	1.20	1.24	1.31	1.50	1.28	1.42	
Gd	3.47	3.13	3.69	3.62	3.88	4.23	4.18	3.86	4.47	4.89	5.12	5.05	
Tb	0.592	0.545	0.614	0.631	0.648	0.723	0.743	0.684	0.765	0.816	0.762	0.832	
Dy	3.50	3.38	3.73	3.71	3.89	4.39	4.55	4.07	4.81	4.90	4.42	4.74	
Ho	0.710	0.704	0.798	0.800	0.805	0.906	0.951	0.857	0.985	0.994	0.856	0.984	
Er	1.93	1.90	2.03	2.02	2.18	2.46	2.57	2.37	2.64	2.59	2.33	2.52	
Tm	0.282	0.284	0.296	0.295	0.315	0.360	0.374	0.352	0.394	0.369	0.340	0.367	
Yb	1.69	1.70	1.82	1.86	1.93	2.21	2.34	2.09	2.46	2.27	2.04	2.26	
Lu	0.241	0.258	0.268	0.262	0.276	0.309	0.350	0.310	0.359	0.328	0.293	0.337	
Hf	2.15	1.89	2.44	2.43	2.41	2.48	2.58	2.45	2.60	2.99	4.28	4.37	
Ta	0.212	0.194	0.268	0.274	0.242	0.216	0.250	0.260	0.286	0.322	0.552	0.596	
Pb	1.36	0.927	1.75	1.40	1.50	0.999	1.28	1.31	1.18	1.02	4.38	8.80	
Th	0.896	0.511	1.16	1.03	0.816	0.629	0.834	0.774	0.817	0.664	4.03	4.39	
U	0.220	0.127	0.216	0.256	0.174	0.173	0.152	0.194	0.191	0.185	1.03	1.05	
<i>Isotope ratios calculated at 60 Ma</i>													
⁸⁷ Sr/ ⁸⁶ Sr ₆₀						0.705004					0.711708		
εSr						6.43					101.59		
¹⁴³ Nd/ ¹⁴⁴ Nd ₆₀						0.512814					0.511796		
εNd						4.93					-14.93		
²⁰⁶ Pb/ ²⁰⁴ Pb ₆₀						17.149					16.950		
²⁰⁷ Pb/ ²⁰⁴ Pb ₆₀						15.094					15.038		
²⁰⁸ Pb/ ²⁰⁴ Pb ₆₀						37.346					37.270		

For explanation of lithological codes, see Table 1. For petrographical notes on the samples, see Table 8c.

Geographical coordinates in WGS 84. First two digits are degrees, then following minutes in decimal form.

Major elements in wt% (XRF analyses). Trace elements in ppm (Zn–Ga: XRF analyses; Rb–U: ICP-MS analyses).

FeO* = total iron as FeO. mg number = 100 × atomic Mg/(Mg+Fe²⁺), with the iron oxidation ratio adjusted to Fe₂O₃/FeO = 0.15.

Table 8b. Chemical analyses of rocks of the Niaquassat Member and possible feeder dykes

Lithology	Middle Niaquassat Member		Upper Niaquassat Member				Possible feeders			Niaquassat Mb feeder
	Basalt		Basalt		Ti-rich top flows		Weakly contaminated basalt dykes			
Lith. code	5311	5311	5321	5321	5321	5321	6181	6181	6281	6281
GGU No.	176622	274419	332898	340817	332894	176615	318753	318707	318824	156570
Deg. W	5455.19	5442.48	5226.30	5240.27	5226.51	5455.73	5227.79	5217.96	5209.12	5445.91
Deg. N	6940.777	7010.613	7030.746	6944.813	7030.736	6941.272	7013.735	7004.028	6949.517	7004.442
Altitude, m	361	323	1897	1306	1977	543	1272	371	10	175
SiO ₂	50.41	49.00	49.08	50.44	48.38	45.10	49.43	49.45	48.23	49.13
TiO ₂	1.78	1.71	2.63	2.69	3.82	5.11	1.60	1.45	1.35	1.41
Al ₂ O ₃	14.07	15.68	12.93	12.73	12.62	11.91	14.60	13.73	13.24	13.80
Fe ₂ O ₃	2.89	6.57	6.58	4.64	4.64	6.69	1.51	1.47	2.14	2.48
FeO	9.54	4.81	8.02	9.80	10.34	10.97	9.42	9.07	8.45	7.66
MnO	0.20	0.18	0.22	0.24	0.23	0.29	0.19	0.17	0.17	0.16
MgO	6.45	6.10	5.91	5.07	5.54	5.36	7.60	11.37	12.64	11.15
CaO	11.04	11.78	10.30	9.42	9.67	9.73	12.04	9.82	10.05	9.37
Na ₂ O	2.37	1.98	2.44	2.42	2.40	2.05	1.94	1.81	1.63	1.76
K ₂ O	0.182	0.113	0.267	0.647	0.630	0.326	0.180	0.365	0.139	0.390
P ₂ O ₅	0.163	0.156	0.268	0.286	0.426	0.646	0.160	0.152	0.150	0.110
Volatiles	0.90	2.51	0.96	1.22	0.80	1.38	1.25	1.01	1.39	1.83
Sum	100.00	100.59	99.60	99.59	99.49	99.56	99.92	99.87	99.58	99.25
FeO*	12.14	10.72	13.94	13.98	14.52	16.99	10.78	10.39	10.38	9.89
mg number	51.80	53.50	46.16	42.32	43.57	38.95	58.78	68.88	71.13	69.51
Zn	94.2	89.7	120	134	138	169	83.3	87.4	83.8	80.3
Cu	91.9	90.3	259	224	323	444	131	78.2	98.7	62.8
Ni	50.9	108	56.6	47.0	75.3	47.0	126	214	319	98.31
Sc	43.6	39.0	49.5	42.8	39.9	42.6	40.7	32.6	33.4	32.4
V	342	313	479	354	442	510	325	288	291	280
Cr	137	375	103	67.6	176	74.5	409	851	926	1151
Ga	19.8	20.8	21.8	22.4	22.5	23.6	19.4	18.9	17.4	17.4
Rb	3.88	0.75	7.57	23.3	12.3	1.88	4.99	8.90	1.61	11.1
Sr	155	184	207	156	207	187	169	185	191	159
Y	33.0	31.2	43.9	53.2	56.5	78.2	28.9	23.4	22.2	21.4
Zr	114	110	185	202	276	411	97.3	104	89.8	98.2
Nb	4.55	4.37	9.93	8.88	21.4	33.9	3.80	4.58	4.06	4.11
Cs	0.118	0.018	0.175	0.590	0.146	0.017	0.126	0.253	1.01	0.450
Ba	67.4	35.9	84.6	120	154	184	46.6	86.2	48.8	79.8
La	6.92	6.59	12.7	13.2	17.8	27.3	5.68	7.41	6.00	7.21
Ce	17.4	16.4	30.9	31.7	43.1	63.7	14.8	18.7	15.5	17.9
Pr	2.62	2.63	4.53	4.61	6.35	9.17	2.28	2.78	2.29	2.44
Nd	13.3	13.0	21.9	23.0	30.7	44.2	11.8	13.4	11.3	11.6
Sm	4.20	4.10	6.50	6.90	8.81	12.1	3.71	3.64	3.22	3.30
Eu	1.43	1.40	2.09	2.08	2.60	3.49	1.30	1.26	1.17	1.14
Gd	5.19	4.88	7.78	8.48	10.4	14.4	4.64	4.27	3.78	3.90
Tb	0.924	0.853	1.30	1.41	1.71	2.36	0.785	0.728	0.657	0.656
Dy	5.67	5.10	7.72	8.77	10.1	13.8	5.14	4.03	3.77	3.89
Ho	1.18	1.08	1.56	1.85	2.01	2.76	1.04	0.820	0.767	0.793
Er	3.30	2.86	4.36	5.04	5.50	7.56	2.79	2.19	1.98	2.12
Tm	0.476	0.423	0.643	0.755	0.781	1.09	0.412	0.322	0.297	0.311
Yb	3.01	2.53	3.91	4.60	4.85	6.71	2.48	1.93	1.86	1.91
Lu	0.429	0.372	0.550	0.655	0.694	0.943	0.374	0.290	0.266	0.267
Hf	3.05	2.98	4.68	5.23	6.72	9.63	2.62	2.72	2.31	2.66
Ta	0.287	0.276	0.560	0.538	1.22	1.88	0.266	0.355	0.280	0.360
Pb	1.97	1.36	2.02	3.08	2.11	2.96	1.17	1.87	1.49	1.75
Th	1.05	0.963	1.49	1.75	2.08	3.18	0.743	1.13	0.828	1.22
U	0.324	0.272	0.437	0.569	0.613	0.844	0.218	0.333	0.239	0.317
<i>Isotope ratios calculated at 60 Ma</i>										
⁸⁷ Sr/ ⁸⁶ Sr ₆₀					0.704381	0.703377	0.703396			
εSr					-2.40	-16.65	-16.38			
¹⁴³ Nd/ ¹⁴⁴ Nd ₆₀					0.512710	0.512883	0.512869			
εNd					2.92	6.29	6.02			
²⁰⁶ Pb/ ²⁰⁴ Pb ₆₀					17.300	18.042	18.151			
²⁰⁷ Pb/ ²⁰⁴ Pb ₆₀					15.142	15.370	15.361			
²⁰⁸ Pb/ ²⁰⁴ Pb ₆₀					37.382	37.792	37.882			

Table 8c. Notes on analysed samples of the Niaqussat Member and possible feeder dykes

332859.	Picrite with well-crystallised doleritic groundmass and abundant microphenocrysts of olivine with tiny enclosed chromites. Zeolites and carbonate in vugs and groundmass. Lowest flow in the Niaqussat Member; Nunavik profile, eastern Nuussuaq.
263973.	Picrite with well-crystallised doleritic groundmass and abundant up to 1 mm olivine phenocrysts with tiny enclosed chromites. Zeolites in vugs and groundmass. Lava flow, Ikorfarsuit profile, Mellemfjord, west Disko.
156625.	Picrite with olivine microphenocrysts. Lava flow 2 m thick, north wall of Rink Dal c. 1.5 km from the coast, north-west Disko.
176642.	Picrite close to magnesian basalt with well-crystallised doleritic groundmass and up to 1 mm large olivine phenocrysts with enclosed chromite crystals. Lava flow 3 m thick, Kingittuusaq profile, outer Nordfjord, West Disko.
340824.	Picrite close to magnesian basalt with well-crystallised doleritic groundmass and scattered up to 1 mm olivine phenocrysts (mostly pseudomorphosed). Rare up to 3 mm glomerocrysts of plagioclase and pseudomorphosed olivine. Traces of tiny chromites. Lava flow 5 m thick, Frederik Lange Dal profile, east Disko.
176603.	Basalt with well-crystallised doleritic groundmass and scattered up to 1 mm phenocrysts of olivine. Lava flow 10 m thick, Sapernuvik profile, west Disko.
264057.	Basalt with well-crystallised groundmass and common up to 2 mm phenocrysts and glomerocrysts of plagioclase and scarce up to 1 mm olivine phenocrysts (pseudomorphosed). Lava flow 12 m thick, Point 1300 m profile, Vesterdalen, west Disko.
274415.	Almost aphyric basalt with very fine-grained groundmass and very scarce microphenocrysts of plagioclase and olivine (pseudomorphosed). Lava flow 14 m thick, 'Point 440 m northern gully' profile, north of Hammer Dal, north-west Disko.
318827.	Basalt with very fine-grained groundmass and scarce <1 mm glomerocrysts of plagioclase and olivine (pseudomorphosed). Uppermost exposed lava flow on plateau, Kvandalen profile, east Disko.
328420.	Basalt with very fine-grained groundmass and widespread phenocrysts and up to 4 mm glomerocrysts of plagioclase, olivine (partly pseudomorphosed) and augite. Lava flow 12 m thick, Alanngup Qaqqai profile, south-west Disko.
362179.	Magnesian basaltic andesite with rare up to 1 cm bodies of native iron rimmed by troilite. Abundant up to 1 mm phenocrysts and microphenocrysts of orthopyroxene and scarce up to 1 mm phenocrysts of olivine, sometimes with chromite. Widespread xenocrysts and microxenoliths of plagioclase and red spinel, and rare xenocrysts of quartz. Lava flow 5 m thick, Qingusaq profile, inner Kvandalen, east Disko.
156571.	Basaltic andesite; thin section lost. Lava flow, north wall of Rink Dal c. 1.5 km from the coast, north-west Disko.
176622.	Basalt with fine-grained groundmass and common phenocrysts and glomerocrysts of plagioclase up to 1.5 mm large and very scarce microphenocrystic augite. Lava flow 8 m thick, Sapernuvik profile, west Disko.
274419.	Basalt with well-crystallised doleritic groundmass, common up to 2 mm glomerocrysts of plagioclase and scarce microphenocrysts of olivine (pseudomorphosed) and augite. Lava flow 8 m thick, 'Point 440 m northern gully' profile, north of Hammer Dal, north-west Disko.
332898.	Basalt with well-crystallised fine-grained groundmass rich in equidimensional Fe-Ti oxide grains. Scattered microphenocrystic plagioclase and augite. Glomerocrysts <1.5 mm of plagioclase and augite. Entablature-dominated lava flow 20 m thick, Point 2080 m profile, eastern Nuussuaq.
340817.	Basalt; thin section lost. Lava flow 15 m thick, Frederik Lange Dal profile, east Disko.
332894.	Evolved high-Ti basalt; thin section lost. Lava flow 20 m thick, Point 2080 m profile, eastern Nuussuaq.
176615.	Evolved high-Ti basalt with fine-grained groundmass rich in Fe-Ti oxide grains. Common phenocrysts of plagioclase, olivine and augite. There are no Fe-Ti oxide microphenocrysts. Most Ti-rich basalt in the Maligât Formation. Lava flow 5 m thick, Sapernuvik profile, west Disko.
318753.	Picrite dyke. Glass chill with abundant microphenocrystic olivine and plagioclase up to 1 mm large. The crystalline groundmass is composed of plagioclase, clinopyroxene, olivine, ilmenite and residuum, and there is abundant microphenocrystic olivine and plagioclase. Dyke 1 m thick cutting lava flows of the Rinks Dal Member. Giesecke Monument, south coast of Nuussuaq.
318707.	Magnesian basalt dyke with well-crystallised doleritic groundmass of plagioclase, clinopyroxene, olivine, Fe-Ti oxides and residuum and scattered olivine phenocrysts up to 1.5 mm and abundant olivine microphenocrysts <0.5 mm large. Dyke 3–4 m thick, striking NE–SW, cutting sediments of the Atane Formation east of Atanikerluk, south Nuussuaq.
318824.	Picrite dyke. The groundmass is well crystallised and composed of plagioclase with characteristic leaf-textured hollow-cored grains, clinopyroxene, olivine, Fe-Ti oxide and residuum. The abundant microphenocrystic olivines (<0.5 mm) are much smaller than the plagioclase grains, and the rock does not therefore appear as porphyritic. Dyke 3.5 m thick, striking 60°NE, shore north of Inngigissoq, east Disko.
156570.	Magnesian basalt feeder dyke for a Niaqussat Member lava flow. Abundant up to 1 mm phenocrysts and microphenocrysts of olivine, a few with chromite. The doleritic groundmass is composed of plagioclase, low- and high Ca clinopyroxene, ilmenite and residuum. North wall of Rink Dal c. 1.5 km from the coast, north-west Disko.

Phenocryst phases as observed in thin section are mentioned in order of decreasing abundance.
 Samples of subaerial lava flows are usually taken in massive columns a few metres above the flow base.

Table 9a. Chemical analyses of rocks of the Sapernuvik Member

Lithology	Basalt			
	5401	5401	5401	5401
Lith. code	5401	5401	5401	5401
GGU No.	176611	176614	176608	176609
Deg. W	5454.77	5455.80	5455.74	5455.48
Deg. N	6942.010	6941.302	6941.734	6941.725
Altitude, m	637.29	559.41	584.05	596.39
SiO ₂	47.37	47.85	49.01	48.96
TiO ₂	0.80	1.11	1.54	1.50
Al ₂ O ₃	16.09	14.69	14.75	14.68
Fe ₂ O ₃	2.57	3.96	3.84	6.04
FeO	6.70	6.92	8.00	5.89
MnO	0.15	0.19	0.19	0.19
MgO	10.59	9.80	7.50	7.37
CaO	12.71	11.21	11.72	12.02
Na ₂ O	1.57	1.71	2.22	2.21
K ₂ O	0.188	0.126	0.248	0.258
P ₂ O ₅	0.062	0.099	0.171	0.171
Volatiles	1.75	2.48	1.33	1.04
Sum	100.55	100.15	100.52	100.33
FeO*	9.01	10.48	11.46	11.32
mg number	70.39	65.41	56.98	56.83
Zn	54.8	73.2	80.1	83.6
Cu	118	227	161	151
Ni	234	189	91	93
Sc	38.6	44.7	35.2	39.9
V	229	270	312	298
Cr	440	465	198	214
Co	51.7	50.5	48.4	48.8
Ga	14.8	15.8	18.5	18.9
Rb	4.82	1.09	1.86	2.93
Sr	142	101	176	178
Y	15.7	23.8	26.8	27.6
Zr	40.4	60.0	83.2	84.2
Nb	1.48	4.16	7.77	8.10
Cs	0.009	0.153	0.009	0.015
Ba	17.7	35.7	74.6	70.8
La	1.82	3.33	6.41	6.64
Ce	5.20	8.82	16.0	15.7
Pr	0.850	1.27	2.42	2.41
Nd	4.87	6.74	11.5	11.5
Sm	1.74	2.44	3.40	3.35
Eu	0.699	0.936	1.25	1.23
Gd	2.22	3.22	4.26	4.16
Tb	0.422	0.617	0.736	0.713
Dy	2.69	3.91	4.59	4.59
Ho	0.585	0.869	0.986	0.957
Er	1.64	2.53	2.63	2.55
Tm	0.238	0.365	0.395	0.400
Yb	1.49	2.35	2.41	2.39
Lu	0.211	0.346	0.367	0.368
Hf	1.16	1.72	2.18	2.33
Ta	0.194	0.244		0.484
Pb	0.317	0.417	0.565	0.680
Th	0.143	0.331	0.620	0.636
U	0.043	0.094	0.143	0.167
<i>Isotope ratios calculated at 60 Ma</i>				
⁸⁷ Sr/ ⁸⁶ Sr ₆₀	0.703382	0.703306		
εSr	-16.58	-17.66		
¹⁴³ Nd/ ¹⁴⁴ Nd ₆₀	0.512971	0.512929		
εNd	7.99	7.18		
²⁰⁶ Pb/ ²⁰⁴ Pb ₆₀	17.669	17.807		
²⁰⁷ Pb/ ²⁰⁴ Pb ₆₀	15.304	15.431		
²⁰⁸ Pb/ ²⁰⁴ Pb ₆₀	37.602	37.608		

Table 9b. Notes on analysed samples of the Sapernuvik Member

176611	Fine-grained basalt with up to 3 mm large phenocrysts of plagioclase and up to 1.5 mm olivine, and up to 3 mm glomerocrysts of plagioclase with resorbed outlines. Third and youngest preserved flow in the Sapernuvik Member; Sapernuvik profile, south-west Disko.
176614	Fine-grained basalt with common 1–2 mm large phenocrysts of plagioclase, olivine and augite, and scattered up to 1 cm large, gabbroic inclusions with augite and plagioclase. Lowest flow in the Sapernuvik Member, Sapernuvik profile, south-west Disko.
176608	Fine-grained basalt with up to 2 mm large glomerocrysts and phenocrysts of plagioclase and olivine (pseudomorphed) and <1 mm large augite. Second flow in the Sapernuvik Member, Sapernuvik profile, south-west Disko.
176609	Fine-grained basalt with sparse phenocrysts and up to 3 mm large glomerocrysts of plagioclase, augite and olivine (pseudomorphed). Central part of second flow in the Sapernuvik Member, Sapernuvik profile, south-west Disko.
Phenocryst phases as observed in thin section are mentioned in order of decreasing abundance.	
Samples of subaerial lava flows were normally collected in massive columns a few metres above the flow base.	

Footnotes, Table 9

For explanation of lithological codes, see Table 1. Geographical coordinates in WGS 84. First two digits are degrees, then follow minutes in decimal form. Major elements in wt% (XRF analyses). Trace elements in ppm (Zn–Ga: XRF analyses; Rb–U: ICP-MS analyses). FeO* = total iron as FeO. mg number = 100 × atomic Mg/(Mg+Fe²⁺), with the iron oxidation ratio adjusted to Fe₂O₃/FeO = 0.15.

Sapernuvis Member

Summary of the main features of the Sapernuvis Member

- The youngest lava flows on Disko and Nuussuaq east of the Itilli fault.
- Only three lava flows preserved in an erosional remnant on southern west Disko; original thickness and extent unknown.
- Conformably overlies lava flows of the upper Niaquassat Member.
- Uncontaminated, relatively magnesian basalts. One flow may include a component of remelted gabbro cumulates.

Lithostratigraphy of the Sapernuvis Member

New member

History. The Sapernuvis Member lava succession is shown on the geological map 1:100 000 Mellemfjord 69 V.1 Nord as unit β_{ol} (Pedersen & Ulf-Møller 1987) and on the geological section along the south coast of Disko (Sapernuvis unit, n_{i5} ; Pedersen *et al.* 2003). The flows were briefly described by Pedersen (1977b, p. 47–48 and table 8 nos 11–13).

Name. After Sapernuvis, a small cove on the west coast of Disko (Fig. 4).

Distribution. The Sapernuvis Member is only preserved within an area measuring 4 × 6 km in a down-thrown, west-dipping fault block on southern west Disko.

Type section. **Sapernuvis** on southern west Disko, on the mountaintop above 560 m (Fig. 14, profile 1; Figs 161 (photograph) and 171 (South Disko section at 0–5 km)).

Thickness. 80 m.

Lithology. Three subaerial lava flows of olivine-microphyric basalt.

Subdivisions. None.

Boundaries. The Sapernuvis Member conformably overlies the lava flows of the Niaquassat Member. The upper boundary is erosional.

Age. Inferred to be Paleocene, 61–60 Ma, magnetochron C26r, based on radiometric dating (Storey *et al.* 1998) of one of the youngest flows in the underlying Niaquassat Member.

Correlation. The Sapernuvis Member is not known to correlate with any other lava succession in the region.

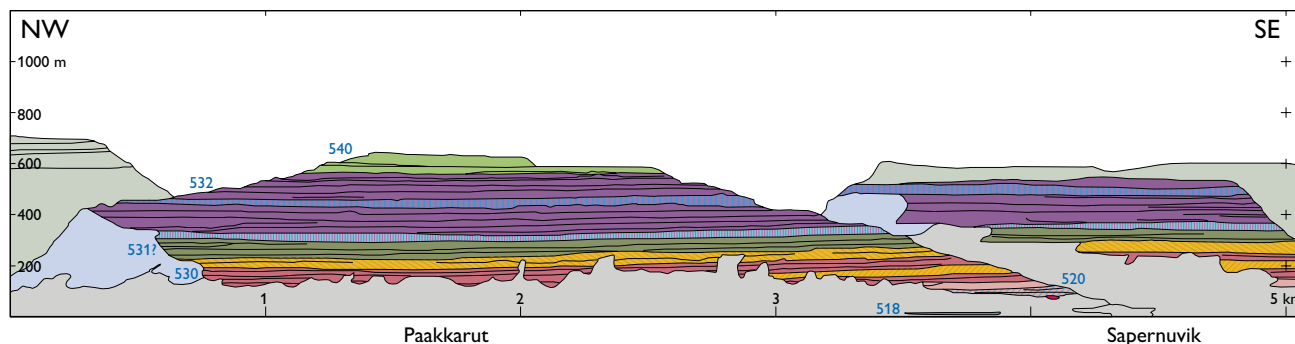


Fig. 171. The type section for the Sapernuvis Member (unit 540) and the upper Niaquassat Member (unit 532), and reference section for the lower and middle Niaquassat Member (units 530 and 531, respectively). Photogrammetrically measured section of the coastal cliff on south-western Disko between Paakkarut and Sapernuvis. Blue three-digit numbers are lithological codes. Slightly modified excerpt from the South Disko section (Pedersen *et al.* 2003). See also photograph in Fig. 161.



Fig. 172. The two lowest lava flows of the Sapernuik Member (540) conformably overlying lava flows of the upper Niaquassat Member (532). The same corrie between Sapernuik and Kingittup Qaqqaa as shown in Fig. 162 but at another place. The numbered samples are taken in the indicated flows but at another locality; the actual sample profile is shown in Fig. 161.

Geology and geochemistry of the Sapernuik Member

The Sapernuik Member (unit 540) comprises only a few lava flows. These are the youngest lava flows preserved on Disko, and they are so compositionally different from all the other flows in the Maligât Formation that they have been assigned the status of a separate member.

The lava flows of the Sapernuik Member cap four separate flat mountaintops on westernmost Disko south of Mellemfjord between Kingittup Qaqqaa and Sapernuik (Figs. 4, 161). The member has only been sampled in the type section. Here, three flows are preserved capping a lava succession that dips 2.5–3°W (Fig. 171). They conformably overlie flows of the upper Niaquassat Member (Fig. 172) and are separated from these by a few decimetres of lateritic claystone. One or two more additional flows may be present on the top plateau of Kingittup Qaqqaa. The member is cut by several basalt dykes, which may have been feeders to inferred lava flows of the younger Svartenhuk and Naqerloq formations (Larsen *et al.* 2016).

Lithologically, the dark grey lavas are fine-grained with phenocrysts of olivine and plagioclase up to a few millimetres in size. One flow also has up to 5 mm large augite phenocrysts. Two of the flows have inclusions of dolerite and gabbro up to a few centimetres in size (Fig. 173).

The four existing analyses of lava flows of the Sapernuik Member are given in Table 9. They have been plotted with the Niaquassat Member in Figs 167–170. The flows are distinctly more magnesian (7.5–10.7 wt% MgO) than the underlying evolved flows of the upper Niaquassat Member. They also have lower SiO₂ and higher CaO and appear not to be crustally contaminated. The highest flow has very high Al₂O₃ (16.3 wt%) and CaO (12.9 wt%) without being plagioclase-accumulative; it also has low FeO* and very low TiO₂ (0.8 wt%) and P₂O₅ (0.06 wt%).

The Sapernuik Member lavas have low contents of several incompatible trace elements and Cr, and highish Sc and Cu contents. The REE patterns have Gd/Lu ratios lower than any other flows in the Maligât Formation,



Fig. 173. Thin section of sparsely olivine-plagioclase phyric basalt of the Sapernuvik Member with a gabbro xenolith 1 cm large, consisting of augite (**cpx**) and plagioclase (**pl**). Sample 176614, Sapernuvik, south-west Disko.

suggesting melt formation at relatively shallow levels. The Al- and Ca-rich flow (sample 176611) has relatively high Rb, K, and Sr contents in accordance with its high normative feldspar content (52%). Larsen & Pedersen (2009) suggested that the Sapernuvik Member lavas include a component of remelted gabbroic cumulates.

Dyke systems of the Nordfjord and Niaqussat members

Summary of the main features of the contaminated dyke systems

- Weakly contaminated small dykes scattered over Disko and Nuussuaq.
- Strongly contaminated large dykes in three major zones on Disko; structurally related to the Disko Gneiss Ridge.
- Composite basalt/andesite dykes up to 80 km long, many with native iron and troilite.
- Magma chambers concentrated on north-west and east Disko.
- Subvolcanic magma chambers and tube-shaped intrusions with native iron and sulfide accumulations.
- Economic geology: Accumulations of native iron and sulfides have been subjected to exploration for Ni and platinum-group elements.

The dyke systems for the Nordfjord and Niaqussat members are treated together here because they are difficult to distinguish from each other and appear to have followed similar patterns.

Weakly contaminated dykes

The basalts and picrites of the Nordfjord and Niaqussat members were presumably erupted mainly, but not solely, west of the Disko Gneiss Ridge. On eastern Disko and south-eastern Nuussuaq there are scattered occurrences of dykes of silica-enriched magnesian basalt with 50–52 wt% SiO₂ and 7.5–13 wt% MgO, very similar to the less contaminated rocks of the Nordfjord and Niaqussat members, indicating that these magmas were also erupted over larger areas east of the Disko Gneiss Ridge (Fig. 174; Larsen & Pedersen 1992). Similar dykes occur on western Disko as single dykes or part of the larger, commonly composite intrusive systems.

Main dyke systems of the strongly contaminated magmas

A considerable number of strongly sediment-contaminated dykes, craters and necks related to the Nordfjord and Niaqussat members have been located on Disko. In contrast, no dykes of this kind are known from Nuussuaq. Many of these rocks carry native iron and sulfides. Except

for two dykes at the coast which were noted in the 1870s, these dykes were first located during the regional geological mapping, and later, as their economic potential became evident (Pedersen 1975c), during systematic prospecting by mining companies (Ulff-Møller 1991). These intrusive systems, in which dykes, feeder dykes, necks and craters are associated, have given rise to spectacular localities with native iron, sulfides and sediment xenoliths. Almost all the intrusions carry xenoliths of magma-modified mudstone and sandstone in various stages of melting and equilibration, indicating that the magmas were emplaced from high-level reservoirs situated within successions of mudstone and sandstone. Many of the dykes are composite, and eruption through such feeders would have formed the composite lava flows found within both the Nordfjord and Niaqussat members.

The dyke systems are shown in Fig. 174. The intrusions have a characteristic distribution pattern apparently influenced by the Disko Gneiss Ridge that extends S–N for about 80 km from the central south coast of Disko to Stordal in the north and continues northwards below exposure level to the Kuugannguaq valley but not farther (Chalmers *et al.* 1999). A number of intrusive systems can be recognised.

System A comprises at least 10–12 composite dykes striking NW–SE to NNW–SSE within a zone *c.* 15 km wide between the central part of Hammer Dal and Morten Porsild Dal on northern Disko. Several craters and volcanic necks are associated with the dyke bodies. The western part of the zone is poorly defined because of the strongly faulted and very poorly exposed areas along the northern west coast of Disko. Particularly important intrusions within system A, described below, are the Hammer Dal, Hanekammen and Nordfjord complexes and the Inner Giesecke Dal intrusion.

System B comprises at least two N–S-striking composite dykes, which extend for more than 50 km along the crest of the Disko Gneiss Ridge between Stordal in the north and the south coast of Disko. One of the dykes, the Killiit dyke, extends for more than 85 km. It originates as a NW–SE-striking dyke within system A north-west of Stordal; south of Stordal it changes strike to N–S and continues for more than 70 km to the south coast of Disko at Killiit.

System C comprises a few dykes striking NW–SE within a 70 km long zone along the north-east coast of Disko,

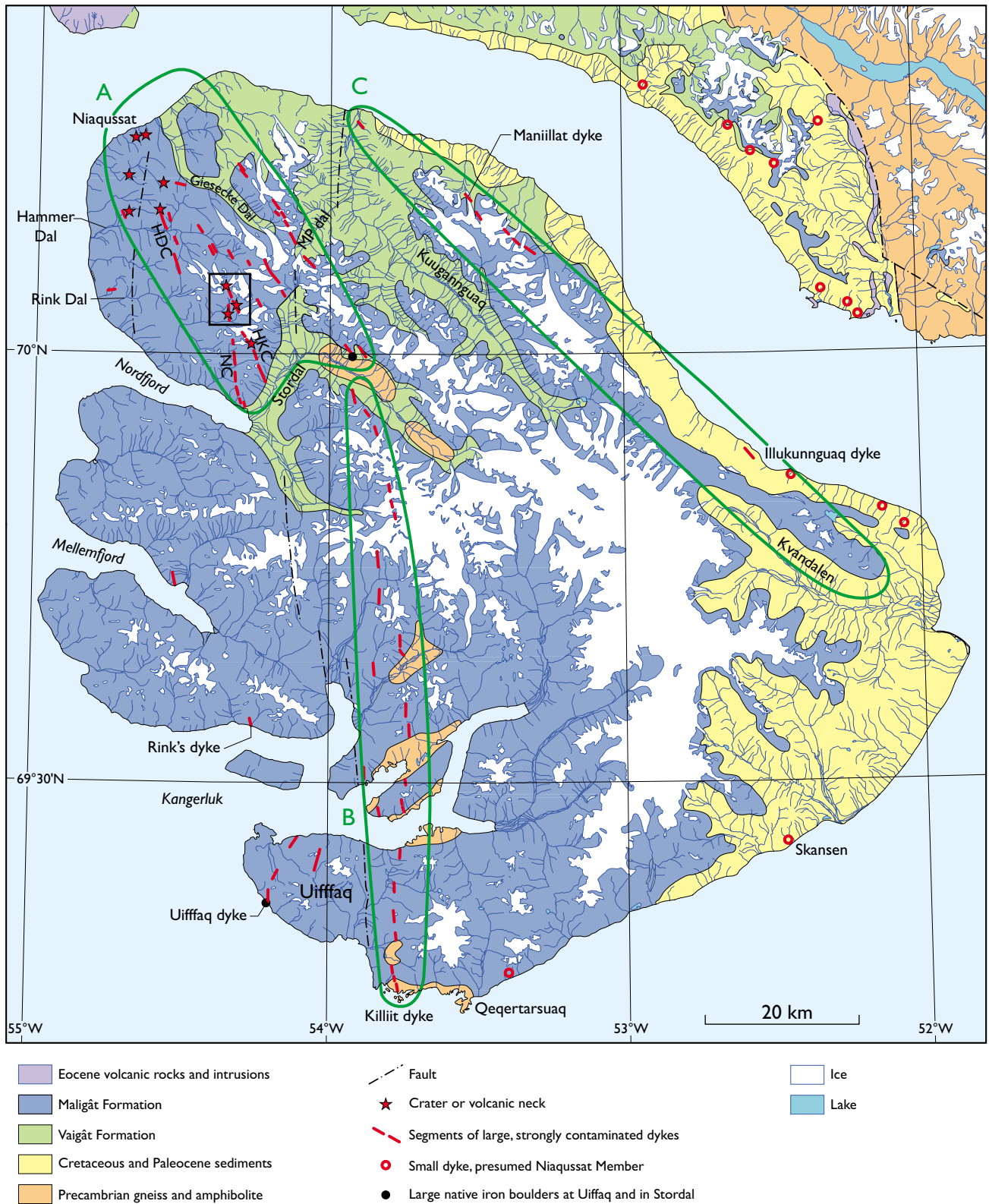


Fig. 174. Geological map of Disko and southern Nuussuaq showing the extension of the three main systems (green outlines A, B, C) of strongly contaminated, commonly native-iron- and sulfide-bearing dykes and craters described in the text. Some specific occurrences are indicated as explained in the legend. **HDC**: Hammer Dal complex. **HKC**: Hanekammen complex. **NC**: Nordfjord complex. **MP dal**: Morten Porsild Dal. The black frame on north-west Disko shows the location of the map in Fig. 181.

semi-parallel to the Vaigat strait. The easternmost dyke exposure is a sulfide-mineralised dyke at Illukunnguaq. It is possible, but not proved, that a large composite, native-iron-bearing lava flow in the Kvandalen area could have been erupted from a system C dyke.

Others comprise a number of small dyke segments striking in various directions from N–S to NNE–SSW to E–W, found between the Uiffaq peninsula west of the Disko Gneiss Ridge in the south and Giesecke Dal in the north. Parts of the areas have not been searched in any detail and are likely to contain many dyke segments, and other areas, such as the outer west coast between Nordfjord and Giesecke Dal, are extensively faulted and poorly exposed. There must also be hidden dykes in the shallow sea offshore western Disko.

Strongly contaminated dykes and lavas are conspicuously absent in the area east of the Disko Gneiss Ridge and south of Kvandalen on eastern Disko. Evidently, the Disko Gneiss Ridge had a confining influence which prevented horizontal flow of magma from the high-level magma reservoirs eastwards via dykes across the ridge. As seen for System B, the stress pattern along the crest of the gneiss ridge and within the overlying older basalts may have forced the magma conduits to change direction from SE-bound to S-bound over distances of more than 50 km. Only north of the Disko Gneiss Ridge (north-east of the Kuugannguaq valley), NW–SE-trending dyke intrusions continued eastwards within system C, allowing strongly contaminated lavas and dykes to be formed on eastern Disko.

The strongly contaminated intrusions yield important information on the sediment–magma reactions in the high-level magma reservoirs and on the sediments that participated in the contamination and redox processes, as well as on the processes in the dyke and feeder systems that led to surface-near mineralisation with native iron and sulfides. For about 100 years (1871–1971), only two intrusions with native iron and sulfide were known: the Uiffaq and Illukunnguaq dykes. An extensive literature exists on the intrusions; the history of the discovery of the intrusions and their native iron bodies is reviewed below in the sections on the individual intrusions.

Intrusions in dyke system A

Hammer Dal complex. This complex illustrates the composite nature of many of the native-iron-bearing intrusions, with an early intrusive pulse of contaminated basalt followed by a later pulse of much more contaminated andesite. The subhorizontal funnel- or tube-shaped intru-

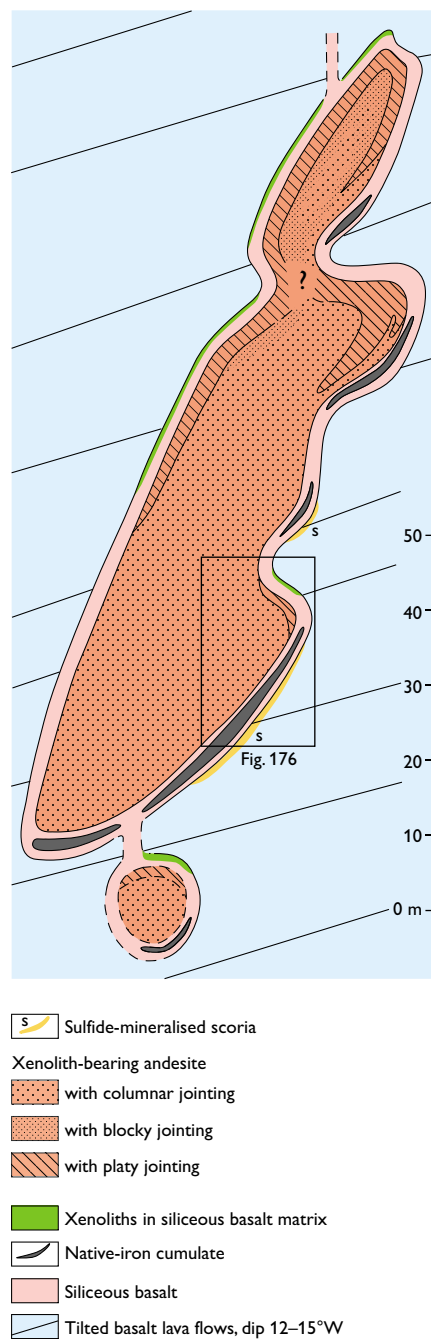


Fig. 175. Funnel-shaped intrusion in the northern segment of the Hammer Dal complex (Fig. 174). See text for description. Photogrammetrically constructed cross section, after Ulf-Møller (1977). For locality, see Fig. 103, loc. 10.

sions interconnected by thin dykes illustrate better than anywhere else the gravitational control of the mineral accumulations, with deposition of the heavy native-iron and sulfide bodies from the basaltic pulse along the lower depressions of the tubes, and accumulation of the much



Fig. 176. The lower part of the funnel-shaped intrusion in the Hammer Dal complex. **s**: the sulfide-mineralised zone. **Fe cum**: the native-iron cumulate zone in Fig. 175. The position of the photo is indicated in Fig. 175.

lighter sediment xenoliths below the hanging walls and roofs of the intrusions.

The Hammer Dal complex was first discovered in 1972 in the northern wall of Hammer Dal about 10 km from the west coast of Disko (Pedersen 1975a). It has been described by Ulff-Møller (1975, 1977, 1983). It displays spectacular cumulates of native iron and nickeliferous pyrrhotite, and accumulations of sediment xenoliths that have floated in the magma. The complex comprises a number of intrusions, which were emplaced into a succession of basalt lava flows of the Rinks Dal Member. The intrusions are situated along a zone that is now oriented 155–160°/80°W after a later westward tilting of the lava succession, with a horizontal extent of at least 7 km. The

complex also comprises a downfaulted transgressive sill about 0.5–1 km east of the main intrusions. A block diagram of the complex is shown in Ulff-Møller (1977, fig. 11). The main intrusions form westerly tilted, funnel-shaped, columnar-jointed masses which vary in thickness from 10 to 40 m; the individual intrusions are interconnected by thin basaltic dykes. The main intrusions widen to between 50 and 100 m in the uppermost, poorly exposed zone, which is probably close to the eruption site that may be a neck or a short feeder dyke.

The best-exposed part is the lowermost intrusion (Figs 175, 176). The inclined body of this has a vertical extent of 129 m and a maximum width of 30 m. It has a marginal zone up to 2–3 m wide of silicic magnesian basalt, in

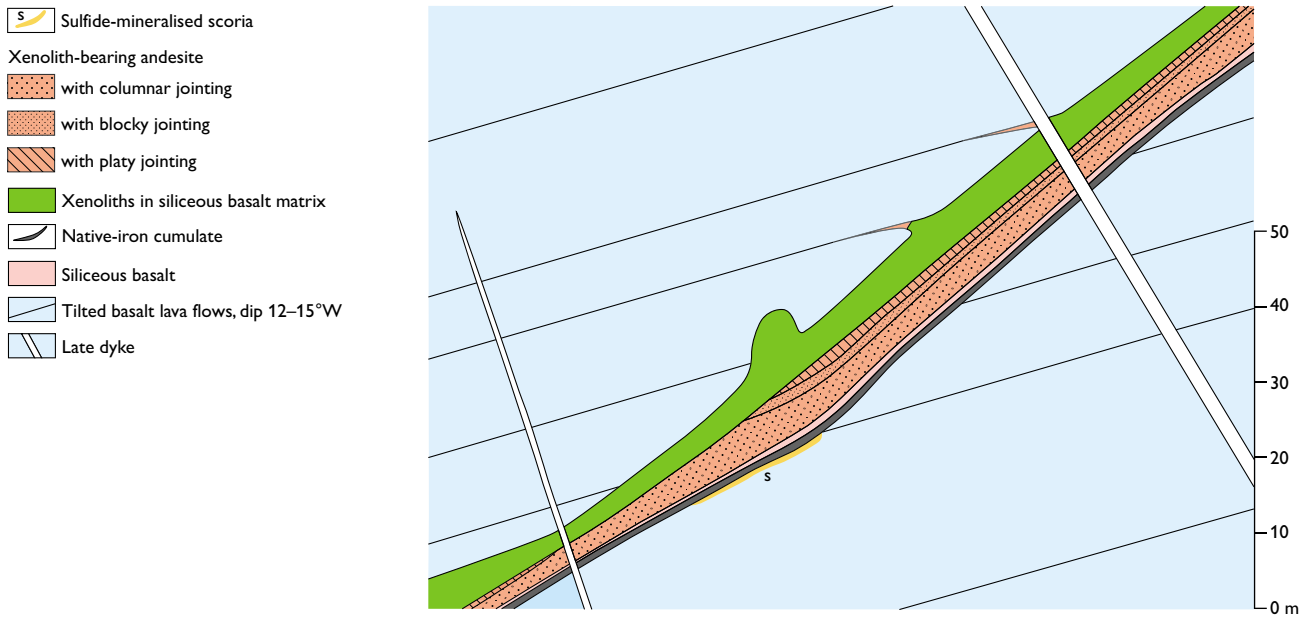


Fig. 177. Transgressive sill east of the main funnel-shaped intrusion of the Hammer Dal complex. See text for description. Photogrammetrically constructed cross section, after Ulf-Møller (1977). For locality, see Fig. 103, loc. 11.



Fig. 178. Transgressive sill east of the main funnel-shaped intrusion of the Hammer Dal complex. The sulfide mineralisation (s) and the native iron cumulate zone (Fe) are indicated. The cross-cutting dyke (d) in the right part of the photo is also seen in the right part of Fig. 177.

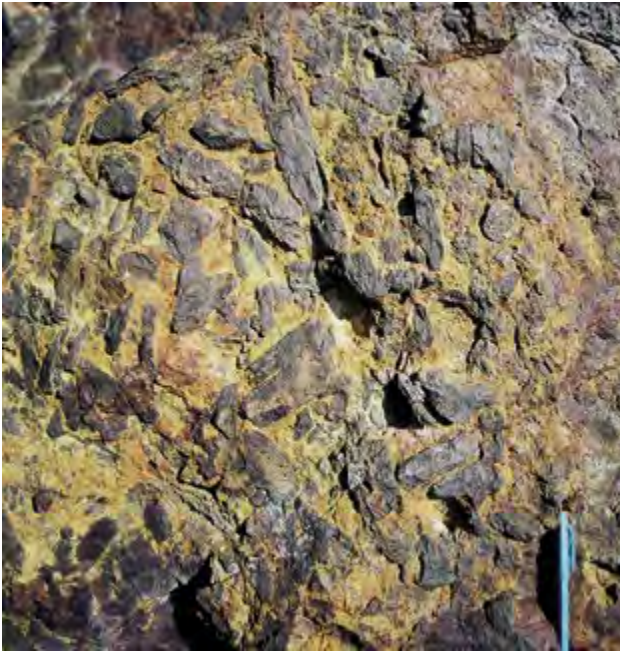


Fig. 179. Sediment xenoliths packed by floating along the upper margin of the transgressive sill of the Hammer Dal complex (Fig. 177). The xenoliths are almost all magma-equilibrated mudstone with graphite. Length of pencil 13 cm.

which native iron accumulated in local depressions. The central part consists of magnesian andesite with native iron (Table 11; Ulf-Møller 1983, table 7).

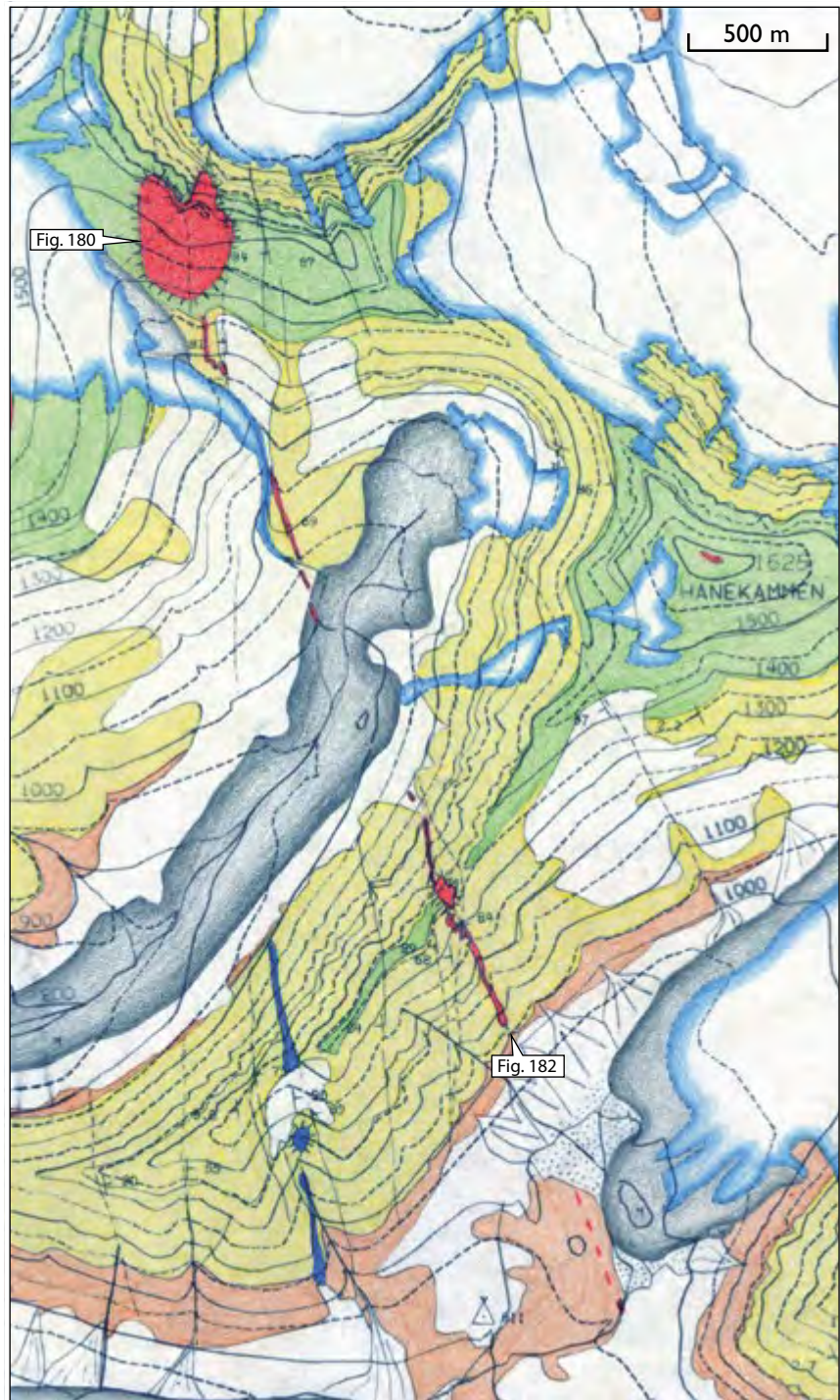
The transgressive sill intrusion east of the main intrusion is up to 10 m thick and is cut by younger, uncontaminated basalt dykes (Figs 177, 178). The sill is composite, like the main intrusions, and has a lower basaltic part with native-iron accumulation and an upper basaltic part; the central part is a fairly silicic graphite andesite with native iron (Ulf-Møller 1983, table 7). Along the lower margin of the transgressive sill, where it cuts across the vesiculated top zone of a basaltic lava flow, a less than 1 m thick zone is developed that is heavily mineralised with nickeliferous pyrrhotite. The basaltic upper margin of the sill is strongly contaminated and packed with sediment xenoliths. Inspection of these sediment accumulations reveals a strong dominance of graphitic, magma-equilibrated mudstone, while sandstone is scarce (Fig. 179).

Hanekammen complex. The Hanekammen complex was discovered in 1972 (Pedersen 1975a) and later investigated by F. Ulf-Møller (Pedersen & Ulf-Møller 1980,



Fig. 180. Volcanic neck of the Hanekammen complex, seen from the west. The 300–400 m wide neck is shown in the upper left part of the map area in Fig. 181.

Fig. 181. Geological map of an area on north-west Disko with the Hanekammen complex necks and dykes (red) and the Nordfjord complex neck and dykes (blue). The surrounding lava succession is the Rinks Dal Member; pale brown: Fe-Ti rich basalt, yellow: aphyric and feldspar-phyric basalt, green: feldspar-phyric basalt. The red lava remnant on the peak Hanekammen is a Nordfjord Member flow. Dark grey is moraine and white with blue margins is ice. Map by Finn Ulff-Møller (1983). The map location is shown in Fig. 174.



Ulff-Møller 1983, p. 28–55 and Ulff-Møller 1990). The complex comprises a number of intrusions. The northernmost part is a prominent volcanic neck *c.* 2.5 km north-west of Hanekammen (Figs 180, 181). It measures 300 × 400 m in cross section and probably represents an eruption site. The neck is composed of basaltic andesite with native iron and is rich in sediment xenoliths. A series

of NNW–SSE-trending dykes extends from this neck for at least 13 km towards south-south-east. In the northern 3 km there are several irregular dyke intrusions, whereas the southern 10 km is a simple *en echelon* dyke which has its southernmost exposure in the western wall of Stordal. The composite intrusions have early marginal pulses ranging from native-iron-bearing, contaminated basalt to



Fig. 182. Dyke and crater of the Hanekammen complex viewed from the south-south-east along the strike of the near-vertical dyke. The dyke (**d**) is seen here to widen upwards into an eruption site with an oxidised crater breccia (**cr**) on the crest of the ridge in the foreground. The larger volcanic neck in Fig. 180 is visible on the ridge in the background. Compare with the map in Fig. 181. Photo: Finn Ulff-Møller.

almost uncontaminated basalt, whereas the later pulses consist of native-iron-bearing basaltic andesite.

The Hanekammen complex has been investigated in detail on the SE-exposed wall of a large ridge extending from the peak Hanekammen towards the south-west. Here, several tube-shaped or irregular, horizontal intrusive bodies are connected into a subvertical dyke that

widens upwards to form an eruption site with crater breccia on the top of the ridge (Fig. 182). The lowermost intrusive body is particularly instructive (Fig. 183; Table 11). It is an irregular intrusion with a marginal zone of native-iron-bearing, silicic basalt which contains a small native-iron cumulus zone, and a later central pulse of native-iron-bearing basaltic andesite which contains chemi-

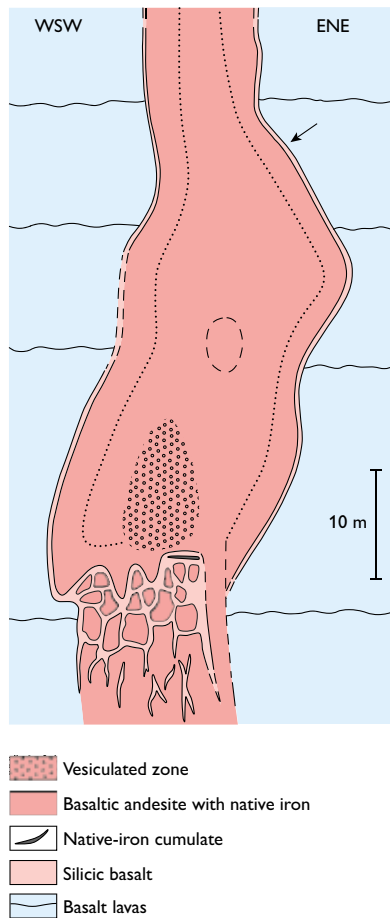


Fig. 183. The lowermost intrusive body of the Hanekammen complex. See text for description. The arrow points to an accumulation of sediment xenoliths in the marginal basalt. Drawing modified from Ulf-Møller (1990). Location indicated in Fig. 182.

cally zoned native-iron bodies. This intrusion was used by Ulf-Møller (1990) to discuss the relation between zoning in the native iron and the dynamics of the process of contamination with crustal rocks.

Nordfjord complex. The Nordfjord complex was discovered in 1979 (Pedersen & Ulf-Møller 1980) and described by Ulf-Møller (1983, p. 56–65). A small outcrop on the north coast of the innermost part of Nordfjord, consisting of silicic basalt with a very rich assemblage of sediment xenoliths, had already been discovered in 1968 (Pedersen 1969).

Exposures are fragmentary. The main exposure has a N–S extent of 1 km and is found on both the north-western and south-eastern wall of the ridge extending south-west from the Hanekammen peak (Fig. 181). It



Fig. 184. The Nordfjord complex in the south wall of Rink Dal, north-western Disko. The complex here forms a subhorizontal, funnel-shaped intrusion with spectacular columnar jointing. The height of the intrusion tube seen is 20 m. Photo: Finn Ulf-Møller.

comprises a composite dyke up to 10 m wide that has locally developed upwards into a brecciated crater pipe with a circular outline and a diameter of *c.* 60 m. Just 70 m below the crater, a tubular subhorizontal intrusion is exposed that has a height of 35 m and a width of at least 25 m. It is composite, and its basaltic marginal part (Table 11) contains small native-iron bodies and a zone with 10–15 cm-sized, coarse-grained plagioclase-olivine nodules. The inner part of the intrusion is a younger pulse of basaltic andesite to andesite with native iron (Table 11). About 2 km south of the crater, on the south wall of Rink Dal, the complex continues as a funnel-shaped, subhorizontal intrusion that shows spectacular columnar jointing (Fig. 184). The core of this part of the intrusion is a native-iron-bearing silicic basalt (Ulf-Møller 1983, table 5, no. 3) similar in composition to the silicic basalt



Fig. 185. The 10 tons native iron boulder found in Stordal in 1985 (Fig. 174). The boulder measures $0.8 \times 1.5 \times 2$ m and comes from a 2 m thick, contaminated basic dyke from which it is slightly displaced due to sliding. The substrate in the photo is a lava flow.

found on the north coast of Nordfjord (Pedersen 1969). This indicates that the Nordfjord complex extends for at least about 12 km.

The chemical compositions of the rocks of the Nordfjord complex are very similar to the most common magnesium-poor basalts and basaltic andesites represented by most of the contaminated lavas of the Nordfjord Member.

Stordal dyke with 10 tons native-iron boulder. For the first time in more than 100 years of research, a new major boulder of native iron was discovered in 1985 (Ulff-Møller 1986). The locality is in the northern wall of Stordal about 3.5 km east-south-east of Point 780 m at 389 m altitude (central Disko section at 33.2 km; Fig. 174). The boulder belongs to a 2 m thick, contaminated basic dyke from which it is slightly displaced due to sliding. It measures $0.8 \times 1.5 \times 2$ m and has an estimated weight of about 10 tons (Fig. 185). A modal and chemical comparison with the large Uiffaq native-iron boulder (Table 10; Ulff-Møller, unpublished data 1990) shows that the Stordal

boulder contains much more troilite (FeS) and much less cohenite (Fe_3C) than the Uiffaq boulder.

The host dyke trends NW–SE and forms part of a small swarm of two to three thin dykes that cut lavas and hyaloclastites of the Vaigat Formation but not the underlying Disko Gneiss Ridge. The dyke belongs to dyke

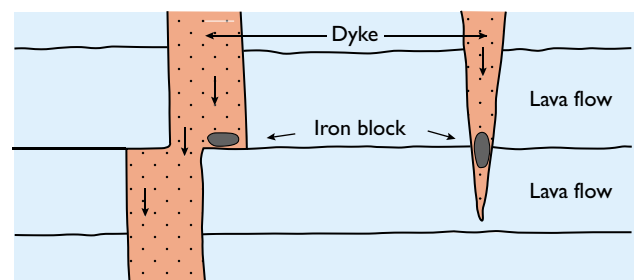


Fig. 186. A model for native iron accumulation in steep intrusions from droplet size to boulder size by gravity accumulation (arrows) at irregularities such as on ledges and in wedges. After Ulff-Møller (1986).

Table 10. Estimated compositions of native iron boulders from Disko

Locality	Stordal	Uiffaq
Year of find	1985	1870
Weight, tons	10	25
<i>Estimated mode, vol.%</i>		
Iron	60	43
Cohenite	7	54
Troilite	30–40	3
Schreibersite	0	Trace
Silicate glass	0.1	0
Chromite	0.01	0
Wüstite	Trace	?
<i>Calculated chemical composition, wt%</i>		
Fe	80	91.6
Co	0.4	0.5
Ni	2	1.8
Cu	0.1	0.16
C	0.5	3.62
P	0.4	0.15
S	10–15	1.09
O	Trace	0.97

Source: Finn Ulff-Møller, personal communication, c. 1990.

system A and is interpreted as the result of horizontal magma transport from a high-level magma reservoir situated within the sedimentary basin north-west of the Disko Gneiss Ridge. The dyke rock is olivine-phyric and contains native iron and many xenoliths of graphite-rich, magma-modified mudstone. Its composition varies between silicic basalt and basaltic andesite (Table 11, samples F062, F066). A model for native-iron accumulation from drops to block size is shown in Fig. 186 (Ulff-Møller 1986).

Inner Giesecke Dal dyke zone. This is the easternmost part of dyke system A. The zone is rather narrow and extends from east of Giesecke Dal in the north-west for more than 22 km to Stordal in the south-east, where it lies east of the Stordal dyke described above (Fig. 174). The zone hosts a number of NW–SE-trending, contaminated dykes that are basaltic at the north-western and south-eastern ends and composite with native-iron-bearing andesitic cores within an 8 km long central part of the zone. The central part is therefore interpreted as the primary upwelling zone for the strongly contaminated magmas from a reservoir within a succession of mudstones and sandstones. These dykes have been investigated and sampled by F. Ulff-Møller (Ulff-Møller 1991), but the results have not been published before.

The northernmost dyke in this zone has been sampled 2–3 km north-west of Point 1460 m north of Giesecke Dal (Fig. 103, loc. 28). It is a NW-trending, 4–5 m thick,



Fig. 187. The northernmost contaminated dyke in the Inner Giesecke Dal dyke zone, 2–3 km north-west of Point 1460 m north of Giesecke Dal (Fig. 174). Length of hammer handle 60 cm. Photo: Finn Ulff-Møller.

regularly columnar-jointed dyke of contaminated basalt (Fig. 187) with about 8.9 wt% MgO.

The southernmost dyke in the zone cuts the Disko Gneiss Ridge and the Vaigat Formation (Fig. 174). It is 8–10 m thick and has fine-grained margins and a crumbling core of more coarse-grained dolerite; from a distance, this gives it the appearance of a double dyke. It consists of contaminated basalt with 11.3 wt% MgO and is rich in graphite-bearing magma-modified mudstone xenoliths 2–7 cm in size.

The central part of the dyke zone hosts one major dyke and several smaller ones, which are all composite with native iron. Within 1 km of the main dyke, the smaller dykes may cut each other at low angles.



Fig. 188. The southernmost exposures of the Inner Giesecke Dal intrusion, *c.* 2 km north-west of Point 1650 m north of Agatfjeldet, at the end of Morten Porsild Dal (Fig. 174). The intrusion forms a segmented composite dyke *c.* 7 m thick, with basaltic to basaltic andesitic margins and an andesitic native-iron-bearing core. Photo: Finn Ulff-Møller.

Inner Giesecke Dal intrusion. The single major dyke in the Inner Giesecke Dal dyke zone is named the Inner Giesecke Dal intrusion. The northernmost, well-exposed part of the Inner Giesecke Dal intrusion is located *c.* 500–600 m west of Point 1560 m north-east of Giesecke Dal (Fig. 103, loc. 29), where it forms a spectacular, native-iron-bearing composite dyke about 10 m thick. The dyke is rich in sediment xenoliths and its core is strongly contaminated and transitional between basaltic andesite and andesite in composition. In the same area a loose boulder with a native-iron cumulate zone more than 0.5 m thick was located, together with other loose blocks with kidney-shaped native-iron bodies with troilite rims 2–3 cm in size.

The central part of the Inner Giesecke Dal intrusion is exposed around the top of the high plateau at Point 1590 m between Giesecke Dal and Morten Porsild Dal (Fig. 103). Here, the intrusion is 12–15 m wide and dips *c.* 70° NE; it has a distinctly rusty colour due to weather-

ing of native iron and sulfide. The dyke is composite with 1–2 m thick basaltic margins and an andesitic core; as an unusual feature, it also contains an inner zone of basalt 1 m thick, which is slightly chilled against the andesite. The marginal basalt contains small native-iron cumulates along the footwall and sediment accumulations along the hanging wall. Another, parallel, composite dyke with native iron occurs *c.* 10 m south-west of the main dyke.

The southernmost exposures of the Inner Giesecke Dal intrusion are situated *c.* 2 km north-west of Point 1650 m north of Agatfjeldet, on walls at the end of Morten Porsild Dal (Fig. 174). Here the intrusion forms a *c.* 7 m thick, segmented, composite dyke dipping 70° NE. It has a basaltic to basaltic andesitic margin *c.* 0.5 m thick, and an andesitic core with up to 1 cm large native-iron bodies (Table 11, nos F045 and F048; Fig. 188). On both sides of the composite intrusion, there are several 1–4 m thick, subparallel basaltic intrusions with sediment xenoliths, and also other intrusions that are only slightly contaminated.

Outer Giesecke Dal dyke. A prominent composite dyke intrusion was discovered by F. Ulf-Møller in 1984 *c.* 8 km south-east of the entrance to Giesecke Dal and *c.* 1.5 km east of the volcanic neck at Point 882 m (Fig. 103, loc. 30). The dyke trends WNW–ESE and is well exposed on both walls of a gully south of Giesecke Dal from where it can be traced eastwards for 3 km. The dyke is up to 25 m thick and composite, with a marginal zone of contaminated basalt up to 7 m thick, which locally contains a native-iron cumulus zone several metres thick, and a core zone of basaltic andesite with native iron and sediment xenoliths.

Small swarm of NW–SE-trending dykes around innermost Hammer Dal. A small swarm of at least five NW–SE-trending dykes discovered by F. Ulf-Møller in 1985 and 1987 in the innermost Hammer Dal area belongs to dyke system A.

A ‘double dyke’ (two closely set parallel dykes) has a main exposure *c.* 3 km NNW of Point 1380 m (Fig. 103, loc. 31). The western dyke is 6–8 m thick and distinctly contaminated (Table 11, no. F074). It is notable for a rich assemblage of xenoliths up to 1 m large of magma-modified sandstone and mudstone and abundant, 2–50 cm large gabbroic nodules. The eastern dyke is 20–30 m thick and only slightly contaminated (Table 11, no. F076). It is composed of medium- to coarse-grained dolerite with light grey residual veins and up to 5 cm large gabbroic xenoliths.

About 1.5–2 km east of the double dyke is another parallel basaltic dyke (Fig. 103, loc. 32; Table 11, no. F162) which is *c.* 5 m thick and contains glomerocrysts up to 1 cm large of plagioclase and abundant xenoliths of sandstone and mudstone. Along the strike and across a glacier, 8 km to the south-east, loose blocks of contaminated basalt from a dyke occur in the talus close to Steenstrup Dal. The basalt contains coarse plagioclase and olivine glomerocrysts and abundant small xenoliths of sandstone and mudstone and is similar to, but less evolved than, the dyke 8 km to the north-west.

About 1.5–2 km farther to the east another composite dyke *c.* 4 m thick is exposed a few kilometres south-west of Point 1610 m (Fig. 103, loc. 33). It strikes NNW–SSE and is composed of a distinctly flow-laminated, contaminated basalt with a core of more silicic, contaminated basalt with disseminated graphite (Table 11, no. F169). A similar, flow-laminated dyke has been traced a few kilometres to the north-west and is probably the same dyke. The flow-lamination is very irregular and discordant to the strike direction of the dyke.

Finally, a NW–SE-trending dyke has been traced south-east of the Point 1610 m plateau between the innermost parts of Hammer Dal and Giesecke Dal (Fig. 103, loc. 34). This dyke is a *c.* 10 m thick, contaminated, evolved dolerite (Table 11, no. F173) with scattered, *c.* 1 cm large xenoliths of plagioclase and graphite, i.e. magma-modified mudstone.

Intrusions in dyke system B

Killiit dyke. The third discovery of a native-iron-bearing intrusion came almost 100 years after the Uiffaq report, when Fundal (1972, 1975) described an 8 m thick basalt dyke with native iron and plagioclase-spinel-graphite xenoliths cutting the Disko Gneiss Ridge at Killiit (old spelling Kitdlit) on the south coast of Disko, 9 km west of Qeqertarsuaq town (Figs 27, 36). Another segment of the dyke at Luciefjeld *c.* 7 km north of the coast cuts basaltic lavas of the Rinks Dal Member but not the underlying gneiss. Based on these observations Fundal (1975) argued that the native iron and the graphite-bearing xenoliths could not be a product of sediment–magma reaction but required a much deeper origin. The same arguments were subsequently pursued by Bird and Weathers (1977) but were later abandoned by Bird *et al.* (1981).

The Killiit dyke was subsequently mapped northwards along the Disko Gneiss Ridge over a distance of more than 80 km (Pedersen 1977c; Ulf-Møller 1979; Pedersen & Ulf-Møller 1980; Ulf-Møller 1983, 1985). In the south the dyke is basaltic (e.g. Pedersen 1979b table 2) and strikes close to N–S. About 65 km north of Killiit it changes direction to NW–SE and becomes composite with a basaltic margin and an andesitic core (Table 11; Ulf-Møller 1985, table 1, nos 2 and 3; Fig. 189). The dyke increases in thickness to 10–15 m towards the north and was clearly emplaced from the north-west. In the northern area, there are several offshoots from the dyke that consist of basalt packed with gneiss xenoliths (Fig. 190). In a limited area, the dyke develops an oxidised, crater-like breccia along one of its margins. From just north of Kangerluk, a *c.* 100 kg native-iron body called the Kitdlit Lens has been described in detail and reveals a complex solidification history (Ulf-Møller 1985). This paper is a major contribution to our knowledge about the native iron.

The present interpretation of the Killiit dyke is that it originated from a high-level magma reservoir within the sedimentary basin north-west of Stordal as a part of dyke system A. The intrusion was emplaced in several pulses, of which the first was a native-iron-bearing basalt magma



Fig. 189. The northern part of the Killiit dyke, 65 km north of Killiit. The dyke (Fe) is here *c.* 15 m thick and cuts lava flows of the Rinks Dal Member. It is composite with a basaltic margin and a *c.* 13 m thick andesitic core; both parts are native-iron-bearing. Locality *c.* 10 km south of Stordal and *c.* 1 km west of Point 1266 m (Figs 6, 174). Photo: Finn Ulff-Møller.



Fig. 190. Offshoot from the Killiit dyke 75 km north of Killiit. The dyke here trends NW and cuts lava flows of the Rinks Dal Member. The apophysis is *c.* 1 m thick and consists of basalt packed with xenoliths of gneiss or arkose. Locality *c.* 1 km east of Point 1578 m in the north-western side of a corrie leading into the south side of Stordal (Figs 6, 174). Photo: Finn Ulff-Møller.

that travelled subhorizontally for more than 85 km towards the south to Killiit, where basalt with sediment xenoliths and native iron has now been found cutting the Disko Gneiss Ridge. When the dyke changed direction to N–S, about 65 km north of the coast it became part of dyke system B. Shortly afterwards, a second pulse of much more contaminated and viscous andesite magma with native iron was emplaced towards the south but became exhausted after having travelled only 15–20 km.

Intrusions in dyke system C

Maniillat dyke. The Maniillat dyke trends NW–SE and runs subparallel with the Vaigat coast on north-eastern Disko for at least 12 km between Maniillat and Pyramiden (Fig. 174). The dyke dips 70–80° NE and is 5–6 m thick in its northern part and around 10 m thick farther south. It cuts both picritic lavas of the Vaigat Formation and basalt flows of the Rinks Dal Member of the Maligât Formation. The dyke has marginal zones of contaminated basalt (Table 11, no. 138235) with olivines up to 2 cm in size and native-iron bodies up to 1 cm in



Fig. 191. The Maniillat dyke (Fig. 174) with an accumulation of closely packed, black sediment xenoliths along its hanging wall. Length of ruler 1 m.

size, beside a range of sediment xenoliths and also sharp-edged xenoliths of uncontaminated basalt with plagioclase phenocrysts. The central, 4–6 m wide part of the dyke (Table 11, no. 138233) has a sharp, but not glassy, contact against the marginal basalt and is composed of andesite with microphenocrysts of olivine and orthopyroxene; it also contains disseminated graphite and xenoliths of magma-modified mudstone. Along the hanging wall, the marginal basalt is particularly rich in sediment xenoliths, and at one locality it contains a 40 cm thick zone of densely packed xenoliths of sandstone, mudstone and coal fragments with an appearance almost like a sediment breccia (Fig. 191). The dyke disappears beneath the glacier- and moraine-filled areas around Qullissat. It is possibly connected to the small dyke segment at Illukunnguaq *c.* 35 km to the south-east (see below).

Illukunnguaq dyke. The second early known intrusion is a 5 m thick basic dyke intruding sandstone of the Atane Formation near the abandoned settlement Illukunnguaq (Igdlukúnguaq) on eastern Disko. The dyke strikes NW–SE and can be followed for about 800 m close to the Vaigat coast (Steenstrup 1874, p. 88, also briefly mentioned by Nordenskiöld 1871). The dyke contained a 28 tons body of nickeliferous pyrrhotite (now nearly mined out) that was described in detail by Pauly (1958). The dyke also contains a range of sediment xenoliths (Fundal 1975). The occurrence shows that the contaminated intrusions have a potential for sulfide mineralisation. The dyke has been described by Ulf-Møller (1983, p. 92–98) who found sulfide blebs with native iron in its glassy chill

zone. An analysis is presented in Table 11, no. 362140. The dyke is now interpreted as part of dyke system C, and it is possible that it acted as feeder for the composite native-iron-bearing lava flow in the lower Niaqussat Member on eastern Disko (Fig. 10, profile 8; Fig. 140).

Other dyke intrusions

Uiffaq dyke. The discovery of three large native-iron boulders (25, 6.5 and 4 tons) on the south-western shore of the Uiffaq peninsula west of Qeqertarsuaq was reported by Nordenskiöld (1871) who interpreted them as iron meteorites. Their unusual composition was reported by Nordström (1871). The history of recovery and research of the native iron is summarised by Sjögren (1916) and an extensive bibliography is given by Bøggild (1953). A memoir based on the largest (25 tons) iron boulder housed in Stockholm (Löfquist & Benedicks 1941) showed that the native iron is dominated by iron carbide (cohenite) and is a cast-iron type. Field observations by Nauckhoff (1872, p. 38) and Steenstrup (1875, fig. 3) suggested the presence of a poorly exposed basaltic dyke at the shore. The host body for the native-iron boulders was finally proved by magnetometer mapping to be a *c.* 7 m thick, approximately N–S-running, composite basaltic dyke (Fundal 1975). Various segments of the dyke have been mapped over a distance of 8 km across the Uiffaq peninsula to its north coast (Pedersen *et al.* 2000); the dyke is shown in Fig. 81. Detailed data on the Uiffaq native iron and sulfide have been presented by Goodrich (1984), Goodrich & Bird (1985) and Howarth *et al.* (2017).

Rink's dyke. For many years, the existence of this dyke was inferred from a sample collected by H. Rink around 1850 on the north coast of Kangerluk. The dyke was rediscovered by F. Ulf-Møller in 1978 (Fig. 174) and briefly described by him (Ulf-Møller 1979, 1983). It is only known to be exposed at the beach where it is vertical, *c.* 4 m thick and strikes N–S. It is composite, with a marginal zone of silicic basalt, a hybrid zone 10–20 cm thick, and a central part 2.5 m thick of basaltic andesite (Table 11). The central part contains numerous 1–10 cm equilibrated sediment xenoliths consisting mainly of plagioclase and graphite. No native iron was observed.

Mellemfjord dyke. This dyke was discovered by AKP in 1974 at Saqqarliit Ilorliit on the north coast of Mellemfjord (Fig. 174) and described by Ulf-Møller (1979, 1983). The dyke is exposed over about 1 km where it is vertical and strikes N–S; it is *c.* 10 m thick at low altitudes but narrows to just 1 m at 700 m a.s.l. The dyke is rich in vesicles. Chemically it is a basaltic andesite (Table 11), probably with a more basic margin. The chilled margin contains sulfide blebs but no native iron.

Concluding remarks on the strongly contaminated dyke systems

The largest and most frequent strongly contaminated intrusions are situated on western and north-western Disko west of the Disko Gneiss Ridge. Therefore, the high-level magma reservoirs within the underlying sediments must have been concentrated in this area, and possibly also beneath the shallow sea north-west of Disko. In addition to the described contaminated intrusions, there are other minor exposures on Disko west of the Disko Gneiss Ridge, and a detailed search, particularly on south-western Disko, would doubtlessly increase the known localities. However, the general picture will most probably not change.

Chemical compositions of the Nordfjord and Niaqussat Member dykes and feeder systems

The intrusions range from only slightly contaminated silicic basalts to strongly crustally contaminated andesites; there are no dacites or rhyolites. The chemical compositions are illustrated in Fig. 192, and representative analyses are shown in Table 11. Most of the contaminated intrusives have compositionally similar counterparts in the lavas of the Nordfjord and Niaqussat members (Figs 145, 147, 167, 169), but some have not, most notably the Killiit dyke which has higher MgO for a given SiO₂ than any other intrusions or lavas.

The weakly contaminated dykes on eastern Disko and Nuussuaq (green dots in Fig. 192) represent an almost normal magma evolution series. In contrast, the large intrusive dyke and crater complexes, such as the Nordfjord complex, the Hanekammen complex and the Killiit dyke, show different compositional evolutions, mainly caused by different compositions of the starting magmas of each system. The Killiit dyke had the most magnesian starting magma (12–13 wt% MgO), the Hanekammen complex was intermediate (9–10 wt% MgO) and the Nordfjord complex was the most evolved (*c.* 8 wt% MgO). The contamination processes comprised sidewall melting, mixing, mineral re-equilibration and reduction (e.g. Ulf-Møller 1990; Larsen & Pedersen 2009), and in each system the contamination led to increasing SiO₂ and K₂O and decreasing MgO, CaO and FeO*, while TiO₂ and P₂O₅ stayed approximately constant. The Cr contents are higher than in uncontaminated magmas because chromite fractionation was delayed by the contamination process (Pedersen 1985), but all the intrusions have a lower degree of Cr-enrichment than the most contaminated rocks of the Vaigat Formation (the Asuk and Kûgánguaq members). Also, no intrusions show Ni-depletion as severe as in the Asuk and Kûgánguaq members, but some native-iron-bearing samples of the Hanekammen complex and the Stordal dyke show Ni-accumulation, presumably in the metallic phase.

There are no compositional differences between dyke systems A, B and C described above. Dyke groups such as the dykes in Giesecke Dal and inner Hammer Dal show widely variable compositions, and the individual dykes must have been generated independently of each other. There are not enough chemical data to characterise the Hammer Dal complex further.

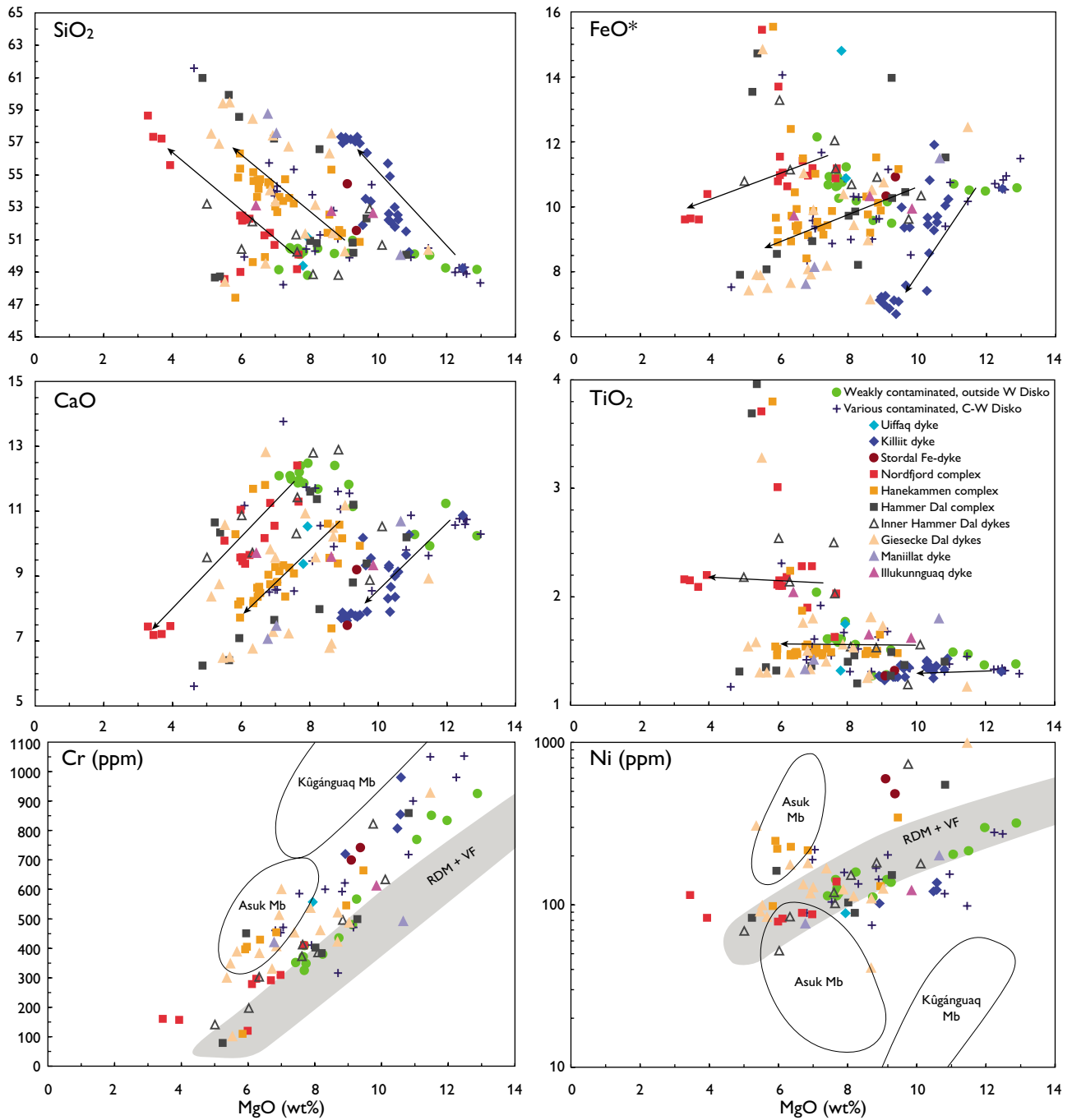


Fig. 192. Variation diagrams of selected major and trace elements for contaminated intrusions of the Nordfjord and Nuaqsat Members. Major element data in wt% oxides recalculated volatile-free. FeO* is total iron as FeO. C–W: central to west. Arrows indicate compositional changes with increasing contamination in the Killiit dyke and the Nordfjord and Hanekammen complexes. The fields for the contaminated Asuk and Kùgànguaq Members of the Vaigat Formation are shown for comparison in the Cr and Ni diagrams. The shaded areas in these two diagrams labelled **RDM + VF** are the fields for the uncontaminated Rinks Dal Member and the uncontaminated parts of the Vaigat Formation.

Table 11a. Chemical analyses of intrusions of the Nordfjord and Niaquassat Members

Intrusion	Hammer Dal complex		Hanekammen complex		Nordfjord complex		Stordal dyke		Inner Giesecke Dal		Inner Hammer Dal swarm	
	Margin	Centre	Margin	Centre	Margin	Centre			Margin	Centre		
Locality	Hammer Dal		Hanekammen		Rink Dal		Stordal		Giesecke Dal		Inner Hammer Dal	
Lith. code	6261	6261	6161	6161	6271	6271	6281	6281	6291	6291	6281	6281
GGU No.	175950	176007	264355	264424	264350	264349	F062	F066	F045	F048	F074	F076
Deg. W	5434.27	5434.27	5419.78	5419.86	5421.8	5421.8	5355.62	5355.62	5404.30	5404.30	5423.43	5423.39
Deg. N	7009.14	7009.15	7002.99	7003.00	7002.7	7002.7	6959.75	6959.75	7006.40	7006.40	7006.91	7006.91
Altitude, m	472	490	1055	1100	1015	1030	385	386	1223	1222	592	587
SiO ₂	49.15	57.55	50.38	53.92	48.42	56.10	50.09	53.01	52.10	58.61	51.00	47.92
TiO ₂	1.37	1.30	1.47	1.43	2.97	2.10	1.281	1.237	1.761	1.281	2.095	1.513
Al ₂ O ₃	13.49	14.35	14.17	16.30	13.54	15.70	14.33	13.91	14.66	15.57	14.93	15.00
Fe ₂ O ₃	0.88	0.00	1.22	0.00	4.06	2.55	11.79	11.18	10.74	8.22	12.11	11.65
FeO	10.52	8.40	9.96	8.73	9.88	7.14						
MnO			0.16	0.12	0.21	0.13	0.145	0.135	0.154	0.116	0.166	0.176
MgO	10.62	5.85	9.37	6.22	5.92	3.38	9.10	8.86	6.84	5.59	6.19	7.94
CaO	10.00	6.97	9.84	7.98	10.91	7.02	8.94	7.28	9.35	6.41	9.52	12.55
Na ₂ O	1.66	2.17	1.99	1.84	2.54	2.32	1.73	1.73	2.05	2.28	2.19	2.04
K ₂ O	0.310	1.400	0.330	0.900	0.260	1.250	0.604	0.845	0.756	1.021	0.491	0.177
P ₂ O ₅	0.120	0.150	0.150	0.180	0.310	0.280	0.156	0.170	0.201	0.187	0.217	0.132
Volatiles	1.63	1.75	1.06	2.09	1.03	1.95	1.53	1.14	0.86	0.35	0.63	0.54
Sum	99.75	99.52	100.10	99.71	100.05	99.92	99.69	99.49	99.47	99.64	99.55	99.64
FeO*	11.31	8.40	11.06	8.73	13.53	9.43	10.61	10.06	9.66	7.40	10.90	10.48
mg number	65.50	58.48	63.15	59.04	46.94	42.02	63.44	64.06	58.87	60.43	53.47	60.51
Zn	79.1	55.7	72.0	53.0	181	99.2	65.4	76.0	87.8	64.2	94.3	73.4
Cu	138	119	148	127	294	114	59.8	171	49.4	55.9	105	161
Ni	548	161	343	228	78.9	115	151	482	128	84.0	84.5	152
Sc	33.8	27.4	31.0	26.9	37.1	30.0	33.5	28.7	32.6	25.7	34.7	37.3
V	284	187	258	213	432	209	308	244	266	185	279	323
Cr	859	450	665	429	120	160	936	742	601	388	303	386
Ga	18.7	19.5	19.6	21.8	24.1	24.9	16.8	19.3	20.9	21.2	22.3	19.4
Rb	6.76	32.2	7.54	26.3	4.77	33.8	3.48	15.8	13.5	39.2	23.2	2.61
Sr	165	185	191	230	243	238	181	192	199	218	215	199
Y	23.5	27.5	23.2	24.2	39.8	34.2	16.5	21.3	24.8	25.3	30.9	23.6
Zr	96.6	192	111	155	181	218	64.5	114	132	190	155	81.1
Nb	4.14	7.84	4.90	7.27	9.08	10.25	2.71	5.13	6.02	8.37	7.32	4.16
Cs	0.237	0.805	0.220	0.763	0.135	0.814	0.128	0.344	0.327	1.04	0.434	0.038
Ba	62.01	304	127	270	53.79	348	39.4	148	145	340	163	28.8
La	7.02	19.5	10.4	18.0	10.1	23.4	4.68	11.7	12.8	21.9	13.3	4.56
Ce	17.16	42.4	24.1	39.6	28.4	51.7	11.9	26.8	30.1	48.3	31.8	12.8
Pr	2.48	5.37	3.19	4.80	4.46	6.60	1.67	3.47	3.85	5.73	4.29	2.06
Nd	11.8	21.7	14.3	19.8	22.3	27.9	8.24	15.2	17.0	23.1	19.5	10.7
Sm	3.35	4.95	3.72	4.38	6.41	6.37	2.34	3.72	4.20	4.96	5.05	3.43
Eu	1.11	1.19	1.19	1.30	2.20	1.65	0.94	1.18	1.30	1.30	1.60	1.25
Gd	4.05	5.35	4.38	4.64	7.37	6.75	2.84	4.02	4.60	5.11	5.74	4.16
Tb	0.674	0.830	0.694	0.741	1.20	1.05	0.471	0.652	0.750	0.798	0.930	0.688
Dy	4.07	4.90	4.32	4.24	7.38	6.24	2.90	3.91	4.48	4.47	5.51	4.31
Ho	0.832	0.989	0.847	0.853	1.46	1.23	0.574	0.775	0.906	0.917	1.12	0.900
Er	2.26	2.64	2.36	2.36	3.91	3.32	1.57	2.07	2.43	2.47	3.01	2.36
Tm	0.323	0.393	0.329	0.334	0.551	0.482	0.216	0.306	0.357	0.364	0.426	0.354
Yb	1.98	2.34	1.99	2.06	3.30	2.95	1.35	1.82	2.09	2.16	2.63	2.07
Lu	0.309	0.370	0.297	0.310	0.510	0.445	0.196	0.264	0.311	0.326	0.391	0.313
Hf	2.52	4.84	2.94	3.98	4.59	5.61	1.74	3.10	3.51	4.92	4.05	2.14
Ta	0.394	0.516	0.453	0.656	0.852	0.898	0.210	0.338	0.405	0.569	0.481	0.272
Pb	2.29	5.23	2.39	4.00	6.54	8.66	1.44	5.35	3.98	5.89	4.28	0.610
Th	1.15	4.59	2.10	4.11	0.799	5.03	0.735	2.42	2.64	5.15	2.52	0.345
U	0.320	1.18	0.509	1.00	0.243	1.23	0.189	0.603	0.680	1.25	0.650	0.113

For explanation of lithological codes, see Table 1. For petrographical notes on the samples, see Table 11c.

Geographical coordinates in WGS 84. First two digits are degrees, then follow minutes in decimal form.

Major elements in wt% (XRF analyses). Trace elements in ppm (Zn–Ga: XRF analyses; Rb–U: ICP-MS analyses).

FeO* = total iron as FeO. $mg\ number = 100 \times \text{atomic Mg}/(\text{Mg} + \text{Fe}^{2+})$, with the iron oxidation ratio adjusted to $\text{Fe}_2\text{O}_3/\text{FeO} = 0.15$.

Table 11b. Chemical analyses of intrusions of the Nordfjord and Niaqussat Members

Intrusion	Inner Hammer Dal swarm			Killiit dyke		Maniillat dyke		Illukunnguaq dyke	Uiffaq dyke	Rink's dyke		Mellemfjord dyke
				Margin	Centre	Margin	Centre			Margin	Centre	
Locality	Inner Hammer Dal			Luciefjeld	Stordal	Maniilat		Illukunnguaq	Uiffaq	Disko	Fjord	Mellemfjord
Lith. code	6281	6281	6281	6171	6171	6281	6281	6281	6281	6281	6281	6281
GGU No.	F162	F169	F173	176669	264338	138235	138233	362140	176683	175156	175164	175005
Deg. W	5420.36	5417.18	5413.78	5346.26	5353.5	5332.25	5332.26	5234.72	5412.18	5416.2	5416.2	5434
Deg. N	7007.09	7006.40	7006.64	6919.306	6956.36	7010.930	7010.93	6953.103	6921.676	6934.1	6934.1	6946
Altitude, m	778	1019	1530	514	755	1059	1066	82	1	4	4	170
SiO ₂	49.05	51.68	50.30	52.09	56.61	48.67	56.66	51.16	50.67	50.92	53.14	54.90
TiO ₂	2.473	1.162	2.454	1.35	1.25	1.75	1.28	1.57	1.73	1.62	1.58	1.45
Al ₂ O ₃	13.22	14.49	12.63	13.81	14.05	13.31	15.36	13.49	14.53	14.36	15.33	14.86
Fe ₂ O ₃	14.36	10.44	13.11	0.00	1.88	3.03	0.90	1.48	3.37	1.38	1.60	0.60
FeO				9.44	5.35	8.45	6.54	8.33	7.74	8.31	7.76	8.26
MnO	0.204	0.138	0.186	0.16	0.14	0.18	0.11	0.15	0.16	0.22	0.18	0.19
MgO	5.86	9.52	7.46	10.48	8.80	10.36	6.54	9.57	7.86	8.83	6.90	7.48
CaO	10.58	8.67	10.11	9.06	7.60	10.38	6.81	9.07	10.43	10.97	8.39	8.47
Na ₂ O	2.26	1.79	2.19	1.82	2.25	2.02	2.34	1.99	2.15	2.19	2.29	2.24
K ₂ O	0.320	0.554	0.487	0.660	0.730	0.250	0.820	0.215	0.435	0.230	0.530	0.520
P ₂ O ₅	0.233	0.136	0.245	0.160	0.140	0.170	0.170	0.183	0.173	0.150	0.180	0.200
Volatiles	1.00	1.34	0.38	0.42	0.99	1.58	2.35	2.97	0.76	1.06	2.08	0.95
Sum	99.56	99.93	99.55	99.45	99.79	99.15	98.88	100.18	100.00	100.24	99.96	100.12
FeO*	12.92	9.40	11.80	9.44	7.04	11.18	7.35	9.66	10.77	9.55	9.20	8.80
mg number	47.84	67.20	56.12	69.19	71.65	65.22	64.28	66.70	59.60	65.15	60.27	63.23
Zn	110	19.3	101	76.6	49.4	95.6	77.1	88.8	84.9	82.7	75.1	77.2
Cu	174	241	94.0	36.2	70.3	162	36.1	24.3	71.8	79.1	110	39.6
Ni	52.1	733	119	42.8	102	201	76.5	123	100	143	218	104
Sc	35.2	25.9	35.7	32.2	26.4	34.5	25.3	31.2	34.6	35.0	29.7	27.0
V	363	221	320	259	204	327	196	265	295	296	227	231
Cr	197	823	373	854	720	492	420	613	557	622	472	586
Ga	22.5	18.7	22.6	18.4	18.0	19.3	20.9	19.7	20.2	19.7	21.2	20.5
Rb	3.89	17.2	13.0	16.1	27.6	3.34	31.6	4.29	8.97	5.37	23.0	23.1
Sr	213	205	198	194	195	188	213	240	207	196	213	236
Y	35.4	20.9	38.2	21.9	24.3	28.2	25.1	27.0	25.8	24.7	25.0	20.1
Zr	149	119	168	123	161	116	185	137	119	105	147	135
Nb	6.74	5.07	7.29	5.30	6.56	5.30	8.11	6.24	5.08	4.40	6.73	6.31
Cs	0.054	0.398	0.218	0.448	0.659	0.107	0.839	1.08	0.160	0.126	0.542	0.714
Ba	65.8	175	94.2	141	247	47.98	300	250	97.8	60.9	205	263
La	8.70	12.6	10.4	10.5	16.2	7.31	20.3	11.2	8.35	7.43	15.7	13.6
Ce	23.6	28.3	27.3	24.6	35.8	19.1	44.1	27.0	20.4	18.6	35.1	29.9
Pr	3.67	3.64	4.15	3.29	4.47	2.95	5.52	3.70	2.94	2.67	4.49	3.95
Nd	18.6	15.6	20.7	14.8	18.8	14.6	22.8	16.7	14.2	12.8	19.3	17.0
Sm	5.55	3.71	6.02	3.81	4.41	4.19	4.87	4.35	3.92	3.62	4.47	3.90
Eu	1.89	1.20	1.89	1.20	1.15	1.46	1.32	1.31	1.36	1.22	1.29	1.30
Gd	6.57	4.04	7.07	4.29	4.63	4.79	5.18	4.79	4.61	4.31	4.92	4.25
Tb	1.07	0.638	1.16	0.672	0.737	0.856	0.801	0.802	0.765	0.698	0.762	0.655
Dy	6.66	3.80	7.05	3.97	4.29	4.79	4.22	4.80	4.71	4.33	4.52	3.85
Ho	1.33	0.770	1.42	0.814	0.850	0.990	0.869	0.956	0.909	0.862	0.908	0.738
Er	3.55	1.98	3.75	2.21	2.30	2.59	2.33	2.47	2.53	2.38	2.42	1.95
Tm	0.495	0.294	0.531	0.320	0.324	0.387	0.337	0.358	0.362	0.338	0.345	0.285
Yb	2.93	1.79	3.16	1.87	2.06	2.33	2.15	2.30	2.15	2.02	2.13	1.74
Lu	0.435	0.259	0.473	0.255	0.314	0.361	0.325	0.345	0.335	0.315	0.324	0.261
Hf	4.05	3.13	4.40	3.23	4.10	3.02	4.56	3.47	3.15	2.76	3.84	3.52
Ta	0.460	0.347	0.474	1.19	0.712	0.478	0.679	0.407	0.398	0.263	0.415	0.372
Pb	1.66	1.04	2.19	2.95	2.70	1.75	6.77	3.03	2.10	1.82	5.35	4.36
Th	0.900	2.59	1.33	2.05	3.73	0.839	4.42	2.12	1.28	1.19	3.55	2.81
U	0.274	0.620	0.374	0.529	0.912	0.249	1.20	0.566	0.345	0.314	0.846	0.688

Table 11c. Notes on analysed samples of intrusions of the Nordfjord and Niaqussat Members

175950	Olivine microphyric basalt with native iron beneath native iron cumulate. Hammer Dal complex, west Disko. Ulf-Møller (1983) table 7 no. 1.
176007	Andesite with native iron from the centre of intrusive body (0.37 wt% carbon). Hammer Dal complex. Ulf-Møller (1983) table 7 no. 6.
264355	Plagioclase-glomerophytic basalt, 20 cm from western contact in the lowermost intrusion of the Hanekammen complex. Northern wall of Rink Dal, west Disko. Ulf-Møller (1983) table 2 no. 3.
264424	Basaltic andesite with native iron from above the centre of the lowermost intrusion in the Hanekammen complex. Northern wall of Rink Dal, west Disko. Ulf-Møller (1983) table 2 no. 11 and Ulf-Møller (1990) table 1 no. 2.
264350	Basalt with native iron from the margin of the northern tube-like intrusion in the Nordfjord complex. Northern wall of Rink Dal, west Disko. Ulf-Møller (1983) table 5 no. 2.
264349	Andesite with native iron from the centre of the northern tube-like intrusion of the Nordfjord complex. Northern wall of Rink Dal, west Disko. Ulf-Møller (1983) table 5 no. 4.
F062	Basalt with native iron from dyke associated with 10 tons native iron boulder in the northern wall of Stordal, central Disko.
F066	Basaltic andesite with native iron from dyke associated with 10 tons native iron boulder in the northern wall of Stordal, central Disko.
F045	Basaltic andesite with native iron from margin of composite dyke (Inner Giesecke Dal dyke), 5 km north-west of Agatfjeldet, north Disko.
F048	Andesite with native iron from centre of composite dyke (Inner Giesecke Dal dyke), same locality as F045.
F074	Basalt from 6–8 m thick, NW-trending basalt dyke from the south-west side of the inner part of Hammer Dal, west Disko.
F076	Basalt 2 m from the margin of 20–30 m thick, NW-trending basalt dyke from the south-west side of the inner part of Hammer Dal, west Disko.
F162	Evolved basalt 0.5 m from margin of 5 m thick, NW-trending composite dyke from gully in the north-eastern wall of Hammer Dal, west Disko.
F169	Basaltic andesite with graphite and sparse native iron from centre of 4 m thick NW-trending, composite dyke south-east of Hammer Dal, west Disko.
F173	Basalt from near the margin of 10 m thick, NW-trending dyke between Hammer Dal and Giesecke Dal, west Disko.
176669	Basaltic andesite with native iron and troilite (0.09 wt% carbon). Chilled margin of the Killiit dyke at Luciefjeld, south Disko. Pedersen (1979b) table 1 no. 1.
264338	Andesite with native iron from the centre of the Killiit dyke south of Stordal, central Disko. Ulf-Møller (1985) table 1 no. 3.
138235	Basalt with native iron from margin of composite dyke (Maniillat dyke), north-east Disko.
138233	Andesite with native iron from centre of composite dyke (Maniillat dyke), same locality as 138235.
362140	Magnesian basaltic andesite from NW-trending basalt dyke associated with a 28 tons pyrrhotite body with traces of native iron. Illukunnguaq, east Disko.
176683	Basalt with native iron from the Uiffaq dyke. Uiffaq, south Disko.
175156	Basalt with native iron from composite dyke (Rink's dyke). North coast of Disko Fjord. Ulf-Møller (1983) table 1 no. 6.
175164	Basaltic andesite with native iron from core of composite dyke (Rink's dyke). Same locality as sample 176156. Ulf-Møller (1983) table 1 no. 7.
175005	Basaltic andesite with native iron from dyke at Saqqarliit Ilorliit. Mellemfjord, west Disko. Ulf-Møller (1983) table 1 no. 4.

Volume relations of the Maligât Formation

In estimating the volume of the Maligât Formation, it must be remembered that it is not well delimited to the west and south; the formation extends below sea level west of Disko and must also have extended south of Disko where it is now removed by erosion. Therefore, measured volumes of the formation are minimum values. On the other hand, the formation is reasonably well delimited to the north and east. The volume calculations presented here are based on a common area comprising all of Disko and Nuussuaq east of the Itilli fault, delimited to the north by the north coast of Nuussuaq, to the west by the Itilli fault and longitude 55°W, to the east by longitude 52°W and to the south by latitude 69°15'N which passes through Qeqertarsuaq town (see e.g. Fig. 4). The area measures close to 18 000 km².

Estimated volumes of the various units of the Maligât Formation within the delimited area are presented in Table 12. The estimates are based on thickness measurements with interpolations in the five geological sections on a scale of 1:20 000 together with thicknesses measured in the many sampled profiles. The numbers were plotted on maps and the thicknesses contoured. On western Disko, the succession dips below sea level and the lower units are extrapolated. In western and central Nuussuaq, extrapolation is also required due to erosion. The values given in Table 12 are rounded figures because of the uncertainties involved, in particular for the more voluminous units. The total volume of the formation within the delimited area is close to 21 200 km³, of which the uncontaminated rocks (Rinks Dal Member) constitute about 13 000 km³ (61%) and the contaminated rocks 8200 km³ (39%) of the succession.

Within the delimited area, the volume of the Rinks Dal Member is reasonably well constrained. It has a pronounced depocentre west of the Disko Gneiss Ridge where the most complete succession with the oldest part is present and thicknesses exceed 1200 m (Fig. 8; Central Disko section). In the north, the lavas gradually overlapped the shield of the earlier Vaigat Formation that rose to the north so that only the upper Rinks Dal Member reached far into Nuussuaq. The upper Rinks Dal Member originally extended east of 52°W, but little is left of it except for small outliers on eastern Nuussuaq. The Rinks Dal Member constitutes between 60% and 66% of the volume of the Maligât Formation. The volumes of the constituent units of the member have been estimated separately (Table 12); with about 7000 km³ the upper Rinks Dal Member constitutes more than half the total volume of the member.

The Nordfjord Member is of large lateral extent (Fig. 12) but of limited thickness and volume (1200 km³) and constitutes only around 6% of the Maligât Formation (Table 12). It has a clear depocentre on north-western Disko where thicknesses reach 350 m and eruption sites, intermediate lavas and acid tuffs are present (Fig. 14). However, over most of the area it is only represented by a few lava flows with combined thicknesses of 30–100 m.

The Niaqussat Member is also of large lateral extent, but its thickness is uncertain because of erosion and removal of much of its upper part. Over much of central and western Nuussuaq (east of the Itilli fault), the member has been completely removed. Erosional remnants are present on eastern Disko with thicknesses up to 180 m in Frederik Lange Dal where the lower, middle and upper

Table 12. Volumes of different parts of the Maligât Formation

Volcanic episode	code	Area (km ²)	Average thickness (m)	Volume (km ³)	% of total
Niaqussat Member	530	18000	600–240, av. 400	7000	33
Nordfjord Member	520	18000	200–30	1200	6
Rinks Dal Member	505–518	18000	1400–200	13000	61
<i>Maligât Formation, total volume</i>		<i>18000</i>	<i>2200–200</i>	<i>21200</i>	<i>100</i>
<i>Units of the Rinks Dal Member</i>					
Upper Rinks Dal Member	514–518	18000	600–200, av. 400	7000	33
Akuarut unit	513	13300	350–0, av. 170	2300	11
Skarvefjeld unit	511	5000	200–0, av. 70	350	2
Lower Rinks Dal Member (excl. 511)	505–512	13300	600–0, av. 250	3500	16

Volumes are measured within an area bounded by the north coast of Nuussuaq, the Itilli Fault, longitudes 55°W and 52°W, and latitude 69°15'N through Qeqertarsuaq town. Thicknesses were contoured, sub-areas measured, and volumes calculated in 100-m thick layers. av.: average.

Niaqussat Member are all present. The best constraint comes from the fact that the upper Niaqussat Member is present with nearly equal thicknesses (150–190 m) in the most complete profile on western Disko (Sapernuvik, Fig. 14) and in the easternmost volcanic outliers on Nuussuaq (Point 2080 m, Fig. 12). In both profiles, the two uppermost flows even have the same slightly changed geochemical character, suggesting that the succession on eastern Nuussuaq is close to the top of the member. In the Sapernuvik area, the entire Niaqussat Member is 500 m thick. The lower Niaqussat Member seems to be thinner in the east where the whole member may have been around 300 m thick. A good estimate of the average thickness of the Niaqussat Member is thus 400 m. This means that the Niaqussat Member originally had a volume of about 7000 km³ and constituted as much as 33% of the Maligât Formation (Table 12). If a thickness of 300 m is used instead, the volume decreases to 5500 km³, i.e. 28% of the Maligât Formation. In any case, the Niaqussat Member originally constituted a considerably larger proportion of the Maligât Formation than it does at present.

Thickness of the removed succession

The average thickness of the Niaqussat Member as estimated above (400 m) means that a succession of about this thickness has been removed over large areas of Disko and Nuussuaq where the member is missing. The original extent and thickness of the Sapernuvik Member is unconstrained but may not have been large. On the other hand, the frequent occurrence throughout Disko and Nuussuaq of dykes with compositions and ages identical to those of the 60–58 Ma Svartenhuk Formation and the 56–54 Ma Naqerloq Formation (Larsen *et al.* 2016) that form the thick basaltic lava successions on Ubekendt Ejland and Svartenhuk Halvø indicate that these lava formations have also been present on Disko and Nuussuaq. This means that the removed succession was probably significantly thicker than 400 m. Uplift studies by Japsen *et al.* (2005, 2009) have indicated that about 1 km of rock succession has been removed from Disko and Nuussuaq, in good agreement with the above.

Crustal contamination of the volcanic rocks

Summary of the main features of the crustal contamination processes

- The contaminants are carbon-bearing mudstones and sandstones of the Nuussuaq Group; these occur abundantly as xenoliths in the contaminated magmas and have the required chemical and isotopic compositions.
- Degrees of contamination vary from 2–5% in the basalts to 10–50% in the basaltic andesites, andesites, dacites and rhyolites. No rocks more evolved than basalt were produced by ordinary fractional crystallisation.
- Magma modification was mainly caused by mixing with partial melts from the sediment sidewall and xenoliths, including transfer of sedimentary sulfur and organic carbon to the melt. Selective exchange of elements, e.g. Ca and Fe, also took place.
- Progressive reduction processes during heating and pressure decrease led to formation of troilite, native iron and graphite.
- Oxygen fugacities varied by as much as eight orders of magnitude from uncontaminated magmas to xenoliths carrying oxygen-deficient, Ti^{3+} -bearing (magnéli) phases.

Crustal contamination of the Nordfjord and Niaqsat member magmas is interpreted to have taken place at two different levels: the basalts became slightly contaminated in deep-seated magma chambers in the lower crust, whereas basaltic andesites, andesites, dacites and rhyolites formed in high-level magma chambers by strong contamination with carbon-bearing mudstones and sandstones (Larsen & Pedersen 2009). A general feature of the strongly contaminated rocks is signs of progressive reduction, delayed or suppressed magnetite crystallisation, unusual mineral zonation patterns, and formation of native iron, sulfides and graphite (e.g. Pedersen 1981). Below, we discuss the character of the contaminants, the degrees of contamination and the contamination processes for the magmas of both the Vaigat and the Maligât formations.

Possible contaminants

On their way through the crust, the magmas could have reacted with both the basement gneisses and the up to 6–8 km thick sediments in the Nuussuaq Basin. Sediment

xenoliths in more or less modified and re-equilibrated states have been found in the contaminated volcanic units, providing direct evidence of the contamination processes. Basement xenoliths are rare, but the possibility of basement contamination cannot be excluded. In the following, compositional data for the possible contaminants are presented in Figs 193–195, and the contamination processes and geochemical changes during contamination are summarised.

Basement

The exposed basement in the Disko Bugt region mainly consists of Archaean orthogneisses of tonalitic to trondhjemitic composition that were reworked during the Proterozoic; other major Archaean units are the Atâ tonalite and the Rodebay granodiorite (Garde & Steenfelt 1999). Another major unit of the basement is the thick succession of Proterozoic metagreywackes in the Karrat Group that occurs over large areas north of Nuussuaq; in the Disko–Nuussuaq region, it may be present at depth within the substrate of the Nuussuaq Basin. Compositional and isotopic data on the various rock units have been published by Kalsbeek *et al.* (1988, 1998), Kalsbeek & Skjernaa (1999) and Kalsbeek & Taylor (1999) but rarely on the same samples. In Table 13, we provide systematic compositional and isotopic data for samples of the different basement units.

The chemical compositions of the basement samples vary within quite narrow limits. The Rodebay granodiorite has distinctly high K_2O (3.5 wt%), Rb, and Ba. The metagreywackes (average of 23 analyses) have higher MgO (3.5 wt%) and lower Na_2O than the igneous basement rocks, but the trace element compositions are not very different. The multi-element patterns (Fig. 195) show a characteristic feature of the metagreywackes: they have higher contents of Zr, Y and the heavy REE than the igneous rocks, presumably because heavy minerals such as zircon are concentrated in the sediments relative to their igneous sources.

Sediments

The exposed sediments in the Nuussuaq Basin are fluvial, deltaic and marine, with fluvial facies dominating in the south-east and marine facies dominating in the north-

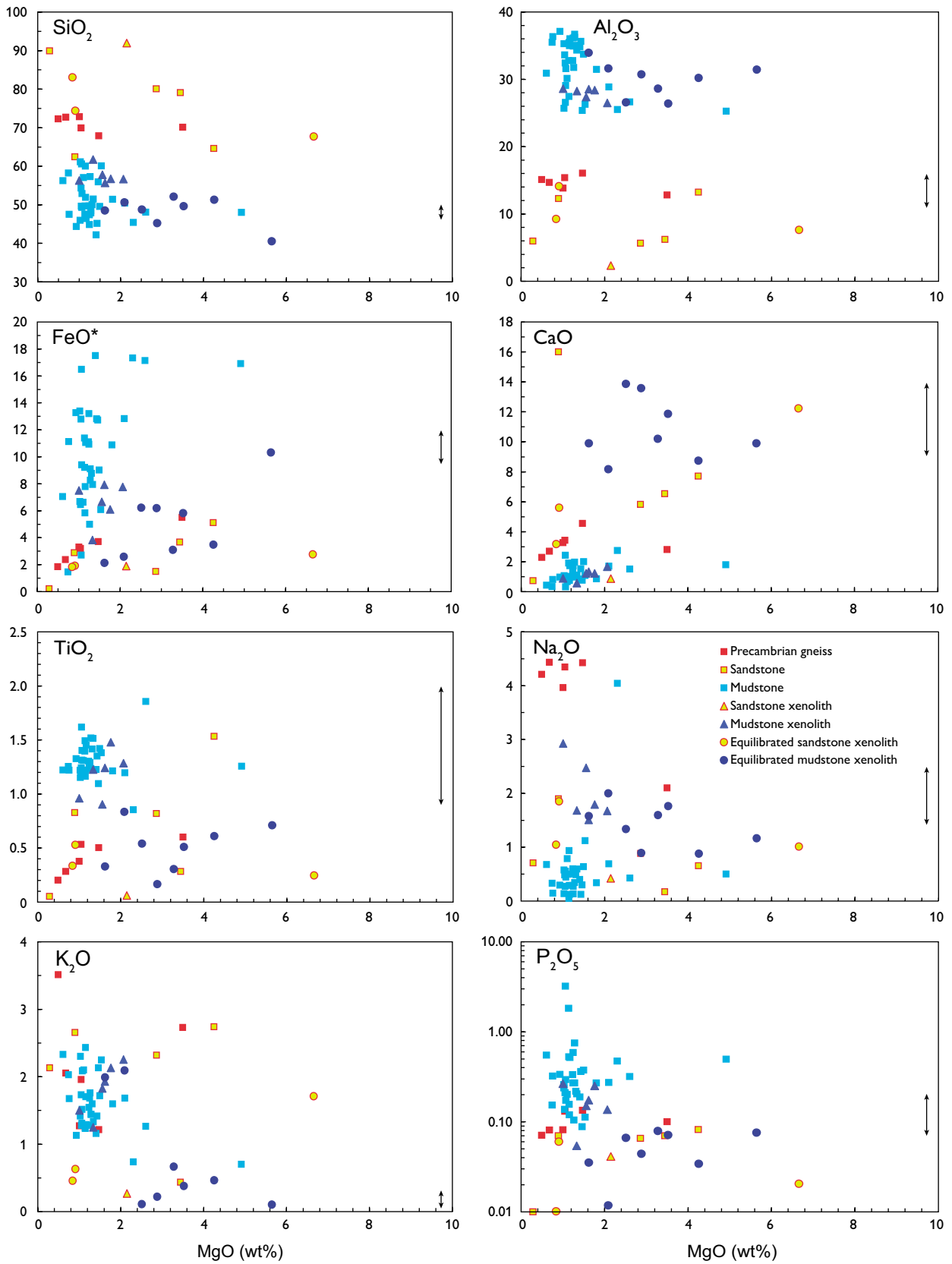


Fig. 193. Major element variation diagrams for possible contaminants of the volcanic rocks. Data in wt% oxides recalculated volatile-free. FeO* is total iron as FeO. Vertical double-headed arrows at the right side of diagrams show the ranges of the respective elements in uncontaminated magmas with 9–18 wt% MgO.

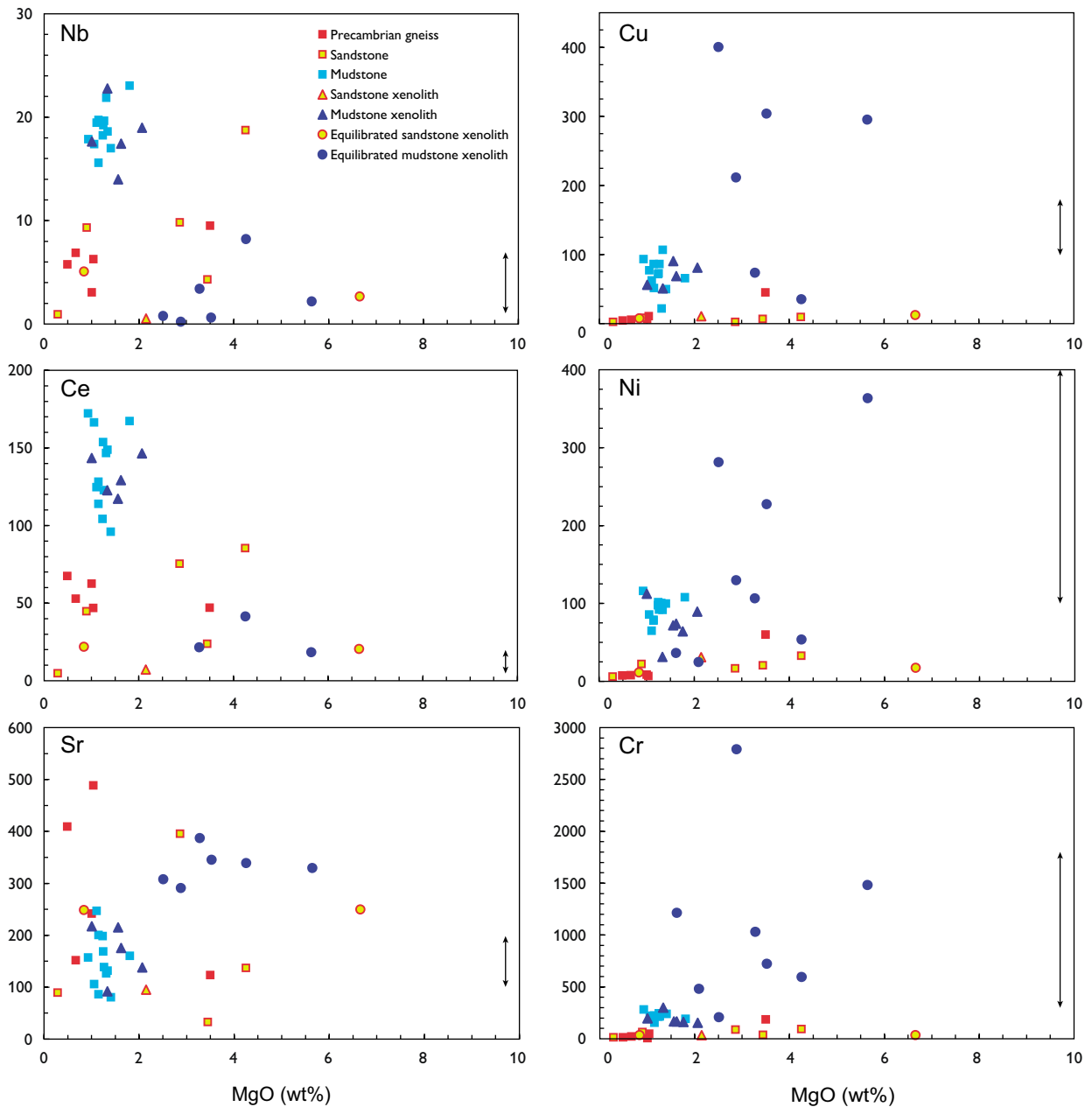


Fig. 194. Selected trace element variation diagrams for possible contaminants of the volcanic rocks. Data in ppm. Vertical double-headed arrows at the right side of diagrams show the ranges of the respective elements in uncontaminated magmas with 9–18 wt% MgO.

west (e.g. G.K. Pedersen & Pulvertaft 1992). The dominant lithology is arkosic sandstone (Schiener 1975). The friable sandstones may be cemented with carbonate, silica or kaolinite. In the fluvial and deltaic successions, the sandstones are interbedded with mudstones and locally with thin coal beds. Thicker, non-marine mudstones (the Atanikerluk Formation, Fig. 5) in the south-east have low sulfur contents (up to 0.1 wt% S) and 6–10 wt% TOC

(G.K. Pedersen *et al.* 1998). Marine mudstones (of the Itilli and Kangilia formations) in the north-west have high sulfur contents (up to 5 wt% S) and mostly 2.5–6 wt% TOC (Christiansen *et al.* 1996, 1997; Bojesen-Koefoed *et al.* 1997). The GRO#3 well on western Nuussuaq penetrated *c.* 3000 m of deep-water marine sediments (Dam *et al.* 2009, fig. 67). The sediments that contaminated the volcanic rocks are situated within the unexposed part of

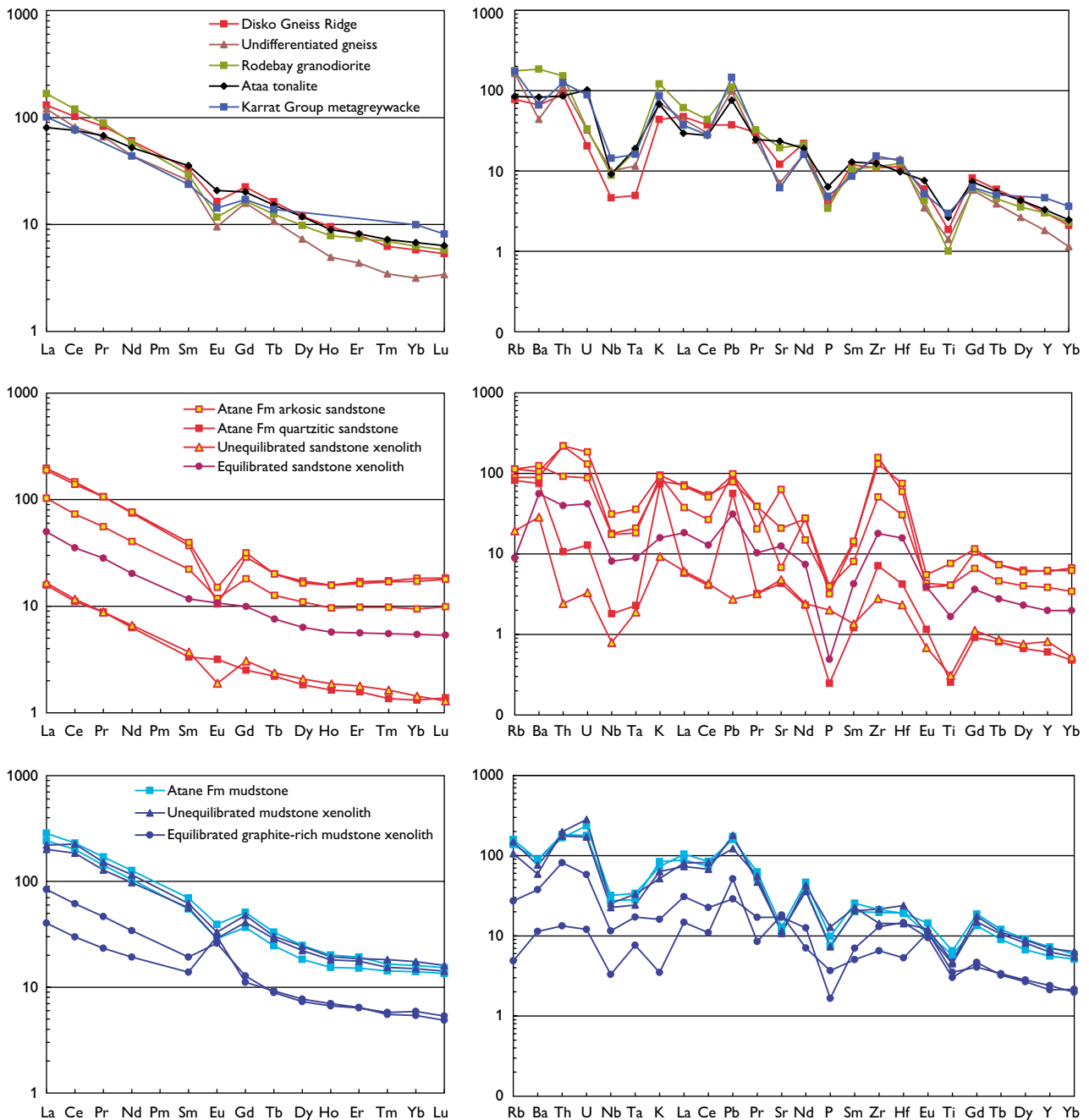


Fig. 195. REE and multi-element diagrams for possible contaminants of the volcanic rocks. Left diagram, chondrite normalised; right diagram, primitive mantle normalised; normalisation factors from McDonough & Sun (1995).

the thick succession but are expected to have lithologies similar to those of the exposed sediments. Chemical analyses of mudstones and sandstones from the Nuussuaq Basin are shown in Table 13. These rocks have high contents of volatiles, 10–25 wt% except for a few sandstones, and the recalculation of analyses to 100% volatile-free makes significant differences.

The recalculated mudstone analyses form a fairly distinct population in Fig. 193. The largest scatter is seen for total iron contents, while a few samples have deviating contents of one or more elements such as Na_2O , K_2O and MgO . The recalculated sandstone analyses show considerable scatter, ranging from a quartzitic sandstone with 90 wt% SiO_2 to more arkosic varieties with lower

Table 13a. Chemical analyses of Precambrian basement, Nuussuaq Basin sediments, and xenoliths

Lithology	Precambrian basement							Mudstone				
	1001	1001	1001	1001	1001	1001	1001	9202	9102	6274	6274	4204
Lith. code	157205	348667	360907	360994	177375	177378	177379	176769	176770	113449	113450	136992
Deg. W	-5332.66	-5032.26	-5044.15	-5025.39	-5145	-5145	-5145	not def.	not def.	5416.36	5416.36	5317.60
Deg. N	6915.94	6949.38	6922.55	7010.89	7115	7115	7115	not def.	not def.	6956.19	6956.19	7011.78
Altitude, m	176.17							not def.	not def.	4.88	4.88	33.25
SiO ₂	71.73	69.34	71.43	71.84	59.96	71.58	72.72	44.85	50.09	53.74	51.03	54.30
TiO ₂	0.37	0.53	0.2	0.28	0.79	0.60	0.54	1.03	0.97	0.84	0.87	1.21
Al ₂ O ₃	13.62	15.24	14.94	14.5	15.94	10.96	11.11	23.68	22.9	25.44	25.91	27.80
Fe ₂ O ₃	1.09	3.53	2.03	2.6	0.74	0.54	0.52			0.62		
FeO	2.28				6.64	4.77	3.55	5.21	4.87	5.63	6.8	7.73
MnO	0.04	0.05	0.02	0.03	0.06	0.10	0.08	0.05	0.04	0.06	0.04	0.04
MgO	0.99	1.04	0.49	0.67	5.14	3.53	2.96	0.87	0.96	1.45	0.91	1.58
CaO	3.22	3.4	2.26	2.66	1.33	5.07	4.79	0.53	0.68	1.13	0.81	1.30
Na ₂ O	3.9	4.31	4.16	4.38	3.46	0.46	0.34	0.62	0.78	2.3	2.65	1.47
K ₂ O	1.25	1.94	3.47	2.03	3.633	1.107	1.734	1.65	2.03	1.7	1.36	1.880
P ₂ O ₅	0.08	0.13	0.07	0.08	0.100	0.095	0.086	0.159	0.13	0.14	0.24	0.170
Volatiles	0.44	0.5	0.2	0.3	1.64	0.99	1.39	20.69	12.26	6.7	9.03	1.48
Sum	99.01	100.01	99.27	99.37	99.43	99.80	99.82	99.34	99.67	99.75	99.65	99.99
Zn	37.5	71.8	62.6	69.1	156	124	94	71.4	68.4	93	110	67
Cu	6.3	10.7	4.3	5.3	91.2	11.5	14	42.2	37.7	84	51	67
Co	49.9	57.9	2	4.8	33.3	48.6	40	16.5	14.8	22	34	25
Ni	7.5	6.5	7.2	7.8	85.7	53.6	54	50.9	50.1	67	102	72
Sc	8.7	4.7	3.6	4.6	23.2	15	15	19.2	14.0	22	25	24
V	30.2	11.8	19.1	28.2	140	109	108	106	126	244	170	142
Cr	7.3	48.1	12.8	20.5	195	217	177	134	131	156	177	163
Ga	13	20.8	17.8	16.7	24	17.2	17	31.2	30.5	33	38	
Rb	46.0	50.4	104	97.5	121	88.8	84	64.7	77.3	82.8	57.4	102
Sr	238	464	384	139	86.8	93.2	123	201	182	213	193	171
Y	12.9	14.1	12.8	7.76	23.2	21	18	24.6	19.7	25.0	27.1	36
Zr	114	104	137	152	133	169	135	173	170	232	134	177
Nb	3.01	5.99	5.77	6.54	10.6	10.5	7.9	16.4	13.5	13.8	15.1	17
Cs	1.38	1.64	0.84	1.70	6.20	6.00	4.70	3.00	2.87	1.67	2.12	
Ba	432	543	1208	288	495	392	366	464	490	471	353	478
La	30.4	18.9	39.3	28.1	29.7	21.1	19.2	53.1	42.7	44.2	47.5	60.6
Ce	61.6	46.0	72.6	49.4	56	42	39	111	88.3	105	125	126
Pr	7.56	6.22	8.14	6.08				12.5	10.4	11.1	12.8	
Nd	27.1	23.7	26.2	19.9	23	19	16	45.7	37.7	41.5	47.9	53
Sm	4.79	5.20	4.29	3.77	4.03	3.41	3.03	8.13	6.31	7.77	8.31	
Eu	0.907	1.16	0.652	0.529	0.9	0.78	0.72	1.74	1.35	1.51	1.69	
Gd	4.39	3.97	3.26	3.11				8.01	6.08	7.57	8.61	
Tb	0.579	0.543	0.445	0.382	0.5	0.5	0.5	0.938	0.689	0.964	0.995	
Dy	2.90	2.88	2.38	1.77				4.80	3.66	5.09	5.43	
Ho	0.512	0.484	0.423	0.266				0.863	0.685	0.923	0.961	
Er	1.25	1.30	1.18	0.691				2.42	1.95	2.62	2.70	
Tm	0.152	0.177	0.170	0.084				0.321	0.280	0.353	0.408	
Yb	0.918	1.08	1.00	0.501	1.71	2.12	1.67	2.04	1.83	2.25	2.55	
Lu	0.129	0.154	0.141	0.083	0.24	0.31	0.23	0.297	0.272	0.325	0.358	
Hf	3.18	2.75	3.50	3.93	2.8	3.8	3.1	4.24	4.16	6.29	3.63	
Ta	0.181	0.699	0.651	0.422	0.8	0.6	0.5	0.981	0.875	0.834	1.11	
Pb	5.53	11.3	16.3	14.7	37.8	17.9	14	18.7	21.9	25.0	16.7	
Th	6.96	6.77	12.0	8.87	11.9	7.9	7	10.4	8.67	12.9	14.3	15.2
U	0.411	2.06	0.669	0.651	2.5	1.2	1.1	3.77	2.60	3.22	5.18	
<i>Isotope ratios calculated at 60 Ma</i>												
⁸⁷ Sr/ ⁸⁶ Sr ₆₀	0.721167	0.713490	0.732382	0.781592	0.81954	0.76145	0.76212		0.725067		0.720346	0.730705
εSr	235.85	126.88	395.03	1093.48	1632.15	807.55	817.05		291.20		224.19	371.22
¹⁴³ Nd/ ¹⁴⁴ Nd ₆₀	0.511068	0.511221	0.510750	0.510909	0.511270	0.511475	0.511469		0.511121		0.511123	
εNd	-29.12	-26.14	-35.32	-32.22	-25.19	-21.19	-21.30		-28.10		-28.05	
²⁰⁶ Pb/ ²⁰⁴ Pb ₆₀	16.948	18.581	14.964	14.878	17.364	18.099	18.878		17.692		17.526	
²⁰⁷ Pb/ ²⁰⁴ Pb ₆₀	15.189	15.389	14.705	14.719	15.493	15.575	15.712		15.192		15.135	
²⁰⁸ Pb/ ²⁰⁴ Pb ₆₀	42.659	37.540	39.379	38.261	36.948	37.681	38.334		37.966		37.873	

For explanation of lithological codes, see Table 1. For petrographical notes on the samples, see Table 13c.
 Geographical coordinates in WGS 84. First two digits are degrees, then follow minutes in decimal form. Not def.: Not definable.
 Major elements in wt% (XRF analyses). Trace elements in ppm (Zn–Ga: XRF and some ICP-MS analyses; Rb–U: ICP-MS analyses).
 Trace elements in 177375–379: XRF and INA analyses; in samples 136992, 113306 and 176506 only XRF analyses.
 High contents of analytical volatiles are due to high contents of TOC and S (see Table 13c).

Table 13b. Chemical analyses of Precambrian basement, Nuussuaq Basin sediments, and xenoliths

Lithology	Sandstone					Magma-equilibrated sediment xenoliths					Buchite	
	2201	4204	2201	2201	2201	4204	6274	6284	4204	5207	5204	
Lith. code	113202	113223	113493	176771	176772	113306	113443	113527	400296	156518.2	176506	
GGU No.	5332.67	5332.79	5314.20	5315	5300.0	5317.69	5416.36	5411.94	5330.08	5446.31	5442.88	
Deg. W	7013.42	7012.92	7010.76	7011	7004.5	7011.81	6956.19	6921.64	7029.95	7007.633	7014.60	
Deg. N	360.19	535.62	3.67			25.64	4.88		1144.77	160	420.21	
Altitude, m	73.29	88.97	87.77	53.61	55.15	46.08	81.84	32.01	45.07	52.47	66.19	
SiO ₂	0.75	0.06	0.05	0.71	1.31	0.27	0.33	0.56	0.54	0.57	0.24	
TiO ₂	5.15	2.24	5.82	10.53	11.31	25.29	9.1	24.83	26.52	16.97	7.46	
Al ₂ O ₃	0.08	1.50		0.92	0.34		0.51		3.40	1.76	0.92	
Fe ₂ O ₃	1.29	0.48	0.2	1.65	4.06	2.74	1.35	8.15	0.00	1.37	1.87	
FeO	0.02	0.03	0.02	0.1	0.09	0.06	0.04	0.09	0.04		0.03	
MnO	2.62	2.08	0.28	0.77	3.63	2.9	0.83	4.46	3.74	0.92	6.51	
MgO	5.32	0.85	0.71	13.73	6.58	9.02	3.12	7.82	7.67	1.64	11.95	
CaO	0.81	0.41	0.69	1.63	0.56	1.41	1.03	0.92	0.77	3.26	0.99	
Na ₂ O	2.12	0.260	2.08	2.28	2.34	0.59	0.45	0.080	0.408	6.150	1.670	
K ₂ O	0.06	0.040		0.07	0.07	0.07	0.01	0.060	0.030	0.120	0.020	
P ₂ O ₅	8.09	2.27	1.89	14.05	14.67	10.47	1.38	19.63	11.69	14.47	2.09	
Volatiles	99.60	99.19	99.51	99.98	100.11	98.93	99.99	98.61	99.87	99.70	99.94	
Sum	Zn	21.0	8.32	7.41	33.9	53.7	63	21.6	126	88.1	40.3	8
	Cu	2.94	10.4	1.45	7.42	10.7	65	7.18	227	29.7	22.0	12
	Co	4.30	18.9	1.77	8.85	8.98	15	3.12	56.3	14.9	6.32	4
	Ni	11.0	30.0	4.73	17.4	23.7	94	12.1	287	47.4	13.9	17
	Sc	8.61	3.93	1.11	8.18	16.2	8.3	5.67	11.8	8.93	9.57	4.6
	V	62.6	227	6.40	32.5	63.1	176	26.7	318	132	72.6	29
	Cr	58.5	34.5	11.7	54.4	78.6	910	33.9	870	569	77.8	35
	Ga	5.64	3.39	5.65	10.9	14.5		9.94	26.9	29.0	23.8	9
	Rb	48.6	11.2	47.9	58.3	57.7	18	5.26	2.31	14.32	83.4	43
	Sr	382	92.3	83.7	1075	115	342	245	285	298	379	244
	Y	25.1	3.40	2.54	14.1	22.8	6	8.43	8.18	8.04	32.4	4.9
	Zr	657	28.4	40.4	294	711	62	184	42.0	123	17.9	311
	Nb	9.94	0.51	1.16	9.86	17.6	3	5.25	1.72	6.67	8.55	2.6
	Cs	0.388	0.166	0.308	0.886	0.809		0.122	0.115	0.467	0.448	
	Ba	569	183	484	705	598	284	363	59.32	219	2653	554
	La	41.5	3.80	3.64	20.9	38.0	10	11.7	7.551	17.5	48.7	9.8
	Ce	78.3	6.91	6.61	38.4	72.9	19	21.3	14.5	33.2	93.2	20
	Pr	8.83	0.791	0.796	4.44	8.42		2.58	1.71	3.79	10.7	
	Nd	30.5	2.91	2.81	15.9	29.7	7	9.13	6.95	13.7	38.8	11
	Sm	4.78	0.531	0.482	2.82	4.98		1.70	1.62	2.50	7.24	
	Eu	0.577	0.103	0.174	0.572	0.723		0.595	1.34	1.29	2.74	
	Gd	5.27	0.590	0.487	3.08	5.38		1.95	1.75	2.23	6.72	
	Tb	0.627	0.082	0.078	0.392	0.619		0.269	0.264	0.282	1.02	
	Dy	3.86	0.495	0.438	2.31	3.46		1.53	1.50	1.58	5.49	
	Ho	0.808	0.099	0.087	0.450	0.731		0.307	0.301	0.319	1.03	
	Er	2.50	0.275	0.245	1.34	2.22		0.887	0.815	0.896	2.71	
	Tm	0.399	0.039	0.033	0.207	0.356		0.135	0.108	0.125	0.390	
	Yb	2.69	0.223	0.206	1.30	2.35		0.863	0.688	0.834	2.21	
	Lu	0.419	0.031	0.033	0.209	0.375		0.130	0.095	0.116	0.321	
	Hf	14.9	0.639	1.16	7.42	18.2		4.40	1.19	3.64	0.818	
	Ta	0.677	0.068	0.083	0.579	1.13		0.324	0.222	0.558	0.568	
	Pb	10.6	0.398	8.223	12.7	12.3		4.60	6.066	3.80	46.0	6
	Th	13.5	0.186	0.831	6.25	14.9	1.95	3.12	0.833	5.70	7.87	4
	U	2.17	0.065	0.256	1.53	3.20		0.837	0.193	1.04	1.43	
<i>Isotope ratios calculated at 60 Ma</i>												
	⁸⁷ Sr/ ⁸⁶ Sr ₆₀	0.718483			0.718084		0.717170	0.717855	0.714886		0.727655	
	εSr	197.75			192.09		179.12	188.84	146.70		327.93	
	¹⁴³ Nd/ ¹⁴⁴ Nd ₆₀	0.510700			0.510962			0.511028	0.511890			
	εNd	-36.30			-31.19			-29.91	-13.09			
	²⁰⁶ Pb/ ²⁰⁴ Pb ₆₀	17.832			16.316			17.226	16.973			
	²⁰⁷ Pb/ ²⁰⁴ Pb ₆₀	15.205			14.954			15.118	15.037			
	²⁰⁸ Pb/ ²⁰⁴ Pb ₆₀	46.498			37.227			37.309	37.297			

Table 13c. Notes on analysed samples of Precambrian basement, sediments of the Nuussuaq Basin, and xenoliths

157205	Gneiss c. 6 m below the contact to the volcanic rocks, Disko Gneiss Ridge below Lyngmarksfjeld, southern Disko.
348667	Atå tonalite, Illuluarsuit Nunataat island east of northern Arveprinsen Eiland.
360907	Rodebay granodiorite, Paakitsup Nunaa c. 25 km north-north-east of Ilulissat.
360994	Undifferentiated gneiss, easternmost Nuussuaq.
177375	Karrat Group metagreywacke, Alfred Wegener Halvø, Uummannaq Fjord.
177378	Karrat Group metagreywacke, Alfred Wegener Halvø, Uummannaq Fjord.
177379	Karrat Group metagreywacke, Alfred Wegener Halvø, Uummannaq Fjord.
176769	Composite of 12 unmetamorphosed Cretaceous to Paleocene mudstone samples from Disko.
176770	Composite of 11 unmetamorphosed Cretaceous to Paleocene mudstone samples from Nuussuaq. Pedersen (1979a), new ICP-MS data. 'Volatiles' include 5.43 wt% TOC and 0.85 wt% S.
113449	Mudstone xenolith, unequilibrated, in Nordfjord Member Fe-andesite dyke, innermost Nordfjord, western Disko. 'Volatiles' include 1.86 wt% TOC and 2.46 wt% S.
113450	Mudstone xenolith, graphite-rich, unequilibrated, in Nordfjord Member Fe-andesite dyke, innermost Nordfjord, western Disko. Pedersen & Larsen (2006), new ICP-MS data. 'Volatiles' include 4.07 wt% TOC and 3.05 wt% S.
136992	Mudstone xenolith, slightly equilibrated, in Fe-andesite lava flow of the Asuk Member at Asuk, northern Disko. Pedersen (1979a). 'Volatiles' include 0.33 wt% TOC and 0.78 wt% S.
113202	Cretaceous sandstone, Maniillat Kussinersuat gully, northern Disko.
113223	Sandstone xenolith in basaltic andesite lava flow of the Asuk Member, Maniillat Kussinersuat gully, northern Disko.
113493	Cretaceous sandstone, quartz-rich, coast south-east of Asuk, northern Disko.
176771	Cretaceous sandstone with muddy streaks, Asuk. Sample collected by K.J.V. Steenstrup 1872.
176772	Cretaceous sandstone with plant imprints, Ritenbenks Kulbrud south of Qullissat. Sample collected by K.L. Giesecke July 17–18 1811 (217 no. 235).
113306	Mudstone xenolith, graphite-rich, equilibrated, in Fe-andesite lava flow from Asuk Member at Asuk, northern Disko. Pedersen (1979a). 'Volatiles' include 6.98 wt% TOC and 0.06 wt% S.
113443	Sandstone xenolith, glass-rich, equilibrated, in Nordfjord Member Fe-andesite dyke, innermost Nordfjord, western Disko.
113527	Mudstone xenolith, graphite-rich, equilibrated, from dyke on Uiffaq, south-west Disko. Sample collected by K.J.V. Steenstrup 1881.
400296	Mudstone xenolith, graphite-rich, equilibrated, in graphite andesite tuff at Ilugissoq, central Nuussuaq. Pedersen & Larsen (2006), new ICP-MS data. 'Volatiles' include 8.83 wt% TOC and 0.03 wt% S.
156518.2	Mudstone xenolith, K ₂ O-rich and graphite-rich, equilibrated, in garnet rhyolite lava block in conglomerate. Sedimentkløften, south side of Hammer Dal, north-west Disko. TOC and S in Table 7.
176506	Sandstone buchite xenolith in Fe-andesite lava flow of the Nordfjord Member at Toornivit, north-west coast of Disko.

SiO₂. The sandstones with more than 5 wt% CaO, three of which also have high MgO (3–4 wt%), are carbonate-cemented. Some of the sandstone samples have very high contents of Zr (up to 1650 ppm recalculated), indicating high contents of detrital zircon grains. Elements such as Y and HREE, which are concentrated in zircon, are therefore also quite high. The arkosic sandstones have LREE contents similar to those of the basement gneisses but significantly increased HREE and Y contents due to relative accumulation of heavy minerals such as zircon (Fig. 195). This 'heavy mineral effect' is more pronounced in the mature sandstones than in the mudstones and the immature Karrat Group metagreywackes. Except for this effect, the multi-element patterns of the sediments are largely similar to those of the meta-igneous basement rocks from which the sediments were ultimately derived. Thus, all samples have high contents of Rb-Ba-Th-U and K-La-Ce, and significant Nb-Ta troughs, Pb peaks, and P and Ti troughs in the multi-element patterns.

Distinction between contaminants

As discussed by Larsen & Pedersen (2009), the Sr, Nd and Pb isotope data enable us to distinguish between the different potential contaminants. The Proterozoic metagreywackes of the Karrat Group have higher ²⁰⁷Pb/²⁰⁴Pb ratios (15.5–15.7) than both the uncontaminated and contaminated magmas (²⁰⁷Pb/²⁰⁴Pb = 15.2–15.5 and 14.9–15.4, respectively), thereby excluding any significant contamination from these rocks. The four local basement orthogneisses analysed in this work have quite variable isotope ratios, and so have other orthogneisses from the region (Kalsbeek & Taylor 1999) which have ⁸⁷Sr/⁸⁶Sr up to >1. In contrast, the sediments of the Nuussuaq Basin have restricted Sr isotopic compositions, which are within the middle range of the orthogneisses, as expected for sediments derived from these gneisses (Fig. 196). In all, the sediments serve very well as possible contaminants, as detailed below. Contamination by basement orthogneisses with relatively low ⁸⁷Sr/⁸⁶Sr cannot be excluded but is not necessary to explain the data.

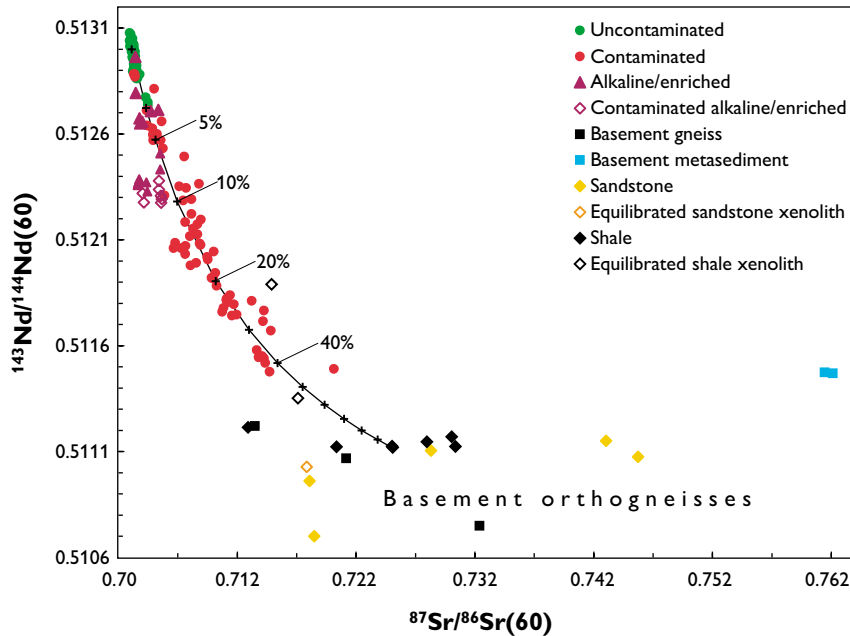


Fig. 196. All Sr and Nd isotope data for the Vaigat and Maligât formations and some possible contaminants (slightly modified from Larsen & Pedersen 2009). Four basement orthogneisses are from Nuussuaq, Disko and the mainland east of Disko (one sample is off scale with $^{87}\text{Sr}/^{86}\text{Sr}(60) = 0.7816$). Other local basement orthogneisses with $^{87}\text{Sr}/^{86}\text{Sr}(60)$ up to >1 are from Kalsbeek & Taylor (1999). The basement metasediments are from the Proterozoic Karrat Group (Kalsbeek *et al.* 1998). The shales and sandstones are Cretaceous sediments from the Nuussuaq Basin. The curve is a mixing curve calculated by bulk mixing of a picrite with 120 ppm Sr, 7 ppm Nd, $^{87}\text{Sr}/^{86}\text{Sr}(60) = 0.7031$, and $^{143}\text{Nd}/^{144}\text{Nd}(60) = 0.5130$ with an average sediment with 230 ppm Sr, 39 ppm Nd, $^{87}\text{Sr}/^{86}\text{Sr}(60) = 0.7250$, and $^{143}\text{Nd}/^{144}\text{Nd}(60) = 0.5111$. Tick marks indicate the amount of sediment (wt%) in the mixture.

Contamination by an enriched lithospheric component in some rocks was identified by Larsen *et al.* (2003) and Larsen & Pedersen (2009). This took place at deep levels before the magmas entered high-level magma chambers and reacted with sediments and is not considered further here.

Degrees of contamination

As shown in Fig. 196 the total Sr-Nd isotope data set conforms well to a simple model of bulk mixing between a picrite and an average sediment. The various contaminated units of both the Vaigat and Maligât formations are shown in details in Fig. 197A. The major contaminated members of the Vaigat Formation require more than about 10% contamination except for the Nuusap Qaqqarsua Member which only requires 5–10% and whose chemical composition is also less modified (Pedersen *et al.* 2017, fig. 156). The Asuk Member rocks are contaminated with up to 40% sediment, which is mudstone-dominated according to Pedersen & Pedersen (1987) and Goodrich & Patchett (1991). The Kûgân-

guaq Member is contaminated with 12–24% sediment, which is sandstone-dominated according to Pedersen & Pedersen (1987).

In contrast the contaminated members of the Maligât Formation (Nordfjord and Niaquassat members) represent a large range of contamination from only 12% to $>50\%$ and *c.* 35%, respectively, in accordance with their large compositional ranges. The most highly contaminated rocks of all are the rhyolites of the Nordfjord Member, which contain around 50% sediment, which is mudstone-dominated according to Pedersen & Pedersen (1987).

Very slight contamination may be difficult to detect. Some samples that are considered contaminated because of small compositional anomalies appear to contain only around 1% contaminant (Fig. 197B). On the other hand, three samples from the low-Ti unit in the Anaanaa Member have Sr-Nd isotope ratios that suggest 2–3% contamination even though their chemical compositions do not match this. This unit is possibly not contaminated, as discussed by Larsen & Pedersen (2009). In general, we consider a sample to be crustally contaminated if it has

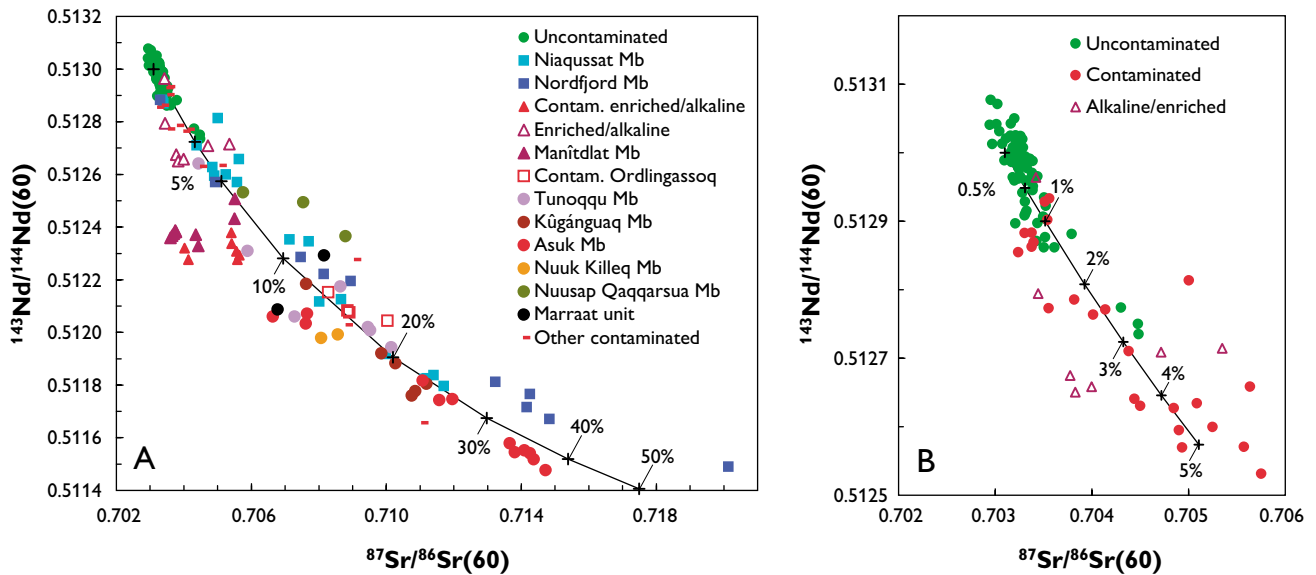


Fig. 197. **A:** Degrees of crustal contamination in the various contaminated units of the Vaigat and Maligât formations. The mixing model is the same as shown in Fig. 196. Tick marks indicate the amount of contaminant (wt%) in the mixture. A model using a parent basalt with slightly higher Nd and Sr instead of a picrite would not change the mixing curvature significantly but would shift the tick marks upwards to require slightly more contaminant. **B:** Enlargement of the less contaminated part of A. Slightly modified from Larsen & Pedersen (2009, fig. 19).

several or all the following characteristics relative to 'normal' rocks: increased SiO_2 , Rb, Ba, Th, K, LREE, Pb, and $^{87}\text{Sr}/^{86}\text{Sr}$, and decreased $^{143}\text{Nd}/^{144}\text{Nd}$. Nb and Zr may not decrease and there need not be any Nb or Zr trough in the multi-element pattern because some sediments have quite high Nb and Zr (up to 17 ppm Nb and 1100 ppm Zr).

An important conclusion of Pedersen & Pedersen (1987) is that no rocks more evolved than basalt were produced by ordinary fractional crystallisation; this is probably the result of very high magma production and throughput rates. More evolved rocks are always contaminated and were produced in local magma chambers with limited or no input of fresh magma. In such chambers the most evolved magmas that were formed were high-Si rhyolites which had fractionated plagioclase, sanidine, Ti-oxide and zircon, judged from the Sr, Ba, Eu, Ti and Zr troughs in the multi-element patterns (Fig. 148).

The minimum MgO content in the parent magma can be estimated from the Cr content in the contaminated magma because chromite crystallisation was delayed by low $f\text{O}_2$ caused by organic compounds from the sediments (Pedersen 1985).

Contamination processes and geochemical changes during contamination

The contamination processes in the magma chambers are very complex and have been dealt with in numerous papers, viz. Melson & Switzer (1966), Pedersen (1978a,b, 1979a,b, 1981, 1985), Ulf-Møller (1979, 1985, 1990), Pedersen & Pedersen (1987), Pedersen & Rønsbo (1987), Goodrich & Patchett (1991), Lightfoot *et al.* (1997) and Larsen & Pedersen (2009). Sediment xenoliths in the volcanic rocks provide direct evidence for the contamination processes, and analyses of slightly to strongly magma-modified and equilibrated xenoliths are included in Table 13.

Mixing and AFC processes

Bulk mixing of disintegrated sediment fragments into the magma took place to some extent, but the major magma modification was caused by mixing with partial melts of the sediment sidewall in high-level magma chambers. As evidenced by pyrometamorphosed and melted xenoliths (buchites), the high temperatures of the magmas induced partial melting of the sidewall, including the loosened xenoliths, and it was these melts, which were of rhyolitic composition, that mixed with the magmas. Analyses of melts from buchites are presented in Table 14. On a vol-

Table 14. Microprobe analyses of glasses in partially melted sediment xenoliths (buchites)

GGU No.	113449		113450		176522		138237		176506		Average glass	
Xenolith type	Mudstone		Mudstone		Mudstone		Sandstone		Sandstone		26 recalculated	
n	6	1 σ	8	1 σ	3	1 σ	2	1 σ	7	1 σ		
SiO ₂	67.94	0.49	66.45	0.52	69.40	0.82	69.20	0.14	73.82	0.86	69.36	73.89
TiO ₂	1.00	0.12	1.23	0.06	1.73	0.31	0.45	0.03	0.26	0.06	0.94	1.00
Al ₂ O ₃	14.79	0.53	15.59	0.23	13.53	1.10	13.35	0.21	11.62	0.25	13.78	14.70
FeO	0.82	0.09	0.25	0.05	2.90	0.87	1.75	0.07	0.14	0.11	1.17	1.25
MnO			0.02	0.02								
MgO	0.54	0.09	0.81	0.10	0.94	0.35	1.30	0.00	0.25	0.14	0.77	0.82
CaO	1.73	0.10	1.27	0.06	0.95	0.65	1.35	0.07	1.83	0.21	1.43	1.52
Na ₂ O	3.03	0.34	3.69	0.95	3.23	0.67	2.85	0.07	2.01	0.11	2.96	3.16
K ₂ O	3.57	0.20	2.40	0.07	2.40	0.36	2.55	0.49	5.84	0.15	3.35	3.56
P ₂ O ₅			0.48	0.05								
Sum	93.41		92.18		95.09		92.80		95.78		94.24	100.00

n: Number of analyses

atile-free basis, these melts contain 72–77 wt% SiO₂ and 6–8 wt% alkalis with high K/Na ratios. The mudstone buchite melts are peraluminous. The calculated result of simple mixing of such a rhyolitic buchite melt into a picrite magma with 15 wt% MgO is shown in Table 15. In the contaminated melt, SiO₂ and K₂O are increased, FeO*, MgO and CaO are decreased, and TiO₂, Al₂O₃, Na₂O and P₂O₅ are nearly unaffected. Such changes can be seen in all the contaminated rocks in West Greenland. The calculated mixture with 10% crustal melt is actually very close in composition to the magmas of the Nuusap Qaqqarsua Member of the Vaigat Formation.

If the contaminated magmas also fractionate, SiO₂ and K₂O will increase further and MgO and CaO will decrease further, whereas the lowered TiO₂ and FeO* will

be counteracted by fractionation-induced increases. Assimilation coupled with fractional crystallisation (AFC) was modelled with Sr isotopes for the contaminated magmas in West Greenland by Pedersen & Pedersen (1987), and bulk mixing was modelled with Sr and Nd isotopes by Goodrich & Patchett (1991), and with trace elements by Lightfoot *et al.* (1997). The isotopes are easily modelled but do not yield much information about other processes, such as assimilation of partial melts and exchange of other elements.

Reduction processes

When sediments are heated by magmas, they lose volatile components to the melt, mainly water but also sulfur and carbon compounds. If the sediments are rich in sulfur and carbon, a chain of P–T-dependent reduction processes takes place in the magma that may ultimately lead to the formation of sulfides, native iron (alloyed with carbon) and graphite. The C–CO–CO₂ buffer equilibrium plays a key role in the processes (e.g. Pedersen 1981). This equilibrium is strongly pressure-dependent (French & Eugster 1965; French 1966; Sato 1978); at pressures very much higher than atmospheric, such as prevails in a magma chamber, the magma may not be very reduced, but by pressure release during high-level intrusion or surface eruption large amounts of oxygen are consumed by this reaction, and liquid sulfide and native iron may form.

The contaminated rocks of the Vaigat and Maligat formations and their xenoliths display a range of oxides, metals and sulfides which indicate that the oxygen fugacities at high temperatures varied by as much as eight orders of magnitude (Fig. 198) from uncontaminated picrites

Table 15. Contamination of picrite by simple mixing with rhyolitic melted sediment

	Picrite	Melt	9:1 mix	Difference	Relative difference, %	400176
SiO ₂	47.5	73.9	50.14	2.64	5.6	49.73
TiO ₂	1.2	1	1.18	-0.02	-1.7	1.2
Al ₂ O ₃	12.5	14.7	12.72	0.22	1.8	12.95
FeO	11.5	1.3	10.48	-1.02	-8.9	10.68
MgO	15	0.8	13.58	-1.42	-9.5	13.11
CaO	10.5	1.5	9.6	-0.9	-8.6	9.92
Na ₂ O	1.5	3.1	1.66	0.16	10.7	1.84
K ₂ O	0.1	3.6	0.45	0.35	350	0.37
P ₂ O ₅	0.1	0.2	0.11	0.01	10	0.1
Sum	99.9	100.1	99.92			99.9

Picrite: simplified typical composition, Naujánguit Member.

Melt: average of five buchite glasses (microprobe analyses), Table 14.

Difference: difference between mixture and picrite.

400176: contaminated lava flow, Nuusap Qaqqarsua Member.

Compare 400176 with the calculated mixture.

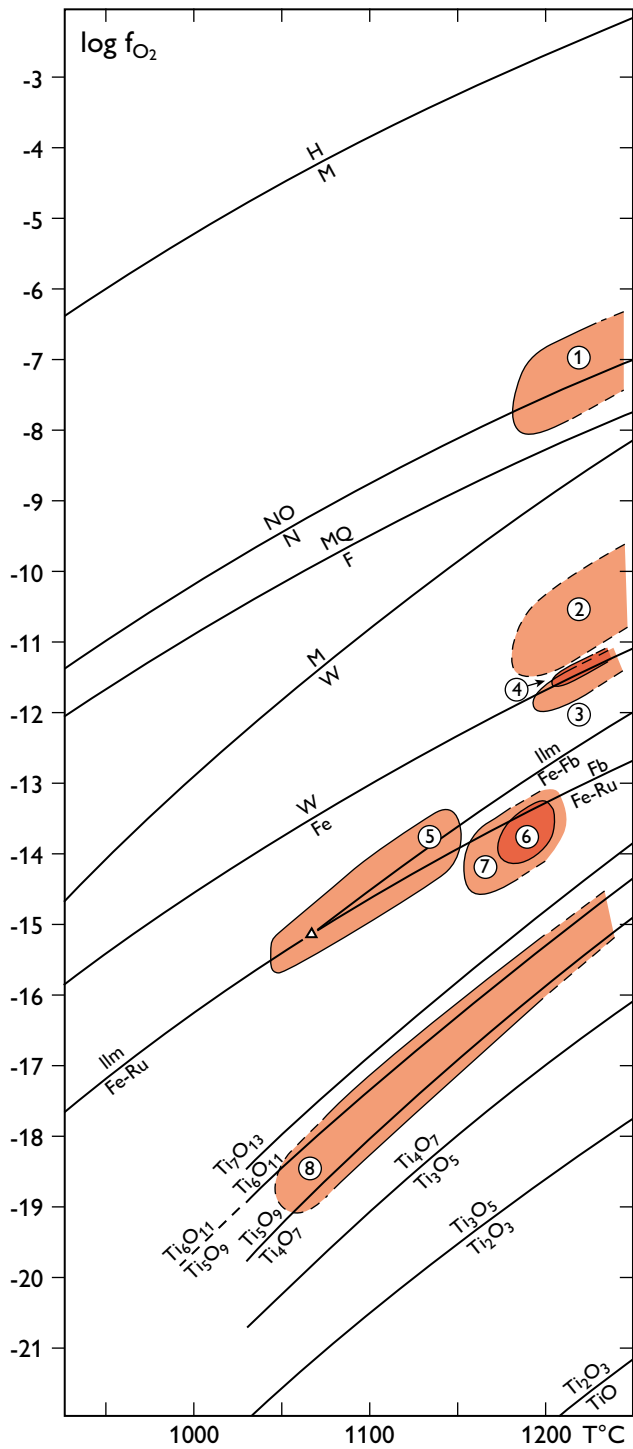


Fig. 198. f_{O_2} - T diagram at 1 bar pressure for a number of investigated volcanic rocks and their xenoliths from the Vaigat and Maligat Formations on Disko and Nuussuaq. A series of oxygen buffer curves are shown as reference curves, with the following abbreviations: **H**: hematite. **M**: magnetite. **NO**: nickel oxide. **N**: nickel metal. **Q**: quartz. **F**: fayalite. **W**: wüstite. **Fe**: metallic iron. **ilm**: ilmenite. **Fb**: ferropseudobrookite. **Ru**: rutile. The stabilities of a number of reduced Ti-oxides are shown with formulae. **Field 1**: Uncontaminated volcanic rocks of the Vaigat Formation (Pedersen 1985). **Field 2**: Kûgánguaq Member, Disko. Magnesian basaltic andesite and magnesian andesite lava flows with very low Fe^{3+} but no native iron and only trace amounts of sulfides; anomalously low Cu and Ni indicate previous sulfide fractionation (Pedersen 1985). **Field 3**: Killiit dyke, Disko. Chilled margin of magnesian basaltic andesite glass with native iron and sulfide globules (Pedersen 1979b). **Field 4**: Asuk Member tuffs in Agatdalen, Nuussuaq. Graphite-rich magnesian andesites with sulfide globules with wüstite and iron metal (Pedersen 1978b). **Field 5**: Andesite and dacite lava flows, Nordfjord Member, Disko, with ilmenite phenocrysts reacted to rutile, iron metal and armalcolite (Pedersen 1981). **Field 6**: Xenolith in native-iron-bearing lava flow, Asuk Member, Disko. Partially melted and chilled mudstone containing native iron, troilite, rutile and armalcolite (Pedersen 1979a). **Field 7**: Magnesian andesite lava flow, Asuk Member, Disko, with native iron and rutile (unpublished). **Field 8**: Xenolith in native-iron-bearing magnesian andesite lava flow, Asuk Member, Disko. Heated and chilled mudstone with oxygen-deficient Ti-oxides (Pedersen & Rønsbo 1987).

and basalts to xenoliths carrying Ti^{3+} -bearing, oxygen-deficient magnetite phases (general formula Ti_nO_{2n-1} , e.g. Pedersen 1978b, 1979a, 1981, 1985; Pedersen & Rønsbo 1987). The formation of native iron can readily be explained by well-known terrestrial reduction processes involving carbon components from sediments, and there is no need to appeal to exotic sources such as Earth's sublithospheric mantle (Bird & Weathers 1977) or iron meteorites (Nordenskiöld 1871; Jones *et al.* 2005).

Exchange of elements

Major elements. Very large decreases in FeO^* (and Ni, Cu and PGE) as seen in the Asuk and Kûgánguaq Member rocks are caused by fractionation of sulfides or native iron. The large decreases in CaO and MgO in many of the contaminated rocks are caused by loss of these elements from the magma into the sidewall. Evidence for this is found in the magma-equilibrated mudstone xenoliths: the highly aluminous mudstones have scavenged CaO and MgO from the magma to form calcic plagioclase and magnesian spinel (Melson & Switzer 1966; Pedersen 1978a). The completely recrystallised and equilibrated xenoliths consist of plagioclase-spinel-corundum-graphite aggregates. Comparison with the exposed sediments (Table 13; Fig. 193) shows that the equilibrated mudstone xenoliths have lost FeO , TiO_2 , K_2O and P_2O_5 , and have gained CaO (in gross amounts), MgO and Na_2O . Even the allegedly unequilibrated mudstone xenoliths seem to have gained Na_2O . Na_2O shows that an element may

participate in counteracting processes: it is both delivered into the magma with the partial melt and scavenged back again through mineral equilibration. Other examples of complex element behaviour are the losses of FeO^* and TiO_2 in the equilibrated xenoliths.

Trace elements. Figure 195 shows that the equilibrated xenoliths have suffered losses of almost the whole range of incompatible trace elements but have gained Sr, which is scavenged with Ca into plagioclase. Eu is not lost because it is retained as Eu^{2+} in the new-formed plagioclase in the xenolith; the rhyolitic partial melt from the xenolith would have had a pronounced negative Eu anomaly without having fractionated plagioclase.

The exchange of incompatible elements between mudstone and picrite magma is illustrated in Fig. 199. The compositional differences between picrite and mudstone are around two orders of magnitude for the most incompatible elements Rb–U (e.g. 0.04 ppm U in picrite, 4 ppm U in mudstone), declining to around one order of magnitude for Pr, and to a factor of <2 for Dy–Yb. The differences between picrite and a rhyolitic partial melt would be even greater. Accordingly, the contaminated magma (a magnesian andesite) has very strongly increased concentrations of the most incompatible elements and almost unchanged concentrations of the least incompatible elements. The Nb–Ta, Sr, P and Ti troughs and Th–U and Pb peaks of the sediment pattern are transferred to the pattern of the contaminated magma. It should be noted that despite the Nb–Ta, Sr and P troughs the contami-

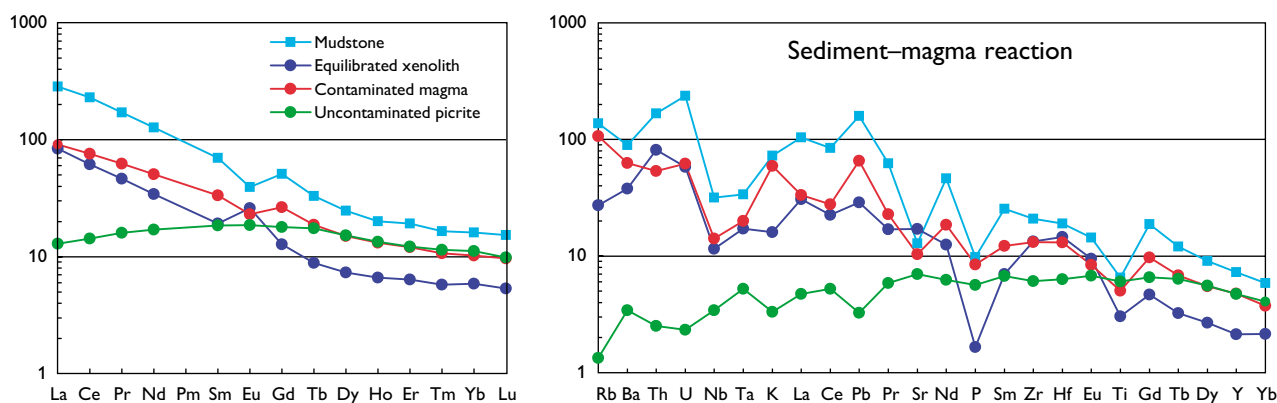


Fig. 199. REE and multi-element diagrams illustrating the behaviour of incompatible elements during crustal contamination. Left diagram: chondrite normalised; right diagram: primitive mantle normalised; normalisation factors from McDonough & Sun (1995). The uncontaminated picrite is of the Naujánúit Member (400139, 16.4 wt% MgO), the contaminated magma is an andesite of the Kûgánguaq Member (135927, 8.5 wt% MgO, 58.4 wt% SiO_2), the equilibrated mudstone xenolith is of the Nordfjord Member (400296) and the unmodified mudstone is a composite of 10 mudstone samples from Disko (176769). Note selective retention of Eu and Sr in the equilibrated xenolith. See text for discussion. Slightly modified from Larsen & Pedersen (2009, fig. 20).

nated magma has not lost these elements, only gained less of them than of the neighbouring elements in the pattern. The Eu trough in the contaminated magma is caused by fixation of Eu^{2+} in the sediment by crystallisation of plagioclase, while the other REE were transferred to the melt. In the case of Pb, a trough in the uncontaminated picrite with 0.5 ppm Pb is turned into a peak in the contaminated magma with 9.5 ppm Pb, illustrating that most of the Pb in the contaminated magma comes from the sediment.

The variation of transition elements in the contaminated rocks (Fig. 147; Pedersen *et al.* 2017, fig. 158) is caused by several mechanisms. Ni, Cu and platinum-group elements (PGE) partition extremely efficiently into sulfide and particularly metal liquid, and a hallmark of sulfide or metal fractionation from a silicate magma is its extremely low contents of Ni and Cu, as seen in the Asuk and Kûgánguaq Member rocks. Some of the Ni- and Cu-depleted rocks carry native iron but other, such as all of the Kûgánguaq Member rocks, do not. This in-

dicates that sulfide or metal fractionation has taken place at depth before eruption (Pedersen 1985; Lightfoot *et al.* 1997). Andesites of the Asuk Member do not show Ni and Cu depletion, presumably because the andesite magma quickly became too viscous to allow metal and sulfide to settle out. Relative enrichment in Cr compared to uncontaminated rocks with similar MgO took place because carbon-induced reduction delayed or prevented precipitation of chromite in the melt (Pedersen 1985).

Except for the effects of native-iron and sulfide accumulation or fractionation, the native-iron-bearing contaminated rocks do not show marked compositional differences from the native-iron-free counterparts. In detail, however, the segregated metal-rich bodies show very complex and unusual mineralogies (e.g. Goodrich 1984; Ulf-Møller 1985, 1989). In rare cases, highly reduced fluids have been preserved as inclusions in olivine in basaltic glass chills and have precipitated hydrocarbon minerals there (Solovova *et al.* 2002).

Concluding remarks

The deposition of the Maligât Formation succeeded that of the Vaigat Formation with little or no time lapse between them, and perhaps they even overlapped in time. The transition was presumably caused by changed tectonic conditions, which resulted in establishment of long-lived, deep-seated magma chambers where the picritic primary magmas, which were still produced (Larsen & Pedersen 2009), were stalled and fractionated to basalt. In this respect, the Maligât Formation is a more normal volcanic succession than the unique, picritic Vaigat Formation.

The Rinks Dal Member magmas represent conditions of quasi-equilibrium in the deep magma chambers, although periods with variable magma residence times may be inferred from the oscillating degrees of fractionation. The Nordfjord Member may represent a period with reduced magma production and therefore greater likelihood for magmas to stall at high crustal levels. The Niaquassat Member reflects a new episode of increased magma production with formation of picrites at its onset but gradually waning to end with quite fractionated basalt magmas. This would have been a suitable end to the magmatic history of the Maligât Formation; however, the existence of the few lava flows of the Sapernuvis Member with a suggestion of remelted gabbro at depth shows that a full record of the magmatic history of the formation is probably not preserved.

The Maligât Formation is confined to the southern part of the Nuussuaq Basin. The contemporaneous evolution in the northern part of the basin (Svartenhuk Halvø) probably did not comprise deposition of volcanic rocks (any age difference between the uppermost Vaigat Formation in the south and in the north is unresolved), but a non-marine sediment horizon of sandstones and mudstones with coal seams was deposited (J.G. Larsen & Grocott 1991; J.G. Larsen & Pulvertaft 2000).

The volcanic activity in the southern part of the Nuussuaq Basin did not terminate with the deposition of the Maligât Formation. Following this, two major volcanic episodes led to the deposition of the late Paleocene basalts of the Svartenhuk Formation and the early Eocene basalts of the Naqerloq Formation, which were both originally present over the whole Nuussuaq Basin from south to north (Larsen *et al.* 2016). These formations contain mass flows and acid tuffs and will be described elsewhere.

Acknowledgements

The results described in this bulletin are based on field work carried out under the auspices of GGU and subsequently GEUS, and with support from the Bureau of Minerals and Petroleum, Government of Greenland. Arktisk Station (University of Copenhagen) in Qeqertarsuaq also provided generous field support. The work was begun in 1968 (AKP) at the suggestion of professor Arne Noe-Nygaard, and over the years we have been indebted to many persons, in particular to the expedition leaders Gilroy Henderson, Feiko Kalsbeek and Flemming Getreuer Christiansen, as well as to department leaders Niels Henriksen, Christian Knudsen and Karen Hanghøj for general GEUS support.

The photogrammetric work was mainly carried out at the Technical University of Denmark in close cooperation with Keld S. Dueholm and with generous support from Ole Mærsk-Møller and Ole Jacobi. We are also grateful for support from Hans Jepsen and Erik Vest Sørensen at the GGU/GEUS photogrammetric laboratory, to Jakob Lautrop for reproduction of countless photographs in the pre-digital age and to Annette Hindø and Willy Weng for technical and geodetic help in the design and production of the geological maps and sections.

Jørgen Kystøl and Ib Sørensen, and in later years Olga Nielsen, at GGU/GEUS's rock geochemical laboratory, and John Bailey at the XRF laboratory of the Geological Institute, University of Copenhagen, maintained the constantly high quality of the chemical analyses of the rocks. Jørgen Bojesen-Koefoed is thanked for the TOC and sulfur analyses.

Jette Halskov prepared the drawings and annotated the photographs, and without her patient and excellent help over several years, this bulletin and its companion on the Vaigat Formation would not have been the same.

We are grateful to the reviewers Richard Wilson and the late Henry Emeleus for their helpful and constructive reviews, and to the scientific bulletin editor Adam Garde for his careful and competent handling of the manuscript.

We are highly indebted to our late friend and colleague Finn Ulf-Møller who took part in the field work during several years and who later, during work for the mining company Greenex, collected invaluable information in areas not visited by us. Special thanks go to the Ulf-Møller family who handed all his field notes, photographs and other unpublished material over to us after his death.

References

- Árting, U.E. 2004: A petrological study of basic dykes and sills of assumed Palaeoproterozoic age in central West Greenland. Unpublished M.Sc. thesis, University of Copenhagen, 121 pp. + appendices.
- Athavale, R.N. & Sharma, P.V. 1975: Paleomagnetic results on Early Tertiary lava flows from West Greenland and their bearing on the evolution history of the Baffin Bay–Labrador Sea region. *Canadian Journal of Earth Sciences* **12**, 1–18.
- Bird, J.M. & Weathers, M.S. 1977: Native iron occurrences of Disko Island, Greenland. *Journal of Geology* **85**, 359–371.
- Bird, J.M., Goodrich, C.A. & Weathers, M.S. 1981: Petrogenesis of Uivfaq Iron, Disko Island, Greenland. *Journal of Geophysical Research* **86**(B12), 11787–11805.
- Bøggild, O.B. 1953: The mineralogy of Greenland. *Meddelelser om Grønland* **149**(3), 442 pp.
- Bojesen-Koefoed, J.A., Christiansen, F.G., Nytoft, H.P. & Dalhoff, F. 1997: Organic geochemistry and thermal maturity of sediments in the GRO#3 well, Nuussuaq, West Greenland. *Danmarks og Grønlands Geologiske Undersøgelse Rapport* **1997/143**, 18 pp.
- Bonow, J.M. 2005: Re-exposed basement landforms in the Disko region, West Greenland – disregarded data for estimation of glacial erosion and uplift modelling. *Geomorphology* **72**, 106–127.
- Bonow, J.M., Japsen, P., Lidmar-Bergström, K., Chalmers, J.A. & Pedersen, A.K. 2006: Cenozoic uplift of Nuussuaq and Disko, West Greenland – elevated erosion surfaces as uplift markers of a passive margin. *Geomorphology* **80**, 325–337.
- Byerly, G. & Swanson, D. 1978: Invasive Columbia River Basalt flows along the northwestern margin of the Columbia Plateau, North-Central Washington. Abstracts, Geological Society of America **10**(3), 98 only.
- Chalmers, J.A. & Pulvertaft, T.C.R. 2001: Development of the continental margins of the Labrador Sea: a review. In: Wilson, R.C.L. *et al.* (eds): Non-volcanic rifting of continental margins: a comparison of evidence from land and sea. Geological Society (London) Special Publication **187**, 77–105.
- Chalmers, J.A., Pulvertaft, T.C.R., Marcussen, C. & Pedersen, A.K. 1999: New insight into the structure of the Nuussuaq Basin, central West Greenland. *Marine and Petroleum Geology* **16**, 197–224.
- Christiansen, F.G., Marcussen, C. & Chalmers, J.A. 1995: Geophysical and petroleum geological activities in the Nuussuaq – Svartehuk Halvø area 1994: promising results for an onshore exploration potential. *Rapport Grønlands Geologiske Undersøgelse* **165**, 32–41.
- Christiansen, F.G., Bojesen-Koefoed, J., Nytoft, H.P. & Laier, T. 1996: Organic geochemistry of sediments, oils and gases in the GANE#1, GANT#1 and GANK#1 wells, Nuussuaq, West Greenland. *Danmarks og Grønlands Geologiske Undersøgelse Rapport* **1996/23**, 35 pp.
- Christiansen, F.G., Bojesen-Koefoed, J. & Laier, T. 1997: Organic geochemistry of sediments and gases in the borehole Umiivik-1, Svartehuk Halvø, West Greenland. *Danmarks og Grønlands Geologiske Undersøgelse Rapport* **1997/33**, 14 pp. + figures and tables.
- Clarke, D.B. 1970: Tertiary basalts of the Baffin Bay: possible primary magma from the mantle. *Contributions to Mineralogy and Petrology* **25**, 203–224.
- Clarke, D.B. & Pedersen, A.K. 1976: Tertiary volcanic province of West Greenland. In: Escher, A. & Watt, W.S. (eds): *Geology of Greenland*, 364–385. Copenhagen: Geological Survey of Greenland.
- Clarke, D.B. & Upton, B.G.J. 1971: Tertiary basalts of Baffin Island: field relations and tectonic setting. *Canadian Journal of Earth Sciences* **8**, 248–258.
- Dam, G. 2002: Sedimentology of magmatically and structurally controlled outburst valleys along rifted volcanic margins; examples from the Nuussuaq Basin, West Greenland. *Sedimentology* **49**, 505–532.
- Dam, G. & Sønderholm, M. 1994: Lowstand slope channels of the Itilli succession (Maastrichtian–Lower Paleocene), Nuussuaq, West Greenland. *Sedimentary Geology* **94**, 49–71.
- Dam, G. & Sønderholm, M. 1998: Sedimentological evolution of a fault-controlled Early Paleocene incised valley system, Nuussuaq Basin, West Greenland. In: Shanley, K.W. & McCabe, P.J. (eds): *Relative role of eustacy, climate, and tectonism in continental rocks*. Society of Economic Palaeontologists and Mineralogists, Special Publication **59**, 109–121.
- Dam, G., Nøhr-Hansen, H., Pedersen, G.K. & Sønderholm, M. 2000: Sedimentary and structural evidence of a new early Campanian rift phase in the Nuussuaq Basin, West Greenland. *Cretaceous Research* **21**, 127–154.
- Dam, G., Pedersen, G.K., Sønderholm, M.S., Midtgaard, H.H., Larsen, L.M., Nøhr-Hansen, H. & Pedersen, A.K. 2009: Lithostratigraphy of the Cretaceous–Paleocene Nuussuaq Group, Nuussuaq Basin, West Greenland. *Geological Survey of Denmark and Greenland Bulletin* **19**, 171 pp.
- Deutsch, E.R. & Kristjansson, L.G. 1974: Palaeomagnetism of the Late Cretaceous-Tertiary volcanics from Disko Island, West Greenland. *Geophysical Journal of the Royal Astronomical Society* **39**, 343–360.
- Drever, H.I. 1953: The origin of some ultramafic rocks: a preliminary survey of the evidence for and against gravitative accumulation of olivine. *Meddelelser fra Dansk Geologisk Forening* **12**, 227–229.
- Drever, H.I. 1956: The geology of Ubekendt Ejland, West Greenland. II. The picritic sheets and dykes of the east coast. *Meddelelser om Grønland* **137**(4), 41pp.
- Ellitsgaard-Rasmussen, K. 1951: A West Greenland globule dike. *Meddelelser fra Dansk Geologisk Forening* **12**, 83–101.
- Fensome, R.A., Nøhr-Hansen, H. & Williams, G.L. 2016: Creta-

- ceous and Cenozoic dinoflagellate cysts and other palynomorphs from the western and eastern margins of the Labrador Sea. *Geological Survey of Denmark and Greenland Bulletin* **36**, 143 pp.
- Fitton, J.G., Saunders, A.D., Larsen, L.M., Hardarson, B.S. & Norry, M.J. 1998: Volcanic rocks from the South-East Greenland margin at 63°N: composition, petrogenesis and mantle sources. In: Saunders, A.D., Larsen, H.C. & Wise, S.H. (eds): *Proceedings of the Ocean Drilling Program, Scientific Results* **152**, 331–350. College Station, TX.
- French, B.M. 1966: Some geological implications of equilibrium between graphite and a C–H–O gas phase at high temperatures and pressures. *Reviews of Geophysics* **4**(2), 223–253.
- French, B.M. & Eugster, H.P. 1965: Experimental control of oxygen fugacities by graphite–gas equilibrium. *Journal of Geophysical Research* **70**, 1529–1539.
- Funck, T., Gohl, K., Damm, V. & Heyde, I. 2012: Tectonic evolution of southern Baffin Bay and Davis Strait: Results from a seismic refraction transect between Canada and Greenland. *Journal of Geophysical Research* **117**, B04107, 24 pp., <http://dx.doi.org/10.1029/2011JB009110>
- Fundal, E. 1972: Det vestgrønlandske jern – geologiens arbejdsfelt og eskimoens værktøj. *Tidsskriftet Grønland* **1972**(4), 97–110.
- Fundal, E. 1975: The Uivfaq dike and related hybrid dikes from southern Disko, West Greenland. *Meddelelser om Grønland* **195**(7), 28 pp.
- Garde, A.A. & Steenfelt, A. 1999: Precambrian geology of Nuussuaq and the area north-east of Disko Bugt, West Greenland. *Geology of Greenland Survey Bulletin* **181**, 6–40.
- Goodrich, C.A. 1984: Phosphoran pyroxene and olivine in silicate inclusions in natural iron-carbon alloy, Disko Island, Greenland. *Geochimica et Cosmochimica Acta* **48**, 1115–1126.
- Goodrich, C.A. & Bird, J.M. 1985: Formation of iron-carbon alloys in basaltic magma at Uivfaq, Disko Island: The role of carbon in mafic magmas. *Journal of Geology* **93**, 475–492.
- Goodrich, C.A. & Patchett, P.J. 1991: Nd and Sr isotope chemistry of metallic iron-bearing, sediment-contaminated Tertiary volcanics from Disko Island, Greenland. *Lithos* **27**, 13–27.
- Gregersen, U. & Bidstrup, T. 2008: Structures and hydrocarbon prospectivity in the northern Davis Strait area, offshore West Greenland. *Petroleum Geoscience* **14**, 151–166.
- Gregersen, U., Hopper, J.R. & Knutz, P.C. 2013: Basin seismic stratigraphy and aspects of prospectivity in the NE Baffin Bay, Northwest Greenland. *Marine and Petroleum Geology* **46**, 1–18.
- Hald, N. 1976: Early Tertiary flood basalts from Hareøen and western Nûgssuaq, West Greenland. *Bulletin Grønlands Geologiske Undersøgelse* **120**, 36 pp.
- Hald, N. 1977: Lithostratigraphy of the Maligât and Hareøen Formations, West Greenland Basalt Group, on Hareøen and western Nûgssuaq. *Rapport Grønlands Geologiske Undersøgelse* **79**, 9–16.
- Hald, N. & Pedersen, A.K. 1975: Lithostratigraphy of the Early Tertiary volcanic rocks of central West Greenland. *Rapport Grønlands Geologiske Undersøgelse* **69**, 17–24.
- Hansen, K. & Pedersen, A.K. 1985: Fission track dating of lower Tertiary rhyolitic glass rocks from Disko. *Rapport Grønlands Geologiske Undersøgelse* **125**, 28–30.
- Heinesen, M. 1987: Nedre tertiære basaltbreccier og undervands-lavstrømme, sydlige Disko, Vestgrønland: Strukturelle, petrografiske og mineralogiske studier. Unpublished MSc thesis, University of Copenhagen, 118 pp. + 3 volumes appendices.
- Henderson, G. 1969: The Precambrian rocks of the Egedesminde–Christianshåb area, West Greenland. *Rapport Grønlands Geologiske Undersøgelse* **23**, 37 pp. + map.
- Henderson, G. 1973: The geological setting of the West Greenland basin in the Baffin Bay region. *Earth Science Symposium on Offshore Eastern Canada. Geological Survey of Canada, Paper* **71-23**, 521–544.
- Holm, P.M., Gill, R.C.O., Pedersen, A.K., Larsen, J.G., Hald, N., Nielsen, T.F.D. & Thirlwall, M.F. 1993: The Tertiary picrites of West Greenland: contributions from ‘Icelandic’ and other sources. *Earth and Planetary Science Letters* **115**, 227–244.
- Howarth, G.H., Day, J.M.D., Pernet-Fisher, J.F., Goodrich, C.A., Pearson, D.G., Luo, Y., Ryabov, V.V. & Taylor, L.A. 2017: Precious metal enrichment in terrestrial native Fe-bearing basalts investigated using laser-ablation ICP-MS. *Geochimica et Cosmochimica Acta* **203**, 343–363.
- Japsen, P., Green, P.F. & Chalmers, J.A. 2005: Separation of Palaeogene and Neogene uplift on Nuussuaq, West Greenland. *Journal of the Geological Society (London)* **162**, 299–314.
- Japsen, P., Bonow, J.M., Green, P.F., Chalmers, J.A. & Lidmar-Bergström, K. 2009: Formation, uplift and dissection of planation surfaces at passive continental margins – a new approach. *Earth Surface Processes and Landform* **34**(5), 683–699, <http://dx.doi.org/10.1002/esp.1766>
- Jones, A.P., Kearsley, A.T., Friend, C.R.L., Robin, E., Beard, A., Tamura, A., Trickett, S. & Claeys, P. 2005: Are there signs of a large Paleocene impact preserved around Disko Bay, West Greenland? Nuussuaq spherule beds origin by impact instead of volcanic eruption? In: Kenkmann, T., Hörz, F. & Deutsch, A. (eds): *Large meteorite impacts III. Geological Society of America, Special Paper* **384**, 281–298.
- Kalsbeek, F. & Skjærnaa, L. 1999: The Archaean Atâ intrusive complex (Atâ tonalite), north-east Disko Bugt, West Greenland. *Geology of Greenland Survey Bulletin* **181**, 103–112.
- Kalsbeek, F. & Taylor, P.N. 1999: Review of isotope data for Precambrian rocks from the Disko Bugt region, West Greenland. *Geology of Greenland Survey Bulletin* **181**, 41–47.
- Kalsbeek, F., Taylor, P.N. & Pidgeon, R.T. 1988: Unreworked Archaean basement and Proterozoic supracrustal rocks from north-eastern Disko Bugt, West Greenland: implications for the nature of Proterozoic mobile belts in Greenland. *Canadian Journal of Earth Sciences* **25**, 773–782.
- Kalsbeek, F., Pulvertaft, T.C.R. & Nutman, A.P. 1998: Geochemistry, age and origin of metagreywackes from the Palaeoproterozoic Karrat Group, Rinkian Belt, West Greenland. *Precambrian Research* **91**, 383–399.
- Kilburn, C.R.J. 2000: Lava flows and flow fields. In: Sigurdsson, H. (ed.): *Encyclopedia of volcanoes*, 291–305. London: Academic Press.

- Klöß, W., Palme, H. & Tobschall, H.J. 1986: Trace elements in natural metallic iron from Disko Island, Greenland. *Contributions to Mineralogy and Petrology* **93**, 273–282.
- Koch, B.E. 1959: Contribution to the stratigraphy of the non-marine Tertiary deposits on the south coast of the Nûgssuaq Peninsula, northwest Greenland, with remarks on the fossil flora. *Meddelelser om Grønland* **162**, 100 pp.
- Larsen, J.G. 1977: Transition from low potassium olivine tholeiites to alkali basalts on Ubekendt Ejland. *Meddelelser om Grønland* **200**(1), 42 pp.
- Larsen, J.G. & Grocott, J. 1991: Geological Map of Greenland, 1:100 000, Svartehuk 71 V.1 Nord. Copenhagen: Geological Survey of Denmark and Greenland.
- Larsen, J.G. & Pulvertaft, T. C. R. 2000: The structure of the Cretaceous–Palaeogene sedimentary-volcanic area of Svartehuk Halvø, central West Greenland. *Geology of Greenland Survey Bulletin* **188**, 40 pp.
- Larsen, L.M. 2006: Mesozoic to Palaeogene dyke swarms in West Greenland and their significance for the formation of the Labrador Sea and the Davis Strait. *Danmarks og Grønlands Geologiske Undersøgelse Rapport* **2006/34**, 69 pp. + appendices.
- Larsen, L.M. & Dalhoff, F. 2007: Composition and significance of igneous rocks dredged in 2006 from the northern Labrador Sea and the Davis Strait. *Danmarks og Grønlands Geologiske Undersøgelse Rapport* **2007/67**, 29 pp. + appendix.
- Larsen, L.M. & Pedersen, A.K. 1988: Investigations of Tertiary volcanic rocks along the south coast of Nûgssuaq and in eastern Disko, 1987. *Rapport Grønlands Geologiske Undersøgelse* **140**, 28–32.
- Larsen, L.M. & Pedersen, A.K. 1989: New geological investigations in eastern Disko: redeposited volcanoclastic sediments with rhyolite from the Nordfjord Member. *Rapport Grønlands Geologiske Undersøgelse* **145**, 45–49.
- Larsen, L.M. & Pedersen, A.K. 1990: Volcanic marker horizons in the Maligât Formation on Disko and Nûgssuaq, and implications for the development of the southern part of the West Greenland basin in the early Tertiary. *Rapport Grønlands Geologiske Undersøgelse* **148**, 65–73.
- Larsen, L.M. & Pedersen, A.K. 1992: Volcanic marker horizons in the upper part of the Maligât Formation on eastern Disko and Nuussuaq, Tertiary of West Greenland: syn- to post-volcanic basin movements. *Rapport Grønlands Geologiske Undersøgelse* **155**, 85–93.
- Larsen, L.M. & Pedersen, A.K. 2000: Processes in high-Mg, high-T magmas: Evidence from olivine, chromite and glass in Palaeogene picrites from West Greenland. *Journal of Petrology* **41**, 1071–1098.
- Larsen, L.M. & Pedersen, A.K. 2009: Petrology of the Paleocene picrites and flood basalts on Disko and Nuussuaq, West Greenland. *Journal of Petrology* **50**, 1667–1711.
- Larsen, L.M., Pedersen, A.K., Sundvoll, B. & Frei, R. 2003: Alkali picrites formed by melting of old metasomatised lithospheric mantle: Manitdlat Member, Paleocene of West Greenland. *Journal of Petrology* **44**, 3–38.
- Larsen, L.M., Pedersen, A.K. & Pedersen, G.K. 2006: A subaqueous rootless cone field at Niuluut, Disko, Paleocene of West Greenland. *Lithos* **92**, 20–32.
- Larsen, L.M., Heaman, L.M., Creaser, R.A., Duncan, A.R., Frei, R. & Hutchison, M. 2009: Tectonomagmatic events during stretching and basin formation in the Labrador Sea and the Davis Strait: evidence from age and composition of Mesozoic to Palaeogene dyke swarms in West Greenland. *Journal of the Geological Society (London)* **166**, 999–1012.
- Larsen, L.M., Pedersen, A.K., Tegner, C., Duncan, R.A., Hald, N. & Larsen, J.G. 2016: Age of Tertiary volcanic rocks on the West Greenland continental margin: volcanic evolution and event correlation to other parts of the North Atlantic Igneous Province. *Geological Magazine* **153**, 487–511, <http://dx.doi.org/10.1017/S0016756815000515>
- Le Maitre, R.W. (ed.) 2002: *Igneous Rocks, A classification and glossary of terms*. 2nd edition. Recommendations of the IUGS subcommission on the systematics of igneous rocks, 236 pp. Cambridge: Cambridge University Press.
- Lightfoot, P.C., Hawkesworth, C.J., Olshevsky, K., Green, A., Doherty, W. & Keays, R.R. 1997: Geochemistry of Tertiary tholeiites and picrites from Qeqertarsuaq (Disko Island) and Nuussuaq, West Greenland with implications for the mineral potential of comagmatic intrusions. *Contributions to Mineralogy and Petrology* **128**, 139–163.
- Löfquist, H. & Benedicks, C. 1941: Det stora Nordenskiöldska Järnblocket från Ovifak: Mikrostruktur och Bildningsätt. *Kungliga Svenska Vetenskapsakademiens Handlingar* **19**(3), 96 pp.
- Lorenzen, J. 1882: Kemisk Undersøgelse af det metalliske Jern fra Grønland samt nogle af de dermed følgende Bjergarter. *Meddelelser om Grønland* **4**(4), 133–172.
- McDonough, W.F. & Sun, S.-S. 1995: The composition of the Earth. *Chemical Geology* **120**, 223–253.
- Melson, W.G. & Switzer, G. 1966: Plagioclase-spinel-graphite xenoliths in metallic iron-bearing basalts, Disko Island, Greenland. *American Mineralogist* **51**, 664–676.
- Midtgaard, H.H. 1996: Inner-shelf to lower-shoreface hummocky sandstone bodies with evidence for geostrophic influenced combined flow, Lower Cretaceous, West Greenland. *Journal of Sedimentary Research* **66**, 343–353.
- Murphy, M.A. & Salvador, A. (eds) 1999: *International Stratigraphic Guide – an abridged version*. International Subcommission on Stratigraphic Classification of IUGS, International Commission on Stratigraphy. *Episodes* **22**(4), 255–271.
- Nauckhoff, G. 1872: Om förekomsten af gediget jern i en basaltgång vid Ovifak i Grönland. Bihang till Kungliga Svenska Vetenskapsakademiens Handlingar **1**(5), 38 pp.
- Nicolau, T. 1900: Untersuchungen an den eisenführenden Gesteinen der Insel Disko. *Meddelelser om Grønland* **24**, 215–248.
- Noe-Nygaard, A. 1974: Cenozoic to recent volcanism in and around the North Atlantic basin. In: Nairn, A.E.M. & Stehli, F.G. (eds): *The ocean basins and margins* **2**, 391–443. New York: Plenum.
- Nordenskiöld, N.A.E. 1871: Redogörelse för en expedition till Grönland år 1870. Öfversikt af Kungliga Svenska Vetenskaps-

- akademiens Förhandlingar, Stockholm **27**(10), 923–1082.
- Nordström, T. 1871: Kemisk undersökning af Meteorjern från Ovi-fak på Grönland. Öfversigt af Kungliga Svenska Vetenskapsakademiens Förhandlingar, Stockholm **28**, 453–462.
- Oakey, G.N. & Chalmers, J.A. 2012: A new model for the Paleogene motion of Greenland relative to North America: Plate reconstructions of the Davis Strait and Nares Strait regions between Canada and Greenland. *Journal of Geophysical Research* **117**, B10401, 28 pp., <http://dx.doi.org/10.1029/2011JB008942>
- Pauly, H. 1958: Igdlukúnguaq nickeliferous pyrrhotite. Meddelelser om Grønland **157**(3), 169 pp. (also *Bulletin of the Geological Survey of Greenland* **17**).
- Pauly, H. 1969: White cast iron with cohenite, schreibersite and sulphides from Tertiary basalts on Disko, Greenland. Meddelelser fra Dansk Geologisk Forening **19**, 8–26.
- Pedersen, A.K. 1969: Preliminary notes on the Tertiary volcanic lavas of northern Disko. Rapport Grønlands Geologiske Undersøgelse **19**, 21–24.
- Pedersen, A.K. 1975a: New mapping in north-western Disko 1972. Rapport Grønlands Geologiske Undersøgelse **69**, 25–32.
- Pedersen, A.K. 1975b: A pillowed sill from the Atanikerdluk area, Nûgssuaq. Rapport Grønlands Geologiske Undersøgelse **69**, 33–34.
- Pedersen, A.K. 1975c: New investigations of the native iron bearing volcanic rocks of Disko, central West Greenland. Rapport Grønlands Geologiske Undersøgelse **75**, 48–51.
- Pedersen, A.K. 1977a: Iron-bearing and related volcanic rocks in the area between Gieseckes Dal and Hammers Dal, north-west Disko. Rapport Grønlands Geologiske Undersøgelse **81**, 5–14.
- Pedersen, A.K. 1977b: Tertiary volcanic geology of the Mellemfjord area, south-west Disko. Rapport Grønlands Geologiske Undersøgelse **81**, 35–51.
- Pedersen, A.K. 1977c: Dyke intrusions along the south coast of Disko. Rapport Grønlands Geologiske Undersøgelse **81**, 57–67.
- Pedersen, A.K. 1978a: Non-stoichiometric magnesian spinels in shale xenoliths from a native iron bearing andesite at Asuk, Disko, Central West Greenland. *Contributions to Mineralogy and Petrology* **67**, 331–340.
- Pedersen, A.K. 1978b: Graphite andesite tuffs resulting from high-Mg tholeiite and sediment reaction; Nûgssuaq, West Greenland. *Bulletin of the Geological Society of Denmark* **27**, Special Issue, 117–130.
- Pedersen, A.K. 1979a: A shale buchite xenolith with armalcolite and native iron in a lava from Asuk, Disko, central West Greenland. *Contributions to Mineralogy and Petrology* **69**, 83–94.
- Pedersen, A.K. 1979b: Basaltic glass with high-temperature equilibrated immiscible sulphide bodies with native iron from Disko, central West Greenland. *Contributions to Mineralogy and Petrology* **69**, 397–407.
- Pedersen, A.K. 1981: Armalcolite-bearing Fe-Ti oxide assemblages in graphite-equilibrated silic volcanic rocks with native iron from Disko, central West Greenland. *Contributions to Mineralogy and Petrology* **77**, 307–324.
- Pedersen, A.K. 1985: Reaction between picrite magma and continental crust: early Tertiary silicic basalts and magnesian andesites from Disko, West Greenland. *Bulletin Grønlands Geologiske Undersøgelse* **152**, 126 pp.
- Pedersen, A.K. & Dueholm, K.S. 1992: New methods for the geological analysis of Tertiary volcanic formations on Nuussuaq and Disko, central West Greenland, using multi-model photogrammetry. In: Dueholm, K.S. & Pedersen, A.K. (eds): Geological analysis and mapping using multi-model photogrammetry. Rapport Grønlands Geologiske Undersøgelse **156**, 19–34.
- Pedersen, A.K. & Larsen, L.M. 1987: Early Tertiary volcanic rocks from eastern Disko and south-eastern Nûgssuaq. Rapport Grønlands geologiske Undersøgelse **135**, 11–17.
- Pedersen, A.K. & Larsen, L.M. 2006: The Ilugissoq graphite andesite volcano, Nuussuaq, central West Greenland. *Lithos* **92**, 1–19.
- Pedersen, A.K. & Pedersen, S. 1987: Sr isotope chemistry of contaminated Tertiary volcanic rocks from Disko, central West Greenland. *Bulletin of the Geological Society of Denmark* **36**, 315–336.
- Pedersen, A.K. & Rønsbo, J.G. 1987: Oxygen deficient Ti oxides (natural magnéli phases) from mudstone xenoliths with native iron from Disko, central West Greenland. *Contributions to Mineralogy and Petrology* **96**, 35–46.
- Pedersen, A.K. & Ulf-Møller, F. 1980: Field work in central west Disko, 1979. Rapport Grønlands Geologiske Undersøgelse **100**, 51–55.
- Pedersen, A.K. & Ulf-Møller, F. 1987: Geological Map of Greenland, 1:100 000, Mellemfjord 69 V.1 Nord. Copenhagen: Geological Survey of Greenland.
- Pedersen, A.K., Larsen, L.M. & Dueholm, K.S. 1993: Geological section along the south coast of Nuussuaq, central West Greenland. 1:20 000 coloured geological sheet. Copenhagen: Geological Survey of Greenland.
- Pedersen, A.K., Larsen, L.M. & Pedersen, G.K. 1996: Filling and plugging of a marine basin by volcanic rocks: the Tunoqu Member of the Lower Tertiary Vaigat Formation on Nuussuaq, central West Greenland. *Bulletin Grønlands Geologiske Undersøgelse* **171**, 5–28.
- Pedersen, A.K., Ulf-Møller, F., Larsen, L.M., Pedersen, G.K. & Dueholm, K.S. 2000: Geological Map of Greenland, 1:100 000, Uiffaq 69 V.1 Syd. Copenhagen: Geological Survey of Denmark and Greenland.
- Pedersen, A.K., Larsen, L.M., Ulf-Møller, F., Pedersen, G.K. & Dueholm, K.S. 2001: Geological Map of Greenland, 1:100 000, Pingu 69 V.2 Nord. Copenhagen: Geological Survey of Denmark and Greenland.
- Pedersen, A.K., Larsen, L.M. & Dueholm, K.S. 2002a: Geological section along the north side of the Aaffarsuaq valley and central Nuussuaq, central West Greenland. 1:20 000 coloured geological sheet. Copenhagen: Geological Survey of Denmark and Greenland.
- Pedersen, A.K., Larsen, L.M., Riisager, P. & Dueholm, K.S. 2002b: Rates of volcanic deposition, facies changes and movements in a dynamic basin: the Nuussuaq Basin, West Greenland, around the C27n–C26r transition. In: Jolley, D.W. & Bell, B.R. (eds): *The North Atlantic Igneous Province: stratigraphy, tectonics, volcan-*

- ic and magmatic processes. Geological Society (London) Special Publication **197**, 157–181.
- Pedersen, A.K., Larsen, L.M., Pedersen, G.K., Heinesen, M.V. & Dueholm, K.S. 2003: Geological section along the south and south-west coast of Disko, central West Greenland. 1:20 000 coloured geological sheet. Copenhagen: Geological Survey of Denmark and Greenland.
- Pedersen, A.K., Larsen, L.M., Pedersen, G.K. & Dueholm, K.S. 2005: Geological section across north central Disko from Nordfjord to Pingu, central West Greenland. 1:20 000 coloured geological sheet. Copenhagen: Geological Survey of Denmark and Greenland.
- Pedersen, A.K., Larsen, L.M., Pedersen, G.K., Sønderholm, M., Midtgaard, H.H., Pulvertaft, T.C.R. & Dueholm, K.S. 2006a: Geological section along the north coast of the Nuussuaq peninsula, central West Greenland. 1:20 000 coloured geological sheet. Copenhagen: Geological Survey of Denmark and Greenland.
- Pedersen, A.K., Larsen, L.M., Pedersen, G.K. & Dueholm, K.S. 2006b: Five slices through the Nuussuaq Basin. Geological Survey of Denmark and Greenland Bulletin **10**, 53–56.
- Pedersen, A.K., Pedersen, G.K., Larsen, L.M., Pulvertaft, T.C.R., Sønderholm, M., & Dueholm, K.S. 2007a: Geological map of the Nuussuaq Basin in southern Nuussuaq, 1:100 000, special map Paatuut, with detailed sections. Copenhagen: Geological Survey of Denmark and Greenland.
- Pedersen, A.K., Pedersen, G.K., Larsen, L.M., Pulvertaft, T.C.R., Sønderholm, M., & Dueholm, K.S. 2007b: Geological map of the south-east coast of Nuussuaq between Ataata Kuua and Saqqaqdalen, central West Greenland, 1:50 000, with detailed sections. Copenhagen: Geological Survey of Denmark and Greenland.
- Pedersen, A.K., Larsen, L.M. & Pedersen, G.K. 2017: Lithostratigraphy, geology and geochemistry of the volcanic rocks of the Vaigat Formation on Disko and Nuussuaq, Paleocene of West Greenland. Geological Survey of Denmark and Greenland Bulletin **39**, 244 pp.
- Pedersen, G.K. & Pulvertaft, T.C.R. 1992: The non-marine Cretaceous of the West Greenland Basin, onshore West Greenland. Cretaceous Research **13**, 263–272.
- Pedersen, G.K., Larsen, L.M., Pedersen, A.K. & Hjortkjær, B.F. 1998: The synvolcanic Naajaat lake, Paleocene of West Greenland. Palaeogeography, Palaeoclimatology, Palaeoecology **140**, 271–287.
- Pedersen, G.K., Andersen, L.A., Lundsteen, E.B., Petersen, H.I., Boejesen-Koefoed, J.A. & Nytoft, H.P. 2006: Depositional environments, organic maturity and petroleum potential of the Cretaceous coal-bearing Atane Formation at Qullissat, Nuussuaq Basin, West Greenland. Journal of Petroleum Geology **29**, 3–26.
- Piasecki, S., Larsen, L.M., Pedersen, A.K. & Pedersen, G.K. 1992: Palynostratigraphy of the Lower Tertiary volcanics and marine clastic sediments in the southern part of the West Greenland Basin: Implications for the timing and duration of the volcanism. Rapport Grønlands Geologiske Undersøgelse **154**, 13–31.
- Rasmussen, T.M. 2002: Aeromagnetic survey in central West Greenland: Project Aeromag 2001. Geology of Greenland Survey Bulletin **191**, 67–72.
- Riisager, J., Riisager, P. & Perrin, M. 1999: Palaeodirectional and palaeointensity results of Paleocene and Eocene basalts from West Greenland. Bulletin of the Geological Society of Denmark **46**, 69–78.
- Riisager, J., Riisager, P. & Pedersen, A.K. 2003: Paleomagnetism of large igneous provinces: case-study from West Greenland, North Atlantic igneous province. Earth and Planetary Science Letters **214**, 409–425.
- Riisager, P. & Abrahamsen, N. 1999: Magnetostratigraphy of Paleocene basalts from the Vaigat Formation of West Greenland. Geophysical Journal International **137**, 774–782.
- Ross, M.E. 1989: Stratigraphic relationships of subaerial, invasive, and intracanyon flows of Saddle Mountains Basalt in the Troy Basin, Oregon, Washington. In: Reidel, S.P. & Hooper, P.R. (eds): Volcanism and tectonism in the Columbia River flood-basalt province. Geological Society of America, Special Paper **239**, 131–142.
- Sato, M. 1978: Oxygen fugacity and the role of gas-forming elements. Geophysical Research Letters **5**, 447–449.
- Saunders, A.D., Fitton, J.G., Kerr, A.C., Norry, M.J. & Kent, R.W. 1997: The North Atlantic Igneous Province. In: Mahoney, J.J. & Coffin, M.L. (eds): Large Igneous Provinces. Geophysical Monograph **100**, 45–93. Washington, D.C.: American Geophysical Union.
- Schiener, E.J. 1975: Sedimentological notes on sandstones from Nûgssuaq, central West Greenland, Rapport Grønlands Geologiske Undersøgelse **69**, 35–44.
- Schmidt, A.G., Riisager, P., Abrahamsen, N., Riisager, J., Pedersen, A.K. & van der Voo, R. 2005: Palaeomagnetism of the Eocene Talerua Member lavas on Hareöen, West Greenland. Bulletin of the Geological Society of Denmark **52**, 27–38.
- Schmincke, H.-U. 1967: Fused tuff and peperites in south-central Washington. Bulletin of the Geological Society of America **78**, 319–330.
- Sjögren, H.J. 1916: Om ovifakjärnet och andra telluriska basaltjärn. Kungliga Svenska Vetenskapsakademiens Årsbok för år 1916, 255–290.
- Skaarup, N. 2002: Evidence for continental crust in the offshore Palaeogene volcanic province, central West Greenland. Geology of Greenland Survey Bulletin **191**, 97–102.
- Skaarup, N. & Pulvertaft, T.C.R. 2007: Aspects of the structure on the coast of the West Greenland volcanic province revealed in seismic data. Bulletin of the Geological Society of Denmark **55**, 65–80.
- Solovova, I.P., Ryabchikov, I.D., Girmis, A.V., Pedersen, A. & Lundsteen, T. 2002: Reduced magmatic fluids in basalt from the island of Disko, central West Greenland. Chemical Geology **183**, 365–371.
- Steenstrup, K.J.V. 1874: Om de kulførende Dannelser på Øen Disko, Hareöen og Syd-Siden af Nûgssuaq's Halvöen i Nord-Grønland. Videnskabelige Meddelelser fra den naturhistoriske Forening i Kjöbenhavn for Aaret 1874, 75–112 + 3 plates.

- Steenstrup, K.J.V. 1875: Om de Nordenskiöldske Jærnmasser og om Forekomsten af gedigent Jærn i Basalt. Videnskabelige Meddelelser fra den naturhistoriske Forening i Kjöbenhavn for Aaret 1875, 284–306 + 2 plates.
- Steenstrup, K.J.V. 1883: Bidrag til Kjendskab til de geognostiske og geographiske Forhold i en Del af Nord-Grønland. Meddelelser om Grønland **4**(5), 173–242.
- Steenstrup, K.J.V. 1900: Beretning om en Undersøgelsesrejse til Øen Disko i Sommeren 1898. Meddelelser om Grønland **24**, 249–306 + plates.
- Storey, M., Duncan, R.A., Pedersen, A.K., Larsen, L.M. & Larsen, H.C. 1998: $^{40}\text{Ar}/^{39}\text{Ar}$ geochronology of the West Greenland Tertiary volcanic province. *Earth and Planetary Science Letters* **160**, 569–586.
- Törnebohm, A.E. 1878: Über die eisenführenden Gesteine von Ovifaq und Assuk in Grönland. Bihang till Kungliga Svenska Vetenskapsakademiens Handlingar **4**(10), 1–22.
- Ulff-Møller, F. 1975: High temperature pyrrhotite and telluric iron mineralisations in western Disko, central West Greenland. Rapport Grønlands Geologiske Undersøgelse **75**, 51–53.
- Ulff-Møller, F. 1977: Native iron bearing intrusions of the Hammers Dal Complex, North-west Disko. Rapport Grønlands Geologiske Undersøgelse **81**, 15–33.
- Ulff-Møller, F. 1979: New investigations of Tertiary lavas and dykes in the area around Disko Fjord, South Disko, central West Greenland. Rapport Grønlands Geologiske Undersøgelse **95**, 30–34.
- Ulff-Møller, F. 1983: Tellurisk jern fra subvulkanske intrusioner på Disko, Grønland. En Petrografisk og kemisk undersøgelse. Unpublished PhD thesis, University of Copenhagen, 124 pp. + appendices.
- Ulff-Møller, F. 1985: Solidification history of the Kitdlit lens: immiscible metal and sulphide liquids from a basaltic dyke on Disko, central West Greenland. *Journal of Petrology* **26**, 64–91.
- Ulff-Møller, F. 1986: Støbejernsblok på 10 tons fundet på Disko. Forskning i Grønland/Tusaat **2/86**, 20–25.
- Ulff-Møller, F. 1989: Exsolution of metallic Pb liquid in a magmatic sulphide–metal lens from Disko, central West Greenland. *Neues Jahrbuch für Mineralogie Abhandlungen* **160**, 193–206.
- Ulff-Møller, F. 1990: Formation of native iron in sediment-contaminated magma. I. A case study of the Hanekammen Complex on Disko Island, West Greenland. *Geochimica et Cosmochimica Acta* **54**, 57–70.
- Ulff-Møller, F. 1991: Magmatic platinum-nickel occurrences in the Tertiary West Greenland Basalt Province: prospecting by Greenex A/S in 1985–1988. Open File Series Grønlands Geologiske Undersøgelse **91/1**, 37 pp.
- Upton, B.G.J. 1988: History of Tertiary igneous activity in the N Atlantic borderlands. In: Morton, A.C. & Parson, L.M. (eds): Early Tertiary volcanism and the opening of the NE Atlantic. Geological Society (London) Special Publication **39**, 429–453.
- Vandenbergh, N., Hilgen, F.J. & Speijer, R.P. 2012: The Paleogene period. In: Gradstein, F.M. *et al.* (eds): The geologic time scale 2012, 855–921. Amsterdam: Elsevier, <http://dx.doi.org/10.1016/B978-0-444-59425-9.00028-7>
- White, J.D.L. & Houghton, B.F. 2006: Primary volcanoclastic rocks. *Geology* **34**, 677–680.

Geological map sheets and sections

Excepting Rosenkrantz et al. (1974, 1976), Pulvertaft (1987) and Pedersen et al. (2008) all these are also included in the reference list because they are referred to in the main text.

- Pedersen, A.K. & Ulff-Møller, F. 1987: Geological Map of Greenland, 1:100 000, Mellemfjord 69 V.1 Nord. Copenhagen: Geological Survey of Greenland.
- Pedersen, A.K., Larsen, L.M. & Dueholm, K.S. 1993: Geological section along the south coast of Nuussuaq, central West Greenland. 1:20 000 coloured geological sheet. Copenhagen: Geological Survey of Greenland.
- Pedersen, A.K., Ulff-Møller, F., Larsen, L.M., Pedersen, G.K. & Dueholm, K.S. 2000: Geological Map of Greenland, 1:100 000, Uiffaq 69 V.1 Syd. Copenhagen: Geological Survey of Denmark and Greenland.
- Pedersen, A.K., Larsen, L.M., Ulff-Møller, F., Pedersen, G.K. & Dueholm, K.S. 2001: Geological Map of Greenland, 1:100 000, Pingu 69 V.2 Nord. Copenhagen: Geological Survey of Denmark and Greenland.
- Pedersen, A.K., Larsen, L.M. & Dueholm, K.S. 2002: Geological section along the north side of the Aaffarsuaq valley and central Nuussuaq, central West Greenland. 1:20 000 coloured geological sheet. Copenhagen: Geological Survey of Denmark and Greenland.
- Pedersen, A.K., Larsen, L.M., Pedersen, G.K., Heinesen, M.V. & Dueholm, K.S. 2003: Geological section along the south and south-west coast of Disko, central West Greenland. 1:20 000 coloured geological sheet. Copenhagen: Geological Survey of Denmark and Greenland.
- Pedersen, A.K., Larsen, L.M., Pedersen, G.K. & Dueholm, K.S. 2005: Geological section across north central Disko from Nordfjord to Pingu, central West Greenland. 1:20 000 coloured geological sheet. Copenhagen: Geological Survey of Denmark and Greenland.
- Pedersen, A.K., Larsen, L.M., Pedersen, G.K., Sønderholm, M., Midtgaard, H.H., Pulvertaft, T.C.R. & Dueholm, K.S. 2006: Geological section along the north coast of the Nuussuaq peninsula, central West Greenland. 1:20 000 coloured geological sheet. Copenhagen: Geological Survey of Denmark and Greenland.
- Pedersen, A.K., Pedersen, G.K., Larsen, L.M., Pulvertaft, T.C.R., Sønderholm, M., & Dueholm, K.S. 2007a: Geological map of the Nuussuaq Basin in southern Nuussuaq, 1:100 000, special map Paatuut, with detailed sections. Copenhagen: Geological Survey of Denmark and Greenland.
- Pedersen, A.K., Pedersen, G.K., Larsen, L.M., Pulvertaft, T.C.R., Sønderholm, M., & Dueholm, K.S. 2007b: Geological map of the south-east coast of Nuussuaq between Ataata Kuua and Saqqaqdalen, central West Greenland, 1:50 000, with detailed sections. Copenhagen: Geological Survey of Denmark and Greenland.

- Pedersen, A.K., Larsen, L.M., Pedersen, G.K. & Dueholm, K.S. 2008: Geological map of the area around Sikillingi, western Nuussuaq, central West Greenland, 1:20 000. Copenhagen: Geological Survey of Denmark and Greenland.
- Pulvertaft, T.C.R. 1987: Geological Map of Greenland, 1:100 000, Agpat 70 V.2 Nord. Copenhagen: Geological Survey of Denmark and Greenland.
- Rosenkrantz, A., Münther, V. & Henderson, G. 1974: Geological map of Greenland, 1:100 000, Agatdal 70 V.1 Nord. København: Grønlands Geologiske Undersøgelse.
- Rosenkrantz, A., Münther, V., Henderson, G., Pedersen, A.K. & Hald, N. 1976: Geological map of Greenland, 1:100 000, Qutdligssat 70 V.1 Syd. København: Grønlands Geologiske Undersøgelse.

Appendix: Place names

The place names mentioned in the text and listed below are shown on the maps in Fig. 1 (regional names) and Figs 4, 6 and 103 (local names and localities).

Aasiaat	Fig. 1	Illuluarsuit Qaqqaa	Fig. 6, 103
Aaffarsuaq	Figs 4, 6	Innerit	Fig. 1
Agatdalen	Fig. 6	Inngigissoq	Figs 4, 6
Agatfjeldet	Fig. 6	Innarsuaq (Skarvefjeld)	Figs 4, 6
Akuarut (Lyngmarksfjeld)	Fig. 6	Inussuk	Fig. 6
Akuliarusersuaq	Figs 4, 6	Ippik	Fig. 6
Akulliit (Mellemfjord)	Figs 4, 6	Itilli (fault)	Figs 1, 4
Akunneq	Fig. 6	Ivisaarqut (Enok Havn)	Fig. 6
Alangup Qaqqai	Fig. 6	Ivissussat Qaqqaat	Figs 4, 6
Apostelfjeld (Navaranaat)	Fig. 6	Jamma	Fig. 6
Aqajaruata Qaqqaa	Figs 4, 6	Jernpynten	Fig. 6
Assoq	Figs 4, 6	Kangerluk	Figs 4, 6
Asuk	Figs 4, 6	Kangersooq (Nordfjord)	Figs 4, 6
Asuutaa	Figs 4, 6	Keglen	Fig. 6
Ataata Kuua	Figs 4, 6	Killerpaat Qaqqarsuat	Fig. 6
Blæsedalen	Fig. 6	Killiit (Fortunebay)	Figs 4, 6
Blåbærdalen	Figs 4, 6	Kingittup Qaqqaa	Fig. 6
Brededal	Figs 4, 6	Kingittuusuaq	Figs 6, 103
Charles Polaris Dal	Fig. 6	Kuannersuit Kuussuat	Fig. 6
Daugaard-Jensen Dal	Figs 4, 6	Kuannersuit Sulluat	Fig. 6
Disko Bugt	Fig. 1	Kuannit	Fig. 6
Disko Gneiss Ridge	Fig. 4	Kuuganguaq	Figs 4, 6
Disko Fjord (Kangerluk)	Figs 4, 6	Kvandalen	Figs 4, 6
Enok Havn (Ivisaarqut)	Fig. 6	Laksedalen	Figs 4, 6
Eqaluit (Nordre Laksebugt)	Figs 4, 6	Luciefjeld	Fig. 6
Eqalunnguaqqat Qaqqaat	Figs 4, 6	Lyngmarksfjeld (Akuarut)	Fig. 6
Eqi	Figs 4, 6	Makittarissagaq	Fig. 6
Eqip Qaqqaa	Figs 4, 6	Maniillat	Fig. 6
Fortunebay (Killiit)	Figs 4, 6	Marraat Qaqqaat	Figs 4, 6
Frederik Lange Dal	Figs 4, 6	Mellemfjord (Akullit)	Figs 4, 6
Gamle Qullissat (Qullissaaqqat)	Fig. 6	Morten Porsild Dal	Fig. 6, 174
Giesecke Dal	Figs 4, 6, 103	Naqerloq	Fig. 6
Giesecke Monument (Uppalluk)	Figs 4, 6	Narsap Qaqqaa	Figs 4, 6
Godhavn (Qeqertarsuaq)	Figs 4, 6	Navaranaat (Apostelfjeld)	Fig. 6
Hammer Dal	Figs 4, 6, 103	Niaqussat	Figs 4, 6
Hanekammen	Figs 4, 6, 103	Niiortuut	Figs 4, 6
Hareøen	Figs 1, 4, 6	Niuluut	Figs 4, 6
Ikorfarsuit	Figs 4, 6	Nordfjord (Kangersooq)	Figs 4, 6
Ikorfat	Figs 4, 6	Nordre Laksebugt (Eqaluit)	Figs 4, 6
Illukasik	Fig. 6	Nunavik	Figs 4, 6
Illukunnguaq	Fig. 6	Nuuk Kangilleq	Fig. 6

Orlingasoq	Figs 4, 6	Saqqarliit Ilorliit	Figs 4, 6
Orpiit Qaqqaat	Figs 4, 6	Saqqarliit Silarliit	Fig. 6
Paatuut	Figs 4, 6	Sedimentkløften	Figs 6, 103
Perlertut Qaqqaat	Figs 4, 6	Sermersuaq	Fig. 6
Pingu	Figs 4, 6	Skarvefjeld (Innarsuaq)	Figs 4, 6
Point 440 m	Figs 6, 103	Skorstensfjeld	Figs 4, 6
Point 500 m	Figs 6, 103	Siniffik	Fig. 6
Point 600 m	Fig. 103	Sorte Hak	Figs 4, 6
Point 780 m	Fig. 6	Sortebærdalen	Figs 4, 6
Point 882 m	Figs 6, 103	Steenstrup Dal	Figs 6, 103
Point 975 m	Fig. 6	Stordal	Figs 4, 6
Point 1014 m	Figs 4, 6	Svartenhuk Halvø	Fig. 1
Point 1025 m	Fig. 6	Tartunaq	Figs 4, 6
Point 1070 m	Figs 6, 103	Tini	Fig. 6
Point 1109 m	Fig. 6	Tuapassuit	Fig. 6
Point 1123 m	Figs 4, 6	Tuapaat	Fig. 6
Point 1132 m	Figs 6, 103	Tuapaat Qaqqaat	Figs 4, 6
Point 1137 m	Figs 6, 103	Tunup Qaqqaa	Figs 4, 6
Point 1266 m	Fig. 6	Ubekendt Ejland	Fig. 1
Point 1300 m	Figs 4, 6	Uiffaq	Figs 4, 6
Point 1380 m	Figs 6, 103	Ukaleqartarfik	Fig. 6
Point 1440 m	Fig. 6	Umiartorfiup Qaqqaa	Fig. 6
Point 1460 m	Figs 6, 103	Umiasat	Figs 4, 6
Point 1510 m	Figs 6, 103	Uppalluk (Giesecke Monument)	Figs 4, 6
Point 1530 m	Figs 4, 6	Uunartuarsuk	Fig. 6
Point 1560 m	Figs 4, 6	Vaigat	Figs 1, 4, 6
Point 1578 m	Figs 4, 6	Vesterdalen	Figs 4, 6
Point 1590 m	Figs 6, 103		
Point 1610 m	Figs 6, 103		
Point 1640 m	Figs 4, 6		
Point 1650 m	Fig. 6		
Point 1722 m	Fig. 6		
Point 1760 m	Fig. 6		
Point 1888 m	Fig. 4, 6		
Point 2000 m	Fig. 6		
Point 2010 m	Fig. 6		
Point 2080 m	Fig. 4, 6		
Puiattussuaq	Fig. 6		
Pyramiden	Figs 4, 6		
Qasigissat (Sælbugten)	Figs 4, 6		
Qasigissat Kuussuat (Vesterdalen)	Figs 4, 6		
Qeqertarsuaq (Godhavn)	Figs 4, 6		
Qingusaaq	Figs 4, 6		
Qullissaaqqat (Gamle Qullissat)	Fig. 6		
Qullissat	Figs 4, 6		
Qunnilik	Fig. 6		
Rink Dal	Figs 4, 6, 103		
Rødeelv	Fig. 6		
Sapernuvik	Figs 4, 6		
Saqqaq	Figs 4, 6		



Danish Ministry
of Energy, Utilities
and Climate

*GEUS is a research and advisory institution in the
Danish Ministry of Energy, Utilities and Climate*

GEOCENTER
DENMARK

*Geocenter Denmark is a formalised cooperation between
Geological Survey of Denmark and Greenland (GEUS),
Department of Geoscience at Aarhus University
and the Geological Museum and Department of
Geosciences and Natural Resource Management
at the University of Copenhagen.*

Lithostratigraphy, geology and geochemistry of the volcanic rocks of the Maligât Formation and associated intrusions on Disko and Nuussuaq, Paleocene of West Greenland

The upper Cretaceous–Tertiary Nuussuaq Basin in West Greenland contains a many kilometres thick succession of siliciclastic sediments and overlying volcanic rocks. The first studies in the early 19th century were centred on the coal and fossils in the sediments and the minerals in the volcanic rocks, including famous occurrences of native iron. The present focus of interest includes modern stratigraphic and volcanological studies to decipher the basin evolution and support hydrocarbon and mineral exploration.

This bulletin presents the lithostratigraphy, geology and geochemistry of the Paleocene volcanic rocks of the Maligât Formation and its related intrusions on Disko and the Nuussuaq peninsula; it concludes with a detailed discussion of the effects of crustal contamination processes. The Maligât Formation is up to 2000 m thick and comprises four formally defined members and 15 chemically defined informal units. It is mainly composed of basalt lavas but also includes basaltic andesite, andesite and dacite flows and rhyolite tuffs. The silicic rocks and intrusions were produced by contamination in high-level magma chambers and commonly contain native iron. The comprehensive descriptions and analyses of each member and unit represent a synthesis of many years of work and are intended to serve as a guide for future studies, including exploration for mineral deposits associated with some units of the formation.

A companion bulletin (volume 39) on the volcanic rocks of the picritic Vaigat Formation that underlies the Maligât Formation was published in 2017.

Printed 2018
ISSN 1604-8156
ISBN 978-87-7871-498-5

De Nationale Geologiske Undersøgelser
for Danmark og Grønland (GEUS)
Geological Survey of Denmark and Greenland

Øster Voldgade 10
DK-1350 Copenhagen K
Denmark

